Charles University

Faculty of Science

Plant Anatomy and Physiology

Functional characterization of plant EXO70 exocyst subunit isoforms and their membrane targeting mechanisms

PhD Thesis

Mgr. Juraj Sekereš

Supervisor:

Ing. Martin Potocký, PhD

Consultants:

Doc. RNDr. Viktor Žárský, PhD

Ing. Přemysl Pejchar, PhD

Declaration

I declare that this work is the result of my own research except as cited in the references. The thesis has not been accepted for any degree and is not currently submitted in the candidature of any other degree.

I understand that my results relate to the rights and obligations of the Act No. 121/2000 Coll., the Copyright Act, as amended, in particular the fact that Charles University in Prague has the right to conclude a licence agreement on the use of this work as a school work pursuant to Section 60 paragraph 1 of the Copyright Act.

In Prague, 4th of July in 2018 Juraj Sekereš

Prohlášení

Prohlašuji, že tato práce je výsledkem experimentů, které jsem vykonal samostatně či ve spolupráci s kolegy, kteří jsou rovněž uvedeni jako spoluautoři na předložených publikacích. Dále prohlašuji, že všechny použité informační zdroje jsou citovány v textu a jsou řádně uvedeny v seznamu literatury. Podaná práce nebyla dříve ani souběžně použita k získání jakéhokoliv titulu v ČR či v zahraničí.

Chápu, že má práce podléhá právům a povinnostem dle zákona č. 121/2000 Sb., autorského zákona, ve znění pozdějších předpisů. Jsem srozuměn s tím, že Univerzita Karlova v Praze může uzavřít licenční smlouvu o užívání této práce jako školní práce podle § 60 odst. 1 autorského zákona.

V Praze, 4. července 2018 Juraj Sekereš

Acknowledgement

First and most of all, I would like to thank Martin Potocký for being good mentor, friend and for virtually saving my ass, probably more than once. I would like to thank The Cloning Master Přemysl Pejchar for the proper initiation into the ancient art of the molecular cloning. I would like to thank Viktor Žárský and Fatima Cvrčková for ongoing inspiring intellectual stimulation. I would like to thank Leopold Butters Stotch, Roman Pleskot and Jitka Ortmannová for continuous supply of interesting conversations and alcohol intoxication. I would like to thank Lukáš Synek for improving my insight in microscopy and travelling. I would like to thank Ivan Kulich and Peter Sabol for all the fruitful scientific discussions during the times of my presence at the faculty. I would like to thank Anamika Rawat for entrusting me the sacred mighty Cheeku. I would like to thank Jana Šťovíčková and Major Haluška for their friendly attitude and occasional supply of free tobacco. I would also like to thank both our technicians, Marta Čadyová and Jana Šťovíčková for all the support provided. I also thank all other members of The Laboratory of Cell Morphogenesis at the Charles University in Prague and the Laboratory of Cell Biology at the Institute of Experimental Botany for contributing to the genuinely positive and nourishing environment I had the honour to be part of. I would like to thank my family and Jarmila Králová for generic moral support and making my life more pleasant. I would like to thank Alexandra Elbakyan for her astonishing bravery in the fight against the broken industry complex pimping the scientific publication process and for saving many hours of my time. I would like to thank the reviewers of this thesis for the just and merciful ordeal. I would like to thank the Grant Agency of the Charles University for financially supporting my research and thus providing me the opportunity to participate in several highly interesting international meetings and to the Czech Science Foundation (GACR) for contributing to my alms. I would like to thank EMBO for funding my participation at courses boosting my training, as well as to the organizers of the courses for allowing me to participate.

Abstract

Vesicle tethering complex exocyst is one of the key regulators of the cell polarity and morphogenesis in eukaryotes. The complex interacts with the secretory vesicle, as well as plasma membrane, and facilitates formation of cis SNARE complex leading into fusion of the vesicle with target destination. Two of the eight exocyst subunits, the SEC3 and EXO70 are known to bind plasma membrane via protein and lipid interactors in Opisthokont model organisms. Genomes of angiosperm plants encode a surprisingly wide repertoire of EXO70 isoforms with over 20 present in both Arabidopsis and diploid tobacco genome. It has been proposed that different EXO70 isoforms would form parts of functionally distinct subtypes of the plant exocyst complex driving membrane trafficking to various membrane domains. Specific interactions of peripheral membrane proteins with particular membrane phospholipids largely contribute to targeting of cellular components to subcellular compartments and membrane domains. This thesis focuses on role of protein-lipid interactions in regulation of plant cell polarity and contributes to functional analysis of the plant EXO70 family diversity. We introduce the topic with the theoretical reviews summarizing role of protein-lipid interactions in establishing plant cell membrane domains at various spatio-temporal scales and role of the exocyst complex at the interface of cytoskeleton and membrane trafficking in eukaryotes. Analyzing the roles of diverse EXO70 isoform within single cell is the core of the first study that systematically compares subcellular localization of the whole EXO70 repertoire using the growing tobacco pollen tube, a well established model system for addressing regulation of plant cell polarity. Transferring the pollen tubes with constructs encoding the tagged native tobacco EXO70 isoforms, we uncovered targeting of the proteins to various compartments, including vesicle-enriched inverted cone, nucleus and two spatially distinct plasma membrane domains overlapping to a different degree with spatial maxima of anionic phospholipids phosphatidylinositol-4,5-bisphosphate and phosphatidic acid. This is followed by the detailed analysis of EXO70A1, the EXO70 isoform expressed across many plant tissues and known to drive polar exocytosis in different cell types. We combined live cell imaging of Arabidopsis root cells and tobacco pollen tubes with in vitro

protein-lipid binding assays and molecular dynamics simulations to demonstrate importance of EXO70A1 direct interaction with anionic phospholipids in membrane targeting of the plant exocyst complex. The thesis further includes functional studies that address the roles of Arabidopsis EXO70A1, EXO70B1 and EXO70B2 isoforms in targeting trafficking to various membrane domains and subcellular compartments, and to which I contributed. In the form of comprehensive review, we discuss our data and the so far published studies addressing the relation between the subcellular localization and function of plant EXO70 isoforms.

Souhrn

Váčkový poutací komplex exocyst patří mezi hlavní regulátory buněčné polarity eukaryot. Tento proteinový komplex propojuje sekretorické váčky s plazmatickou membránou a reguluje vznik cis SNARE komplexu, jehož formování pohání fúzi membrány váčku s cílovou membránou. Výzkum funkce komplexu exocyst u kvasinkových a savčích buněk ukázal, že dvě z jeho osmi podjednotek, SEC3 a EXO70, poutají komplex k plazmatické membráně díky přímým interakcím se specifickými proteiny a membránovými fosfolipidy. Podjednotka exocystu EXO70 je v genomech krytosemenných rostlin kódována velkým počtem paralogů, v případě modelových rostlin huseníčku a tabáku se jedná o více než 20 genů. Rozdílné izoformy EXO70 pravděpodobně tvoří součást funkčně odlišných typů komplexu exocyst a regulují jejich zacílení do rozličných membránových domén, jelikož specifické interakce periferních membránových proteinů s různými fosfolipidy obecně přispívají k nasměrování proteinů do cílových organel a membránových domén. Tato práce se zaměřuje na funkci specifických interakcí proteinů a lipidů v rámci regulace buněčné polarity u rostlin a přispívá k objasnění rozmanitosti izoforem podjednotky exocystu EXO70 v rostlinných buňkách. Úvodní přehledné články přinášejí recentní shrnutí souhry proteinů a lipidů v ustálení membránových domén rostlinných buněk na různých časových a prostorových škálách a funkce poutacího komplexu exocyst na rozhraní cytoskeletu a váčkového membránového transportu. Studium rozdílné role podjednotek EXO70 v rámci buňky je jádrem první systematické studie srovnávající buněčnou lokalizaci všech izoforem EXO70 v klíčící pylové láčce tabáku, klasickém modelovém systému pro výzkum regulace buněčné polarity rostlin. Transformovali jsme pylové láčky tabáku konstrukty kódujícími fluorescenčně značené izoformy EXO70 a pozorovali lokalizaci do různých buněčných kompartmentů, jako například subapikální oblast cytoplazmy bohatá na membránové váčky, buněčné jádro a dvě rozdílné domény plazmatické membrány s různým obsahem fosfatidylinositol-4,5-bisfosfátu a fosfatidové kyseliny. Na tuto studii navazuje podrobná analýza široce exprimované isoformy EXO70A1, která je nezbytná pro polarizovanou exocytózu v mnoha rostlinných pletivech. Pomocí pokročilé fluorescenční mikroskopie, biochemických analýz a počítačových simulací interakcí EXO70A1 s lipidy jsme ukázali, že EXO70A1

interaguje s vybranými záporně nabitými fosfolipidy a tyto interakce jsou nezbytné pro zacílení komplexu exocyst do míst buněčné sekrece. Práce dále zahrnuje výsledky několika projektů popisujících funkci izoforem EXO70A1, EXO70B1 a EXO70B2 v rámci buněčného transportu do specifických membránových domén a vakuoly u modelového organizmu *Arabidopsis thaliana*, na jejichž řešení jsem se podílel. V rámci diskuse představujeme důkladnou studii shrnující známé poznatky o vztahu vnitrobuněčné lokalizace a biologické funkce izoforem EXO70 u rostlin.

Table of Contents

Introduction

In the following reports, I have addressed the issues of cell biology, the interplay of lipids and proteins in establishing and maintenance of plant cell polarity and the role of the vesicle tethering complex exocyst as the interaction machine at the interface of cytoskeleton and membrane trafficking.

PAPER 1:

Title: 180 Years of the Cell: From Matthias Jakob Schleiden to the Cell Biology of the Twenty-First Century

Authors: Juraj Sekereš and Viktor Žárský

Rationale of the report: We have explored the concept of the cell and its paradigmatic implications since the birth of the Cell Theory in 19th century, through establishment of modern molecular biology till recent trends in cell biology synthesizing reductionist and holistic approaches like modular and systems biology and attempts for in vivo biochemistry as a way to understand fine dynamic structure and self-organization of the cytoplasm. Special focus was also dedicated to the development of the concept of biological membranes from the early disputes over cell boundaries including debates between proponents of the Cell Theory and the Protoplasmic Theory concepts through discovery of the phospholipid bilayer till modern approaches appreciating crucial impact of phospholipid composition on membrane properties and addressing membrane heterogeneity at fine spatio-temporal scales.

My contribution: I wrote most of the manuscript with many pieces of fruitful conceptual contribution from Dr. Viktor Žárský.

Published in: Concepts in Cell Biology - History and Evolution Plant Cell Monographs book series, volume 23: p7-37, doi: 10.1007/978-3-319-69944-8_2

PAPER 2:

Title: The song of lipids and proteins: dynamic lipid-protein interfaces in the regulation of plant cell polarity at different scales.

Authors: Juraj Sekereš, Roman Pleskot, Přemysl Pejchar, Viktor Žárský and Martin Potocký

Rationale of the report: We have summarized the contemporary point of view on the interplay of proteins and lipids in the establishment and maintenance of plant plasma membrane domains at various scales. We emphasized the complementary role of proteins and lipids in constituting biological functions of the membranes and put strong focus on necessity to combine independent methodical approaches, namely advanced fluorescent microscopy, biochemistry and computational simulations, for the proper understanding of the cell membranes.

My contribution: I wrote several chapters of the review, namely the part about phosphoinositides, the text on the role of sterols and very-long-chain fatty acids, as well as the text about membrane microdomains and advanced microscopy techniques used for their studying. All authors collectively participated in finalizing of the manuscript.

Published in: Journal of Experimental Botany 66(6):1587-98, doi: 10.1093/jxb/erv052

PAPER 3:

Title: The exocyst at the interface between cytoskeleton and membranes in eukaryotic cells.

Authors: Lukáš Synek, Juraj Sekereš and Viktor Žárský

Rationale of the report: We summarized current insight in function of exocyst complex as the interaction machine contributing to polarized secretion by connecting cytoskeleton, secretory vesicle and plasma membrane via plethora of specific protein-protein and protein-lipid interactions, mostly characterized in yeast and mammalian cells. We also reviewed known experiments addressing plant exocyst interactions with the cytoskeleton and addressed potential implications of the Opisthokont data on exocyst-cytoskeleton interactions for plant cell biology.

My contribution: Me, Lukáš Synek and Viktor Žárský contributed equally to the manuscript.

Published in: Frontiers in Plant Science 4:543, doi: 10.3389/fpls.2013.00543

Chapter 2
180 Years of the Cell: From Matthias Jakob Schleiden to the Cell Biology of the Twenty-First Century

Juraj Sekeres and Viktor Zarsky

Abstract The fact that the form and function of organisms results from the collective action of cells, the structural and functional units of life, is undoubtedly one of the most important foundations of contemporary biology. Here, we provide a glimpse of the key discoveries and accompanying theoretical disputes that led from the discovery of the cellular structure of organisms, through elaboration of a tool set enabling study of cell phenomena at the molecular level in a mechanistic framework, to the latest theoretical and methodological trends in addressing cellular organization as the methodological and interpretational framework for addressing the phenomena of life. We also emphasize how views of cell structure and function prevailing during particular eras were influenced by methodological constraints at the time and how previously disregarded concepts returned to mainstream biology as a result of novel techniques that could provide more detailed insight into the structure and dynamics of cellular components.

2.1 Theoretical and Methodical Foundations of Cell Theory

Various ideas, first in the form of mythological narratives, on the origins and basis of life have existed since the dawn of humankind. Some of the first modern ideas on the substance of life and its developmental program being confined to a small piece of living organism came from Aristotle in the fourth century BC. On the basis of empirical experience of egg development and plant vegetative reproduction, he postulated "entelchy" as a driving principle that leads organisms toward fulfilling their form and potential (Welch and Clegg 2010). Until the seventeenth century, the

J. Sekeres (✉) • V. Zarsky
Laboratory of Cell Biology, Institute of Experimental Botany, Czech Academy of Science, Prague 6, Czech Republic

Laboratory of Cell Morphogenesis, Department of Experimental Plant Biology, Faculty of Science, Charles University, Prague 2, Czech Republic
e-mail: juro.seky@gmail.com; viktor.zarsky@natur.cuni.cz

V.P. Sahi, F. Baluška (eds.), *Concepts in Cell Biology - History and Evolution*, Plant Cell Monographs 23, https://doi.org/10.1007/978-3-319-69944-8_2

developing science of biology only rarely sought the causes of live phenomena in the fine structure of organisms. Prominent trends such as French morphology and German *Naturphilosophie* looked for explanation of body plans and structures in abstract ideal forms toward which organisms are driven (Radl 1930); the approach was largely orthogonal to later and contemporary mechanistic views of life.

Idealistic concepts accompanied biology further, but a gradual shift toward empiricism and mechanistic tendencies in science appeared in the eighteenth century. The trend included revival of atomism, a theory that claims that properties of matter are given by the small indivisible particles it is composed of (Harris 2000). It is important to note that advances resulting in formulation of cell theory were not only led by technological improvements in microscopy, but also by a change in theoretical focus. Many scholars already had the idea that observed tissues were aggregates of more basic units, even before looking through microscopes (Harris 2000). Another important philosophical inspiration (quite distinct from common early analogies between cells and atoms or crystals, and much closer to the contemporary perception of cells) came from G.W. Leibniz (1646–1716). His idea established the often unrecognized basis of cell theory. In the idea of fully autonomous self-reproducing "monads," developed in a critical discourse with the Cartesian mechanistic view of the universe, Leibniz stated that if living organisms were machines their parts would not merely be simple mechanical pieces of matter but smaller machines themselves. Importantly, the dynamics of monads is driven from the inside. This idea stimulated the concept of German philosopher Lorenz Oken (1779–1851) that all organisms are composed of "infusoria" and "Urbläschen" (primordial bubbles) as basic life units; this speculation directly preceded the works of the first empirical cell biologists (Canguilhem 2008; Harris 2000). However, it was only the invention and improvement of microscopes that enabled direct observation of the material basis and composition of organisms.

Based on early observations, the composition of tissues as fibers, globules, or twisted cylinders was postulated (Harris 2000). In the eighteenth century, Albrecht von Haller, inspired by atomism, speculated that fibers composed of strings of atoms were the basic structural elements of the body: "For the fiber is for the physiologist what the straight line for the geometrician, and from this fibre all shapes surely arise" (in Harris 2000). Robert Hooke was active in many fields of natural sciences in the second half of the seventeenth century and is considered to be the father of the term "cell" in biology. He used this term to describe the structures he saw with his simple microscope in slices of plant cork tissue because they resembled honeycomb cells (*cellulae* in Latin). At that time, cells were conceived as hollow and regarded as "avenues of communication, channels for conveyance of juices" (in Welch and Clegg 2010).

2.2 From Schleiden to Virchow: Formation of Cell Theory Tenets

More and more nineteenth century scientists were convinced that plant tissues were generally composed of cells, but Matthias Jakob Schleiden (1804–1881) made the first attempt to use cellular composition as a unifying explanatory principle in botany (Harris 2000). Schleiden wanted to establish botany on a firm ground as a more exact science, leaving behind the speculative tradition of German *Naturphilosophie*. Schleiden was mechanistically oriented and, like many of his contemporaries, inspired by Isaac Newton's physics. He used crystal-like metaphors for conceptualizing the self-organization of organisms. He also emphasized inductive and empirical approaches, as well as the importance of following ontogeny (reflecting specification or differentiation of initial simpler general forms into more complex elaborated ones) in order to properly understand plant tissues. Schleiden's efforts resulted in the formulation of a general rule that all plant tissues are composed of a single basic element, the polyhedral cell. He would subsequently call for "condemnation of every theory that explains processes in a plant otherwise than as combination of processes in individual cells" (in Radl 1930).

The cell wall as the boundary and structural element was still considered more important than the internal content, although the nucleus was already known and described. It was named in 1833 by Robert Brown who, however, did not recognize the general presence of nuclei in all cells. Such an opinion is understandable considering that the cell wall is morphologically the most conspicuous structure in differentiated plant cells and is often the functional determinant of the particular tissue. Moreover, the crucial importance of cell wall mechanics and its integration with the plant cell membrane and cytoplasmic core are currently well-recognized features of plant body organization. Schleiden was unclear about the ontogenic origin of cells; therefore, an extracellular protoplasm or sap played a role in his concept of cell formation. He postulated condensation of nuclei from this material and formation of cellular matter around them. Cells were formed from nuclei as growing vesicles until they touched each other (Harris 2000; in Radl 1930). Later in development, they mostly formed around nuclei inside other cells (Lombard 2014). Schleiden considered nuclei in mature cells dispensable and often reabsorbed (Harris 2000).

Because of the absence of distinct cell walls and difficulties in sample preparation, the cellular nature of animal bodies was less clear. Animal cells were studied, for example in developing embryos. However, the general empirical supposition postulated formation of the animal body from cells during early development, but not necessarily in its adult state. Henri Dutrochet (1776–1847) advocated a materialistic worldview and aimed to identify vital phenomena in animals and plants (Harris 2000). He claimed that both plant and animal tissues were composed of "vesicles" and "globules," although he probably could not observe animal cells. Although Dutrochet's morphological view of cells was largely erroneous, he was probably the first to perceive cells as basic physiological units of metabolic

exchange with selective inflow of nutrients and outflow of waste. He also suggested the existence of the same underlying principles in animal and plant tissues: "[If] phenomena are tracked down to their origins, the differences are seen to disappear and an admirable uniformity of plan is revealed" (in Harris 2000).

The first claim of the widespread presence of "Kornchen" analogous to plant cells in animal tissues, backed by countless histological observations, was made by Bohemiam Jan Evangelista Purkyně/Purkinje (Harris 2000). He claimed that animal tissues were universally composed of cells, fibers, and fluids. Purkyně was also one of the first (following Dutrochet) to emphasize the functional significance of cells and facilitated the transition from "histomorphology" to "histophysiology" (Harris 2000), particularly through comprehensive studies of ciliary movements in several animal tissues. Unlike Schwann, who put most emphasis on the nucleus, Purkyně also focused on the active content of the cell, the "protoplasm" (see Sect. 2.3).

Theodor Schwann (1810–1882) got most credit for extending cell theory to animal tissue because he made stronger (although not always correct) claims than Purkyně (Harris 2000). Inspired by Schleiden's conclusions, as well as the similarity between animal notochord cells and plant cells discovered by Schwann's teacher Johannes Müller (Harris 2000), Schwann accumulated a vast number of examples of embryonic and adult animal tissues consisting of cells and claimed cellular origin as the unifying ontogenic principle for animals as well as plants (Radl 1930). Schwann was not certain about the exact origin of individual cells and postulated their origin either from homogenous life matter (possibly through first generating a nucleus) or from inside other cells, around their nuclei. According to Schwann, cells could thus originate inside or outside other cells (Harris 2000; Lombard 2014). Inspired by Schleiden, Schwann claimed that formation of cells from liquid via nuclei was a mechanistic crystallization-like process (Harris 2000).

Several different ideas about the mechanism of new cell generation coexisted and many scientists accepted that different mechanisms could work in different organisms and tissues (Harris 2000). Discovery of binary cell fission by Barthélemy Dumortier and Hugo von Mohl was of outstanding importance, although both admitted the plurality of mechanisms of cell formation. Franz Unger (1800–1870) was the first to oppose Schleiden's aggregation/crystallization idea openly. He disregarded "cytoblasts" as source of cells and postulated that binary division was the most common mechanism of plant cell division (Harris 2000). Within a few years, sufficient empirical evidence had accumulated to abandon Schleiden's concept of cell formation. Because of technical difficulties, it took much longer to accumulate precise observations of animal cell formation. Robert Remak (1815–1865) proposed the first explicit unifying theory of cell division in both plants and animals. Remak developed novel hardening agents that allowed him to carry out extensive studies of cell formation in many animal tissues. He concluded that extracellular formation of cells does not occur in animal tissues and that binary division is the universal mechanism of cell formation. Development is thus a sequence of binary divisions followed by morphological modifications; furthermore, the egg itself is a cell. Remak also proposed that the same rules governed cell

division in both pathologic and embryonic tissues (in direct opposition to Müller's theory of specific malignant tumor formation). Remak categorically opposed Schleiden and Schwann, particularly their analogies between cells and crystals: "It is hardly necessary to make special mention of the similarity or disparity of cells and crystals, for, in the light of the facts that I have discussed, the two structures offer no points of comparison" (in Harris 2000).

Rudolf Virchow (1821–1902), strongly inspired by Remak and spreading Remak's ideas, consolidated cell theory with his famous statement "*Omnis cellula e cellula*," reflecting the origin of existing cells from other cells and describing ontogeny as a gradual process of binary divisions from a fertilized egg to adult tissues. Classical cell theory thus stood on three major tenets:

1. All living organisms are composed of one or more cells.
2. The cell is the basic unit of structure and function in all organisms.
3. All cells arise from preexisting cells.

The history of discoveries leading to a unified picture of cell division (and the relationship between nucleus and cytoplasm during formation of new cells) is an excellent example of how the choice of methods and model system can influence the inferred theory. This aspect has always constrained experimental biology and is still relevant in our time. From the contemporary point of view (i.e., retrospective judgement), ideas about extracellular formation and crystallization around nuclei might seem obscure. However, one must acknowledge that many conclusions were based on observations of fixed tissues prone to artifacts and providing only a static view of underlying dynamic phenomena. The presence of open mitosis in both animals and plants (Sazer et al. 2014) made deciphering the relationships between "sap" (cytoplasm), nucleus, and cell division even more complicated until the nature of chromosomes was understood.

Moreover, some of the tissues used in the past as model systems are nowadays known as rather exceptional cases. Even original observations of plant tissues by Schleiden involved endosperm syncytium undergoing cellularization, which might have given him the wrong impression of cell formation (Harris 2000). Many early conclusions were also misled by mistaking starch grains (forming inside cells) for nuclei. On the other hand, Dumortier and von Mohl were able to make their outstanding discovery through observing an ideal model system for study of binary cell division—the filamentous alga *Conferva (Draparnaldia by contemporary nomenclature)* with cells dividing at the termini of filaments. Cartilage was repeatedly used as argument for the acellular origin of animal cells (Harris 2000). Developing embryos, which enabled direct observation of unfixed dividing cells in time, were the source both of support for a model of binary cell division and of erroneous judgment. Although many authors (working mostly with amphibian models) correctly interpreted the partitioning of egg as progressive cell division, French biologist Quatrefages de Bréau claimed in the middle of the nineteenth century that the development of gastropod embryos involves formation of cells within cells. Quatrefages de Bréau was probably driven by an attempt to support Schwann's model. Even Dumortier, who discovered binary division in *Conferva*

(Draparnaldia by contemporary nomenclature), acknowledged the possible formation of cells within cells and even formation of cells from acellular material after observing gastropod development (Harris 2000). Large yolky embryos with unequal cleavage were also source of confusion, as in the case of Carl Vogt who claimed that *Alytes* frog embryo furrowing was independent of formation of new cells.

In the light of incongruent fragmentary observations, it was honest of many contemporary scientists in the nineteenth century to acknowledge the plurality of animal cell formation mechanisms (Harris 2000). Strong universal claims required systematic comparison of many different tissues and improved techniques, as performed by Remak. Although he opposed ideas that involved intracellular formation of cells, he admitted that it was often not sloppiness of observation or ill judgment that lead to incorrect conclusions, but accidental choice of problematic material such as cartilage or muscle fiber. However, even Remak made an erroneous conclusion regarding nuclear division, possibly because of observation of static fixed specimens and a bias toward making an analogy between binary cell division and binary nuclear division. Karl Bogislaus Reichert (1811–1883) observed dissolution of nuclei during division of red blood cells, which he used as an argument for Schwann's concept of de novo nuclei formation and against the concept of binary cell division. Remak claimed that he had failed to reproduce Reichert's observation of nucleus dissolution in dividing red blood cells. Reichert's ideas about cell formation were generally wrong but some of his observations were correct, whereas Remak's ideas about cell formation were generally right but some of his observations were wrong. Remak occasionally observed nuclear dissolution but interpreted it as an artifact. Both Remak and Virchow supported a model of nuclear binary division that involved formation of grooves, constriction, and division of one nucleus into two. Some scientists advocated Remak's and Virchow's models, whereas others referred to nuclear dissolution ("Reichert's doctrine"), often with interpretations close to Schwann's original ideas about cell formation (Harris 2000).

2.3 Protoplasmic Concepts and Early Criticisms of Newly Established Cell Theory

Cell theory was popular with reductionists, who attempted to comprehend fundamental life phenomena by studying simple structural components. Technological improvements such as the oil immersion lens, Purkyně's microtome technique (Harris 2000), and novel fixation and staining methods (McIntosh and Hays 2016) led to countless observations of cells and their contents in the nineteenth century. Criticism of cell theory also existed and, in extreme cases, many histological discoveries were accused of being staining and/or fixation artifacts. Skepticism over the universality of cell theory often cited the existence of cells without nuclei,

multinuclear syncytia, and large amounts of extracellular material in adult tissues as evidence against cell theory. Nevertheless, all of these phenomena were ultimately understood as developmental products of cells. One of the last bitter arguments about the general validity of cell theory was over the nature of nervous tissue. "Reticulate theory" considered the nervous tissue as a continuous uninterrupted network, because of observation limits set by contemporary microscopes. Yet, cell theory envisaged nervous tissue as consisting of individual cells as in other tissues (the "neuronal doctrine"). Ramon y Cajal demonstrated the latter to be true by using a staining method that randomly marked only a few neurons within the tissue, clearly indicating discontinuity in the neuronal network (Radl 1930).

In addition to claims that cell theory cannot universally explain the functioning of organisms and that many observed structures might be fixation artifacts, cell theory was also repeatedly accused of being insufficient or even not relevant to understand the universal properties of life. Some of these incongruences were formulated in various forms of "protoplasmic theory," which either complemented cell theory by closing a conceptual gap between the cell surface and cellular contents or competed with cell theory by completely shifting focus from cells as a mere building bricks to the living substance inside the cell. The term "protoplasm" was introduced by Jan Evangelista Purkyně/Purkinje in 1839, well before Hugo von Mohl and in a very similar sense (Janko and Štrbáňová 1988; Harris 2000; Zárský 2012; Liu 2016). Hugo von Mohl was critical of Schleiden's and Schwann's focus on understanding cells in terms of boundaries and building blocks and disliked analogies between cells and crystals. He redefined the cell's function as more based on internal organization and formulated his protoplasmic theory in 1846 (Liu 2016).

Ferdinand Cohn proposed in 1850 that "plants and animals were analogous not only because of their construction from cells, but also, at a more fundamental level, by virtue of a common substance, protoplasm, filling the cavities of those cells" (Welch and Clegg 2010; Liu 2016). He thus connected von Mohl's concept with the earlier idea of "sarcode," a contractile substance proposed by Félix Dujardin to provide the life basis of unicellular eukaryotes (Liu 2016). The tendency to look for basic attributes of life (irritability, sensibility, contractility, reproduction, etc.) in the properties of protoplasm was not uncommon, and protoplasm itself was compared to an "elementary organism." Anatomist Max Schultze suggested in the middle of the nineteenth century that the true basis of life would be found by studying protoplasm, not the cell (Welch and Clegg 2010) and redefined the cell as a "clump of protoplasm" around a nucleus (Liu 2016).

Some authors regarded the cell as a nonliving envelope and focused on studying protoplasm as the "naked state of living matter" (Welch and Clegg 2010). For example, E.B.Wilson did not claim protoplasm to be the only living element inside the cell: "Protoplasm deprived of nuclear matter has lost, wholly or in part, one of the most characteristic vital properties, namely, the power of synthetic metabolism, yet we still speak of it as 'living', because it may for a long time perform some of the other functions, manifesting irritability and contractility, and showing also definite coordination of movements" (as in the enucleated protozoan) (Wilson

1899). He also disregarded strong versions of reductionism that searched for a single basic element of life in "any single substance or structural element of the cell," because "life in its full sense is the property of the cell-system as a whole rather than of any one of its separate elements." His theory is thus not atomistic or reductionistic but puts a strong focus on the properties of protoplasm by claiming "that the continuous substance is the most constant and active element and that which forms the fundamental basis of the system, transforming itself into granules, drops, fibrillae or networks in accordance with varying physiological needs" (Wilson 1899). Yet, Wilson prophetically admitted that he could not achieve any clear general conclusion because the basis of all phenomena lies in the "invisible organization of a substance which seems to the eye homogenous." He believed that "ultramicroscopic bodies," molecules, groups of molecules, and micellae formed the basis of protoplasmic organization (Wilson 1899).

2.4 Discovery of Organelles: Increasing Appreciation of Cellular Content

Along with protoplasmic concepts involving the actions of micelles, drops, and tiny fibrillae, the presence of larger structures localized within cells was more and more recognized and emphasized, including the notion of smaller living units present inside cells, inspired by Leibnitz's theory of spontaneity and hierarchy of monads (see Sect. 2.1). Franz Unger described moving structures in pollen cytoplasm as an "army of monads full of inner vitality, full of an inner self-determination that revealed itself in their movements" (in Harris 2000). Observations of large unicellular eukaryotes such as amoebae and ciliates further stimulated thoughts about subcellular structures with specialized functions, analogous to macroscopic bodies. In 1884, Karl August Mobius suggested the term "organulum" (little organ) for such structures because they form parts of one cell, whereas true organs of multicellular animals consist of many cells. The term was later transformed into "organelle" and its meaning was expanded to cover subcellular structures of both unicellular and multicellular organisms (Schuldiner and Schwappach 2013).

An important breakthrough was made by van Benden and Boveri at the end of the nineteenth century. They discovered the autonomous life cycle of the centrosome and concluded that the structure had a life of its own; Boveri described the centrosome as a special organ of cell division (Harris 2000). Whitman perceived the cell as a "colony of simpler units, nucleus, centrosome, and so on," much as a higher organism is colony of cells (Whitman 1893). In 1882, Julius Sachs wrote that "chlorophyl bodies" (chloroplasts) behaved like autonomous organisms that divide to adjust their number to the size of growing leaves (Kutschera and Niklas 2005). In 1883, Andreas Schimper noticed the similarity between chloroplasts and cyanobacteria and proposed the symbiotic cyanobacterial origin of plastids (Taylor 1987). In 1890, Altmann postulated the universal presence of "bioblasts" (named

"mitochondria" by German microbiologist Benda in 1898) and discovered that they had same staining properties as bacteria; he concluded that they were modified bacteria (Ernster and Schatz 1981; Kutschera and Niklas 2005).

This idea of the endosymbiotic origin of chloroplasts and xenobiotic origin of eukaryotic cells as an evolutionary amalgam of once-independent organisms was further elaborated by Konstantin Mereschkowsky between 1905 and 1920 (Taylor 1987; Kutschera and Niklas 2005), but was not generally accepted until its revival in the 1970s. With improved microscopes and staining methods, novel organelles were added to the nuclei, chloroplasts, and vacuoles known from earlier observations (Ernster and Schatz 1981). With the discovery of "ergatoplasm" (later named "endoplasmic reticulum") in 1897 and the Golgi apparatus one year later, most large common components of the cell "inventory" were known by the end of the nineteenth century (Ernster and Schatz 1981).

2.5 Disputes over Cell Boundaries

For a living system, the existence and properties of a boundary to the outside world are as important as the properties of its internal composition. Yet, the presence and identity of a boundary between cells and the outside environment was not clear in the nineteenth century and (especially from the contemporary perspective) was largely neglected by proponents of both cell and protoplasmic points of view. Schwann assumed that surfaces/membranes always limit the mobility in/out of a cell, even if invisible, and this could be inferred from the Brownian motion of cell components, which do not escape the cell volume as delimited by the surface structure. Generally, however, comparison of the cell surfaces of plant cells (with walls) and animal cells were confusing and the terms "wall" and "membrane" were often used interchangeably. True membranes were impossible to detect with nineteenth century histology techniques. Thus, in the second half of the nineteenth century, little attention was paid to membranes and, if present, they were considered unessential secondary structures originating from hardening of the cell surface. Max Schulze, the proponent of protoplasmic theory, was also an eager opponent of the membrane concept (Lombard 2014). He postulated, in place of cells, small blebs of contractile protoplasm immiscible with water. Detected membranes were simply the result of protoplasm hardening caused by contact with the outside environment or an artifact of degeneration and the hallmark of dead cellular material.

The main support for the membrane concept came from osmotic studies. Hewson published experiments on the swelling and shrinking of blood cells as early as 1773. In the first half of the nineteenth century, Dutrochet explained plant turgescence by osmosis via a border with "chemical sieves" (Harris 2000; Lombard 2014). The first artificial membranes were created by precipitation of copper ferrocyanide (from potassium ferrocyanide and copper sulfate) and were thus named precipitation membranes. Together with the contemporary colloidal concept

of cell interiors and ideas about cell membranes originating through surface hardening, the existence of artificial precipitation membranes fueled belief that the surface of colloidal protoplasm precipitates and forms an osmotic barrier. Overton's pioneering experiments (published between 1895 and 1900) showed cell volume changes in more than 500 different solutions and allowed him to conclude that a barrier distinct from the plant cell wall must exist and is made of ether-soluble components (i.e., is hydrophobic). He suggested cholesterol and phospholipids as possible candidates. In combination with works on electrophysiology and microinjection experiments, acceptance of the plasma membrane as a real structure was established in the early twentieth century (Harris 2000; Lombard 2014).

2.6 Toward Cellular Determinants of Heredity

A clear picture of nuclear division formed only after the mitotic spindle and chromosomes were discovered and understood. Recurrent observations eventually led to the consensus that nuclei disassemble and reassemble during cell division. Strassburger proposed homology of plant and animal cell division before the end of the nineteenth century (Harris 2000). In the 1870s, details of cell division events were repeatedly observed and, in 1879, Walter Flemming coined the term "mitotic process" and described its basic chronology. Flemming also introduced the term "chromatin" and was the first to describe longitudinal division of chromosomes in both animal and plant cells. He was a sharp critic of the direct nuclear division concept advocated by Remak and Virchow, but at the same time fully acknowledged the continuity of nuclear material during cell division by expanding Virchow's statement into "*Omnis nucleus e nucleo*."

At that time, there was also a major effort to localize the material determinants of heredity. Many great biologists of the nineteenth century, even if not working with cells themselves, postulated such particles (Darwin postulated gemulae; Haeckel, plastiduls; Spencer, physiological units; de Vries, pangenes; Galton, strips, etc.) and thus stimulated the search for them (Radl 1930). Cumulative descriptive work helped characterize the progression of cell division and behavior of chromosomes in sufficient detail that biological interpretations and manipulative experiments were possible. As early as 1885, the concept of chromosomal loops as storage place for hereditary information was proposed by A. Weissmann (McIntosh and Hays 2016) and helped to explain the phenomena of meiosis and recombination (Harris 2000). The work of Theodor Boveri (1862–1915) not only definitively demonstrated chromosome function in heredity, but also shifted work from solely combination of observations and deduction to the introduction of manipulative experiments (Harris 2000). His experiments with sea urchin embryos involved polyspermy and manipulation of early embryo cleavage, resulting in blastomeres with unequal chromosome distribution. Boveri discovered that the fate of blastomeres correlated with introduced chromosomal abnormalities and deduced that different chromosomes carry different genetic loads. After the rediscovery of

Mendel's laws, Boveri was the first to point out the similarity between segregation of elements, as proposed by Mendel, and physical segregation of chromosomes (Harris 2000). The first concept of genes was purely phenomenological and did not necessarily ask for the material agent of heredity. Later, in the light of mechanistic trends, a material component responsible for transmission of genetic information was envisaged. Boveri proposed that the material basis of Mendel's laws of inheritance lay in the properties of chromosomes and thus contributed to the development of molecular genetics in the twentieth century (Harris 2000).

2.7 Cells in Tissues: Early Holistic and Reductionist Experimental Approaches

Since the early days of cell theory, many scientists have stressed that organisms are more than just an assembly of their parts, and that functional aspects of life should be studied in the context of the whole developing embryo/organism. Attitudes ranged from sharp criticism of cell doctrine as insufficient and misleading, through attempts to introduce novel organizing principles that would supplement and coordinate the action of cells, to a systematic attempt to understand developing embryos purely from the collective interactions of individual cells.

T.H. Huxley put forward a physiological interpretation of the cell in opposition to Schleiden's and Schwann's morphological concept. He claimed that "the cell-theory of Schleiden and Schwann" was not only "based upon erroneous conceptions of structure," but it also led "to errors in physiology" (Richmond 2000). He particularly disliked that "cell doctrine" overstated the assumption of anatomic individuality of cells and felt that cells should be studied in their mutual relation in the context of development, because the entire life history of an organism is "dominated by development" (Richmond 2000). Whitman stated that "the fact that physiological unity is not broken by cell-boundaries is confirmed in so many ways that it must be accepted as one of the fundamental truths in biology" (Whitman 1893). Sachs advocated the organism-standpoint and considered the presence of cells, although a general phenomenon of life, to be of secondary importance and only one of the many manifestation of formative life forces (Whitman 1893). The idea of Sachs that growth and change of plant forms is primary and that planes of cell division are secondary and dependent on overall growth (Radl 1930) was also shared by de Bary, who coined the famous statement: "The plant forms cells, the cells do not form plants" (Thompson 1917).

Major attempts at causal analysis of embryonic development as a result of collective interaction of individual cells crystallized into the discipline of *Entwicklungsmechanik* (developmental mechanics in the sense of natural causation), enthusiastically advocated by Wilhelm Roux (Radl 1930; Sander 1991). Roux shifted focus from speculations based purely on descriptive observations to manipulative experiments in a quest for causal explanation of development by

combination of individual acting forces (Priven and Alfonso-Goldfarb 2009; Sander 1991). Based on his experiments with amphibian embryos, Roux advocated a mosaic concept of development, stating that cells of the early embryo determine the position of later parts of the organism.

Other scientists proposed different concepts of development, largely because they used other model systems, such as cnidarians and early developing embryos that display an astonishing capacity for regeneration and a certain degree of invariance of morphogenesis with respect to the number of cells participating. Such experiments suggested that cells of the same lineage can have different fates and cells of different lineages the same fate, depending on the position they acquire within the embryo. Whitman claimed that "Comparative embryology reminds us at every turn that the organism dominates cell-formation, using for the same purpose one, several, or many cells, massing its material and directing its movements, and shaping its organs, as if cells did not exist, or as if they existed only in complete subordination to its will" (Whitman 1893). Some of the trends even resulted in the search for holistic principles that precede formation of cells and organize actions of cells across the whole developing organism.

Hans Driesch also attempted to break the continuous process of animal morphogenesis into its ultimate elements (first principles) at the outset of his career (Sander 1992a). In a visionary manner, he considered development to "start with a few ordered manifoldnesses," which would gradually "create, by interactions, new manifoldnesses," which "acting back upon the original ones (manifoldnesses) provoke new differences." "With each response, a new cause is immediately provided, and a new specific reactivity for further specific responses." (Sander 1992a). Parts of the developing embryo thus constitute a gradual conversion of states and receptivity to other stimuli. Governed by the nucleus, organogenetic chemicals are formed in the cytoplasm, which acts as intermediaries between external stimuli and the nucleus. A cascade of stimuli between cells and their partial activations drive development of the organism (Sander 1992a). Later in his life, Driesch became critical of overestimating the explanatory potential cell theory (Whitman 1893) and even revoked some of his original positions (Sander 1992b). Experiments with cnidarians, acrasid slime molds, plants, and echinoderm embryos (Markoš 2002; Sander 1992b) led him to search for fundamental laws determining the spatiotemporal coordinating system that leads cells into form (Priven and Alfonso-Goldfarb 2009; Sander 1993). Driesch advocated a mathematical and physical approach (Priven and Alfonso-Goldfarb 2009) but also wanted biology to be a science with autonomy and thus searched for organization principles, around which the undergoing chemical and physical phenomena are constituted (Priven and Alfonso-Goldfarb 2009). His conclusion that contemporary chemistry and physics were not sufficient to explain embryogenesis could in fact be extended until the 1970s, when cell research incorporated advances in cybernetics and genetics (Roth 2011). Driesch put strong emphasis on teleology in development (Sander 1992b) and unsuccessfully tried to formulate entelechy as a new collective physical quantity (Markoš 2002; Priven and Alfonso-Goldfarb

2009), specific for organisms, which might be analyzed using mathematical approaches (Priven and Alfonso-Goldfarb 2009).

Driesch's attempt to uncover laws of organization typical for biology was further developed by Alexander Gurwitsch (Beloussov 1997; Markoš 2002). Gurwitsch studied developing shark brain, fungal fruiting bodies, and composite flowers and arrived at the general conclusion that the overall shape repeatedly develops in an exact manner despite fluctuations in the shape and growth rate of individual parts. He also thought that the outline of a part or a whole embryo can be formulated mathematically more precisely than the shape and arrangements of their internal components (Beloussov 1997). Looking for a supracellular principle that orders and coordinates cells over the embryo, and inspired by contemporary developments in physics, he formulated the concept of a "species-specific field" that organizes morphogenesis (Beloussov 1997; Markoš 2002). Cells produce the field that extends to and affects an extracellular space and, at the same time, the field acts back on the cells. Fields from cells form an aggregate field, which depends on the configuration of the multicellular whole and there is feedback between the field and its morphogenetic consequences (Markos 2002). The interdependence between cell properties and their coordinates of position within a developing organism should be precise and mathematically simple (Beloussov 1997). Gurwitsch even attempted to define the field in vectorial manner (as a geometric description, not in a strictly physical sense), where cells followed the vectors of the field (Markoš 2002).

By the 1930s, many crucial discoveries in experimental embryology had been accomplished. Many studies involved isolation and recombination of embryonic parts and mapping of the differentiation and inductive potential of the isolated parts of embryos and the effects of parts transplanted onto other embryos, including interspecific transplants (Oppenheimer 1966; Gilbert et al. 1996). Phenomena such as the inductive potential of neural folds and establishment of limb polarity were intensively studied. Hans Spemann reintroduced the term "field of organization" to describe the inductive properties of the amphibian dorsal blastopore (Gilbert et al. 1996), conceptually building upon Driesch's concept of a "harmonious equipotential system." The concept of a field was thus still vital and, in 1939, Paul Weiss postulated that field is the key organizing principle of embryology; developmental phenomena have field properties and components of fields are connected by a web of interactions (Gilbert et al. 1996). Field concepts in the 1930s experimental embryology were materialistic. Weiss claimed that field has physical existence and is bound by physical substrates from which morphogenesis arises and should be the object of research like any other physical phenomena. The morphogenetic field was supposed to become the basic paradigm of embryology in its attempt to discover the laws of morphogenesis (Gilbert et al. 1996).

2.8 Establishment of Molecular Biology

Details of the birth and early history of biochemistry are beyond the scope of this review. However, we mention several key discoveries and concepts because the paradigm and methodology elaborated by biochemists largely influenced the advent of modern cell biology, especially in the twentieth century. Although most German scientists studying cells focused on their structure and formation, the French naturalist Francois Vincent Raspail (1794–1878) was interested in the chemistry of cells. He analyzed the chemical composition of cells by adopting chemical combustion analysis for small samples (microburning) and developed staining procedures to detect starch, albumin, silica, mucin, sugar, chlorides, and iron. He also stressed that that the cell is itself a microlaboratory, carefully balancing catabolism and anabolism (Harris 2000). In 1833, Payen and Persoz purified a thermolabile fraction able to breakdown starch into sugar. Such "agents" were later named enzymes by Wilhelm Kuhne. In 1893, Eduard Buchner was able to replicate the whole yeast fermentation process by a cell-free extract. Thomas Burr Osborne systematically crystallized proteins and demonstrated a vast diversity of protein species (Kyne and Crowley 2016). In 1926, James Sumner managed to isolate and crystallize an enzyme (urease) for the first time. He redissolved urease from the crystal (thus free of any small compounds potentially co-purified from the cell) and showed its catalytic activity, also demonstrating the proteinaceous (and biopolymer) nature of enzymes (Quastel 1985; Kyne and Crowley 2016).

The initial approach of biochemistry was thus orthogonal to that of microscopy. The properties of life would be studied outside of the organismal context, irrespective of the structural principles in the intact body. The aim was to replicate life or life-like processes in an isolated system with a minimal set of components and thus isolate the underlying substances in order to understand the ongoing properties and changes of matter. Parts of the "protoplasmic" concept were dropped or overshadowed by the advent of classical biochemistry, which focused on isolated molecules in buffered water solutions of simple composition (Kyne and Crowley 2016). The simplified "bag of enzymes in solution" perception of cell content, where molecules randomly encounter each other and follow the law of mass action, was criticized at the outset of the science of biochemistry. It was suggested that catalytic agents act as part of an integral and dynamic proteinaceous network in the cell. However, the original focus of early biochemistry on enzymes as catalytic agents provided a unified mechanistic tool set for characterizing subsets of cellular components and phenomena (Welch and Clegg 2010; Kyne and Crowley 2016). Molecular biology is currently understood as based on molecular genetics, but before the ability to modify genetic information was acquired, it was biochemistry that established the first true molecular-level reductionist description of some life processes.

Synthesis of Mendelian and chromosomal heredity theories in the early twentieth century put genes into the spatial context of location on chromosomes and stimulated institutionalization of genetics as a discipline. As a result of the

successful reductionist approach and the immediate economic impact on breeding, there was a common tendency to put genetics into the center of a mechanistic biology framework (Gayon 2016). For example, developmental genetics arose as an alternative program that competed with established experimental embryology (instead of being proposed as a complementary approach). Both the concept of gene used by geneticists and the concept of field used by embryologists were abstract and both were considered to have a physical basis, although understood only vaguely. At that time, genes were still considered to be associated with the action of proteins, possibly enzymes (Oppenheimer 1966; Gilbert et al. 1996). Genocentric tendencies were thus evident in biology at least two decades before the tenets of molecular biology were consolidated. The concept of field as an organizing principle was eventually abandoned, largely because biochemical techniques to examine field phenomena in detail were not available, whereas techniques for study of gene expression in model systems gradually appeared (Gilbert et al. 1996). Despite continuous attempts to interpret life in a holistic framework or perspective, reductionist approaches prevailed in biology as a pragmatic framework for finding mechanistic explanations of complex phenomena.

Genetics, biochemistry, and biophysics developed independently for some time, but started to converge after the 1930s. Key experiments on genetic regulation of *Neurospora* biochemistry in the 1940s showed that each step in a metabolic pathway is controlled by a single gene and this led to the "one gene–one enzyme hypothesis," which suggested that each gene acts directly as an enzyme or determines the specificity of an enzyme (Gayon 2016). This further stimulated perception of the gene as a central unit of biological function and much of the attention turned to the relationship between nucleic acid and protein macromolecules and the search for the molecular basis of heredity. Introduction of novel techniques such as X-ray crystallography and ultracentrifugation helped to turn the focus from colloidal theories to biopolymers and their structures.

Recapitulating the great endeavors of twentieth century molecular biology is beyond the scope of this review and is thoroughly described elsewhere (e.g., Rheinberger 2010). Most importantly, the material basis of hereditary information in the form of nucleotide sequences of nucleic acids was discovered and the genetic code solved, uncovering the relationship between a gene sequence and the protein macromolecule it encodes. Discoveries of the basic principles of molecular biology further stimulated the search for genes responsible for all sorts of processes in living organisms.

With basic metabolic pathways mapped, biochemists became interested in the regulation of metabolism. After the pioneering research of Jacques Monod (1910–1974) on the regulation of biochemical pathways and gene expression (Pardee and Reddy 2003), the concepts of positive feedback, negative feedback, allosteric regulation, cooperativity, induction of enzymes, control by repression, nonlinear regulation, cross-inhibition, and boolean integration of regulatory processes became the standard vocabulary of molecular biology (Monod 1972; Pardee and Reddy 2003). Parallels between molecular biology and cybernetics were thus grounded (Monod 1972), although ideas about cell signaling and gene expression at

the time were rooted in biochemistry and simple cybernetic relations. Newly developed tools shifted the focus onto study of individual genes and their protein products or simple signaling, genetic, and biochemical pathways. It was understood that other components such as extracellular matrix (ECM) components and membrane lipid composition also play important roles (Monod 1972) but, because of technological difficulties, they were neglected in comparison with research performed on DNA and proteins. These molecules were understood to be localized inside cells but more focus was put on understanding their function at a molecular level than on their cellular functions in terms of structural organization of the cells.

2.9 Biological Membranes in the Twentieth Century: From Discovery of Lipid Bilayers to the Fluid Mosaic Model

Despite initial neglect of the cell barrier in the nineteenth century, the nature of biological membranes became an important topic in twentieth century cell biology. In 1925, Gorter and Grendel performed a pioneering experiment addressing the structural nature of the plasma membrane. They picked erythrocytes, cells devoid of internal membranes, as the model system and showed that the ratio of monolayer area formed from extracted lipids and erythrocyte surface area was 2:1, suggesting the bilayer nature of the plasma membrane (Lombard 2014). It is noteworthy that the experiment was criticized for several shortcomings, including neglecting the protein components of the plasma membrane and wrong calculation of erythrocyte surface. It is now believed that several experimental errors reciprocally cancelled each other, leading to the correct conclusion. However, the validity of this early model can only be appreciated in the light of much later experiments. Regardless of the criticism, the immediate impact of the lipid bilayer hypothesis was to open discussion on the molecular nature of membrane structure. Trends based on Traube precipitation membranes and Overton lipid membranes were both popular. In terms of molecule permeability prediction, a crucial component of the former was pore size and of the latter, hydrophobicity. The unifying theories assumed membranes to be lipid layers interrupted by pores. The mixed roles of lipids and proteins in the function of membranes were acknowledged, but their relative contribution was a controversial issue (Lombard 2014).

In addition to the iconic character of the search for molecular heredity determinants and solving the differential role of proteins and nucleic acids in the nucleus, another key question in twentieth century cell biology was the nature of protein and lipid interplay in the functioning of biological membranes. Various models involved mixtures of lipid and protein fractions within or between postulated layers of the membrane. Interestingly, one of the concepts dominating membrane research for decades was the “paucimolecular model,” which postulated a lipid layer sandwiched between two protein layers. The model was based on measurement of surface tension between echinoderm/teloostei cells and an oil layer, as well as the

structure of myelinized axons. The surface tension experiments were soon criticized for using triacylglycerol instead of native membrane phospholipids, and for using myelinized axons as representative model for a general cell membrane. Nevertheless, the concept became popular for a long time and early low quality electron microscopy (EM) images were interpreted as supporting the paucimolecular membrane model. As in many other cases, a well-intended set of experiments and choice of model system led to wrong assumptions that persisted for decades (Lombard 2014).

Mosaic models of the plasma membrane were also popular. Speculations involving fat-like parts and protoplasmic-like parts, a mixture of sieve-like and solvent elements, were supported by permeability experiments at the beginning of the twentieth century. Permeability experiments also suggested that "pore" diameter could change according to the hydration of the pore, pH, metabolic activity, and cell type but the molecular mechanisms of membrane properties were unclear. Even the breakthrough experiments of Hodgkin and Huxley on membrane excitability (1952) were phenomenological and the mechanism of differential membrane permeability toward Na^+ and K^+ ions was not known (Lombard 2014). Because hydrated Na^+ ions are larger than hydrated K^+ ions, selective protein agents facilitating Na^+ transport were difficult to imagine. Lipid-based carriers specific for Na^+ were postulated. Furthermore, several arguments against the lipid nature of plasma membranes were based on its high water permeability. These conundrums were eventually solved in the context of a delicate structure of the potassium channel and the late discovery of aquaporins, membrane proteins that facilitate water permeability.

The fluid mosaic model dominated the membrane field in the 1970s. It was compatible with most contemporary experiments and predicted future observations; the model remained basically unaltered for next few decades. One of its main advantages over several competing models was compatibility with the thermodynamics of protein–lipid and lipid–lipid binding within membranes, largely based on hydrophobic interactions (Singer 2004; Lombard 2014). The general focus on proteins was fostered by tools developed for molecular biology, resulting in membrane proteins being the primary target of research looking for molecular agents of particular membrane functions. Lipids were considered to be passive structural elements that mostly ensured fluidity of proteins within the membrane. Such an idea is still advocated in many textbooks.

2.10 Insights into Cell Ultrastructure and Organelle Origin in the Twentieth Century

The classical descriptive endeavor of cell theory continued during the twentieth century with the disciplines of histology and cytology. The methodological barrier of microscopy was broken in the 1930s by the introduction of electron microscopy.

In combination with novel fixation, sectioning, and staining techniques, it became possible to image subcellular structures with the precision of tens of nanometers. First EM images of mitochondria immediately revealed the presence of a double membrane with inner membrane folds, named cristae (Ernster and Schatz 1981). In 1953, EM helped rediscover the endoplasmic reticulum (Schuldiner and Schwappach 2013). EM not only served as a tool for discovering novel details of subcellular structures, but also brought independent confirmation of conclusions on some older conundrums or questions. For example, several competing models of plasma membrane structure existed and Fischer still opposed membrane theory in 1921, arguing that membranes were invisible even when boundaries of cells were visible (see Sect. 2.9). EM eventually confirmed the presence of a plasma membrane lipid bilayer even in bacterial cells, where its presence had been debated for a long time (Lombard 2014). The generally accepted neuronal theory was also unequivocally confirmed by visualizing the synaptic cleft, a small space between neighboring neural cells. The high spatial resolution enabled detection of novel fine branching structures connecting other cellular components (Welch and Clegg 2010). This microtrabecular network was considered the "basic solid component of cytoplasm," but was also deemed a fixation artifact by many opponents. The concept of solid/liquid phases and heterogeneity of cytoplasm thus became hot topic for some time but then disappeared, only to come back in recent years (Welch and Clegg 2010).

The idea of symbiogenesis (introduced by Mereschkowsky) as the appearance of evolutionary novelties, including novel cell organelles, was revived by Lynn Margulis in the 1970s (Taylor 1987; Chapman and Margulis 1998; Kutschera and Niklas 2005). Margulis also propagated the concept of serial endosymbiosis, stating that modern eukaryotic cells originated by multiple successive symbiogenetic events of once independent organisms (Taylor 1987), and the idea that symbiogenetic events were a common driving force in eukaryotic speciation (Kutschera and Niklas 2005). With employment of molecular biology techniques, support for the endosymbiotic origin of mitochondria and plastids soon accumulated and the paradigm of eukaryotic cell evolution shifted from gradual accumulation of changes as the only mechanism to the possibility of abrupt acquisition of organelles (Taylor 1987). Revival of the symbiogenetic organelle concept and the idea of the eukaryotic cell as a product of cellular fusion between Archea and Eubacteria (Kutschera and Niklas 2005) points to the crucial role of cooperative processes in the evolution of life and to the fact that the evolution of cells could not be fully understood as a simple progressive, incremental process but involved singularities with crucial macroevolutionary impact.

2.11 Formation of Modern Cell Biology and Methodical Trends in Twenty-First Century Cell Biology

Whereas nineteenth century biology had to decide which of the big theories were correct, late twentieth century cell biology was marked by the trend to put together the discoveries of genetics, molecular biology, biochemistry, and cytology into a congruent whole. Top-down (more and more detailed observation of tissue ultrastructure) and bottom-up (examining the properties of smallest functional components in the form of molecules and their relationships) approaches were eventually used together as a common tool set of a unified scientific field. Many processes were attributed to specific genes and their protein products. Proteins were successfully mapped into biochemical, signaling, and gene regulatory pathways. With the help of cell fractionation techniques and EM, combined with antibody staining, it became possible to map biochemical pathways and protein activities to specific subcellular compartments (Schuldiner and Schwappach 2013). The ability to maintain, grow, and manipulate cells outside organisms (a relatively simple task for plant cells), together with the expansion of live cell imaging techniques, especially discovery of genetically encoded fluorescent proteins, led to countless observations of dynamic processes in living cells. Cells have always been perceived as dynamic entities, but the new techniques allowed observation of molecular processes in vivo with the proper spatial and temporal context.

Emphasis has gradually shifted from the role of individual genes to how the actions of individual components within the cell collectively contribute to a particular process. This trend does not negate the earlier discoveries of twentieth century molecular biology in any sense, but demonstrates the importance of studying molecular components within live cells, taking into account structural and dynamic properties of the cellular environment. The cell has thus re-emerged as both a biological and an interpretational platform, connecting molecular mechanisms with macroscopic phenomena.

Several technological trends are typical for cell biology in this new millennium. First, improved techniques now allow cellular components and processes to be followed with greater and greater precision. The resolution of fluorescence microscopes is increasing in time and space, beyond the limitation imposed by the diffraction barrier (Wollman et al. 2015). The classical resolution limit of light microscopy has been surmounted by combination of fluorescence technologies and specialized fluorophore excitation methods. These techniques, along with sophisticated computer analyses, allow almost angstrom (Å) resolution in specific cases (Zeng and Xi 2016). Structural analyses of large macromolecular machines such as the ribosome (Yusupova and Yusupov 2017) and nuclear pore (Beck and Hurt 2017) are not uncommon. Fast tools for intracellular manipulation, such as optical tweezers (Ritchie and Woodside 2015), optogenetically activated proteins (Toettcher et al. 2011), and small photoactivated molecules (Hoglinger et al. 2014), now supplement traditional genetic and pharmacological tools.

Some of the new techniques are helping to bridge traditional approaches. For example, correlative light and electron microscopy enables live cell imaging. High resolution EM data can be acquired for a specific part of the cell after rapid freezing of the sample at a chosen time point (Kobayashi et al. 2016). During imaging mass spectrometry, specific regions of a cell/tissue are separately analyzed by mass spectrometry, which is thus enriched with spatial information (Asano et al. 2016). Analyses of protein structural properties, previously obtained by in vitro measurements, can be performed within the cellular environment in some cases (Schwamborn et al. 2016). Another dominant trend of contemporary cell biology is increasing experimental throughput with the help of automatized data acquisition and processing. Such tendencies were largely introduced for sequencing of whole genomes and transcriptomes but "omics" approaches are becoming widespread in connection with most techniques, including fluorescence microscopy (Mattiazzi Usaj et al. 2016), cell sorting (Warkiani et al. 2015), electron microscopy (Eberle et al. 2015), and structural biology (Grabowski et al. 2016).

2.12 Modular Cell Biology

It has become evident that, although some simple cellular functions are executed by a single molecular component (potassium transport through the plasma membrane via a membrane channel, metabolite conversion by a specialized enzyme), most cellular functions (growth regulation, cell differentiation, chemotaxis) arise from the interactions of many components (Hartwell et al. 1999). After decades of characterizing individual cell components and trends for their total catalogization, focus is now shifting from identifying individual parts to understanding their relationships, spatiotemporal associations, and collective behavior. Systems biology approaches rely on combining high-throughput data generated by various omics and quantitative computational analyses to generate new integrated insights into how individual parts produce emergent phenomena. Precise definition and methodology of systems biology is not unified and often elusive (Simpson 2016), but the main emphasis is on deducing the properties of interaction networks governing cellular processes. Ongoing debate exists about the need to change perception and scientific language if we are to understand cellular functions.

The concept of "modular biology" (closely linked with the concept of synthetic biology) is based on the realization that omics approaches alone are unable to uncover and understand the "design" or "engineering" (in a functional sense) principles of living organisms (Hartwell et al. 1999). Yuri Lazebnik has called for a new formalized language that is better suited to comprehend modules in living systems (Lazebnik 2002). Inspired by Hartwell et al. (1999), he uses the putative example of an effort to understand the functions of a radio and repair it using the methodology of molecular biology: dissecting the functioning system into a pile of random smaller parts or describing the effects of their removal (as in classical developmental genetics). Such an approach would undoubtedly lead to

identification of a few components that are crucial for functioning, and replacement of which would repair the radio if those components had been damaged. However, this procedure is futile if the individual components are functional but not tuned properly. Similarly, the quest of the pharmaceutical industry to find "miracle drugs" by identifying "critical molecular targets" does not often work because the malfunction may be the result of improper "tuning" of the whole system rather than damage to the critical molecular target.

On the other hand, the formal language of electronics (with components such as triggers and amplifiers) used by engineers provides direct insight into processes that the components are wired to perform. The analogy is not entirely fair because engineers have designed artifacts from first principles and formulated suitable language on the way, whereas the reverse-engineering approach of molecular biology meets systems that have evolved on their own for billions of years in complex environments. Nevertheless, biologists could learn more from taking an engineering perspective. Even the original models of gene expression regulation were inspired by Boolean logic, and many modern machines are now complex enough to foster further dialogue between biology and engineering, at least in the realm of signal transmission, processing, and interpretation (Csete and Doyle 2002). The concepts of amplification, adaptation (short and long term), robustness, insulation, attractors, bistability, waves and oscillations, memory switches, filtering, pattern recognition, discrimination of time series, hysteresis, complex logic gate operations, error correction, and coincidence detection should become staple parts of cell biology vocabulary. Cellular modules reflecting these concepts, rather than individual molecules, are of primary interest in understanding collective cell phenomena (Hartwell et al. 1999; Klipp and Liebermeister 2006; Lim et al. 2013; Mast et al. 2014). Novel bioinformatic methods can be used to search for similar network motifs, and it can be experimentally tested whether similar motifs play the same role in different contexts (Lim et al. 2013). The general functions of positive feedback (bistability, memory, switch-like behavior) and negative feedback (noise resistance, input-induced steady state) have been known for a long time (Lim et al. 2013).

The list of common motifs and architectures associated with specific functions in cells is now being expanded. For example, coherent feedforward loops often act as persistence detectors, which switch "on" only when the input persists for minimal amount of time (Lim et al. 2013). If the set of solutions for a particular problem is small enough, more analogies between artificial systems and cells should be possible to find and a table of frequent motifs with their functions established (Lim et al. 2013). There are even calls for verification of these rules by building minimal biological processing networks, with the use of a "synthetic biology" as the ultimate proof of understanding (Mast et al. 2014). However, it should be emphasized that networks and their motifs in living systems have their own specificities, because they often evolved to play multiple roles and work in unstable environments (Klipp and Liebermeister 2006). Yet, many modern artifacts are not dominated by minimal function but by modular buildup, which ensures robustness and further evolvability, so more similarities with evolving living systems could be

discovered in the future (Csete and Doyle 2002). The languages of modular cell biology and molecular cell biology are complementary, because the same functional motifs studied by modular biology can be implemented by many different molecular agents: "Cell biology is in transition from a science that was preoccupied with assigning functions to individual proteins or genes, to one that is now trying to cope with the complex sets of molecules that interact to form functional modules" (Hartwell et al. 1999).

2.13 Cells in Tissues: Molecular and Modular Mechanisms of Morphogenesis

Contemporary biology is again realizing the importance of an old wisdom that multicellular animals and plants are not composed of cells in a brick-like manner, but that tissues form specialized domains by cell growth, division, and differentiation. In addition to focusing on individual cell activity in this process, the dynamic integrated whole of the organism that produces and controls cells should be considered. As in cell biology, attempts have been made to understand multicellular developing systems in terms of the information processing networks of signaling pathways and gene expression regulation (Davidson 2010). It is also understood that, along with regulatory modules embodied in protein–protein interactions and gene promoter structures, the dynamic shape of tissue needs to be taken in account. For example, gradients of signaling molecules are dynamically reshaped by changes in tissue shape (Bollenbach and Heisenberg 2015). Therefore, each specific type of cell within an organism can be fully understood only within the context of its specific position within a tissue and its function. Bottom-up molecular and modular approaches must be complemented by top-down concepts that take into account the structure of developing tissues (Levin 2012).

Understanding both the modular and interconnected nature of living systems has allowed revival of the supracellular concept of field in developmental biology and its re-formulation in a framework compatible with molecular biology (Gilbert et al. 1996; Levin 2012). Such modular fields, displaying both autonomy and hierarchy and interacting with each other, have been proposed as mediators between genotype and phenotype in both ontogeny and evolution. Unlike some early field concepts, these fields are based on genetically defined interactions between cells. Their hierarchy and establishment are influenced by genetic information, but the field concept allows a shift of focus to the supracellular level of organization (Gilbert et al. 1996).

For a long time, the ECM was considered a passive material that filled the space between cells (Rozario and DeSimone 2010). Now it is understood as a dynamic repository of signaling molecules. The ECM can inhibit or facilitate signal spreading (Yan and Lin 2009; Rozario and DeSimone 2010), as well as store the morphogens and release them upon proteolytic degradation or stimulation by

additional signals (Rozario and DeSimone 2010). Moving cells reorganize the structure and position of ECM and ECM tracks the drive direction of cell migration (Rozario and DeSimone 2010). The actions of cells and ECM are thus bidirectional and complementary. More than a century after Roux defined a program of developmental mechanics, mechanical concepts are becoming the hallmark of mainstream developmental biology.

A program ridiculed by early developmental geneticists for not having achieved any mechanical understanding (Gilbert et al. 1996) now works fully within the framework of molecular biology. Developmental biology can also focus on mechanical aspects of development as a result of technological advances such as optical tweezers (Le et al. 2016), laser ablation of selected cells within tissue (Polacheck and Chen 2016), and atomic force microscopy to measure quantitatively the mechanical properties of cell/ECM surfaces at microscale resolution (Alcaraz et al. 2017). An increasing number of studies have demonstrated how the mechanical signaling within interconnected cellular–ECM nets strongly regulates growth, gene expression, and differentiation (Heisenberg and Bellaïche 2013), including mechanical aspects of regulation of cellular invasivity in normal development and in cancer establishment (Parekh and Weaver 2016).

2.14 Insights into Cytoplasm Structure in the Twenty-First Century

Together with the established tradition of associating cellular processes with membrane-bound organelles, attempts to comprehend the structure and properties of cytoplasm have reemerged 100 years after the decline of protoplasmic concepts, as nicely expressed in a quotation by T. Mitchison (2010): "Nothing epitomizes the mystery of life more than the spatial organization and dynamics of the cytoplasm."

The aqueous phase of the cytoplasm is not a bag of freely diffusing enzymes, as often wrongly perceived in the light of classical biochemistry, but is crowded with macromolecules. Diffusive transport and partitioning of macromolecules and organelles in cytoplasm is highly restricted by steric hindrance and by unexpected binding interactions (Luby-Phelps 2013). High viscosity and crowding are thought to play major roles in the mobility of cytoplasmic components. Mobility measurements by modern techniques indeed show behavior different from mere passive diffusion. Oddly, small proteins often move faster than inert molecules (Ross 2016). Weak interactions with surrounding cytoplasmic components possibly enhance their mobility. Recent advances have accumulated sufficient evidence for the existence of membraneless or "naked" compartments in the cytoplasm. Such compartments are formed by multivalent weak interactions between low complexity repeat domains and/or distorted hydrophobic domains (Luby-Phelps 2013; Uversky 2017). Self-interaction of domains ensures phase separation of the components from the rest of the cytoplasm. Upon formation of such a compartment by

polyvalent interacting proteins, monovalent interacting partners can enter the compartment and concentrate there.

Membraneless droplets could play a role in concentrating components of a cellular pathway without the need for a membrane barrier or other cage. Individual droplets of the same kind can split and coalesce, and components are constantly exchanged with the soluble pool (Weber and Brangwynne 2012). These structures thus possess a high level of internal dynamics and are characterized by liquid-like behavior, such as dripping, fusion, wetting, and the ability to become reversibly deformed when encountering a physical barrier (Uversky 2017). Droplets of different kinds (each based on a different self-interaction domain) can coexist within the cytoplasm without mixing together. Many such compartments are ribonucleoprotein granules consisting of long multivalent RNA molecules and specific RNA-binding proteins (Weber and Brangwynne 2012). Formation of membraneless compartments is condition-dependent, reversible, and controlled, including by posttranslational modification (Uversky 2017). The environment of these compartments is even more crowded than the rest of the cytoplasm (Uversky 2017). The combination of phase separation and molecular crowding can even trap together proteins with extremely low copy number (Wolde and Mugler 2014). The effects of crowding on the dynamics of signaling pathways, gene regulation networks, and metabolic networks are still not well understood, but crowding alters the diffusion of proteins and the kinetics of biochemical reactions (due to entropic changes), often in nonlinear dependence on the concentrations of molecules involved (Wolde and Mugler 2014).

Some of the ideas involving aqueous phase separation as a self-organizing mechanism trace back to 1899 or possibly earlier. E.B. Wilson proposed at the end of nineteenth century that non-membrane-bound compartments such as P-granules and Cajal bodies could be explained by the principles of colloid chemistry (Luby-Phelps 2013). Membraneless protein bodies of crystalline or quasicrystalline organization, probably formed by self-assembly, have also been known for some time. The shells of such compartments are permeable for small metabolites but otherwise keep the inside isolated from the rest of the cytoplasm (O'Connell et al. 2012). Most of these structures were discovered in bacterial cells, but examples from eukaryotes have also been described. In addition to the well-known polymerization of actin and tubulin into cytoskeletal fibers, some metabolic enzymes such as CTP synthase also tend to form fibers. Large-scale fluorescence microscopy screens revealed the localization of many supposedly cytoplasmic yeast proteins in fibers. The studies avoided overexpression artifacts and were supported by additional methods such as mass spectrometry for selected candidates (O'Connell et al. 2012). Packing of many proteins into as-yet uncharacterized structures is thus becoming evident.

Various roles for protein fibers and foci have been proposed, including efficient allosteric regulation, shielding of metabolic intermediates and their channeling into complex pathways, and storage of inactive proteins. Each of these functions has been demonstrated in particular cases but, for most proteins, the impact of assembly into aggregates is not known and the impact of the highly organized structure of the

cytoplasm is currently not well documented or understood. However, it is clear that certain emergent physicochemical properties of the cell interior cannot be revealed by reductionist experiments with a few isolated components. A challenge for postreductionist biochemistry is to study biochemical phenomena far from chemical equilibrium and under physiologically relevant conditions (i.e., inside cells, in complex cell extracts, or in crowded solutions) (Kyne and Crowley 2016).

2.15 Lipid and Membrane Research in the Twenty-First Century

Although support for the widespread existence of membraneless compartments in cells is accumulating, modern research also demonstrates the vital role of biological membranes. In interplay with cytoplasmic components, membranes expand the mechanisms of cell compartmentalization and functional regulation with additional layers of complexity. Lipids, although previously overlooked as mere passive components of membranes, are now appreciated as crucial determinants of membrane properties at different scales and are a key research topic in modern cell biology (Mouritsen and Bagatolli 2015). Improved lipidomic analyses demonstrate that the diversity of lipids could match the diversity of protein species in a eukaryotic cell and that the catalogue of lipid diversity is still expanding (Saliba et al. 2015). One year after the formulation of the fluid mosaic model of plasma membranes, it was hypothesized that more stable domains exist within evenly mixed membranes (Sezgin et al. 2017). This "lipid-raft" hypothesis, based on biochemical extractions indicating stable sphingolipid and sterol-enriched compartments within membranes, was never fully accepted. However, the expanded computational, biophysical, and biochemical tool set, including molecular dynamic simulations and advanced spectroscopic methods (Sezgin and Schwille 2011, 2012; Gumí-Audenis et al. 2016; Sommer 2013), is leading to better understanding of membrane heterogeneity at different spatial and temporal levels. Like macromolecules in cytoplasm, membrane components show anomalous diffusion and undergo clustering (Honigmann and Pralle 2016). Transient self-organized domains driven by segregation of components are reported at scales from a few molecules to micrometers. Moreover, the cortical actin cytoskeleton obviously fine tunes the organization of microdomains, not only by acting as a boundary to membrane protein diffusion but also by influencing lipid organization and phase transition, which can be further facilitated or suppressed by actin (depending on other specific conditions) (Honigmann and Pralle 2016). The existence of a fine actin–spectrin network has been observed in red blood cells and recently demonstrated in neurons with the help of super-resolution microscopy (D'Este et al. 2016), indicating a general cellular phenomenon. Fast local rearrangements of the domains as a result of feedback between the local phosphoinositide composition and actin cytoskeleton are also possible (Honigmann and Pralle 2016). Like the cytoplasmic cortex, the

ECM is believed to influence the mobility of membrane proteins, which has been demonstrated in the case of selective limiting of the mobility of plant plasma membrane proteins by the cell wall (Martinière et al. 2012). Differences in local lipid composition regulate the function of membrane proteins, and a substantial fraction of membrane lipids are bound to transmembrane proteins in the form of a hydrophobic solvation shell instead of being freely mobile within the bilayer (Poveda et al. 2017). The effects of lipid composition on the physical properties of a membrane are complex and difficult to predict. For example, cholesterol can increase or decrease local membrane fluidity depending on the other components (Schmid 2017).

Computational and experimental tools now allow assessment of the effect of specific compositions on membrane physical properties and protein structure in different situations (Poveda et al. 2017). Once cytoplasmic proteins are recruited to the membrane, the dimensionality of their mobility is reduced from three to two dimensions, increasing their effective concentration by orders of magnitude. Membranes thus serve as interaction platforms for proteins, which can be further fine-tuned by segregating interaction partners to specific microdomains (Honigmann and Pralle 2016; Stoeger et al. 2016). Membranes are now also understood to serve as tunable capacitors for integration and storage of information in the form of accumulation of specific signaling phospholipid species (Stoeger et al. 2016). Coincidence detection of more lipid species, or a specific lipid together with a protein interaction partner, regulates protein binding to the microdomains and membranes of different organelles (Saliba et al. 2015). Large-scale protein–protein interaction maps are now being complemented by high-throughput screens testing protein–membrane interactions and their dependence on the complex composition of the membrane and biophysical properties such as curvature (Saliba et al. 2015). The dynamic effects of lipid composition on cellular processes have been difficult to study, because membrane composition is subject to tight and fast regulation in the form of phospholipid headgroup modification, fatty acyl chain transfer, and movement of lipids between membrane leaflets (Sekereš et al. 2015). Furthermore, lipid transfer proteins in connection with membrane contact sites are being studied as regulated highways for lipid transport. Such a transport mechanism is possibly much faster than vesicular transport, previously considered to be the major agent of lipid movement between compartments (Jain and Holthuis 2017). Emerging technologies such as optogenetic activation of lipid-modifying enzymes (Idevall-Hagren and De Camilli 2015) and photoactivation of caged phospholipids (Hoglinger et al. 2014) now enable monitoring the effect of membrane composition changes on cellular processes at the physiological spatiotemporal scale.

2.16 Into the Unknown: The Future of Cell Biology

In addition to the increasing resolution and coverage of molecular measurements, discovery of some previously unknown fundamental components and mechanisms has been achieved. Discovery of RNA interference in the 1990s reshaped the perception of gene expression regulation and fostered growing interest in noncoding RNA species (Deniz and Erman 2016). There are also factors that probably have a large impact but are difficult to measure and factors whose existence we do not even suspect, the true "dark matter of cell biology" (Ross 2016). Examples of the former are the properties of intrinsically disordered proteins, small intracellular and intercellular DNA species, weak interactions impossible to detect using traditional biochemical methods, and intracellular distribution of ion species. The latter factors could be undiscovered protein–protein interaction motifs, exotic phases, undetected types of small molecules existing at low copy numbers, unknown posttranslational modifications, or new modes of collective behavior of biomolecules. With further improvement of available tools, it is possible that previously abandoned and possibly forgotten concepts in the framework of molecular biology will be revived, as happened with endosymbiotic theories and epigenetics. Cell biologists will continue to use the combination of top-down and bottom-up approaches. Detailed mechanistic characterization of individual components will be combined with large-scale systems level approaches, enabling identification of novel functional cellular modules. The future of cell biology (and of biology as a whole) also lies in capturing life processes simultaneously at different spatiotemporal scales and the integration of results into multiscale models, so that the relationship between the interactions of individual components and collective emergent phenomena can be understood.

Acknowledgments This work was funded by the project Ministry of Education of the Czech Republic/MSMT project NPUI LO1417. Part of the income of Juraj Sekeres was provided by the Grant Agency of the Czech Republic project 17-27477S. We would like to thank Peter Sabol for critical reading of the manuscript.

References

Alcaraz J, Otero J, Jorba I, Navajas D (2017) Bidirectional mechanobiology between cells and their local extracellular matrix probed by atomic force microscopy. Semin Cell Dev Biol. doi: https://doi.org/10.1016/j.semcdb.2017.07.020

Asano S, Engel BD, Baumeister W (2016) *In situ* cryo-electron tomography: a post-reductionist approach to structural biology. J Mol Biol 428(2 Pt A):332–343

Beck M, Hurt E (2017) The nuclear pore complex: understanding its function through structural insight. Nat Rev Mol Cell Biol 18(2):73–89

Beloussov LV (1997) Life of Alexander G. Gurwitsch and his relevant contribution to the theory of morphogenetic fields. Int J Dev Biol 41:771–779

Bollenbach T, Heisenberg CP (2015) Gradients are shaping up. Cell 161(3):431–432

Canguilhem G (2008) Knowledge of life. Fordham University Press, New York
Chapman MJ, Margulis L (1998) Morphogenesis by symbiogenesis. Int Microbiol 1(4):319–326
Csete ME, Doyle JC (2002) Reverse engineering of biological complexity. Science 295 (5560):1664–1669
D'Este E, Kamin D, Velte C, Göttfert F, Simons M, Hell SW (2016) Subcortical cytoskeleton periodicity throughout the nervous system. Sci Rep 6:22741
Davidson EH (2010) Emerging properties of animal gene regulatory networks. Nature 468 (7326):911–920
Deniz E, Erman B (2016) Long noncoding RNA (lincRNA), a new paradigm in gene expression control. Funct Integr Genomics 17:135–143
Eberle AL, Mikula S, Schalek R, Lichtmann J, Knothe Tate ML, Zeidler D (2015) High-resolution, high-throughput imaging with a multibeam scanning electron microscope. J Microsc 259(2):114–120
Ernster L, Schatz G (1981) Mitochondria: a historical review. J Cell Biol 91(3 Pt 2):227s–255s
Gayon J (2016) From Mendel to epigenetics: history of genetics. C R Biol 339(7–8):225–230
Gilbert SF, Opitz JM, Raff RA (1996) Resynthesizing evolutionary and developmental biology. Dev Biol 173(2):357–372
Grabowski M, Niedzalkowska E, Zimmerman MD, Minor W (2016) The impact of structural genomics: the first quindecennial. J Struct Funct Genomics 17(1):1–16
Gumí-Audenis B, Costa L, Carlá F, Comin F, Sanz F, Giannotti MI (2016) Structure and nanomechanics of model membranes by atomic force microscopy and spectroscopy: insights into the role of cholesterol and sphingolipids. Membranes (Basel) 6(4):58
Harris H (2000) The birth of the cell. Yale University Press, New Haven. isbn:0-300-08295-9
Hartwell LH, Hopfield JJ, Leibler S, Murray AW (1999) From molecular to modular cell biology. Nature 402(6761 Suppl):C47–C52
Heisenberg CP, Bellaïche Y (2013) Forces in tissue morphogenesis and patterning. Cell 153 (5):948–962
Hoglinger D, Nadler A, Schultz C (2014) Caged lipids as tools for investigating cellular signaling. Biochim Biophys Acta 1841(8):1085–1096
Honigmann A, Pralle A (2016) Compartmentalization of the cell membrane. J Mol Biol 428(24 Pt A):4739–4748
Idevall-Hagren O, De Camilli P (2015) Detection and manipulation of phosphoinositides. Biochim Biophys Acta 1851(6):736–745
Jain A, Holthuis JCM (2017) Membrane contact sites, ancient and central hubs of cellular lipid logistics. Biochim Biophys Acta 1864(9):1450–1458
Janko J, Štrbáňová S (1988) Věda Purkyňovy doby [The science of Purkyně's time]. Academia, Prague
Klipp E, Liebermeister W (2006) Mathematical modeling of intracellular signaling pathways. BMC Neurosci 7(Suppl 1):S10
Kobayashi S, Iwamoto M, Haraguchi T (2016) Live correlative light-electron microscopy to observe molecular dynamics in high resolution. Microscopy 65(4):296–308
Kutschera U, Niklas KJ (2005) Endosymbiosis, cell evolution and speciation. Theory Biosci 124:1–24
Kyne C, Crowley PB (2016) Grasping the nature of the cell interior: from physiological chemistry to chemical biology. FEBS J 283(16):3016–3028
Lazebnik Y (2002) Can a biologist fix a radio? Or, what I learned while studying apoptosis. Cancer Cell 2(3):179–182
Le S, Liu R, Lim CT, Yan J (2016) Uncovering mechanosensing mechanisms at the single protein level using magnetic tweezers. Methods 94:13–18
Levin M (2012) Morphogenetic fields in embryogenesis, regeneration, and cancer: non-local control of complex patterning. Biosystems 109(3):243–261
Lim WA, Lee CM, Tang C (2013) Design principles of regulatory networks: searching for the molecular algorithms of the cell. Mol Cell 49(2):202–212

Liu D (2016) The cell and protoplasm as container, object, and substance, 1835–1861. J Hist Biol. doi:https://doi.org/10.1007/s10739-016-9460-9
Lombard J (2014) Once upon a time the cell membranes: 175 years of cell boundary research. Biol Direct 9:32
Luby-Phelps K (2013) The physical chemistry of cytoplasm and its influence on cell function: an update. Mol Biol Cell 24(17):2593–2596
Markoš A (2002) Readers of the book of life: contextualizing developmental evolutionary biology. Oxford University Press, Oxford
Martinière A, Lavagi I, Nageswaran G, Rolfe DJ, Maneta-Peyret L, Luu DT, Botchway SW, Webb SE, Mongrand S, Maurel C, Martin-Fernandez ML, Kleine-Vehn J, Friml J, Moreau P, Runions J (2012) Cell wall constrains lateral diffusion of plant plasma-membrane proteins. Proc Natl Acad Sci U S A 109(31):12805–12810
Mast FD, Ratushny AV, Aitchison JD (2014) Systems cell biology. J Cell Biol 206(6):695–706
Mattiazzi Usaj M, Styles EB, Verster AJ, Friesen H, Boone C, Andrews BJ (2016) High-content screening for quantitative cell biology. Trends Cell Biol 26(8):598–611
McIntosh JR, Hays T (2016) A brief history of research on mitotic mechanisms. Biology (Basel) 5 (4):55
Mitchison TJ (2010) Remaining mysteries of the cytoplasm. Mol Biol Cell 21(22):3811–3812
Monod J (1972) Chance and necessity: an essay on natural philosophy of modern biology. Vintage Books, New York
Mouritsen OG, Bagatolli LA (2015) Lipid domains in model membranes: a brief historical perspective. Essays Biochem 57:1–19
O'Connell JD, Zhao A, Ellington AD, Marcotte EM (2012) Dynamic reorganization of metabolic enzymes into intracellular bodies. Annu Rev Cell Dev Biol 28:89–111
Oppenheimer JM (1966) The growth and development of developmental biology. In: Locke M (ed) Major problems in developmental biology. Academic, New York, pp 1–27. doi:https://doi.org/10.1016/B978-0-12-395618-7.50005-6
Pardee AB, Reddy PG (2003) Beginnings of feedback inhibition, allostery and multi-protein complexes. Gene 321:17–23
Parekh A, Weaver AM (2016) Regulation of invadopodia by mechanical signaling. Exp Cell Res 343(1):89–95
Polacheck WJ, Chen CS (2016) Measuring cell-generated forces: a guide to the available tools. Nat Methods 13(5):415–423
Poveda JA, Marcela Giudici A, Lourdes Renart M, Morales A, González-Ros JM (2017) Towards understanding the molecular basis of ion channel modulation by lipids: mechanistic models and current paradigms. Biochim Biophys Acta 1859(9 Pt B):1507–1516
Priven SW, Alfonso-Goldfarb AM (2009) Mathematics Ab Ovo: Hans Driesch and Entwicklungsmechanik. Hist Philos Life Sci 31:35–54
Quastel JH (1985) The development of biochemistry in the 20th century. Mol Cell Biochem 69 (1):17–26
Radl E (1930) The history of biological theories. Oxford University Press, Oxford (in German 1905 and 1909, 2nd edn. 1913; in Czech 1909 and 2006)
Rheinberger HJ (2010) A short history of molecular biology. In: Lorenzano P, Rheinberger H-J, Ortiz E, Galles CD (eds) History and philosphy of science and technology, Vol 2. EOLSS, Oxford, pp 1–31
Richmond ML (2000) T.H. Huxley's criticism of German cell theory: an epigenetic and physiological interpretation of cell structure. J Hist Biol 33(2):247–289
Ritchie DB, Woodside MT (2015) Probing the structural dynamics of proteins and nucleic acids with optical tweezers. Curr Opin Struct Biol 34:43–51
Ross JL (2016) The dark matter of biology. Biophys J 111(5):909–916
Roth S (2011) Mathematics and biology: a Kantian view on the history of pattern formation theory. Dev Genes Evol 221(5–6):255–279

Rozario T, DeSimone DW (2010) The extracellular matrix in development and morphogenesis: a dynamic view. Dev Biol 341(1):126–140
Saliba AE, Vonkova I, Gavin AC (2015) The systematic analysis of protein-lipid interactions comes of age. Nat Rev Mol Cell Biol 16(12):753–761
Sander K (1991) Landmarks in developmental biology: Wilhelm Roux and his programme for developmental biology. Roux Arch Dev Biol 200(1):1–3
Sander K (1992a) Hans Driesch the critical mechanist: "Analytische Theorie der organischen Entwicklung". Roux Arch Dev Biol 201(6):331
Sander K (1992b) Hans Driesch's "philosophy really ab ovo", or why to be a vitalist. Roux Arch Dev Biol 202(1):1–3
Sander K (1993) Entelechy and the ontogenetic machine – work and views of Hans Driesch from 1895 to 1910. Roux Arch Dev Biol 202(2):67–69
Sazer S, Lynch M, Needleman D (2014) Deciphering the evolutionary history of open and closed mitosis. Curr Biol 24(22):R1099–R1103
Schmid F (2017) Physical mechanisms of micro- and nanodomain formation in multicomponent lipid membranes. Biochim Biophys Acta 1859(4):509–528
Schuldiner M, Schwappach B (2013) From rags to riches – the history of the endoplasmic reticulum. Biochim Biophys Acta 1833(11):2389–2391
Schwamborn K, Kriegsmann M, Weichert W (2016) MALDI imaging mass spectrometry – from bench to bedside. Biochim Biophys Acta 1865(7):795–816
Sekereš J, Pleskot R, Pejchar P, Žárský V, Potocký M (2015) The song of lipids and proteins: dynamic lipid-protein interfaces in the regulation of plant cell polarity at different scales. J Exp Bot 66(6):1587–1598
Sezgin E, Schwille P (2011) Fluorescence techniques to study lipid dynamics. Cold Spring Harb Perspect Biol 3(11):a009803
Sezgin E, Schwille P (2012) Model membrane platforms to study protein-membrane interactions. Mol Membr Biol 29(5):144–154
Sezgin E, Levental I, Mayor S, Eggeling C (2017) The mystery of membrane organization: composition, regulation and roles of lipid rafts. Nat Rev Mol Cell Biol 18(6):361–374
Simpson MR (2016) Systems biology: impressions from a newcomer graduate student in 2016. Adv Physiol Educ 40(4):443–445
Singer SJ (2004) Some early history of membrane molecular biology. Annu Rev Physiol 66:1–27
Sommer B (2013) Membrane packing problems: a short review on computational membrane modeling methods and tools. Comput Struct Biotechnol J 5:e201302014
Stoeger T, Battich N, Pelkmans L (2016) Passive noise filtering by cellular compartmentalization. Cell 164(6):1151–1161
Taylor FJR (1987) An overview of the status of evolutionary cell symbiosis theories. Ann N Y Acad Sci 503:1–16
Thompson D'A (1917) On growth and form. Cambridge University Press, Cambridge
Toettcher JE, Voigt CA, Weiner OD, Lim WA (2011) The promise of optogenetics in cell biology: interrogating molecular circuits in space and time. Nat Methods 8(1):35–38
Uversky VN (2017) Intrinsically disordered proteins in overcrowded milieu: membrane-less organelles, phaseseparation, and intrinsic disorder. Curr Opin Struct Biol 44:18–30
Warkiani ME, Wu L, Tay AK, Han J (2015) Large-volume microfluidic cell sorting for biomedical applications. Annu Rev Biomed Eng 17:1–34
Weber SC, Brangwynne CP (2012) Getting RNA and protein in phase. Cell 149(6):1188–1191
Welch GR, Clegg JS (2010) From protoplasmic theory to cellular systems biology: a 150-year reflection. Am J Physiol Cell Physiol 298(6):C1280–C1290
Whitman CO (1893) The inadequacy of the cell-theory of development. J Morphol 8:639–658
Wilson EB (1899) The structure of protoplasm. Science 10:33–45
Wolde PR, Mugler A (2014) Importance of crowding in signaling, genetic, and metabolic networks. Int Rev Cell Mol Biol 307:419–442

Wollman AJ, Nudd R, Hedlund EG, Leake MC (2015) From Animaculum to single molecules: 300 years of the light microscope. Open Biol 5(4):150019

Yan D, Lin X (2009) Shaping morphogen gradients by proteoglycans. Cold Spring Harb Perspect Biol 1(3):a002493

Yusupova G, Yusupov M (2017) Crystal structure of eukaryotic ribosome and its complexes with inhibitors. Philos Trans R Soc Lond Ser B Biol Sci 372(1716). doi:https://doi.org/10.1098/rstb.2016.0184

Zárský V (2012) Jan Evangelista Purkyně/Purkinje (1787–1869) and the establishment of cellular physiology – Wrocław/Breslau as a central European cradle for a new science. Protoplasma 249(4):1181

Zeng Z, Xi P (2016) Advances in three-dimensional super-resolution nanoscopy. Microsc Res Tech 79(10):893–898

Journal of Experimental Botany, Vol. 66, No. 6 pp. 1587–1598, 2015
doi:10.1093/jxb/erv052 Advance Access publication 25 February 2015

REVIEW PAPER

The song of lipids and proteins: dynamic lipid–protein interfaces in the regulation of plant cell polarity at different scales

Juraj Sekereš[1,2], Roman Pleskot[1,3], Přemysl Pejchar[1], Viktor Žárský[1,2] and Martin Potocký[1,*]

[1] Institute of Experimental Botany, v. v. i., Academy of Sciences of the Czech Republic, Rozvojová 263, 16502 Prague 6, Czech Republic
[2] Department of Experimental Plant Biology, Faculty of Science, Charles University in Prague, Viničná 5, 12844 Prague 2, Czech Republic
[3] Institute of Organic Chemistry and Biochemistry, v. v. i., Academy of Sciences of the Czech Republic, Flemingovo náměstí 2, 16610 Prague 6, Czech Republic

* To whom correspondence should be addressed. E-mail: potocky@ueb.cas.cz

Received 19 November 2014; Revised 13 January 2015; Accepted 27 January 2015

Abstract

Successful establishment and maintenance of cell polarity is crucial for many aspects of plant development, cellular morphogenesis, response to pathogen attack, and reproduction. Polar cell growth depends on integrating membrane and cell-wall dynamics with signal transduction pathways, changes in ion membrane transport, and regulation of vectorial vesicle trafficking and the dynamic actin cytoskeleton. In this review, we address the critical importance of protein–membrane crosstalk in the determination of plant cell polarity and summarize the role of membrane lipids, particularly minor acidic phospholipids, in regulation of the membrane traffic. We focus on the protein–membrane interface dynamics and discuss the current state of knowledge on three partially overlapping levels of descriptions. Finally, due to their multiscale and interdisciplinary nature, we stress the crucial importance of combining different strategies ranging from microscopic methods to computational modelling in protein–membrane studies.

Key words: Cell polarity, endocytosis, exocytosis, membrane trafficking, membrane domain, microscopy, phosphatidic acid, phosphatidylinositol (4,5)-bisphosphate, pollen tube.

Introduction

Polar cell growth is one of the most fundamental processes in plant development. It determines cellular morphogenesis and ultimately defines plant phenotype. Membrane trafficking, especially exo- and endocytosis, is of crucial importance for the establishment and maintenance of cell polarity. Most processes of membrane trafficking involve membrane–protein interfaces. In this review, we aim to emphasize the critical importance of protein–membrane crosstalk in the determination of plant cell polarity and to summarize the role of membrane lipids in the regulation of membrane traffic. Since this is a topic of an inherently complex multiscale nature, for the sake of clarity we will describe this continuum in three partially overlapping spatial categories, which roughly relate to the readouts of particular research techniques: (i) membrane domains corresponding to confocal laser-scanning microscopy (CLSM) imaging with a resolution >1 μm or classical biochemical techniques; (ii) membrane domains describing processes taking place on a submicrometer scale, typically

Abbreviations: BFA, brefeldin A; CG, coarse-grained; CLC, clathrin light chain; CLSM, confocal laser-scanning microscopy; CME, clathrin-mediated endocytosis; DAG, diacylglycerol; GFP, green fluorescent protein; mbC, methyl-β-cyclodextrin; MD, molecular dynamics; PA, phosphatidic acid; PI, phosphatidylinositol; PI4P, phosphatidylinositol 4-phosphate; PLC, phospholipase C; PLD, phospholipase D; PM, plasma membrane; PPI, phosphoinositide; TIRF/VAEM, total internal reflection fluorescence/variable angle epifluorescence microscopy; VLCFA, very-long-chain fatty acid, wild type.

observed with advanced optical microscopy techniques such as super-resolution, spinning-disk or total internal reflection fluorescence/variable angle epifluorescence microscopy (TIRF/VAEM); and (iii) membrane dynamics at the nanometer level, where molecular details of individual lipid–lipid and protein–lipid molecular interactions can be addressed primarily by computational approaches such as molecular dynamics simulations (Fig. 1). Due to space limitations, we do not cover most reports relying on highly advanced physical–chemical approaches (such as solid state nuclear magnetic resonance, X-ray scattering, surface plasmon resonance, FTIR spectroscopy) and we focus mainly on methods allowing the visualization of protein–membrane interface dynamics in polar membrane trafficking.

While protein complexes involved in exocytosis and endocytosis are relatively well known across eukaryotes, data on the involvement of lipid membrane components lag significantly behind, despite the obvious fact that membrane fusion processes must also involve phospholipids. This is especially true for exocytosis, where there are few data directly showing mechanistic role of phospholipids, even for animal/yeast models, and where only indirect evidence exists for plant cells. Here, we review our current knowledge of the dynamic protein–membrane interface in plant cells at different scales and point out the molecular mechanisms possibly shared with other eukaryotic models.

A game of membranes: cellular 'macrodomains' in plant cell polarity

Membrane components often differ not only among different organelles of a cell but also among different regions of the single cell plasma membrane (PM, Alassimone *et al.*, 2010). Notoriously known examples involve the large membrane domains of polarized cells. Animal epithelial cells have a drastically different composition of the apical and basolateral membranes in terms of both lipids and proteins. The diffusion barrier formed by tight junctions prevents the membrane domains from mixing (Nicolson, 2014). In plants, at least four distinct membrane domains with different compositions can co-exist in one cell (Žárský *et al.*, 2009; Alassimone *et al.*, 2010)-the apical, basal, inner lateral and outer lateral domains. The endodermal/exodermal casparian strip is an example of a cell-type-specific plant cell polar domain (Roppolo *et al.*, 2010).

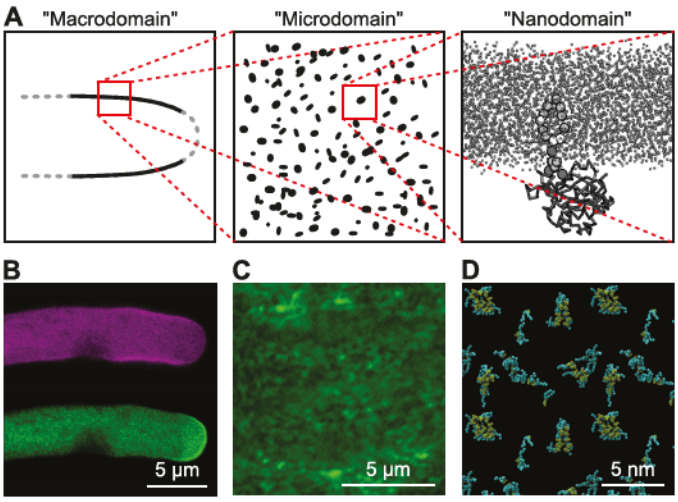

Fig. 1. Diagram of the different levels of lipid–protein dynamics. (A) Schematic cartoon illustration depicting the different scales of lipid–protein domains. (B) Membrane domains corresponding to CLSM imaging with resolution >1 µm or classical biochemical techniques; pollen tube transiently expressing PA and PI(4,5)P_2 marker is shown as the example. (C) Membrane domains describing processes taking place on a submicrometer scale, with the example of exocyst subunit localization at the PM visualized by spinning-disk confocal microscopy (courtesy of Dr Lukas Synek). (D) Membrane dynamics at the nanometer level, with the example of CG-MD of PI(4,5)P_2 clustering simulated with the MARTINI force-field (Marrink *et al.*, 2007).

Polar exocytosis, selective endocytosis, limitation of the diffusion rate, and the presence of diffusion barriers can all play a role in membrane protein polarity establishment and maintenance (Kleine-Vehn *et al.*, 2011). Limiting diffusion of membrane proteins by their attachment to the cell wall is an important mechanism of plant membrane protein polarization (Martinière *et al.*, 2012).

The discovery of the rapid changes in the spatio-temporal dynamics of minor signalling lipids (and their interacting proteins) brought about new challenges in finding approaches through which such changes can be visualized and quantified. Thanks to the existence of protein modules that selectively recognize distinct phospholipids, rapid changes in their levels and distribution can be monitored by CLSM (Balla and Várnai, 2002; Vermeer and Munnik, 2013). Although this technique is one of the few that provides information on lipid dynamics in live cells with subcellular resolution, it has also limitations that need to be taken into account when interpreting the data (Balla, 2007). The most importantly, it is not yet clear whether all pools of a particular lipid are visualized by the marker constructs. They may recognize the lipid in a very specific context and not image the whole population of the studied lipid in every cellular compartment. It is therefore imperative to remember that the absence of evidence is not evidence of absence, and to interpret the data with caution. Alongside imaging of protein–lipid dynamics *in vivo*, microscopic studies of giant unilamellar vesicles are excellent model systems for the determination of membrane properties and protein–lipid interactions on the macrodomain scale. Membrane phase separation, lipid sorting, membrane rigidity, and stretching elasticity have been studied using these giant unilamellar vesicles (Zhao and Lappalainen, 2012).

A feast for phosphoinositides: rare but powerful master players in the membrane

Phosphoinositides (PPIs) comprise a group of phospholipids consisting of the backbone molecule phosphatidylinositol (PI) and its mono-, bis-, or tris-phosphorylated derivatives. A variety of lipid kinases reversibly phosphorylate positions 3, 4, and 5 on the inositol ring so that three modifications results in seven PPI species. PPIs have been implicated in a plethora of processes and their classic 'textbook' role is to serve as substrates for the generation of secondary messengers (typically diacylglycerol (DAG) and inositol 1,4,5-trisphosphate

produced from phosphatidylinositol 4,5-bisphosphate). In exocytosis, PPIs function more as 'local' organizers of membrane domains and regulators of membrane deformation and sorting machineries (Thole and Nielsen, 2008), or in the control of cytoskeletal dynamics (Pleskot *et al.*, 2014). This can be also achieved by the very 'regional' character of PPI metabolism, where various kinases and phosphatases are located on various organelles, thus creating distinct pools of different PPIs (Boutté and Moreau, 2014).

In plant cells, five of the seven PPIs were detected. Phosphatidylinositol 3,4,5-trisphosphate (PIP_3) has never been detected in plant cells, and the reported detection of plant phosphatidylinositol 3,4-bisphosphate $PI(3,4)P_2$ was most probably a misinterpretation of then unknown $PI(3,5)P_2$ (Meijer and Munnik, 2003). Simon *et al.* (2014) used different genetically encoded biosensors to characterize localization of PPIs within *Arabidopsis* root epidermal cells, showing that $PI(4,5)P_2$ is localized almost exclusively at the PM and that phosphatidylinositol 4-phosphate (PI4P) exhibits a gradient of increasing localization from the Golgi apparatus to post-Golgi compartments to the PM. During cell division, the PI4P marker showed strong labelling of the cell plate (Vermeer *et al.*, 2009). The role of PI4P and $PI(4,5)P_2$ in polar growth has been studied most extensively in plant-tip growing cells, pollen tubes, and root hairs. The PI4P marker is enriched at the tips of emerging and growing root hairs (Vermeer *et al.*, 2009). Similarly, the $PI(4,5)P_2$ marker localizes to the tip of both root hairs (van Leeuwen *et al.*, 2007) and pollen tubes (Ischebeck *et al.*, 2011; Potocký *et al.*, 2014). Polar localization and gradients of phospholipids are sustained by restricted localization and the activity of PI-converting enzymes (Heilmann and Heilmann, 2014; Helling *et al.*, 2006).

PI4P has traditionally been understood only as a precursor for the synthesis of $PI(4,5)P_2$. However, recent lines of evidence showing PI4P as an important organizer of membrane trafficking put this molecule back into the spotlight. While in animals regulated secretion relies on $PI(4,5)P_2$, constitutive secretion appears to be mostly under the control of PI4P, generated from PI by the phosphatidylinositol 4-kinases (PI4Ks). In mammals, four different PI4K isoforms have been identified so far. Two of these, PI4KIIα and PI4KIIIβ, are localized to the Golgi, which appears to be the organelle where PI4P has a prominent and direct role. Indeed, many PI4P-binding proteins have been identified at the Golgi, such as clathrin adaptors and lipid-transfer proteins (D'Angelo *et al.*, 2008). In yeast, two PI4K isoforms are present, Pik1p (type IIIα of PI4K present at the Golgi and nucleus) and Stt4p (type IIIβ of PI4K localized to the PM) serving as primary sources of PI4P for secretion (Audhya *et al.*, 2000).

In *Arabidopsis*, the only known enzymes with PI4K activity belong to the IIIβ type. In contrast to yeast, disruption of both plant IIIβ PI4Ks does not lead to lethality, although the double mutant displays disturbed morphology of root hairs. PI4P production and membrane trafficking are further linked by the interaction of PI4Kβ1 with the small GTPase RabA4b, which controls post-Golgi trafficking to the PM (Preuss *et al.*, 2006). Interestingly, while PI4Kβ1 co-localizes with RabA4b in the TGN-like compartment, the majority of PI4P resides at the PM (Vermeer *et al.*, 2009). This apparent ambiguity was solved by identification of the *root-hair-defective 4* (*rhd4*) mutant. In *Arabidopsis*, RHD4 is required for normal root hair development and encodes a Sac1p-like PI4P-selective phosphatase. RHD4/SAC7 also co-localizes with RabA4b and PI4Kβ1 and probably functions as the regulator of PI4P levels, restricting the levels of PI4P to the vesicles at the tips of growing root hairs. In *rhd4* mutant plants, loss of the phosphatase activity results in PI4P accumulation, leading to mislocalization and accumulation of PI4P-labelled secretory vesicles (Thole *et al.*, 2008).

The *Arabidopsis* genome contains 11 paralogues of PI4P 5-kinases (PIP5K, Heilmann and Heilmann (2014)) divided into a type A subfamily with a domain structure similar to mammalian and yeast enzymes (PIP5K10 and -11) and a type B subfamily with N-terminal Lin and MORN domains. PIP5K1, -2, -7, -8, and -9 are expressed ubiquitously in most vegetative tissues, PIP5K3 is trichoblast and root hair specific, and PIP5K2, -4, -5, -6, -10 and -11 are also expressed in pollen (Ischebeck *et al.*, 2008, 2011; Kusano *et al.*, 2008; Sousa *et al.*, 2008; Stenzel *et al.*, 2008; Zhao *et al.*, 2010). Both mutations and overexpressions of PIP5K paralogues cause various defects in tip growing cells. This indicates the necessity of fine-tuned PI-converting machinery in tip growing cells (Ischebeck *et al.*, 2010).

Localization of PIP5K3 in growing root hairs is apical (Kusano *et al.*, 2008; Stenzel *et al.*, 2008) and the root hairs of *pip5k3* mutants are shorter and swollen. *Arabidopsis* root hairs overexpressing PIP5K1, -2, or -3 (Ischebeck *et al.*, 2013; Stenzel *et al.*, 2008) are also short and swollen.

Localization of all fluorescently tagged pollen-expressed PIP5K isoforms 2, 4, 5, 6, 10, and 11 in tobacco pollen share similar characteristics. In growing cells, PIP5Ks are localized in the subapical region, while in non-growing cells, the localization is also expanded into the very tip (Ischebeck *et al.*, 2008, 2010, 2011; Stenzel et al., 2008, 2012; Zhao *et al.*, 2010). Pollen from *pip5k4* mutant *Arabidopsis* plants has a lower germination rate and slower growth with the occasional occurrence of branched pollen tubes. The germination rate is even more reduced in *pip5k4 pip5k5* double mutant *Arabidopsis* pollen (Ischebeck *et al.*, 2008). There are two types of phenotype associated with PIP5K overexpressors. PIP5K2, -10, and -11 overexpression causes swelling of the tobacco pollen tube tip (Ischebeck *et al.*, 2011; Stenzel *et al.*, 2012), while overexpression of PIP5K4, -5, and -6 results into pollen tube waving, tip branching or invagination of the tip membrane with detachment from the cell wall ('protoplast trapping', Ischebeck *et al.*, 2008, 2010; Sousa *et al.*, 2008; Stenzel *et al.*, 2012; Zhao *et al.*, 2010).

The protoplast-trapping phenotype of PIP5K4 and -5 overexpressors is associated with increased pectin deposition. Pollen tubes with low overexpression of PIP5K6 grow slower and show slightly slower targeting of receptor-like kinase to the membrane, indicating slower exocytosis. In contrast, *Arabidopsis* PIP5K6 RNAi pollen and tobacco PIP5K6 overexpressors have impaired FM dye internalization and recruit less clathrin heavy chain to the PM. Simultaneous expression

of dominant-negative clathrin heavy chain alleviates the phenotype of strong PIP5K6 overexpressors, indicating that the phenotype is caused by accumulation of aborted endocytotic events (Zhao *et al.*, 2010). In summary, disruption of the delicate PI(4,5)P_2 balance probably influences both exocytosis and endocytosis in the pollen tube tip.

The pollen tip-swelling phenotype of PIP5K2, -10, and -11 mutants/overexpressors is actin related, and the mechanism responsible for altered actin structure and swelling seems to be activation of the small GTPase NtRac5 (Ischebeck *et al.*, 2010). A domain deletion and domain swapping study by Stenzel *et al.* (2012) identified regions of B-type PIP5Ks responsible for membrane localization and different overexpression phenotypes of PIP5K2 and PIP5K5/PIP5K6. These regions differ from the catalytic domain and could facilitate protein–protein interactions driving PIP5Ks in specific signalling contexts.

Besides systematic investigations of PI(4,5)P_2 and PIP5Ks in tip growth, their role in recycling of PIN auxin transporters has been addressed. Growth and gravitropic phenotypes of *pip5k1* (Ischebeck *et al.*, 2013), *pip5k2* (Mei *et al.*, 2012; Ischebeck *et al.*, 2013), and mostly *pip5k1 pip5k2* (Mei *et al.*, 2012; Ischebeck *et al.*, 2013; Tejos *et al.*, 2014) double mutants indicate defective auxin transport. *pip5k2* mutants showed reduced FM4-64 internalization, which could be rescued by external addition of PI(4,5)P_2. FM4-64 accumulation was more sensitive to brefeldin A (BFA, Mei *et al.*, 2012). In the *pip5k2* mutant background, PIN2–green fluorescent protein (GFP) and PIN3–GFP are more readily accumulated in BFA bodies and retained in the bodies after BFA washout (Mei *et al.*, 2012). In the *pip5k1 pip5k2* double mutant, PIN2 polarization is disrupted. Overexpression of PIP5K1 and PIP5K2 also causes auxin-related growth defects and reduced PIN2 localization to the PM with internalization/retention in bodies. Endocytotic cycling of PIN1 and PIN2 is impaired in the *pip5k1 pip5k2* double mutant (Ischebeck *et al.*, 2013). Localization of PIP5K1 and PIP5K2 in root cells is enriched at the apical and basal membrane in several root tissues (Ischebeck *et al.*, 2013; Tejos *et al.*, 2014). PM enrichment at the apical and basal membrane can also be observed for PI4P and PI(4,5)P_2 (Ischebeck *et al.*, 2013; Tejos *et al.*, 2014). Intact PI(4,5)P_2 metabolism with precise spatial distribution of PI(4,5)P_2- and PI(4,5)P_2-forming enzymes is thus important for both internalization and exocytosis of PIN proteins. It is noteworthy that the EXO70 subunit of the secretory vesicle tethering complex exocyst directly binds PI(4,5)P_2 in mammals and yeasts (He *et al.*, 2007; Liu *et al.*, 2007). The *Arabidopsis* homologue EXO70A1 has a conserved PI(4,5)P_2 binding site (Žárský *et al.*, 2009) and plays a role in PIN delivery to the PM (Janková Drdová *et al.*, 2013).

The spatial restriction and steady-state levels of PI(4,5)P_2 can be also regulated by controlled hydrolysis via either phospholipases or phosphatases with fundamentally different physiological consequences. Cleavage by phospholipases gives rise to secondary messengers that propagate and amplify signalling, whereas dephosphorylation controls PI(4,5)P_2 steady-state levels and turns off its function. Indeed, in animal endocytosis, dephosphorylation removes PI(4,5)P_2 from internalized membranes, thus restricting the localization of PI(4,5)P_2 to the PM without coupling the endocytic reaction to the generation of signalling metabolites (Cremona *et al.*, 1999). In the *Arabidopsis* genome, several genes from the 5PTase phosphatase family have been implicated in PI(4,5)P_2 breakdown. This family includes FRA3, a member of the plant type II 5PTase subfamily with highest substrate affinity towards PI(4,5)P_2, which controls actin organization and secondary cell-wall synthesis in fibre cells (Zhong *et al.*, 2004), and 5PTase9, implicated in the regulation of endocytosis after salt stress (Golani *et al.*, 2013). Furthermore, plants also possess the SAC (suppressor of actin) family, which contains both 4- and 5-specific phosphatase activities. Besides the previously mentioned PI4P-specific SAC7/RHD4, SAC9 is also implicated in PI(4,5)P_2 cleavage and is involved in the regulation of this lipid in stress responses (Williams *et al.*, 2005). Other members of the SAC family were shown to cleave the 3-phosphate group and were implicated in vacuolar fusion (Nováková *et al.*, 2014).

PI–phospholipase C (PLC) cleaves PI(4,5)P_2 into diacylglycerol (DAG) and inositol 1,4,5-trisphosphate in a calcium-dependent manner. Although most plant PI–PLC studies have focused on its role in stress responses (Meijer and Munnik, 2003), PI–PLC was also shown to be important for the polar growth of pollen tubes. In both *Petunia* and tobacco, PI–PLC is localized to the PM but excluded from the very apex (Dowd *et al.*, 2006; Helling *et al.*, 2006). Together with the distribution of PIPK isoforms, this seem to restrict PI(4,5)P_2 distribution to the apex of tip growing cells. Intriguingly, a signalling role of DAG in plant cells is not obvious. Meijer and Munnik (2003) showed that DAG in plant cells is rapidly phosphorylated by DAG kinase to phosphatidic acid (PA), which plays active roles in plant signalling processes. However, data showing DAG as a signalling platform in plants are emerging (Helling *et al.*, 2006; Pejchar *et al.*, 2010; Pejchar *et al.*, 2015).

Phosphatidic acid: simple but still powerful

PA represents the simplest glycerophospholipid, consisting of a hydrophobic DAG body and a single phosphate as the polar hydrophilic headgroup. Although PA can be produced by two distinct pathways (see Pleskot *et al.*, 2012a), its production by proteins from the phospholipase D (PLD) family is by far the most investigated. While the functions of PA in various stress responses (Testerink and Munnik, 2011) and cytoskeletal regulation (Pleskot *et al.*, 2012b, 2013) are well described, molecular details about its direct involvement in plant cell polarity are still scarce and are mostly confined to pharmacological studies and circumstantial evidence (Potocký *et al.*, 2003; Monteiro *et al.*, 2005; Pleskot *et al.*, 2012a). In recent work, Potocký *et al.* (2014) visualized PA in living pollen tubes utilizing a PA biosensor derived from the PA-binding domain of yeast Spo20p. The authors found that PA localized in the subapical region of tobacco pollen tube PM and partially overlapped with the signal for PI(4,5)P_2. To the best of our knowledge, this is the only evidence of PA localization and dynamics in the living plant cells.

Interestingly, PLDζ2, a member of the PLD subfamily most closely related to animal PLDs, emerged as a regulator of auxin transport by affecting vesicle trafficking (Li and Xue, 2007). *Arabidopsis pldζ2* mutants have a less pronounced gravitropic response, root growth, and hypocotyl elongation in response to external auxin than wild-type (WT) plants. Overexpression of PLDζ2 or externally added PA stimulates a root gravitropic response and FM internalization, while *n*-butanol, a PLD inhibitor, inhibits it. PLDζ2 overexpressors are less sensitive to the inhibitory effect of BFA on root growth, hypocotyl elongation, and gravitropism, and also form BFA bodies less frequently than WT controls. PA treatment and PLDζ2 overexpression stimulate PIN2 return to the PM from BFA bodies after BFA washout. These results show that PLDζ2-generated PA facilitates both exocytosis and endocytosis. A negative halotropic response-growth of the root away from soil regions with a high-salt concentration-is preceded by asymmetrical relocalization of PIN2 in *Arabidopsis* (Galvan-Ampudia *et al.*, 2013) with PIN2 internalization by clathrin-mediated endocytosis (CME). The process involves PLDζ2-mediated clathrin light chain (CLC) recruitment (Galvan-Ampudia *et al.*, 2013).

Minor acidic phospholipids regulate both exocytosis and endocytosis in plant cells and their local concentrations need to be fine-tuned for proper cell morphogenesis. The mechanisms involved are often unknown, but both $PI(4,5)P_2$ (Martin, 2014) and PA (Liu *et al.*, 2013) directly bind various components of the exocytotic and endocytotic pathways in Opisthokont systems. Many of the interactions probably exist in plants as well. Minor acidic phospholipids also regulate cytoskeleton dynamics (Pleskot *et al.*, 2013, 2014), which in turn affects trafficking.

Clash of sterols: from membrane rigidity to endocytic deformations

Besides selected phospholipid species, sterols have also been shown to be indispensable for proper trafficking in plant cells. Mild concentrations of filipin are suitable for sterol staining, whereas cells treated with higher concentrations sequester sterols from the membrane and inhibit sterol-dependent endocytosis (Boutté *et al.*, 2011). Sterols are distributed along the whole PM (Boutté *et al.*, 2011), within the cell plate (Men *et al.*, 2008), and in various endosomal compartments (Grebe *et al.*, 2003). Filipin staining of root hairs and pollen tubes showed enrichment in the prospective root hair outgrowth site and growing root hair and pollen tube tip (Liu *et al.*, 2009; Ovečka *et al.*, 2010). Proper sterol composition is required for endocytosis-driven maintenance of PIN2 polarity (Men *et al.*, 2008). In BFA-treated cells, sterols get trapped in BFA bodies together with PIN2 (Grebe *et al.*, 2003), and both PIN2 and FM4-64 internalization to BFA bodies is inhibited by high concentrations of filipin (Men *et al.*, 2008). Disruption of sterol synthesis by genetic or pharmacological methods also affects post-cytokinetic sequestration of KNOLLE from the cell plate, and KNOLLE diffuses from the plate to lateral membranes in the sterol biosynthesis *cpi1* mutant and in fenpropimorph-treated cells (Boutté *et al.*, 2009; Frescatada-Rosa *et al.*, 2014). In *Picea meyeri* pollen tubes, disruption of membrane sterols leads to partial shifting of NOX and reactive oxygen species production activity away from the tip (Liu *et al.*, 2009). This is probably due to impaired endocytosis, which restricts NOX at the pollen tube tip. Use of ratiometric lipid order sensing dye (Frescatada-Rosa *et al.*, 2014; Zhao *et al.*, 2014) showed that the lipid order of the PM is higher than that of endosomes (Zhao *et al.*, 2014) but lower than the lipid order of the cell plate (Frescatada-Rosa *et al.*, 2014). A *cpi1* mutant background and sterol synthesis inhibitors decrease the cell plate lipid order. Besides erroneous recruitment of endocytic machinery to the cell plate with decreasing order, the lipid order remains similar to that of the PM without functional DRP1A at the cell plate. There is thus mutual feedback between high lipid order maintenance and functional endocytosis at the cell plate (Frescatada-Rosa *et al.*, 2014).

A storm of very-long-chain fatty acids (VLCFAs): the impact of VLCFAs

Besides head groups, the tail composition of membrane lipids plays an important role in membrane trafficking. In *Arabidopsis*, both exocytosis of selected membrane proteins (Markham *et al.*, 2011) and proper cytokinesis (Molino *et al.*, 2014) require lipids with VLCFAs. LOH1 and LOH3 ceramide synthases are responsible for VLCFA sphingolipid synthesis in *Arabidopsis*, and both can be inhibited simultaneously with fumonisin B1 (FB1, Markham *et al.*, 2011; Molino *et al.*, 2014). FB1 treatment inhibits polar auxin transport, and newly synthesized AUX1 and PIN1 accumulate in TGN-positive intracellular bodies after FB1 treatment, without reaching the PM, indicating a defect in the exocytotic pathway (Markham *et al.*, 2011). Molino *et al.* (2014) showed that glycosphingolipids with VLCFAs enhance the membrane vesicle fusion rate *in vitro*. FB1 treatment also affects the later stages of cytokinesis and leads to accumulation of Golgi-derived vesicles at the cell plate. Fusion of RabA2 and VHAa1 normally occurring during late cytokinesis is slower in FB1-treated cells (Molino *et al.*, 2014). Interestingly, trafficking of some membrane proteins (PIN2, aquaporin PIP2, and LTi6b) is not affected by FB1 (Markham *et al.*, 2011).

The winds of traffic: the dynamic nature of membrane 'microdomains'

In addition to the long-known examples of large co-existing membrane domains in a single eukaryotic cell, recent methodically advanced studies clearly demonstrate membrane heterogeneity at a smaller spatial scale and the presence of many co-existing stable membrane microdomains with distinct composition (Spira *et al.*, 2012; Jarsch *et al.*, 2014). For many years, the idea of such microdomains was mostly represented by the so-called 'lipid raft theory'. As an extension to the original fluid mosaic concept of biological membranes, this postulated the existence of more rigid sterol- and sphingolipid-enriched fractions floating within

the rest of the membrane, which behaves in a fluid mosaic manner (Nicolson, 2014). Protein partitioning into these domains was originally tested biochemically by its presence in isolated non-ionic detergent-resistant fractions of the PM. The concept of lipid rafts has been criticized in terms of its possible artefact nature, and both the spatial and temporal dimensions of these microdomains have been discussed extensively. With the advent of super-resolution microscopy and other techniques allowing high spatiotemporal observations inside cells, evidence of multiple long-lived co-existing microdomains within one membrane is accumulating. As reported by Nicolson (2014), control of membrane microorganization may be more complex than previously thought, and many types of membrane-associated cytoskeletal structures probably exist, some of them being less susceptible to cytoskeleton-disrupting drugs. Microdomains could form due to partitioning into sterol- and sphingolipid-enriched membrane fractions, but interactions of proteins with other lipid species, protein–protein interactions, lipid clustering, confinement by the cytoskeleton, and other mechanisms seem to play a role in PM heterogeneity regulation at small spatial dimensions.

Increasing availability and usage of high-end microscopy approaches is bringing new insights into protein localizations in plant cells. Fine spatial information with regard to localization and partitioning into different PM microdomains can now be observed directly. TIRF/VAEM microscopy is being used increasingly to observe events near the membrane and in the cortical cytoplasm (Konopka and Bednarek, 2008). Use of super-resolution microscopy in plant science is also emerging; structured illumination was used for dynamic localization of cortical microtubules (Komis *et al.*, 2014), and stimulated emission depletion (STED) was successfully applied to visualize remorins (Demir *et al.*, 2013) and PIN cycling (Kleine-Vehn *et al.*, 2011). Techniques like single-molecule tracking, fluorescence correlation spectroscopy (H. Li *et al.*, 2011) and fluorescence energy resonance transfer/fluorescence lifetime imaging (FRET/FLIM; Jarsch *et al.*, 2014) are also appearing in plant cell biology. We will not cover the details of high-end fluorescent microscopy techniques with regard to membrane microdomain organization, as the topic has been reviewed elsewhere (Owen and Gaus, 2013).

A number of different biochemical methods for identification of lipid–protein interactions on the micrometer scale have been described. For the first identification of novel lipid-binding proteins, lipid affinity beads assay were used to isolate candidate proteins from cell extracts followed by proteomic analysis (Lim *et al.*, 2002). To identify less abundant lipid-binding proteins, additional purification and fractionation steps should be done (McLoughlin *et al.*, 2013). Where a lipid-binding protein is presumed (e.g. containing a known lipid-binding domain), the lipid–protein interaction can be verified and particular lipid-binding specificity can be detected by a so-called protein–lipid overlay, a method that is fast, cheap, and requires only small amount of protein (Munnik and Wierzchowiecka, 2013). However, the main disadvantage of both methods is that the lipids presented are not in their natural form, which may lead to false results. Thus, the interaction of lipid and candidate proteins should be further confirmed by co-sedimentation with large unilamellar vesicles, a method that enables analysis of protein–lipid binding affinity and specificity (Julkowska *et al.*, 2013).

A large-scale study comparing yeast PM proteins covering different functional categories and types of membrane anchor (Spira *et al.*, 2012) combined TIRF microscopy and deconvolution to address protein distribution heterogeneity. The distribution of all tested proteins turned out to be heterogeneous, with different patterns ranging from patches to networks. The patterns of transmembrane proteins were stable within minutes, whereas peripheral proteins (and lipid markers) turned out to be highly dynamic. Co-localization of tested proteins was addressed and revealed the presence of many co-existing domains. Various microdomains were shown to require a specific membrane lipid composition and/or actin-based structures for their existence (Spira *et al.*, 2012).

Recent systematic work on mapping localization of 20 *Arabidopsis* membrane proteins by TIRF/VAEM microscopy demonstrated multiple co-existing microdomains in plant cell PM (Jarsch *et al.*, 2014). This demonstration of possible (and cell-type-specific) microdomain co-existence within the PM is of outstanding importance, since current practice is to use co-localization with remorin or flotillin to prove that the studied protein resides in 'microdomains'. Therefore, the frequently used tag of 'membrane microdomain-associated protein' may be a rather vague category.

The mechanistic basis of localization of plant proteins into microdomains is not clear. It is possible that polar exocytosis, regulated endocytosis and restricted diffusion—the mechanisms responsible for asymmetric localization into large membrane domains—act in the sorting of proteins into microdomains as well. In the case of remorin At4g00670, FRAP experiments have indicated the stability of the microdomain and targeted delivery of the microdomain-resident protein. In Opisthokont systems, diffusion barriers at a small spatial scale can be formed by fine cortical cytoskeletal structures (Nicolson, 2014) and the decoration of cytoskeletal fibres may represent a general protein micropatterning mechanism. Indeed, remorin Atg13920 localizes into a filament-like pattern, which is sensitive to oryzalin treatment (Jarsch *et al.*, 2014). Other mechanisms for keeping plant membrane proteins in specific microdomains may be limiting of the diffusion by binding to the cell wall or partitioning into areas of specific lipid composition and clustering with other proteins. Typically, post-translational modifications like acylations affect protein partitioning into the microdomains, as was shown for remorin SYMREM1 (Konrad *et al.*, 2014) and small GTPase ROP6 (Sorek *et al.*, 2010).

The differential lipid composition of plant microdomains still needs to be addressed. Furt *et al.* (2010) reported existence of $PI(4,5)P_2$ clusters within the PM of tobacco BY2 cells. However, such clusters may be induced solely by Triton X-100, used for membrane extraction (van Rheenen *et al.*, 2005). The functional significance of plant membrane microdomains is often not clear. A lipid microenvironment can influence the functional properties of membrane proteins, as was shown by

Spira *et al.* (2012), and is also generally known for membrane channels (Coskun and Simons, 2011). Microdomains may have distinct mechanical properties due to specific membrane composition and thus facilitate membrane deformations during membrane trafficking, and can harbour protein–protein interactions (Jarsch *et al.*, 2014).

The concept of microdomains is of course complementary rather than exclusive to investigation of differences in membrane composition in large plant cell domains (apical, outer, lateral, etc.). The composition of large membrane domains/regions can also mirror the prevalence of a particular microcompartment. FRAP measurements of protein kinetics in the apical membrane of Madin–Darby canine kidney (MDCK) epithelial cells by Meder *et al.* (2006) showed that, in comparison with the PM of fibroblasts, 'raft' proteins freely diffuse within the MDCK apical membrane and 'non-raft' proteins are dispersed into isolated microdomains within this 'macrodomain'. The apical domain of MDCK epithelial cells thus behaves like one big 'percolated raft'. Similarly, many plant membranes seem to contain floating microdomains enriched in sterols but in some cases, like the PM of plasmodesmata sleeves, the whole membrane seems to be enriched in sterols and has some 'raft'-like properties (Raffaele *et al.*, 2009). Similarly, the sterol-enriched domains at the apex of tip growing cells (Liu *et al.*, 2009; Ovečka *et al.*, 2010) and pathogen penetration sites (Bhat *et al.*, 2005) could be formed by local enrichment of sterol-based microdomains.

Advanced optical microscopy in the analysis of PM dynamics

In recent years, TIRF/VAEM and spinning-disk imaging of *Arabidopsis* root cells has been applied to gain detailed insight into the spatial organization of membrane trafficking in plant cells. Most of the addressed process seems to be CME. Plant CME involves basic components previously described in the Opisthokont model systems [namely adaptor protein complex 2 (AP-2), clathrin triskelion, and dynamin-related proteins] driving endocytosis site selection, vesicle formation, and vesicle scission, respectively. Moreover, the recently described TPLATE complex drives endocytosis initiation in plant cells (Van Damme *et al.*, 2011; Gadeyne *et al.*, 2014). All of the basic CME machinery components localize into distinct puncta within the PM with some, although limited, lateral diffusion and a similar lifetime due to appearing and disappearing within the PM plane (Konopka and Bednarek, 2008; Gadeyne *et al.*, 2014).

Despite rich evidence of the importance of minor phospholipid species in CME, plant cell biologists are only beginning to address this issue in the context of spatial organization within the membrane. Ischebeck *et al.* (2013) showed a decrease in CLC foci density and an increase in their size in *pip5k1 pip5k2* double mutants compared with the situation in WT plants. Careful studies involving genetic and pharmacological tools and spinning-disk/TIRF/VAEM analysis of spatiotemporal phospholipid probes behaviour should be performed in future with regard to the role of minor phospholipids in the organization and kinetics of endocytosis and exocytosis. Some novel methodical limitations might arise by addressing co-localization at the fine spatiotemporal level. For example, as pointed out by Heilmann and Heilmann (2014), interacting proteins can mask phospholipid species if they bind and make them inaccessible for phospholipid probes. Different probes may also bind particular phospholipids only in specific cellular contexts (Balla *et al.*, 2000). Genetic and pharmacological alterations (also discussed below) might also alter the behaviour of proteins not typically interacting with affected phospholipid species. Localization and dynamics changes can be the result of altered membrane partitioning into microdomains due to compositional alterations. Studies on the widely used polarized trafficking models of PIN1 and PIN2 will also have to be supplemented more often with other membrane proteins (e.g. aquaporins, see also below), because apical and basal membranes, where most of the PIN2 and PIN1 population occurs, are not accessible for TIRF/VAEM studies and are difficult to access with spinning-disk microscopy.

Recently, R. Li *et al.* (2012) identified a clathrin-independent endocytosis pathway in plants, associated with flotillin 1 (Flot1). Both confocal and immunoelectron microscopy show that Flot1 is associated with the detergent-resistant fraction of the PM and does not co-localize with CLC. Knockdown of Flot1 results into a decrease of PM lipid order, so Flot1 could be required directly for the formation of sterol-enriched microdomains (Zhao *et al.*, 2014). TIRF/VAEM-visualized Flot1 foci have limited lateral diffusion and mostly appear and disappear in the membrane plane. Flot1 and CLC foci display opposite sensitivity to methyl-β-cyclodextrin (mbC) and tyrphostin A23 (TyrA23) with CLC dynamics being altered by TyrA23 and being mbC insensitive, and with Flot1 foci dynamics being mbC sensitive. LatB and even more oryzalin treatment decreases the Flot1 foci diffusion coefficient (R. Li *et al.*, 2012).

X. Li *et al.* (2011), Wang *et al.* (2013), and Hao *et al.* (2014) brought more insight into the spatial aspects of endocytosis, addressing both the role of CME and clathrin-independent endocytosis of selected 'cargo' proteins, namely PIP2,1 aquaporin, ammonium transporter AMT1;3, and reactive oxygen species regulator RbohD, respectively.

Dual-colour TIRF/VAEM observations showed that part of RbohD foci co-localize with CLC and part of the foci co-localize with Flot1 (Hao *et al.*, 2014). NaCl treatment induces rapid RbohD internalization, and a combination of fluorescence cross-correlation spectroscopy (with CLC or Flot1) and pharmacology indicates that CME is the major pathway for internalization, but a substantial part of RbohD is also internalized via a clathrin-independent, Flot1-associated pathway. Inhibition of either pathway also increases the amount of foci at the membrane and decreases their diffusion rate under normal osmotic conditions.

AMT1;3 NH_4^+ carrier availability at the PM is regulated by NH_4^+ accessibility (Wang *et al.*, 2013). A high ammonium concentration results in AMT1;3-selective endocytosis, which is preceded by aggregation of transporters into clusters. CLC- and Flot1 co-localization experiments and pharmacological (TyrA23 and mbC) treatments have demonstrated the utilization of both clathrin-dependent and

clathrin-independent pathways in AMT1;3 internalization, with the clathrin-dependent pathway being prevalent.

X. Li *et al.* (2011) carefully analysed single-molecule (or up to a tetrameric complex) behaviour of PIP2;1 aquaporin. Disruption of sterol-rich microdomains by mbC causes aggregation of the transporters. The sterol synthesis inhibitor fenpropimorph and sphingolipid synthesis inhibitor PPMP have a similar effect. While endocytosis accompanying constitutive PIP2;1 cycling is driven solely by the clathrin pathway, NaCl-induced endocytosis involves both CME and Flot1 pathways with the clathrin-dependent pathway being prevalent (X. Li *et al.*, 2011).

As described above, the proteins clearly partition into sterol-dependent microdomains but also localize to other PM fractions. The universal implication suggesting protein restriction into rafts due to its presence in the detergent-resistant membrane extract might thus be an overinterpretation. It is also noteworthy that fenpropimorph treatment can influence the dynamics of CME components (Konopka and Bednarek, 2008; Konopka *et al.*, 2008). The previously mentioned studies relied mostly on specific disruption of CME or clathrin-independent endocytosis by TyrA23 or sterol microdomain-disrupting agents, respectively. However, if sterol microdomain disruption affects CME as well, single-molecule studies of protein partitioning and endocytosis will be more difficult to interpret than is currently assumed.

Recently, Fendrych *et al.* (2013) performed a pioneering study of plant exocytosis spatial details, which addressed the EXO70A1, EXO84b, SEC8, and SEC6 subunits of the vesicle-tethering complex exocyst. Individual subunits co-localized in distinct highly dynamic spots different from the endocytotic puncta labelled by DRP1C. These spots did not move within the optical plane but appeared and disappeared in the plane. Most of the exocytotic foci thus do not correspond to vesicles but contain dynamic exocyst particles or membrane microdomains where these particles are targeted. The foci decrease in density and partly cluster into clumps after prolonged actin disruption. Similar localization and dynamics were also shown for the SEC3a exocyst subunit (Zhang *et al.*, 2013). As both SEC3 and EXO70 subunits of the exocyst directly bind $PI(4,5)P_2$ in Opisthokont models (He *et al.*, 2007; Liu *et al.*, 2007; Zhang *et al.*, 2008), $PI(4,5)P_2$-enriched microdomains could be important in exocyst recruitment. Detailed localization studies of exocytotic machinery components together with genetic and pharmacological disruptions of selected lipid species formation will be of outstanding importance in order to understand the role of membrane microdomains in spatial exocytosis organization.

It is also important to note that when studied only by diffraction-limited microscopy without additional methods, like single fluorophore quantification and bleaching, 'microdomain localization' can represent different phenomena. Diffraction-limited spots can harbour clusters of proteins (that may localize together due to partitioning into a lipid islet) but also single protein–protein complexes. Some of the patches described by Spira *et al.* (2012) and Jarsch *et al.* (2014) might thus represent randomly distributed proteins at certain density.

A dance with molecules: molecular dynamics (MD) simulations as the 'computational microscope'

To describe the role of protein–lipid interplay in cell polarity, it is important to understand the mechanistic details of lipid-, lipid-protein, and protein–protein interactions. Although we have experienced major progress in experimental techniques, their resolution is still limited for the description of events that underline processes in the biological membranes (Manna *et al.*, 2014). Over the last 20 years, molecular simulations and especially MD have become a valuable tool to study membrane and protein systems. Together with the increase in computational power and better algorithms, MD results have reached time and length scales directly comparable with experiments and they thus represent a complementary tool to the experimental methods. Moreover, they enable us to probe the system of interest at the single-molecule level (Bennett and Tieleman, 2013).

In MD simulations, the system is represented as an ensemble of particles that follow the laws of classical physics, and time evolution of the system is obtained by the numerical solution of Newtonian equations (Manna *et al.*, 2014). A crucial part of MD simulations is the force field, which describes interactions between parts of the simulated systems in terms of a potential energy function, which is composed of two types of interaction, bonded and non-bonded (Manna *et al.*, 2014). Typical simulated times for all-atom simulations are hundreds of nanoseconds, but simulations reaching microseconds have been also reported (Deleu *et al.*, 2014). The simulation times can be further increased to tens of microseconds and even to milliseconds using a coarse-grained (CG) force field, in which groups of atoms are represented as a one particle (Ingólfsson *et al.*, 2014a).

Biophysical principles of membrane domain formation elucidated by MD simulations

CG-MD simulations have been used to address the formation of lipid nanodomains or 'rafts' (reviewed by Bennett and Tieleman, 2013). Several studies have shown phase separation of ternary mixtures composed of various lipid species with results matching experimental observations (Risselada and Marrink, 2008; Schäfer and Marrink, 2010; Perlmutter and Sachs, 2011). Recently, the model of the mammalian PM containing 63 different lipid species was published showing the transient occurrence of lipid domains on a microsecond scale (Ingólfsson *et al.*, 2014b). Interestingly, the authors observed clustering of phosphoinositides in the inner leaflet of the PM. The combination of an experimental and computational approach was used successfully to study the effect of polyunsaturated lipids on mammalian endocytosis (Pinot *et al.*, 2014). The authors found that polyunsaturated lipids increased the ability of dynamin and endophilin to deform and vesiculate membranes by reducing the energetic cost of membrane bending and fission.

The raft hypothesis suggests that the formation of lipid nanodomains would influence the distribution and activity of

membrane proteins. It was shown that ionic proteins indeed cluster with PI(4,5)P_2 molecules, using CG-MD and STED microscopy (van den Bogaart *et al.*, 2011). Different small GTPases were shown to be partitioned into the specific lipid domains based on the type of their lipid anchor (Janosi and Gorfe, 2010; Z. Li *et al.*, 2012; de Jong *et al.*, 2013). The mechanism of membrane targeting of diverse peripheral membrane proteins or their domains has been revealed using both all-atom MD and CG-MD simulations (Stansfeld and Sansom, 2011; Pleskot *et al.*, 2012b). Several recent papers have demonstrated the effect of protein on the distribution of specific lipids in the lipid bilayer (Kalli *et al.*, 2013; Charlier *et al.*, 2014; Jefferys *et al.*, 2014). Moreover, proteins such as the BAR domain or EXO70p can induce the membrane curvature, as was shown both computationally and experimentally (Arkhipov *et al.*, 2008; Zhao *et al.*, 2013).

Many peripheral membrane proteins are not specific towards one lipid species but instead recognize multiple targets in the membrane leading to conditional binding (Moravcevic *et al.*, 2012). It was shown that phosphatidylethanolamine enhances protein–PA interactions by increasing the negative curvature of the membrane and thus facilitating the insertion of hydrophobic amino acid residues into the lipid bilayer (Kooijman *et al.*, 2007). Lipid distribution is also affected by specific interactions with ions: PI(4,5)P_2 molecules were shown to form clusters via their interaction with divalent cations, particularly Ca^{2+} (reviewed by Wang *et al.*, 2014).

A dream of exocytosis: concluding remarks

Although a substantial amount of data has been acquired about the organization, dynamics, and general importance of lipids at the macrodomain level, we still know surprisingly little about the identity and role of lipids in constituting distinct microdomains in plant cells. Over the last decade, the existence of membrane microdomains in plant cells has been firmly established, and it has been shown that there is substantial diversity in their composition, mobility, and stability. With the general availability of advanced microscopic methods and the wealth of mutants affecting polar membrane trafficking, it is necessary to cross the barrier to this other level of protein–membrane interactions studies. At the same time, recent advances in chemical biology provide us with a number of specific drugs interfering with the proteins and lipids involved in cell polarity. To this end, it will be extremely beneficial to study the effect of both established and novel chemical inhibitors at the microdomain level in living cells. Last but not least, we feel that in order to get a novel insight into protein–membrane interactions in plant biology, it is crucially important to combine experimental data with computational studies.

Both exocytosis and endocytosis have been shown to require specific lipid production in selected cases. It is noteworthy that most studies analysing the role of PPIs or sterols in membrane traffic are endocytosis -biased. It is often impossible to distinguish exocytosis-related defects, endocytosis-related defects, or a combination of both from each other without specific experiments. Many cell polarity phenotypes associated with altered lipid levels are thus probably the result not only of endocytosis but also of exocytosis alteration.

Acknowledgements

The work in the authors' laboratory is supported by the Czech Science Foundation grant GA13-19073S to MP. A part of the income of VŽ is covered by the MŠMT ČR project NPUI LO1417. The authors thank Dr Lukáš Synek (IEB, Czech Republic) for the picture taken by the spinning-disk confocal microscope. The authors also thank the developers of the Linux operation system and the open-source software used in the preparation of this study, particularly Inkscape and Gimp.

References

Alassimone J, Naseer S, Geldner N. 2010. A developmental framework for endodermal differentiation and polarity. *Proceedings of the National Academy of Sciences, USA* **107,** 5214–5219.

Arkhipov A, Yin Y, Schulten K. 2008. Four-scale description of membrane sculpting by BAR domains. *Biophysical Journal* **95,** 2806–2821.

Audhya A, Foti M, Emr SD. 2000. Distinct roles for the yeast phosphatidylinositol 4-kinases, Stt4p and Pik1p, in secretion, cell growth, and organelle membrane dynamics. *Molecular Biology of the Cell* **11,** 2673–2689.

Balla T. 2007. Imaging and manipulating phosphoinositides in living cells. *Journal of Physiology* **582,** 927–937.

Balla T, Bondeva T, Várnai P. 2000. How accurately can we image inositol lipids in living cells? *Trends in Pharmacological Sciences* **21,** 238–241.

Balla T, Várnai P. 2002. Visualizing cellular phosphoinositide pools with GFP-fused protein-modules. *Science's STKE 2002* , pl3.

Bennett WFD, Tieleman DP. 2013. Computer simulations of lipid membrane domains. *Biochimica et Biophysica Acta* **1828,** 1765–1776.

Bhat RA, Miklis M, Schmelzer E, Schulze-Lefert P, Panstruga R. 2005. Recruitment and interaction dynamics of plant penetration resistance components in a plasma membrane microdomain. *Proceedings of the National Academy of Sciences, USA* **102,** 3135–3140.

Boutté Y, Frescatada-Rosa M, Men S, *et al*. 2009. Endocytosis restricts *Arabidopsis* KNOLLE syntaxin to the cell division plane during late cytokinesis. *EMBO Journal* **29,** 546–558.

Boutté Y, Men S, Grebe M. 2011. Fluorescent *in situ* visualization of sterols in *Arabidopsis* roots. *Nature Protocols* **6,** 446–456.

Boutté Y, Moreau P. 2014. Modulation of endomembranes morphodynamics in the secretory/retrograde pathways depends on lipid diversity. *Current Opinion in Plant Biology* **22,** 22–29.

Charlier L, Louet M, Chaloin L, Fuchs P, Martinez J, Muriaux D, Favard C, Floquet N. 2014. Coarse-grained simulations of the HIV-1 matrix protein anchoring: revisiting its assembly on membrane domains. *Biophysical Journal* **106,** 577–585.

Coskun U, Simons K. 2011. Cell membranes: the lipid perspective. *Structure* **19,** 1543–1548.

Cremona O, Di Paolo G, Wenk MR, *et al*. 1999. Essential role of phosphoinositide metabolism in synaptic vesicle recycling. *Cell* **99,** 179–188.

D'Angelo G, Vicinanza M, Di Campli A, De Matteis MA. 2008. The multiple roles of PtdIns(4)*P*—not just the precursor of PtdIns(4,5)P_2. *Journal of Cell Science* **121,** 1955–1963.

de Jong DH, Lopez CA, Marrink SJ. 2013. Molecular view on protein sorting into liquid-ordered membrane domains mediated by gangliosides and lipid anchors. *Faraday Discussions* **161,** 347–363.

Deleu M, Crowet J-M, Nasir MN, Lins L. 2014. Complementary biophysical tools to investigate lipid specificity in the interaction between bioactive molecules and the plasma membrane: a review. *Biochimica et Biophysica Acta* **1838,** 3171–3190.

Demir F, Horntrich C, Blachutzik JO, *et al*. 2013. *Arabidopsis* nanodomain-delimited ABA signaling pathway regulates the anion channel SLAH3. *Proceedings of the National Academy of Sciences, USA* **110,** 8296–8301.

Dowd PE, Coursol S, Skirpan AL, Kao T-h, Gilroy S. 2006. *Petunia* phospholipase C1 is involved in pollen tube growth. *The Plant Cell* **18,** 1438–1453.

Fendrych M, Synek L, Pečenková T, Janková Drdová E, Sekereš J, de Rycke R, Nowack MK, Žárský V. 2013. Visualization of the exocyst complex dynamics at the plasma membrane of *Arabidopsis thaliana*. *Molecular Biology of the Cell* **24,** 510–520.

Frescatada-Rosa M, Stanislas T, Backues SK, Reichardt I, Men S, Boutté Y, Jürgens G, Moritz T, Bednarek SY, Grebe M. 2014. High lipid order of Arabidopsis cell-plate membranes mediated by sterol and DYNAMIN-RELATED PROTEIN1A function. *The Plant Journal* **80,** 745–757.

Furt F, König S, Bessoule J-J, *et al*. 2010. Polyphosphoinositides are enriched in plant membrane rafts and form microdomains in the plasma membrane. *Plant Physiology* **152,** 2173–2187.

Gadeyne A, Sánchez-Rodríguez C, Vanneste S, *et al*. 2014. The TPLATE adaptor complex drives clathrin-mediated endocytosis in plants. *Cell* **156,** 691–704.

Galvan-Ampudia CS, Julkowska MM, Darwish E, Gandullo J, Korver RA, Brunoud G, Haring MA, Munnik T, Vernoux T, Testerink C. 2013. Halotropism is a response of plant roots to avoid a saline environment. *Current Biology* **23,** 2044–2050.

Golani Y, Kaye Y, Gilhar O, Ercetin M, Gillaspy G, Levine A. 2013. Inositol polyphosphate phosphatidylinositol 5-phosphatase9 (At5PTase9) controls plant salt tolerance by regulating endocytosis. *Molecular Plant* **6,** 1781–1794.

Grebe M, Xu J, Möbius W, Ueda T, Nakano A, Geuze HJ, Rook MB, Scheres B. 2003. *Arabidopsis* sterol endocytosis involves actin-mediated trafficking via ARA6-positive early endosomes. *Current Biology* **13,** 1378–1387.

Hao H, Fan L, Chen T, Li R, Li X, He Q, Botella MA, Lin J. 2014. Clathrin and membrane microdomains cooperatively regulate RbohD dynamics and activity in *Arabidopsis*. *The Plant Cell* **26,** 1729–1745.

He B, Xi F, Zhang X, Zhang J, Guo W. 2007. Exo70 interacts with phospholipids and mediates the targeting of the exocyst to the plasma membrane. *EMBO Journal* **26,** 4053–4065.

Heilmann M, Heilmann I. 2014. Plant phosphoinositides-complex networks controlling growth and adaptation. *Biochimica et Biophysica Acta* doi: 10.1016/j.bbalip.2014.1009.1018 (in press).

Helling D, Possart A, Cottier S, Klahre U, Kost B. 2006. Pollen tube tip growth depends on plasma membrane polarization mediated by tobacco PLC3 activity and endocytic membrane recycling. *The Plant Cell* **18,** 3519–3534.

Ingólfsson HI, Lopez CA, Uusitalo JJ, de Jong DH, Gopal SM, Periole X, Marrink SJ. 2014*a*. The power of coarse graining in biomolecular simulations. *Wiley Interdisciplinary Reviews: Computational Molecular Science* **4,** 225–248.

Ingólfsson HI, Melo MN, van Eerden FJ, Arnarez C, Lopez CA, Wassenaar TA, Periole X, de Vries AH, Tieleman DP, Marrink SJ. 2014*b*. Lipid organization of the plasma membrane. *Journal of the American Chemical Society* **136,** 14554–14559.

Ischebeck T, Stenzel I, Heilmann I. 2008. Type B phosphatidylinositol-4-phosphate 5-kinases mediate Arabidopsis and *Nicotiana tabacum* pollen tube growth by regulating apical pectin secretion. *The Plant Cell* **20,** 3312–3330.

Ischebeck T, Stenzel I, Hempel F, Jin X, Mosblech A, Heilmann I. 2011. Phosphatidylinositol-4,5-bisphosphate influences Nt-Rac5-mediated cell expansion in pollen tubes of *Nicotiana tabacum*. *The Plant Journal* **65,** 453–468.

Ischebeck T, Vu LH, Jin X, Stenzel I, Löfke C, Heilmann I. 2010. Functional cooperativity of enzymes of phosphoinositide conversion according to synergistic effects on pectin secretion in tobacco pollen tubes. *Molecular Plant* **3,** 870–881.

Ischebeck T, Werner S, Krishnamoorthy P, *et al*. 2013. Phosphatidylinositol 4,5-bisphosphate influences PIN polarization by controlling clathrin-mediated membrane trafficking in *Arabidopsis*. *The Plant Cell* **25,** 4894–4911.

Janková Drdová E, Synek L, Pečenková T, Hála M, Kulich I, Fowler JE, Murphy AS, Žárský V. 2013. The exocyst complex contributes to PIN auxin efflux carrier recycling and polar auxin transport in Arabidopsis. *The Plant Journal* **73,** 709–719.

Janosi L, Gorfe A. 2010. Importance of the sphingosine base double-bond geometry for the structural and thermodynamic properties of sphingomyelin bilayers. *Biophysical Journal* **99,** 2957–2966.

Jarsch IK, Konrad SS, Stratil TF, Urbanus SL, Szymanski W, Braun P, Braun KH, Ott T. 2014. Plasma membranes are subcompartmentalized into a plethora of coexisting and diverse microdomains in *Arabidopsis* and *Nicotiana benthamiana*. *The Plant Cell* **26,** 1698–1711.

Jefferys E, Sansom MS, Fowler PW. 2014. NRas slows the rate at which a model lipid bilayer phase separates. *Faraday Discussions* **169,** 209–223.

Julkowska MM, Rankenberg JM, Testerink C. 2013. Liposome-binding assays to assess specificity and affinity of phospholipid-protein interactions. *Methods in Molecular Biology* **1009,** 261–271.

Kalli AC, Morgan G, Sansom MS. 2013. Interactions of the auxilin-1 PTEN-like domain with model membranes result in nanoclustering of phosphatidyl inositol phosphates. *Biophysical Journal* **105,** 137–145.

Kleine-Vehn J, Wabnik K, Martinière A, *et al*. 2011. Recycling, clustering, and endocytosis jointly maintain PIN auxin carrier polarity at the plasma membrane. *Molecular Systems Biology* **7,** 540.

Komis G, Mistrik M, Šamajová O, Doskočilová A, Ovečka M, Illés P, Bartek J, Šamaj J. 2014. Dynamics and organization of cortical microtubules as revealed by superresolution structured illumination microscopy. *Plant Physiology* **165,** 129–148.

Konopka CA, Backues SK, Bednarek SY. 2008. Dynamics of *Arabidopsis* dynamin-related protein 1C and a clathrin light chain at the plasma membrane. *The Plant Cell* **20,** 1363–1380.

Konopka CA, Bednarek SY. 2008. Comparison of the dynamics and functional redundancy of the Arabidopsis dynamin-related isoforms DRP1A and DRP1C during plant development. *Plant Physiology* **147,** 1590–1602.

Konrad SS, Popp C, Stratil TF, Jarsch IK, Thallmair V, Folgmann J, Marín M, Ott T. 2014. *S*-Acylation anchors remorin proteins to the plasma membrane but does not primarily determine their localization in membrane microdomains. *New Phytologist* **203,** 758–769.

Kooijman EE, Tieleman DP, Testerink C, Munnik T, Rijkers DTS, Burger KNJ, de Kruijff B. 2007. An electrostatic/hydrogen bond switch as the basis for the specific interaction of phosphatidic acid with proteins. *Journal of Biological Chemistry* **282,** 11356–11364.

Kusano H, Testerink C, Vermeer JEM, Tsuge T, Shimada H, Oka A, Munnik T, Aoyama T. 2008. The *Arabidopsis* phosphatidylinositol phosphate 5-kinase PIP5K3 is a key regulator of root hair tip growth. *The Plant Cell* **20,** 367–380.

Li G, Xue HW. 2007. *Arabidopsis PLDζ2* regulates vesicle trafficking and is required for auxin response. *The Plant Cell* **19,** 281–295.

Li H, Cao Z, Zhang Y, Lau C, Lu J. 2011. Simultaneous detection of two lung cancer biomarkers using dual-color fluorescence quantum dots. *Analyst* **136,** 1399–1405.

Li R, Liu P, Wan Y, *et al*. 2012. A membrane microdomain-associated protein, *Arabidopsis* Flot1, is involved in a clathrin-independent endocytic pathway and is required for seedling development. *The Plant Cell* **24,** 2105–2122.

Li X, Wang X, Yang Y, Li R, He Q, Fang X, Luu DT, Maurel C, Lin J. 2011. Single-molecule analysis of PIP2;1 dynamics and partitioning reveals multiple modes of *Arabidopsis* plasma membrane aquaporin regulation. *The Plant Cell* **23,** 3780–3797.

Li Z, Janosi L, Gorfe AA. 2012. Formation and domain partitioning of H-ras peptide nanoclusters: effects of peptide concentration and lipid composition. *Journal of the American Chemical Society* **134,** 17278–17285.

Lim Z-Y, Thuring JW, Holmes AB, Manifava M, Ktistakis NT. 2002. Synthesis and biological evaluation of a PtdIns(4,5)P_2 and a phosphatidic acid affinity matrix. *Journal of the Chemical Society, Perkin Transactions* **1,** 1067–1075.

Liu J, Zuo X, Yue P, Guo W. 2007. Phosphatidylinositol 4,5-bisphosphate mediates the targeting of the exocyst to the plasma membrane for exocytosis in mammalian cells. *Molecular Biology of the Cell* **18,** 4483–4492.

Liu P, Li R-L, Zhang L, Wang Q-L, Niehaus K, Baluška F, Šamaj J, Lin J-X. 2009. Lipid microdomain polarization is required for NADPH oxidase-dependent ROS signaling in *Picea meyeri* pollen tube tip growth. *The Plant Journal* **60,** 303–313.

Liu Y, Su Y, Wang X. 2013. Phosphatidic acid-mediated signaling. In: Capelluto DGS, ed. *Lipid-mediated protein signaling* . Dordrecht: Springer, 159–176.

Manna M, Róg T, Vattulainen I. 2014. The challenges of understanding glycolipid functions: an open outlook based on molecular simulations. *Biochimica et Biophysica Acta* **1841,** 1130–1145.

Markham JE, Molino D, Gissot L, Bellec Y, Hématy K, Marion J, Belcram K, Palauqui JC, Satiat-JeuneMaître B, Faure JD. 2011. Sphingolipids containing very-long-chain fatty acids define a secretory pathway for specific polar plasma membrane protein targeting in *Arabidopsis*. *The Plant Cell* **23,** 2362–2378.

Marrink SJ, Risselada HJ, Yefimov S, Tieleman DP, de Vries AH. 2007. The MARTINI force field: coarse grained model for biomolecular simulations. *Journal of Physical Chemistry B* **111,** 7812–7824.

Martin TFJ. 2014. PI(4,5)P_2-binding effector proteins for vesicle exocytosis. *Biochimica et Biophysica Acta* doi: 10.1016/j.bbalip.2014.1009.1017 (in press),

Martinière A, Lavagi I, Nageswaran G, *et al*. 2012. Cell wall constrains lateral diffusion of plant plasma-membrane proteins. *Proceedings of the National Academy of Sciences, USA* **109,** 12805–12810.

McLoughlin F, Arisz SA, Dekker HL, Kramer G, de Koster CG, Haring MA, Munnik T, Testerink C. 2013. Identification of novel candidate phosphatidic acid-binding proteins involved in the salt-stress response of *Arabidopsis thaliana* roots. *Biochemical Journal* **450,** 573–581.

Meder D, Moreno MJ, Verkade P, Vaz WLC, Simons K. 2006. Phase coexistence and connectivity in the apical membrane of polarized epithelial cells. *Proceedings of the National Academy of Sciences, USA* **103,** 329–334.

Mei Y, Jia WJ, Chu YJ, Xue HW. 2012. *Arabidopsis* phosphatidylinositol monophosphate 5-kinase 2 is involved in root gravitropism through regulation of polar auxin transport by affecting the cycling of PIN proteins. *Cell Research* **22,** 581–597.

Meijer HJG, Munnik T. 2003. Phospholipid-based signaling in plants. *Annual Review of Plant Biology* **54,** 265–306.

Men S, Boutté Y, Ikeda Y, Li X, Palme K, Stierhof Y-D, Hartmann M-A, Moritz T, Grebe M. 2008. Sterol-dependent endocytosis mediates post-cytokinetic acquisition of PIN2 auxin efflux carrier polarity. *Nature Cell Biology* **10,** 237–244.

Molino D, Van der Giessen E, Gissot L, *et al*. 2014. Inhibition of very long acyl chain sphingolipid synthesis modifies membrane dynamics during plant cytokinesis. *Biochimica et Biophysica Acta* **1841,** 1422–1430.

Monteiro D, Liu Q, Lisboa S, Scherer GEF, Quader H, Malhó R. 2005. Phosphoinositides and phosphatidic acid regulate pollen tube growth and reorientation through modulation of $[Ca^{2+}]_c$ and membrane secretion. *Journal of Experimental Botany* **56,** 1665–1674.

Moravcevic K, Oxley CL, Lemmon MA. 2012. Conditional peripheral membrane proteins: facing up to limited specificity. *Structure* **20,** 15–27.

Munnik T, Wierzchowiecka M. 2013. Lipid-binding analysis using a fat blot assay. *Methods in Molecular Biology* **1009,** 253–259.

Nicolson GL. 2014. The Fluid-Mosaic Model of Membrane structure: still relevant to understanding the structure, function and dynamics of biological membranes after more than 40 years. *Biochimica et Biophysica Acta* **1838,** 1451–1466.

Nováková P, Hirsch S, Feraru E, *et al*. 2014. SAC phosphoinositide phosphatases at the tonoplast mediate vacuolar function in *Arabidopsis*. *Proceedings of the National Academy of Sciences, USA* **111,** 2818–2823.

Ovečka M, Berson T, Beck M, Derksen J, Šamaj J, Baluška F, Lichtscheidl IK. 2010. Structural sterols are involved in both the initiation and tip growth of root hairs in *Arabidopsis thaliana*. *The Plant Cell* **22,** 2999–3019.

Owen DM, Gaus K. 2013. Imaging lipid domains in cell membranes: the advent of super-resolution fluorescence microscopy. *Frontiers in Plant Science* **4,** 503.

Pejchar P, Potocký M, Novotná Z, Veselková Š, Kocourková D, Valentová O, Schwarzerová K, Martinec J. 2010. Aluminium ions inhibit formation of diacylglycerol generated by phosphatidylcholine-hydrolysing phospholipase C in tobacco cells. *New Phytologist* **188,** 150–160.

Pejchar P, Potocký M, Krčková Z, Brouzdová J, Daněk M, Martinec J. 2015. Non-specific phospholipase C4 mediates response to aluminum toxicity in Arabidopsis thaliana. *Frontiers in Plant Science* **6**, 66, doi: 10.3389/fpls.2015.00066.

Perlmutter JD, Sachs JN. 2011. Interleaflet interaction and asymmetry in phase separated lipid bilayers: molecular dynamics simulations. *Journal of the American Chemical Society* **133,** 6563–6577.

Pinot M, Vanni S, Pagnotta S, Lacas-Gervais S, Payet LA, Ferreira T, Gautier R, Goud B, Antonny B, Barelli H. 2014. Polyunsaturated phospholipids facilitate membrane deformation and fission by endocytic proteins. *Science* **345,** 693–697.

Pleskot R, Li J, Žárský V, Potocký M, Staiger CJ. 2013. Regulation of cytoskeletal dynamics by phospholipase D and phosphatidic acid. *Trends in Plant Science* **18,** 496–504.

Pleskot R, Pejchar P, Bezvoda R, Lichtscheidl IK, Wolters-Arts M, Marc J, Žárský V, Potocký M. 2012*a*. Turnover of phosphatidic acid through distinct signalling pathways affects multiple aspects of tobacco pollen tube tip growth. *Frontiers in Plant Science* **3,** 54, doi: 10.3389/fpls.2012.00054.

Pleskot R, Pejchar P, Staiger CJ, Potocký M. 2014. When fat is not bad: the regulation of actin dynamics by phospholipid signaling molecules. *Frontiers in Plant Science* **5,** 5, doi: 10.3389/fpls.2014.00005.

Pleskot R, Pejchar P, Žárský V, Staiger CJ, Potocký M. 2012*b*. Structural insights into the inhibition of actin-capping protein by interactions with phosphatidic acid and phosphatidylinositol (4,5)-bisphosphate. *PLoS Computational Biology* **8,** e1002765.

Potocký M, Eliáš M, Profotová B, Novotná Z, Valentová O, Žárský V. 2003. Phosphatidic acid produced by phospholipase D is required for tobacco pollen tube growth. *Planta* **217,** 122–130.

Potocký M, Pleskot R, Pejchar P, Vitale N, Kost B, Žárský V. 2014. Live-cell imaging of phosphatidic acid dynamics in pollen tubes visualized by Spo20p-derived biosensor. *New Phytologist* **203,** 483–494.

Preuss ML, Schmitz AJ, Thole JM, Bonner HK, Otegui MS, Nielsen E. 2006. A role for the RabA4b effector protein PI-4Kβ1 in polarized expansion of root hair cells in *Arabidopsis thaliana*. *Journal of Cell Biology* **172,** 991–998.

Raffaele S, Bayer E, Lafarge D, *et al*. 2009. Remorin, a Solanaceae protein resident in membrane rafts and plasmodesmata, impairs *Potato virus X* movement. *The Plant Cell* **21,** 1541–1555.

Risselada HJ, Marrink SJ. 2008. The molecular face of lipid rafts in model membranes. *Proceedings of the National Academy of Sciences, USA* **105,** 17367–17372.

Roppolo D, De Rybel B, Tendon VD, Pfister A, Alassimone J, Vermeer JEM, Yamazaki M, Stierhof Y-D, Beeckman T, Geldner N. 2010. A novel protein family mediates Casparian strip formation in the endodermis. *Nature* **473,** 380–383.

Schäfer LV, Marrink SJ. 2010. Partitioning of lipids at domain boundaries in model membranes. *Biophysical Journal* **99,** L91–L93.

Simon MLA, Platre MP, Assil S, van Wijk R, Chen WY, Chory J, Dreux M, Munnik T, Jaillais Y. 2014. A multi-colour/multi-affinity marker set to visualize phosphoinositide dynamics in Arabidopsis. *The Plant Journal* **77,** 322–337.

Sorek N, Segev O, Gutman O, *et al*. 2010. An *S*-acylation switch of conserved G domain cysteines is required for polarity signaling by ROP GTPases. *Current Biology* **20,** 914–920.

Sousa E, Kost B, Malhó R. 2008. *Arabidopsis* phosphatidylinositol-4-monophosphate 5-kinase 4 regulates pollen tube growth and polarity by modulating membrane recycling. *The Plant Cell* **20,** 3050–3064.

Spira F, Mueller NS, Beck G, von Olshausen P, Beig J, Wedlich-Söldner R. 2012. Patchwork organization of the yeast plasma membrane into numerous coexisting domains. *Nature Cell Biology* **14,** 640–648.

Stansfeld PJ, Sansom MS. 2011. Molecular simulation approaches to membrane proteins. *Structure* **19,** 1562–1572.

Stenzel I, Ischebeck T, König S, Hołubowska A, Sporysz M, Hause B, Heilmann I. 2008. The type B phosphatidylinositol-4-phosphate 5-kinase 3 is essential for root hair formation in *Arabidopsis thaliana*. *Plant Cell* **10,** 124–141.

Stenzel I, Ischebeck T, Quint M, Heilmann I. 2012. Variable regions of PI4P 5-kinases direct PtdIns(4,5)P_2 towards alternative regulatory functions in tobacco pollen tubes. *Frontiers in Plant Science* **2,** 114.

Tejos R, Sauer M, Vanneste S, *et al*. 2014. Bipolar plasma membrane distribution of phosphoinositides and their requirement for auxin-mediated cell polarity and patterning in *Arabidopsis*. *The Plant Cell* **26,** 2114–2128.

Testerink C, Munnik T. 2011. Molecular, cellular, and physiological responses to phosphatidic acid formation in plants. *Journal of Experimental Botany* **62,** 2349–2361.

Thole JM, Nielsen E. 2008. Phosphoinositides in plants: novel functions in membrane trafficking. *Current Opinion in Plant Biology* **11,** 620–631.

Thole JM, Vermeer JEM, Zhang YL, Gadella TWJ, Nielsen E. 2008. *ROOT HAIR DEFECTIVE4* encodes a phosphatidylinositol-4-phosphate phosphatase required for proper root hair development in *Arabidopsis thaliana*. *The Plant Cell* **20,** 381–395.

Van Damme D, Gadeyne A, Vanstraelen M, Inzé D, Van Montagu MCE, De Jaeger G, Russinova E, Geelen D. 2011. Adaptin-like protein TPLATE and clathrin recruitment during plant somatic cytokinesis occurs via two distinct pathways. *Proceedings of the National Academy of Sciences, USA* **108,** 615–620.

van den Bogaart G, Meyenberg K, Risselada HJ, *et al*. 2011. Membrane protein sequestering by ionic protein–lipid interactions. *Nature* **479,** 552–555.

van Leeuwen W, Vermeer JEM, Gadella TWJ, Jr, Munnik T. 2007. Visualization of phosphatidylinositol 4,5-bisphosphate in the plasma membrane of suspension-cultured tobacco BY-2 cells and whole Arabidopsis seedlings. *The Plant Journal* **52,** 1014–1026.

van Rheenen J, Mulugeta Achame E, Janssen H, Calafat J, Jalink K. 2005. PIP_2 signaling in lipid domains: a critical re-evaluation. *EMBO Journal* **24,** 1664–1673.

Vermeer JE, Munnik T. 2013. Using genetically encoded fluorescent reporters to image lipid signalling in living plants. *Methods in Molecular Biology* **1009,** 283–289.

Vermeer JEM, Thole JM, Goedhart J, Nielsen E, Munnik T, Gadella Jr TWJ. 2009. Imaging phosphatidylinositol 4-phosphate dynamics in living plant cells. *The Plant Journal* **57,** 356–372.

Wang Q, Zhao Y, Luo W, Li R, He Q, Fang X, De Michele R, Ast C, von Wirén N, Lin J. 2013. Single-particle analysis reveals shutoff control of the *Arabidopsis* ammonium transporter AMT1;3 by clustering and internalization. *Proceedings of the National Academy of Sciences, USA* **110,** 13204–13209.

Wang Y-H, Slochower DR, Janmey PA. 2014. Counterion-mediated cluster formation by polyphosphoinositides. *Chemistry and Physics of Lipids* **182,** 38–51.

Williams ME, Torabinejad J, Cohick E, Parker K, Drake EJ, Thompson JE, Hortter M, DeWald DB. 2005. Mutations in the Arabidopsis phosphoinositide phosphatase gene *SAC9* lead to overaccumulation of PtdIns(4,5)P_2 and constitutive expression of the stress-response pathway. *Plant Physiology* **138,** 686–700.

Žárský V, Cvrčková F, Potocký M, Hála M. 2009. Exocytosis and cell polarity in plants—exocyst and recycling domains. *New Phytologist* **183,** 255–272.

Zhang X, Orlando K, He B, Xi F, Zhang J, Zajac A, Guo W. 2008. Membrane association and functional regulation of Sec3 by phospholipids and Cdc42. *Journal of Cell Biology* **180,** 145–158.

Zhang Y, Immink R, Liu C-M, Emons AM, Ketelaar T. 2013. The Arabidopsis exocyst subunit SEC3A is essential for embryo development and accumulates in transient puncta at the plasma membrane. *New Phytologist* **199,** 74–88.

Zhao H, Lappalainen P. 2012. A simple guide to biochemical approaches for analyzing protein–lipid interactions. *Molecular Biology of the Cell* **23,** 2823–2830.

Zhao X, Li R, Lu C, Baluška F, Wan Y. 2014. Di-4-ANEPPDHQ, a fluorescent probe for the visualisation of membrane microdomains in living *Arabidopsis thaliana* cells. *Plant Physiology and Biochemistry* **87,** 53–60.

Zhao Y, Liu J, Yang C, *et al*. 2013. Exo70 generates membrane curvature for morphogenesis and cell migration. *Developmental Cell* **26,** 266–278.

Zhao Y, Yan A, Feijó JA, Furutani M, Takenawa T, Hwang I, Fu Y, Yang ZB. 2010. Phosphoinositides regulate clathrin-dependent endocytosis at the tip of pollen tubes in Arabidopsis and tobacco. *The Plant Cell* **22,** 4031–4044.

Zhong R, Burk DH, Morrison III WH, Ye ZH. 2004. *FRAGILE FIBER3*, an Arabidopsis gene encoding a type II inositol polyphosphate 5-phosphatase, is required for secondary wall synthesis and actin organization in fiber cells. *The Plant Cell* **16,** 3242–3259.

frontiers in
PLANT SCIENCE

MINI REVIEW ARTICLE
published: 02 January 2014
doi: 10.3389/fpls.2013.00543

The exocyst at the interface between cytoskeleton and membranes in eukaryotic cells

Lukáš Synek[1], Juraj Sekereš[1,2] and Viktor Žárský[1,2] *

[1] Laboratory of Cell Biology, Institute of Experimental Botany, Academy of Sciences of the Czech Republic, Prague, Czech Republic
[2] Laboratory of Plant Cell Biology, Department of Experimental Plant Biology, Faculty of Science, Charles University in Prague, Prague, Czech Republic

Edited by:
Christopher J. Staiger, Purdue University, USA

Reviewed by:
Andreas Nebenführ, University of Tennessee, USA
Frantisek Baluska, University of Bonn, Germany

***Correspondence:**
Viktor Žárský, Laboratory of Plant Cell Biology, Department of Experimental Plant Biology, Faculty of Science, Charles University in Prague, Vinicna 5, 12844 Prague, Czech Republic
e-mail: zarsky@ueb.cas.cz

Delivery and final fusion of the secretory vesicles with the relevant target membrane are hierarchically organized and reciprocally interconnected multi-step processes involving not only specific protein–protein interactions, but also specific protein–phospholipid interactions. The exocyst was discovered as a tethering complex mediating initial encounter of arriving exocytic vesicles with the plasma membrane. The exocyst complex is regulated by Rab and Rho small GTPases, resulting in docking of exocytic vesicles to the plasma membrane (PM) and finally their fusion mediated by specific SNARE complexes. In model Opisthokont cells, the exocyst was shown to directly interact with both microtubule and microfilament cytoskeleton and related motor proteins as well as with the PM via phosphatidylinositol 4,5-bisphosphate specific binding, which directly affects cortical cytoskeleton and PM dynamics. Here we summarize the current knowledge on exocyst-cytoskeleton-PM interactions in order to open a perspective for future research in this area in plant cells.

Keywords: exocyst, actin cytoskeleton, microtubule cytoskeleton, phospholipids, myosin, small GTPases, Exo70, secretion

THE EXOCYST AS A REGULATORY HUB IN THE ACTIVE CELL CORTEX

Polarized surface growth in eukaryotic cells involves interactions between the cytoskeleton and membrane transport pathways. The last steps of the secretory pathway taking place in the vicinity of the plasma membrane (PM) are regulated by an array of small GTPases, the exocyst tethering complex, and SNARE proteins. The exocyst is a protein complex comprising eight subunits (Sec3, Sec5, Sec6, Sec8, Sec10, Sec15, Exo70, and Exo84) engaged in docking and tethering of secretory vesicles, providing a spatial and temporal regulation of exocytosis (Hsu et al., 1996; TerBush et al., 1996) and interacting directly or indirectly with membranes, cytoskeletal proteins, as well as with small GTPases from the Rab, Ral, and Rho subfamilies and many other proteins in the cell cortex (Wu et al., 2008). As such, the exocyst seems to act as an integrating hub in the cell cortex, mainly in the context of exocytosis. In general, proper exocyst function is essential for polar growth and cell morphogenesis, including invadopodia, lamellipodia, and neuronal dendrites formation in animal cells, bud growth in budding yeast, and cytokinesis in fission yeast (reviewed in Heider and Munson, 2012; Vaškovičová et al., 2013; **Figure 1**). A growing number of papers document functions of the plant exocyst in similar processes with high demand for exocytosis, including root hair growth, hypocotyl cell elongation, cytokinesis, seed coat formation and papilla formation after a pathogen attack in plants (Synek et al., 2006; Hála et al., 2008; Fendrych et al., 2010; Kulich et al., 2010; Pecenkova et al., 2011; Vaškovičová et al., 2013).

THE EXOCYST AND ACTIN CYTOSKELETON

Deep insight into exocyst functions and their mechanisms came from genetic studies on budding yeast, where the exocyst was originally discovered as a protein complex (Novick et al., 1980; TerBush et al., 1996). In budding yeast cells, secretory vesicles are transported along formin- and Arp2/3-generated actin cables. A common model of the exocyst action suggests that most exocyst subunits arrive to the PM in association with secretory vesicles and cannot localize properly after disruption of the actin cytoskeleton (Boyd et al., 2004; Bendezú et al., 2012). However, Sec3p and part of the Exo70p population can reach its destination, a newly forming bud, independently of the actin cytoskeleton probably via direct association with Rho GTPases (Boyd et al., 2004). Therefore, Sec3p and Exo70p are supposed to act as landmarks of sites for the exocyst localization and action (Finger et al., 1998; Boyd et al., 2004).

Mutations in several exocytosis-related genes cause actin cytoskeleton defects in budding yeast, leading subsequently to impaired cell growth and morphogenesis and also to an mRNA transport and polarization defect that is actin-dependent (Aronov and Gerst, 2004). The identified genes included those encoding *SEC10* and *SEC15* exocyst components and *CDC42* and *RHO3* GTPases regulating the exocyst polar targeting (Wu et al., 2008).

An interesting reciprocal relationship was observed during cell wounding response, where Sec3p and the Bni1p formin are degraded in order to eliminate competition for secretory vesicles required to repair the damaged membrane and cell wall, which are arriving along the pre-polarized cytoskeleton directing current polarized growth. The Bnr1p formin and the Exo70p exocyst subunit relocalize to the damage site followed by redistribution of the Myo2p myosin and delivery of new material (Kono et al., 2012).

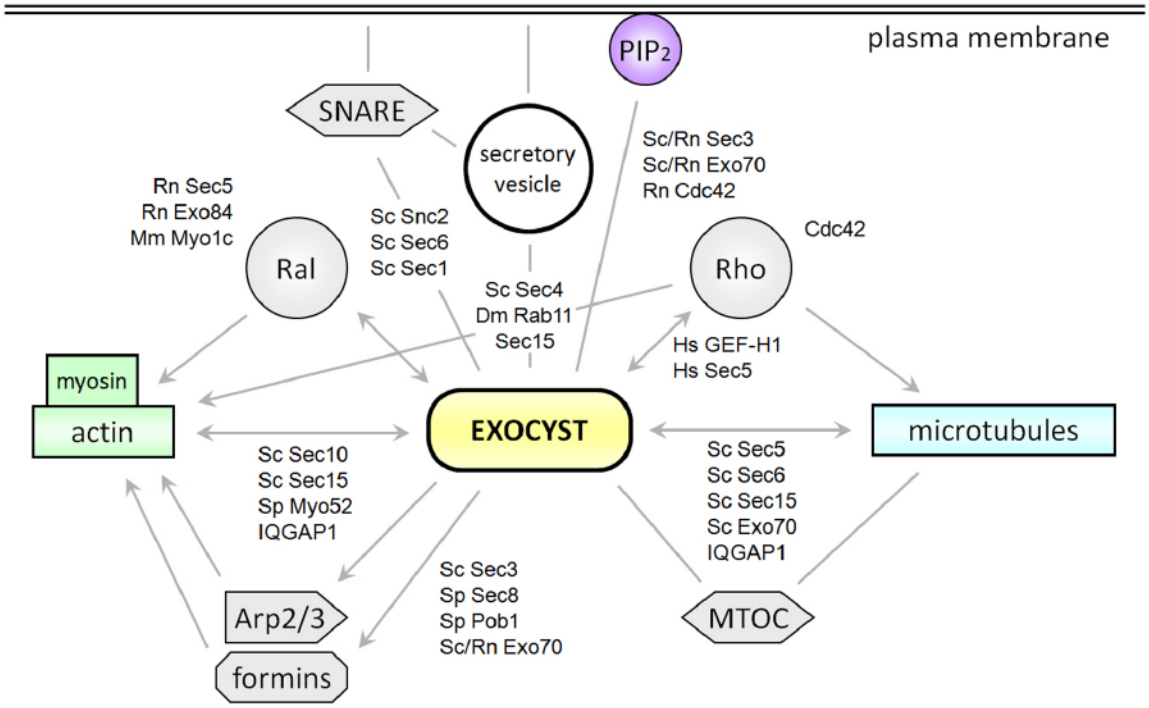

FIGURE 1 | Interactions of the exocyst complex with the cytoskeleton, plasma membrane, and associated proteins. Scheme of exocyst interactions described in the text, including the key players Ral and Rho GTPases, SNARE proteins, formins, and the Arp2/3 actin-nucleating complex, microtule-organizing center (MTOC) and phosphatidylinositol 4,5-bisphosphate (PIP_2) at the plasma membrane. Dm, *Drosophila melanogaster*; Mm, *Mus musculus*; Hs, *Homo sapiens* Rn, *Ratus norwegicus*; Sc, *Saccharomyces cerevisiae*; Sp, *Schizosaccharomyces pombe*.

In budding yeast, cell polarity and polarized exocytosis is coordinated also by the Rho3p GTPase (Adamo et al., 1999), which can regulate both actin polarity and transport of exocytic vesicles from mother cell to the bud, as well as vesicle docking to the PM. While the Rho3p vesicle delivery function is mediated by Myo2p, the docking requires Exo70p (Adamo et al., 1999).

In the fission yeast *Schizosaccharomyces pombe*, the actin cytoskeleton is dispensable for proper exocyst localization and polarized growth (Bendezú and Martin, 2011; Snaith et al., 2011). While actin-independent polar transport in budding yeasts might be constrained by the narrow bud neck, and bud growth requires motor-driven transport along actin cables, the open cylindrical shape of fission yeast cells may allow actin-independent vesicle transport (Bendezú and Martin, 2011). However, the exocyst and actin cytoskeleton share at least two common upstream regulators – Cdc42 (Estravís et al., 2011) and Pob1 (Nakano et al., 2011).

The polar exocyst localization and formation of actin cables are dependent on and mutually coupled by Pob1 via its interaction with the For3 formin and the Sec8 exocyst subunit, respectively. Simultaneous deletion of For3 and Sec8 results in isotropic growth, indicating a functional redundancy between microfilaments and the exocyst in cell polarization (Bendezú and Martin, 2011). In contrast, although unable to divide properly, *sec8 exo70* and *sec6 sec8* double mutants are still capable of polarized growth (Bendezú and Martin, 2011).

Although all fission yeast exocyst subunits can localize to cell poles largely independently of the actin cytoskeleton, at least Sec3, Sec5, and Exo70 (most probably as a part of the complete exocyst complex) are more efficiently transported to the cell apex by the Myo52 myosin V along microfilaments (Snaith et al., 2011; Bendezú et al., 2012). Either functional Sec3 or Exo70 is essential for viability and proper localization of other exocyst subunits, suggesting that, as in budding yeast, these two components act as exocyst tethers at the PM (Bendezú et al., 2012). A polarization pathway involving the exocyst relocalization and actin repolarization downstream of Cdc42 also participates in fission yeast mating (Bendezú and Martin, 2013).

Unexpectedly, the fission yeast Sec3 not only acts in exocytosis but also marks sites for actin recruitment and controls overall actin organization via direct binding of For3 (Jourdain et al., 2012). Mutants in Sec3 exhibit lack of microfilaments, depolarized actin patches, and disassembly of the cytokinetic actomyosin ring probably due to a failure in polarization of the For3 formin.

The Exo70 exocyst subunit also interacts both *in vitro* and *in vivo* with the yeast and rat Arpc1/Arc40 subunit of the Arp2/3 complex, a key regulator of actin polymerization. Inhibition of the Exo70 function in rat kidney cells blocks formation of actin-based membrane protrusions and affects cell migration (Zuo et al., 2006), pointing to yet unknown capacity of Exo70 to regulate the actin organization and coordinating thus actin cytoskeleton with membrane trafficking during cell migration. Exo70 was recently shown to promote Arp2/3-driven microfilament nucleation and branching (Liu et al., 2012). Because both the

exocyst and Arp2/3 complexes are well conserved across eukaryotes, including plants, their interaction is likely to be conserved as well.

In mammalian cells, actin organization, as well as membrane trafficking, cell growth and differentiation, is regulated by RalA and RalB, ubiquitous small GTPases from the Ras superfamily (Feig et al., 1996). Activated (GTP-bound) RalA forms a stable complex with the exocyst via binding to Sec5 (Brymora et al., 2001; Sugihara et al., 2002; Fukai et al., 2003) and Exo84 (Moskalenko et al., 2003; Jin et al., 2005) exocyst subunits in human and rat cells. Specific inhibition of the Sec5 activity blocks filopodia formation in 3T3 cells, a dynamic process that is highly dependent on actin reorganization and that can be normally induced by RalA or cytokines via Cdc42 (Sugihara et al., 2002). This inhibitory effect could not be attributed to disrupted secretion, since inhibition of secretion by brefeldin A did not affect filopodia formation (Sugihara et al., 2002), indicating that the exocyst-RalA complex may regulate actin reorganization independently of vesicle transport. Both RalA-Sec5 and RalA-Exo84 interactions are necessary for proper regulation of the actin cytoskeleton dynamics, as documented by different morphological consequences of uncoupling these interactions in PC-3 cells, such as defects in lamellipodia formation, rounder cells or extended spindles (Hazelett and Yeaman, 2012). RalA also interacts with the actin cytoskeleton via Myo1c, suggesting its function as a cargo receptor for the Myo1c motor (Chen et al., 2007). Taken together, the exocyst complex as an immediate effector of RalA obviously integrates the secretory pathway and actin cytoskeleton near the PM in mammalian cells (**Figure 1**).

Cells of mouse oocytes can use secretory (Rab11-positive) vesicles associated with the exocyst components via the Rab11–Sec15 interaction (Wu et al., 2005) as adaptable, motorized network nodes regulating the dynamics and density of microfilaments in a myosin Vb-dependent manner (Holubcová et al., 2013). Such an actin modulation is essential for asymmetric positioning of the meiotic spindle and thus for the development of a fertilizable egg in mammals.

Although we can find no dynamic membrane protrusions analogous to filopodia in plant cells, fine F-actin meshwork is essential for polar growth of root hairs, pollen tubes, or stigmatic papillae and this type of growth demanding precise regulation of exocytosis is also strongly dependent on the exocyst function (Yalovsky et al., 2008; Vaškovičová et al., 2013).

Ral GTPases are specific to animals – in plant cells, as in yeast, only homologs to Rho GTPases (called also Rac in animals) are present and due to some plant specific features they are called Rop (Rho of plant). Rop GTPases were clearly implied in the cortical cytoskeleton regulation mostly possibly via plant specific Rop-interacting adaptors (RICs; Fu et al., 2001; Yalovsky et al., 2008). Very significant for the speculations on plant exocyst-cytoskeleton links is a dominant land-plant specific way of Rop activation mediated by specific PRONE-GEF (plant-specific ROP nucleotide exchanger – GDP/GTP exchange factor) regulated by interacting receptor-like kinases (RLKs) that allow for very efficient cortical activation of Rop GTPases in response to plethora of different stimuli including changes in cell wall mechanics (Mucha et al., 2011). Moreover, the first Rop-exocyst interaction observed in plants is not direct – several GTP-bound Rops interact with the Sec3 exocyst subunit in *Arabidopsis* via a plant specific adaptor protein ICR1 which is implied in the regulation of auxin polar transport (Lavy et al., 2007; Hazak et al., 2010; see further). These features along with plant specific transmembrane anchorage of plant F-actin nucleating formins (Cvrčková, 2013; in this issue) indicate that the cortical wiring between actin cytoskeleton and exocytosis in plants will be quite specific.

THE EXOCYST AND TUBULIN CYTOSKELETON

Microtubules are not essential for exocytosis in budding yeast and no functional link with the exocyst complex has been documented so far (Hammer and Sellers, 2012). In rat kidney cells, however, Exo70 co-localizes with microtubules and the mitotic spindle, and *in vitro*, the exocyst complex reconstituted from recombinant subunits inhibits tubulin polymerization. However, deletions of any of Sec5, Sec6, Sec15, or Exo70 exocyst subunits diminished the inhibition activity. Surprisingly, Exo70 itself could inhibit tubulin polymerization, albeit the exocyst complex lacking the Exo70 subunit did not lose its activity completely. On the other hand, when Exo70 was overexpressed, the microtubule network became disrupted and filopodia-like PM protrusions were formed (Wang et al., 2004).

The protrusion formation is consistent with an observation in *Xenopus* neurons, where a local disassembly of microtubules by focal application of nocodazole induced an addition of a new membrane material at the affected site (Zakharenko and Popov, 1998).

In undifferentiated PC12 neuronal cells, the exocyst complex is associated with microtubules as well as microtubule organizing centers and can be co-immunoprecipitated with microtubules from the total rat brain lysate (Vega and Hsu, 2001). However, upon activation of neuronal differentiation, the exocyst redistributes from perinuclear localization to the growing neurite characterized by high exocytic activity at the PM. The subcellular exocyst localization was affected by treatment with microtubule-disrupting drugs, but not actin-disrupting drugs. These results support a possibility that the exocyst complex acts as a modulator of microtubules to mediate vesicle targeting in animal cells.

It is expected that also in respect to microtubular cytoskeleton-secretory pathway relationship the plant cells will have specific features due to the obvious dependence of the final steps of exocytosis and membrane recycling in plants on the actin cytoskeleton and very possibly exocytosis permissive feature of even dense cortical microtubuli (see below). However, both cytoskeletal systems in plant cells strongly interact (e.g., via specific actin nucleating formins) so that in the real biological context it will be challenging to separate their functions.

INTERPLAY BETWEEN THE EXOCYST AND BOTH TYPES OF CYTOSKELETON

In contrast to budding yeast, typical vertebral cells use microtubules for long-range cargo transport and microfilaments for short-range transport in cell cortex during later steps of vesicles traffic (Hammer and Sellers, 2012). Several studies pinpoint the potential importance of the exocyst in transition of cargo from microtubules to microfilaments.

Mammalian cell migration involves cooperative reorganization of the actin and microtubule cytoskeletons under the control of Rho GTPases (de Curtis and Meldolesi, 2012). Proper localization and activity of the exocyst is promoted by microtubule-associated GEF-H1, a GTP exchange factor for the RhoA actin activator, in HeLa cells (Pathak et al., 2012). Microtubule depolymerization results in the activation of GEF-H1, which further activates RhoA (Krendel et al., 2002). Importance of this regulation was documented experimentally on the cleavage furrow formation during cytokinesis (Birkenfeld et al., 2007) and on actin dynamics during cell migration (Nalbant et al., 2009). The depletion of GEF-H1 led to accumulation of Rab11-positive secretory vesicles within the cells and to mislocalization of Exo70 and Sec8 exocyst subunits (Pathak et al., 2012). GEF-H1 also directly binds the Sec5 exocyst subunit in a RalA GTPase-dependent manner; the interaction is stronger with free GEF-H1 than with its microtubule associated form (Pathak et al., 2012). The Sec5-GEF-H1 interaction promotes RhoA activation, which then regulates exocyst localization and possibly its assembly, as well as actin polymerization. Exocyst thus first helps to activate RhoA, which subsequently assists functioning of the exocyst, resulting in a positive feedback (Pathak et al., 2012).

Interestingly, despite the different mechanisms of cytokinesis between plants and animals/fission yeast (contraction versus building of a cell plate), the exocyst is involved in both types of cytokinesis (Fendrych et al., 2010).

IQGAP1 is another important regulator of both actin and microtubular cytoskeleton associated with the exocyst. The active RhoA and Cdc42 trigger association of Sec3 and Sec8 exocyst subunits with IQGAP1. This interaction is essential for MT1-MMP protease localization at invadopodia and thus for proper invadopodia functioning (Sakurai-Yageta et al., 2008). IQGAP1 stimulates actin bundling (White et al., 2012) and directly interacts with microtubule plus end binding protein CLIP-170 in neurons (Swiech et al., 2011).

EXOCYST INTERACTION WITH CELLULAR MEMBRANES

As mentioned earlier, in budding yeast, Sec3p and part of Exo70p population can reach newly forming bud also independently of microfilaments (Boyd et al., 2004). They bind the PM directly via phospholipid phosphatidylinositol 4,5-bisphosphate (PIP_2) and indirectly by association with Rho GTPases (He et al., 2007; Zhang et al., 2008; Wu et al., 2010; **Figure 1**). Sec15p binds to the membrane of secretory vesicles via the Sec4p Rab GTPase (Guo et al., 1999) and Sec6p binds Snc2p, a vesicle-associated SNARE protein (Shen et al., 2013). Sec6p also contributes to anchor the exocyst complex at sites of secretion – possibly via interaction with PM-associated proteins (Songer and Munson, 2009). Besides facilitating exocytosis by interactions with Sec9p, a Qbc exocytic t-SNARE protein (Sivaram et al., 2005), and with Sec1, a protein from the Sec1/Munc18 family regulating SNARE functions (Morgera et al., 2012), the exocyst also interacts with the vesicles transporting myosin Myo2p (also a known Sec4p interactor) via the Sec15p subunit that directly binds the motor and allows for its release after vesicle tethering (Jin et al., 2011; Donovan and Bretscher, 2012).

In fission yeast, Sec6 and Sec8 exocyst subunits localize to cell tips largely independent of the actin cytoskeleton, but in a Cdc42 and PIP_2-dependent manner. Thus, the fission yeast long-range cytoskeletal transport and PIP_2-dependent exocyst represent parallel morphogenetic modules downstream of Cdc42, raising the possibility of similar mechanisms in other organisms (Bendezú and Martin, 2013). Bendezú et al. (2012) showed that Sec3 and Exo70 tether the exocyst complex arriving with secretory vesicles by direct binding to PIP_2 and Rho GTPases at the cell poles. In absence of the Myo52 motor protein, vesicles with the entire exocyst can still reach the cell pole by random movement, but less efficiently. In absence of both Sec3 and Exo70, vesicles and the rest of the exocyst fail in delivery and tethering and form aggregates. Also in plants Sec3 subunit of exocyst interacts with membrane lipids (Bloch et al., in preparation).

Very recently Zhao et al. (2013) discovered that Exo70 alone, through an oligomerization-based manner, can generate membrane curvatures *in vitro* independent of the exocyst function. This represents a mechanism creating protrusions even in the absence of actin, albeit it is not clear to what extent stimulated actin polymerization, membrane delivery, and membrane deformation contribute to cell shape changes *in vivo* including formation of membrane protrusions. Thus, Exo70 as a membrane-bending protein may couple the actin dynamics and PM remodeling in morphogenesis.

The exocyst is also essential for large-particle phagocytosis (Mohammadi and Isberg, 2013), Salmonella invasion into host cells (Nichols and Casanova, 2010) and formation of tunneling nanotubes – recently discovered structures connecting cytoplasm of animal cells (Ohno et al., 2010; Mukerji et al., 2012; Schiller et al., 2013). Each of these events could combine all three mechanisms mentioned above. Membrane-deforming ability of Exo70 could function well beyond the cell cortex-associated events, since the exocyst participates in many cellular processes (reviewed in Heider and Munson, 2012; Liu and Guo, 2012).

PERSPECTIVES ON THE EXOCYST–CYTOSKELETON INTERFACE IN ENDOMEMBRANE BIOGENESIS IN PLANTS

Regulation of the cytoskeleton structure and dynamics in plant cells is very much affected by the cell wall, implying close proximity between secretory pathway, cell wall biogenesis and cortical cytoskeleton. These cellular systems are regulated by small GTPases, especially from the ARF, RAB, and ROP families, major regulators of the cell polarity and morphogenesis closely related to their fungal or animal counterparts (Vaškovičová et al., 2013). Work in the laboratory of Shaul Yalovsky (Lavy et al., 2007; Hazak et al., 2010) showed that the SEC3 exocyst subunit interacts with an activated (GTP-bound) ROP at the PM via ICR1, a founding member of the ICR/RIP protein family (Li et al., 2008; Mucha et al., 2010). RIP3 (also known as MIDD1) interacts in a GTP-bound manner with ROPs and also with the Kinesin-13A to regulate the microtubular dynamics (Mucha et al., 2010). RIP3 is a crucial negative regulator of cortical microtubules in the patterning of secondary cell wall thickening directed by the ROP11 GTPase module (Oda and Fukuda, 2012). At PM sites, where cortical microtubules are locally destabilized, the localized exocytosis-dependent secondary cell wall thickening is blocked (Oda and Fukuda, 2012).

While local destabilization of cortical microtubules seems to stimulate exocytosis in animal cells (see above Zakharenko and Popov, 1998), dense microtubule cortical domains of somatic plant cells are often the cortical domains of highest secretory activity, as in xylem thickening or seed coat epidermal cells with a volcano-like cell wall thickening, where highly polarized delivery of pectins is targeted to extremely dense cortical microtubule domains (McFarlane et al., 2008; Oda and Fukuda, 2012). The exocytosis of pectins into pectin-accumulating pockets depends on exocyst function, implying a possibility that microtubule-rich domains might be a general cortical target recognized by EXO70s or other exocyst subunits, functioning as putative PM landmarks for exocytosis targeting (Žárský et al., 2009; Kulich et al., 2010). Extensive proliferation of the EXO70 gene in land plants (e.g., *Arabidopsis* in endowed with 23 EXO70 paralogs) possibly provides a potential for fine targeting into specific cortical areas (Synek et al., 2006; Cvrčková et al., 2012).

On the contrary, dense cortical microfilament meshwork might block exocytosis in both animal and plant cells (Valentijn et al., 1999; Žárský et al., 2009). For instance, a dense subapical F-actin fringe separating actively growing tip from the rest of the tobacco pollen tube might also be a mechanical obstacle for exocytosis (Lovy-Wheeler et al., 2005). The exocyst is also accumulated at the tip of growing pollen tubes and is obviously involved in exocytosis (Hála et al., 2008). The transport and delivery of secretory vesicles in plant cells is likely to depend on both microfilaments and an interaction of some exocyst subunits with the PM phosphoinositides, like in the case of yeast and animal cells (see above). Phosphoinositide binding was indeed predicted for several *Arabidopsis* EXO70 paralogs based on yeast and animal models (Žárský et al., 2009) and currently proved both biochemically and cytologically in our laboratory for the *Arabidopsis* SEC3 exocyst subunit (Bloch et al., in preparation).

The dynamics of several exocyst subunits at the PM, as monitored by TIRF microscopy in *Arabidopsis* epidermal cells, was unaffected by actin or microtubule cytoskeleton disruption after short (10 min) treatment with inhibitors, however, prolonged actin cytoskeleton disruption (1 h) resulted in exocyst redistribution and aggregation at the PM and impaired dynamics (Fendrych et al., 2013). This is consistent with microfilament involvement not only in the delivery but also in spatial distribution of secretory vesicles and endomembrane compartments (Staehelin and Moore, 1995).

Interestingly, exocyst complexes show almost no lateral movement within the PM in both plant and animal cells, as analyzed by the TIRF microscopy, and very similar time of persistence at the PM of about 10 s was recorded (Fendrych et al., 2013; Rivera-Molina and Toomre, 2013). Similarly, the KAT1 channel is localized inside the PM within positionally stable microdomains, which last, however, for 10s of minutes, in contrast to dynamics of the exocyst (Sutter et al., 2006). It is possible that some transmembrane proteins, e.g., plant-specific transmembrane formins (Martiniere et al., 2011; Cvrčková, 2013; in this issue) create, together with specific membrane lipids, functional clusters stabilized against the lateral movement in the PM. These transmembrane proteins might be immobilized by the binding extracellular domains in the cell wall matrix and provide landmarks for the delivery of secretory vesicles (Martinière et al., 2012).

CONCLUSION

Direct as well as a circumstantial evidence accumulated over the years concerning interactions and cooperation between the exocyst and cytoskeleton indicates that the exocyst, cytoskeleton, and membrane traffic meet at the active cellular cortex. The exocyst serves an important role in co-ordination of the vesicle trafficking with the cytoskeleton in eukaryotes, in addition to its canonical role in exocytosis. In plant cells, however, we have currently only limited and indirect evidence for this regulatory interplay, urging further research in this direction.

ACKNOWLEDGMENTS

This work was supported by the Czech Science Foundation (GACR project GPP501/11/P853) and EU-ITN grant No. 238640-PLANTORIGINS. The authors thank F. Cvrčková for critical reading of the manuscript.

REFERENCES

Adamo, J. E., Rossi, G., and Brennwald, P. (1999). The Rho GTPase Rho3 has a direct role in exocytosis that is distinct from its role in actin polarity. *Mol. Biol. Cell* 10, 4121–4133. doi: 10.1091/mbc.10.12.4121

Aronov, S., and Gerst, J. E. (2004). Involvement of the late secretory pathway in actin regulation and mRNA transport in yeast. *J. Biol. Chem.* 279, 36962–36971. doi: 10.1074/jbc.M402068200

Bendezú, F. O., and Martin, S. G. (2011). Actin cables and the exocyst form two independent morphogenesis pathways in the fission yeast. *Mol. Biol. Cell* 22, 44–53. doi: 10.1091/mbc.E10-08-0720

Bendezú, F. O., and Martin, S. G. (2013). Cdc42 explores the cell periphery for mate selection in fission yeast. *Curr. Biol.* 23, 42–47. doi: 10.1016/j.cub.2012.10.042

Bendezú, F. O., Vincenzetti, V., and Martin, S. G. (2012). Fission yeast Sec3 and Exo70 are transported on actin cables and localize the exocyst complex to cell poles. *PLoS ONE* 7:e40248. doi:10.1371/journal.pone.0040248

Birkenfeld, J., Nalbant, P., Bohl, B. P., Pertz, O., Hahn, K. M., and Bokoch, G. M. (2007). GEF-H1 modulates localized RhoA activation during cytokinesis under the control of mitotic kinases. *Dev. Cell* 12, 699–712. doi: 10.1016/j.devcel.2007.03.014

Boyd, C., Hughes, T., Pypaert, M., and Novick, P. (2004). Vesicles carry most exocyst subunits to exocytic sites marked by the remaining two subunits, Sec3p and Exo70p. *J. Cell Biol.* 167, 889–901. doi: 10.1083/jcb.200408124

Brymora, A., Valova, V. A., Larsen, M. R., Roufogalis, B. D., and Robinson, P. J. (2001). The brain exocyst complex interacts with RalA in a GFP-dependent manner: identification of a novel mammalian Sec3 gene and a second Sec15 gene. *J. Biol. Chem.* 276, 29792–29797. doi: 10.1074/jbc.C10 0320200

Chen, X. W., Leto, D., Chiang, S. H., Wang, Q., and Saltiel, A. R. (2007). Activation of RalA is required for insulin-stimulated Glut4 trafficking to the plasma membrane via the exocyst and the motor protein Myo1c. *Dev. Cell* 13, 391–404. doi: 10.1016/j.devcel.2007.07.007

Cvrčková, F. (2013). Formins and membranes: anchoring cortical actin to the cell wall and beyond. *Front. Plant Sci.* 4:436. doi: 10.3389/fpls.2013.00436

Cvrčková, F., Grunt, M., Bezvoda, R., Hála, M., Kulich, I., Rawat, A., et al. (2012). Evolution of the land plant exocyst complexes. *Front. Plant Sci.* 3:159. doi: 10.3389/fpls.2012.00159

de Curtis, I., and Meldolesi, J. (2012). Cell surface dynamics – how Rho GTPases orchestrate the interplay between the plasma membrane and the cortical cytoskeleton. *J. Cell Sci.* 125, 4435–4444. doi: 10.1242/jcs. 108266

Donovan, K. W., and Bretscher, A. (2012). Myosin-V is activated by binding secretory cargo and released in coordination with Rab/exocyst function. *Dev. Cell* 23, 769–781. doi: 10.1016/j.devcel.2012.09.001

Estravís, M., Rincón, S. A., Santos, B., and Pérez, P. (2011). Cdc42 regulates multiple membrane traffic events in fission yeast. *Traffic* 12, 1744–1758. doi: 10.1111/j.1600-0854.2011.01275.x d

Feig, L. A., Urano, T., and Cantor, S. (1996). Evidence for a Ras/Ral signaling cascade. *Trends Biochem. Sci.* 21, 438–441. doi: 10.1016/S0968-0004(96)10058-X

Fendrych, M., Synek, L., Pecenková, T., Drdová, E. J., Sekeres, J., de Rycke, R., et al. (2013). Visualization of the exocyst complex dynamics at the plasma membrane of *Arabidopsis thaliana*. *Mol. Biol. Cell* 24, 510–520. doi: 10.1091/mbc.E12-06-0492

Fendrych, M., Synek, L., Pecenkova, T., Toupalova, H., Cole, R., Drdova, E., et al. (2010). The *Arabidopsis* exocyst complex is involved in cytokinesis and cell plate maturation. *Plant Cell* 22:3053–3065. doi: 10.1105/tpc.110.074351

Finger, F. P., Hughes, T. E., and Novick, P. (1998). Sec3p is a spatial landmark for polarized secretion in budding yeast. *Cell* 92, 559–571. doi: 10.1016/S0092-8674(00)80948-4

Fukai, S., Matern, H. T., Jagath, J. R., Scheller, R. H., and Brunger, A. T. (2003). Structural basis of the interaction between RalA and Sec5, a subunit of the sec6/8 complex. *EMBO J.* 22, 3267–3278. doi: 10.1093/emboj/cdg329

Fu, Y., Wu, G., and Yang, Z. (2001). Rop GTPase-dependent dynamics of tip-localized F-actin controls tip growth in pollen tubes. *J. Cell Biol.* 152, 1019–1032. doi: 10.1083/jcb.152.5.1019

Guo, W., Roth, D., Walch-Solimena, C., and Novick, P. (1999). The exocyst is an effector for Sec4p, targeting secretory vesicles to sites of exocytosis. *EMBO J.* 4, 71–80.

Hála, M., Cole, R., Synek, L., Drdová, E., Pečenková, T., Nordheim, A., et al. (2008). An exocyst complex functions in plant cell growth in *Arabidopsis* and tobacco. *Plant Cell* 20, 1330–1345. doi: 10.1105/tpc.108.059105

Hammer, J. A., and Sellers, J. R. (2012). Walking to work: roles for class V myosins as cargo transporters. *Nat. Rev. Mol. Cell. Biol.* 13, 13–26. doi: 10.1038/nrm3248

Hazak, O., Bloch, D., Poraty, L., Sternberg, H., Zhang, J., Friml, J., et al. (2010). A RHO scaffold integrates the secretory system with feedback mechanisms in regulation of auxin distribution. *PLoS Biol.* 8:e1000282. doi:10.1371/journal.pbio.1000282

Hazelett, C. C., and Yeaman, C. (2012). Sec5 and Exo84 mediate distinct aspects of RalA-dependent cell polarization. *PLoS ONE* 7:e39602. doi: 10.1371/journal.pone.0039602

He, B., Xi, F., Zhang, X., Zhang, J., and Guo, W. (2007). Exo70 interacts with phospholipids and mediates the targeting of the exocyst to the plasma membrane. *EMBO J.* 26, 4053–4065. doi: 10.1038/sj.emboj.7601834

Heider, M. R., and Munson, M. (2012). Exorcising the exocyst complex. *Traffic* 13, 898–907. doi: 10.1111/j.1600-0854.2012.01353.x

Holubcová, Z., Howard, G., and Schuh, M. (2013). Vesicles modulate an actin network for asymmetric spindle positioning. *Nat. Cell Biol.* 15, 937–947. doi: 10.1038/ncb2802

Hsu, S. C., Ting, A. E., Hazuka, C. D., Davanger, S., Kenny, J. W., Kee, Y., et al. (1996). The mammalian brain rsec6/8 complex. *Neuron* 6, 209–219.

Jin, R., Junutula J. R., Matern H. T., Ervin K. E., Scheller R. H., and Brunger A. T. (2005). Exo84 and Sec5 are competitive regulatory Sec6/8 effectors to the RalA GTPase. *EMBO J.* 24, 2064–2074. doi: 10.1038/sj.emboj.7600699

Jin, Y., Sultana, A., Gandhi, P., Franklin, E., Hamamoto, S., Khan, A. R., et al. (2011). Myosin V transports secretory vesicles via a Rab GTPase cascade and interaction with the exocyst complex. *Dev. Cell* 21, 1156–1170. doi: 10.1016/j.devcel.2011.10.009

Jourdain, I., Dooley, H. C., and Toda, T. (2012). Fission yeast sec3 bridges the exocyst complex to the actin cytoskeleton. *Traffic* 13, 1481–1495. doi: 10.1111/j.1600-0854.2012.01408.x

Kono, K., Saeki, Y., Yoshida, S., Tanaka, K., and Pellman, D. (2012). Proteasomal degradation resolves competition between cell polarization and cellular wound healing. *Cell* 150, 151–164. doi: 10.1016/j.cell.2012.05.030

Krendel, M., Zenke, F. T., and Bokoch, G. M. (2002). Nucleotide exchange factor GEF-H1 mediates cross-talk between microtubules and the actin cytoskeleton. *Nat. Cell Biol.* 4, 294–301. doi: 10.1038/ncb773

Kulich, I., Cole, R., Drdová, E., Cvrčková, F., Soukup, A., Fowler, J., et al. (2010). *Arabidopsis* exocyst subunits SEC8 and EXO70A1 and exocyst interactor ROH1 are involved in the localized deposition of seed coat pectin. *New Phytol.* 188, 615–625. doi: 10.1111/j.1469-8137.2010.03372.x

Lavy, M., Bloch, D., Hazak, O., Gutman, I., Poraty, L., Sorek, N., et al. (2007). A Novel ROP/RAC effector links cell polarity, root-meristem maintenance, and vesicle trafficking. *Curr. Biol.* 17, 947–952. doi: 10.1016/j.cub.2007.04.038

Li, S., Gu, Y., Yan, A., Lord, E., and Yang, Z. B. (2008). RIP1 (ROP Interactive Partner 1)/ICR1 marks pollen germination sites and may act in the ROP1 pathway in the control of polarized pollen growth. *Mol. Plant* 1, 1021–1035. doi: 10.1093/mp/ssn051

Liu, J., and Guo, W. (2012). The exocyst complex in exocytosis and cell migration. *Protoplasma* 249, 587–597. doi: 10.1007/s00709-011-0330-1

Liu, J., Zhao, Y., Sun, Y., He, B., Yang, C., Svitkina, T., et al. (2012). Exo70 stimulates the Arp2/3 complex for lamellipodia formation and directional cell migration. *Curr. Biol.* 22, 1510–1515. doi: 10.1016/j.cub.2012.05.055

Lovy-Wheeler, A., Wilsen, K. L., Baskin, T. I., and Hepler, P. K. (2005). Enhanced fixation reveals the apical cortical fringe of actin filaments as a consistent feature of the pollen tube. *Planta* 221, 95–104. doi: 10.1007/s00425-004-1423-2

Martiniere, A., Gayral, P., Hawes, C., and Runions, J. (2011). Building bridges: formin1 of *Arabidopsis* forms a connection between the cell wall and the actin cytoskeleton. *Plant J.* 66, 354–365. doi: 10.1111/j.1365-313X.2011.04497.x

Martinière, A., Lavagi, I., Nageswaran, G., Rolfe, D. J., Maneta-Peyret, L., Luu, D. T., et al. (2012). Cell wall constrains lateral diffusion of plant plasma-membrane proteins. *Proc. Natl. Acad. Sci. U.S.A.* 109, 12805–12810. doi: 10.1073/pnas.1202040109

McFarlane, H. E., Young, R. E., Wasteneys, G. O., and Samuels, A. L. (2008). Cortical microtubules mark the mucilage secretion domain of the plasma membrane in *Arabidopsis* seed coat cells. *Planta* 227, 1363–1375. doi: 10.1007/s00425-008-0708-2

Mohammadi, S., and Isberg, R. R. (2013). Cdc42 interacts with the exocyst complex to promote phagocytosis. *J. Cell Biol.* 200, 81–93. doi: 10.1083/jcb.201204090

Morgera, F., Sallah, M. R., Dubuke, M. L., Gandhi, P., Brewer, D. N., Carr, C. M., et al. (2012). Regulation of exocytosis by the exocyst subunit Sec6 and the SM protein Sec1. *Mol. Biol. Cell* 23, 337–346. doi: 10.1091/mbc.E11-08-0670

Moskalenko, S., Tong, C., Rosse, C., Mirey, G., Formstecher, E., Daviet, L., et al. (2003). Ral GTPases regulate exocyst assembly through dual subunit interactions. *J. Biol. Chem.* 278, 51743–51748. doi: 10.1074/jbc.M308702200

Mucha, E., Hoefle, C., Hückelhoven, R., and Berken, A. (2010). RIP3 and AtKinesin-13A - a novel interaction linking Rho proteins of plants to microtubules. *Eur. J. Cell. Biol.* 89, 906–916. doi: 10.1016/j.ejcb.2010.08.003

Mucha, E., Fricke, I., Schaefer, A., Wittinghofer, A., and Berken, A. (2011). Rho proteins of plants-functional cycle and regulation of cytoskeletal dynamics. *Eur. J. Cell Biol.* 90, 934–943. doi: 10.1016/j.ejcb.2010.11.009

Mukerji, J., Olivieri, K. C., Misra, V., Agopian, K. A., and Gabuzda, D. (2012). Proteomic analysis of HIV-1 Nef cellular binding partners reveals a role for exocyst complex proteins in mediating enhancement of intercellular nanotube formation. *Retrovirology* 9:33. doi: 10.1186/1742-4690-9-33

Nakano, K., Toya, M., Yoneda, A., Asami, Y., Yamashita, A., Kamasawa, N., et al. (2011). Pob1 ensures cylindrical cell shape by coupling two distinct Rho signaling events during secretory vesicle targeting. *Traffic* 12, 726–739. doi: 10.1111/j.1600-0854.2011.01190.x

Nalbant, P., Chang, Y. C., Birkenfeld, J., Chang, Z. F., and Bokoch, G. M. (2009). Guanine nucleotide exchange factor-H1 regulates cell migration via localized activation of RhoA at the leading edge. *Mol. Biol. Cell* 20, 4070–4082. doi: 10.1091/mbc.E09-01-0041

Nichols, C. D., and Casanova, J. E. (2010). Salmonella-directed recruitment of new membrane to invasion foci via the host exocyst complex. *Curr. Biol.* 20, 1316–1320. doi: 10.1016/j.cub.2010.05.065

Novick, P., Field, C., and Schekman, R. (1980). Identification of 23 complementation groups required for post-translational events in the yeast secretory pathway. *Cell* 21, 205–215. doi: 10.1016/0092-8674(80)90128-2

Oda, Y., and Fukuda, H. (2012). Secondary cell wall patterning during xylem differentiation. *Curr. Opin. Plant Biol.* 15, 38–44. doi: 10.1016/j.pbi.2011.10.005

Ohno, H., Hase, K., and Kimura, S. (2010). M-Sec: emerging secrets of tunneling nanotube formation. *Commun. Integr. Biol.* 3, 231–233. doi: 10.4161/cib.3.3.11242

Pathak, R., Delorme-Walker, V. D., Howell, M. C., Anselmo, A. N., White, M. A., Bokoch, G. M., et al. (2012). The microtubule-associated Rho activating factor GEF-H1 interacts with exocyst complex to regulate vesicle traffic. *Dev. Cell* 23, 397–411. doi: 10.1016/j.devcel.2012.06.014

Pecenkova, T., Hala, M., Kulich, I., Kocourkova, D., Drdova, E., Fendrych, M., et al. (2011). The role for the exocyst complex subunits Exo70B2 and Exo70H1 in the plant-pathogen interaction. *J. Exp. Bot.* 62, 2107–2116. doi: 10.1093/jxb/erq402

Rivera-Molina, F., and Toomre, D. (2013). Live-cell imaging of exocyst links its spatiotemporal dynamics to various stages of vesicle fusion. *J. Cell Biol.* 201, 673–680. doi: 10.1083/jcb.201212103

Sakurai-Yageta, M., Recchi, C., Le Dez, G., Sibarita, J. B., Daviet, L., Camonis, J., et al. (2008). The interaction of IQGAP1 with the exocyst complex is required for tumor cell invasion downstream of Cdc42 and RhoA. *J. Cell Biol.* 181, 985–998. doi: 10.1083/jcb.200709076

Schiller, C., Diakopoulos, K. N., Rohwedder, I., Kremmer, E., von Toerne, C., Ueffing, M., et al. (2013). LST1 promotes the assembly of a molecular machinery responsible for tunneling nanotube formation. *J. Cell Sci.* 126, 767–777. doi: 10.1242/jcs.114033

Shen, D., Yuan, H., Hutagalung, A., Verma, A., Kümmel, D., Wu, X., et al. (2013). The synaptobrevin homologue Snc2p recruits the exocyst to secretory vesicles by binding to Sec6p. *J. Cell Biol.* 202, 509–526. doi: 10.1083/jcb.201211148

Sivaram, M. V., Saporita, J. A., Furgason, M. L., Boettcher, A. J., and Munson, M. (2005). Dimerization of the exocyst protein Sec6p and its interaction with the t-SNARE Sec9p. *Biochemistry* 44, 6302–6311. doi: 10.1021/bi048008z

Snaith, H. A., Thompson, J., Yates, J. R., and Sawin, K. E. (2011). Characterization of Mug33 reveals complementary roles for actin cable-dependent transport and exocyst regulators in fission yeast exocytosis. *J. Cell Sci.* 124, 2187–2199. doi: 10.1242/jcs.084038

Songer, J. A., and Munson, M. (2009). Sec6p anchors the assembled exocyst complex at sites of secretion. *Mol. Biol. Cell* 20, 973–982. doi: 10.1091/mbc.E08-09-0968

Staehelin, L. A., and Moore, I. (1995). The plant golgi apparatus: structure, functional organization and trafficking mechanisms. *Annu. Rev. Plant Physiol. Plant Mol. Biol.* 46, 261–288. doi: 10.1146/annurev.pp.46.060195.001401

Sugihara, K., Asano, S., Tanaka, K., Iwamatsu, A., Okawa, K., and Ohta, Y. (2002). The exocyst complex binds the small GTPase RalA to mediate filopodia formation. *Nat. Cell Biol.* 1, 73–78. doi: 10.1038/ncb720

Sutter, J. U., Campanoni, P., Tyrrell, M., and Blatt, M. R. (2006). Selective mobility and sensitivity to SNAREs is exhibited by the *Arabidopsis* KAT1 K+ channel at the plasma membrane. *Plant Cell* 18, 935–954. doi: 10.1105/tpc.105.038950

Swiech, L., Blazejczyk, M., Urbanska, M., Pietruszka, P., Dortland, B. R., Malik, A. R., et al. (2011). CLIP-170 and IQGAP1 cooperatively regulate dendrite morphology. *J. Neurosci.* 31, 4555–4568. doi: 10.1523/JNEUROSCI.6582-10.2011

Synek, L., Schlager, N., Eliáš, M., Quentin, M., Hauser, M. T., and Žárský, V. (2006). AtEXO70A1, a member of a family of putative exocyst subunits specifically expanded in land plants, is important for polar growth and plant development. *Plant J.* 48, 54–72. doi: 10.1111/j.1365-313X.2006.02854.x

TerBush, D. R., Maurice, T., Roth, D., and Novick, P. (1996). The Exocyst is a multiprotein complex required for exocytosis in *Saccharomyces cerevisiae*. *EMBO J.* 15, 6483–6494.

Valentijn, K. M., Gumkowski, F. D., and Jamieson, J. D. (1999). The subapical actin cytoskeleton regulates secretion and membrane retrieval in pancreatic acinar cells. *J. Cell Sci.* 112, 81–96.

Vaškovičová, K., Žárský, V., Rösel, D., Nikolič, M., Buccione, R., Cvrčková, F., et al. (2013). Invasive cells in animals and plants: searching for LECA machineries in later eukaryotic life. *Biol. Direct* 8:8. doi: 10.1186/1745-6150-8-8

Vega, I. E., and Hsu, S. C. (2001). The exocyst complex associates with microtubules to mediate vesicle targeting and neurite outgrowth. *J. Neurosci.* 21, 3839–3848.

Wang, S., Liu, Y., Adamson, C. L., Valdez, G., Guo, W., and Hsu, S. C. (2004). The mammalian exocyst, a complex required for exocytosis, inhibits tubulin polymerization. *J. Biol. Chem.* 279, 35958–35966. doi: 10.1074/jbc.M313778200

White, C. D., Erdemir, H. H., and Sacks, D. B. (2012). IQGAP1 and its binding proteins control diverse biological functions. *Cell. Signal* 24, 826–834. doi: 10.1016/j.cellsig.2011.12.005

Wu, S., Mehta, S. Q., Pichaud, F., Bellen, H. J., and Quiocho, F. A. (2005). Sec15 interacts with Rab11 via a novel domain and affects Rab11 localization in vivo. *Nat. Struct. Mol. Biol.* 12, 879–885. doi: 10.1038/nsmb987

Wu, H., Rossi, G., and Brennwald, P. (2008). The ghost in the machine: small GTPases as spatial regulators of exocytosis. *Trends Cell Biol.* 18, 397–404. doi: 10.1016/j.tcb.2008.06.007

Wu, H., Turner, C., Gardner, J., Temple, B., and Brennwald, P. (2010). The Exo70 subunit of the exocyst is an effector for both Cdc42 and Rho3 function in polarized exocytosis. *Mol. Biol. Cell* 21, 430–442. doi: 10.1091/mbc.E09-06-0501

Yalovsky, S., Bloch, D., Sorek, N., and Kost, B. (2008). Regulation of membrane trafficking, cytoskeleton dynamics and cell polarity by ROP/RAC GTPases. *Plant Phys.* 147, 1527–1543. doi: 10.1104/pp.108.122150

Zakharenko, S., and Popov, S. (1998). Dynamics of axonal microtubules regulate the topology of new membrane insertion into the growing neurites. *J. Cell Biol.* 143, 1077–1086.

Žárský, V., Cvrčková, F., Potocký, M., and Hála, M. (2009). Exocytosis and cell polarity in plants - exocyst and recycling domains. *New Phytol.* 183, 255–272. doi: 10.1111/j.1469-8137.2009.02880.x

Zhang, X., Orlando, K., He, B., Xi, F., Zhang, J., Zajac, A., et al. (2008). Membrane association and functional regulation of Sec3 by phospholipids and Cdc42. *J. Cell Biol.* 180, 145–158. doi: 10.1083/jcb.200704128

Zhao, Y., Liu, J., Yang, C., Capraro, B. R., Baumgart, T., Bradley, R. P., et al. (2013). Exo70 generates membrane curvature for morphogenesis and cell migration. *Dev. Cell* 26, 266–278. doi: 10.1083/jcb.200704128

Zuo, X., Zhang, J., Zhang, Y., Hsu, S. C., Zhou, D., and Guo, W. (2006). Exo70 interacts with the Arp2/3 complex and regulates cell migration. *Nat. Cell Biol.* 8, 1383–1388.

Conflict of Interest Statement: The authors declare that the research was conducted in the absence of any commercial or financial relationships that could be construed as a potential conflict of interest.

Received: 31 October 2013; paper pending published: 18 November 2013; accepted: 12 December 2013; published online: 02 January 2014.

Citation: Synek L, Sekereš J and Žárský V (2014) The exocyst at the interface between cytoskeleton and membranes in eukaryotic cells. Front. Plant Sci. 4:543. doi: 10.3389/fpls.2013.00543

This article was submitted to Plant Traffic and Transport, a section of the journal Frontiers in Plant Science.

Aims of the thesis

My experimental work revolved mostly around the mechanisms of targeting plant exocyst complex to various plasma membrane domains and subcellular compartments. I contributed to the functional understanding of EXO70 gene family expansion in plants by following these aims:

Aim 1:

Systematically employ the model system of growing tobacco pollen tube to explore subcellular targeting of EXO70 isoforms. Analyze the expression of EXO70 isoforms in tobacco pollen and compare the behavior of native pollen isoforms with isoforms not normally expressed in pollen upon ectopic expression of the fluorescently tagged versions of EXO70 isoforms. Use overexpression experiments to reveal functional characteristics of selected isoforms in growing pollen tubes.

Aim 2:

Use the widely expressed and functionally characterized canonical EXO70 isoform, the EXO70A1, as a model candidate for detailed analysis of the plant EXO70 membrane targeting mechanisms with particular focus on molecular interactions of EXO70A1 with membrane phospholipids.

Aim 3:

Contribute to the functional characterization of selected *Arabidopsis thaliana* EXO70 paralogs in different tissues and during specific cellular and physiological processes.

Results

During my doctoral training, I have followed the above stated research aims by contributing to following papers, which are either published, submitted for publication or in the state of final preparation for submission, as stated:

Aim 1:

PAPER 4:

Title: Analysis of Exocyst Subunit EXO70 Family Reveals Distinct Membrane Polar Domains in Tobacco Pollen Tubes.

Authors: Juraj Sekereš, Přemysl Pejchar, Jiří Šantrůček, Nemanja Vukašinović, Viktor Žárský and Martin Potocký

Rationale of the report: We systematically analyzed expression and subcellular localization of all tobacco EXO70 isoforms in growing tobacco pollen tubes by spinning disk confocal microscopy. Selected isoforms localized to specific domains of the pollen tube plasma membrane, apical vesicle-rich inverted cone region, nucleus, and cytoplasm. NtEXO70A1a and NtEXO70B1 occupied two distinct and mutually exclusive plasma membrane domains, both overlapping to a different degree with maxima of phosphatidylinositol 4,5-bisphosphate and phosphatidic acid. The overexpression of major pollen-expressed A-class and C-class EXO70 isoforms resulted in growth arrest and characteristic phenotypic deviations of tip swelling and apical invaginations. The A-class EXO70 isoforms localized to focused subapical plasma membrane region known to be the place of exocytosis in tobacco pollen tube and thus plays a role in bulk secretion. On the other hand, C-class EXO70 isoforms localized to cytoplasm under all tested conditions and probably play regulatory role. The function of the NtEXO70B1 in tobacco pollen is unclear but it might contribute to the endocytosis or an alternative minor secretory pathway.

My contribution: I performed all the experimental work included in the publication with the following exceptions: Přemysl Pejchar and Nemanja Vukašinović cloned part of the constructs, Martin Potocký helped me with the phylogenetic analysis and Jiří Šantrůček performed the proteomic expression analysis of EXO70 isoforms in tobacco pollen. I designed the experiments and analyzed results together with Martin Potocký and Viktor Žárský. I wrote the manuscript with assistance of Martin Potocký and Přemysl Pejchar with Viktor Žárský contributed to finalization of the manuscript.

Published in: Plant Physiology 173(3):1659-1675, doi: 10.1104/pp.16.01709

Aim 2:

PAPER 5:

Title: Molecular architecture of the Arabidopsis exocyst complex reveals EXO70A1 as the key subunit required for targeting of the plant exocyst to the plasma membrane through the direct interaction with anionic phospholipids.

Authors: Lukáš Synek*, Juraj Sekereš*, Roman Pleskot, Klára Aldorfová, Edita Janková-Drdová, Vedrana Marković, Jitka Ortmannová, Tamara Pečenková, Přemysl Pejchar, Martina Růžičková, Hana Soukupová, Jiří Šantrůček, Nemanja Vukašinović, Viktor Žárský, and Martin Potocký

* the authors contributed equally to the results of the work

Rationale of the report: The work includes systematic analysis of plant exocyst architecture by coimmunoprecipitation, which demonstrated similar architecture to yeast and mammalian exocyst with two evolutionary conserved subcomplexes. The work confirms the crucial role of the EXO70A1 subunit for targeting of the exocyst complex to plasma membrane, as well as an autonomous potential of the EXO70A1 to bind plasma membrane upon disruption of the complex. Furthermore, it unravels the mechanism of EXO70A1 plasma membrane targeting by combination of fluorescent live cell imaging, *in vitro* protein-lipid binding assays and molecular dynamics simulations. We show that EXO70A1 is capable of binding various anionic

phospholipids, namely phosphatidic acid, phosphatidylinositol-4-phosphate and phosphatidylinositol-4,5-bisphosphate *in vitro* and *in vivo* and that the particular lipid species responsible for EXO70A1 recruitment differ among tissues.

My contribution: I performed the experiments addressing *in vivo* interactions of WT variant of tobacco NtEXO70A1a with phosphatidylinositol-4,5-bisphosphate and phosphatidic acid in growing tobacco pollen tubes. I performed imaging and subsequent analysis of Arabidopsis EXO70A1 interaction with outer lateral plasma membrane in control plants, *pip5k1pip5k2* double mutant background and in plants treated by selected inhibitors of phospholipid metabolism. I demonstrated inability of mutated NtEXO70A1a to bind plasma membrane in growing tobacco pollen under various conditions, which indicates that the same key positively charged lysine residues are vital for interaction of EXO70A1 with anionic phospholipids in both Arabidopsis and tobacco. I also wrote substantial part of the manuscript.

Manuscript is being finalized for submission

Aim 3:

PAPER 6:

Title: Visualization of the exocyst complex dynamics at the plasma membrane of Arabidopsis thaliana.

Authors: Matyáš Fendrych, Lukáš Synek, Tamara Pečenková, Edita Drdová-Janková, Juraj Sekereš, Riet de Rycke, Moritz K. Nowack and Viktor Žárský

Rationale of the report: The study provides first detailed high resolution examination of plant exocyst dynamics at the outer lateral root membrane. It demonstrates altered exocyst dynamics after prolonged disruption of the actin cytoskeleton and confirms the crucial role of EXO70A1 for proper localization of selected core exocyst subunit, the SEC6.

My contribution: I contributed to FRAP measurements and the analysis of EXO84b:GFP dynamics under control conditions and upon disruption of actin or microtubule cytoskeleton.

Published in: Molecular Biology of the Cell 24(4):510-20, doi: 10.1091/mbc.E12-06-0492

PAPER 7:

Title: Arabidopsis exocyst subcomplex containing subunit EXO70B1 is involved in autophagy-related transport to the vacuole.

Authors: Ivan Kulich, Tamara Pečenková, Juraj Sekereš, Ondřej Smetana, Matyáš Fendrych, Ilse Foissner, Margit Höftberger and Viktor Žárský

Rationale of the report: The work focused on the specific role of one of the 23 Arabidopsis EXO70 paralogs, the EXO70B1. Exo70B1 mutant plants hyperaccumulate salicylic acid, which results into hypersensitive reaction. Subsequent analysis revealed that EXO70B1 plays role in autophagy and autophagy-related trafficking to the vacuole.

My contribution: I designed and performed the initial starvation experiments linking EXO70B1 with canonical autophagic pathway. I imaged and quantified vacuolar accumulation of EXO70B1-positive bodies under normal conditions and upon ER stress.

Published in: Traffic 14(11):1155-65, doi: 10.1111/tra.12101

PAPER 8:

Title: Microtubule-dependent targeting of the exocyst complex is necessary for xylem development in Arabidopsis.

Authors: Nemanja Vukašinović, Yoshihisa Oda, Přemysl Pejchar, Lukáš Synek, Tamara Pečenková, Anamika Rawat, Juraj Sekereš, Martin Potocký and Viktor Žárský

Rationale of the report: The work combined fluorescent live cell imaging, genetics and protein-protein interaction analysis to address mechanisms of exocyst complex targeting to sites of prospective secondary cell deposition in maturating xylem. The study concluded that exocyst is inevitable for proper secondary cell wall deposition in xylem and gets recruited to target membrane domains in microtubule-dependent manner due to direct interaction of several exocyst subunits with COG2, which itself indirectly interacts with microtubules via tissue specific protein linkers VETH1 and VETH2.

My contribution: I was involved in the study design, experiments planning, interpreting the results and writing the manuscript.

Published in: New Phytologist 213(3):1052-1067, doi: 10.1111/nph.14267

PAPER 9:

Title: Exocyst complex mediates non-host resistance against powdery mildew in Arabidopsis

Authors: Jitka Ortmannová, Tamara Pečenková, Juraj Sekereš, Ivan Kulich, Jiří Šantrůček and Viktor Žárský

Rationale of the report: The work provides detailed analysis of role of plant exocyst during plant cell defence reaction against pathogenic fungi and focuses on specialized function of the EXO70B2 as the EXO70 isoform upregulated upon pathogen attack and driving the exocyst-regulated vesicular trafficking to the sites of secretory papilla and extrahaustorial encasement deposition. The study also demonstrates role of exocyst in well characterized SYP121-mediated vesicle secretion and provides data on direct interaction between the EXO70B2 and SYP121.

My contribution: I provided the *sec5a-1* mutant and the SEC5a:GFP line. I participated in finalizing of the manuscript.

Submitted to Molecular Plant

Analysis of Exocyst Subunit EXO70 Family Reveals Distinct Membrane Polar Domains in Tobacco Pollen Tubes[1][OPEN]

Juraj Sekereš, Přemysl Pejchar, Jiří Šantrůček, Nemanja Vukašinović[2], Viktor Žárský, and Martin Potocký*

Institute of Experimental Botany, Czech Academy of Sciences, Prague 6, Czech Republic (J.S., P.P., N.V., V.Ž., M.P.); Department of Experimental Plant Biology, Faculty of Science, Charles University, Prague 2, Czech Republic (J.S., V.Ž.); and Department of Biochemistry and Microbiology, University of Chemistry and Technology, Prague 6, Czech Republic (J.Š.)

ORCID IDs: 0000-0002-4876-5454 (J.S.); 0000-0003-0488-7465 (P.P.); 0000-0002-5301-0339 (V.Ž.); 0000-0002-3699-7549 (M.P.).

The vesicle-tethering complex exocyst is one of the crucial cell polarity regulators. The EXO70 subunit is required for the targeting of the complex and is represented by many isoforms in angiosperm plant cells. This diversity could be partly responsible for the establishment and maintenance of membrane domains with different composition. To address this hypothesis, we employed the growing pollen tube, a well-established cell polarity model system, and performed large-scale expression, localization, and functional analysis of tobacco (*Nicotiana tabacum*) EXO70 isoforms. Various isoforms localized to different regions of the pollen tube plasma membrane, apical vesicle-rich inverted cone region, nucleus, and cytoplasm. The overexpression of major pollen-expressed EXO70 isoforms resulted in growth arrest and characteristic phenotypic deviations of tip swelling and apical invaginations. NtEXO70A1a and NtEXO70B1 occupied two distinct and mutually exclusive plasma membrane domains. Both isoforms partly colocalized with the exocyst subunit NtSEC3a at the plasma membrane, possibly forming different exocyst complex subpopulations. NtEXO70A1a localized to the small area previously characterized as the site of exocytosis in the tobacco pollen tube, while NtEXO70B1 surprisingly colocalized with the zone of clathrin-mediated endocytosis. Both NtEXO70A1a and NtEXO70B1 colocalized to different degrees with markers for the anionic signaling phospholipids phosphatidylinositol 4,5-bisphosphate and phosphatidic acid. In contrast, members of the EXO70 C class, which are specifically expressed in tip-growing cells, exhibited exocytosis-related functional effects in pollen tubes despite the absence of apparent plasma membrane localization. Taken together, our data support the existence of multiple membrane-trafficking domains regulated by different EXO70-containing exocyst complexes within a single cell.

The pollen tube is a structure indispensable for angiosperm sexual reproduction. The tube germinates from a pollen grain after it lands on the stigma of a pistil within a flower. During its growth through the pistil, the pollen tube needs to overcome, depending on the plant species, millimeters to centimeters of transmitting tract distance (Lora et al., 2016) so that sperm cells can be brought to the embryo sac. Overcoming such a long distance is enabled by a special type of polar growth called tip growth, the local delivery of cell materials to a focused growth site, forming an elongated cellular structure. Because of such extreme polar growth, pollen tubes are used as an important model system of cell polarity, and many fundamental cell polarity regulators like ROP GTPases and plant phospholipid-modifying enzymes were first characterized in pollen tubes and later appeared to play an analogous function in other cell types (Qin and Dong, 2015).

Plant cells have several polar membrane domains with different composition (Žárský et al., 2009; Łangowski et al., 2010, 2016), and additional polarized structures arise during the response to pathogens and symbionts (Dörmann et al., 2014). One of the key components regulating cell polarity is the exocyst complex. It is a heterooctameric protein complex (TerBush et al., 1996) that is shared across eukaryotes (Vaškovičová et al., 2013; Martin-Urdiroz et al., 2016) and that tethers secretory vesicles to the plasma

[1] This work was supported by the Czech Science Foundation (grant nos. GA13-19073S and GA15-24711S), the Grant Agency of Charles University (grant no. 394815), the Ministry of Education, Youth, and Sport of the Czech Republic (grant no. NPUI LO1417 to V.Ž. and Specific University Research grant no. 20/2016 to J.Š.), and the Operational Programme Prague – Competitiveness (grant no. CZ. 2.16/3.1.00/21519 to the Institute of Experimental Botany).

[2] Present address: Department of Plant Systems Biology, VIB, 9052 Ghent, Belgium.

* Address correspondence to potocky@ueb.cas.cz.

The author responsible for distribution of materials integral to the findings presented in this article in accordance with the policy described in the Instructions for Authors (www.plantphysiol.org) is: Martin Potocký (potocky@ueb.cas.cz).

J.S. and M.P. conceived the project, designed the experiments, analyzed the data, and wrote the article with contributions of all the authors; J.S. performed most of the experiments with contributions from P.P. and N.V.; J.Š. performed mass spectrometry analysis; V.Ž. initiated the research topic; M.P., P.P., and V.Ž. supervised the experiments.

[OPEN] Articles can be viewed without a subscription.
www.plantphysiol.org/cgi/doi/10.1104/pp.16.01709

membrane (PM) and regulates their subsequent fusion. In animal and yeast model systems, many molecular interactions involved in exocyst function have already been discovered: EXO70 and SEC3 drive exocyst to the target site by interaction with phosphatidylinositol 4,5-bisphosphate (PIP_2) and small GTPases of the Rho family (He et al., 2007; Liu et al., 2007; Wu et al., 2010; Pleskot et al., 2015), both budding yeast (*Saccharomyces cerevisiae*) Sec15p (France et al., 2006) and Exo70p interact with the cell polarity determinant Bem1p (Liu and Novick, 2014), SEC15 interacts with secretory vesicle-associated Rab GTPases (Wu et al., 2005) and promotes myosin motor release after vesicle fusion with the PM (Donovan and Bretscher, 2015), and budding yeast Sec6p binds SNARE proteins and promotes SNARE complex assembly (Dubuke et al., 2015) and also binds the SNARE interactor Sec1p (Morgera et al., 2012). Besides facilitating canonical exocytosis, exocyst in opisthokonts plays a role in other processes such as fission yeast (*Schizosaccharomyces pombe*) cytokinesis (Wang et al., 2002, 2016), midbody scission (Chen et al., 2006), and the formation of tunneling nanotubes (Hase et al., 2009), and the animal exocyst subcomplex also contributes to the initiation of autophagy (Bodemann et al., 2011).

We previously discovered the exocyst complex in plants (Eliáš et al., 2003) and have unraveled some of its functions, like pectin deposition in seed coats (Kulich et al., 2010), recycling of auxin transporters (Drdová et al., 2013), cell plate initiation and maturation during cytokinesis (Fendrych et al., 2010), tip growth (Cole et al., 2005; Bloch et al., 2016), and defense against pathogen infection (Pečenková et al., 2011). One of the most striking findings was the presence of many paralogs encoding the EXO70 subunit in plant genomes (Eliáš et al., 2003; Cvrčková et al., 2012). Besides the trivial explanation that different EXO70 paralogs could play equivalent roles in different cell types, it was hypothesized that various EXO70 isoforms would coexist within a single cell type and regulate exocytosis to different PM domains (Žárský et al., 2009; Žárský and Potocký, 2010). Besides different lateral mobility and regulated endocytosis, targeted exocytosis was postulated as a key mechanism responsible for the presence of polar membrane domains with different composition. Thus, different activated cortical domains, docking platforms for exocytotic vesicles, could drive the secretion to different parts of the PM by employing different EXO70 isoforms and connected intracellular secretory machinery (diverse recycling endosomes, Rab GTPase, and SNARE protein isoforms, etc.; Žárský et al., 2009).

While exocyst acts as a complex in budding yeast (TerBush et al., 1996; Heider et al., 2016) and plant cells (Hála et al., 2008) and its subunits should be studied in the context of the whole complex, it also makes sense to analyze plant EXO70 proteins separately and infer valuable results with biological relevance. First, the EXO70 subunit is involved in the targeting of the whole complex. Localization of tagged EXO70 alone should reflect the localization where it can drive the rest of the complex. EXO70 proteins are subject to regulated proteolytic degradation (Samuel et al., 2009; Stegmann et al., 2012; Žárský et al., 2013), and exchange of different EXO70 isoform levels probably acts as a fast switch of secretion to polar domains preferred by different EXO70s. Second, some EXO70s may act as part of the exocyst subcomplex (Kulich et al., 2013) or could have functions completely independent of the rest of the exocyst, as was shown for animal EXO70 (Zuo et al., 2006; Dellago et al., 2011; Liu et al., 2012; Zhao et al., 2013). Due to the large number of predicted EXO70 protein interactors, EXO70 isoforms possibly serve as an important component of cell polarity-directing machines (Žárský et al., 2009). Systematic study of the subcellular localization of different EXO70 isoforms is thus of utmost importance.

Due to the large number of plant EXO70 paralogs, distinct intracellular localization of EXO70 protein isoforms to different membrane domains or other compartments was mapped only in some instances. Arabidopsis (*Arabidopsis thaliana*) AtEXO70B1 was shown to play a role in autophagy and localizes to internal compartments starting at the endoplasmic reticulum and directed to the Golgi-independent vacuolar pathway (Kulich et al., 2013). EXO70I was recently demonstrated to be important for the formation of the periarbuscular membrane subdomain during arbuscular mycorrhizal symbiosis in *Medicago trunculata* (Zhang et al., 2015). For most EXO70 paralogs, the available studies are based on genetic approaches combined with cytological analyses. This way, AtEXO70H4 was shown to be indispensable for correct trichome cell wall thickening and callose deposition (Kulich et al., 2015). The results of gene-silencing experiments suggest that the EXO70F-like subunits are essential in resistance to fungal penetration in barley (*Hordeum vulgare*; Ostertag et al., 2013). To our knowledge, no study simultaneously showing the localization of more EXO70 isoforms in a single cell has been published so far.

In the context of plant cell polarity research, the extremely polarized growing pollen tube represents a great model system for large-scale analyses due to easy transiently tagged protein expression and the availability of vast transcriptomic and proteomic data sets. Indeed, some PM domains are larger and better separated from each other in this cell type (Sekereš et al., 2015). Zones of active endocytosis (Derksen et al., 1995; Moscatelli et al., 2007) and exocytosis (Bove et al., 2008; Idilli et al., 2013; Luo et al., 2016) are very well separated. A previous study attempting to systematically examine the localization of exocyst components in tobacco (*Nicotiana tabacum*) BY-2 cells (Chong et al., 2010) resulted in the aggregation of tagged proteins into clusters caused by overexpression in many cases. Contrary to Chong et al. (2010), we also decided to study autologous tobacco proteins instead of Arabidopsis homologs, so that conditions would be as native as possible.

The aim of our study was to perform a systematic analysis of the localization and functional properties of EXO70 isoforms in growing tobacco pollen tubes. We demonstrate a distinct localization for several EXO70 isoforms and show that selected pollen-expressed isoforms induce specific morphological phenotypes upon overexpression. We provide evidence that isoforms NtEXO70A1a and NtEXO70B1 localize to distinct, mutually exclusive domains of the pollen tube PM and display different degrees of colocalization with markers for the anionic signaling phospholipids PIP_2 and phosphatidic acid (PA). Both isoforms colocalize with the exocyst subunit NtSEC3a at the PM and are possibly part of distinct subpopulations of exocyst complex particles.

RESULTS

All Major Angiosperm EXO70 Clades Are Present in Solanaceae Genomes

Plant EXO70s constitute an expanded gene family divided into nine clades that are present in most angiosperm groups (Cvrčková et al., 2012). We initiated a detailed study of tobacco EXO70 proteins by bioinformatic analysis that confirmed the presence of all major EXO70 clades in the Solanaceae, including tobacco (Fig. 1). It should be noted that tobacco is amphidiploid with two nearly identical copies of most genes in its genome (one from each parental species). For the sake of clarity, we further present data from only the one diploid gene set. An exhaustive BLAST analysis of the tobacco genome draft, together with searches in the genomes of the tobacco parental species *Nicotiana sylvestris* and *Nicotiana tomentosiformis* and the closely related tomato (*Solanum lycopersicum*), uncovered 24 EXO70 genes in a diploid tobacco gene set. In congruence with previous observations from other plant genomes (Synek et al., 2006; Cvrčková et al., 2012), most EXO70 genes outside clades A and I are intronless. While tobacco EXO70 genes can be easily sorted into the same clades as Arabidopsis EXO70 genes, one-to-one orthology relations cannot be established in most cases (Fig. 1). During the evolution from the last common ancestor of the Solanaceae and Brassicaceae, some genes have undergone duplications only in Solanaceae (e.g. ancestral EXO70C1 into NtEXO70C1a and NtEXO70C1b) while others have duplicated only in the lineage leading to Brassicaceae (e.g. ancestral EXO70A2 into AtEXO70A2 and AtEXO70A3). However, in the case of some isoforms (AtEXO70C2/NtEXO70C2, AtEXO70E2/NtEXO70E2, and AtEXO70F/NtEXO70F), clear orthology relationships can be inferred.

Multiple EXO70 Isoforms Are Expressed in Germinating Pollen

After compiling the repertoire of tobacco EXO70 genes, we investigated EXO70 isoforms that are expressed in tobacco pollen. We analyzed the transcription of tobacco EXO70 genes by reverse transcription (RT)-PCR amplification of EXO70 fragments from cDNA mixtures prepared from imbibed pollen, germinating pollen, and growing pollen tubes. Due to the high similarity of the gene-coding regions in the T and S genomes of amphidiploid tobacco, primer pairs were designed so that they would discriminate between particular isoforms indicated in Figure 1 but would not discriminate between copies from parental species. Furthermore, three members of the NtEXO70H3-4a subclade (Fig. 1) were not discriminated either, because of their extreme similarity at the nucleic acid level. RT-PCR analysis has shown that 10 EXO70s are transcribed in at least one stage of pollen germination or pollen tube growth (Fig. 2). Since the correlation between the transcription level and the protein abundance is often weak, we further investigated EXO70 expression in tobacco pollen at the protein level. Total cytoplasmic protein extract was separated by SDS protein electrophoresis, and proteins of around 70 kD were analyzed by mass spectrometry. Although this approach was not sensitive enough to detect all pollen isoforms, it uncovered the most abundant EXO70s. Table I summarizes the results of four independent mass spectrometry reads from two different biological replicates and shows that EXO70 clades A and C represent dominant subfamilies in growing pollen tubes.

Several EXO70 Isoforms Localize to Distinct Compartments in Growing Tobacco Pollen Tubes

In order to get a first insight into the putative functions of pollen EXO70s, we fused 20 different tobacco EXO70 isoforms to the C terminus of yellow fluorescent protein (YFP) under the control of the LAT52 promoter (nucleotide sequences of our clones are provided in Supplemental File S1) and performed detailed subcellular localization analyses by spinning disk confocal microscopy. Since the transient expression of constructs results in variable levels of expression among different pollen tubes, we focused on pollen tubes that exhibited low levels of expression of the transgenic constructs (as assessed by fluorescence intensity readout) and normal growth rate (~3–5 μm min^{-1}). Our observations are summarized in Figure 3 for pollen-expressed isoforms and in Supplemental Figure S1 for isoforms not natively expressed in pollen. In systems where binding properties of EXO70 to membrane were well characterized, EXO70 was demonstrated to be a peripheral membrane protein (He et al., 2007). Thus, it is not surprising that, besides distinct subcellular patterns of different isoform localization, most tagged EXO70 isoforms also exhibit strong cytoplasmic fluorescence. These observations provided several noteworthy conclusions.

(1) NtEXO70A1a localized to the small but very distinct PM region adjacent to the pollen tube tip (Fig. 3; Supplemental Movie S1). In contrast, NtEXO70A2 was concentrated in an area near the pollen tube tip but did

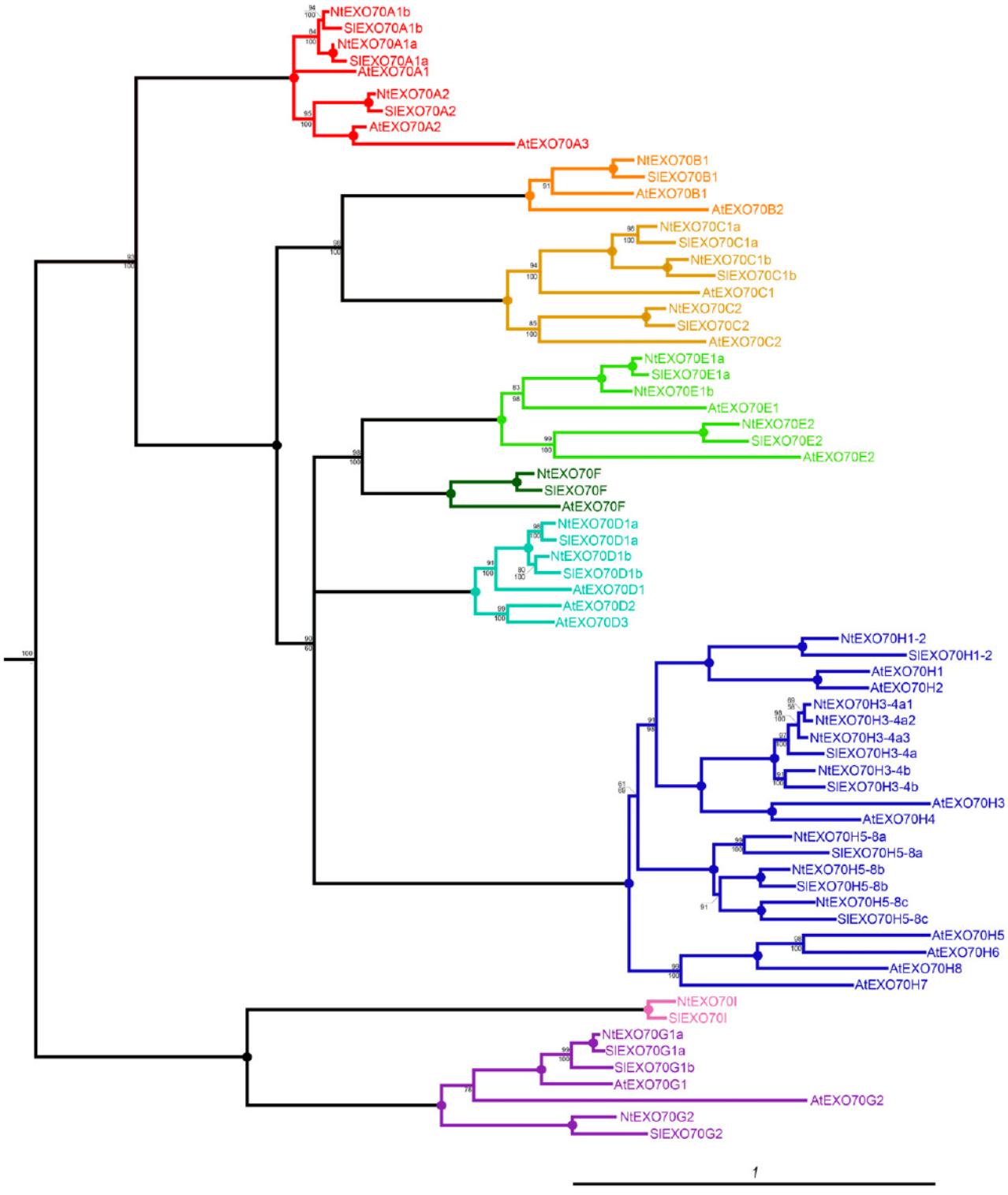

Figure 1. Phylogenetic relationship of EXO70 proteins from Arabidopsis (At), tobacco (Nt), and tomato (Sl). The tree represents the protein maximum likelihood phylogeny, where numbers at nodes correspond to the approximate likelihood ratio test with SH (Shimodaira-Hasegawa)-like support from maximum likelihood (top) and posterior probabilities from Bayesian analysis (bottom). Circles represent 100% support by both methods, and branches were collapsed if the inferred topology was not supported by both methods. The tree was rooted using human EXO70 as an outgroup. The scale bar indicates the rate of substitutions per site.

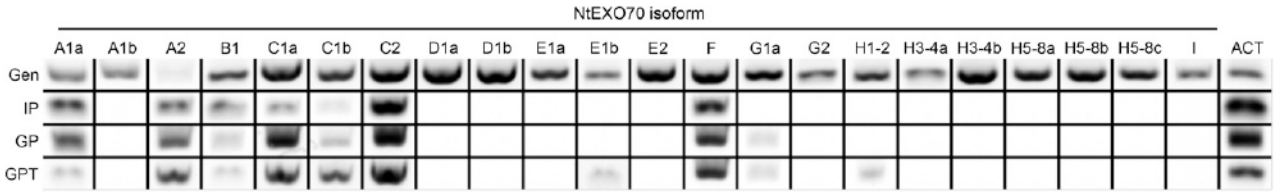

Figure 2. Several EXO70 isoforms are expressed in tobacco pollen and growing pollen tubes. Semiquantitative RT-PCR analysis is shown for the EXO70 family in tobacco imbibed pollen (IP), germinating pollen (GP), and growing pollen tube (GPT), with genomic DNA (Gen) used for the control amplification. Actin (ACT) was amplified as a control from the same premix solution. The image shown was assembled from two independent experiments for each tissue. Combinations that did not result in the presence of an active band are represented by blank spaces.

not localize to the PM in most pollen tubes observed. Only occasionally did NtEXO70A2 display PM localization comparable to NtEXO70A1a (Fig. 3). Surprisingly, NtEXO70A1b, the closest homolog of NtEXO70A1a (sharing 90% identical residues with NtEXO70A1a; Supplemental Fig. S2), was localized in growing pollen tubes evenly throughout the cytoplasm and only rarely in the manner observed for NtEXO70A2. To our knowledge, PM localization of NtEXO70A1b in growing pollen tubes has never been observed. (2) We observed a very distinct localization pattern for YFP:NtEXO70B1, which localizes to a broader subapical PM region but is excluded from the area near the pollen tube tip (Fig. 3; Supplemental Movie S2). (3) Rather surprisingly, all members of the pollen-enriched C class localized exclusively in the cytoplasm. (4) We further discovered that NtEXO70E1b localizes to the inverted-cone region at the pollen tube tip, the zone enriched with secretory and recycling vesicles (Derksen et al., 1995). (5) NtEXO70E2 localized to mobile spots in the cytoplasm (Supplemental Fig. S1; Supplemental Movie S3). Because NtEXO70E2 is not expressed in pollen and aggregation to puncta is a common overexpression artifact, the localization pattern of NtEXO70E2 in the growing pollen tube is probably an artifact. (6) While tagged NtEXO70G1a localizes only to the cytoplasm upon very low levels of expression, in pollen tubes with slightly increased expression and slightly decreased growth rate, NtEXO70G1a decorates the subapical membrane and fibrillar structures, likely actin fibers (Supplemental Fig. S3; Supplemental Movie S4). (7) Unexpectedly, fluorescently tagged NtEXO70H1-2 and NtEXO70H5-8b localized predominantly to the nucleus. Since other tagged EXO70 isoforms do not exhibit nuclear fluorescence despite frequent strong cytoplasmic signals and the nuclear signal is stronger than the cytoplasmic signal, we can conclude that targeting to the nucleus is an active, isoform-specific process and not the result of a passive entry or degradation of the YFP-fused protein. In the case of NtEXO70H1-2, the tendency of nuclear import is so strong that almost no cytoplasmic signal can be detected.

Because the transient expression of fluorescently tagged proteins in growing tobacco pollen tubes does not allow a direct way to prove the functionality of the tagged proteins by rescue of the mutant phenotype (as is possible in the case for Arabidopsis mutants stably transformed with tagged proteins of interest), we decided to further verify that the subcellular localization of the N-terminally tagged NtEXO70 isoforms reflects the behavior of the native proteins by examining the subcellular localization of C-terminally YFP-tagged NtEXO70B1. NtEXO70B1:YFP displayed a nearly identical subcellular distribution to YFP:EXO70B1 (Supplemental Fig. S4A).

In summary, we observed a distinct localization pattern for several tobacco EXO70 isoforms. Interestingly, membrane binding was observed only for natively expressed pollen isoforms, and clear differences could be seen even between closely related EXO70 paralogs (e.g. NtEXO70A1a versus NtEXO70A1b and NtEXO70E1a versus NtEXO70E1b; Fig; 3; Supplemental Fig. S1). Most other nonpollen EXO70 isoforms also showed cytoplasm-only localization in pollen tubes (Supplemental Fig. S1). This strongly suggests that the nonoverlapping localizations observed for pollen NtEXO70 isoforms A1a, B1, and E1b reflect their functional significance.

NtEXO70A1a and NtEXO70B1 Occupy Mutually Exclusive Parts of the PM in Growing Tobacco Pollen Tubes, and Both Overlap with Exocyst Subunit NtSEC3a PM Localization

The localization of tagged NtEXO70A1a and NtEXO70B1 (Fig. 3) strongly suggested that the proteins inhabit mutually exclusive PM domains in the growing tobacco pollen tube. To analyze this in more detail, we transiently cotransformed tobacco pollen with YFP-tagged NtEXO70A1a and monomeric red fluorescent protein (mRFP)-tagged NtEXO70B1. In growing pollen tubes with low levels of transgene expression, besides their cytoplasmic signal, the tagged EXO70 proteins indeed localized to distinct membrane zones (Fig. 4). We repeatedly observed a similar pattern of localization and quantified the distance of onset and end of EXO70 localization from the pollen tube apex (Fig. 4). Please note that, although onset and end of localization were variable among the pollen tube population, NtEXO70A1a and NtEXO70B1 did not overlap in the vast majority of pollen tubes. End of

Table I. *Incidence of EXO70 isoform detection in the proteomic expression analysis*

Isoform	Total No. of Peptides
NtEXO70A2	14
NtEXO70C1a	25
NtEXO70C1b	5
NtEXO70C2	7

NtEXO70A1a and onset of NtEXO70B1 localization were separated by less than 1 μm (n = 49). Recently published work (Bloch et al., 2016) characterized the localization and mechanism of membrane binding of the exocyst subunit SEC3 to a broader region near the tobacco pollen tube tip. In order to elucidate the relation of NtEXO70A1a and NtEXO70B1 to other components of the exocyst complex, we compared the distribution of the membrane signals of YFP:NtEXO70A1a and YFP:NtEXO70B1 with the exocyst subunit NtSEC3a:YFP. Interestingly, typical NtSEC3a:YFP localization partially overlaps with both YFP:NtEXO70A1a and YFP:NtEXO70B1 localization (Fig. 5A). We also investigated the distribution of the membrane signal of YFP:NtEXO70A1a, YFP:NtEXO70B1, and NtSEC3a:YFP along the annular surface of growing tobacco pollen tubes using optical sectioning. As documented by orthogonal views, these experiments also showed the partial overlap of NtSEC3a with both NtEXO70A1a and NtEXO70B1 and indicated that, in pollen tubes, the fluorescence signal of exocyst subunits at the PM seems to be mostly continuous (Fig. 5B). The observed relation between NtEXO70A1a, NtEXO70B1, and NtSEC3a also was corroborated by measuring equatorial distances of onset and end of YFP:NtEXO70A1a, YFP:NtEXO70B1, and NtSEC3a:YFP membrane localization from the pollen tube apex (Fig. 5C). This was further supported by a colocalization analysis of tobacco pollen tubes expressing mRFP:NtEXO70B1 and NtSEC3a:YFP (Supplemental Fig. S4B). The membrane signal of mRFP:NtEXO70B1 and NtSEC3a:YFP largely overlapped, but the signal of NtSEC3a:YFP clearly reached farther to the tip, probably to the zone of NtEXO70A1a membrane localization.

The Zone of Active Clathrin-Mediated Endocytosis Maximum Is Distinct from the NtEXO70A1a PM Localization and Largely Overlaps with NtEXO70B1 Membrane Localization

The unexpected localization of NtEXO70B1 in the pollen tube subapex far from textbook sites of secretion prompted us to further analyze its distribution. We noted that the localization of NtEXO70B1 resembled the previously described maximum of clathrin-mediated endocytosis (Derksen et al., 1995; Moscatelli et al., 2007). To confirm this, we used an mRFP-tagged dynamin-related protein from Arabidopsis (AtDRP1C; Konopka and Bednarek, 2008) as a marker of clathrin-mediated endocytosis and visualized it together with YFP-tagged NtEXO70B1. Similar patterns of localization were

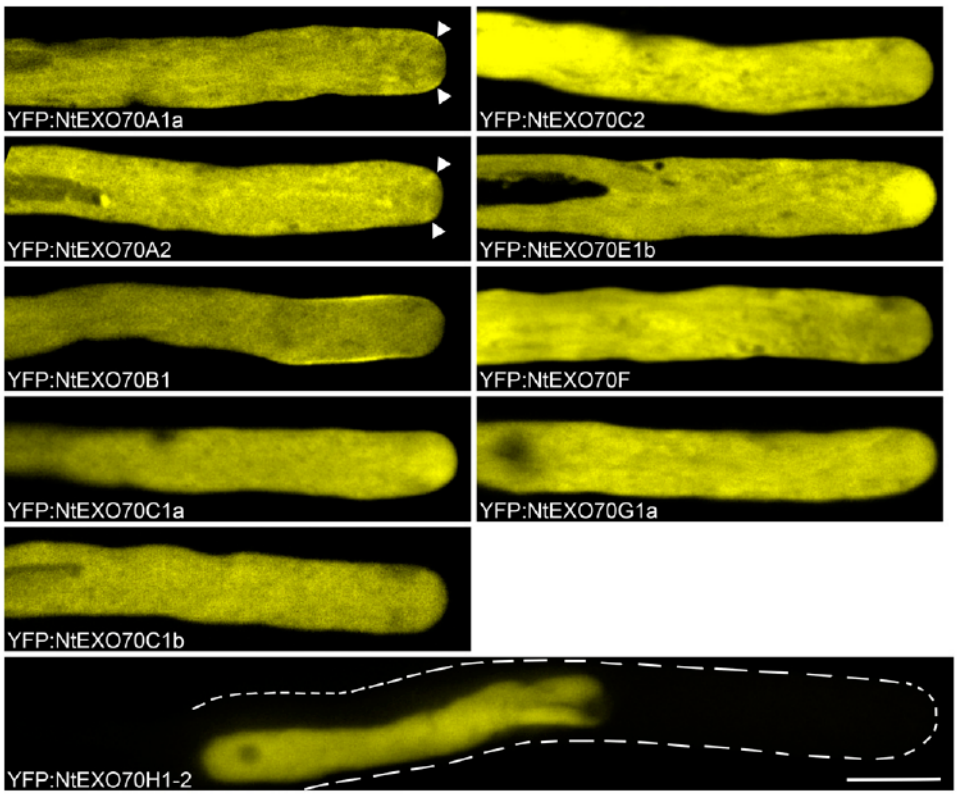

Figure 3. Localization of natively pollen-expressed EXO70 isoforms in growing tobacco pollen tubes. Selected YFP-tagged tobacco EXO70 isoforms were transiently expressed in tobacco pollen tubes, and their subcellular localization was examined by spinning disk confocal microscopy. Growing pollen tubes with low expression levels of the transgene are shown. The images shown are representative for 20 or more transformed pollen tubes observed in at least two independent experiments for NtEXO70F, NtEXO70G1a, and NtEXO70H1-2 and for 30 or more transformed pollen tubes in three or more independent experiments for the rest of the isoforms. Arrowheads mark small areas of membrane localization for NtEXO70A1a and concentration of signal in the corresponding area for NtEXO70A2. In the case of NtEXO70H1-2, the contour of the pollen tube is marked because of negligent cytoplasmic signal due to nuclear accumulation of the signal. Bar = 10 μm.

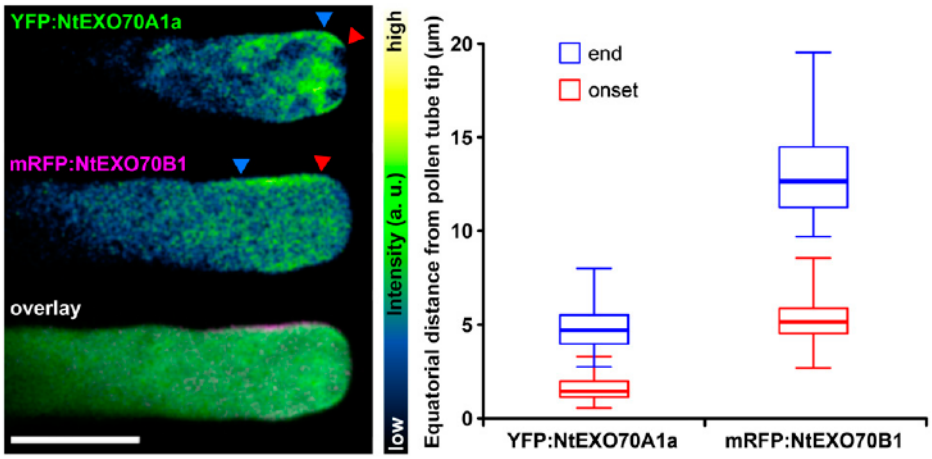

Figure 4. Mutually exclusive localization of NtEXO70A1a and NtEXO70B1 in growing tobacco pollen tubes. YFP:NtEXO70A1a and mRFP:NtEXO70B1 were transiently coexpressed in tobacco pollen tubes, and their subcellular localization was examined by spinning disk confocal microscopy with representative results shown (left). Images of individual channels are represented using a color intensity code in order to display local enrichment of the YFP/mRFP signal. In the overlay, YFP is represented by green, mRFP by magenta, and white indicates the overlapping signal. Red and blue arrowheads mark the onset and end of the particular membrane signal, measured in middle optical sections as the equatorial distance from the pollen tube apex (right; $n = 25$). a.u., Arbitrary unit. Bar = 10 μm.

observed repeatedly, and distances of membrane localization onset and end from the apex were quantified (Fig. 6). In healthy growing pollen tubes with low levels of transgene expression, areas of NtEXO70B1 and AtDRP1C membrane localization largely overlapped. The onset of membrane localization was almost identical for both proteins, and the membrane localization of AtDRP1C was more extended. On the other hand, colocalization of YFP:NtEXO70A1a and AtDRP1C:mRFP demonstrated that the observed membrane localization of the two constructs is mutually exclusive (Supplemental Fig. S5).

NtEXO70A1a and NtEXO70B1 Exhibit Different Degrees of Overlap with Genetically Encoded Markers for Anionic Signaling Phospholipids

Budding yeast (He et al., 2007) and animal (Liu et al., 2007) EXO70 were demonstrated to directly bind PIP_2 at the PM. Recently, the affinity of the SEC3 exocyst subunit toward PIP_2 and its biological relevance, previously known from opisthokonts (Zhang et al., 2008), were confirmed in plants (Bloch et al., 2016). Amino acid residues identified as responsible for opisthokont EXO70 lipid binding are conserved to different degrees among plant EXO70 isoforms (Žárský et al., 2009). Thus, it is probable that the local lipid composition of the PM is responsible for the differential binding of different EXO70s. In the light of this hypothesis, we transiently cotransformed tobacco pollen with YFP-tagged EXO70s and mRFP-tagged genetically encoded lipid markers for PA and PIP_2. In growing pollen tubes with low levels of transgene expression, NtEXO70A1a (Fig. 7) and NtEXO70B1 (Fig. 8) displayed different degrees of overlap with PA (mRFP:2Spo20p-PABD) and PIP_2 (mRFP:$2PH_{PLC\delta1}$) markers. Membrane YFP:NtEXO70A1a was fully included within the range of mRFP:$2PH_{PLC\delta1}$ signal in every pollen tube observed. Interestingly, the very tip covered by mRFP:$2PH_{PLC\delta1}$ but devoid of mRFP:2Spo20p-PABD was devoid of YFP:NtEXO70A1a as well (Fig. 7). This was confirmed by the quantification of YFP:NtEXO70A1a and mRFP:2Spo20p-PABD membrane signal onset distances from the pollen tube tip, which appeared to be the same (Fig. 7). Note that, although the onset and end of localization were variable among pollen tube population, the YFP:NtEXO70A1a signal never reached closer to the very tip than mRFP:2Spo20p-PABD in individual pollen tubes. Although with current tools we cannot equivocally say whether the YFP:EXO70A1a signal membrane localization matches the maximum of mRFP:$2PH_{PLC\delta1}$ signal, it is clear that the mRFP:$2PH_{PLC\delta1}$ signal always completely covers the area of PM YFP:EXO70A1a localization. The YFP:NtEXO70B1 membrane signal matched the area of mRFP:2Spo20p-PABD signal maximum and also largely overlapped with mRFP:$2PH_{PLC\delta1}$ (Fig. 8).

Major Pollen EXO70 Isoforms Inhibit Pollen Tube Growth upon Overexpression

Overexpression of the protein of interest in the tobacco pollen tube is often used to infer a protein's function (Ischebeck et al., 2008). To test the physiological role of most prevalent tobacco pollen EXO70 isoforms, we analyzed the effect of their overexpression on pollen tube growth. From the A clade of EXO70 proteins, the most expressed isoform (NtEXO70A2) and the isoform with the most distinct subcellular localization (NtEXO70A1a) were selected for functional characterization. From the C clade, we chose the two most

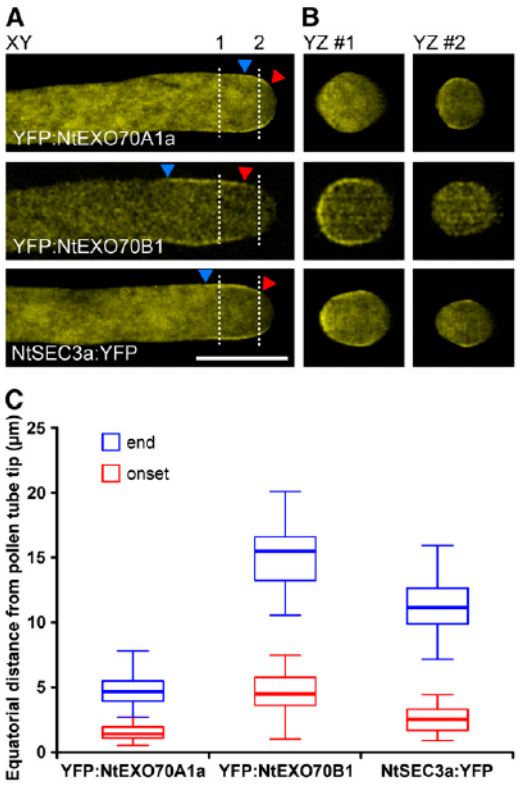

Figure 5. Membrane NtSEC3a localization overlaps with both NtEXO70A1a and NtEXO70B1 localization. YFP:NtEXO70A1a, YFP:NtEXO70B1, and NtSEC3a:YFP were expressed individually in tobacco pollen tubes, and their subcellular localization was examined by optical sectioning using spinning disk confocal microscopy. The main image shows a single optical section at the *x-y* plane (A), and dashed lines indicate where the stack was sectioned to show the *y-z* planes (B). Red and blue arrowheads mark the onset and end of the particular membrane signal, measured as the equatorial distance from the pollen tube apex (C; $n \geq 15$). Bar = 10 μm.

expressed isoforms at the protein level: NtEXO70C1a and NtEXO70C2. When overexpressed, all four of these isoforms significantly impaired pollen tube growth. The transformed tubes grew to about half of the length of the control pollen tubes overexpressing YFP:GUS (Fig. 9). To rule out a possible nonspecific effect caused by the overexpression of membrane trafficking-related protein, we also analyzed the overexpression effect of YFP:NtEXO70E1a, a selected isoform that is neither expressed in pollen nor exhibits specific subcellular localization (Fig. 2; Supplemental Fig. S1). Pollen tubes overexpressing YFP:NtEXO70E1a elongated almost identically to the tubes overexpressing YFP:GUS, which strongly indicates that the ability of a particular EXO70 isoform to inhibit pollen growth upon overexpression correlates with its physiological role in pollen growth. We did not observe any effect of NtEXO70B1 overexpression (Fig. 9), probably because YFP-tagged NtEXO70B1 (regardless of the YFP position) loses its distinct membrane localization and forms artificial aggregates in cytoplasm once the level of expression reaches a certain threshold (Supplemental Fig. S4A). Thus, in the case of NtEXO70B1, overexpression cannot be used to assess the physiological functionality of the protein.

Overexpression of Major Pollen EXO70 Isoforms in Growing Pollen Tubes Results into Distinct Morphological Phenotypes

After demonstrating the functional significance of selected pollen isoforms in pollen tube growth, we further aimed to infer more about the role of these proteins from phenotypic changes in pollen tubes overexpressing particular constructs. Such an approach was demonstrated repeatedly as a successful method to get insight into the functions of proteins of interest in pollen tube polar growth (Ischebeck et al., 2008, 2011; Stenzel et al., 2012). Thus, we carefully investigated pollen tube morphology upon overexpression of selected YFP-tagged EXO70 isoforms that strongly inhibited pollen tube growth, namely NtEXO70A1a, NtEXO70A2, NtEXO70C1a, and NtEXO70C2. Despite the high inherent variability in the population of transformed pollen tubes, several distinct phenotypic categories induced by the overexpression of YFP:EXO70s could be assigned by careful examination of a large data set of transformed pollen tubes (Fig. 10). We compared these effects with mild alterations inevitably caused by high overexpression of a control construct encoding YFP:GUS. The overview of different phenotypic category occurrence is summarized in Figure 10. Generally, mild overexpression of pollen EXO70s (as assessed by fluorescence level; Supplemental Fig. S6) induced the expansion of the pollen tube apical region. Even though the extended tip phenotype also was observed occasionally in the control set overexpressing YFP:GUS, the incidence of the phenotype and the severity of tip expansion were significantly lower than in the population of EXO70-overexpressing pollen tubes. Strong overexpression of EXO70 isoforms from both the A and C classes resulted in the formation of apical invaginations (Fig. 10). Note that the observed phenotypic categories of pollen tubes overexpressing particular isoforms do not necessarily represent a succession order (e.g. pollen tubes overexpressing NtEXO70A2 with the morphology classified as category 2 would not necessarily change morphology to category 3 given enough time to develop).

During a systematic localization study of EXO70 isoforms in growing pollen tubes with low transgene expression, cells with high levels of YFP-tagged EXO70 isoforms (as assessed by level of fluorescence; Supplemental Fig. S6) also were often observed, because of the variable nature of transgene expression in the transiently transformed pollen population. A similar trend to that reported for the overexpression of NtEXO70C1a and NtEXO70C2 (Fig. 10) also was observed in pollen tubes overexpressing NtEXO70C1b. Also, YFP:NtEXO70A1b was seen occasionally to be recruited to the tip PM upon overexpression but did so

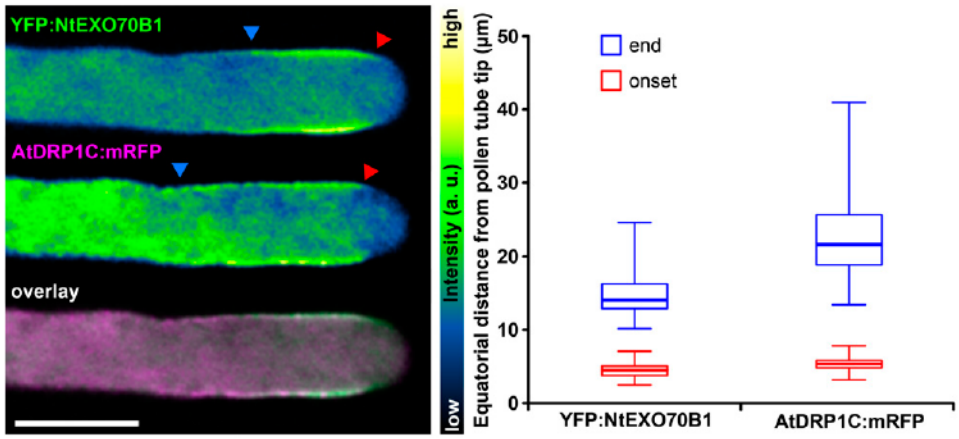

Figure 6. Overlap of NtEXO70B1 localization and the zone of clathrin-mediated endocytosis maximum marked by AtDRP1C. YFP:NtEXO70B1 and AtDRP1C:mRFP were transiently coexpressed in tobacco pollen tubes, and their subcellular localization was examined by spinning disk confocal microscopy with representative results shown (left). Images of individual channels are represented using a color intensity code in order to display local enrichment of the YFP/mRFP signal. In the overlay, YFP is represented by green, mRFP by magenta, and white indicates the overlapping signal. Red and blue arrowheads mark the onset and end of the particular membrane signal, measured as the equatorial distance from the pollen tube apex (right; $n = 50$). a.u., Arbitrary unit. Bar = 10 μm.

far less frequently than YFP:NtEXO70A1a or YFP:NtEXO70A2. However, the apical invagination phenotype was never observed outside A- and C-class EXO70 proteins, and strong membrane recruitment upon EXO70 overexpression was never observed outside the A class. Furthermore, the morphology of cells overexpressing nonpollen YFP:EXO70 isoforms was comparable to that of cells overexpressing YFP:GUS. It is noteworthy that, while the overexpression of A-class EXO70 isoforms resulted in increased membrane recruitment of the tagged proteins to the pollen tube membrane tip and induced invaginations, C-class EXO70 isoforms never localized to the PM, even upon strong overexpression (Fig. 10). This indicated completely different molecular mechanisms of A- and C-class EXO70 action in pollen tube tip growth. In order to further test this hypothesis, we attempted to recruit NtEXO70C2 to the PM by increasing the levels of a minor acidic phospholipid in situ. We chose PIP_2 as a candidate phospholipid because it was demonstrated previously to recruit EXO70 to the PM in budding yeast and mammalian cells (He et al., 2007; Liu et al., 2007)

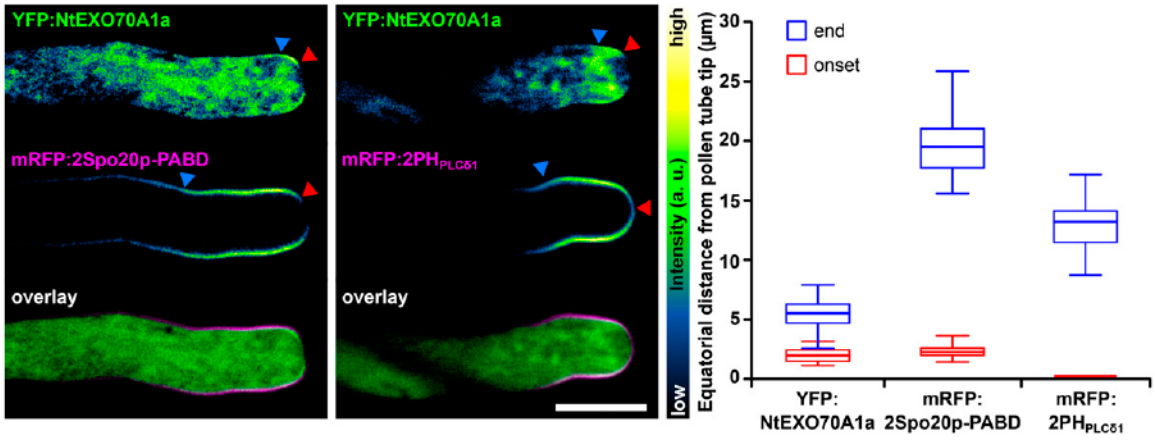

Figure 7. Colocalization of NtEXO70A1a with lipid markers in growing tobacco pollen tubes. NtEXO70A1a was transiently coexpressed together with the PA marker mRFP:2Spo20p-PABD (left) and the PIP_2 marker mRFP:$2PH_{PLC\delta1}$ (middle), and the subcellular localization of the constructs was examined by spinning disk confocal microscopy. Images of individual channels are represented using a color intensity code in order to display local enrichment of the YFP/mRFP signal. In the overlays, YFP is represented by green, mRFP by magenta, and white indicates the overlapping signal. Red and blue arrowheads mark the onset and end of the particular membrane signal, measured as the equatorial distance from the pollen tube apex (right; $n \geq 13$). The onset value for mRFP:$2PH_{PLC\delta1}$ was set to zero because it always covers the very tip of the pollen tube PM. Bar = 10 μm.

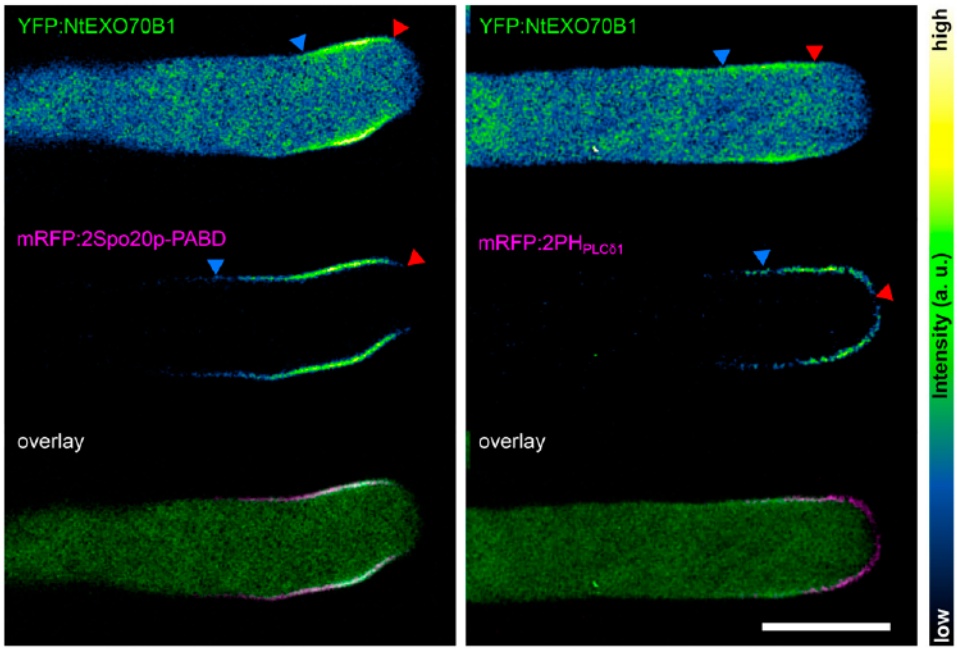

Figure 8. Colocalization of NtEXO70B1 with lipid markers in growing tobacco pollen tubes. NtEXO70B1 was transiently coexpressed together with the PA marker mRFP:2Spo20p-PABD (left) and the PIP_2 marker mRFP:$2PH_{PLC\delta1}$ (right), and the subcellular localization of the constructs was examined by spinning disk confocal microscopy with representative results shown. Images of individual channels are represented using a color intensity code in order to display local enrichment of the YFP/mRFP signal. In the overlays, YFP is represented by green, mRFP by magenta, and white indicates the overlapping signal. Red and blue arrowheads mark the onset and end of the particular membrane signal. a.u., Arbitrary unit. Bar = 10 μm.

and the enzymes catalyzing the conversion of phosphatidylinositol 4-phosphate into PIP_2 are well characterized in plant cells, including tobacco pollen tubes (Ischebeck et al., 2008, 2013). As the positive control, we used NtSEC3a as a bona fide peripheral membrane protein binding PIP_2. Plant SEC3 was demonstrated recently to directly bind PIP_2 in plant cells, including growing tobacco pollen tubes, with the molecular mechanism of PIP_2 well characterized and supported by both in vitro and in vivo experiments (Bloch et al., 2016). We transformed the pollen tubes with a high amount of the cyan fluorescent protein-tagged phosphatidylinositol 4-phosphate 5-kinase 5 (PIP5K5:CFP, Ischebeck et al., 2008) in order to rapidly increase the PIP_2 level in situ and low amount of NtSEC3a or NtEXO70C2 so that exocyst subunits would not perturb cellular morphology by themselves and only serve as a readout of their membrane-binding properties. The morphological aberrations of the pollen tubes observed (Supplemental Fig. S7) are thus the sole result of PIP5K5 overexpression, as reported previously (Ischebeck et al., 2008). In the case of NtSEC3a, we repeatedly observed strong recruitment of the protein to the PM upon increased levels of PIP_2 with increased PM-cytoplasm signal ratio (Supplemental Fig. S7). On the other hand, NtEXO70C2 was never recruited to the PM after increasing PIP_2 level, which confirms the notion that C-class EXO70 isoforms do not bind the PM.

DISCUSSION

Previous studies clearly demonstrated the involvement of exocyst in plant cell polarity regulation, including polar tip growth (Cole et al., 2005; Synek et al., 2006; Hála et al., 2008). The significance of EXO70 family diversity in angiosperms (Eliáš et al., 2003; Cvrčková et al., 2012) has become one of the key topics in understanding plant cell polarity regulation (Žárský et al., 2009). However, most studies carried out to date were limited to Arabidopsis and none involved expression, localization, and functional study of EXO70 family diversity within a single cell. Here, we attempted to overcome these shortcomings by systematic investigation of tobacco EXO70 isoforms in tobacco pollen tubes, a cell type particularly favorable for analyses of genes regulating cell morphogenesis and membrane traffic.

First, we performed a phylogenetic analysis of the EXO70 family in Solanaceae and studied it in the context of previous findings (Eliáš et al., 2003; Cvrčková et al., 2012). All nine angiosperm EXO70 clades are present in Solanaceae genomes, with 22 members in the diploid tomato genome and 24 members in the diploid tobacco genome. As summarized in Figure 1, in some cases, clear orthologs between Arabidopsis and Solanaceae isoforms can be detected. In other instances, the EXO70 genes have undergone a few independent duplications in lineages leading to Brassicaceae and Solanaceae. Most striking examples of independent duplications were detected for the H clade. Noteworthy, the rate of substitution detected between EXO70 genes from tobacco and its parental species (*N. sylvestris* and *N. tomentosiformis*) was very low for A-clade EXO70s and highest for H-clade EXO70s (data not shown). This underpins the relatively high evolutionary rate of the H-clade EXO70s and offers insight for a future study of EXO70 family evolution in plants.

Furthermore, we analyzed the expression of EXO70 family members in tobacco pollen at the transcript level in three different stages of pollen germination and by a

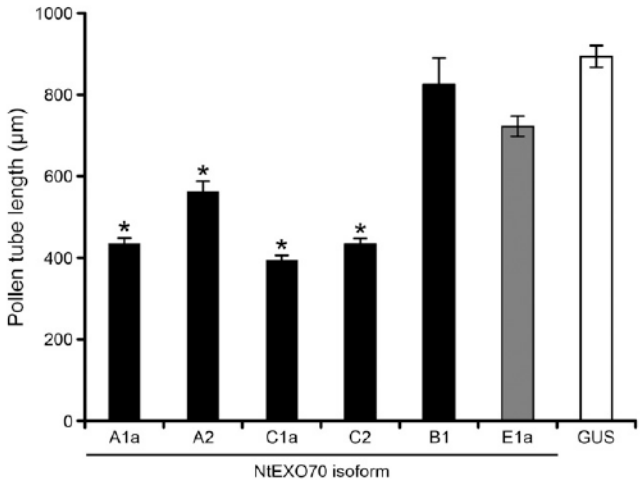

Figure 9. Overexpression of the major pollen EXO70 class members inhibits pollen tube growth. Tobacco pollen tubes transiently expressing high levels (5 μg of DNA) of selected tagged EXO70 isoforms and control (YFP-tagged GUS) were imaged 8 h after biolistic transformation by epifluorescence microscopy, and pollen tube lengths were determined. At least 100 cells from at least two independent transformations were measured for each construct. Asterisks indicate significant differences ($P < 0.001$) from the corresponding controls (GUS and NtEXO70E1a) according to ANOVA followed by posthoc multiple mean comparison test with Tukey contrasts using the multcomp R package. Data represent means of 100 or more pollen tubes ± SE.

proteomic approach. In total, transcripts of 10 genes from seven clades were detected (Fig. 2). Proteomic analysis identified the presence of NtEXO70A2 and all three members of the EXO70 C clade. Compared with known EXO70 family expression analyses of Arabidopsis pollen, the following picture can be drawn. At the transcript level, AtEXO70A2, AtEXO70C1, AtEXO70C2, AtEXO70F, AtEXO70G2, AtEXO70H3, and AtEXO70H5 can be detected in Arabidopsis pollen (Winter et al., 2007; Loraine et al., 2013; L. Synek, unpublished data), with C-clade EXO70s having the highest level of expression. Pollen expression of AtEXO70A2, AtEXO70C1, and AtEXO70C2 was further confirmed at the protein level (Grobei et al., 2009), with the prevalence of C-clade isoforms in the proteome, followed by AtEXO70A2. Together with our data obtained in tobacco, these results suggest that A- and C-clade EXO70s are the major angiosperm pollen isoforms. The importance of NtEXO70B1 (see below) for pollen growth in angiosperms outside the Solanaceae remains to be confirmed. Both tobacco and Arabidopsis express H-class EXO70s in pollen, although the particular isoforms differ, probably due to the rapid evolution of H-class EXO70s. Lower expression of certain isoforms suggests that they play marginal or regulatory roles.

We then investigated the subcellular localization of 20 EXO70 isoforms in growing tobacco pollen tubes by spinning disk confocal microscopy. NtEXO70A1a and NtEXO70B1 localized to distinct PM domains, as discussed below.

NtEXO70E1b localized to the inverted cone region, the structure where secretory/recycling vesicles accumulate (Hepler and Winship, 2015). NtEXO70E1b might play a regulatory role in earlier steps of the secretory pathway. However, biological interpretations of NtEXO70E1b localization to the inverted cone should be considered with caution due to the low native expression of NtEXO70E1b in tobacco pollen.

Interestingly, NtEXO70G1a decorated fibrillar structures resembling actin and the subapical membrane. This is similar to the subcellular localization of NET2A, a member of a newly discovered actin-interactor family, in Arabidopsis pollen (Deeks et al., 2012). NET superfamily proteins mediate the interaction of actin and various membranes in plant cells. In opisthokonts, exocyst interacts directly with both actin and the microtubule cytoskeleton (Synek et al., 2014), animal EXO70 was shown previously to interact directly with the Arp2/3 complex and regulate actin polymerization (Zuo et al., 2006; Liu et al., 2012), and EXO70 directly binds membrane in budding yeast and mammalian cells (He et al., 2007; Liu et al., 2007). Thus, NtEXO70G1a (or G-class EXO70s generally) might regulate part of the actin cytoskeleton and its interaction with the PM. The functions of G-clade EXO70s remain largely unexplored, and future studies are required to confirm our conclusions regarding NtEXO70G1a.

We further observed the accumulation of NtEXO70E2 in distinct bodies with little cytoplasmic localization. It is probable that NtEXO70E2 has the property of forming artificial structures when overexpressed. The expression of AtEXO70E2 is largely restricted to a few tissues like stomata (eFP browser), and the function of AtEXO70E2 is still not known. Since NtEXO70E2 is not natively expressed in pollen, the localization of tagged NtEXO70E2 is probably an artifact, and its native biological function remains to be established.

Surprisingly, two members of the rapidly evolving H class, NtEXO70H1-2 and NtEXO70H5-8b, exhibit strong enrichment in the nucleus with respect to the cytoplasm (NtEXO70H1-2 signal is almost absent from the cytoplasm). Since NtEXO70H1-2 is present in tobacco pollen, we believe that the nuclear localization of the tagged NtEXO70H1-2 reflects the native behavior of the protein. Furthermore, interactors of closely related Arabidopsis AtEXO70H1 identified by high-throughput screen include transcription factors (Žárský et al., 2013), and animal EXO70 was shown previously to shuttle into the nucleus and interact with spliceosomal components (Dellago et al., 2011). It is not clear whether ancestral eukaryotic EXO70 played a role in the nucleus among other processes or whether such a function was independently secondarily acquired for animal EXO70 and selected plant EXO70s. Our findings epitomize the previous notion that plant EXO70 proteins should be investigated not only in the light of the exocyst complex but also with the possibility of autonomous exocyst-independent function (Žárský et al., 2013).

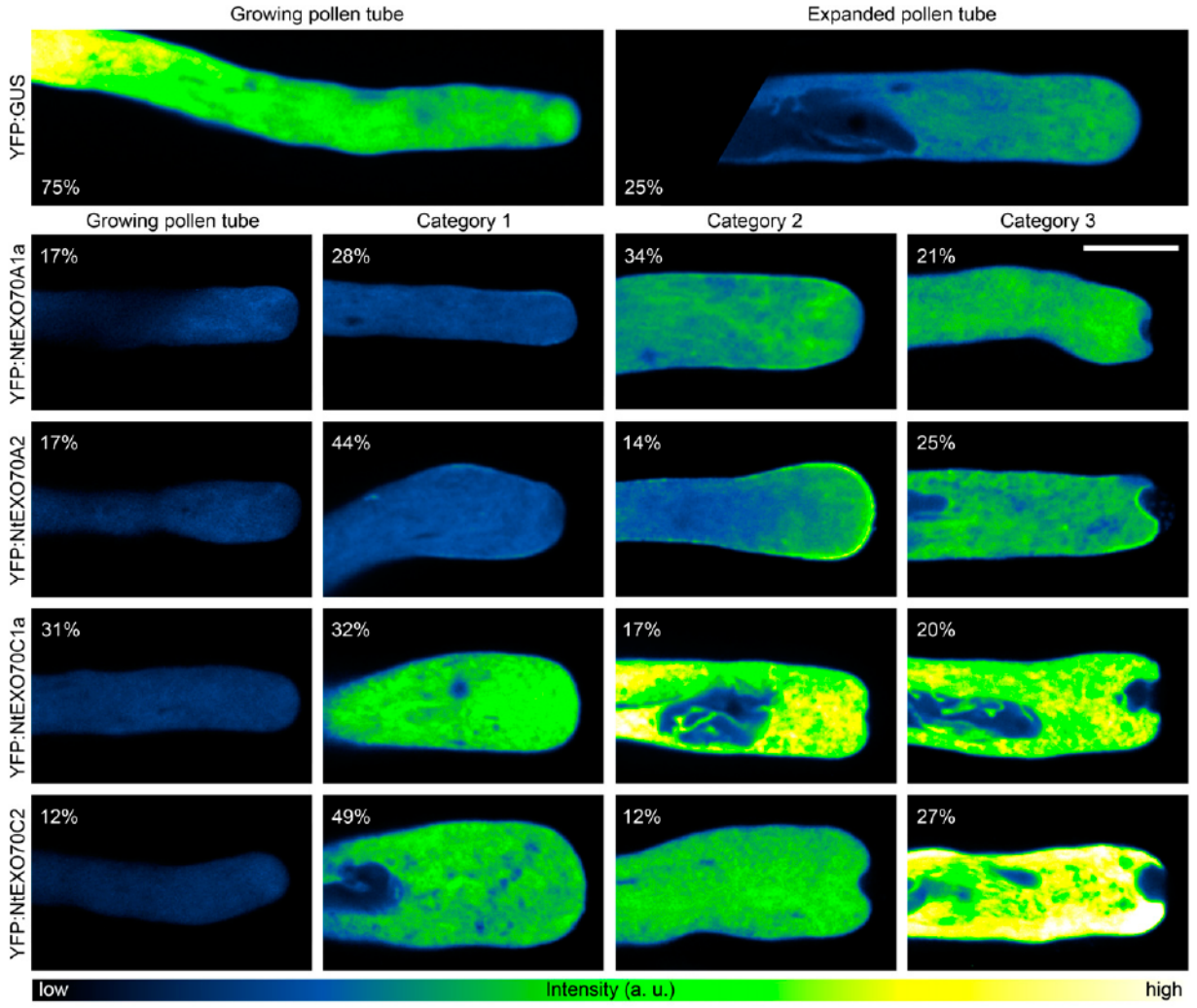

Figure 10. Effects of major pollen EXO70 isoform overexpression on the phenotypes of tobacco pollen tubes. Tobacco pollen tubes transiently expressing high levels of selected tagged EXO70 isoforms were imaged 8 h after biolistic transformation by spinning disk confocal microscopy. For each EXO70 isoform, pollen tubes were classified into four phenotypic categories (with the percentage of occurrence shown for each image). Control pollen tubes expressing YFP:GUS could be classified only into two categories. Images are displayed using a color intensity code with the same upper limit set for all images (see "Materials and Methods"), and the representative images thus reflect differences in signal intensity between the individual pollen tubes. The data are based on 33 or more transformed pollen tubes observed for each construct in three independent experiments. a.u., Arbitrary unit. Bar = 10 μm.

One of the key aims of this study was to use the polar tip-growing pollen tube as a universal model system to categorize the subcellular localization of the whole spectrum of the EXO70 family. Surprisingly, tagged versions of almost all isoforms not natively expressed in pollen localized only to the cytoplasm. Even in the case of closely related isoforms like NtEXO70E1a and NtEXO70E1b, the pollen-expressed isoform displayed distinct localization to the inverted cone while the isoform not expressed in pollen did not. Moreover, we observed very different localization for three closely related isoforms of the A clade. Even upon overexpression, the nonpollen NtEXO70A1b localized to the PM only rarely, while pollen isoforms from the A clade displayed a significant tendency to bind PM near the pollen tube tip (Figs. 3 and 10). Thus, coincident interactions with cell-specific protein partners are probably indispensable for the proper targeting of EXO70 isoforms. Small GTPases are important for budding yeast and animal EXO70 targeting (Wu et al., 2008; Pleskot et al., 2015). Plant EXO70s have been shown to interact with ROH1 (Kulich et al., 2010), and NOI family proteins might play a role in EXO70 membrane targeting (Afzal et al., 2013; Sabol et al, 2017). Given our observations, it is paramount to study EXO70s in cell types where they are natively expressed.

NtEXO70A1a, NtEXO70A2, NtEXO70C1a, and EXO70C2 significantly inhibited pollen tube growth

upon overexpression, in contrast to YFP:GUS and NtEXO70E1a, a nonpollen isoform, used as controls. This is in agreement with the notion that EXO70 isoforms not natively expressed in pollen do not have functional properties there, probably due to the lack of tissue-specific protein interactors. We continued with more detailed analysis focused on morphological phenotypes of pollen tubes overexpressing major pollen EXO70s. Such an approach has been applied previously to elucidate the functions of proteins of interest in pollen tubes (Ischebeck et al., 2008, 2010; Stenzel et al., 2012). All four analyzed EXO70 isoforms induced distinct changes in pollen tube tips (Fig. 10). In each case, strong overexpressors displayed apical membrane invaginations. Such invaginations were reported previously as a result of the overexpression of phospholipid-modifying enzymes and are generally interpreted as a hallmark of disrupted cell polarity (Ischebeck et al., 2008; Stenzel et al., 2012). Previously, this phenotype was interpreted as a consequence of excessive endocytosis (Zhao et al., 2010), but it is often difficult to distinguish between an imbalance in exocytosis and endocytosis in plant cells without very detailed studies (Sekereš et al., 2015).

In striking contrast to YFP-tagged A-class EXO70s, C-class EXO70s never localized to the PM, even under conditions of strong overexpression or upon an increased intracellular PIP_2 level induced by the overexpression of PIP5K5. This suggests mutually exclusive roles of the two EXO70 families. Pollen tube tip swelling was described previously as a consequence of Rac-type GTPase overexpression (Klahre et al., 2006) and has been attributed to changes in the actin cytoskeleton (Fu et al., 2001). Although tip swelling of the C-class EXO70 overexpressors is much less pronounced than in the case of Rac-type GTPase overexpression, C-class EXO70s might regulate actin properties, similar to animal EXO70 (Zuo et al., 2006; Liu et al., 2012). Another possible interpretation could be that EXO70 C-class isoforms play the negative regulatory function of exocyst membrane binding. The proteins are overly similar to A-class EXO70s but lack the ability to bind membrane. In Arabidopsis, C-class EXO70s are expressed specifically in tip-growing cells: root hairs and pollen. Tip-growing cells grow relatively fast and need to focus exocytosis to a small area near the growing tip. It is possible that exocyst is bound by C-class EXO70 isoforms not capable of targeting the complex and secretory vesicle to the membrane in most of the cell body. In the tip, where A-class EXO70s bind to the PM, possibly due to local lipid and protein interactors, the secretory vesicle would be allowed to fuse with the PM and deliver the cargo. Exchange of the EXO70 isoform of exocyst was already proposed as an important cellular reaction to changing conditions (Žárský et al., 2013), but it also could act as a spatial regulatory event after exocyst relocalization within the cell. This model also is supported by the fact that AtEXO70C1 and AtEXO70C2 are expressed in a nonstoichiometric manner with respect to the exocyst subunits in Arabidopsis (eFP browser), and C-class EXO70s are prevalent over A-class EXO70s in the pollen proteome (Grobei et al., 2009; this study). Thus, an inhibitory C class without membrane-binding properties is prevalent in cytoplasm and could prevent ectopic vesicle fusion before vesicles reach the tip where A-class EXO70s reside. Therefore, overexpression of C-class EXO70s would cause an imbalance in exocytosis regulation, resulting in the described phenotypes.

Most importantly, we demonstrated the localization of NtEXO70A1a and NtEXO70B1 to two distinct, mutually exclusive domains of the pollen tube PM (Fig. 4). The small area of NtEXO70A1a localization corresponds to the previously described area of exocytosis maximum in the pollen tube (Bove et al., 2008; Idilli et al., 2013; Luo et al., 2016). This localization is in accordance with previous characterizations of Arabidopsis EXO70A1 as the isoform generally responsible for exocytosis in many plant tissues (Synek et al., 2006; Hála et al., 2008; Samuel et al., 2009; Kulich et al., 2010; Drdová et al., 2013; Fendrych et al., 2013; Zhang et al., 2016; Vukašinović et al., 2017). In accordance with the published observations, NtEXO70A1a localizes both to the cytoplasm and to the specific area of the PM. The enrichment of PM signal with respect to the cytoplasmic signal in growing pollen tubes was less pronounced compared with tissues like Arabidopsis rhizodermis and stigmatic papillae (Samuel et al., 2009; Zhang et al., 2016). Generally, the ratio of membrane to the cytoplasmic population of EXO70A1 differs among various cell types. For example, previous observations regarding the AtEXO70A1 distribution in Arabidopsis root tissues demonstrated a strong enrichment of GFP:AtEXO70A1 at the outer lateral PM of rhizodermal cells but significantly weaker apolar membrane enrichment of GFP:AtEXO70A1 in root cortical cells (Zhang et al., 2016). The overall abundance of the cytoplasmic NtEXO70A1a population in growing tobacco pollen tubes might be caused by the fact that the membrane domain of NtEXO70A1a localization and cellular secretion is very small and focused. Thus, a high concentration of the peripheral membrane protein targeting the secretion could facilitate its dynamic recruitment to this focused area.

According to previous findings, the role of EXO70B1 in plants is more complex. It is important for autophagy and autophagy-derived transport to the vacuole (Kulich et al., 2013) but also was shown to localize to the PM during light-induced stomatal opening when ectopically expressed in fava bean (*Vicia faba*) protoplasts (Hong et al., 2016). EXO70B1 also was suggested to be involved in unconventional secretion in specific circumstances like defense against pathogen attack (Žárský et al., 2013; Kulich and Žárský, 2014). Although it is an extremely useful model system for examining the membrane-binding properties of peripheral membrane proteins in plant cells, the tobacco pollen tube is still limited by the impossibility of directly testing the functionality of fluorescently tagged proteins by rescuing the phenotype in a mutant background. Thus, we verified our observations of N-terminal YFP:NtEXO70

fusion proteins by examining the subcellular localization of the C-terminally YFP-tagged NtEXO70B1, which confirmed the previous observation of the corresponding N-terminally tagged protein (Supplemental Fig. S4A). Moreover, AtEXO70B1 was demonstrated previously to rescue the mutant phenotype in Arabidopsis (Kulich et al., 2013). We thus conclude that the observed localization patterns of tagged EXO70 isoforms are biologically relevant.

There are several possible hypotheses explaining the localization of NtEXO70B1 to the subapical region of the pollen tube posterior to the zone of NtEXO70A1a localization. First, NtEXO70B1 might drive an unconventional secretory pathway delivering a specific cargo, alternative to the bulk secretion driven by NtEXO70A1a. This would be in accordance with the general model involving exocytosis to different membrane domains by different EXO70 isoforms (Žárský et al., 2009). Indeed, both NtEXO70A1a and NtEXO70B1 overlap with NtSEC3a at the PM (Fig. 5; Supplemental Fig. S4B). This supports the idea that both EXO70s can act as part of a complex together with other exocyst subunits. One possible mechanism would involve the dynamic replacement of NtEXO70A1a by NtEXO70B1 after cargo delivery. Alternatively, there can be two subpopulations of NtSEC3a-containing exocyst particles: one binding NtEXO70A1a and the other binding NtEXO70B1. This would also explain why the previously described membrane signal of NtSEC3a (Bloch et al., 2016) seems rather broad in comparison with the narrow area of bulk exocytosis in the tobacco pollen tube (Bove et al., 2008; Idilli et al., 2013; Luo et al., 2016). Second, NtEXO70B1 also could play a role in pollen tube endocytosis. Large-scale analysis previously suggested exocyst to be an important linking hub between exocytosis and endocytosis in budding yeast cells (Jose et al., 2015). After delivering secretory cargo to the PM, exocyst or its subcomplex could orchestrate subsequent endocytic recycling. NtEXO70B1 localizes to the area where most of the clathrin-mediated endocytic recycling occurs (Derksen et al., 1995; Moscatelli et al., 2007). This is further supported by colocalization studies with a clathrin endocytosis marker, AtDRP1C, that largely overlaps with NtEXO70B1, and the subapical onset of the membrane localization is identical for both proteins. Importantly, the zone of clathrin endocytosis visualized by DRP1C does not overlap with the region decorated by NtEXO70A1a (Supplemental Fig. S5). Third, subapical NtEXO70B1 could play an exocyst-independent role in pollen tube membrane traffic by assisting membrane remodeling similar to animal Exo70p (Zhao et al., 2013).

Notably, the distinct localization of NtEXO70A1a and NtEXO70B1 also may reflect their different phospholipid-binding properties. As proposed previously (Potocký et al., 2014), the near-subapical overlap of PA and PIP_2 could define a distinct domain responsible for the recruitment of certain effectors. Since onsets of NtEXO70A1a and PA marker localization are identical and membrane NtEXO70A1a signal also overlaps with PIP_2 localization (Fig. 7), it is possible that the membrane recruitment of NtEXO70A1a requires the simultaneous detection of both PA and PIP_2. Conversely, NtEXO70B1 localization is largely excluded from the PIP_2-decorated apex and corresponds to the area of the pollen tube strongly decorated by the PA marker. Thus, it is probable that the local phospholipid composition of the PM fine-tunes the membrane affinity toward selected EXO70 isoforms. Protein interactors also are likely to be involved, because A-class EXO70 isoforms display different affinity toward the target PM domain, even though they share amino acid residues predicted to bind minor acidic phospholipids (Žárský et al., 2009).

We conclude that the diversity of EXO70 isoforms in plant cells can play a role in targeting different exocyst complexes or subcomplexes to specific PM domains, but EXO70 isoforms also can be involved in processes not related to membrane trafficking, possibly acting outside the exocyst complex. C-class EXO70 proteins, specifically expressed in tip-growing cells, do not directly bind membrane and probably have a regulatory function. Our results also strongly indicate that EXO70 isoforms need to be studied in cell types in which they are normally expressed. Two of the studied isoforms, NtEXO70A1a and NtEXO70B1, occupy mutually exclusive areas of the pollen tube PM. They exhibit different localization patterns toward the endocytosis marker and lipid probes, and both overlap with the exocyst subunit NtSEC3 at the PM. Since specific interactions with membrane lipids may be important for the membrane recruitment of these isoforms, functional and pharmacological studies will be used in the future to elucidate causal relationships between the distribution of different minor acidic phospholipids and the recruitment of particular EXO70 isoforms.

MATERIALS AND METHODS

Sequence and Phylogenetic Analyses

Tobacco (*Nicotiana tabacum*) and tomato (*Solanum lycopersicum*) EXO70 sequences were identified by BLAST searches against corresponding genome databases at the Sol Genomics Network database (https://solgenomics.net) with multiple members of the AtEXO70 family as input query sequences. In most cases, default search parameters were used with occasional modifications (word size 2, scoring matrix BLOSUM45). Multiple alignments were constructed with MAFFT algorithms in E-INS-i mode (Katoh and Toh, 2008) and manually adjusted. Conserved sequence blocks were concatenated, giving alignment with 70 sequences and 588 positions. The maximum likelihood method using the PhyML program (Guindon and Gascuel, 2003) was employed for phylogeny inference with the LG matrix, γ-corrected for among-site rate variation with four rate site categories plus a category for invariable sites, with all parameters estimated from the data. Bayesian tree searches were performed using MrBayes 3.1 (Ronquist and Huelsenbeck, 2003) with a WAG amino acid model, where the analysis was performed in four runs with six chains and 1,000,000 generations, and trees were sampled every 100 generations. All four runs asymptotically approached the same stationarity after the first 200,000 generations, which were omitted from the final analysis.

RT-PCR Expression Analysis

RNA from freshly hydrated pollen, germinating pollen (hydrated and incubated in liquid medium [Klahre et al., 2006] for 40 min), and growing pollen tubes (hydrated and incubated in liquid medium for 3 h) of tobacco was isolated

using the RNeasy Kit (Qiagen). Residual DNA was removed with the Turbo DNA-free Kit (Thermo Fisher), and the RNA was transcribed to cDNA using the Transcriptor High Fidelity cDNA Synthesis Kit (Roche). Primers for specific detection of EXO70 paralogs (Supplemental Table S1) were used for subsequent PCR analysis, and tobacco actin was used as the control gene as described by Bosch et al. (2005).

Proteomic Expression Analysis

Pollen tubes were cultivated in liquid medium (Klahre et al., 2006) for 2 h at 150 rpm. They were subsequently vacuum filtered, resuspended in lysis buffer (Potocký et al., 2012), and lysed by sonication. Lysed tubes were centrifuged three times (8,000*g*, 10 min, 4°C) to get the crude extract. Crude extract protein samples were separated on 10% SDS-PAGE gels, and the band corresponding to 70 kD was cut. Alternatively, the peripheral membrane protein fraction was prepared according to McLoughlin et al. (2013), proteins were separated by 10% SDS-PAGE, and the lane was cut into three bands. After in-gel digestion with trypsin, eluted peptides were identified using UHPLC Dionex Ultimate3000 RSLC nano (Dionex) connected with the mass spectrometer ESI-Q-TOF Maxis Impact (Bruker). Measurements were carried out in positive ion mode with precursor ion selection in the range of 400 to 1,400 mass-to-charge ratio; up to 10 precursor ions were selected for fragmentation from each mass spectrometry spectrum. Peak lists were extracted from raw data by Data Analysis version 4.1 (Bruker Daltonics) and uploaded to the data management system Proteinscape (Bruker Daltonics). For protein identification, the Mascot server (version 2.4.1; Matrix Science) was used with a custom-made database containing tobacco variety K326 and SwissProt proteins.

Molecular Cloning

Most EXO70 coding sequences are intronless and were amplified from tobacco genomic DNA (prepared using Plant DNAzol reagent; Thermo Fisher). EXO70s from the A clade were amplified from a mix of tobacco leaf and pollen cDNA (for preparation, see "RT-PCR Expression Analysis"). AtDRP1C was cloned from Arabidopsis (*Arabidopsis thaliana*) cDNA. Primers used for molecular cloning together with specific restriction sites are listed in Supplemental Table S2. For N-terminal YFP and mRFP fusions, EXO70 isoforms were cloned into pWEN240 (LAT52:YFP-GA5-MCS:NOS) and pHD222 (LAT52:MCS-GA5-mRFP:NOS) vectors, respectively (Klahre et al., 2006). For C-terminal mRFP fusion of AtDRP1C, we used the pHD223 vector (LAT52:mRFP-GA5-MCS:NOS; Klahre et al., 2006).

Pollen Transformation and Microscopic Analysis

Expression vectors were transferred into tobacco pollen grains germinating on solid culture medium by particle bombardment using a helium-driven particle-delivery system (PDS-1000/He; Bio-Rad) as described previously (Kost et al., 1998). Particles were coated with 1 μg of DNA for subcellular protein localization studies and with 5 μg of DNA for overexpression studies. When two constructs were coexpressed, particles were coated with 1 μg of each DNA plasmid (unless explicitly stated). For observation of subcellular protein localization, 6- to 8-h-old pollen tubes were observed. For overexpression analyses, 8- to 10-h-old pollen tubes were used. For measurement of pollen tube growth inhibition, we used an upright wide-field microscope (Zeiss Axioimager, HPX120V excitation, with camera Axiocam 506 mono) with Achromat 5× dry (numerical aperture = 0.16) objective. For the observation of subcellular protein localization and detailed studies of overexpression-induced phenotypes, we used a spinning disk confocal microscope (Yokogawa CSU-X1 on Nikon Ti-E platform, laser box Agilent MLC400, with sCMOS camera Andor Zyla) with Lense Plan Apochromat 60× WI (numerical aperture = 1.2) objective and 488- and 561-nm laser lines.

Quantitative Image Analysis

For measurements of the equatorial distance of the onset and end of membrane signal, we subtracted background signal and then manually measured the distances from the tip of pollen tubes along the pollen tube membrane (using segmented line and length measurements in ImageJ software). Data are presented as box plots where the horizontal line in the box represents the median, the top and bottom lines of the box represent the 75th and 25th percentiles, and the top-most and bottom-most lines represent extreme values. For evaluation of the effect of EXO70 isoform overexpression on pollen tube morphology and presentation of pollen tubes with typical morphological phenotypes, we applied the following criteria on all images (obtained with the same acquisition setup): the background signal was subtracted, the maximum value of the intensity scale was set to 2,500 (an arbitrary value we empirically found to cover the whole intensity spectrum of signal even for very strong representative overexpressors), and a color intensity code was used to present the processed images. For the quantitative evaluation of YFP-tagged protein overexpression, we measured maximum intensity values of individual images.

Accession Numbers

Sequence data from this article can be found in the GenBank/EMBL data libraries under accession numbers NtExo70A1a, KY499241; NtEXO70A1b, KY499242; NtEXO70A2, KY499243; NtEXO70B1, KY499244; NtExo70C1a, KY499245; NtEXO70C1b, KY499246; NtEXO70C2, KY499247; NtEXO70D1a, KY499248; NtExo70D1b, KY499249; NtEXO70E1a, KY499250; NtEXO70E1b, KY499251; NtEXO70E2, KY499252; NtEXO70F, KY499253; NtEXO70G1a, KY499254; NtEXO70G2, KY499255; NtEXO70H1-2, KY499256; NtEX070H3-4b, KY499257; NtEXO70H5-8a, KY499258; NtEXO70H5-8b, KY499259; NtEXO70H5-8c, KY499260.

Supplemental Data

The following supplemental materials are available.

Supplemental Figure S1. Localization of nonpollen EXO70 isoforms in growing tobacco pollen tubes.

Supplemental Figure S2. Comparison of the NtEXO70A1a and NtEXO70A1b amino acid sequences.

Supplemental Figure S3. Localization of YFP:NtEXO70G1a in growing tobacco pollen tubes with different expression levels.

Supplemental Figure S4. Localization of YFP:NtEXO70B1 and NtEXO70B1:YFP in growing tobacco pollen tubes with different expression levels and colocalization of NtEXO70B1 with NtSEC3a.

Supplemental Figure S5. Mutually exclusive localization of NtEXO70A1a and AtDRP1C in growing tobacco pollen tubes.

Supplemental Figure S6. Fluorescence signal intensity distribution in pollen tubes overexpressing major pollen N-terminally YFP-tagged EXO70 isoforms or the YFP:GUS control.

Supplemental Figure S7. Overexpression of PIP5K5 results in increased NtSEC3a recruitment to the PM in pollen tubes but does not recruit NtEXO70C2 to the PM.

Supplemental Table S1. Primers used for RT-PCR expression analysis of the EXO70 family.

Supplemental Table S2. Primers used for molecular cloning.

Supplemental Movie S1. Localization of YFP:NtEXO70A1a in a growing tobacco pollen tube.

Supplemental Movie S2. Localization of YFP:NtEXO70B1 in a growing tobacco pollen tube.

Supplemental Movie S3. Localization of YFP:NtEXO70E2 in a growing tobacco pollen tube.

Supplemental Movie S4. Localization of YFP:NtEXO70G1a in a growing tobacco pollen tube.

Supplemental File S1. Nucleotide sequences of EXO70 clones used in this study.

ACKNOWLEDGMENTS

We thank Dr. Ingo Heilmann and colleagues for providing the plasmid encoding PIP5K5:CFP and Dr. Roman Pleskot for careful and critical reading of the article, including useful comments.

Received November 4, 2016; accepted January 10, 2017; published January 12, 2017.

LITERATURE CITED

Afzal AJ, Kim JH, Mackey D (2013) The role of NOI-domain containing proteins in plant immune signaling. BMC Genomics **14:** 327

Bloch D, Pleskot R, Pejchar P, Potocký M, Trpkošová P, Cwiklik L, Vukašinović N, Sternberg H, Yalovsky S, Žárský V (2016) Exocyst SEC3 and phosphoinositides define sites of exocytosis in pollen tube initiation and growth. Plant Physiol **172:** 980–1002

Bodemann BO, Orvedahl A, Cheng T, Ram RR, Ou YH, Formstecher E, Maiti M, Hazelett CC, Wauson EM, Balakireva M, et al (2011) RalB and the exocyst mediate the cellular starvation response by direct activation of autophagosome assembly. Cell **144:** 253–267

Bosch M, Cheung AY, Hepler PK (2005) Pectin methylesterase, a regulator of pollen tube growth. Plant Physiol **138:** 1334–1346

Bove J, Vaillancourt B, Kroeger J, Hepler PK, Wiseman PW, Geitmann A (2008) Magnitude and direction of vesicle dynamics in growing pollen tubes using spatiotemporal image correlation spectroscopy and fluorescence recovery after photobleaching. Plant Physiol **147:** 1646–1658

Chen XW, Inoue M, Hsu SC, Saltiel AR (2006) RalA-exocyst-dependent recycling endosome trafficking is required for the completion of cytokinesis. J Biol Chem **281:** 38609–38616

Chong YT, Gidda SK, Sanford C, Parkinson J, Mullen RT, Goring DR (2010) Characterization of the Arabidopsis thaliana exocyst complex gene families by phylogenetic, expression profiling, and subcellular localization studies. New Phytol **185:** 401–419

Cole RA, Synek L, Žárský V, Fowler JE (2005) SEC8, a subunit of the putative Arabidopsis exocyst complex, facilitates pollen germination and competitive pollen tube growth. Plant Physiol **138:** 2005–2018

Cvrčková F, Grunt M, Bezvoda R, Hála M, Kulich I, Rawat A, Žárský V (2012) Evolution of the land plant exocyst complexes. Front Plant Sci **3:** 159

Deeks MJ, Calcutt JR, Ingle EK, Hawkins TJ, Chapman S, Richardson AC, Mentlak DA, Dixon MR, Cartwright F, Smertenko AP, et al (2012) A superfamily of actin-binding proteins at the actin-membrane nexus of higher plants. Curr Biol **22:** 1595–1600

Dellago H, Löscher M, Ajuh P, Ryder U, Kaisermayer C, Grillari-Voglauer R, Fortschegger K, Gross S, Gstraunthaler A, Borth N, et al (2011) Exo70, a subunit of the exocyst complex, interacts with SNEV (hPrp19/hPso4) and is involved in pre-mRNA splicing. Biochem J **438:** 81–91

Derksen J, Rutten T, Lichtscheidl IK, de Win AHN, Pierson ES, Rongen G (1995) Quantitative analysis of the distribution of organelles in tobacco pollen tubes: implications for exocytosis and endocytosis. Protoplasma **3:** 267–276

Donovan KW, Bretscher A (2015) Tracking individual secretory vesicles during exocytosis reveals an ordered and regulated process. J Cell Biol **210:** 181–189

Dörmann P, Kim H, Ott T, Schulze-Lefert P, Trujillo M, Wewer V, Hückelhoven R (2014) Cell-autonomous defense, re-organization and trafficking of membranes in plant-microbe interactions. New Phytol **204:** 815–822

Drdová EJ, Synek L, Pečenková T, Hála M, Kulich I, Fowler JE, Murphy AS, Žárský V (2013) The exocyst complex contributes to PIN auxin efflux carrier recycling and polar auxin transport in Arabidopsis. Plant J **73:** 709–719

Dubuke ML, Maniatis S, Shaffer SA, Munson M (2015) The exocyst subunit Sec6 interacts with assembled exocytic SNARE complexes. J Biol Chem **290:** 28245–28256

Eliáš M, Drdová E, Žiak D, Bavlnka B, Hála M, Cvrčková F, Soukupová H, Žárský V (2003) The exocyst complex in plants. Cell Biol Int **27:** 199–201

Fendrych M, Synek L, Pečenková T, Drdová EJ, Sekereš J, de Rycke R, Nowack MK, Žársky V (2013) Visualization of the exocyst complex dynamics at the plasma membrane of Arabidopsis thaliana. Mol Biol Cell **24:** 510–520

Fendrych M, Synek L, Pečenková T, Toupalová H, Cole R, Drdová E, Nebesárová J, Sedinová M, Hála M, Fowler JE, et al (2010) The *Arabidopsis* exocyst complex is involved in cytokinesis and cell plate maturation. Plant Cell **22:** 3053–3065

France YE, Boyd C, Coleman J, Novick PJ (2006) The polarity-establishment component Bem1p interacts with the exocyst complex through the Sec15p subunit. J Cell Sci **119:** 876–888

Fu Y, Wu G, Yang Z (2001) Rop GTPase-dependent dynamics of tip-localized F-actin controls tip growth in pollen tubes. J Cell Biol **152:** 1019–1032

Grobei MA, Qeli E, Brunner E, Rehrauer H, Zhang R, Roschitzki B, Basler K, Ahrens CH, Grossniklaus U (2009) Deterministic protein inference for shotgun proteomics data provides new insights into Arabidopsis pollen development and function. Genome Res **19:** 1786–1800

Guindon S, Gascuel O (2003) A simple, fast, and accurate algorithm to estimate large phylogenies by maximum likelihood. Syst Biol **52:** 696–704

Hála M, Cole R, Synek L, Drdová E, Pečenková T, Nordheim A, Lamkemeyer T, Madlung J, Hochholdinger F, Fowler JE, et al (2008) An exocyst complex functions in plant cell growth in *Arabidopsis* and tobacco. Plant Cell **20:** 1330–1345

Hase K, Kimura S, Takatsu H, Ohmae M, Kawano S, Kitamura H, Ito M, Watarai H, Hazelett CC, Yeaman C, et al (2009) M-Sec promotes membrane nanotube formation by interacting with Ral and the exocyst complex. Nat Cell Biol **11:** 1427–1432

He B, Xi F, Zhang X, Zhang J, Guo W (2007) Exo70 interacts with phospholipids and mediates the targeting of the exocyst to the plasma membrane. EMBO J **26:** 4053–4065

Heider MR, Gu M, Duffy CM, Mirza AM, Marcotte LL, Walls AC, Farrall N, Hakhverdyan Z, Field MC, Rout MP, et al (2016) Subunit connectivity, assembly determinants and architecture of the yeast exocyst complex. Nat Struct Mol Biol **23:** 59–66

Hepler PK, Winship LJ (2015) The pollen tube clear zone: clues to the mechanism of polarized growth. J Integr Plant Biol **57:** 79–92

Hong D, Jeon BW, Kim SY, Hwang JU, Lee Y (2016) The ROP2-RIC7 pathway negatively regulates light-induced stomatal opening by inhibiting exocyst subunit Exo70B1 in Arabidopsis. New Phytol **209:** 624–635

Idilli AI, Morandini P, Onelli E, Rodighiero S, Caccianiga M, Moscatelli A (2013) Microtubule depolymerization affects endocytosis and exocytosis in the tip and influences endosome movement in tobacco pollen tubes. Mol Plant **6:** 1109–1130

Ischebeck T, Stenzel I, Heilmann I (2008) Type B phosphatidylinositol-4-phosphate 5-kinases mediate *Arabidopsis* and *Nicotiana tabacum* pollen tube growth by regulating apical pectin secretion. Plant Cell **20:** 3312–3330

Ischebeck T, Stenzel I, Hempel F, Jin X, Mosblech A, Heilmann I (2011) Phosphatidylinositol-4,5-bisphosphate influences Nt-Rac5-mediated cell expansion in pollen tubes of *Nicotiana tabacum*. Plant J **65:** 453–468

Ischebeck T, Vu LH, Jin X, Stenzel I, Löfke C, Heilmann I (2010) Functional cooperativity of enzymes of phosphoinositide conversion according to synergistic effects on pectin secretion in tobacco pollen tubes. Mol Plant **3:** 870–881

Ischebeck T, Werner S, Krishnamoorthy P, Lerche J, Meijón M, Stenzel I, Löfke C, Wiessner T, Im YJ, Perera IY, et al (2013) Phosphatidylinositol 4,5-bisphosphate influences PIN polarization by controlling clathrin-mediated membrane trafficking in *Arabidopsis*. Plant Cell **25:** 4894–4911

Jose M, Tollis S, Nair D, Mitteau R, Velours C, Massoni-Laporte A, Royou A, Sibarita JB, McCusker D (2015) A quantitative imaging-based screen reveals the exocyst as a network hub connecting endocytosis and exocytosis. Mol Biol Cell **26:** 2519–2534

Katoh K, Toh H (2008) Recent developments in the MAFFT multiple sequence alignment program. Brief Bioinform **9:** 286–298

Klahre U, Becker C, Schmitt AC, Kost B (2006) Nt-RhoGDI2 regulates Rac/Rop signaling and polar cell growth in tobacco pollen tubes. Plant J **46:** 1018–1031

Konopka CA, Bednarek SY (2008) Comparison of the dynamics and functional redundancy of the Arabidopsis dynamin-related isoforms DRP1A and DRP1C during plant development. Plant Physiol **147:** 1590–1602

Kost B, Spielhofer P, Chua NH (1998) A GFP-mouse talin fusion protein labels plant actin filaments *in vivo* and visualizes the actin cytoskeleton in growing pollen tubes. Plant J **16:** 393–401

Kulich I, Cole R, Drdová E, Cvrčková F, Soukup A, Fowler J, Žárský V (2010) Arabidopsis exocyst subunits SEC8 and EXO70A1 and exocyst interactor ROH1 are involved in the localized deposition of seed coat pectin. New Phytol **188:** 615–625

Kulich I, Pečenková T, Sekereš J, Smetana O, Fendrych M, Foissner I, Höftberger M, Žárský V (2013) Arabidopsis exocyst subcomplex containing subunit EXO70B1 is involved in autophagy-related transport to the vacuole. Traffic **14:** 1155–1165

Kulich I, Vojtíková Z, Glanc M, Ortmannová J, Rasmann S, Žárský V (2015) Cell wall maturation of Arabidopsis trichomes is dependent on exocyst subunit EXO70H4 and involves callose deposition. Plant Physiol **168:** 120–131

Kulich I, Žárský V (2014) Autophagy-related direct membrane import from ER/cytoplasm into the vacuole or apoplast: a hidden gateway also for secondary metabolites and phytohormones? Int J Mol Sci **15:** 7462–7474

Łangowski L, Růzicka K, Naramoto S, Kleine-Vehn J, Friml J (2010) Trafficking to the outer polar domain defines the root-soil interface. Curr Biol **20:** 904–908

Łangowski Ł, Wabnik K, Li H, Vanneste S, Naramoto S, Tanaka H, Friml J (2016) Cellular mechanisms for cargo delivery and polarity maintenance at different polar domains in plant cells. Cell Discov **2:** 16018

Liu D, Novick P (2014) Bem1p contributes to secretory pathway polarization through a direct interaction with Exo70p. J Cell Biol **207:** 59–72

Liu J, Zhao Y, Sun Y, He B, Yang C, Svitkina T, Goldman YE, Guo W (2012) Exo70 stimulates the Arp2/3 complex for lamellipodia formation and directional cell migration. Curr Biol **22:** 1510–1515

Liu J, Zuo X, Yue P, Guo W (2007) Phosphatidylinositol 4,5-bisphosphate mediates the targeting of the exocyst to the plasma membrane for exocytosis in mammalian cells. Mol Biol Cell **18:** 4483–4492

Lora J, Hormaza JI, Herrero M (2016) The diversity of the pollen tube pathway in plants: toward an increasing control by the sporophyte. Front Plant Sci **7:** 107

Loraine AE, McCormick S, Estrada A, Patel K, Qin P (2013) RNA-seq of Arabidopsis pollen uncovers novel transcription and alternative splicing. Plant Physiol **162:** 1092–1109

Luo N, Yan A, Yang Z (2016) Measuring exocytosis rate using corrected fluorescence recovery after photoconversion. Traffic **17:** 554–564

Martin-Urdiroz M, Deeks MJ, Horton CG, Dawe HR, Jourdain I (2016) The exocyst complex in health and disease. Front Cell Dev Biol **4:** 24

McLoughlin F, Arisz SA, Dekker HL, Kramer G, de Koster CG, Haring MA, Munnik T, Testerink C (2013) Identification of novel candidate phosphatidic acid-binding proteins involved in the salt-stress response of Arabidopsis thaliana roots. Biochem J **450:** 573–581

Morgera F, Sallah MR, Dubuke ML, Gandhi P, Brewer DN, Carr CM, Munson M (2012) Regulation of exocytosis by the exocyst subunit Sec6 and the SM protein Sec1. Mol Biol Cell **23:** 337–346

Moscatelli A, Ciampolini F, Rodighiero S, Onelli E, Cresti M, Santo N, Idilli A (2007) Distinct endocytic pathways identified in tobacco pollen tubes using charged nanogold. J Cell Sci **120:** 3804–3819

Ostertag M, Stammler J, Douchkov D, Eichmann R, Hückelhoven R (2013) The conserved oligomeric Golgi complex is involved in penetration resistance of barley to the barley powdery mildew fungus. Mol Plant Pathol **14:** 230–240

Pečenková T, Hála M, Kulich I, Kocourková D, Drdová E, Fendrych M, Toupalová H, Žársky V (2011) The role for the exocyst complex subunits Exo70B2 and Exo70H1 in the plant-pathogen interaction. J Exp Bot **62:** 2107–2116

Pleskot R, Cwiklik L, Jungwirth P, Žárský V, Potocký M (2015) Membrane targeting of the yeast exocyst complex. Biochim Biophys Acta **1848:** 1481–1489

Potocký M, Pejchar P, Gutkowska M, Jiménez-Quesada MJ, Potocká A, Alché JdeD, Kost B, Žárský V (2012) NADPH oxidase activity in pollen tubes is affected by calcium ions, signaling phospholipids and Rac/Rop GTPases. J Plant Physiol **169:** 1654–1663

Potocký M, Pleskot R, Pejchar P, Vitale N, Kost B, Žárský V (2014) Live-cell imaging of phosphatidic acid dynamics in pollen tubes visualized by Spo20p-derived biosensor. New Phytol **203:** 483–494

Ronquist F, Huelsenbeck JP (2003) MrBayes 3: Bayesian phylogenetic inference under mixed models. Bioinformatics **19:** 1572–1574

Qin Y, Dong J (2015) Focusing on the focus: what else beyond the master switches for polar cell growth? Mol Plant **8:** 582–594

Sabol P, Kulich I, Žárský V (2017) RIN4 recruits the exocyst subunit EXO70B1 to the plasma membrane. J Exp Bot doi/10.1093/jxb/erx007

Samuel MA, Chong YT, Haasen KE, Aldea-Brydges MG, Stone SL, Goring DR (2009) Cellular pathways regulating responses to compatible and self-incompatible pollen in *Brassica* and *Arabidopsis* stigmas intersect at Exo70A1, a putative component of the exocyst complex. Plant Cell **21:** 2655–2671

Sekereš J, Pleskot R, Pejchar P, Žárský V, Potocký M (2015) The song of lipids and proteins: dynamic lipid-protein interfaces in the regulation of plant cell polarity at different scales. J Exp Bot **66:** 1587–1598

Stegmann M, Anderson RG, Ichimura K, Pečenková T, Reuter P, Žárský V, McDowell JM, Shirasu K, Trujillo M (2012) The ubiquitin ligase PUB22 targets a subunit of the exocyst complex required for PAMP-triggered responses in Arabidopsis. Plant Cell **24:** 4703–4716

Stenzel I, Ischebeck T, Quint M, Heilmann I (2012) Variable regions of PI4P 5-kinases direct PtdIns(4,5)P_2 toward alternative regulatory functions in tobacco pollen tubes. Front Plant Sci **2:** 114

Synek L, Schlager N, Eliáš M, Quentin M, Hauser MT, Žárský V (2006) AtEXO70A1, a member of a family of putative exocyst subunits specifically expanded in land plants, is important for polar growth and plant development. Plant J **48:** 54–72

Synek L, Sekereš J, Žárský V (2014) The exocyst at the interface between cytoskeleton and membranes in eukaryotic cells. Front Plant Sci **4:** 543

TerBush DR, Maurice T, Roth D, Novick P (1996) The exocyst is a multiprotein complex required for exocytosis in Saccharomyces cerevisiae. EMBO J **15:** 6483–6494

Vaškovičová K, Žárský V, Rösel D, Nikolič M, Buccione R, Cvrčková F, Brábek J (2013) Invasive cells in animals and plants: searching for LECA machineries in later eukaryotic life. Biol Direct **8:** 8

Vukašinović N, Oda Y, Pejchar P, Synek L, Pečenková T, Rawat A, Sekereš J, Potocký M, Žárský V (2017) Microtubule-dependent targeting of the exocyst complex is necessary for xylem development in Arabidopsis. New Phytol **213:** 1052–1067

Wang H, Tang X, Liu J, Trautmann S, Balasundaram D, McCollum D, Balasubramanian MK (2002) The multiprotein exocyst complex is essential for cell separation in Schizosaccharomyces pombe. Mol Biol Cell **13:** 515–529

Wang N, Lee IJ, Rask G, Wu JQ (2016) Roles of the TRAPP-II complex and the exocyst in membrane deposition during fission yeast cytokinesis. PLoS Biol **14:** e1002437

Winter D, Vinegar B, Nahal H, Ammar R, Wilson GV, Provart NJ (2007) An "Electronic Fluorescent Pictograph" browser for exploring and analyzing large-scale biological data sets. PLoS ONE **2:** e718

Wu H, Rossi G, Brennwald P (2008) The ghost in the machine: small GTPases as spatial regulators of exocytosis. Trends Cell Biol **18:** 397–404

Wu H, Turner C, Gardner J, Temple B, Brennwald P (2010) The Exo70 subunit of the exocyst is an effector for both Cdc42 and Rho3 function in polarized exocytosis. Mol Biol Cell **21:** 430–442

Wu S, Mehta SQ, Pichaud F, Bellen HJ, Quiocho FA (2005) Sec15 interacts with Rab11 via a novel domain and affects Rab11 localization in vivo. Nat Struct Mol Biol **12:** 879–885

Žárský V, Cvrčková F, Potocký M, Hála M (2009) Exocytosis and cell polarity in plants: exocyst and recycling domains. New Phytol **183:** 255–272

Žárský V, Kulich I, Fendrych M, Pečenková T (2013) Exocyst complexes multiple functions in plant cells secretory pathways. Curr Opin Plant Biol **16:** 726–733

Žárský V, Potocký M (2010) Recycling domains in plant cell morphogenesis: small GTPase effectors, plasma membrane signalling and the exocyst. Biochem Soc Trans **38:** 723–728

Zhang C, Brown MQ, van de Ven W, Zhang ZM, Wu B, Young MC, Synek L, Borchardt D, Harrison R, Pan S, et al (2016) Endosidin2 targets conserved exocyst complex subunit EXO70 to inhibit exocytosis. Proc Natl Acad Sci USA **113:** E41–E50

Zhang X, Orlando K, He B, Xi F, Zhang J, Zajac A, Guo W (2008) Membrane association and functional regulation of Sec3 by phospholipids and Cdc42. J Cell Biol **180:** 145–158

Zhang X, Pumplin N, Ivanov S, Harrison MJ (2015) EXO70I is required for development of a sub-domain of the periarbuscular membrane during arbuscular mycorrhizal symbiosis. Curr Biol **25:** 2189–2195

Zhao Y, Liu J, Yang C, Capraro BR, Baumgart T, Bradley RP, Ramakrishnan N, Xu X, Radhakrishnan R, Svitkina T, et al (2013) Exo70 generates membrane curvature for morphogenesis and cell migration. Dev Cell **26:** 266–278

Zhao Y, Yan A, Feijó JA, Furutani M, Takenawa T, Hwang I, Fu Y, Yang Z (2010) Phosphoinositides regulate clathrin-dependent endocytosis at the tip of pollen tubes in *Arabidopsis* and tobacco. Plant Cell **22:** 4031–4044

Zuo X, Zhang J, Zhang Y, Hsu SC, Zhou D, Guo W (2006) Exo70 interacts with the Arp2/3 complex and regulates cell migration. Nat Cell Biol **8:** 1383–1388

Molecular architecture of the Arabidopsis exocyst complex reveals EXO70A1 as the key subunit required for targeting of the plant exocyst to the plasma membrane through the direct interaction with anionic phospholipids.

Lukáš Synek[a*], Juraj Sekereš[ab*], Roman Pleskot[a], Klára Aldorfová[ab], Edita Janková-Drdová[a], Vedrana Marković[ab], Jitka Ortmannová[ab], Tamara Pečenková[a], Přemysl Pejchar[a], Martina Růžičková[a], Hana Soukupová[a], Jiří Šantrůček[c], Nemanja Vukašinović[a], Viktor Žárský[ab#], and Martin Potocký[a#]

[a] *Institute of Experimental Botany, v.v.i., Academy of Sciences of the Czech Republic, 165 02 Prague, Czech Republic*

[b] *Department of Experimental Plant Biology, Faculty of Science, Charles University in Prague, 128 44 Prague, Czech Republic*

[c] *Department of Biochemistry and Microbiology, Faculty of Food and Biochemical Technology, 166 28, University of Chemistry and Technology, Prague*

[*] the authors contributed equally to the results of the work

[#] corresponding authors

Abstract

Polarized vesicular trafficking facilitates identity of polar membrane domains, which is essential for many vital processes of plant cells including transport of nutrients and signalling molecules, cell wall deposition and tissue morphogenesis, as well as defence against pathogens and interactions with symbiotic organisms. Vesicle tethering complex is one of the major cell polarity regulators in eukaryotes. Despite being well characterized in yeast and mammalian model systems, the molecular details of exocyst complex targeting in plants have so far remained

elusive. Our study combined genetics, molecular pharmacology, advanced live cell imaging, in vitro protein-lipid binding assays and computational molecular dynamics to uncover mechanisms of plant exocyst targeting with respect to phospholipid composition of the target membrane. We provide comprehensive analysis of plant exocyst architecture based on mass spectrometry proteomic measurements, which demonstrates evolutionary conservation of most interactions known from yeast and mammalian systems forming the two exocyst subcomplexes. We further confirmed the key function of the EXO70A1 subunit in targeting of the plant exocyst complex. Based on *in vitro* experiments, we then identified the anionic phospholipids phosphatidylinositol 4,5-bisphosphate, phosphatidylinositol 4 phosphate and phosphatidic acid as direct interactors of the EXO70A1. We subsequently confirmed key role of these phospholipids in EXO70A1 recruitment to the plasma membrane in both Arabidopsis and tobacco. We confirmed that together with the phosphatidylinositol 4,5-bisphosphate essential for exocyst targeting in other eukaryotes, phosphatidylinositol 4 phosphate and phosphatidic acid are crucial for this process as unique determinants of the plant plasma membrane identity.

Introduction

Eukaryotic cell plasma membrane (PM) is spatially segregated into domains of distinct function and composition at different scales, which is essential for many vital functions, including cell morphogenesis, symbiotic interactions and reaction to pathogens (Dörmann et al., 2014; Sekereš et al., 2015; Konrad and Ott, 2015). One of the key mechanisms contributing to establishment and maintenance of the polarity is localized exocytosis, which is orchestrated by precise regulation of the cytoskeleton and other secretory pathway components by an arsenal of small GTPases and their effectors, mainly the octameric vesicle tethering complex exocyst (Žárský et al., 2013; Synek et al., 2014). The exocyst regulates many cellular processes that employ polarity establishment and propagation, including yeast budding, maintenance of basolateral domain of animal epithelia and neurite outgrowth, as well as final stages of cytokinesis in yeast and mammalian cells (Martin-Urdiroz et al., 2016). Furthermore, some exocyst subunits play a role

in secretion-independent processes like autophagy (Bodemann et al., 2011) and mRNA splicing (Awasthi et al., 2001; Dellago et al., 2011). Mechanisms of exocyst function are best explored in budding yeast, where the complex facilitates contact of secretory vesicle and PM, due to Sec15p subunit direct interaction with vesicle-bound Rab GTPase Sec4p (Guo et al., 1999) and binding of Sec3p together with Exo70p to phosphatidylinositol 4,5-bisphosphate (PIP_2) (He et al., 2007; Zhang et al., 2008; Pleskot et al., 2015) and protein interactors (Robinson et al., 1999; Guo et al., 2001; Zhang et al., 2001) at the PM. The exocyst further facilitates formation of membrane fusion driving trans-SNARE complex due to interaction of t-SNARE Sso2 with Sec3p (Yue et al., 2017) and Sec9p with Sec6p (Sivaram et al., 2005), as well as recruitment of SNARE regulator SM protein Sec1 by the Sec6p subunit (Morgera et al., 2012). Sec15p also acts as one of the adaptors for myosin V in the yeast (Jin et al., 2011; Donovan and Bretscher, 2015). An emerging model of the complex based on partially solved structures of several exocyst subunits (Munson and Novick, 2006; Moore et al., 2007; Yamashita et al., 2010; Chen et al., 2017), protein interaction map, cryo-electron microscopy (Heider et al., 2016; Mei et al., 2018) and fluorescent microscopy (Picco et al., 2017) assumes that interlaced rod-like exocyst subunits align longitudinally at core of the complex with distant parts kept flexible and available for molecular interactions.

Exocyst complex is also involved in plethora of cell polarity governing processes in plant cells, including pectin secretion (Kulich et al., 2010), tip growth of root hairs (Synek et al., 2006; Pečenková et al., 2017) and pollen tubes (Cole et al., 2005), auxin transporter PIN exocytosis (Drdová et al., 2013), hypocotyl elongation (Hála et al., 2008), cell wall maturation (Vukašinović et al., 2017; Kulich et al., 2018) and interaction with pathogens (Pečenková et al., 2011; Ortmannová et al., 2018), as well as with fungal symbionts (Genre et al., 2012). Exocyst also plays essential role in plant cytokinesis initiation and cell plate maturation (Fendrych et al., 2013; Rybak et al., 2014). Like in case of growing yeast buds (TerBush and Novick, 1995), tight junctions in mammalian epithelial cells (Yeaman et al., 2004) and tips of growing neurites in neuronal cells (Vega and Hsu, 2001), the subcellular localization of plant exocyst correlates with the site of ongoing vesicle fusion, in contrast to t-SNARE protein SYP132, that is distributed evenly along the PM in plant cells (Fendrych et al., 2013). Fluorescently tagged exocyst subunits

are thus excellent reporters of exocytosis in space and time. In plants, they are enriched at outer lateral PM of root epidermis (Fendrych et al., 2013), near pollen tube tip (Hála et al., 2008; Bloch et al., 2016; Sekereš et al., 2017) and at sites of xylem (Vukašinović et al., 2017) and endodermis secondary cell wall deposition (Kalmbach et al., 2017). At higher resolution level, the exocyst visualization reveals dynamic foci representing "hot-spots" for exocytosis below the PM of root epidermis (Fendrych et al., 2013). Strikingly, while EXO70 is encoded by single gene in yeast and animal cells, many EXO70 isoforms exist in angiosperms (Eliáš et al., 2003; Žárský et al. 2009, Cvrčková et al. 2012). While some of the EXO70 isoforms are involved in tissue-specific secretion (Kulich et al., 2015), reaction to biotic stress (Pečenková et al., 2011; Ortmannová et al., 2018) or play regulatory role (Sekereš et al., 2017; Synek et al., 2017), most secretory processes regulated by canonical Arabidopsis exocyst complex seem to employ the EXO70A1 isoform. Mutant plants with missing EXO70A1 phenocopy secretory defects of core exocyst subunit mutants like seed coat deposition (Kulich et al., 2010), hypocotyl elongation (Synek et al., 2006), PIN protein recycling (Drdová et al., 2013) and stigmatic papillae growth (Safavian et al., 2015). Moreover, EXO70A1 is expressed in most tissues (Synek et al., 2006) and subcellular localizations of GFP-tagged core exocyst subunits and of EXO70A1 are identical in many cell types (Fendrych et al., 2010; Fendrych et al., 2013; Vukašinović et al., 2017; Kalmbach et al., 2017). Among the plethora Arabidopsis EXO70 isoforms, we have thus focused on function of EXO70A1 in plant exocyst architecture and targeting in this study.

Mechanism of exocyst membrane targeting involving direct interaction of EXO70 with phosphatidylinositol 4,5-bisphosphate (PIP_2) and specific PM protein interactors is well documented in Opisthokonts (He et al., 2007; Liu et al., 2007; Zhao et al., 2013), including atomistic details of PIP_2 binding and clustering by the yeast Exo70p (Pleskot et al., 2015). Near full-length of yeast, mouse and Arabidopsis EXO70 structures have already been solved based on crystallographic data (Dong et al., 2005; Hamburger et al., 2006; Moore et al., 2007).

While PIP_2-dependent recruitment is one of the most common mechanisms governing localization of peripheral membrane proteins to PM in Opisthokonts (Kolay et al., 2016), other anionic phospholipids like PA, PS and PI4P might be at least equally important as PIP_2 in

constituting plant PM lipid signature (Platre and Jaillais, 2017; Pleskot et al., 2014; Simon et al., 2016; Platre et al., 2018). This opens interesting opportunity for comparative studies uncovering both differences and conserved mechanisms of cell polarity regulation among different eukaryotic lineages. Although plant cell biology generally lags behind animal and yeast research, the advanced tools for investigating protein-lipid interactions including *in vitro* lipid binding assays and employment of computational biochemistry are starting to be applied in plant systems, like in case of actin capping protein (Pleskot et al., 2012b) and the exocyst subunit SEC3a (Bloch et al., 2016).

In this study we demonstrated a conserved evolutionary architecture of the exocyst complex and we refined the interaction map of the EXO70A1-containing plant exocyst complex architecture and confirmed essential role of the EXO70A1 for plant exocyst plasma membrane targeting. We further combined genetics, live cell imaging, biochemistry, structural protein homology modelling and molecular dynamics simulations to unravel molecular mechanism of the EXO70A1 membrane recruitment and role of specific phospholipid species in this process.

Results

Analysis of plant exocyst complex *in vivo* molecular architecture reveals presence of two conserved modules

Our previous research has uncovered multitude of pairwise interactions between the plant exocyst subunits with use of the yeast two-hybrid system (Hála et al., 2008; Fendrych et al., 2010; Vukašinović et al., 2017). In order to further refine our insight into plant exocyst molecular architecture, we utilized available collection of Arabidopsis lines, as well as lines newly created for the purpose of this study, expressing GFP-tagged exocyst subunits and performed immunoprecipitation using the tagged exocyst subunits as baits followed by mass spectrometry analysis of the isolated protein interactors. While Arabidopsis genomes encodes 23 different EXO70 isoforms, we focused on the EXO70A1 in our investigation of the exocyst

architecture. This isoform is widely expressed (Synek et al., 2006, Hála et al., 2008), sequentially and structurally close to the yeast and animal EXO70 (Žárský et al., 2009; Zhang et al., 2016) and exhibits the same subcellular localization in root cells as the core exocyst subunits observed so far (Fendrych et al., 2010; Drdová et al., 2013; Fendrych et al., 2013), so it is the best EXO70 candidate for investigation of the canonical plant exocyst complex. Immunoprecipitate of each bait contained at least two other exocyst subunits (Fig. 1). The peptide score matrix of the mass spectrometry results suggests tight association of subunits within 2 clusters with one cluster composed of SEC6, SEC8, SEC5a and SEC3a protein and the other one involving SEC15b, SEC10a/b, EXO84b and the EXO70A1 subunit. While presence of an exocyst subunit in mass spectrometry readout does not imply direct interaction with the particular bait, the higher peptide score of a specific pair of subunits suggests proximity of the subunits within the complex. Interestingly, systematic analysis of purified yeast exocyst complex (Heider et al., 2016), which was further supported *in vivo* by the PICT imaging approach in budding yeast (Picco et al., 2017) and by visible immunoprecipitation assay in animal cells (Katoh et al., 2015), demonstrated presence of two four-subunit modules with the same subunit composition as the clusters we identified when analyzing the plant exocyst. Our co-immunoprecipitation data corresponded well with the known binary interactions described earlier for both yeast and plant exocyst subunits, i.e. SEC15b-SEC10a/b, SEC6-SEC8, EXO70A1-EXO84b-ΔC (Fig.1, see also Hála et al., 2008; Fendrych et al., 2013; Vukašinović et al., 2017). Interestingly, EXO70A1 was the only subunit able to pull-down most of the exocyst subunits with strong peptide score for interactions with subunits of the (EXO70A1-EXO84b-SEC10-SEC15b) subcomplex. Summed up, our data show that the modular composition of exocyst complex together with the most of the binary interactions between subunits are conserved between ophistokonts and plants.

EXO70A1 is essential for plant exocyst targeting to the plasma membrane

Both EXO70 and SEC3 subunits of the exocyst are known to contribute to the exocyst recruitment to PM in Opisthokonts (He et al., 2007; Liu et al., 2007; Zhang et al., 2008; Pleskot et al., 2015). Interestingly, our previous work addressing function of the SEC3 subunit within the

plant exocyst showed that the complex is still functional when the SEC3a lipid binding capability is abolished (Bloch et al., 2016) and the roles of SEC3a subunit unrelated to membrane phospholipid binding, like the stabilization of the complex, are thus sufficient for the exocyst functionality at least in some plant tissues. This stimulated us to explore the role of EXO70A1 in PM targeting of the plant exocyst in detail. We showed previously that the dotted pattern of SEC6:GFP PM signal is virtually lost in the *exo70A1-2* mutant background (Fendrych et al., 2013). Figure 2 shows that all tested exocyst subunits (SEC3, SEC6, SEC8, SEC10a and EXO84b), representing both structural subcomplexes of the exocyst, lost their PM localization in *exo70A1-2 mutant background*. Interestingly, we could observe tagged exocyst subunits in intracellular structures of unknown identity in the *mutant* background (Fig. 2). We suspected that the subunits form a partial complex in these structures, so we tested whether core exocyst subunits retained capacity to coexist in the *exo70A1* mutant background. We co-expressed SEC10b:mRFP with EXO84b:GFP under their native promoters in the wild-type or *exo70A1* mutant background. In wild-type cells, SEC10b:mRFP and EXO84b:GFP fully co-localized at the PM but in *exo70A1* cells, both proteins were relocated to the intracellular structures, where they also fully colocalized (Supplementary Fig. 1). We also used mass spectrometry to analyze co-immunoprecipitate for which GFP:SEC8 in *exo70A1* mutant background served as the bait. As expected, the mass spectrometry readout contained peptides from other exocyst subunits (Supplementary Fig. 1). We were further interested whether the intracellular structures constituted artificial precipitates of incomplete exocyst particles or cellular compartments of unknown identity. We first enquired if the structures would contain proteins outside of the exocyst complex, so we examined intracellular localization of the GFP-tagged version of KEULE (Steiner et al., 2016), a known interactor of plant exocyst (Wu et al., 2013). Like the core exocyst subunits, KEULE was relocalized into intracellular structures in the *exo70A1-2* mutant background (Supplementary Fig. 2). We were further enquired whether the structures constitute internal membrane-enclosed compartments or their coalescence, so we introduced several organelle marker lines expressing tagged Rab proteins (Geldner et al., 2009) into *exo70A1-2* mutant background and compared their subcellular localization between the mutant and WT background (Supplementary Fig. 2). We observed altered TGN/recycling endosomal

compartments, which suggest that the bodies accumulating exocyst subunits in the *exo70A1-2* mutant have TGN/recycling endosome identity.

Having demonstrated that EXO70A1 is indispensable for exocyst recruitment to PM in root cells and the exocyst gets mislocalized in the *exo70A1* mutant background, we decided to test ability of the EXO70A1 to autonomously bind PM *in vivo*. We introduced GFP-tagged EXO70A1 and other subunits into *exo84b-1* background and observed localization of the subunits upon exocyst destabilization caused by the absence of EXO84b subunit (Fig. 2). While the localization of SEC6:GFP and GFP:SEC8 was completely cytoplasmic upon the complex destabilization, GFP:EXO70A1 retained some PM localization despite the severe growth phenotype and altered cellular morphology of the *exo84b* mutant (Fendrych et al., 2010). Interestingly, the SEC10a:GFP was still present at PM, but it relocalized from the outer lateral domain to the basal and apical PM of root epidermal cells (Fig. 2). Taken together, our data strongly suggest that EXO70A1 is indispensable for the native localization of the whole complex to PM and capable of direct interaction with PM independently on the rest of the complex.

Full-length EXO70A1 is required for exocyst targeting to plasma membrane and functional complementation of *exo70A1* mutants

After confirming essential function of EXO70A1 in targeting of the exocyst to PM, we wanted to further elucidate molecular details of EXO70A1 membrane recruitment. Based on solved structure of yeast (Hamburger et al., 2006), mammalian (Moore et al., 2007) and partial Arabidopsis EXO70 (Zhang et al., 2016), we identified four distinct regions corresponding to described ABCD EXO70 subdomains in Arabidopsis EXO70A1. We cloned a series of truncated versions of EXO70A1 lacking one or two out of its four domains (ABC-, -BCD, --CD; Supplementary file S1) into the same expression vector as previously used for preparation of GFP-tagged full-length EXO70A1 (ABCD) (Fendrych et al., 2010). All versions were tagged with GFP at their N-termini, which results in functional version of the protein capable to complement the mutant phenotype in case of full length EXO70A1 (Drdova EJ et al., 2013). To

achieve stable expression, we introduced the constructs to heterozygous mutants for the *exo70A1-2* allele. We used the model system of root epidermal outer lateral PM domain of upper meristematic and transition zone, to which are exocyst subunits strongly recruited under normal conditions, for localization analysis of dissected EXO70A1 versions. In contrast to the full-length EXO70A1, none of the truncated variants was able to effectively localize to the outer lateral PM of young root epidermal cells (Fig. 3). Localization of GFP:EXO70A1(ABC-) and GFP:EXO70A1(--CD) was cytoplasmic without any PM signal. GFP:-BCD localized mostly to the cytoplasm but faint signal along the PM could be detected in some cells, albeit without the polarized localization at outer lateral PM. We further confirmed inability of truncated EXO70A1 versions to bind lateral PM of root epidermis by high-resolution spinning disk confocal imaging focused just beneath PM, where EXO70A1 and core exocyst subunits colocalize in dynamic foci representing putative exocytotic sites (Fendrych et al., 2013). In order to unambiguously focus the imaging to the area of endocytosis and exocytosis beneath PM, we crossed lines expressing GFP-tagged full length and truncated EXO70A1 with a transgenic line expressing DRP1C:mOrange (dynamin-related protein involved in endocytosis; Konopka and Bednarek, 2008). While the full length GFP:EXO70A1 formed distinct puncta beneath PM, the truncated ABC- and -CD versions were indeed completely detached from the PM (Fig. 3). In summary, we deduce that only the A domain is potentially dispensable for the EXO70A1-PM interaction, while domains B, C, D are essential. The A domain, however, improves the interaction and seems to underlie proper EXO70A1 association with the rest of the exocyst complex, which might explain the different distribution pattern at the PM observed for -BCD. The necessity of all four EXO70A1 domains for the proper PM localization suggests that both PM binding and interaction with other exocyst subunits are inevitable for proper EXO70A1 targeting. In order to dissect which domains act in interactions with other exocyst subunits, we performed a yeast two hybrid (Y2H) test between the subunits previously demonstrated to directly interact with the EXO70A1 in Y2H and truncated variants of the EXO70A1 (Fig. 4). While the full length EXO70A1 and the variant missing the D domain retained full capacity to interact with both SEC3a and N-terminal part of the EXO84b (EXO84bΔC), the AB-- variant has dramatically reduced capacity to interact with the EXO84bΔC and most importantly, the --CD variant of

EXO70A1 completely lost the capacity for interaction with the core exocyst subunits. These results demonstrate that while N-terminal part of the EXO70A1 is sufficient for interaction with other exocyst subunits, the C-terminal part is dispensable for this process and probably serves for interaction with PM *in vivo*.

We have previously demonstrated that full-length EXO70A1 tagged with GFP, regardless whether at the N- or C-terminus, can functionally compensate for the loss of native EXO70A1 in *exo70A1* mutants (Drdová et al., 2013). To evaluate if the GFP-tagged truncated versions are still at least partially functional, we analyzed the offspring of heterozygous mutants for the *exo70A1-2* allele expressing the truncated protein versions. All GFP-positive seedlings (5-d-old) were transferred to soil for further analysis of their morphology. We found that all putative mutant seedlings developed their mutant phenotype typical for adult *exo70A1* homozygous plants (Fig. 3). Individuals that exhibited the wild-type phenotype were confirmed to be wild types or heterozygotes by PCR genotyping, indicating that in contrast to full-length EXO70A1, none of the truncated versions was able to functionally complement the mutation in EXO70A1.

EXO70A1 is not required for exocyst-mediated vesicle trafficking to maturing the cell plate

The exocyst was documented to play essential role in plant cytokinesis, where it probably functions in delivery of specific vesicles. Core exocyst subunits and EXO70A1 localize to the cell plate primer and maturing post-cytokinetic cell walls (Fendrych et al., 2010; Rybak et al., 2014). Therefore, after observation of the compromised localization of truncated versions at the PM, we inspected their localization in forming cell plate. The -BCD version fully localized to the maturing cell plates, while the ABC- and --CD versions displayed weaker localization to the cell plate in part of the observed dividing cells. Surprisingly, all versions were thus capable to localize to the maturing post-cytokinetic cell walls similarly to the full-length EXO70A1, indicating a different mean of the EXO70A1 recruitment to these cellular structures that to PM (Fig. 3). Moreover, the SEC3A subunit was observed properly localize to maturing cell plate in *exo70A1-2* mutant background, confirming that the exocyst complex properly reaches the cell

plate in absence of the EXO70A1 (Supplementary Fig. S3). These observations are in concert with only mild and transient cytokinetic phenotype of the *exo70A1* mutant compared to strong cytokinetic phenotype of the core subunit mutant *exo84b-1* (Fendrych et al., 2010).

EXO70A1 shows high affinity to the acidic phospholipids *in vitro* and *in vivo*

Having confirmed the essential role of EXO70A1 in targeting plant exocyst to PM, we further investigated molecular mechanism of EXO70A1 interaction with the membrane. Yeast and animal EXO70s were previously demonstrated to be recruited to PM with contribution of direct binding to PIP_2, a phospholipid determinant of Opisthokont PM identity. Our previous work suggested possible interaction of EXO70A1 with both PIP_2 and PA, because the tobacco NtEXO70A1a localizes to the region where PIP_2 and PA maxima overlap in growing tobacco pollen tube (Sekereš et al., 2017). Recent study addressing the role of phospholipid species as determinants of plant PM identity indicated crucial role of PI4P with possible contribution of PA and PS in Arabidopsis root cells (Simon et al., 2016, Platre et al., 2018). Therefore, we tested capability of EXO70A1 to directly bind the negatively charged PM phospholipids via cosedimentation assay with large unilamellar vesicles (LUV) of specific phospholipid composition. Using recombinant GST:EXO70A1 purified from E.coli lysates, we performed the LUV co-sedimentation assay to uncover potential to bind negatively charged phospholipids. We used vesicles containing a mixture of phosphatidylethanolamine (PE) and phosphatidylcholine (PC) with portions of anionic phospholipids, namely PS (20%), PA (20%), PI4P (5%) and PIP_2 (5%). We found that GST:EXO70A1 interacted with all of them, with preference towards PA, PI4P and PIP_2 (Fig. 5).

We utilized two independent strategies to assess lipid binding properties of plant EXO70A1 *in vivo*. We first employed a fast model system - the growing tobacco pollen tube. Our previous work already demonstrated that tobacco ortholog of Arabidopsis EXO70A1, the NtEXO70A1a, binds to specific domain of plasma membrane near the pollen tube tip, where high levels of both PIP_2 and PA overlap (Sekeres et al., 2017). To supplement our previous descriptive observations with functional experiments, we decided to monitor enhanced NtEXO70A1a recruitment to PM

in tobacco pollen tubes with either elevated PIP_2 or elevated PA. Several isoforms of plant PI4P-5 kinases producing PIP_2 from PI4P have been functionally characterized (Ischebeck et al., 2008; 2010; Stenzel et al., 2008; 2012) and for some isoforms, their ability to increase PIP_2 content upon overexpression in tobacco pollen tube was directly demonstrated by monitoring enhanced PM localization of PLC PH domain, the PIP_2 probe (Sousa et al., 2008; Zhao et al., 2010). We have also previously confirmed *in vivo* interaction of the tobacco exocyst subunit SEC3 with PIP_2 by monitoring increased PM recruitment of the protein in tobacco pollen tube upon PIP5K5 overexpression (Sekereš et al., 2017). Furthermore, we have recently characterized delta subfamily of tobacco PA-producing phospholipase D enzymes and demonstrated that overexpression of PLDδ3 results in specific recruitment of the Spo20 PA marker to PM in growing tobacco pollen tube (Pejchar et al., in prep). We were thus able to apply established toolset for testing EXO70A1 interaction with PIP_2 and PA in tobacco pollen tubes. We transformed tobacco pollen with low amount of the construct encoding NtEXO70A1a, the closest homolog of Arabidopsis EXO70A1, so that EXO70 expression would not perturb cellular morphology by itself and only serve as a readout of its membrane-binding properties, together with high amount of either cyan fluorescent protein-tagged phosphatidylinositol 4-phosphate 5-kinase 5 (PIP5K5:CFP, Ischebeck et al., 2008), high amount of monomeric red fluorescent protein (mRFP)-tagged NtPLDδ3, or high amount of mRFP-tagged NtPLDδ3 K693R mutant with reduced catalytic activity (Pejchar et al., in prep). We monitored NtEXO70A1a PM localization by spinning disk confocal microscopy and quantified the results (Fig. 6). In agreement with the result of *in vitro* lipid-binding assay, both elevated level of PIP_2 and elevated level of PA resulted into increased recruitment of NtEXO70A1a to the PM when compared to control pollen tubes expressing only NtEXO70A1a or coexpressing NtEXO70A1a with NtPLDδ3 K693R with reduced catalytic activity (Fig. 6). In a few instances, we were able to directly observe formation of PLDδ3 overexpression-induced invagination in live time and observe immediate NtEXO70A1a recruitment to the structure, thus eliminating possibility that the NtEXO70A1a PM recruitment is a secondary effect of perturbed pollen tube tip growth (Supplementary fig. S4; Supplementary movie 1).

Next, we decided to investigate the role of the anionic phospholipids in EXO70A1 PM recruitment in Arabidopsis root epidermal cells. Since phenotype of *pip5k1pip5k2* double mutant plants (Ischebeck et al., 2013) strongly resembles phenotype of the *exo70A1* mutant (Synek et al. 2006, Drdová et al., 2013) including longevity and reduced apical dominance, we immediately suspected PIP_2 to play essential role in EXO70A1 recruitment in Arabidopsis sporophyte tissues. To test this hypothesis, we crossed the line expressing GFP:EXO70A1 with plants homozygous for *pip5k2* mutation and heterozygous for *pip5k1* mutation (*pip5k1pip5k2* double mutants are infertile; Ischebeck et al., 2013). In the next generation, we compared GFP:EXO70A1 subcellular localization in root cells of *pip5k1pip5k2* double mutants (identified according to growth phenotype and subsequently confirmed by genotyping) and control plants by spinning disk confocal microscopy (Fig. 7). Surprisingly, GFP:EXO70A1 localization in *pip5k1pip5k2* double mutants matched localization pattern observed in control plants and no reduced EXO70A1 PM binding in the double mutant plants was observed. To investigate potential weak localization phenotype, we measured the ratio of signal intensity at the outer lateral PM and in the underlying cortical cytoplasm as a hallmark of EXO70A1-PM affinity. However, no significant difference between control and double mutant plants was measured (Fig. 7). In order to test the role of other anionic phospholipids in EXO70A1 PM recruitment in Arabidopsis root cells, we applied established pharmacological inhibitors of phospholipid modifying enzymes. It was previously shown that PM localization of the PA probe Spo20 (Platre et al., 2018) and the PI4P probe PH-FAPP1 (Simon et al., 2016) is completely lost upon application of DGK inhibitor R59022 and PI4P inhibitor PAO, respectively. We thus treated GFP:EXO70A1 expressing seedlings with R59022, PAO or combination of both inhibitors, monitored EXO70A1 localization in root cells and compared the results with control DMSO treated seedlings (Fig. 7). EXO70A1 recruitment to the outer lateral membrane was mildly but significantly reduced upon R59022 treatment, drastically decreased after PAO treatment and completely lost when combination of both inhibitors was applied. Besides the documented loss of outer lateral PM signal (Fig. 7), reduction (PAO treatment) and loss of PM localization (combined treatment) was also observed in the case of apical, basal and inner lateral PM. Our results thus uncovered

complementary contribution of PI4P and PA in the EXO70A1 PM recruitment in Arabidopsis root epidermis and cortex and negligible role of the PIP_2 in this process.

Conserved C-terminal lysine residues are crucial for PM recruitment of EXO70A1 by interaction with acidic phospholipids

We recently used available structural data on yeast Exo70p and characterized its interaction with the membrane containing PIP_2 by the means of coarse-grained molecular dynamics simulations (Pleskot et al., 2015). We took an advantage of this approach to elucidate structural details of the interaction between Arabidopsis EXO70A1 and a membrane containing anionic phospholipids. To this end, we constructed a model of Arabidopsis EXO70A1 (amino acid residues 67-630) using homology-based modelling approach with the crystallized near full-length yeast and mammalian EXO70 structures together with partial Arabidopsis EXO70A1 structure (pdb codes 2PFV, 2PFT and 4RL5, respectively) used as templates.

Having a reliable model of the almost full-length Arabidopsis EXO70A1, we performed series of coarse-grained molecular dynamics simulations (MD). The advantage of CG force fields is that they enable to simulate bigger systems for longer times and thus they are a valuable tool to study biological phenomena. To study the association of EXO70A1 with a membrane, we performed four independent CG-MD simulations. Out of the three anionic phospholipids interacting with EXO70A1 *in vitro*, the PIP2, PI4P and PA, the interaction with PA *in vivo* was confirmed in both biological systems tested, namely the tobacco pollen tube and Arabidopsis root epidermis. Furthermore, the PI4P and PIP2 bear more negative charge than the PA and would thus constitute less stringent option for the MD simulation testing capacity of individual amino acid residues of the EXO70A1 for its membrane recruitment by anionic phospholipids. Therefore, we chose PA as the anionic lipid species used in simulations elucidating details of EXO70A1 recruitment by the PM anionic phospholipids. In all performed simulations (each of the 1 μs length), we observed binding of EXO70A1 to the lipid bilayer containing PA. After 1 μs, the whole molecule of EXO70A1 associated with the membrane via several PA-binding sites in a

similar manner as its yeast counterpart with the membrane containing PIP_2 (Fig.8, Pleskot et al., 2015). Similarly to yeast Exo70p, the analysis of the amino acid residues involved in the interaction of EXO70A1 with PA revealed that the highest number of interacting positively charged residues is located at the C-terminal part, a region corresponding to the domains C and D of the EXO70 (Fig. 8).

In order to confirm the proposed theoretical conclusions acquired using CG-MD simulations, we prepared EXO70A1 constructs with the five lysine residues mostly interacting with PA molecules (K393, K462, K549, K607, K611; Fig. 8) substituted for glutamate residues using site-directed mutagenesis on the full-length EXO70A1 CDS. Such substitutions inverted positive surface of the protein to negative, as revealed by structural homology modeling (Fig. 9). We prepared N-terminal GST fusion of the mutated EXO70A1, expressed the protein in E.coli, purified the protein and performed LUV co-sedimentation assays. In contrast to the WT EXO70A1, EXO70A1-(5x)K/E lost the ability to specifically bind PA *in vitro* (Fig. 9). To test the essential function of the candidate EXO70A1 residues for the protein recruitment to PM *in planta*, we then prepared wild-type and *exo70A1* lines stably expressing the mutated EXO70A1 tagged with GFP at the N-terminus using the same vector as previously employed for the expression of full-length and truncated EXO70A1 versions. As predicted, substitutions of the key lysine residues for glutamate resulted in complete loss of EXO70A1 PM binding. In agreement with experiments involving truncated EXO70A1 versions, the GFP:EXO70A1 with mutated key residues was not capable to fully complement the *exo70A1* mutant (Fig. 10).

In order to test evolutionary conserved role of the lysine residues critical for PM binding between Arabidopsis and tobacco, we prepared (5x)K/E version of the tobacco NtEXO70A1a, analogous to the Arabidopsis EXO70A1-(5x)K/E variant. When transiently expressed, YFP:NtEXO70A1a-(5x)K/E displays complete loss of PM signal when compared to WT YFP:NtEXO70A1a in both growing pollen tubes and in pollen tubes overexpressing the particular construct (Fig. 11). Moreover, while overexpression of PIP5K5 or PLDδ3, as also presented in Fig. 6, leads to enhanced recruitment of YFP:NtEXO70A1a to PM, it does not

recruit YFP:NtEXO70A1a-(5x)K/E to PM (Fig. 11) even in the pollen tubes with strong morphological deviations caused by elevated level of particular phospholipids. These phenotypes are known to result from the strong elevation of PIP2 (Ischebeck et al., 2008) or PA (Pejchar et al., in prep) level. The fact that even in the extremely deformed pollen tubes with split growth apex or membrane invaginations due to the elevated PA/PIP2 level are unable to recruit the YFP:NtEXOA1a-(5x)K/E to the plasma membrane fully supports notion that the key evolutionary conserved residues play essential role in EXO70A1 binding to acidic phospholipids. Unlike the WT EXO70A1, the mutated EXO70A1 thus cannot bind anionic phospholipids and the same amino acid residues are essential for the interaction with acidic phospholipids in Arabidopsis and tobacco.

Discussion

Our comprehensive *in vivo* protein-protein interaction analysis of the plant exocyst demonstrated presence of two evolutionary conserved modules known from the Opisthokont model systems. After improving the known interaction map of plant exocyst complex, we further focused on mechanisms of its targeting. Mutated versions of SEC3a incapable of PIP_2 binding were previously shown to nevertheless be able to reach PM in Arabidopsis pollen, probably due to membrane targeting of whole exocyst complex by the EXO70 subunit (Bloch et al., 2016). This suggests essential role of EXO70 for plant exocyst PM targeting and only auxiliary function of SEC3 in the process. We have indeed confirmed that functional EXO70A1 is crucial for the delivery of other exocyst subunits including SEC3 to PM in epidermal and cortical root cells. On the other hand, core exocyst subunits properly localize to maturing cell plate even in absence of EXO70A1, which is in concert with only mild and transient cytokinetic phenotype of *exo70A1* mutant (Fendrych et al., 2013). In differentiating xylem, exocyst localizes to the sites of secondary cell deposition via indirect interaction with cortical microtubules, which involves EXO70A1 but is partly functional in *exo70A1* mutant due to tethering to VETH-COG2 by other exocyst subunits (Vukašinović et al., 2017). On the other hand, exocyst targeting to prospective casparian strip is dependent on EXO70A1, which was documented by GFP:SEC8

mislocalization in *exo70A1* mutant plants (Kalmbach et al., 2017). EXO70A1 thus plays essential role in exocyst targeting in some but not all scenarios, depending on cell types and membrane domains involved. The complex can be targeted by other EXO70 isoforms or by interaction of core subunits with specific protein partners like in case of developing xylem (Vukašinović et al., 2017).

While PIP_2 is widely recognized as part of animal and yeast PM identity barcode responsible for EXO70 recruitment (Platre and Jaillais, 2017), EXO70A1 is capable to directly bind several anionic phospholipids with strong affinity towards PA, PI4P and PIP_2 *in vitro* and *in vivo*. PI4P was also shown to interact with animal and yeast EXO70 but with 10x (Liu et al., 2007) and 20x (He et al., 2007) lower affinity when compared to PIP_2-mediated interaction, respectively. Role of PI4P in recruitment of Opisthokont exocyst to PM is thus considered negligible due to localization of most PI4P cellular pool at Golgi apparatus (Platre and Jaillais, 2017). On the other hand, plant plasma membrane contains substantial pool of PI4P, largely responsible for its negative charge (Simon et al., 2016). Lipidomic analyses uncovered comparable PIP_2 and PI4P content in tobacco leaf and BY2 PM fractions (Furt et al., 2010) and 5:1 PI4P:PIP_2 ratio in Arabidopsis seedlings (Ischebeck et al., 2013) and Arabidopsis leaf PM fraction (König et al., 2008), further suggesting importance of PI4P as a PM hallmark recruiting effector proteins. Indeed, we observed dramatic loss of EXO70A1 membrane signal in root tissues upon pharmacological quenching of PI4P.

Studies addressing Opisthokont EXO70s affinity towards phospholipids never included PA, partly due to negligible levels of PA in non-stimulated animal cells (Zeniou-Meyer et al., 2007) and partly due to small emphasize put on role of PA in PM organization and regulation. On the other hand, several past years of plant cell research have brought substantial evidence for vital contribution of PA to plant PM composition. Lipidomics of tobacco leaf and BY2 cell PM fraction demonstrated 5-10 times higher PA than PIP_2 content (Furt et al., 2010) and PA level in plant tissues further rises during biotic and abiotic stresses (Testerink and Munnik, 2011). Importance of plant PA signaling is also reflected by expansion of genes encoding PA producing

enzymes in plant evolution (Pleskot et al., 2012a). Several candidate PA interactors, including components of signaling pathways, endocytic machinery and cytoskeletal regulators, were identified in proteomic screens of plant tissues under normal and stressed conditions (Testerink et al., 2004; McLoughlin et al., 2013). Direct interaction of selected plant proteins with PA was subsequently reported (Choudhury and Pandey, 2017; Ufer et al., 2017) and in case of two SnRK2 protein kinases (Julkowska et al., 2015) and the microtubule regulator MAP65-1 (Zhang et al., 2012) specificity for PA over other anionic phospholipids was documented. Interestingly, the actin capping protein, which is generally regulated by PIP_2 in eukaryotes, also interacts with PA in plants (Huang et al., 2006), due to lineage specific features of the plant protein that drive the interaction (Pleskot et al., 2012b).

We discovered partial contribution of DGK produced PA in EXO70A1 recruitment to root epidermis PM. It is possible that PA plays more significant role in exocyst recruitment during exocytosis as response to stress factors and environmental stimuli, which involves increased PA production (Testerink and Munnik, 2011). PA producing PLDζ subfamily plays role in various root tropisms and membrane trafficking that underlies these reactions at the cellular level (Galvan-Ampudia et al., 2013; Li et al., 2006; Li and Xue, 2007; Taniguchi et al., 2010). PLDζ2 is clearly involved in exocytosis (Li and Xue, 2007) and it is thus probable that PLD-produced PA contributes to exocyst recruitment during reaction to environmental stimuli. Our results bring further piece of accumulating evidence that during plant evolution PA has complemented and in some cases overtaken role played by PIP_2 in other eukaryotes, as previously hypothesized (Pleskot et al., 2014).

Several PLD and DGK isoforms are expressed in germinating pollen and PA is vital for growth of pollen tube (Pleskot et al., 2012; Pejchar et al., in prep), where it accumulates in subapical region (Potocký et al., 2014). Tobacco EXO70A1a was previously observed in domain where the PA rich region overlaps with PIP_2 maximum (Sekereš et al., 2017). It is thus not surprising that experimental elevation of either of the lipids results in dramatic NtEXO70A1a recruitment to pollen tube PM. On the other hand, EXO70A1 PM recruitment is not affected in root cells of

PIP_2 deficient *pip5k1pip5k2* double mutant. While this mutant resembles phenotype of *exo70A1* caused by impaired PIN exocytosis (Drdová et al., 2013), the *pip5k1pip5k2* plants normally recruit EXO70A1 to PM, so their phenotype is probably result of impaired PIN endocytosis, as originally proposed (Ischebeck et al., 2013; Tejos et al., 2014).

It is evident that while EXO70A1 protein is capable to bind various acidic phospholipids, it is recruited to PM *in vivo* by different particular lipid species depending on cell type, namely PI4P and PA in root epidermis and PIP_2 together with PA in growing pollen tube. PIP_2 also probably plays role in EXO70A1 rexruitment to microdomain of prospective Casparian strip deposition, since both PIP_2 marker Tubby and EXO70A1 accumulate at the site prior to localized CASP protein secretion in differentiating endodermis (Kalmbach et al., 2017).

Using MD simulation with virtual membrane composed of 20% PA and 80% PC, we identified EXO70A1 amino acid residues biologically relevant for interaction with all 3 major PM anionic phospholipids. EXO70A1 (5x)K/E mutant lost ability to interact with both root epidermal membrane (normally driven by PA and PI4P) and pollen tube tip (normally driven by PA and PIP_2). We proved that the same residues are required for EXO70A1 PM interaction in Arabidopsis and tobacco. Since Brassicaceae and Solanaceae belong to different clades of core eudicots (Chase et al., 2016), the mechanism is probably conserved among most angiosperms.

It is not clear, whether PA, PI4P and PIP_2 play redundant role in EXO70A1 attraction based on net negative charge of the lipids regardless of their identity or whether specific combination of the lipids can act synergistically in EXO70A1 recruitment to PM, as suggested by NtEXO70A1a localization to region of PA and PIP_2 overlap in pollen tube (Sekereš et al., 2017). To tackle this issue in the future, quantitative measurements of EXO70A1 interaction with liposomes containing different ratios of more anionic phospholipids combined will be required. Clearly, molecularly yet unidentified protein factors also contribute to the exocyst PM targeting and we thus hypothesize that EXO70A1 targeting is driven by coincident detection of lipids and tissue-specific protein interaction partners. Such coincident detection is a general mechanism of

fine-tuned protein recruitment to target organelles and membrane microdomains (Saliba et al., 2015) and is known to be involved in animal (Liu et al., 2007; Dupraz et al., 2009) and yeast EXO70 targeting (Robinson et al., 1999; He et al., 2007; Wu et al., 2010). Indeed, from two closely related tobacco paralogs, NtEXO70A1a natively expressed in pollen localizes to distinct PM domain in pollen tube, while its closest homolog NtEXO70A1b, normally not present in pollen, does not localize to PM when ectopically expressed in pollen tube (Sekereš et al., 2017), despite the fact that it shares all positively charged lysine and arginine residues with the NtEXO70A1a. It thus seems that protein interactor specific for NtEXO70A1a supplements lipid-based interaction with PM and makes it strong enough to recruit the EXO70. Role of protein interaction partner RIN4 was recently shown in PM recruitment of the EXO70B1 isoform (Sabol et al., 2017).

Our pioneering work addressing PM targeting of EXO70A1 opens door for future comparative studies focused on specific interactions of other plant EXO70 isoforms with lipids. Pieces of evidence supporting original hypothesis that different EXO70 isoforms localize to distinct membrane domains of plant cell (Žárský et al., 2009) have recently accumulated (Sekereš et al., 2017; Kulich et al., 2018; Ortmannová et al., submitted). At least part of this specificity will definitely be explained by differential interaction of EXO70 isoforms with particular lipid species.

While EXO70A1 drives general secretion to many plant cell PM domains, subcellular localization of other isoforms is more focused. It is thus also possible that lipid interactions of some EXO70s will be more specific, unlike interaction of EXO70A1 with different anionic phospholipids. For example, membrane domain of NtEXO70B1 largely overlaps with PA maximum (Sekereš et al., 2017), suggesting potential selectivity towards PA. Since some EXO70 isoforms function in different compartments than PM, like involvement of Arabidopsis EXO70B1 in autophagy (Kulich et al., 2013), interactions with non PM lipids, like phosphatidylinositol 3-phosphate, are also possible.

In summary, our study shows that while overall architecture of the exocyst complex is conserved between plants and Opisthokonts, the mechanism of exocyst targeting to target membrane is fine tuned to the molecular identity of the plant plasma membrane by ability of the EXO70A1 to bind not only PIP2 but also PI4P and PA, which are contributing to plant PM negative charge and molecular identity. Our approach combining advanced fluorescent live cell imaging, in vitro lipid binding assays and computational molecular dynamics also provides blueprint for future studies analyzing molecular mechanisms of peripheral membrane proteins targeting in plant cells.

Materials and methods

Molecular cloning

The following constructs were prepared de novo for the sake of this study with the use of the primers summarized in the Supplementary table S1:

Constructs encoding GFP-tagged exocyst subunits and their truncated/mutated variants used for preparation of stable Arabidopsis lines:

In order to prepare the pSEC3a::SEC3a:GFP construct, we amplified SEC3a coding sequence using the SEC3-F and SEC3-R primers, as well as the SEC3a promoter using the SEC3aP-F and SEC3aP-R primers and subsequently introduced the fragments into pB7m34GW destination vector by Gateway BP reaction. To prepare the pSEC15b::GFP:SEC15b construct, we used the Three Fragment Multisite Gateway strategy. First, we PCR amplified the SEC15b native promoter and cloned it into pDONR™ P4-P1R using pENTR™ 5′-TOPO®TA Cloning® Kit (Invitrogen) and amplified SEC15b coding sequence with primers SEC15b-F and SEC15b-R and cloned it into pDONR™ P2R-P3 using BP reaction (Invitrogen). Subsequently, we performed LR reaction (Invitrogen) and introduced the promoter with the coding sequence into the pB7m34GW destination vector. Both point-mutated and truncated versions of EXO70A1 were cloned in analogous way to the full-length (wild-type) version published previously (Drdova et al., 2013). The altered coding sequence of Arabidopsis EXO70A1 (At5g03540) was always bordered with *Spe*I sites on both ends during PCR amplification (a STOP codon was also introduced when needed) and inserted into the *Xba*I site in a modified pBAR1 vector containing GFP upstream of the polylinker to produce *p35S::GFP:EXO70A1* and its mutated variants. Point-mutated versions of *EXO70A1* were generated by series of PCR reactions (primers referred in the Supplementary File 2) using the intermediate PCR products as megaprimers for the subsequent PCR reactions with the final product cloned into pBAR1. In the protein sequence, the five lysine residues 339, 462, 549, 607, 611 were mutated to glutamate residues, respectively to generate version indicated as *EXO70A1-5xE*. Protein and nucleotide sequences of WT and mutated EXO70A1 variants are listed in Supplementary File 2.

Constructs for yeast two hybrid test:

Truncated EXO70A1 versions (AB--, ABC-, -BCD, and --CD) were PCR-amplified and cloned with a STOP codon into the pGBKT7 vector (Clontech) using *Eco*RI and *Sal*I restriction enzymes to produce GAL4 Binding domain fusions (BD-EXO70A1Δ).

Constructs for expression of EXO70A1 and its mutated variant in E.coli cells:

In order to improve solubility of the expressed protein, we PCR-amplified the *EXO70A1* coding sequence excluding the very N-terminal part of the EXO70A1 (the first 69 triplets), similarly to the previous studies involving expression and purification of EXO70 protein in bacterial cells (Hamburger et al., 2006; Moore et al., 2007 and Zhang et al., 2015). The sequence was bordered with *Eco*RI and *Sal*I restriction sites and cloned into the pGEX4T-2 vector (Sigma) to produce a GST:EXO70A1Δ1-69 fusion protein (nucleotide sequence is provided in the Supplementary File 1). The point-mutated variant *EXO70A1-5xE* was cloned analogically using the same primers with the previously prepared XXX construct encoding *EXO70A1-5xE* used as the template.

Constructs used for transient tobacco pollen transformation:

The (5x)K/E point-mutated version of the YFP:NtEXO70A1a was generated analogically to the Arabidopsis EXO70 mutant variant with primers complementary to the tobacco NtEXO70A1a coding sequence (Supplementary file 2). Previously published YFP:NtEXO70A1a - encoding construct (Sekeres et al., 2017) was used as the PCR template. Analogically to the published WT variant of NtEXO70A1a, the newly created mutant variant was introduced into the pWEN240 vector (Klahre et al., 2006).

Plant material and growth conditions

Together with the previously published Arabidopsis lines pEXO84b:EXO84b:GFP, pSEC6:SEC6:GFP, pSEC8:GFP:SEC8 (Fendrych et al., 2010), 35S:GFP:EXO70A1 (Drdova EJ et al., 2013), SEC10a:GFP (Vukasinovic et al., 2017) and Ub:SEC5a:GFP (Ortmannova et al., unpublished), following novel constructs (for details, see Molecular cloning section) were introduced into WT and mutant Arabidopsis lines using the *Agrobacterium tumefaciens* – mediated transformation by floral dip method (Clough and Bent, 1998):

35S::GFP:EXO70A1(-BCD)

35S::GFP:EXO70A1(ABC-)

35S::GFP:EXO70A1(--CD)

p35S::GFP:EXO70A1-(5x)K/E

pSEC3a:SEC3a:GFP

pSEC15b:GFP:SEC15b

In order to analyse localization the GFP-tagged exocyst subunits and their mutated/truncated versions in mutant backgrounds, we used previously published lines *exo70A1-2* (Synek et al., 2006), *exo84b-1* (Fendrych et al., 2010) and the *pip5k1pip5k2* double mutant (Ischebeck et al., 2013). Due to drastically reduced or absent fertility of these mutant lines, the corresponding constructs were transformed into heterozygous plants. The homozygot plants for subsequent analysis were selected based on the phenotype and subsequently confirmed by genotyping. Primers used for genotyping of the mutant lines were the same as used in the original studies characterizing the mutant lines (Synek et al., 2006; Fendrych et al., 2010; Ischebeck et al., 2013). For the analysis of growth phenotype of the mutant lines expressing GFP-tagged versions of EXO70A1, seeds were surface sterilized (70% ethanol for 3 min, 10% commercial bleach for 10 min, and rinsed three times in sterile distilled water) and vernalized for 3 days at 4°C. The seeds were then germinated on vertical ½× MS1 agar plates (half-strength Murashige and Skoog salts [Duchefa Biochemie] supplemented with 1% sucrose, vitamin mixture and 1.6% Plant agar [Duchefa Biochemie]) at 21°C and 16 h of light per day. Seven-day-old seedlings were transferred into turf pellets (Jiffy Products International, Norway) and grown again at 22°C and 16 h of light per day.

Co-immunoprecipitation and mass spectrometry analysis

For analysis of *in vivo* interactions within the exocyst complex by co-immunoprecipitation, we used 10 days old *Arabi*dopsis seedlings (1 g of seedlings for each isolation). Protein interactors of GFP-tagged exocyst subunits and of free GFP expressing line used as a negative control were isolated using the μMACS GFP-tagged protein isolation kit (Miltenyi Biotec), according to the

manufacturer's instructions. The protocol was modified in a way that the provided wash buffers were substituted with the Sec6/8 buffer (Hála et al., 2008) during the wash steps. Bound proteins were eluted with 100 µL of the preheated elution buffer and flash frozen in liquid nitrogen until further analysis.

After in-gel digestion with trypsin, eluted peptides were identified using UHPLC Dionex Ultimate3000 RSLC nano (Dionex) connected with the mass spectrometer ESI-Q-TOF Maxis Impact (Bruker). Measurements were carried out in positive ion mode with precursor ion selection in the range of 400 to 1,400 mass-to-charge ratio; up to 10 precursor ions were selected for fragmentation from each mass spectrometry spectrum. Peak lists were extracted from raw data by Data Analysis version 4.1 (Bruker Daltonics) and uploaded to the data management system Proteinscape (Bruker Daltonics). For protein identification, the Mascot server (version 2.4.1; Matrix Science) was used with a custom-made database containing tobacco variety K326 and SwissProt proteins.

Confocal microscopy and image analysis of the Arabidopsis root cells

Seeds were surface sterilized (70% ethanol for 3 min, 10% commercial bleach for 10 min, and rinsed three times in sterile distilled water) and vernalized for 3 days at 4°C. The seeds were then germinated on vertical ½× MS1 agar plates (half-strength Murashige and Skoog salts [Duchefa Biochemie] supplemented with 1% sucrose, vitamin mixture and 1.6% Plant agar [Duchefa Biochemie]) at 21°C and 16 h of light per day. The epidermal root cells of 4-5 days old seedlings expressing wild-type, truncated or point-mutated GFP:EXO70A1 were examined using a spinning disc confocal microscope (Yokogawa CSU-X1 on Nikon Ti-E platform, Agilent MLC400 laser box, Zyla sCMOS camera by Andor, NIS Elements 4.1 software). An Plan Apochromat 60x/1.2 water immersion lens was used for overview of GFP:EXO70A1 localization in the root tissue, while a Plan Apochromat 100x/1.4 Oil lens for details of plasma-membrane localization. Seedlings grown vertically on ½× MS1 agar plates were transferred with a small block of agar underneath into a chambered coverglass Lab-Tek II (Thermo Scientific) with a drop of water and placed upside-down. The GFP (and mOrange)

fluorescence was recorded using the Zyla camera (Andor) at 1s exposure time, 4× averaging, with the fluorophores excited by 488 and 561 laser lines, respectively.

For the determination of the dissociation index of GFP:EXO70A1 signal at the outer lateral plasma membrane under various conditions, we first manually measured average pixel intensity of the plasma membrane signal and average pixel intensity of the small part of cytoplasm just beneath the outer lateral plasma membrane using the polygon selection in ImageJ software. We then divided the average cortical cytoplasm pixel intensity by average plasma membrane pixel intensity to obtain PM dissociation index of the particular cell in analogous manner as published/used previously (Barbosa et al., 2016).

Yeast two-hybrid assay

The yeast two-hybrid assay employed the MATCHMAKER GAL4 Two-Hybrid System 3 (Clontech) following manufacturer's protocols. Cells of the AH109 yeast strain were always stepwise transformed with one of the *BD:EXO70A1* truncated versions as well as full-length *EXO70A1* or empty pGBKT7 vector, and after selection (-TRP) by one of exocyst subunits (*SEC3a, SEC5a, SEC6, SEC8, SEC10b, SEC15b, EXO70A1, EXO84b-N*, *EXO84b-C*) fused with the GAL4 Activation domain in the pGADT7 vector (Clontech). *BD:EXO70A1* (full-length) and exocyst subunits fused to *AD* were generated previously by Hala et al. (2008) and Fendrych et al. (2010). Double transformed cells for all 6x9 combinations were selected on -Leu-Trp medium. Single colonies were then scale-diluted in sterile distilled water and dropped by 10 µl onto -Ade-His-Leu-Trp selective medium to reveal protein interactions.

Expression and purification of recombinant GST:EXO70A1

GST:EXO70A1Δ69 and GST:EXO70A1Δ69-(5x)K/E encoding pGEX4T-2 constructs were transformed into *Escherichia coli* ArcticExpress (DE3) RIL cells with Codon Plus technology (Stratagene). Bacterial culture was grown in LB medium (50 ml for wild-type or 5 l for mutated version) supplemented with ampicillin (50 mg/l) at 37°C until OD_{600} reached 0.5–0.8, then transferred to 12°C and protein expression was induced for 24 hours by 1 mM isopropyl β-D-thiogalactoside. Cells were harvested by centrifugation and resuspended in 5 ml or 35 ml of

lysis buffer (25 mM Tris, 250 mM NaCl, 5 mM beta-mercaptoethanol, protease inhibitors cocktail (Roche), pH 8.0) in the case of wild-type or mutated version, respectively. After disruption of cells by sonication, the lysate was cleared by centrifugation and soluble fraction was loaded on a Glutathione-agarose column (Sigma), washed twice with 10 ml of lysis buffer to remove non-specifically bound proteins, and finally the WT or mutated GST:EXO70A1Δ69 protein was eluted by 0.25 ml of 1M Tris-HCl (pH 8.8) supplemented with 30mM glutathione.

Protein-lipid binding assay

We analyzed binding of EXO70A1 and its (5x)K/E mutant variant to large unilamellar vesicles (LUV) of various lipid composition according to Koojiman et al., 2008 using total amount of 400 nmol of lipids and 1 µg of the particular protein.

Pollen Transformation and Microscopic Analysis

Expression vectors were transferred into tobacco pollen grains germinating on solid culture medium by particle bombardment using a helium-driven particle-delivery system (PDS-1000/He; Bio-Rad) as described previously (Kost et al., 1998). Particles were coated with 1 µg of DNA for subcellular protein localization of the NtEXO70A1a and its mutated varians and with 5 µg of DNA of the particular phospholipid modifying enzymes for experiments testing role of phospholipids in NtEXO70A1a recruitment to the plasma membrane. For imaging of NtEXO70A1a and its mutated variant alone under condition of overexpression, we coated the particles with 5 µg of the particular constructs. 8- to 10-h-old pollen tubes were used for the observations. Imaging was performed with a spinning disk confocal microscope (Yokogawa CSU-X1 on Nikon Ti-E platform, laser box Agilent MLC400, with sCMOS camera Andor Zyla) with Lense Plan Apochromat 60× WI (numerical aperture = 1.2) objective and the 488 laser line.

For measurements of the total length of NtEXO70A1a membrane signal under various conditions, we subtracted background signal and then manually measured the length of the

pollen tube membrane covered with the YFP signal (using segmented line and length measurements in ImageJ software).

Structural homology modelling

3D model of near full-length Arabidopsis EXO70A1 (aa 69-630) was predicted using mouse (PDB code 2PFT) and partial Arabidopsis (PDB code 4RL5) structures as a template. Multiple structure-sequence alignment of 231 EXO70 sequences from multiple eukaryotic lineages was used as a starting point for the prediction using MODELLER 9v8 software. 100 generated models were evaluated with internal Modeller ranking algorithms (DOPE-HR, molpdf and Z) and ten best models were further evaluated using PSVS (http://psvs-1_5-dev.nesg.org), Prosa (https://prosa.services.came.sbg.ac.at/prosa.php) and WhatIf (http://swift.cmbi.ru.nl) algorithms. The best model scored comparable to or even better than experimental template structures (e.g. Prosa scores for Arabidopsis EXO70A1 model, 2PFT and 4RL5 were -11.74, -10.99 and -6.79, respectively, lower is better).

Coarse-grained molecular dynamics simulations

To simulate EXO70A1 interaction with the lipid bilayer, we performed several molecular dynamics (MD) simulations. In this approach, the simulated system is considered as an ensemble of interacting particles, which are assumed to obey the laws of classical mechanics and their movement can be thus derived from numerical solution of Newton's equations of motion. Interactions in the system are described by force field in terms of potential energy function. To this end, we used the MARTINI coarse-grained (CG) force field (Marrink et al., 2007, Monticelli et al., 2008; Periole et al., 2009), which is based on four-to-one mapping; on average four heavy atoms plus associated hydrogens are represented by a single interaction center, the CG particle. To convert the structure of EXO70A1 to the MARTINI v2.1 CG representation, we utilized the martinize.py script and we used the ELNEDYN representation with r_c=0.9 nm and f_c= 500 kJ $mol^{-1}nm^{-2}$ (de Jong et al., 2013). The MARTINI CG model for 1-palmitoyl-2-oleoylphosphatidylcholine (PC) and 1-palmitoyl-2-oleoylphosphatidic acid (PA) was taken from (Ingólfsson et al., 2014). The program GROMACS 4.5.0 was used for all MD

simulations (Hess et al., 2008). Lennard-Jones and electrostatic interactions were shifted to 0 between 9 and 12 A and between 0 and 12 A, respectively. A relative dielectric constant of 15 was used. Simulations were run in NPT ensemble. The temperature of protein, lipids, and solvent was coupled separately at 310 K using the Berendsen algorithm, with coupling constant 1.0 ps. The system pressure was coupled using the same algorithm with coupling constant 3.0 ps, compressibility of 3.0, and reference pressure of 1 bar. Simulations were performed using a 20 fs integration time step. Initially, protein was placed 2.5 nm apart the membrane, which was prepared by the insane.py script (Ingólfsson et al., 2014), equilibrated and dehydrated before the addition of the protein. Subsequently, we added standard MARTINI water and Na+ ions to ensure electroneutrality of the system. The whole system was energy minimized using steepest descent method up to maximum of 500 steps and production runs were performed for 1000 ns. Standard Gromacs tools as well as in-house codes were used for analysis. The VMD program was used to prepare figures (Humphrey et al., 1996).

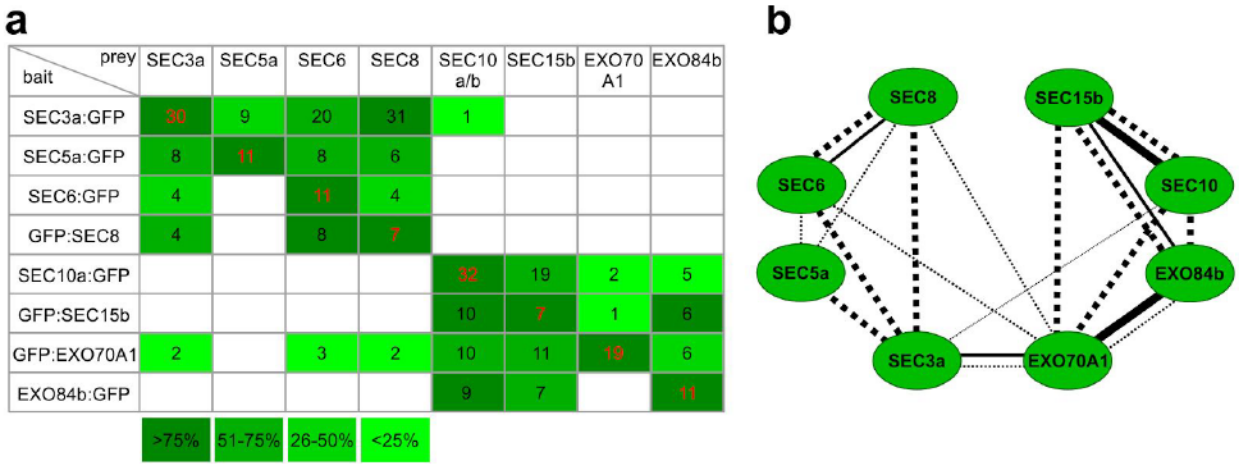

Figure 1: Plant exocyst complex consists of two loosely-connected subcomplexes. a Co-immunoprecipitation of Arabidopsis exocyst complex. Individual GFP-tagged exocyst subunits were used as baits and interacting proteins were isolated using the µMACS protein isolation kit and identified with LC-MS/MS. Numbers of identified peptides are shown with self-identified bait proteins depicted in red. Color-code indicates the relative interaction propensity based on identified peptides normalized to bait-protein identification. **b** Schematic spoke-model of the Arabidopsis exocyst complex. Dashed lines represent interactions found via co-immunoprecipitation, solid lines represent previously published Y2H interactions. Thick and thin lines depict interactions found in both or one bait-prey pairs, respectively.

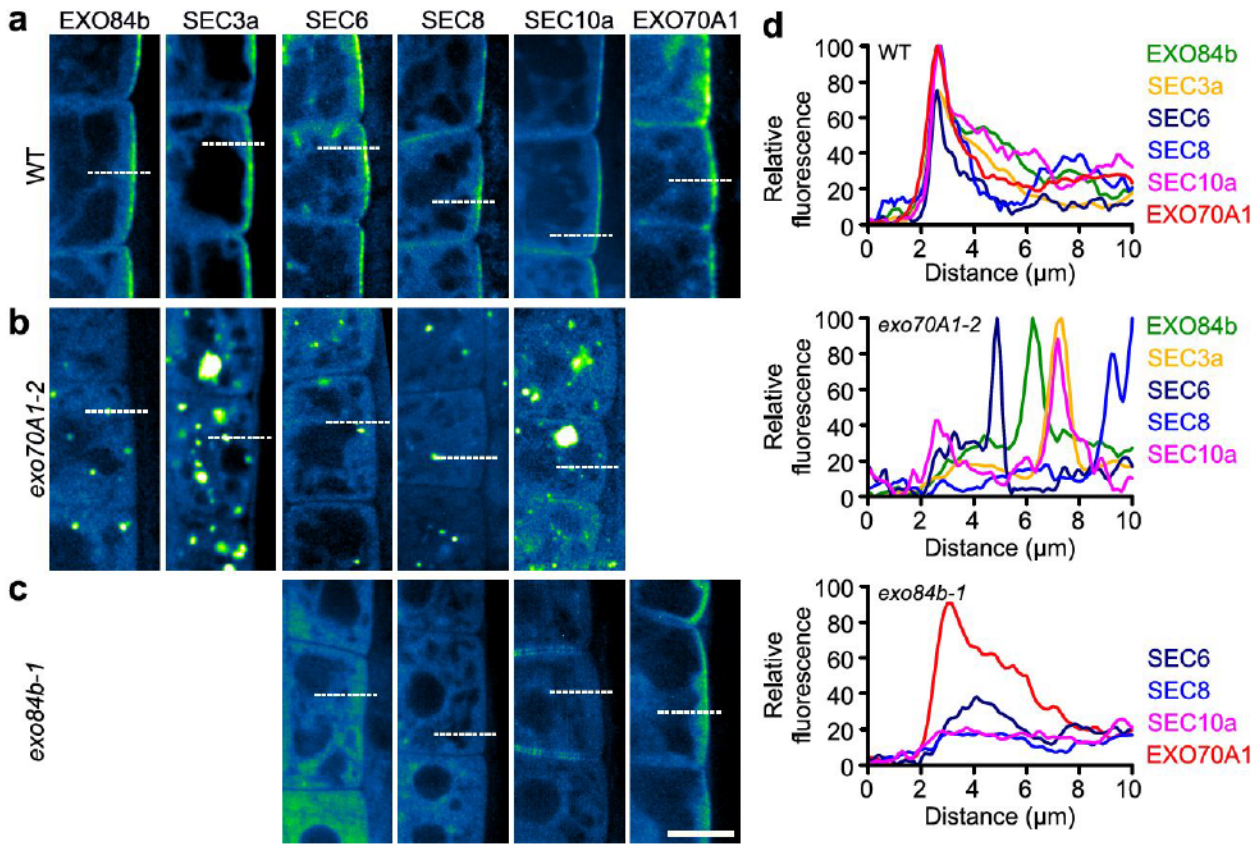

Figure 2: EXO70A1 is required for correct targeting of Arabidopsis exocyst complex to plasma membrane. a Exocyst subunits preferentially localize to outer lateral plasma membrane domain in root epidermal cells. **b** In *exo70A1-2* mutant, exocyst is detached from the plasma membrane and accumulates in intracellular compartments. **c** EXO70A1 can still bind outer lateral plasma membrane in *exo84b-1* mutant, while other subunits from both subcomplexes are cytoplasmic or relocalize to the baso-apical membrane. **d** Relative fluorescence intensity profiles normalized to cytosolic signal from cells shown in **a-c.** Typical cells from several independent lines are shown. EXO84b, *pEXO84b::EXO84b:GFP*; SEC3, *pSEC3::SEC3:GFP*; SEC6, *pSEC6::SEC6:GFP*; SEC8, *pSEC8::GFP:SEC8*; SEC10a, *pSEC10a::SEC10a:GFP*; EXO70A1, p*35S::GFP:EXO70A1*. Bar = 10 µm.

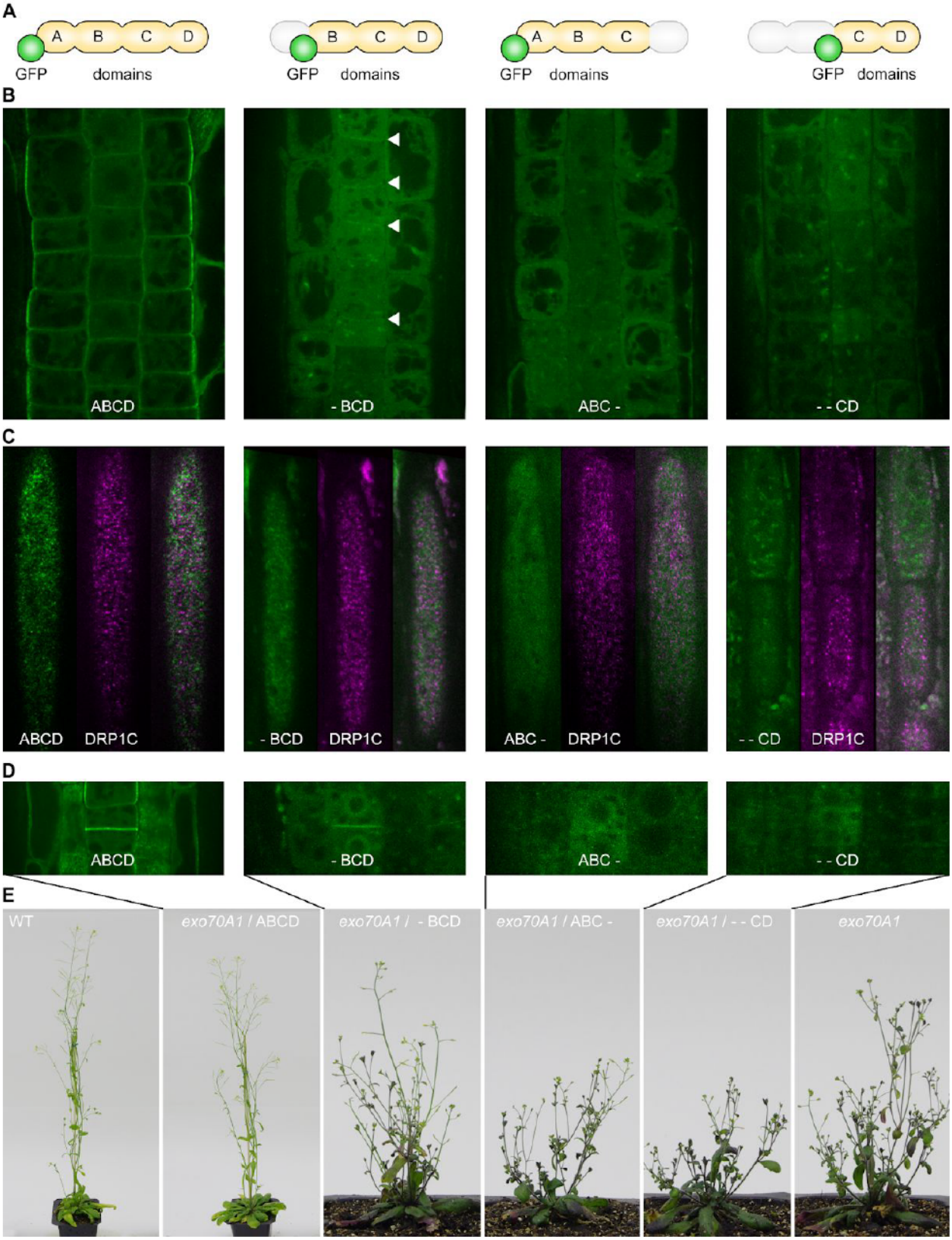
A
A B C D
GFP domains
B C D
GFP domains
A B C
GFP domains
C D
GFP domains
B
ABCD
- BCD
ABC -
- - CD
C
ABCD DRP1C
- BCD DRP1C
ABC - DRP1C
- - CD DRP1C
D
ABCD
- BCD
ABC -
- - CD
E
WT
exo70A1 / ABCD
exo70A1 / - BCD
exo70A1 / ABC -
exo70A1 / - - CD
exo70A1

Figure 3. Full length EXO70A1 is required for the proper PM localization and functional complementation of the *exo70A1* mutant. From left to right, subcellular localization and functional capabilities of full length EXO70A1 and its -BCD, ABC- and --CD variants are presented. **a** schematic representations of the full length and truncated EXO70A1 variants. **b** subcellular localizations of the GFP-tagged EXO70A1 versions. **c** co-localization of GFP-tagged variants of EXO70A1 with mOrange-tagged DRP1C in cortex of root epidermal cells indicating capability of the particular EXO70A1 constructs to bind plasma membrane. **d** localization of the WT and truncated EXO70A1 versions to maturing cell plate. E growth phenotypes of plants expressing variants of GFP"EXO70A1 in the *exo70A1-2* background. WT columbia Arabidopsis plants and *exo70A1-2* plants are displayed as reference.

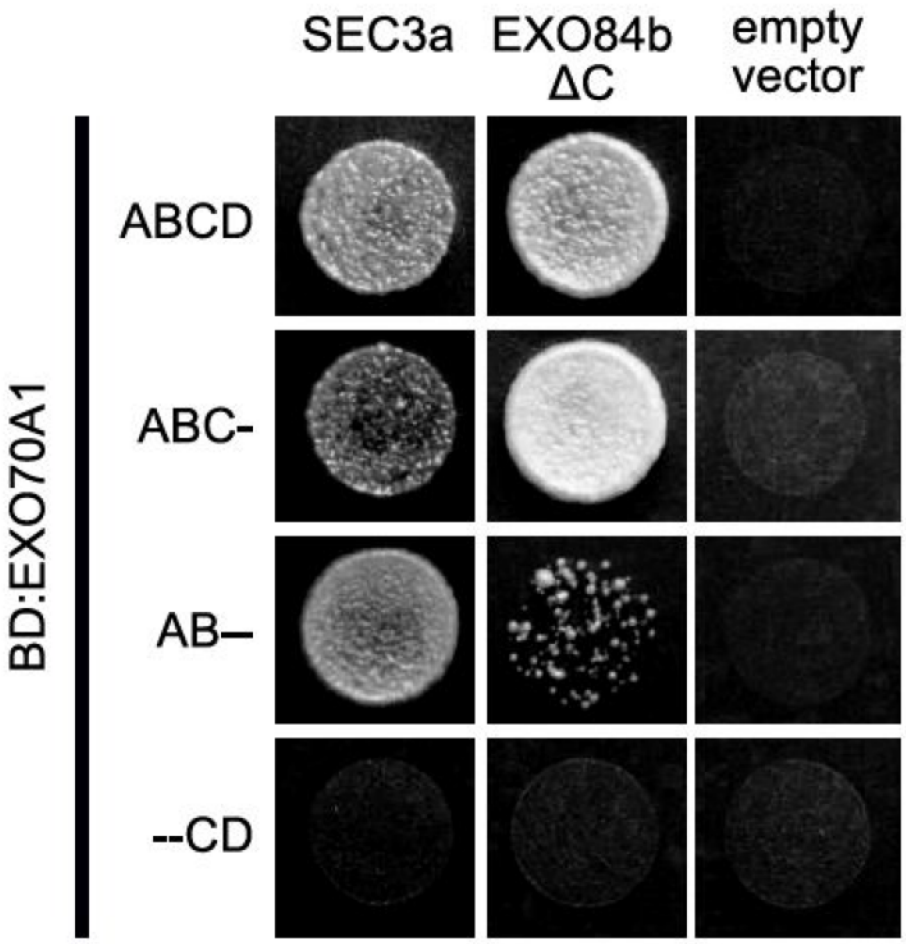

Figure 4. N-terminal domains of EXO70A1 drive its interaction with the core exocyst subunits. The ABC- variant of EXO70A1 retains capability of the full length protein to interact with SEC3A and the N terminal part of the EXO84b in the Y2H assay. The AB-- variant of the EXO70A1 retains full capacity of the EXO70A1 to interact with the SEC3A and partially interacts with the N terminal part of EXO84b in Y2H assay. The --CD variant of EXO70A1 does not interact with the selected core exocyst subunits. The representative combinations of AD and BD Y2H test constructs were selected according to previously characterized interaction pairs of the full length EXO70A1 with core subunits that avoid self-activation of any of the used constructs in the Y2H assay (Hala et al., 2008; Fendrych et al., 2010).

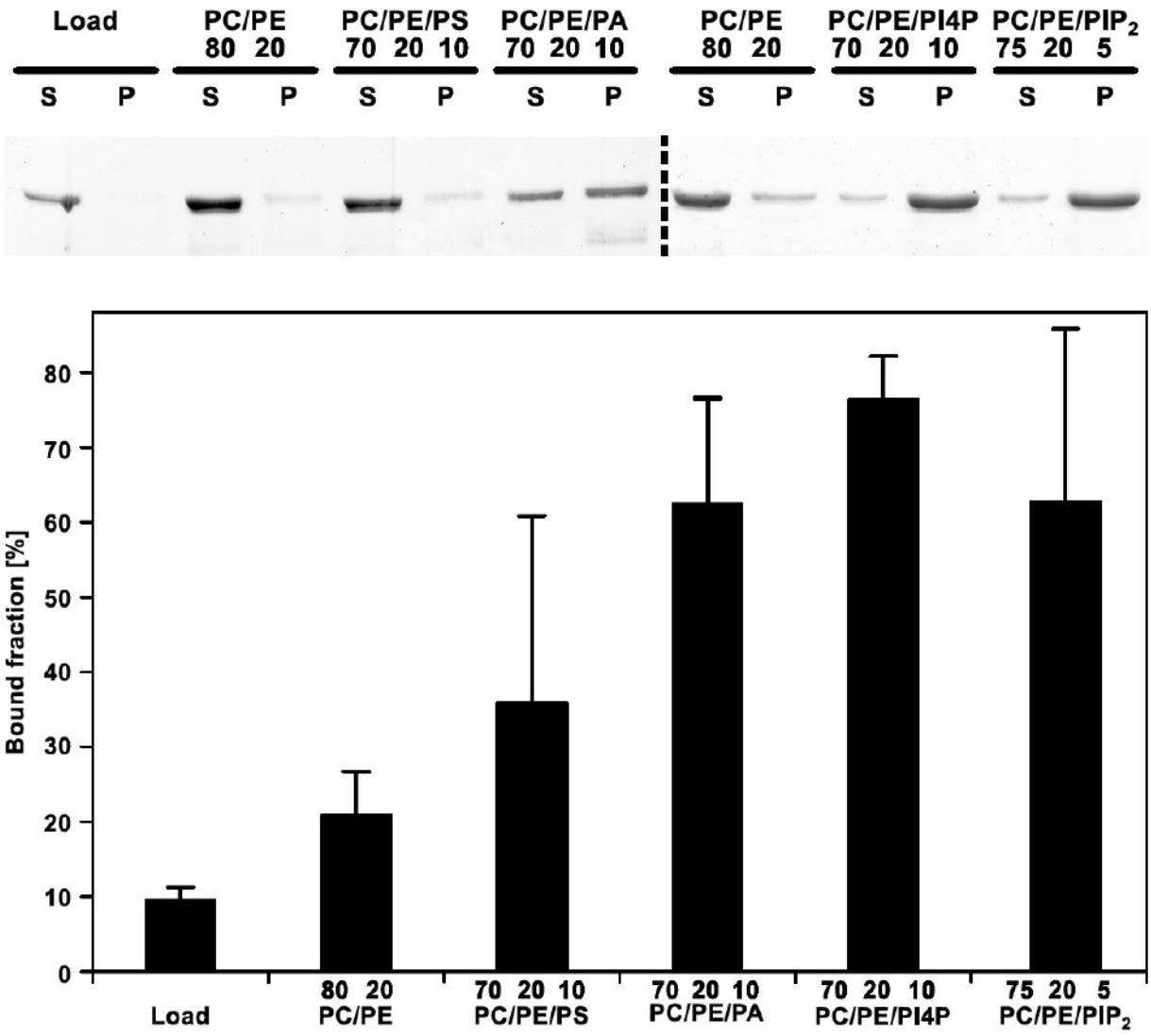

Figure 5. EXO70A1 binds negatively-charged phospholipids *in vitro*. 200 nm large unilamellar vesicles (LUVs) containing PC/PE (80/20%), PC/PE/PS (60/20/20%), PC/PE/PA (60/20/20%), PC/PE/PI4P (70/20/10%) and PC/PE/PIP2 (75/20/5%) were incubated with purified recombinant GST:EXO70A1. After centrifugation, proteins in the supernatant (S) and pellet (P) were subjected to SDS–PAGE and visualized by Coomassie Blue staining. Membrane-bound EXO70A1 fractions (mean ± SE from 3-5 independent experiments) were quantified by densitometry using the ImageJ software.

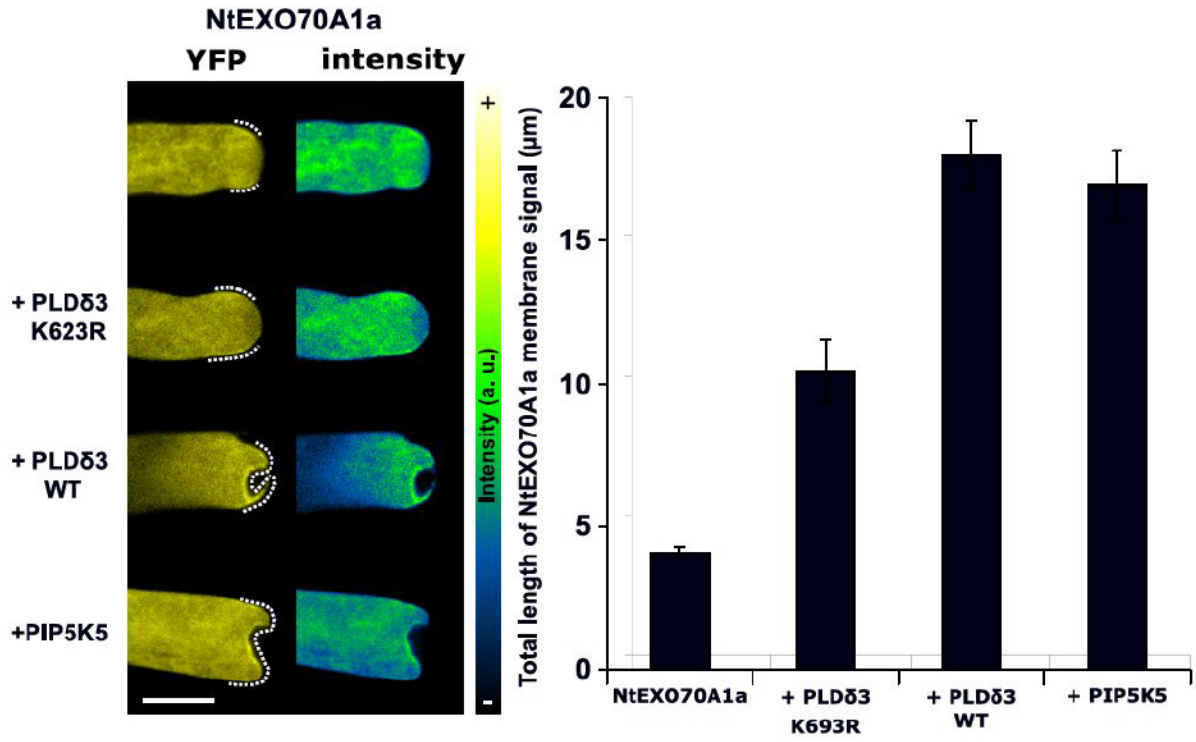

Figure 6: Phosphatidylinositol 4,5-bisphosphate and phosphatidic acid recruit EXO70A1 to plasma membrane *in vivo*. YFP:NtEXO70A1a was transiently expressed in tobacco pollen tubes either alone or together with particular lipid-modifying enzymes. Elevation of either PIP2 or PA level leads to the increased plasma membrane recruitment of the EXO70A1a in tobacco pollen tube when compared with control pollen tubes not expressing a phospholipid modifying enzyme or pollen tubes expressing partly catalytically inactive variant (K623R) of the phospholipase Dδ3. Left: Subcellular localization of YFP:NtEXO70A1a in tobacco pollen tube visualized in yellow (left part) and using a color intensity code in order to display local enrichment of the YFP signal (right part). From top to bottom, representative pollen tubes expressing YFP:NtEXO70A1a only and co-expressing YFP:NtEXO70A1a with partly catalytically inactive variant (K623R) of the phospholipase Dδ3, WT variant of the phospholipase Dδ3 or phosphatidylinositol-4-phosphate 5 kinase. Right: Quantification of total length of the plasma membrane covered with the YFP:NtEXO70A1a signal in pollen tubes expressing either YFP:NtEXO70A1a alone or together with the indicated lipid-modifying

enzymes. Both pollen tubes expressing YFP:NtEXO70A1a alone and coexpresing the construct with mutated phospholipase Dδ3 variant significantly differed from the pollen tubes expressing YFP:NtEXO70A1a together with fully functional phospholipid-modifying enzymes ($P < 0.001$) according to ANOVA followed by post hoc multiple mean comparison test with Tukey contrasts using the multcomp R package. Each dataset represents mean of 16 or more pollen tubes ± SE. a.u., Arbitrary unit. Bar = 10 μm.

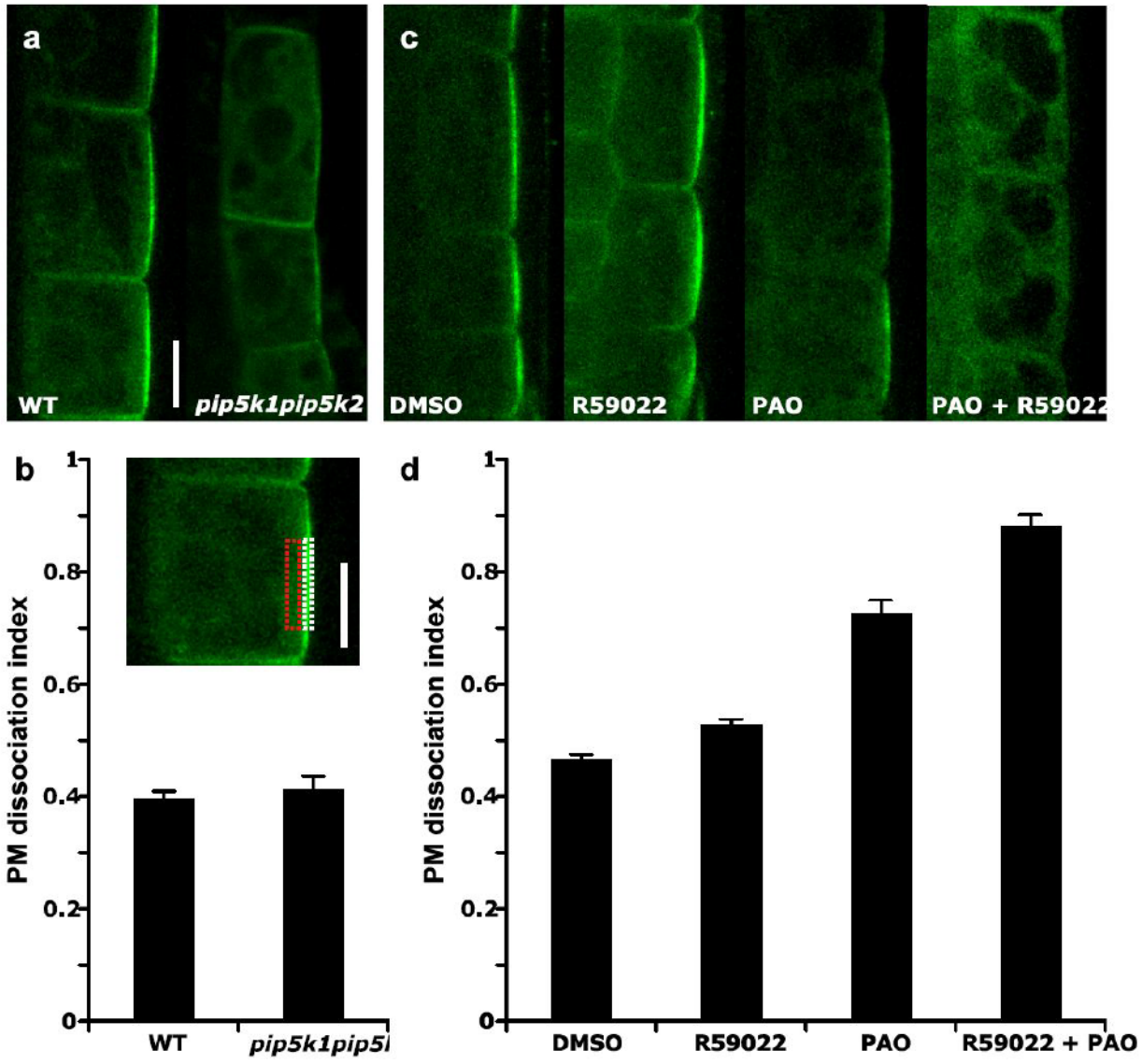

Figure 7: Plasma membrane localization of EXO70A1 in Arabidopsis root cells is dependent on phosphatidylinositol 4-phosphate and diacylglycerol kinase-produced pool of phosphatidic acid.

a GFP:EXO70A1 recruitment to the outer lateral membrane domain of Arabidopsis rhizodermal cells is unaffected in *pip5k1pip5k2* double mutant plants when compared to control plants. **b** Plasma membrane (PM) dissociation index determined as the ratio between the average signal detected in the cortical cytoplasm beneath the outer lateral plasma membrane domain (region

encircled by the red dotted rectangle) and the average signal at the outer lateral plasma membrane domain (the region encircled by white dotted rectangle). PM dissociation index of GFP:EXO70A1 does not significantly differ between WT and *pip5k1pip5k2* double mutant plants. Each dataset represents mean of 28 or more root cells ± SE. **c** GFP:EXO70A1 recruitment to the outer lateral domain of Arabidopsis rhizodermal plasma membrane is significantly reduced upon inhibition of diacylglycerol kinases, massively reduced after reduction of phosphatidylinositol 4-phosphate concentration and completely lost upon simultaneous inhibition of diacylglycerol kinases and phosphatidylinositol 4-kinases. **d** PM dissociation index of GFP:EXO70A1 upon pharmacological inhibition of phospholipid modifying enzymes. All sets significantly differed from each other ($P < 0.001$) according to ANOVA followed by posthoc multiple mean comparison test with Tukey contrasts using the multcomp R package. Each dataset represents mean of 80 or more root cells ± SE. Bars = 10 μm.

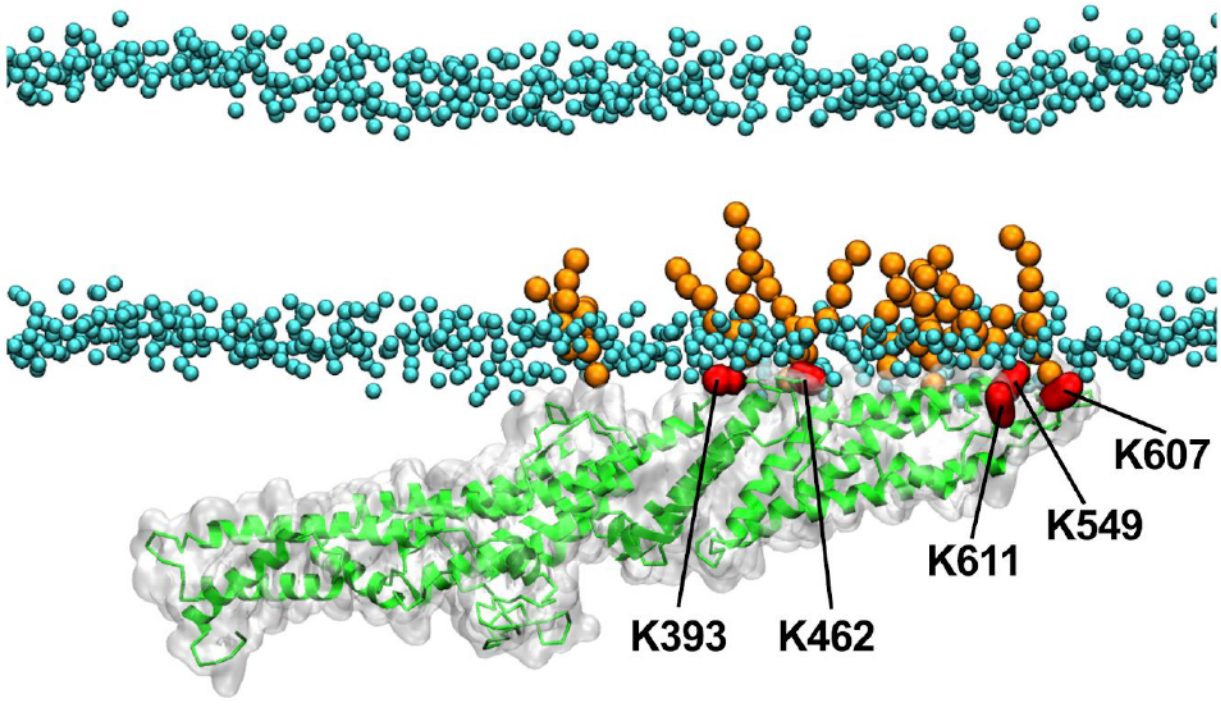
K607
K549
K611
K393
K462

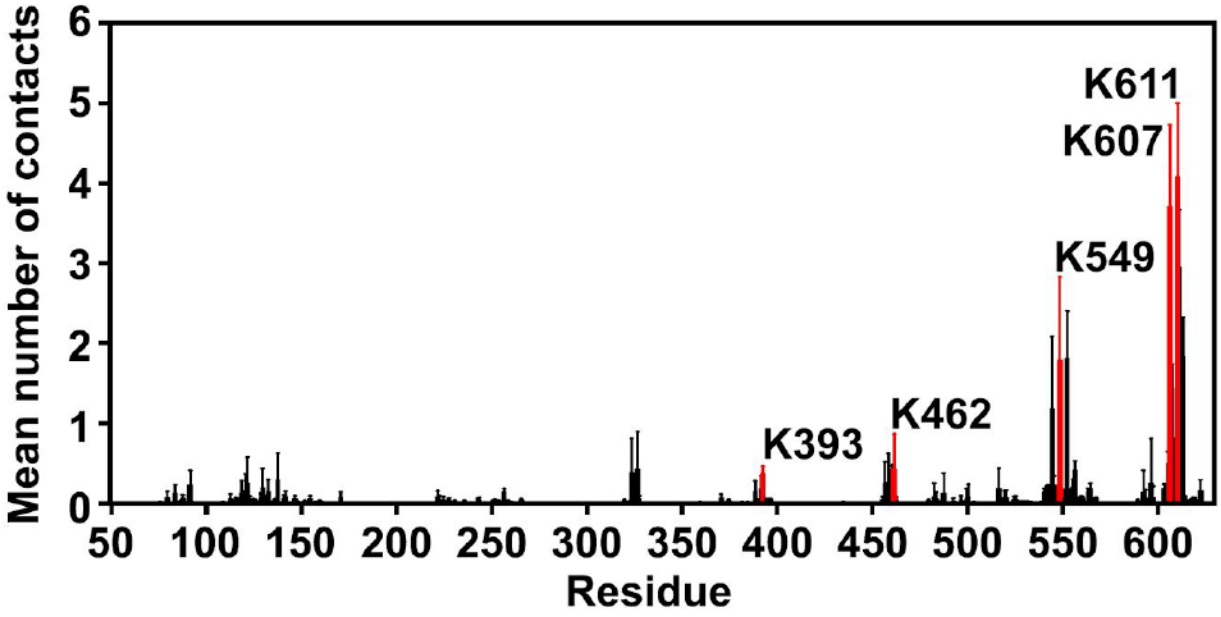
Mean number of contacts
0
1
2
3
4
5
6
50
100
150
200
250
300
350
400
450
500
550
600
Residue
K611
K607
K549
K462
K393

Figure 8: Molecular dynamic simulations reveal the key residues indispensable for interaction of EXO70A1 with anionic phospholipids. Top: Representative snapshot from the molecular dynamic simulation of EXO70A1 (in green) and the lipid bilayer containing phosphatidic acid (PA). The key basic amino acid residues of EXO70A1 interacting with PA are highlighted in red. Only PA molecules in the distance of 0.8 nm from the protein after 1000 ns are shown in orange. Choline headgroup atoms of phosphatidylcholine are shown in van der Waals representation (cyan). Water molecules and ions are not shown for the sake of clarity. Bottom: The mean number of EXO70A1-PA contacts per amino acid residue. The contacts were defined as the number of PA phosphate groups within 0.8 nm of protein atoms.

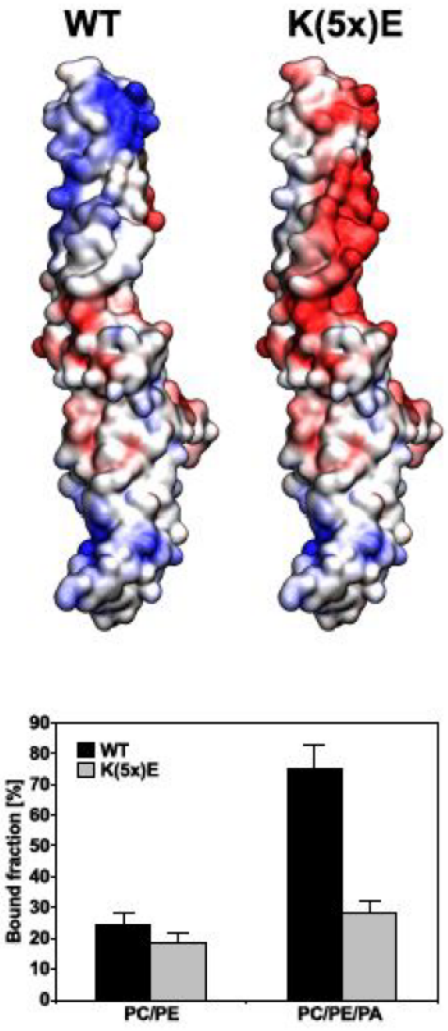

Figure 9: K(5x)E mutant of EXO70A1 displays altered surface charge distribution and loses capability to interact with anionic phospholipids. Top: Structural homology models of the WT EXO70A1 and the K(5x)E mutant version of the EXO70A1 demonstrating altered surface charge distribution of the mutant variant. Indicated electrostatic potential mapped onto the solvent accessible surfaces spans from -5 (red) to +5 (blue) kbT/ec. Bottom: the K(5x)E EXO70A1 loses capability to bind PA-containing vesicles *in vitro*.

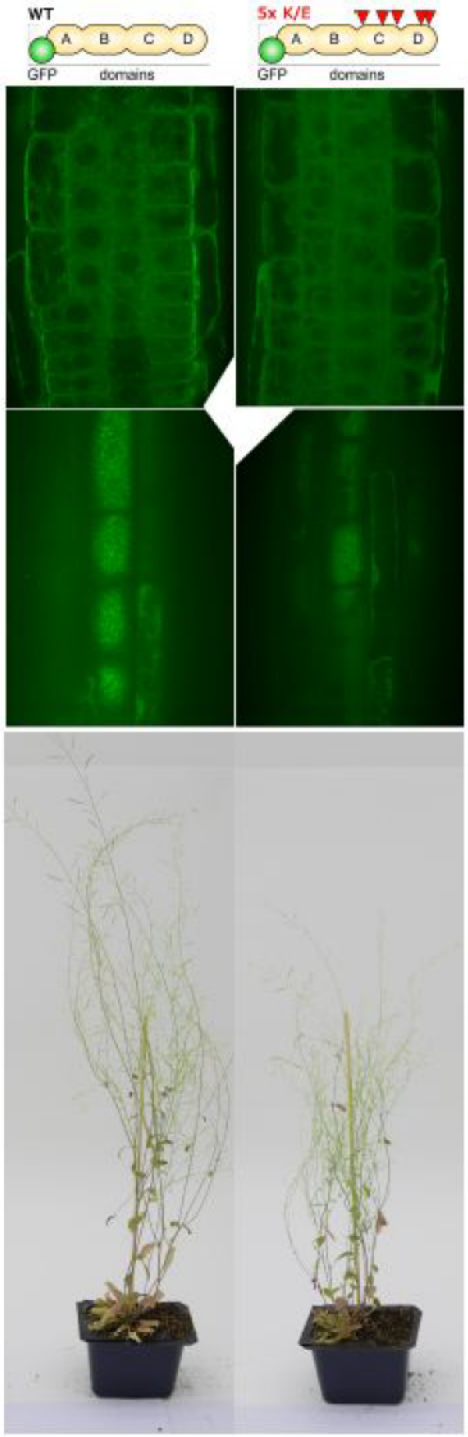
WT
A
B
C
D
GFP
domains
5x K/E
A
B
C
D
GFP
domains

Figure 10: K(5x)E EXO70A1 mutant loses the capability to bind plasma membrane and fully complement the *exo70A1-2* mutant phenotype. The lysine residues predicted by the molecular dynamics simulation are essential for EXO70A1 recruitment to plasma membrane and for the function of EXO70A1 in targeting of the exocyst complex. Left: GFP:EXO70A1 properly localizes to the outer lateral plasma membrane of the Arabidopsis root cells and complements growth phenotype of the *exo70A1-2* mutant. Right: The GFP:EXO70A1 with the K(5x)E amino acid substitution loses capacity to bind plasma membrane and leads to only partial growth phenotype complementation when introduced into the *exo70A1-2* mutant background.

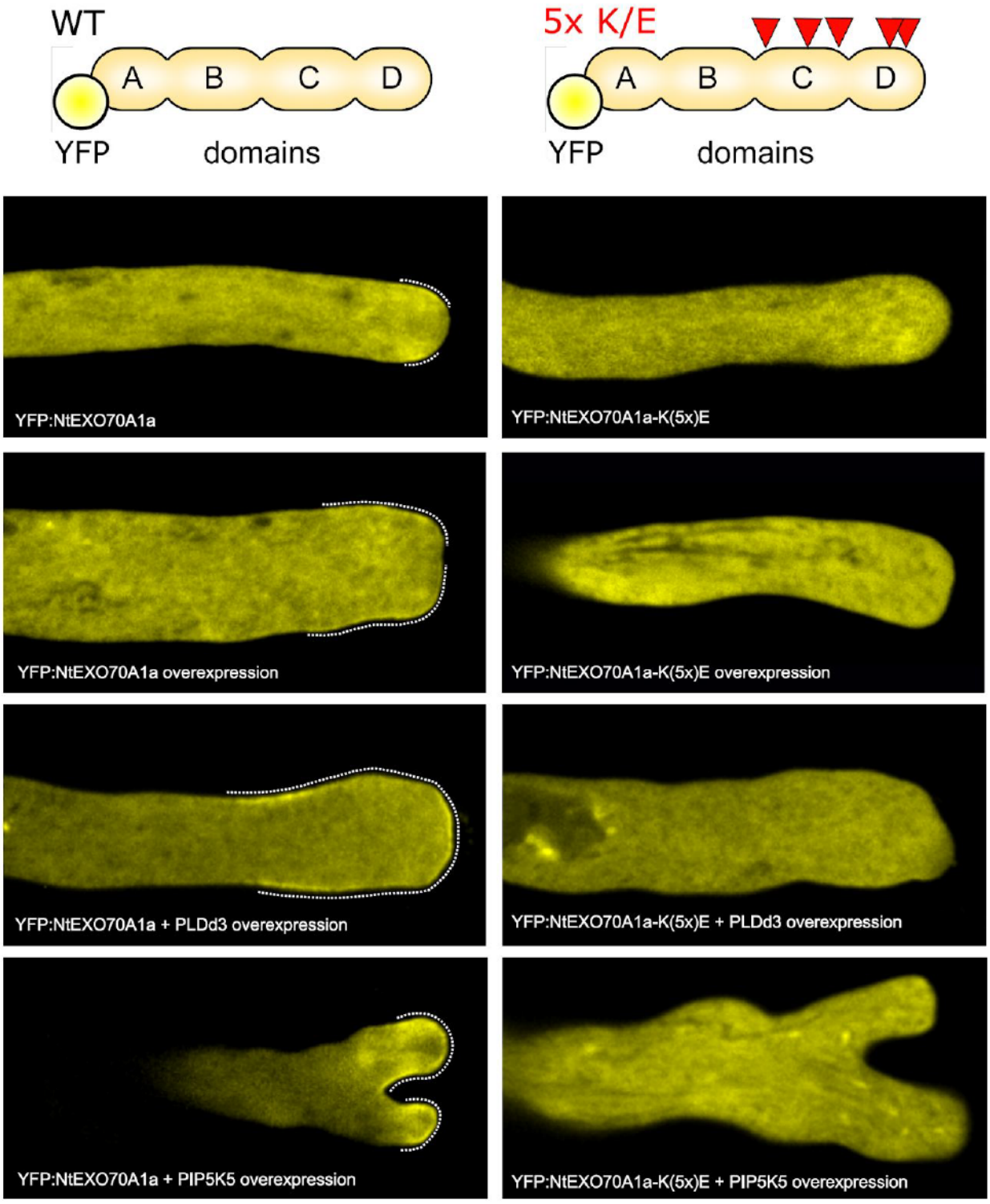
WT
A
B
C
D
YFP
domains
5x K/E
A
B
C
D
YFP
domains
YFP:NtEXO70A1a
YFP:NtEXO70A1a-K(5x)E
YFP:NtEXO70A1a overexpression
YFP:NtEXO70A1a-K(5x)E overexpression
YFP:NtEXO70A1a + PLDd3 overexpression
YFP:NtEXO70A1a-K(5x)E + PLDd3 overexpression
YFP:NtEXO70A1a + PIP5K5 overexpression
YFP:NtEXO70A1a-K(5x)E + PIP5K5 overexpression

Figure 11. Specific lysine residues are required for the interaction of NtEXO70A1a with anionic phospholipids in tobacco pollen tube. The lysine residues predicted by the molecular dynamics simulation are essential for NtEXO70A1a affinity towards acidic phospholipids in tobacco pollen tube, as displayed by localization of the wild-type YFP:NtEXO70A1a (left column) and localization of the mutated YFP:NtEXO70A1a-K(5x)E (right column) in tobacco pollen tube under various conditions. While the wild type fluorescently tagged NtEXO70A1a localizes to plasma membrane under physiological conditions in growing tobacco pollen tubes, in tobacco pollen tubes overexpressing NtEXO70A1a and in pollen tubes with elevated PIP2 or PA level due to overexpression of enzymes producing the particular lipids, the mutated NtEXO70A1a-K(5x) variant does not bind plasma membrane neither at physiological conditions nor when the NtEXO70A1a or anionic phospholipid producing enzymes are overexpressed. The images shown are representative for 15 or more transformed pollen tubes observed in at least two independent experiments. Bar = 10 μm.

a

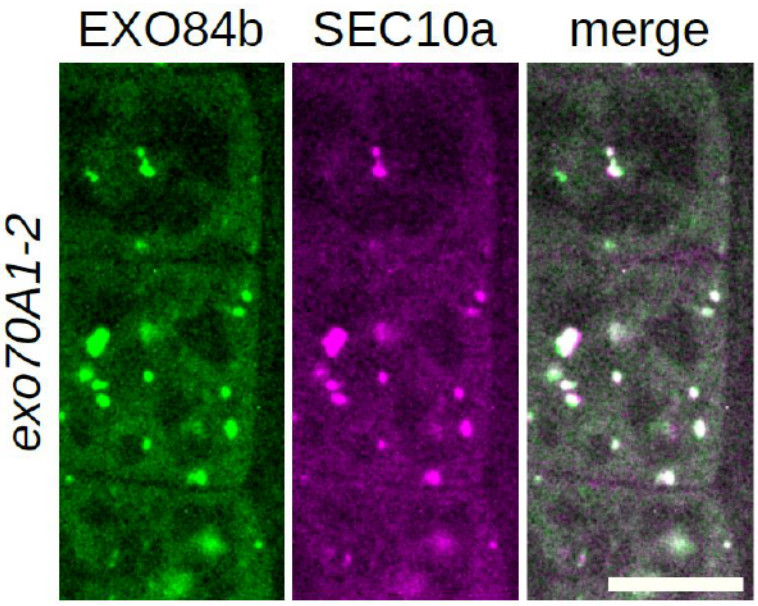

b

prey / bait	SEC3a	SEC5a	SEC6	SEC8	SEC10 a/b	SEC15b	EXO70 A1	EXO84b
GFP:SEC8 in *exo70A1-2*	3		4	4				

Supplementary figure S1. Core exocyst subunits remain in complex in *exo70A1-2* mutant cells. a EXO84 and SEC10a colocalize in *exo70A1-2* induced intracellular compartments. **b** Co-immunoprecipitation analysis of GFP-tagged SEC8 in *exo70A1-2* mutant background. Numbers of identified peptides are shown with self-identified SEC8 depicted in red. EXO84b, *pEXO84b::EXO84b:GFP*; SEC8, *pSEC8::GFP:SEC8*; SEC10a, *pSEC10a::SEC10a:mCherry*. Bar = 10 µm.

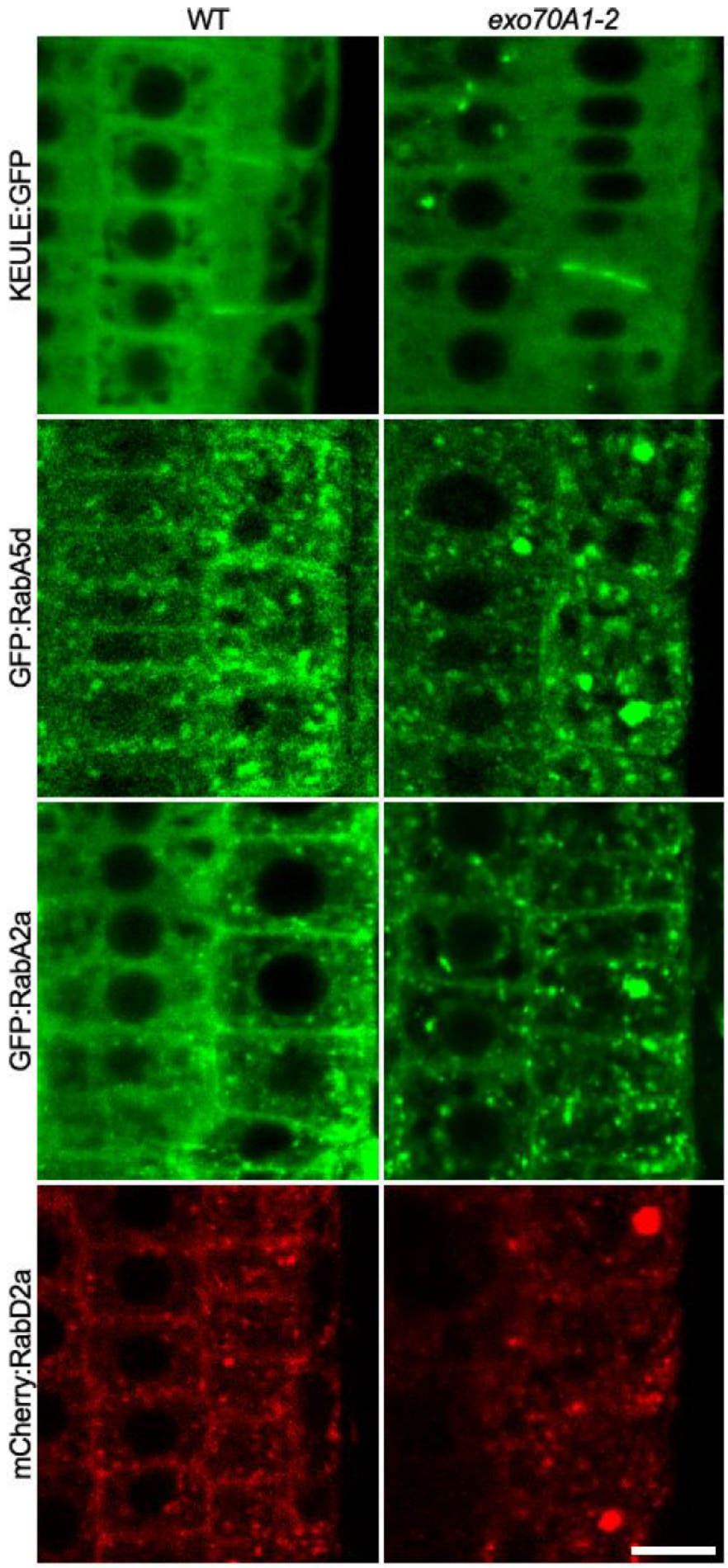
WT
exo70A1-2
KEULE:GFP
GFP:RabA5d
GFP:RabA2a
mCherry:RabD2a

Supplementary figure S2. Multiple endomembrane associated proteins relocalize to the intracellular compartment in *exo70A1-2* mutant while keeping targeting to the cell-plate. a cell-plate specific Sec1/Munc18 protein KEULE:GFP **b** Recycling endosome-specific small GTPase GFP:RabA5d. **c** TGN/endosome-localized small GTPase GFP:RabA2a. **d** Golgi/endosomal-localized small GTPase mCherry:RabD2a.

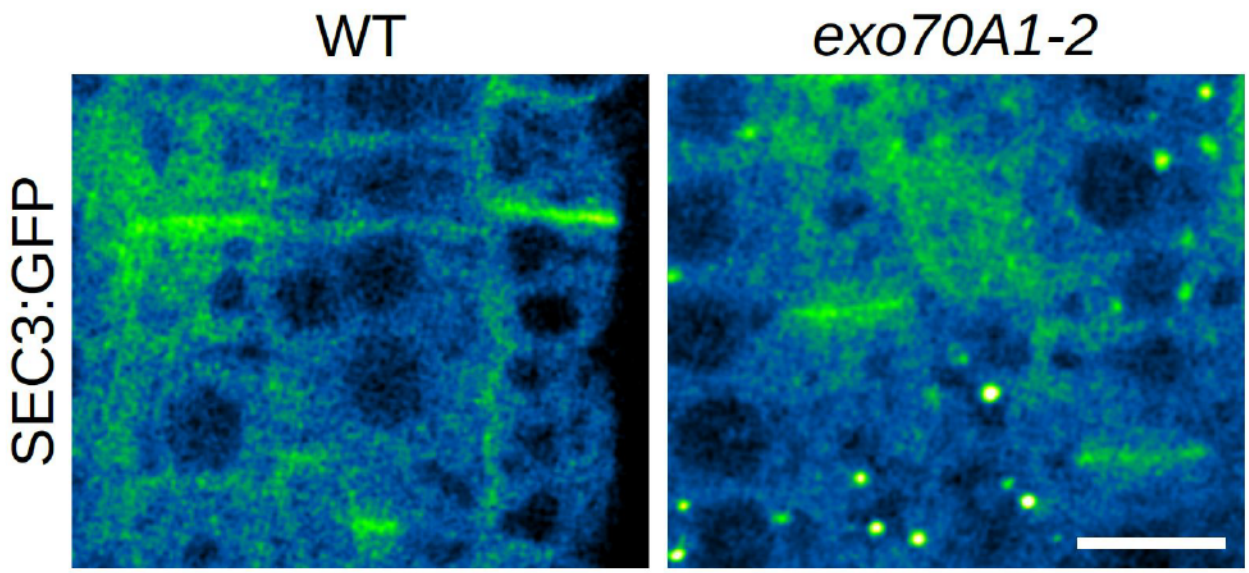

Supplementary figure S3. Core exocyst subunit SEC3a (*pSEC3a::SEC3a:GFP*) retains its cell-plate localization in *exo70A1-2* mutant background.

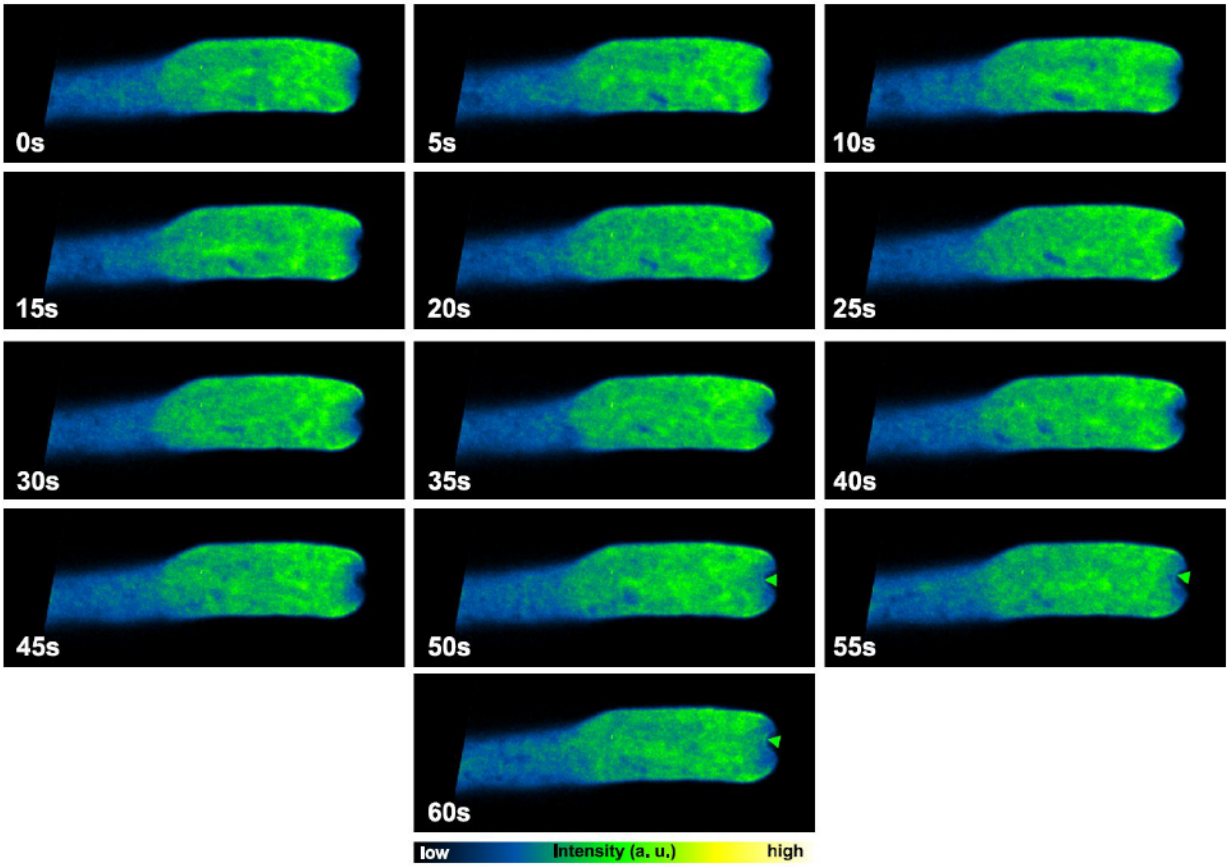

Supplementary figure S4. Development of the PLDδ3 overexpression - induced plasma membrane invagination of tobacco pollen tube resulting in rapid plasma membrane recruitment of NtEXO70A1a with time intervals of the imaging indicated. Bar = 10 μm.

Insert	Forward primer	Reverse primer	Restriction/recombination sites	Target vector
pSEC3	ATAGAAAAGTTGAATTTCTCTGTCTCTACTCTCTAATATTT	TTGTACAAACTTGATGTTGTTGTTGCGGATC	attb1, attb4	pB7m34GW
SEC3	AAAAAAGCAGGCTATGGCGAAATCAAGCGC	CAAGAAAGCTGGGTACATGGAAGCCAGAAGTCC	attb1, attb2	pB7m34GW
pSEC15b	TTGTCGACGCGATTGCTTTTTGCCATGC	TGTTTTATCTCCGATTAGGTAAAAG	SalI, NotI	pENTR1a
SEC15b	ATGCAATCGTCGAAAGGAC	TTGCGGCCGCGAGAGACCAACGAATCATCAACA	SalI, NotI	pDONR
EXO70A1 full-length	ATCACTAGTATGGCTGTTGATAGC	TATACTAGTTTACCGGCGTGGTTCATT	SpeI, SpeI	pBAR1:GFP
EXO70A1 -BCD	ATAACTAGTAGTAAAGCGGTGGAGCC	TATACTAGTTTACCGGCGTGGTTCATT	SpeI, SpeI	pBAR1:GFP
EXO70A1 - - CD	TACTGGATCCAAAGGGAAAGCATGC	TAATGGATCCTTACCGGCGTGGTTC	BamHI, BamHI	pBAR1:GFP
EXO70A1 ABC-	ATCACTAGTATGGCTGTTGATAGC	TACACTAGTTTAGCCTAACAAATCCTT	SpeI, SpeI	pBAR1:GFP
EXO70A1 -BCD	ATGAATTCAGTAAAGCGGTGGAGCCTG	ATGTCGACTACCGGCGTGGTTCATT	EcoRI, SalI	pGBKT7
EXO70A1 - - CD	ATGAATTCAAAGGGAAAGCATGCCTCGAAATTA	ATGTCGACTACCGGCGTGGTTCATT	EcoRI, SalI	pGBKT7
EXO70A1 ABC-	ATGAATTCGCCATGGCTGTTGATAGCAGA	ATGTCGACTAGCCTAACAAATCCTTGGC	EcoRI, SalI	pGBKT7
EXO70A1 AB - -	ATGAATTCGCCATGGCTGTTGATAGCAGA	ATGTCGACTACCCTTTGAAAATTGTCTCAATC	EcoRI, SalI	pGBKT7
EXO70A1Δ69	ACGGAATTCTTAAGGCTGCTGAAGTTATTTTG	TAGTCGACTTACCGGCGTGGTTCATTC	EcoRI, SalI	pGEX4T-2
EXO70A1Δ69-5xE	ACGGAATTCTTAAGGCTGCTGAAGTTATTTTG	TAGTCGACTTACCGGCGTGGTTCATTC	EcoRI, SalI	pGEX4T-2

Final mutated EXO70A1 variant	Primer sequence
Arabidopsis EXO70A1 (5x)K/E	ATAACTAGTGCCATGGCTGTTGATAGC
Arabidopsis EXO70A1 (5x)K/E	TGAGAAAGATGCTACAGCGACTGCTGTTCTAGATGGA
Arabidopsis EXO70A1 (5x)K/E	GTGTGTCAATGCAGGATCTGCGTACTGTTTCGATTTTCCG
Arabidopsis EXO70A1 (5x)K/E	GTTTCAAGAGGATTATTAGCAGAGAGGTTCAAGATGTTC
Arabidopsis EXO70A1 (5x)K/E	CTTTGGTTGAGAGTGGGGCGAATCCTCAGGCATACATAAAGTATACAGCTGAAGA
Arabidopsis EXO70A1 (5x)K/E	TATACTAGTTTACCGGCGTGGTTCATT
Tobacco NtEXO70A1a (5x)K/E	TAGCCGGCATGGGTATGCCAAGAAACAC

Tobacco NtEXO70A1a (5x)K/E	CTGTCGAGAAAGATGCAACCGAGACCGCCGTATCAGATGG
Tobacco NtEXO70A1a (5x)K/E	GGAACAAGTTAGTAAGAGCTGGATCCTCATACTGCTTAGATTTCCCATCCA
Tobacco NtEXO70A1a (5x)K/E	GGAGTTTCAAGAGCGCTTGTAGAGGAAAGGTTGAAGACTTTCAATATTCA
Tobacco NtEXO70A1a (5x)K/E	GCCAATGGTTGAGAATGGTGAGAATCCCCAAGAGTATATCAGGTACTCGGCTGAAGAT
Tobacco NtEXO70A1a (5x)K/E	TAGGGCCCTCATCGTTTTGGCTCATTC

Supplementary file S2. Tables of the primers used for direct cloning of the novel constructs used in this study (top) and the primers used for introducing point mutations into Arabidopsis EXO70A1 and tobacco NtEXO70A1a (bottom).

References

Awasthi, S., Palmer, R., Castro, M., Mobarak, C. D. & Ruby, S. W. New Roles for the Snp1 and Exo84 Proteins in Yeast Pre-mRNA Splicing. *Journal of Biological Chemistry* **276,** 31004–31015 (2001).

Barbosa, I. C. R. *et al.* Phospholipid composition and a polybasic motif determine D6 PROTEIN KINASE polar association with the plasma membrane and tropic responses. *Development* **143,**4687–4700 (2016).

Bloch, D. *et al.* Exocyst SEC3 and phosphoinositides define sites of exocytosis in pollen tube initiation and growth. *Plant Physiology* (2016). doi:10.1104/pp.16.00690

Bodemann, B. O. *et al.* RalB and the Exocyst Mediate the Cellular Starvation Response by Direct Activation of Autophagosome Assembly. *Cell* **144,** 253–267 (2011).

The Angiosperm Phylogeny Group, Chase, M. W., Christenhusz, M. J. M., Fay, M. F., Byng, J. W., Judd, W. S., Soltis, D. E., Mabberley, D. J., Sennikov, A. N., Soltis, P. S., Stevens, P. F. An update of the Angiosperm Phylogeny Group classification for the orders and families of flowering plants: APG IV. *Botanical Journal of the Linnean Society* **181,** 1-20 (2016).

Choudhury, S. R. & Pandey, S. Phosphatidic acid binding inhibits RGS1 activity to affect specific signaling pathways in Arabidopsis. *The Plant Journal* **90,**466–477 (2017).

Cole, R. A. SEC8, a Subunit of the Putative Arabidopsis Exocyst Complex, Facilitates Pollen Germination and Competitive Pollen Tube Growth. *Plant Physiology* **138,**2005–2018 (2005).

Cvrčková, F. *et al.* Evolution of the Land Plant Exocyst Complexes. *Frontiers in Plant Science* **3,** (2012).

Chen, J. *et al.*Crystal structure of Sec10, a subunit of the exocyst complex. *Scientific Reports* **7,**40909 (2017).

Cvrčková, F. & Žárský, V. Old AIMs of the exocyst: evidence for an ancestral association of exocyst subunits with autophagy-associated Atg8 proteins. *Plant Signaling & Behavior* **8,**(2013).

Dellago, H. *et al.* Exo70, a subunit of the exocyst complex, interacts with SNEVhPrp19/hPso4and is involved in pre-mRNA splicing. *Biochemical Journal* **438,**81–91 (2011).

Ding, Y. *et al.* Exo70E2 is essential for exocyst subunit recruitment and EXPO formation in both plants and animals. *Molecular Biology of the Cell* **25,**412–426 (2014).

Dong, G., Hutagalung, A., Fu, C., Novick, P. & Reinisch, K. The structures of exocyst subunit Exo70p and the Exo84p C-terminal domains reveal a common motif. (2005). doi:10.2210/pdb2b1e/pdb

Donovan, K. W. & Bretscher, A. Tracking individual secretory vesicles during exocytosis reveals an ordered and regulated process. *The Journal of Cell Biology* **210,**181–189 (2015).

Dörmann, P. *et al.* Cell-autonomous defense, re-organization and trafficking of membranes in plant-microbe interactions. *New Phytologist* **204,**815–822 (2014).

Drdová, E. J. *et al.* The exocyst complex contributes to PIN auxin efflux carrier recycling and polar auxin transport in Arabidopsis. *The Plant Journal* **73,**709–719 (2013).

Dupraz, S. *et al.* The TC10-Exo70 Complex Is Essential for Membrane Expansion and Axonal Specification in Developing Neurons. *Journal of Neuroscience* **29,**13292–13301 (2009).

Eliáš, M. The exocyst complex in plants. *Cell Biology International* **27,**199–201 (2003).

Fendrych, M. *et al.* The Arabidopsis Exocyst Complex Is Involved in Cytokinesis and Cell Plate Maturation. *The Plant Cell* **22,**3053–3065 (2010).

Fendrych, M. *et al.* Visualization of the exocyst complex dynamics at the plasma membrane of Arabidopsis thaliana. *Molecular Biology of the Cell* **24,**510–520 (2013).

Clough, S. J. & Bent, A. F. Floral dip: a simplified method for Agrobacterium-mediated transformation of Arabidopsis thaliana. *The Plant Journal* **16,**735–743 (1998).

Furt, F. *et al.* Polyphosphoinositides Are Enriched in Plant Membrane Rafts and Form Microdomains in the Plasma Membrane. *Plant Physiology* **152,**2173–2187 (2010).

Galvan-Ampudia, C. S. *et al.* Halotropism Is a Response of Plant Roots to Avoid a Saline Environment. *Current Biology* **23,**2044–2050 (2013).

Geldner, N. *et al.* Rapid, combinatorial analysis of membrane compartments in intact plants with a multicolor marker set. *The Plant Journal* **59,**169–178 (2009).

Genre, A. *et al.* Multiple Exocytotic Markers Accumulate at the Sites of Perifungal Membrane Biogenesis in Arbuscular Mycorrhizas. *Plant and Cell Physiology* **53,**244–255 (2011).

Guo, W., Roth, D., Walch-Solimena, C. & Novick, P. The exocyst is an effector for Sec4p, targeting secretory vesicles to sites of exocytosis. *The EMBO Journal* **18,**1071–1080 (1999).

Guo, W., Tamanoi, F. & Novick, P. Spatial regulation of the exocyst complex by Rho1 GTPase. *Nature Cell Biology* **3,**353–360 (2001).

Hála, M. *et al.* An Exocyst Complex Functions in Plant Cell Growth in Arabidopsis and Tobacco. *The Plant Cell Online* **20,**1330–1345 (2008).

Hamburger, Z., Hamburger, A., West, A. & Weis, W. Crystal Structure of the S. cerevisiae Exocyst Component Exo70p. (2005). doi:10.2210/pdb2b7m/pdb

He, B., Xi, F., Zhang, X., Zhang, J. & Guo, W. Exo70 interacts with phospholipids and mediates the targeting of the exocyst to the plasma membrane. *The EMBO Journal* **26,**4053–4065 (2007).

Heider, M. R. *et al.* Subunit connectivity, assembly determinants and architecture of the yeast exocyst complex. *Nature Structural & Molecular Biology* **23,**59–66 (2015).

Hess, B., Kutzner, C., Spoel, D. V. D. & Lindahl, E. GROMACS 4: Algorithms for Highly Efficient, Load-Balanced, and Scalable Molecular Simulation. *Journal of Chemical Theory and Computation* **4,**435–447 (2008).

Huang, S., Gao, L., Blanchoin, L. & Staiger, C. J. Heterodimeric Capping Protein from Arabidopsis Is Regulated by Phosphatidic Acid. *Molecular Biology of the Cell* **17,**1946–1958 (2006).

Humphrey, W., Dalke, A. & Schulten, K. VMD: Visual molecular dynamics. *Journal of Molecular Graphics* **14,**33–38 (1996).

Ingólfsson, H. I. *et al.* Lipid Organization of the Plasma Membrane. *Journal of the American Chemical Society* **136,**14554–14559 (2014).

Ischebeck, T., Stenzel, I. & Heilmann, I. Type B Phosphatidylinositol-4-Phosphate 5-Kinases Mediate Arabidopsis and Nicotiana tabacum Pollen Tube Growth by Regulating Apical Pectin Secretion. *The Plant Cell Online* **20,**3312–3330 (2008).

Ischebeck, T. *et al.* Functional Cooperativity of Enzymes of Phosphoinositide Conversion According to Synergistic Effects on Pectin Secretion in Tobacco Pollen Tubes. *Molecular Plant* **3,**870–881 (2010).

Ischebeck, T. *et al.* Phosphatidylinositol 4,5-Bisphosphate Influences PIN Polarization by Controlling Clathrin-Mediated Membrane Trafficking in Arabidopsis. *The Plant Cell* **25,**4894–4911 (2013).

Jin, Y. *et al.* Myosin V Transports Secretory Vesicles via a Rab GTPase Cascade and Interaction with the Exocyst Complex. *Developmental Cell* **21,**1156–1170 (2011).

Jong, D. H. D. *et al.* Improved Parameters for the Martini Coarse-Grained Protein Force Field. *Journal of Chemical Theory and Computation* **9,** 687–697 (2012).

Julkowska, M. M. *et al.* Identification and functional characterization of the Arabidopsis Snf1-related protein kinase SnRK2.4 phosphatidic acid-binding domain. *Plant, Cell & Environment* **38,**614–624 (2014).

Kalmbach, L. *et al.* Transient cell-specific EXO70A1 activity in the CASP domain and Casparian strip localization. *Nature Plants* **3,**17058 (2017).

Katoh, Y., Nozaki, S., Hartanto, D., Miyano, R. & Nakayama, K. Architectures of multisubunit complexes revealed by a visible immunoprecipitation assay using fluorescent fusion proteins. *Journal of Cell Science* **128,**2351–2362 (2015).

Klahre, U., Becker, C., Schmitt, A. C. & Kost, B. Nt-RhoGDI2 regulates Rac/Rop signaling and polar cell growth in tobacco pollen tubes. *The Plant Journal* **46,**1018–1031 (2006).

Kolay, S., Basu, U. & Raghu, P. Control of diverse subcellular processes by a single multi-functional lipid phosphatidylinositol 4,5-bisphosphate [PI(4,5)P2]. *Biochemical Journal* **473,**1681–1692 (2016).

Konopka, C. A. & Bednarek, S. Y. Comparison of the Dynamics and Functional Redundancy of the Arabidopsis Dynamin-Related Isoforms DRP1A and DRP1C during Plant Development. *Plant Physiology* **147,**1590–1602 (2008).

Kooijman, E. E. *et al.* An Electrostatic/Hydrogen Bond Switch as the Basis for the Specific Interaction of Phosphatidic Acid with Proteins. *Journal of Biological Chemistry* **282,**11356–11364 (2007).

König, S., Hoffmann, M., Mosblech, A. & Heilmann, I. Determination of content and fatty acid composition of unlabeled phosphoinositide species by thin-layer chromatography and gas chromatography. *Analytical Biochemistry* **378,**197–201 (2008).

Konrad, S. S. & Ott, T. Molecular principles of membrane microdomain targeting in plants. *Trends in Plant Science* **20,**351–361 (2015).

Kost, B., Spielhofer, P. & Chua, N.-H. A GFP-mouse talin fusion protein labels plant actin filaments in vivo and visualizes the actin cytoskeleton in growing pollen tubes. *The Plant Journal* **16,**393–401 (1998).

Kulich, I. *et al.* Arabidopsis exocyst subunits SEC8 and EXO70A1 and exocyst interactor ROH1 are involved in the localized deposition of seed coat pectin. *New Phytologist* **188,**615–625 (2010).

Kulich, I. *et al.* Arabidopsis exocyst subcomplex containing subunit EXO70B1 is involved in the autophagy-related transport to the vacuole. *Traffic* (2013). doi:10.1111/tra.12101

Kulich, I. *et al.* Cell Wall Maturation of Arabidopsis Trichomes Is Dependent on Exocyst Subunit EXO70H4 and Involves Callose Deposition. *Plant Physiology* **168,**120–131 (2015).

Kulich, I. *et al.* Exocyst Subunit EXO70H4 Has a Specific Role in Callose Synthase Secretion and Silica Accumulation. *Plant Physiology* **176,**2040–2051 (2018).

Li, M., Qin, C., Welti, R. & Wang, X. Double Knockouts of Phospholipases Dzeta1 and Dzeta2 in Arabidopsis Affect Root Elongation during Phosphate-Limited Growth But Do Not Affect Root Hair Patterning. *Plant Physiology* **140,**761–770 (2006).

Li, G. & Xue, H.-W. Arabidopsis PLDzeta2 Regulates Vesicle Trafficking and Is Required for Auxin Response. *The Plant Cell* **19,**281–295 (2007).

Liu, J., Zuo, X., Yue, P. & Guo, W. Phosphatidylinositol 4,5-Bisphosphate Mediates the Targeting of the Exocyst to the Plasma Membrane for Exocytosis in Mammalian Cells. *Molecular Biology of the Cell* **18,**4483–4492 (2007).

Marrink, S. J., Risselada, H. J., Yefimov, S., Tieleman, D. P. & Vries, A. H. D. The MARTINI Force Field: Coarse Grained Model for Biomolecular Simulations. *The Journal of Physical Chemistry B* **111,**7812–7824 (2007).

Martin-Urdiroz, M., Deeks, M. J., Horton, C. G., Dawe, H. R. & Jourdain, I. The Exocyst Complex in Health and Disease. *Frontiers in Cell and Developmental Biology* **4,**(2016).

Mcloughlin, F. *et al.* Identification of novel candidate phosphatidic acid-binding proteins involved in the salt-stress response of Arabidopsis thaliana roots. *Biochemical Journal* **451,**(2013).

Mei, K. *et al.* Cryo-EM Structure of the Exocyst Complex. *Nature structural & molecular biology* (2018). doi:10.2210/pdb5yfp/pdb

Monticelli, L. *et al.* The MARTINI Coarse-Grained Force Field: Extension to Proteins. *Journal of Chemical Theory and Computation* **4,** 819–834 (2008).

Moore, B. & Xu, Z. The Crystal Structure of Mouse Exo70 Reveals Unique Features of the Mammalian Exocyst. (2007). doi:10.2210/pdb2pft/pdb

Morgera, F. *et al.* Regulation of exocytosis by the exocyst subunit Sec6 and the SM protein Sec1. *Molecular Biology of the Cell* **23,**337–346 (2012).

Munson, M. & Novick, P. The exocyst defrocked, a framework of rods revealed. *Nature Structural & Molecular Biology* **13,**577–581 (2006).

Oda, Y., Iida, Y., Nagashima, Y., Sugiyama, Y. & Fukuda, H. Novel Coiled-Coil Proteins Regulate Exocyst Association with Cortical Microtubules in Xylem Cells via the Conserved Oligomeric Golgi-Complex 2 Protein. *Plant and Cell Physiology* **56,**277–286 (2014).

Ortmannová, J., Pečenková, T., Sekereš, J., Kulich, I., Šantrůček, J., Žárský, V. Exocyst complex mediates non-host resistance against powdery mildew in Arabidopsis. *Submitted to Molecular plant*

Pečenková, T. *et al.* The role for the exocyst complex subunits Exo70B2 and Exo70H1 in the plant–pathogen interaction. *Journal of Experimental Botany* **62,**2107–2116 (2011).

Pečenková, T. *et al.* Early Arabidopsis root hair growth stimulation by pathogenic strains of Pseudomonas syringae. *Annals of Botany* **120,**437–446 (2017).

Pejchar, P. , Sekereš, J., Potocký, M. Molecular characterization of pollen-preferred phospholipase Dδ family in tobacco. *In prep*

Periole, X., Cavalli, M., Marrink, S.-J. & Ceruso, M. A. Combining an Elastic Network With a Coarse-Grained Molecular Force Field: Structure, Dynamics, and Intermolecular Recognition. *Journal of Chemical Theory and Computation* **5,** 2531–2543 (2009).

Picco, A. *et al.* The In Vivo Architecture of the Exocyst Provides Structural Basis for Exocytosis. *Cell* **168,** (2017).

Platre, M. P. & Jaillais, Y. Anionic lipids and the maintenance of membrane electrostatics in eukaryotes. *Plant Signaling & Behavior* **12,**(2017).

Platre, M. P. *et al.* A combinatorial lipid code shapes the electrostatic landscape of plant endomembranes. (2018). doi:10.1101/278135

Pleskot, R. *et al.* Turnover of Phosphatidic Acid through Distinct Signaling Pathways Affects Multiple Aspects of Pollen Tube Growth in Tobacco. *Frontiers in Plant Science***3,**(2012).

Pleskot, R., Pejchar, P., Žárský, V., Staiger, C. J. & Potocký, M. Structural Insights into the Inhibition of Actin-Capping Protein by Interactions with Phosphatidic Acid and Phosphatidylinositol (4,5)-Bisphosphate. *PLoS Computational Biology* **8,**(2012).

Pleskot, R., Pejchar, P., Staiger, C. J. & Potocký, M. When fat is not bad: the regulation of actin dynamics by phospholipid signaling molecules. *Frontiers in Plant Science* **5,**(2014).

Pleskot, R., Cwiklik, L., Jungwirth, P., Žárský, V. & Potocký, M. Membrane targeting of the yeast exocyst complex. *Biochimica et Biophysica Acta (BBA) - Biomembranes* **1848,**1481–1489 (2015).

Potocký, M. *et al.* Live-cell imaging of phosphatidic acid dynamics in pollen tubes visualized by Spo20p-derived biosensor. *New Phytologist* **203,**483–494 (2014).

Robinson, N. G. G. *et al.* Rho3 of Saccharomyces cerevisiae, Which Regulates the Actin Cytoskeleton and Exocytosis, Is a GTPase Which Interacts with Myo2 and Exo70. *Molecular and Cellular Biology* **19,** 3580–3587 (1999).

Rybak, K. *et al.*Plant Cytokinesis Is Orchestrated by the Sequential Action of the TRAPPII and Exocyst Tethering Complexes. *Developmental Cell* **29,**607–620 (2014).

Sabol, P., Kulich, I. & Žárský, V. RIN4 recruits the exocyst subunit EXO70B1 to the plasma membrane. *Journal of Experimental Botany* **68,**3253–3265 (2017).

Saliba, A.-E., Vonkova, I. & Gavin, A.-C. The systematic analysis of protein–lipid interactions comes of age. *Nature Reviews Molecular Cell Biology* **16,**753–761 (2015).

Safavian, D. *et al.* RNA silencing of exocyst genes in the stigma impairs the acceptance of compatible pollen in Arabidopsis. *Plant Physiology*(2015). doi:10.1104/pp.15.00635

Sekereš , J., Pleskot, R., Pejchar, P., Žárský, V. & Potocký, M. The song of lipids and proteins: dynamic lipid-protein interfaces in the regulation of plant cell polarity at different scales. *Journal of Experimental Botany* **66,**1587–1598 (2015).

Sekereš, J. *et al.* Analysis of Exocyst Subunit EXO70 Family Reveals Distinct Membrane Polar Domains in Tobacco Pollen Tubes. *Plant Physiology* **173,** 1659–1675 (2017).

Simon, M. L. A. *et al.* A PtdIns(4)P-driven electrostatic field controls cell membrane identity and signalling in plants. *Nature Plants* **2,**16089 (2016).

Sivaram, M. V. S., Saporita, J. A., Furgason, M. L. M., Boettcher, A. J. & Munson, M. Dimerization of the Exocyst Protein Sec6p and Its Interaction with the t-SNARE Sec9p†. *Biochemistry* **44,**6302–6311 (2005).

Sousa, E., Kost, B. & Malho, R. Arabidopsis Phosphatidylinositol-4-Monophosphate 5-Kinase 4 Regulates Pollen Tube Growth and Polarity by Modulating Membrane Recycling. *The Plant Cell Online* **20,**3050–3064 (2008).

Steiner, A. *et al.* The Membrane-Associated Sec1/Munc18 KEULE is Required for Phragmoplast Microtubule Reorganization During Cytokinesis in Arabidopsis. *Molecular Plant* **9,**528–540 (2016).

Stenzel, I. *et al.* The Type B Phosphatidylinositol-4-Phosphate 5-Kinase 3 Is Essential for Root Hair Formation in Arabidopsis thaliana. *The Plant Cell Online* **20,**124–141 (2008).

Stenzel, I., Ischebeck, T., Quint, M. & Heilmann, I. Variable Regions of PI4P 5-Kinases Direct PtdIns(4,5)P2 Toward Alternative Regulatory Functions in Tobacco Pollen Tubes. *Frontiers in Plant Science* **2,**(2012).

Synek, L. *et al.* AtEXO70A1, a member of a family of putative exocyst subunits specifically expanded in land plants, is important for polar growth and plant development. *The Plant Journal* **48,** 54–72 (2006).

Synek, L., Sekereš, J. & Žárský, V. The exocyst at the interface between cytoskeleton and membranes in eukaryotic cells. *Frontiers in Plant Science* **4,**(2014).

Synek, L. *et al.* EXO70C2 Is a Key Regulatory Factor for Optimal Tip Growth of Pollen. *Plant Physiology* **174,**223–240 (2017).

Taniguchi, Y. Y., Taniguchi, M., Tsuge, T., Oka, A. & Aoyama, T. Involvement of Arabidopsis thaliana phospholipase Dζ2 in root hydrotropism through the suppression of root gravitropism. *Planta* **231,**491–497 (2009).

Tejos, R. *et al.* Bipolar Plasma Membrane Distribution of Phosphoinositides and Their Requirement for Auxin-Mediated Cell Polarity and Patterning in Arabidopsis. *The Plant Cell* **26,**2114–2128 (2014).

Terbush, D. R. Sec6, Sec8, and Sec15 are components of a multisubunit complex which localizes to small bud tips in Saccharomyces cerevisiae. *The Journal of Cell Biology* **130,**299–312 (1995).

Testerink, C. *et al.* Isolation and identification of phosphatidic acid targets from plants. *The Plant Journal* **39,**527–536 (2004).

Testerink, C. & Munnik, T. Molecular, cellular, and physiological responses to phosphatidic acid formation in plants. *Journal of Experimental Botany* **62,**2349–2361 (2011).

Tzfadia, O. & Galili, G. The Arabidopsis exocyst subcomplex subunits involved in a golgi-independent transport into the vacuole possess consensus autophagy-associated atg8 interacting motifs. *Plant Signaling & Behavior* **8,**(2013).

Ufer, G., Gertzmann, A., Gasulla, F., Röhrig, H. & Bartels, D. Identification and characterization of the phosphatidic acid-binding A. thaliana phosphoprotein PLDrp1 that is regulated by PLDα1 in a stress-dependent manner. *The Plant Journal* **92,**276–290 (2017).

Vega, I. E. & Hsu, S.-C. The Exocyst Complex Associates with Microtubules to Mediate Vesicle Targeting and Neurite Outgrowth. *The Journal of Neuroscience* **21,**3839–3848 (2001).

Vukašinović, N. *et al.* Microtubule-dependent targeting of the exocyst complex is necessary for xylem development in Arabidopsis. *New Phytologist* **213,**1052–1067 (2016).

Wu, J. *et al.*Regulation of Cytokinesis by Exocyst Subunit SEC6 and KEULE in Arabidopsis thaliana. *Molecular Plant* **6,**1863–1876 (2013).

Wu, H., Turner, C., Gardner, J., Temple, B. & Brennwald, P. The Exo70 Subunit of the Exocyst Is an Effector for Both Cdc42 and Rho3 Function in Polarized Exocytosis. *Molecular Biology of the Cell* **21,**430–442 (2010).

Yamashita, M. *et al.*Structural basis for the Rho- and phosphoinositide-dependent localization of the exocyst subunit Sec3. *Nature Structural & Molecular Biology* **17,**180–186 (2010).

Yeaman, C. Mechanism of recruiting Sec6/8 (exocyst) complex to the apical junctional complex during polarization of epithelial cells. *Journal of Cell Science* **117,**559–570 (2004).

Yue, P. *et al.* Sec3 promotes the initial binary t-SNARE complex assembly and membrane fusion. *Nature Communications* **8,**14236 (2017).

Žárský, V., Cvrčková, F., Potocký, M. & Hála, M. Exocytosis and cell polarity in plants - exocyst and recycling domains. *New Phytologist* **183,**255–272 (2009).

Žárský, V., Kulich, I., Fendrych, M. & Pečenková, T. Exocyst complexes multiple functions in plant cells secretory pathways. *Current Opinion in Plant Biology* **16,**726–733 (2013).

Zeniou-Meyer, M. *et al.* Phospholipase D1 Production of Phosphatidic Acid at the Plasma Membrane Promotes Exocytosis of Large Dense-core Granules at a Late Stage. *Journal of Biological Chemistry* **282,**21746–21757 (2007).

Zhang, X. *et al.* Cdc42 Interacts with the Exocyst and Regulates Polarized Secretion. *Journal of Biological Chemistry* **276,**46745–46750 (2001).

Zhang, X. *et al.* Membrane association and functional regulation of Sec3 by phospholipids and Cdc42. *The Journal of Cell Biology* **180,**145–158 (2008).

Zhang, Q. *et al.* Phosphatidic Acid Regulates Microtubule Organization by Interacting with MAP65-1 in Response to Salt Stress in Arabidopsis. *The Plant Cell* **24,**4555–4576 (2012).

Zhang, C. *et al.* Endosidin2 targets conserved exocyst complex subunit EXO70 to inhibit exocytosis. *Proceedings of the National Academy of Sciences* **113,** (2015).

Zhao, Y. *et al.* Phosphoinositides Regulate Clathrin-Dependent Endocytosis at the Tip of Pollen Tubes in Arabidopsis and Tobacco. *The Plant Cell* **22,**4031–4044 (2010).

Zhao, Y. *et al.* Exo70 Generates Membrane Curvature for Morphogenesis and Cell Migration. *Developmental Cell* **26,**266–278 (2013).

Visualization of the exocyst complex dynamics at the plasma membrane of *Arabidopsis thaliana*

Matyáš Fendrych[a,*], Lukáš Synek[a], Tamara Pečenková[a,b], Edita Janková Drdová[a], Juraj Sekereš[a], Riet de Rycke[c], Moritz K. Nowack[c], and Viktor Žárský[b]
[a]Institute of Experimental Botany, Academy of Sciences of the Czech Republic, 165 02 Prague 6, Czech Republic;
[b]Department of Experimental Plant Biology, Faculty of Science, Charles University, 128 44 Prague 2, Czech Republic;
[c]VIB Department of Plant Systems Biology, Ghent University, 9052 Gent, Belgium

ABSTRACT The exocyst complex, an effector of Rho and Rab GTPases, is believed to function as an exocytotic vesicle tether at the plasma membrane before soluble *N*-ethylmaleimide–sensitive factor attachment protein receptor (SNARE) complex formation. Exocyst subunits localize to secretory-active regions of the plasma membrane, exemplified by the outer domain of *Arabidopsis* root epidermal cells. Using variable-angle epifluorescence microscopy, we visualized the dynamics of exocyst subunits at this domain. The subunits colocalized in defined foci at the plasma membrane, distinct from endocytic sites. Exocyst foci were independent of cytoskeleton, although prolonged actin disruption led to changes in exocyst localization. Exocyst foci partially overlapped with vesicles visualized by VAMP721 v-SNARE, but the majority of the foci represent sites without vesicles, as indicated by electron microscopy and drug treatments, supporting the concept of the exocyst functioning as a dynamic particle. We observed a decrease of SEC6–green fluorescent protein foci in an *exo70A1* exocyst mutant. Finally, we documented decreased VAMP721 trafficking to the plasma membrane in *exo70A1* and *exo84b* mutants. Our data support the concept that the exocyst-complex subunits dynamically dock and undock at the plasma membrane to create sites primed for vesicle tethering.

Monitoring Editor
Patrick J. Brennwald
University of North Carolina

Received: Jul 2, 2012
Revised: Dec 17, 2012
Accepted: Dec 19, 2012

INTRODUCTION

Plant surfaces are products of secretory pathways. The final decisive step in secretion is exocytosis, resulting in the fusion of membrane vesicles with the plasma membrane (PM) and delivery of the vesicle content to the cell surface—the apoplast. All of the different "direct secretion" systems at the PM (e.g., ion transporters, cellulose synthases, and ABC transporters responsible, among others, for cell wall modifications) are brought to the PM by exocytosis. An intricate balance between exocytosis and endocytosis (i.e., membrane recycling) is the basis for proper PM system functioning (Battey *et al.*, 1999). Despite its importance, we know surprisingly little about mechanistic details of plant exocytosis.

The secretory vesicle life cycle includes its budding from the donor membrane, transport, and finally tethering and fusion with the destination membrane (Cai *et al.*, 2007). The vesicle–target membrane fusion is achieved by a coordinated action of tethering factors and soluble *N*-ethylmaleimide–sensitive factor attachment protein receptor (SNARE) proteins (Söllner *et al.*, 1993). The tethering machinery includes Rab GTPases, coiled-coil tethering proteins, and multisubunit tethering complexes. Vesicle tethering precedes the membrane fusion catalyzed by SNARE proteins by bridging the vesicle and the PM (reviewed in Bröcker *et al.*, 2010). Distinct phases of exocytic vesicle tethering and docking at the target membrane have been described in detail in animal cells, but such a resolution has not been achieved in plants, and therefore we use the term "tethering" sensu lato. The exocyst is an octameric protein complex that tethers vesicles to the PM and is composed of the SEC3, SEC5, SEC6, SEC8 SEC10, SEC15, EXO70, and EXO84 subunits in

This article was published online ahead of print in MBoC in Press (http://www.molbiolcell.org/cgi/doi/10.1091/mbc.E12-06-0492) on January 2, 2013.

*Present address: VIB Department of Plant Systems Biology, Ghent University, 9052 Gent, Belgium.

Address correspondence to: Matyáš Fendrych (fendrych@ueb.cas.cz).

Abbreviations used: PM, plasma membrane; VAEM, variable-angle epifluorescence microscopy.

animals, yeast, and plants (Heider and Munson, 2012). In yeast, the exocyst binds the vesicle via interaction of the Sec15 subunit with the vesicle-associated Sec4 Rab GTPase (Guo *et al.*, 1999b). Attachment of the exocyst to the PM is achieved by interactions with Cdc42, Rho1, and Rho3 GTPases in yeast (Robinson *et al.*, 1999; Guo *et al.*, 2001; Zhang *et al.*, 2001) and possibly via the ROP/RAC effector ICR1 in *Arabidopsis* (Lavy *et al.*, 2007). In yeast, the exocyst is further linked to the PM by direct binding of Exo70 and Sec3 subunits to phosphatidylinositol 4,5-bisphosphate (He *et al.*, 2007; Zhang *et al.*, 2008) and by interaction of Sec6 with the Sec9 t-SNARE (Sivaram *et al.*, 2005). In *Arabidopsis*, the EXO70B2 exocyst subunit interacts with the SNAP33 SNARE (Pečenková *et al.*, 2011). Organisms defective in exocyst subunits typically suffer from secretion defects (Novick *et al.*, 1980; Guo *et al.*, 1999a). *Arabidopsis* exocyst mutants are indeed defective in seed coat pectin exocytosis, pollen tube, root hair, and hypocotyl growth. In addition, the exocyst complex localizes to secretory-active PM domains in plant cells, similar to the situation in other eukaryotes (Cole *et al.*, 2005; Hála *et al.*, 2008; Žárský *et al.*, 2009; Fendrych *et al.*, 2010; Kulich *et al.*, 2010). Both facts suggest a role for the exocyst in exocytosis in plant cells.

As the action of the exocyst depends on its precise localization to the PM, the data indicate localization of the bulk of exocyst proteins to membrane domains associated with high secretion activity (Finger *et al.*, 1998; Lipschutz *et al.*, 2000; Gromley *et al.*, 2005; Fendrych *et al.*, 2010). Detailed analysis of the exocyst localization at the PM is lacking. Whereas endocytosis was characterized by visualizing the assembly of clathrin light chain and dynamin-related proteins at single endocytic sites in *Arabidopsis* (Konopka and Bednarek, 2008a; Konopka *et al.*, 2008; Fujimoto *et al.*, 2010), there is no similar framework for exocytic events. The exocyst is considered a vesicle-tethering machinery. However, when the exocyst subunits are recruited to secretory vesicles and to the PM, whether the exocyst actually colocalizes with secretory vesicles, and the dynamics of the exocyst at the PM are not known. To fill this gap, we use a combination of advanced microscopy techniques and genetic and pharmacological experiments in *Arabidopsis* plants expressing fluorescently tagged exocyst subunits and *Arabidopsis* exocyst mutants.

RESULTS

Exocyst subunits colocalize in distinct foci at the plasma membrane

In *Arabidopsis thaliana*, green fluorescent protein (GFP)–tagged exocyst subunits SEC6, SEC8, EXO70A1, and EXO84b are enriched at the outer PM of root epidermal cells and localize strongly to post-cytokinetic cell plate membranes (Figure 1A; Fendrych *et al.*, 2010). The PM signal is not homogeneous, and we occasionally observed dim spots at high magnification using the confocal laser scanning microscope (CLSM). To achieve higher spatial resolution and to separate the signal of exocyst subunits at the PM from the fluorescence of subunits in cytoplasm, we used variable-angle epifluorescence microscopy (VAEM; Konopka and Bednarek, 2008b), which enables illumination of objects in close proximity to the microscope slide. We examined roots of *Arabidopsis* seedlings expressing SEC6-GFP, GFP-SEC8, and EXO84b-GFP under the control of genomic promoters and EXO70A1-GFP under the control of the constitutive 35S promoter (Fendrych *et al.*, 2010). Functionality of the exocyst-subunit localizations is corroborated by the ability of EXO84b, EXO70A1, and SEC8 GFP-fusion proteins to complement mutations in the respective genes (Fendrych *et al.*, 2010; Kulich *et al.*, 2010). We observed localization of GFP signal into distinct foci at the PM (Figure 1B). In the meristematic zone it was sometimes difficult to distinguish individual foci, and therefore we determined the density of the foci in elongation and maturation zones (Figure 1C). Density decreased from the root meristematic zone to the maturation zone from ~1.6 to 1.3 foci/μm^2; this difference was statistically significant for the EXO84b, EXO70A1, and SEC8 subunits (analysis of variance, $\alpha = 0.05$).

To test whether exocyst subunits colocalize in the PM foci, we crossed *Arabidopsis* plants expressing GFP-tagged exocyst subunits with plants expressing monomeric red fluorescent protein (mRFP)–tagged SEC6 or EXO84b subunits. The mRFP- and GFP-labeled foci colocalized in ~37% (Figure 2, A and B). We also observed a high proportion (~50%) of only GFP-labeled foci and a small proportion (~7–17%) of only mRFP-labeled foci in all combinations (Figure 1, D and E). Probably due to silencing of the GFP-EXO70A1 transgene, we were unable to obtain any GFP-EXO70A1 and mRFP-positive plants in the progeny of the respective crosses. Patterns of endocytic events in *Arabidopsis* epidermal cells when visualized by dynamin-related proteins (DRP) and the clathrin light chain protein fusions (Konopka and Bednarek, 2008a; Konopka *et al.*, 2008) resemble that of exocyst foci. We therefore analyzed possible colocalization of DRP1C-mOrange with GFP-SEC8 and found that it was low, ~10%, similar to the colocalization of exocyst foci caused by a random overlap (Figure 1, D and E, and Supplemental Figure S1A).

Taken together, the results show exocyst subunits colocalized in the PM foci that were clearly distinct from endocytic sites marked by DRP1C.

Dynamics of exocyst foci and dependence on the cytoskeleton

The exocyst-labeled foci displayed limited spatial motility that preceded or followed dwelling of the foci at the PM. The signal usually appeared and remained localized to an identical site and vanished eventually (Figure 2A and Supplemental Videos S1 and S2). To monitor the foci behavior in time, we used kymographic representations of the time series, where the bona fide exocytic events appear as a straight line (Figure 2A). The signal intensity typically increased after its appearance, and later decreased before its disappearance. There was no prevailing pattern of signal maxima or minima during the event. Exocyst subunits colocalized in the foci during the whole event (Figure 2B).

The median lifetime (represented by the length of straight lines in kymographs) of exocyst foci in cells of elongation and root hair zones as determined from kymographs was 9.4, 13.3, 9.3, and 11.8 s for SEC6, SEC8, EXO70A1, and EXO84b, respectively. The lifetime distribution was similar for all exocyst subunits tested (Figure 2D).

To assess the exocyst turnover at the PM and to measure the turnover of the bulk of exocyst subunits, we performed fluorescence recovery after photobleaching (FRAP) experiments using CLSM. We infer from the FRAP curves that the mobile fraction of exocyst subunits is high, representing ~90% (Figure 2C). The fluorescence recovery half-time was 23.4 ± 8.9, 19.9 ± 9.6, 38.1 ± 17.3, and 36.0 ± 6.5 s for the SEC6, SEC8, EXO70A1, and EXO84b subunit, respectively (± represents SD). The FRAP experiments show that the exocyst subunits cycle between cytoplasm and PM approximately on the order of tens of seconds for all four subunits studied. The FRAP values were higher than the foci lifetimes, which can be caused by the fact that the laser also bleaches populations of foci in adjacent focal planes.

The exocyst is known to be sensitive to actin disruption in yeast cells (Boyd *et al.*, 2004). First, we analyzed the possible colocalization of the exocyst (represented by EXO84b-GFP) with the actin marker Lifeact-mRFP (Riedl *et al.*, 2008) and found no significant

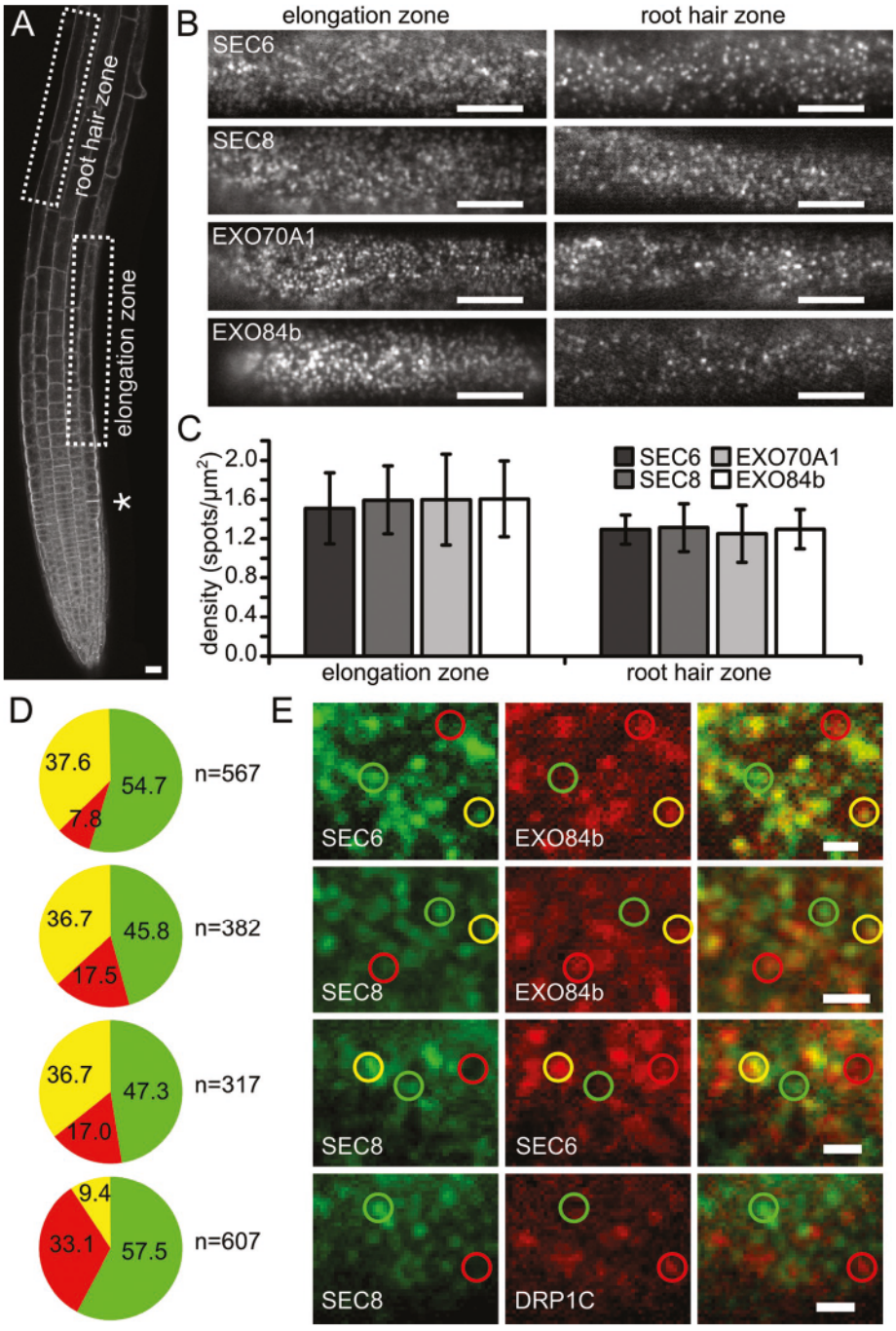

FIGURE 1: Exocyst subunits colocalize in distinct foci at the plasma membrane. (A) CLSM section of *Arabidopsis* root expressing EXO84b-GFP. The signal decorates outer epidermal PM. In recently divided cells, the exocyst is focused on the maturing cell walls (asterisk). (B) Exocyst subunits form distinct foci at the PM when observed by VAEM. Foci appearance is shown in the PM of outer epidermal root cells in elongation (left) and root hair zones (right). Scale bars, 10 μm. (C) Exocyst foci density in root epidermal cells; $n \geq 10$ cells for each column; error bars, SDs. (D) Quantification (%) of the exocyst subunits and DRP1C colocalizations in *Arabidopsis* root epidermal cells. Pairs indicated in E were evaluated. Green, red, and yellow colors represent GFP only, mRFP only, and their colocalization, respectively. (E) Localization of SEC6, SEC8, and EXO84b exocyst subunits. Green, red, and yellow circles denote GFP-only, mRFP-only, and GFP- and mRFP-positive foci, respectively. Scale bars, 1 μm.

colocalization (Figure 3A). Second, upon 10 min of actin disruption by latrunculin B (latB), the exocyst appearance remained unaffected. After 1-h latB treatment, exocyst foci were still present; however, in some cells the foci aggregated into clusters (Figure 3C). The effect was more obvious when using the CLSM, as the latB effect was pronounced in the epidermal cells below the lateral root cap, and these cells are inaccessible for VAEM. The exocyst aggregated into cell corners and formed clusters of intensive signal in epidermal cells in the elongation zone (Figure 3E).

The exocyst is known to associate with microtubules (MT) in animals (Vega and Hsu, 2001; Wang *et al.*, 2004). However, we did not observe any significant colocalization when EXO84b-mRFP was expressed with the MAP4-GFP MT marker (Marc *et al.*, 1998; Figure 3B). The exocyst appearance at the PM remained unchanged after either 10-min or 1-h MT disruption by amiprophos methyl (Figure 3, B and D).

We further examined possible cytoskeletal drug effect on the EXO84b-GFP turnover at the PM using FRAP. Whereas 1-h MT disruption had no obvious effect, 1-h actin disruption led to a significant retardation of exocyst recruitment to the PM (Figure 3G).

These data indicate that although cytoskeletal systems are not essential for exocyst localization at the PM in the short term, long-term actin disruption leads to changes in exocyst localization and its dynamics at the PM.

Do all exocyst foci harbor secretory vesicles?

The exocyst complex is supposed to function as a vesicle–PM tethering machinery. To address the mechanism of exocyst-complex function, we asked whether the observed exocyst foci also harbor secretory vesicles tethered to the PM. We attempted to visualize secretory vesicles using the secretory marker secGFP (Batoko *et al.*, 2000) but did not observe any vesicle-like events using VAEM (unpublished data). Exocytic vesicles harbor v-SNARE proteins that eventually form SNARE complexes with their PM counterparts. Therefore we tagged VAMP721—a v-SNARE (R-SNARE) expressed in root cells (Uemura *et al.*, 2004; Lipka *et al.*, 2007), which has been used as a marker of exocytosis in plants (Genre *et al.*, 2012)—with GFP and expressed the fusion protein in *Arabidopsis* under the control of its native promoter. Using CLSM, we observed signal in endosomal compartments and a PM signal that was strong at the outer PM of root epidermal cells (Figure 4A). The fusion protein also labeled growing cell plates (Supplemental Figure S1B). The GFP-VAMP721 signal localized to the PM and also to distinct foci, likely vesicles (Allersma *et al.*, 2004), when observed by VAEM. The putative vesicles were moving beneath the PM, and a subpopulation of the foci was tethered at the PM. Dwelling of some foci followed or preceded their movement (Figure 4A). It is possible that

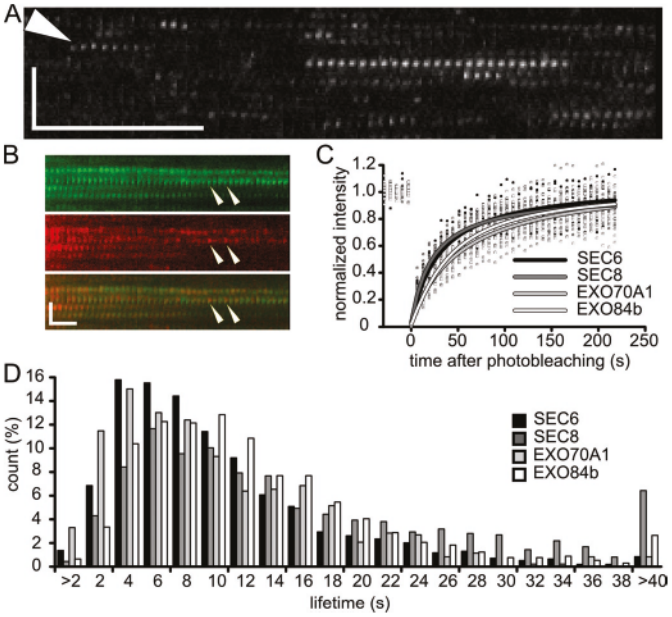

FIGURE 2: **Exocyst foci dynamics. (A) A kymographic representation of EXO84b-GFP at the PM of an elongating root epidermal cell. Arrowhead points to lateral movement of EXO84b-GFP in the vertical direction. Horizontal and vertical bars represent 5 s and 3 µm, respectively. (B) A kymographic representation of SEC6-GFP and EXO84b-mRFP colocalization in the exocyst foci. Recruitment of new EXO84b-mRFP molecules is apparent (arrowheads). The horizontal and vertical bars represent 10 s and 2 µm, respectively. (C) FRAP of exocyst subunits at lateral PM of elongating root epidermal cells. Each curve was constructed from ≥10 FRAP experiments; the individual measurements are represented by dots. (D) Histogram showing distribution of exocyst foci lifetimes measured in kymographs; $n \geq 600$ foci for each subunit.**

these foci correspond to exocytic and endocytic foci, but we were unable to distinguish between the two types of events.

The pattern of the GFP-VAMP721 foci resembled that of exocyst foci (Figure 4, A and B). We tested the colocalization between GFP-VAMP721 and the exocyst—represented by EXO84b-mRFP, as this construct proved reliable and had stronger signal than SEC6-mRFP. EXO84b-mRFP colocalized with GFP-VAMP721 at the lateral PM but not in the endosome-like compartments when observed by CLSM (Supplemental Figure S1C). When VAEM was used, exocyst foci colocalized with the GFP-VAMP721 putative vesicles tethered at the PM in 21.6% of the foci observed (Figure 4, D and E), whereas the colocalization caused by a random overlap was 10.6%. A portion of the exocyst foci is thus associated with putative secretory vesicles. However, the question remains whether the remaining foci also tether vesicles.

We further attempted to visualize a PM-localized t-SNARE protein. The SYP132 t-SNARE (Qa-SNARE) is expressed ubiquitously during all plant developmental stages, suggesting that it could be involved in constitutive PM trafficking (Uemura *et al.*, 2004; Enami *et al.*, 2009). GFP-tagged SYP132 appeared as a PM signal using CLSM (Figure 4C; Kato *et al.*, 2010). With VAEM, the SYP132-GFP signal localized to motile foci of high density, probably representing SYP132 protein clusters (Figure 4C). Unlike the exocyst subunits, it was difficult to distinguish individual foci and thus impossible to determine their actual density. When we compared the kymographs of exocyst subunits and the SYP132 foci (Figure 4, B and C), it was obvious that SYP132 foci exhibited substantially higher motility, and we did not observe any long-lasting exocyst-like foci in the case of SYP132. Due to the motility and short SYP132 dwelling times, the potential colocalization would not be observable in the time resolution achieved during the sequential imaging of the green and red channels.

If all exocyst foci do tether a membrane-bound vesicle, these would be discernible using electron microscopy. High-pressure freezing, automated freeze-substitution electron microscopy (HPF-AFS) is commonly used to analyze endomembrane processes (Seguí-Simarro *et al.*, 2004), as the sample is fixed within a fraction of a second, thus preserving all endomembrane structures. We fixed the epidermal cells of *Arabidopsis* root tips using HPF-AFS and examined the lateral PM for the presence of tethered vesicles. In total, we analyzed 93.6 µm of the lateral PM of epidermal root cells (Figure 4H). The sections examined were 60 nm thick. The approximate diameter of secretory vesicles in *Arabidopsis* is 50–70 nm (Seguí-Simarro *et al.*, 2004; Ketelaar *et al.*, 2008). Therefore the area of lateral PM examined is roughly 11.2 µm^2 (the length examined multiplied by the sum of the section thickness and the vesicle diameter, as a vesicle cut in half while sectioning will be visible in the micrograph). If all exocyst foci harbored vesicles, we would observe ~18 vesicles (the area examined multiplied by the exocyst foci density, 1.6 µm^{-2}), but instead we observed only 3 vesicles in the vicinity of the lateral PM of epidermal cells (Figure 4, F–I). Recently it was reported (Wang *et al.*, 2010) that the exocyst associates with double-membrane structures that are secreted into the apoplast; however, we observed only structures distantly resembling these compartments—the paramural bodies often found in corners of epidermal cells (Figure 4F).

To test the hypothesis that the exocyst localizes to the PM even without the presence of a vesicle, we used an approach with a higher throughput than transmission electron microscopy imaging and blocked exocytosis using the ARF-GEF inhibitor brefeldin A (BFA), which causes the aggregation of the *trans*-Golgi network and partially inhibits exocytosis (Geldner *et al.*, 2003; Teh and Moore, 2007). After 2-h treatment of 4-d seedlings with 50 µM BFA, the GFP-VAMP721 signal in root epidermal cells aggregated in so-called BFA compartments, and its intensity on the PM decreased, indicating that exocytosis was inhibited (Figure 5). On the contrary, EXO84b, EXO70A1, SEC6, and SEC8 GFP-tagged exocyst subunits did not exhibit such behavior, and their signal persisted completely at the PM (Figure 5). Note that the analysis of VAMP721 VAEM images was very difficult due to the signal of the endomembrane compartments present beneath the plasma membrane. After BFA treatment of VAMP721, the PM signal decreased, whereas the underlying endomembrane particles were still present; therefore we did not analyze the BFA-treated samples using VAEM but used confocal microscopy instead.

In summary, the partial colocalization with the VAMP721 v-SNARE, the lack of tethered vesicles at the lateral PM as examined by HPF-AFS, and the insensitivity of the exocyst to BFA demonstrate that the exocyst foci represent sites of exocyst complex docking at the PM that occur also without the presence of secretory vesicles. Thus the exocyst foci probably form at preexisting sites capable of vesicle tethering.

Exocytosis is decreased in exocyst mutants

The exocyst is an octameric protein complex, and loss-of-function mutations of its subunits result in developmental defects, implying that it needs all of its components for proper functioning. To test whether exocyst foci are altered in cells lacking one of the exocyst components, we expressed the SEC6-GFP subunit in the *exo70A1* exocyst mutant (Synek *et al.*, 2006). We compared

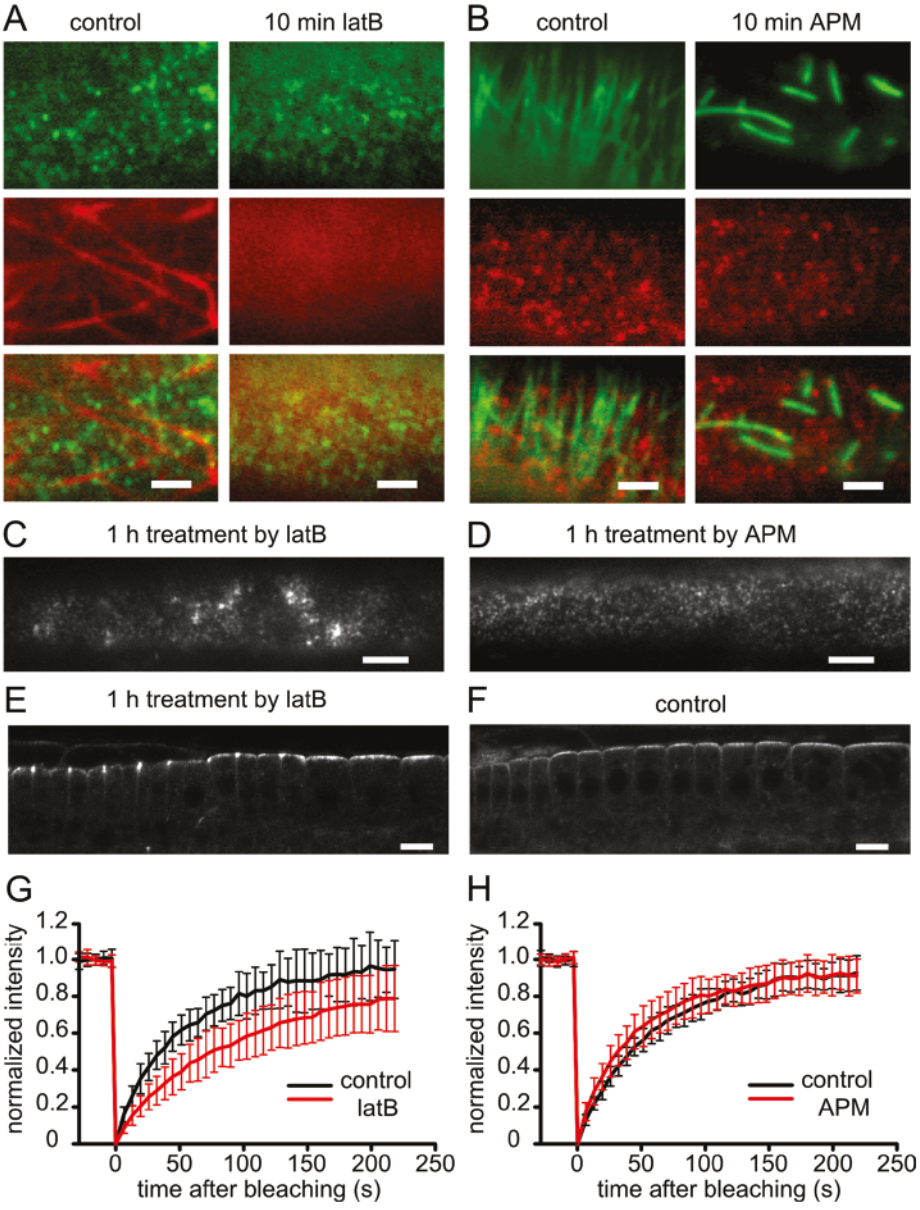

FIGURE 3: EXO84b-GFP and cytoskeleton in root epidermal cells. (A) EXO84B-GFP (green) does not colocalize with actin as visualized by Lifeact-mRFP (red). Short-term actin disruption (10 min, right) does not influence the appearance of exocyst foci. Scale bars, 2 μm. (B) Localization of EXO84b-mRFP (red) and microtubules (green, MAP4-GFP). After 10-min APM treatment, microtubules are disrupted, whereas exocyst foci remain unaffected. Scale bars, 2 μm. (C, D) EXO84b-GFP foci 1 h after disruption of actin (C) and microtubule (D) cytoskeleton. Scale bars, 5 μm. (E, F) EXO84b-GFP in CLSM root sections 1 h after disruption of actin (E) and control (F). Hyperpolarization of the exocyst signal is obvious in E. Scale bars, 10 μm. (G, H) FRAP curves demonstrate retarded recovery of EXO84b-GFP at the PM of the epidermal root cells upon 1-h treatment by latB (G). MT disruption had no effect. Error bars, SDs; $n = 12$ (controls), 20 (latB and APM treatments).

phenotypically wild-type plants (heterozygous and wild type with respect to the *exo70A1* allele) with the mutants. In the latter, the PM incidence of SEC6-GFP foci was decreased, as manifested in a conspicuously decreased density of the foci at the lateral PM of the elongation zone (Figure 6, A and B). The foci sometimes formed clusters at the PM, which were never observed in wild-type controls (Figure 6A).

If the exocyst foci indeed represent PM sites with vesicle-tethering capacity, then the decrease in exocyst foci density should result in decreased exocytosis. In root epidermal cells, GFP-tagged VAMP721 is partitioned between the PM and endomembrane compartments. The strong signal at the lateral PM likely results from intensive exocytosis (Figure 4A). The ratio of the PM and endomembrane signals can then be used as an approximation for ongoing exocytosis. Therefore we examined GFP-VAMP721 in *exo84b* and *exo70A1* exocyst mutants. The *exo84b-1* and *exo84b-2* mutants are dwarf plants with pleiotropic developmental defects (Fendrych *et al.*, 2010). In both lines, the GFP-VAMP721 localization differed dramatically from the wild type: the lateral PM signal was lost, and the protein was present in the cytoplasm and the endomembranes (Figure 6C). We further analyzed the localization of GFP-VAMP721 in the *exo70A1* mutant, which is less severely affected, and its cell types can be directly compared with wild type. In *exo70A1*, lateral PM-domain localization typically decreased and the signal in the endomembrane compartments increased, although some mutant cells resembled wild-type cells. To quantify this observation, we determined the ratio of the lateral PM-domain signal to the entire cytoplasmic signal. This ratio was lower in *exo70A1* mutants than in phenotypically wild-type siblings and wild-type plants (Figure 6D). We were unable to compare the GFP-VAMP721 signal using VAEM microscopy, as the endomembrane compartments accumulated below the PM in the mutant plants hamper such an analysis, similar to the situation in BFA-treated samples (see earlier discussion).

In summary, the absence of the EXO70A1 subunit leads to a decreased recruitment of the SEC6 subunit to the PM. This indicates that the exocyst-docking function was impaired in the *exo70A1*-mutant plants. In turn, exocytosis decreased in these plants, as inferred from the localization of GFP-VAMP721. A plausible explanation of this effect is that the cells face difficulties in exocytosis due to the inability to tether vesicles to the PM. Such inability may well explain morphological and developmental defects of the *exo70A1* mutant.

DISCUSSION

Exocyst localization was described in various model organisms as intense signal in secretory-active PM domains; in *Arabidopsis* roots, the exocyst decorated strongly the outer PM of elongating epidermal cells. The outer epidermal cell domain defines the root–soil interface, and it is a site of active secretion of pectinaceous mucilage (Willats *et al.*, 2001; Langowski *et al.*, 2010). The role of the exocyst in pectinaceous mucilage secretion in the seed coat was described by Kulich *et al.* (2010), and a similar role likely holds in the case of

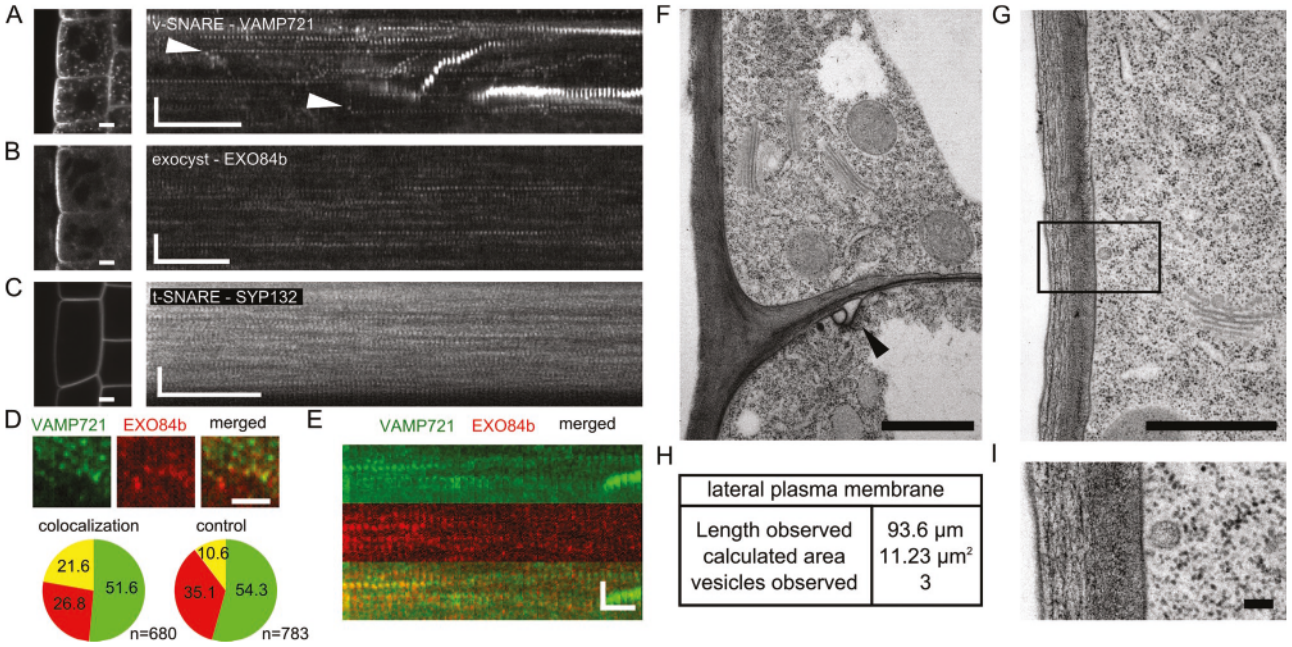

FIGURE 4: Colocalization of exocyst foci with vesicle marker and electron microscopy analysis of the lateral plasma membrane of root epidermal cells. (A–C) Comparison of VAMP721 (A), exocyst foci (B), and SYP132-GFP (C) CLSM localization (left) and dynamics visualized by VAEM (right). GFP-VAMP721 localizes to epidermal PM and endosomes and EXO84b-GFP signal is prominent at the outer epidermal PM, whereas SYP132-GFP is evenly distributed along the entire PM; the seemingly stronger signal of the intercellular membranes results from summing of the adjacent PM signal. Kymographs demonstrate that VAMP721 and exocyst label PM-localized foci with similar appearance (A, B). VAMP721 foci dwelling at the PM are preceded by movement of the foci (arrowheads). Motile foci and endosomes are visible in the kymograph (B). SYP132-GFP (C) is highly dynamic compared with EXO84b-labeled foci. Scale bars, 5 µm (left); horizontal and vertical bars (right) represent 5 s and 3 µm, respectively. (D) Colocalization of GFP-VAMP721 and EXO84b-mRFP foci (scale bar, 2 µm), and quantification (%) of the colocalization (left). The random overlap quantification is shown on the right. Note the weak PM signal of GFP-VAMP721 apart from the larger foci. (E) Kymographic representation of the colocalization between GFP-VAMP721 and EXO84b-mRFP; horizontal and vertical bars represent 10 s and 2 µm, respectively. (F, G) HPF-AFS electron microscopy analysis of the lateral PM of *Arabidopsis* root epidermal cells. (H) Table summarizing the length and area of lateral PM analyzed and number of visible vesicles. From the actual vesicle number observed it is clear that only a subset of exocyst foci are tethering a vesicle. Numerous Golgi and endomembranes are apparent in F, but no vesicles are tethered below the lateral PM. In the lower cell, paramural bodies are present (arrowhead). An example of vesicle tethered at the PM is shown in G; note also the presence of numerous vesicles in the cytoplasm close to the Golgi. (I) Magnified inset from (G); the distance of the vesicle from the PM is 23 nm. Scale bars, 1 µm in F and G and 100 nm in I.

the root epidermis. In postmitotic cells, the exocyst refocuses to the maturing cell wall, another domain with high secretion demands (Fendrych *et al.*, 2010). Here, using VAEM, we achieved a new level of spatiotemporal resolution and characterized the exocyst dynamics in PM-localized foci.

We showed that SEC6-, SEC8-, and EXO84b-positive foci colocalize. There was, however, also a significant proportion of GFP-only labeled foci. For technical reasons, GFP and mRFP channels were imaged sequentially, resulting in an approximately 1-s delay between imaging of the two channels, explaining part of the noncolocalizing foci. Although the mRFP-tagged protein expression was driven by the 35S constitutive promoter, the expression levels were low, and the localization pattern was very similar when compared the 35S promoter with the native-promoter–driven constructs (EXO84b-RFP, SEC6-RFP). In fact, the mRFP signal hit the detection limit of the microscope setup. The mRFP protein has a lower quantum yield and bleaches faster than GFP (Dixit *et al.*, 2006), and in our microscope setup, the mRFP signal was photobleached rapidly, explaining another part of the GFP-only–labeled foci. It is also possible that GFP-tagged subunits are incorporated into exocyst complexes more easily than the mRFP-tagged ones, perhaps due to the weak ability of the GFP to dimerize (Zacharias *et al.*, 2002). The exocyst foci (represented by SEC8) differed from the endocytic sites marked by dynamin-related protein 1C (Konopka and Bednarek, 2008a; Konopka *et al.*, 2008). The density of the foci was similar for all exocyst subunits tested, and it decreased with the distance from the root apical meristem.

We further tested the dependence of exocyst localization and dynamics on actin and MT cytoskeletons. Although the exocyst was shown to localize to MT in opisthokont cells (Vega and Hsu, 2001; Wang *et al.*, 2004), we observed neither significant colocalization nor an effect of MT disruption on exocyst foci appearance. The immediate exocyst localization was actin independent, but long-term actin disruption led to changes in exocyst foci appearance and dynamics. This was probably due to unequal distribution of the foci and compartments that are sources of exocytic vesicles. The delivery of cellulose–synthase complexes to the PM was not microtubule dependent (Gutierrez *et al.*, 2009), and similar to our results, upon actin disruption, the pattern of distribution of the complexes at the PM was disrupted, likely reflecting the irregular distribution of

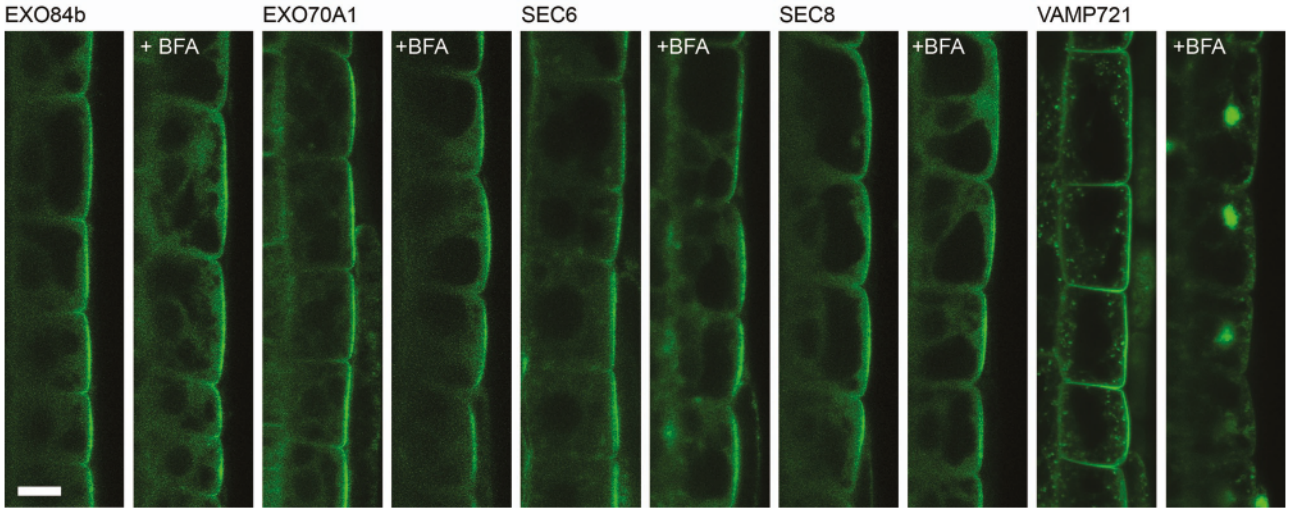

FIGURE 5: The exocyst is insensitive to brefeldin A treatment. Plants expressing exocyst subunits and VAMP721 GFP fusions were treated with BFA for 2 h as indicated. The exocyst subunits remained localized on the lateral PM in the root epidermal cells, whereas the VAMP721 aggregated in BFA compartments. Scale bars, 10 µm.

vesicle-producing compartments (Crowell *et al.*, 2009; Gutierrez *et al.*, 2009). These results agree with the notion that fission yeast polarity and morphogenesis are cooperatively guided by actin and the exocyst, albeit in a redundant manner (Bendezú and Martin, 2010). In addition, it seems that the fission yeast exocyst holocomplex is delivered to the growing ends of cells by the F-actin network (Bendezú *et al.*, 2012).

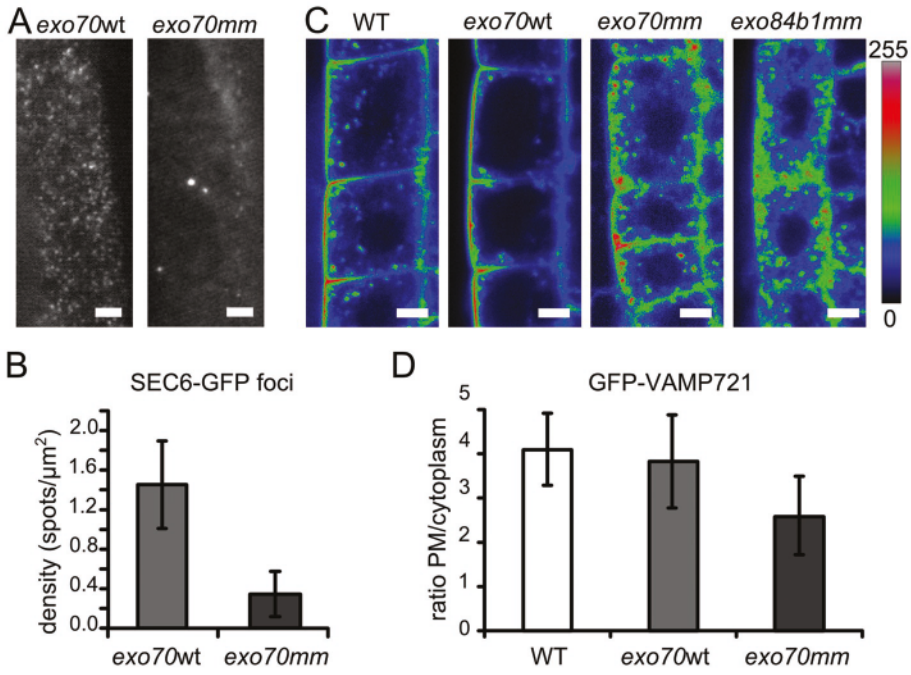

FIGURE 6: Mutations in exocyst subunits decrease the incidence of exocyst foci at the PM and lead to a decrease in exocytosis. (A) SEC6-GFP exocyst foci in wild-type and *exo70A1*-mutant root epidermal cells; scale bars, 2 µm. (B) quantification of SEC6-GFP foci density in *exo70A1* wild-type and mutant cells; error bars, SDs; $n = 23$ and 12 cells for *exo70A1mm* and exo70A1 wild type, respectively. (C) GFP-VAMP721 localizes to the lateral PM and endomembranes in the wild type and *exo70A1* phenotypic wild-type cells. In *exo70A1* and *exo84b1* exocyst mutants, GFP-VAMP721 localization to the lateral PM decreases, and, in turn, the signal of endomembrane compartment increases. Calibration bar of the color coding is shown on the right; scale bars, 5 µm. (D) Quantification of the lateral PM domain/cytoplasmic signal intensity ratio in wild-type, *exo70A1* wild-type, and *exo70A1* mutants. The *exo84b* mutants were not quantified due to the lack of signal at the PM. $n = 48$ cells in 18 seedlings (wild type), $n = 54$ cells in 18 seedlings (*exo70A1* wild type), and $n = 45$ cells in 16 seedlings (*exo70A1* mutants); error bars, SDs.

The assembly and dynamics of exocyst subunits has been a matter of a debate. The seminal model of Peter Novick, based on yeast data, proposes consecutive assembly of exocyst subcomplexes on the vesicle (mediated by Sec15–Sec4 interaction) and on the target PM domain (Sec3 and Exo70). Full complex assembly then results in vesicle tethering (Bröcker *et al.*, 2010). Alternatively, the exocyst might function as a particle preassembled at the plasma membrane that is activated by Rho GTPases to trigger tethering (Wu *et al.*, 2008). The latter model is also supported by the finding that after specific mutations of the yeast Sec6 subunit, the exocyst is released from PM as a complete particle (Songer and Munson, 2009). Theoretically, the exocyst assembly could be observed by colocalization of differentially labeled subunits in the PM foci. Nevertheless, this was impossible using our microscope setup due to the low time resolution caused by sequential imaging. However, the fact that dynamics and density at the PM were similar for all subunits tested, including EXO70A1—which would be expected to "wait" as a landmark at the PM based on the consecutive assembly model—supports the hypothesis of the exocyst function as a preassembled particle. This inference is strengthened by the fact that the exocyst subunits were present at the PM even without the tethered vesicle (also upon addition of BFA). A recent report on the preassembled exocyst holocomplex (including the

Sec3 subunit) delivered to the PM by F-actin in fission yeast strongly supports the possibility of the exocyst holocomplex functioning as a particle in vesicle tethering (Bendezú *et al.*, 2012).

Our study in plants presents data showing that the exocyst localized in distinct foci. The intriguing question is whether exocyst foci correspond to secretory vesicles tethered to the PM in *Arabidopsis* cells. We found only partial colocalization with the secretory vesicle marker VAMP721 v-SNARE. Capturing of exocytosis events by electron microscopy is very rare. In plants, vesicle tethering has not been addressed in detail, but there are reports showing vesicles or vesicle clusters associated with the PM (Toyooka *et al.*, 2009). As a complementary approach to fluorescence microscopy, we used electron microscopy to analyze the number of vesicles actually tethered at the PM. Tethering might occur at distance greater than half of the vesicle size, but the presumed exocyst dimensions are ~13 × 30 nm (Hsu *et al.*, 1998); therefore the tethered vesicle should be visible in the proximity of PM connected to the exocyst foci. Our electron microscopy results demonstrated that there are fewer vesicles tethered at the PM than there are exocyst foci. Therefore we conclude that either vesicles are bound to the exocyst foci for a very short time or only a subset of exocyst foci actually tether a vesicle during its existence. We are not able to distinguish between these two possibilities; in both scenarios, the exocyst is present at the PM even without the actual presence of a secretory vesicle. This conclusion is further supported by the insensitivity of exocyst-subunit PM localization to BFA treatment. This indicates that although exocytosis decreased, exocyst subunits were still able to dock at the PM.

We further compared the localization of the PM-localized SYP132 t-SNARE with the exocyst (Uemura *et al.*, 2004; Enami *et al.*, 2009). In animal cells, syntaxins assemble into clusters at sites of secretory granules (Barg *et al.*, 2010). We hoped to elucidate the time at which t-SNAREs associate with the fusion site and the portion of the putative exocytic foci that actually end up in a successful vesicle fusion. Comparison of SYP132 and exocyst foci localization showed that the t-SNARE is ubiquitously present throughout the entire PM, whereas the exocytic sites are selected by the exocyst complex located at secretory-active domains (Žárský *et al.*, 2009).

Finally, we analyzed exocyst localization in a mutant of the EXO70A1 exocyst subunit, a highly expressed member of the *Arabidopsis* EXO70 family (Synek *et al.*, 2006). In this mutant, density of exocyst foci at the PM decreased substantially, indicating that exocyst function is likely reduced in mutant cells. The hypothesis that the marked decrease of exocyst foci resulted in decreased exocytosis was supported by a decrease of a secretory vesicle marker (VAMP721-GFP) at the PM of the *exo*70A1 and *exo*84b mutants, suggesting impaired exocytosis in these cells. This result agrees with the work of Tsuboi *et al.* (2005), who showed decreased vesicle docking in exocyst-mutant cells.

In summary, we provided insights into the dynamics of exocyst-complex subunits docking at the plant plasma membrane. We propose that the exocyst serves to increase vesicle-tethering probability at PM domains and is able to localize—most probably as a particle—to the PM without the associated vesicle.

MATERIALS AND METHODS

Optical microscopy

We used a Leica DMI6000 microscope (Leica Microsystems, Vienna, Austria) with total internal reflection fluorescence illumination and an HCX PL APO 100.0×/1.46 oil objective. The penetration depth was set to 90–250 nm, roughly corresponding to angles of 64–61°, and the exposure time to ~80–200 ms (300 ms for mRFP and mOrange). Note that the set penetration depths do not necessarily reflect the actual physical penetration depths, due to the intricate optical system of interfaces with various refractive indexes: the glass–medium, medium–cell wall, and cell wall–cytoplasm interfaces. Excitation at 488 nm and the GFP filter were used for imaging of GFP. Excitation at 488 and 560 nm, the QuadP-T cube, and 525/36 and 600/32 filters were used for GFP/mRFP and GFP/mOrange sequential imaging. Relative focus correction was used for colocalization imaging to compensate for the fact that different wavelengths appear at different focal depths. The system, equipped with a DFC350FXR2 camera, was controlled by LAS AF software (Leica).

FRAP experiments were performed using the Zeiss LSM 5 DUO CLSM (Zeiss, Jena, Germany) with the Zeiss C-Apochromat 40×/1.2 water-corrected objective. All images were acquired using identical settings: image size was 500 × 200 pixels; the region of interest (70 × 20 pixels) was bleached using 10 iterations of a 489-nm laser at 100% laser power; and 5 and 35 frames by 6.5-s steps were acquired before and after bleaching, respectively.

HPF-AFS and electron microscopy

Root tips of 5-d-old seedlings of *A. thaliana* were excised, immersed in 20% (wt/vol) bovine serum albumin, and frozen immediately in a high-pressure freezer (EM PACT; Leica Microsystems). Freeze substitution was carried out using a Leica EM AFS (Leica Microsystems) in dry acetone containing 0.1% uranyl acetate, 1% (wt/vol) OsO_4, and 0.2% glutaraldehyde over a 4-d period as follows: −90°C for 54 h, 2°C/h increase for 15 h, −60°C for 8 h, 2°C/h increase for 15 h, and −30°C for 8 h. Samples were then slowly warmed to 4°C, infiltrated stepwise over 3 d at 4°C in Spurr's resin, and embedded in capsules. The polymerization was performed at 70°C for 16 h. Ultrathin sections were made using an ultramicrotome (Leica EM UC6) and poststained in a Leica EM AC20 for 40 min in uranyl acetate at 20°C and for 10 min in lead stain at 20°C. Grids were viewed with a JEM 1010 transmission electron microscope (JEOL, Tokyo, Japan) operating at 80 kV.

Molecular cloning

SEC6 and EXO84b were transferred into pK7RWG2 (Karimi *et al.*, 2002) binary vector by the LR Clonase II enzyme mix (Invitrogen, Carlsbad, CA).

Lifeact marker (Riedl *et al.*, 2008) was amplified using Lifeact5 and Lifeact3 primers in a reaction without a template DNA. The product was further reamplified using attB1 and attB2 primers to flank it with the attB sites. Resulting product was transferred into the pDONR207 vector (Invitrogen) using the BP Clonase II (Invitrogen) and further to the pK7RWG2 vector by the LR Clonase II (Invitrogen).

VAMP721 (AT1G04750) was cloned by the three-template PCR method (Tian *et al.*, 2004). The VAMP721 promoter region and VAMP721 gene were amplified from *A. thaliana* genomic DNA by using P1 and P2, and P5 and P6 primers, respectively; the GFP gene was amplified from the pGWB6 vector (Nakagawa *et al.*, 2007) by using P3 and P4 primers. In a subsequent PCR, resulting products were mixed and amplified using attB1 and attB2 primers. Product of this three-template reaction was transferred into pDONR207 and further to the pGWB1 binary vector (Nakagawa *et al.*, 2007) by BP Clonase II and LR Clonase II enzyme mix, respectively. The construct was verified by sequencing; the promoter region lacked the initial 400 base pairs, resulting in ~800–base pair promoter region. GFP-VAMP721 was transformed into *A. thaliana* expressing EXO84b-mRFP using the floral dip method.

Lifeact5	AAAAAAGCAGGCTCCACCATGGGTGTCGCA-GATTTGATCAAGAAATTC
Lifeact3	AGAAAGCTGGGTCTTCTTCCTTTGAGATGCTTTC-GAATTTCTTGATCA
attB1	GGGGACAAGTTTGTACAAAAAAGCAGGCT
attB2	GGGGACCACTTTGTACAAGAAAGCTGGGT
P1	AAAAAGCAGGCTAACGAAACCTAAGAACACCAC
P2	GCCCTTGCTCACCATTTTTTCTTTACCT-TAAATCTCC
P3	TAAGGTAAAGAAAAAATGGTGAGCAAGGGCGAG
P4	GGCCCCAGCGGCCGCAGCAGCACCAGCGTA-CAGCTCGTCCATGCC
P5	CTGCTGCGGCCGCTGGGGCCATGGCGCAA-CAATCGTTGATC
P6	AGAAAGCTGGGTCTTAACACTTAAACCCATG-GCAAAC

TABLE 1: **Primers used.**

All PCRs were performed using the Phusion polymerase (Finnzymes, Thermo Scientific, Vantaa, Finland). Primers used are listed in Table 1.

Plant material

The Columbia-0 ecotype of *A. thaliana* was transformed using the floral dip method (Clough and Bent, 1998).

Seeds of *A. thaliana* expressing SYP132 were kindly provided by M. H. Sato (Graduate School of Life and Environmental Sciences, Kyoto Prefectural University, Japan) and DRP1C-mOrange by S. Bednarek (Department of Biochemistry, University of Wisconsin–Madison).

F1 generation of crosses between plants expressing GFP- and mRFP- or GFP- and mOrange-tagged proteins was used for evaluation of possible colocalization; in the case of VAMP721–EXO84b colocalization, T2-generation seedlings were used. To observe SEC6-GFP foci in the *exo70A1* mutant, we transformed the *exo70A1-1* line with the SEC6-GFP construct using the floral dip method. In the T2 generation, phenotypically homozygous plants were selected and compared with phenotypically wild-type siblings.

Four-day-old *Arabidopsis* plantlets grown on vertical agar plates were transferred with a block of agar beneath into a minute droplet of half-strength Murashige and Skoog medium (½ MS) supplemented with 1% (wt/vol) sucrose in a LabTekII chambered coverglass and observed. Five-day-old seedlings were used for FRAP experiments.

For cytoskeleton treatment, 10 mM latrunculin B (Molecular Probes, Eugene, OR) in dimethyl sulfoxide and 100 mM amiprophos methyl (APM; Sigma-Aldrich, St. Louis, MO) in ethanol were used. Seedlings were transferred into ½ MS containing a 1:1000 dilution of the appropriate drug or equivalent volume of the solvent in controls, incubated for 10 min or 1 h, respectively, and observed.

The BFA experiment was conducted as follows: 4-d-old seedlings expressing GFP-tagged exocyst subunits or VAMP721, respectively, were treated with 50 mM brefeldin A diluted 1:1000 in ½ MS liquid medium. Images of epidermal cells at root transition zone were taken after 2-h treatment.

Image analysis

All images were analyzed using ImageJ software (National Institutes of Health, Bethesda, MD). Root growth was compensated using the CorrectStackDrift.txt macro (http://rsbweb.nih.gov/ij/macros/examples/). Density of foci was determined in a rectangle of ~50 μm^2 using the Cell Counter ImageJ plug-in. GFP/mRFP and GFP/mOrange colocalization was analyzed as follows: the first three images in a time series were averaged to enhance the signal of the stable foci. Only cell areas where both channels were focused properly were used for evaluation. Random overlap was determined in images where one of the channels was shifted by 30 pixels. Colocalization was determined by evaluating each labeled spot by eye in the assayed area and counted using the Cell Counter ImageJ plug-in.

Kymographs were constructed from five-pixel-wide rectangles from each time point concatenated consecutively. To determine exocyst dynamics, series obtained in 0.5-s intervals were used to ensure proper coverage of both the short-time and the long-lasting events; lengths of exocytic events were measured manually in kymographs.

FRAP images were corrected for root growth, and intensities were normalized as follows:

$$I_t = \left[(A_t/C_t) - (A_b/C_b)\right] / \left[\mathrm{Av} - (A_b/C_b)\right]$$

where A_t is the intensity in the bleached area at time t; C_t is the intensity in the control, nonbleached area; A_b and C_b are the intensities in the bleached and unbleached areas, respectively, immediately after the bleaching; and Av is the average A_t/C_t intensity ratio in the five frames before bleaching.

Electron micrographs of epidermal root cells were checked for the presence of vesicles in the PM vicinity, and the outer PM length was measured.

Evaluation of GFP-VAMP721 intensities at the PM and cytoplasm was achieved by creating a region of interest encompassing the entire cytoplasm and lateral PM domain, respectively; mean intensity was recorded, and the ratio was calculated.

All data were processed using the Gnumeric spreadsheet (http://projects.gnome.org/gnumeric/), and FRAP curves were fitted using Gnuplot (www.gnuplot.info/) with the equation

$$f(x) = a + b^{*}\arctan[c(x - d)]$$

Figures were assembled in ImageJ, GIMP (www.gimp.org/), and Inkscape (www.inkscape.org) software, and histograms were adjusted to obtain the best signal-to-noise ratio.

ACKNOWLEDGMENTS

This work was supported by Grant Agency of the Czech Republic/Czech Science Foundation Projects P305/11/1629. We thank Martin Potocký and Jan Petrášek for helpful discussions, Pavel Hejbal for help with Gnuplot, and S. Bednarek for kindly providing experimental material. M.F. thanks the developers of Ubuntu Linux, Gnome, GIMP, and Inkscape.

REFERENCES

Allersma MW, Wang L, Axelrod D, Holz RW (2004). Visualization of regulated exocytosis with a granule-membrane probe using total internal reflection microscopy. Mol Biol Cell 15, 4658–4668.

Barg S, Knowles M, Chen X, Midorikawa M, Almers W (2010). Syntaxin clusters assemble reversibly at sites of secretory granules in live cells. Proc Natl Acad Sci USA 107, 20804–20809.

Batoko H, Zheng HQ, Hawes C, Moore I (2000). A rab1 GTPase is required for transport between the endoplasmic reticulum and Golgi apparatus and for normal Golgi movement in plants. Plant Cell 12, 2201–2218.

Battey N, James N, Greenland A, Brownlee C (1999). Exocytosis and endocytosis. Plant Cell 11, 643–660.

Bendezú FO, Martin SG (2010). Actin cables and the exocyst form two independent morphogenesis pathways in the fission yeast. Mol Biol Cell 22, 44–53.
Bendezú FO, Vincenzetti V, Martin SG (2012). Fission yeast Sec3 and Exo70 are transported on actin cables and localize the exocyst complex to cell poles. PLoS One 7, e40248.
Boyd C, Hughes T, Pypaert M, Novick P (2004). Vesicles carry most exocyst subunits to exocytic sites marked by the remaining two subunits, Sec3p and Exo70p. J Cell Biol 167, 889–901.
Bröcker C, Engelbrecht-Vandré S, Ungermann C (2010). Multisubunit tethering complexes and their role in membrane fusion. Curr Biol 20, R943–R952.
Cai H, Reinisch K, Ferro-Novick S (2007). Coats, tethers, Rabs, and SNAREs work together to mediate the intracellular destination of a transport vesicle. Dev Cell 12, 671–682.
Clough SJ, Bent AF (1998). Floral dip: a simplified method for *Agrobacterium*-mediated transformation of *Arabidopsis thaliana*. Plant J 16, 735–743.
Cole RA, Synek L, Žárský V, Fowler JE (2005). SEC8, a subunit of the putative *Arabidopsis* exocyst complex, facilitates pollen germination and competitive pollen tube growth. Plant Physiol 138, 2005–2018.
Crowell EF, Bischoff V, Desprez T, Rolland A, Stierhof Y-D, Schumacher K, Gonneau M, Höfte H, Vernhettes S (2009). Pausing of Golgi bodies on microtubules regulates secretion of cellulose synthase complexes in *Arabidopsis*. Plant Cell 21, 1141–1154.
Dixit R, Cyr R, Gilroy S (2006). Using intrinsically fluorescent proteins for plant cell imaging. Plant J 45, 599–615.
Enami K, Ichikawa M, Uemura T, Kutsuna N, Hasezawa S, Nakagawa T, Nakano A, Sato MH (2009). Differential expression control and polarized distribution of plasma membrane-resident SYP1 SNAREs in *Arabidopsis thaliana*. Plant Cell Physiol 50, 280–289.
Fendrych M *et al.* (2010). The *Arabidopsis* exocyst complex is involved in cytokinesis and cell plate maturation. Plant Cell 22, 3053–3065.
Finger FP, Hughes TE, Novick P (1998). Sec3p is a spatial landmark for polarized secretion in budding yeast. Cell 92, 559–571.
Fujimoto M, Arimura S, Ueda T, Takanashi H, Hayashi Y, Nakano A, Tsutsumi N (2010). *Arabidopsis* dynamin-related proteins DRP2B and DRP1A participate together in clathrin-coated vesicle formation during endocytosis. Proc Natl Acad Sci USA 107, 6094–6099.
Geldner N, Anders N, Wolters H, Keicher J, Kornberger W, Muller P, Delbarre A, Ueda T, Nakano A, Jürgens G (2003). The *Arabidopsis* GNOM ARF-GEF mediates endosomal recycling, auxin transport, and auxin-dependent plant growth. Cell 112, 219–230.
Genre A, Ivanov S, Fendrych M, Faccio A, Žárský V, Bisseling T, Bonfante P (2012). Multiple exocytotic markers accumulate at the sites of perifungal membrane biogenesis in *Arbuscular mycorrhizas*. Plant Cell Physiol 53, 244–255.
Gromley A, Yeaman C, Rosa J, Redick S, Chen C-T, Mirabelle S, Guha M, Sillibourne J, Doxsey SJ (2005). Centriolin anchoring of exocyst and SNARE complexes at the midbody is required for secretory-vesicle-mediated abscission. Cell 123, 75–87.
Guo W, Grant A, Novick P (1999a). Exo84p is an exocyst protein essential for secretion. J Biol Chem 274, 23558–23564.
Guo W, Roth D, Walch-Solimena C, Novick P (1999b). The exocyst is an effector for Sec4p, targeting secretory vesicles to sites of exocytosis. EMBO J 18, 1071–1080.
Guo W, Tamanoi F, Novick P (2001). Spatial regulation of the exocyst complex by Rho1 GTPase. Nat Cell Biol 3, 353–360.
Gutierrez R, Lindeboom JJ, Paredez AR, Emons AMC, Ehrhardt DW (2009). *Arabidopsis* cortical microtubules position cellulose synthase delivery to the plasma membrane and interact with cellulose synthase trafficking compartments. Nat Cell Biol 11, 797–806.
Hála M *et al.* (2008). An exocyst complex functions in plant cell growth in *Arabidopsis* and tobacco. Plant Cell 20, 1330–1345.
He B, Xi F, Zhang X, Zhang J, Guo W (2007). Exo70 interacts with phospholipids and mediates the targeting of the exocyst to the plasma membrane. EMBO J 26, 4053–4065.
Heider M, Munson M (2012). Exorcising the exocyst complex. Traffic 13, 898–907.
Hsu SC, Hazuka CD, Roth R, Foletti DL, Heuser J, Scheller RH (1998). Subunit composition, protein interactions, and structures of the mammalian brain sec6/8 complex and septin filaments. Neuron 20, 1111–1122.
Karimi M, Inzé D, Depicker A (2002). GATEWAY vectors for *Agrobacterium*-mediated plant transformation. Trends Plant Sci 7, 193–195.
Kato N, Fujikawa Y, Fuselier T, Adamou-Dodo R, Nishitani A, Sato MH (2010). Luminescence detection of SNARE–SNARE interaction in *Arabidopsis* protoplasts. Plant Mol Biol 72, 433–444.
Ketelaar T, Galway ME, Mulder BM, Emons AMC (2008). Rates of exocytosis and endocytosis in *Arabidopsis* root hairs and pollen tubes. J Microsc 231, 265–273.
Konopka CA, Backues SK, Bednarek SY (2008). Dynamics of *Arabidopsis* dynamin-related protein 1C and a clathrin light chain at the plasma membrane. Plant Cell 20, 1363–1380.
Konopka CA, Bednarek SY (2008a). Comparison of the dynamics and functional redundancy of the Arabidopsis dynamin-related isoforms DRP1A and DRP1C during plant development. Plant Physiol 147, 1590–1602.
Konopka Ca, Bednarek SY (2008b). Variable-angle epifluorescence microscopy: a new way to look at protein dynamics in the plant cell cortex. Plant J 53, 186–196.
Kulich I, Cole R, Drdová E, Cvr ková F, Soukup A, Fowler J, Žárský V (2010). *Arabidopsis* exocyst subunits SEC8 and EXO70A1 and exocyst interactor ROH1 are involved in the localized deposition of seed coat pectin. New Phytol 188, 615–625.
Langowski L, R ži ka K, Naramoto S, Kleine-Vehn J, Friml J (2010). Trafficking to the outer polar domain defines the root-soil interface. Curr Biol 20, 904–908.
Lavy M, Bloch D, Hazak O, Gutman I, Poraty L, Sorek N, Sternberg H, Yalovsky S (2007). A novel ROP/RAC effector links cell polarity, root-meristem maintenance, and vesicle trafficking. Curr Biol 17, 947–952.
Lipka V, Kwon C, Panstruga R (2007). SNARE-ware: the role of SNARE-domain proteins in plant biology. Annu Rev Cell Dev Biol 23, 147–174.
Lipschutz JH, Guo W, O'Brien LE, Nguyen YH, Novick P, Mostov KE (2000). Exocyst is involved in cystogenesis and tubulogenesis and acts by modulating synthesis and delivery of basolateral plasma membrane and secretory proteins. Mol Biol Cell 11, 4259–4275.
Marc J, Granger C, Brincat J, Fisher D, Kao T, McCubbin A, Cyr R (1998). A GFP-MAP4 reporter gene for visualizing cortical microtubule rearrangements in living epidermal cells. Plant Cell 10, 1927–1940.
Nakagawa T, Kurose T, Hino T, Tanaka K, Kawamukai M, Niwa Y, Toyooka K, Matsuoka K, Jinbo T, Kimura T (2007). Development of series of gateway binary vectors, pGWBs, for realizing efficient construction of fusion genes for plant transformation. J Biosci Bioeng 104, 34–41.
Novick P, Field C, Schekman R (1980). Identification of 23 complementation groups required for post-translational events in the yeast secretory pathway. Cell 21, 205–215.
Pečenková T, Hála M, Kulich I, Kocourková D, Drdová E, Fendrych M, Toupalová H, Žárský V (2011). The role for the exocyst complex subunits Exo70B2 and Exo70H1 in the plant–pathogen interaction. J Exp Bot 62, 2107–2116.
Riedl J *et al.* (2008). Lifeact: a versatile marker to visualize F-actin. Nat Methods 5, 605–607.
Robinson NGG, Guo L, Imai J, Toh-e A, Matsui Y, Tamanoi F (1999). Rho3 *of Saccharomyces cerevisiae*, which regulates the actin cytoskeleton and exocytosis, is a GTPase which interacts with Myo2 and Exo70. Mol Cell Biol 19, 3580–3587.
Seguí-Simarro JM, Austin JR 2nd, White EA, Staehelin LA (2004). Electron tomographic analysis of somatic cell plate formation in meristematic cells of *Arabidopsis* preserved by high-pressure freezing. Plant Cell 16, 836–856.
Sivaram MVS, Saporita JA, Furgason MLM, Boettcher AJ, Munson M (2005). Dimerization of the exocyst protein Sec6p and its interaction with the t-SNARE Sec9p. Biochemistry 44, 6302–6311.
Söllner T, Whiteheart SW, Brunner M, Erdjument-Bromage H, Geromanos S, Tempst P, Rothman JE (1993). SNAP receptors implicated in vesicle targeting and fusion. Nature 362, 318–324.
Songer JA, Munson M (2009). Sec6p anchors the assembled exocyst complex at sites of secretion. Mol Biol Cell 20, 973–982.
Synek L, Schlager N, Eliáš M, Quentin M, Hauser MT, Žárský V (2006). AtEXO70A1, a member of a family of putative exocyst subunits specifically expanded in land plants, is important for polar growth and plant development. Plant J 48, 54–72.
Teh O-K, Moore I (2007). An ARF-GEF acting at the Golgi and in selective endocytosis in polarized plant cells. Nature 448, 493–496.
Tian GW *et al.* (2004). High-throughput fluorescent tagging of full-length *Arabidopsis* gene products in planta. Plant Physiol 135, 25–38.
Toyooka K, Goto Y, Asatsuma S, Koizumi M, Mitsui T, Matsuoka K (2009). A mobile secretory vesicle cluster involved in mass transport from the Golgi to the plant cell exterior. Plant Cell 21, 1212–1229.

Tsuboi T, Ravier Ma, Xie H, Ewart M-A, Gould GW, Baldwin Sa, Rutter GA (2005). Mammalian exocyst complex is required for the docking step of insulin vesicle exocytosis. J Biol Chem 280, 25565–25570.
Uemura T, Ueda T, Ohniwa RL, Nakano A, Takeyasu K, Sato MH (2004). Systematic analysis of SNARE molecules in *Arabidopsis*: dissection of the post-Golgi network in plant cells. Cell Struct Funct 29, 49–65.
Vega IE, Hsu SC (2001). The exocyst complex associates with microtubules to mediate vesicle targeting and neurite outgrowth. J Neurosci 21, 3839–3848.
Wang J, Ding Y, Hillmer S, Miao Y, Lo SW, Wang X, Robinson DG, Jiang L (2010). EXPO, an exocyst-positive organelle distinct from multivesicular endosomes and autophagosomes, mediates cytosol to cell wall exocytosis in *Arabidopsis* and tobacco cells. Plant Cell 22, 4009–4030.
Wang S, Liu Y, Adamson CL, Valdez G, Guo W, Hsu SC (2004). The mammalian exocyst, a complex required for exocytosis, inhibits tubulin polymerization. J Biol Chem 279, 35958–35966.
Willats WG, McCartney L, Knox JP (2001). In-situ analysis of pectic polysaccharides in seed mucilage and at the root surface of *Arabidopsis thaliana*. Planta 213, 37–44.
Wu H, Rossi G, Brennwald P (2008). The ghost in the machine: small GTPases as spatial regulators of exocytosis. Trends Cell Biol 18, 397–404.
Zacharias DA, Violin JD, Newton AC, Tsien RY (2002). Partitioning of lipid-modified monomeric GFPs into membrane microdomains of live cells. Science 296, 913–916.
Žárský V, Cvrčková F, Potocký M, Hála M (2009). Exocytosis and cell polarity in plants— exocyst and recycling domains. New Phytol 183, 255–272.
Zhang X, Bi E, Novick P, Du L, Kozminski KG, Lipschutz JH, Guo W (2001). Cdc42 interacts with the exocyst and regulates polarized secretion. J Biol Chem 276, 46745–46750.
Zhang X, Orlando K, He B, Xi F, Zhang J, Zajac A, Guo W (2008). Membrane association and functional regulation of Sec3 by phospholipids and Cdc42. J Cell Biol 180, 145–158.

Traffic 2013; 14: 1155–1165

doi:10.1111/tra.12101

Arabidopsis Exocyst Subcomplex Containing Subunit EXO70B1 Is Involved in Autophagy-Related Transport to the Vacuole

Ivan Kulich[1,2], Tamara Pečenková[1,2], Juraj Sekereš[1], Ondřej Smetana[1,2], Matyáš Fendrych[2], Ilse Foissner[3], Margit Höftberger[3] and Viktor Žárský[1,2,*]

[1] Department of Experimental Plant Biology, Faculty of Sciences, Charles University, Prague, Czech Republic
[2] Institute of Experimental Botany, Academy of Sciences of the Czech Republic, Prague, Czech Republic
[3] Department of Cell Biology, Division of Plant Physiology, University of Salzburg, Salzburg, Austria

**Corresponding author: Viktor Žárský, viktor@natur.cuni.cz*

Autophagic transport to the vacuole represents an endomembrane trafficking route, which is widely used in plants, not only during stress situations, but also for vacuole biogenesis and during developmental processes. Here we report a role in autophagic membrane transport for EXO70B1 – one of 23 paralogs of *Arabidopsis* EXO70 exocyst subunits. EXO70B1 positive compartments are internalized into the central vacuole and co-localize with autophagosomal marker ATG8f. This internalization is boosted by induction of autophagy. Loss of function (LOF) mutations in *exo70B1* cause reduction of internalized autopagic bodies in the vacuole. Mutant plants also show ectopic hypersensitive response (HR) mediated by salicylic acid (SA) accumulation, increased nitrogen starvation susceptibility and anthocyanin accumulation defects. Anthocyanin accumulation defect persists in *npr1x exo70B1* double mutants with SA signaling compromised, while ectopic HR is suppressed. EXO70B1 interacts with SEC5 and EXO84 and forms an exocyst subcomplex involved in autophagy-related, Golgi-independent membrane traffic to the vacuole. We show that EXO70B1 is functionally completely different from EXO70A1 exocyst subunit and adopted a specific role in autophagic transport.

Key words: Arabidopsis, autophagy, EXO70, EXO70B1, exocyst, Golgi-independent, hypersensitive response, salicylic acid

Received 20 January 2013, revised and accepted for publication 10 August 2013, uncorrected manuscript published online 14 August 2013, published online 17 September 2013

The plant vacuole is a very diverse and dynamic organelle with many sub-types and complicated endomembrane trafficking relationships depending on the tissue type and external conditions (1,2). In general, two major types of vacuoles are distinguished: protein storage and lytic vacuoles. In differentiated cells, these vacuoles normally fuse into a large central vacuole (3). The best mapped and understood transport pathway into the vacuole is Golgi-dependent transport via the prevacuolar compartment/MVB, which represents an important junction between the plasma membrane (PM), the trans-Golgi network/early endosome (TGN/EE) and the vacuole (4). For specific types of protein storage vacuoles, and recently also for anthocyanins (5) a direct pathway from the endoplasmic reticulum (ER) to vacuole bypassing the Golgi apparatus (GA) was described via precursor accumulating vesicles (reviewed in 6). This pathway overlaps with ER-to-vacuole protein-sorting route (of some storage proteins), where anthocyanins can be visualized in ER-bodies and in green fluorescent protein (GFP)-Chi labeled vacuoles. As Brefeldin A has no effect on anthocyanin accumulation, this mechanism is Golgi-independent (7). This pathway is also likely to include autophagic steps, as ATG mutants show some anthocyanin accumulation defects (7).

There are obviously more unconventional types of transport into the vacuole, often involving autophagy and autophagy-related mechanisms. The canonical autophagy, known as macroautophagy, is the best-characterized autophagy pathway. It involves engulfment of cellular components resulting into autophagosome formation with two membranes of the phagophore, which later fuses with a lytic vacuole. It is known to be especially induced by nitrogen and carbon starvation (8–10). From studies on non-plant organisms we know that the term autophagy includes several mechanisms with the different membrane contributions to build up the phagophore – ER being an important starting compartment for this process (11,12). Plants with defective components of the autophagic pathway display leaf chlorosis and have impaired survival under both carbon and nitrogen starvation (7) and defense against pathogens were observed when compared to WT plants (see Refs. 13,14). Anthocyanin accumulation defects are not severe, as there are two alternative import pathways for anthocyanins into the vacuole: (A) – a direct transmembrane transport of anthocyanins via GST-ligandins tonoplast transporters (LT pathway), and (B) – vesicle dependent autophagy-related pathway of anthocyanin containing vesicles from ER into the vacuolar lumen (VT pathway, 5). The LT transport can be effectively inhibited by various drugs as, e.g. 1-chloro-2-4-dinitrobenzene (CDNB) or DL-Buthionine-(S,R)-sulfoximine (BSO) to study specifically VT transport (5). In these experiments, anthocyanin synthesis can be boosted artificially by addition of its precursor naringenin to culture media; naringenin is a

product of chalcone isomerase, downstream of chalcone synthase (5).

Importantly, *Arabidopsis* autophagy (*atg)* mutants display early senescence phenotype, which can be suppressed by mutation in *npr1-1* – an essential component of salicylic acid (SA) signaling pathway or by NahG transgene (SA degradation) (15). Genes for core components of autophagy pathway are conserved and expressed constitutively in plants which implies their essential housekeeping function; however, they are strongly upregulated in a response to starvation (16–18).

Recently, a new surprising player in the process of autophagy emerged. Octameric complex exocyst was originally discovered as a tethering complex between vesicles and PM prior to exocytosis, driven by the SNARE complex is initiated (19,20). In mammalian epithelial cells, SEC5 and EXO84 are accumulated in distinct membrane organelles and along with the small GTPase RalB act as a regulatory switch, promoting autophagosome assembly under amino acid deprivation. Upon starvation RalB GTPase is activated, binds to the inactive (in context of autophagy) exocyst subcomplex which loses SEC5 subunit and incorporates EXO84 instead and allows phosphorylation of ULK1 and activation of other autophagosome formation regulators (BECN 1, ATG14L and VPS15/VPS34) and autophagosome initiation (21). In plants, exocyst complex genes are conserved and some subunits have evolved into large gene families over the land plant evolution – especially the EXO70 family (22,23). While the role of exocyst in secretion and polarized cell growth is well established in plants (24–27), we report here that specific version of a exocyst complex harboring EXO70B1 along with EXO84b and SEC5 subunits is an important regulator of autophagosome formation and autophagy-related Golgi-independent import into the vacuole in plants.

Results

Arabidopsis exo70B1 mutant plants show ectopic hypersensitive reaction due to SA hyper accumulation

We have investigated exocyst vesicle tethering complex subunit *EXO70B1* gene function (encoded by single exon) in two GABIKAT 3′-end loss of function (LOF) insertional lines: GK-114C03 and GK-156G02 – *exo70B1-1* and *exo70B1-2*, respectively. Phenotypic deviations of these two lines were identical. Therefore, we have picked only *exo70B1-2* allele for our following experiments. As a positive control for evaluation of autophagic phenotypic deviations, we have used *atg5* mutant. Unfortunately, the previously published mutant *atg5-1* was unavailable from the community, therefore we have obtained and characterized a new allele (SALK_020601) and named it *atg5-3. The atg5-3* mutation is located in the start codon of the ATG5 CDS and it showed phenotypic deviations matching fully the deviations described for the *atg5-1* mutant (15). The presence of a minor PCR product is likely not an indication of a functional transcript (Figure 1B).

Reverse transcription-polymerase chain reaction (RT-PCR) analysis of the *exo70b1-2* mutant line has revealed, that this line is a knock-down mutant, lacking the 3′ terminal part of the mRNA (Figure 1B,C). Thirty-five days after germination (DAG), the leaves of *exo70B1-2* mutants become epinastic, twisted and small spontaneous lesions appear on the mutant leaves (Figure 1A). These symptoms also appear on axenic plants grown *in vitro*, excluding involvement of pathogen interaction in phenotypic deviations incidence (Figure S1C, Supporting Information). Lesions spread and result in death of most of leaves. This is slightly different in the *atg5-3* mutant, where progress of programmed cell death caused no lesions, but early yellowing of the whole leaves (Figure 1A). Eventually, a few small leaves grow from the center of the rosette, giving *exo70B1* mutants a dwarfed appearance. Interestingly, the development of lesions on *exo70B1* mutants is dependent on light dosage. Intensities over 750 $\mu M/m^2/s$ PAR (photosynthetically active radiation) fully rescued mutants from the lesion formation (Figure S1A). Lesion appearance on *exo70B1* mutants indicates that ectopic hypersensitive response (HR) might occur. We have tested HR presence by three methods: detection of apoptotic DNA fragmentation by terminal deoxynucleotidyl transferase dUTP nick end labeling (TUNEL) on the *exo70B1-2* sections; semi-quantitative RT-PCR of cell death markers; and phytohormone analysis together with the suppression of lesion formation by *npr1-1* mutation (Figures 1 and S1B). HR markers, which we have tested in *exo70B1-2* mutant, included vacuolar processing enzymes (VPEs) and PR1. We detected dramatic up-regulation of PR1, slight up-regulation of αVPE, while γVPE mRNA was similarly present in both mutant and WT, as expected in plants 20 DAG (Figure 1D) (28). Expression of PR1 genes is induced by SA accumulation; therefore we estimated levels of SA and other acidic phytohormones in leaves of mutant plants. Not only SA, but also levels of several acidic hormones [including jasmonic acid (JA) and abscisic acid (ABA)] and their derivates were increased, except for gibberellic acid and its derivates (Figure 1C). To further prove, that lesion formation is due to hyper accumulation of SA and SA-dependent signaling, we crossed the *exo70B1-2* mutant with the *npr1-1* – mutant insensitive to SA. Double mutant plants *exo70B1-2/npr1-1* lost the characteristic appearance of *exo70B1-2* plants (Figure 1A). But similarly like in the *atg5-1* mutant (15), early yellowing of leaves, with chlorotic shoots, was still visible. This is logical, since the *npr1* mutation does knock-down SA signaling, but not hyper accumulation of SA (Figure 1A). Thus, we conclude, that *exo70B1* mutant ectopic hypersensitive reaction is caused by hyper accumulation of SA in the *exo70B1* mutant plants. This conclusion fits with TUNEL staining, which has revealed massive genomic DNA fragmentation, as is expected during HR (Figure S1B).

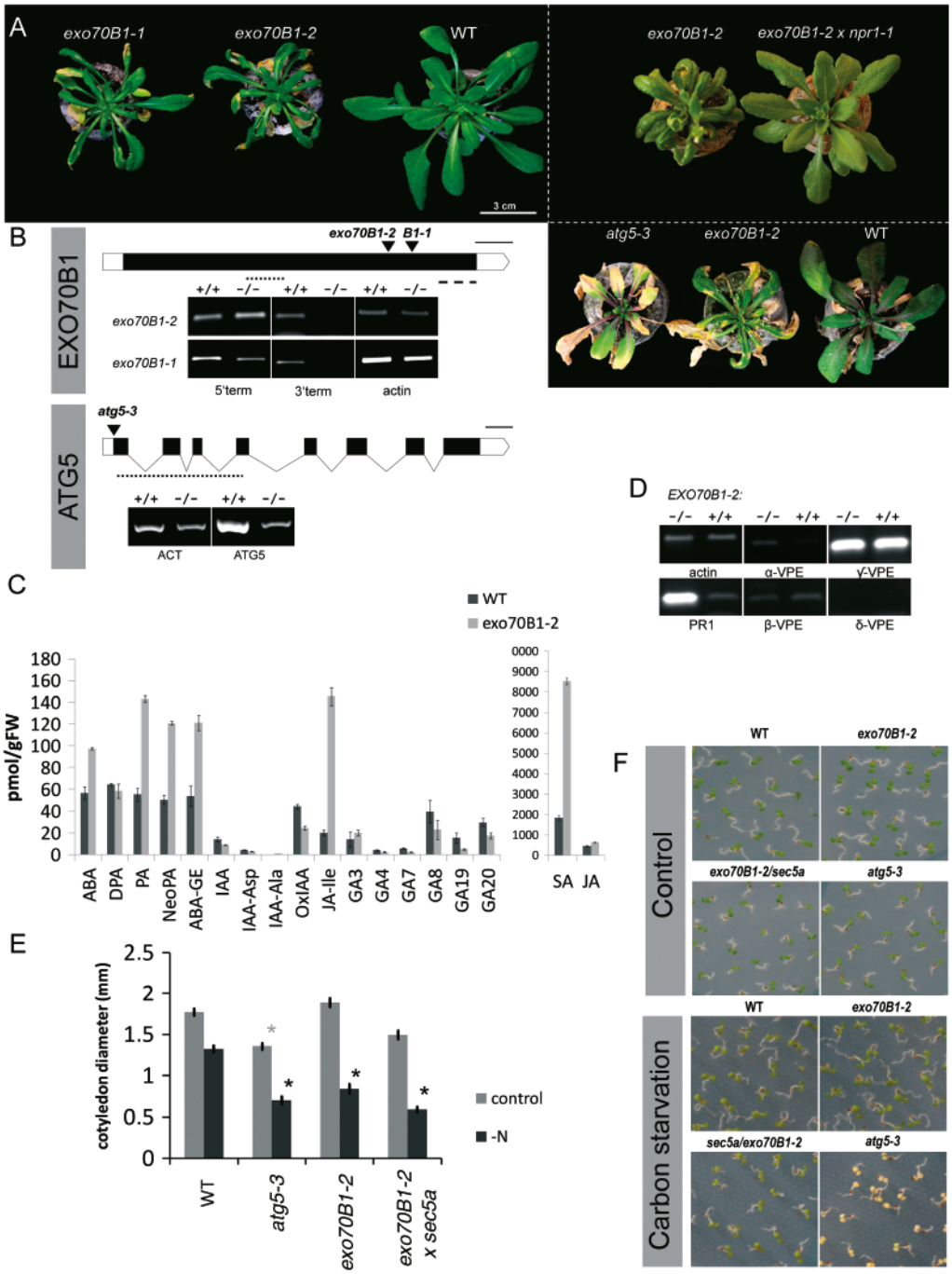

Figure 1: T-DNA insertional mutants used in this study – ***exo70B1-1* and *exo70B1-2*.** Both exhibit the same phenotypes, including ectopic HR lesions formation on leaves, which can be suppressed by crossing with *npr1-1*. Comparison of *exo70B1-2* with *atg5-3* mutant. Plants were grown in standard conditions (see *Materials and Methods*) (A). Insertional lines named *exo70B1-1*, *exo70B1-2* and *atg5-3* disrupt CDS as indicated. Dotted and dashed lines represent 5′-terminal and 3′-fragments, which were amplified in RT-PCR, where (+/+) stands for WT and (–/–) for mutant. Actin was used as a control (B). Selected phytohormones and related substances analysis showing several differentially accumulated compounds in mutant plats (C). Hyperaccumulated salicylic acid (SA; C) corresponds to strong PR1 mRNA induction visualized by semiquantitavie RT-PCR (D). Cotyledon size of nitrogen starved seedlings of *exo70B1-2* mutant and *exo70B1-2/sec5a-1* double mutant compared to WT and *atg5-3*. Stars indicate significant change compared to the WT (E). *exo70B1-2* mutant and *exo70B1-2/sec5a-1* double mutant survive 6 days of carbon starvation unlike *atg5-3* (F). ABA, abscisic acid; DPA, dihydrophaseic acid; PA, phaseic acid; NeoPA, Neophaseic acid; ABA-GE, ABA-glucose ester; IAA, indole-3-acetic acid; IAA-Asp, IAA-aspartate; IAA-Ala, IAA-alanine; OxIAA, oxo-IAA; SA, salicylic acid; JA, jasmonic acid; JA-Ile, JA-isoleucine; GAn, Gibberellin n.

exo70B1-2 mutant seedlings are hypersensitive to nitrogen starvation, but not to the carbon starvation

In next steps, we compared the *exo70B1-2* mutant with the autophagic mutant *atg5-3* stressed by nitrogen and carbon starvation. Seedlings of *exo70B1-2* were affected by nitrogen starvation more than WT plants and showed decreased size of cotyledons, similarly like the *atg5-3* mutant. This difference was enhanced in homozygous plants of the double mutant, formed when we crossed the *exo70B1-2* mutant with another mutation in exocyst subunit – *sec5a-1* (26) (Figure 1E).

As it was shown previously the *atg5-1* mutant is highly susceptible to carbon starvation and cannot recover after 6 days of the starvation treatment (14). Similarly, *atg5-3* seedlings also have not survived 6 days carbon starvation. In contrast, the *exo70B1-2* mutant, or *sec5/exo70B1-2* double mutant have survived this treatment just like the WT control (Figure 1F). This however, was different, when we repeated the experiment with adult plants, which failed to recover and have died just like *atg5-3* (data not shown). This could be a result of boosted progress of hypersensitive cell death due to SA hyperaccumulation rather than inability to remobilize nutrients.

Vesicular trafficking of anthocyanins into the vacuole is compromised in exo70B1-2 mutant

In strong light, an ectopic hypersensitive reaction in *exo70B1* mutants does not appear (see above), but – *exo70B1-2* plants show strongly decreased anthocyanin pigment accumulation. We have observed this phenotype in 30-day old rosettes transferred for 7 days to anthocyanin inductive conditions – both sunlight (long day) and short day (100 $\mu M/m^2/s$ PAR) with additional soft UV irradiation (see *Materials and Methods*). To estimate anthocyanin pigment content, we have measured absorption of methanol eluate from leaves at 400–600 nm (anthocyanin absorption peaks at 530 nm). In *exo70B1* mutant plants, the amount of anthocyanin was dramatically reduced to almost undetectable levels in both light conditions (Figure 2A). Similar, but less dramatic phenotypic deviation was observed on 6 days old etiolated seedlings, where anthocyanin accumulation was induced by 3% sucrose (Figure 2B). Decreased anthocyanin accumulation in *exo70B1* mutants indicates that either synthesis, or at least one of the two described anthocyanin transport pathways to the vacuole (GST-ligandin versus VT pathway) is crippled. To distinguish between these possibilities, we used treatments with naringenin – product of chalcone isomerase, downstream of chalcone synthase (CHS) and with CDNB – a substrate of GSTs, which saturates (i.e. competitively inhibits) vacuolar GST-ligandin dependent pathway. Naringenin treatment is crucial to rule out defects in anthocyanin synthesis, as MAMP (microbe associated molecular pattern) triggered immunity (MTI) was recently shown to down regulate CHS on both transcription and translation/protein levels suppressing anthocyanin accumulation (29).

When the seedlings supplied by naringenin were pretreated by 0.1 mM CDNB, anthocyanin accumulation was fully suppressed in *exo70B1-2* mutant, whereas there was only partial suppression in WT control (Figure 2D). Thus, chemical inhibition of the LT pathway reveals the defect of the vesicular transport (VT) of anthocyanins in *exo70B1-2* mutant. Mutant *exo70B1-2* rescued by *npr1-1* from necrotic lesion formation fully retained the anthocyanin accumulation defect (Figure 2E). This further supports the hypothesis that the anthocyanin accumulation phenotype is not a secondary phenotype caused by SA hyperaccumulation. To be sure that the defect is downstream of CHS, we also performed semi-quantitative RT-PCR on the CHS transcript. In *exo70B1-2* mutant seedlings induced by 3% sucrose for different time periods, CHS mRNA was induced similarly as in the WT (Figure 2F).

YFP-EXO70B1 complements the exo70B1-2 mutation and co-localizes with anthocyanin containing compartments

To investigate subcellular localization of EXO70B1, we created N-terminal YFP and EOS fusion proteins under the ubiquitin (UBQ) promoter (YFP-EXO70B1 and EOS-EXO70B1) and transformed them into the *exo70B1-2* heterozygous plants (to be able to get segregating progeny for mutant complementation). Despite the fact, that there was overall very little fluorescence, the EOS-EXO70B1 construct successfully complemented the mutant phenotype of *exo70B1-2* (Figure S2A). As was indicated in (30), YFP-EXO70B1 localizes into small, mostly static spherical bodies, slightly visible also in DIC. We took advantage of autofluorescent properties of anthocyanin pigments (5) and detected anthocyanin pigment co-localization with YFP-EXO70B1 in etiolated hypocotyls, where anthocyanin synthesis was induced by 3% sucrose. Co-localization was well visible 12 h after addition of sucrose. Later on, the signal was hard to track due to the strong vacuolar background (Figure 3).

EXO70B1-positive compartments are internalized into the vacuole and co-localize with the ATG8f-positive autophagosomal membrane bodies in Arabidopsis

YFP-EXO70B1 positive bodies could be visualized inside of the central vacuole, after vacuole alkalinization by concanamycin A (ConcA). To investigate the relationship of these bodies with autophagic bodies, we have used tunicamycin (TM), which was recently shown to strongly induce ER stress triggered autophagy in *Arabidopsis* (31). The amount of intravacuolar YFP-EXO70B1 bodies after ConcA treatment was significantly increased by addition of TM (Figure 4B). Hence, YFP-EXO70B1 positive bodies have autophagic character. To confirm this, we generated stable transformants with YFP-EXO70B1 and the autophagic marker ATG8f-RFP (32). As shown in Figure 4A, ATG8f-RFP co-localized with YFP-EXO70B1 in both the cytoplasm and in the vacuole after ConcA treatment

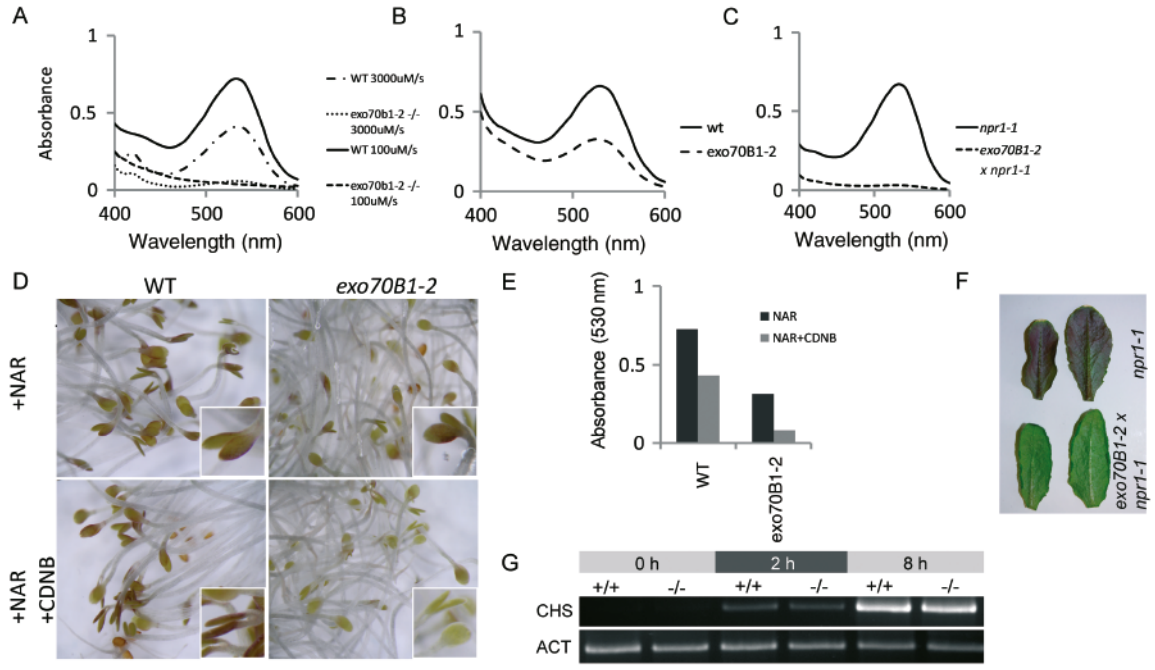

Figure 2: Absorption spectra of methanol eluate from dry leaves of *exo70B1-2* mutant and WT indicating very distinct differences in anthocyanin accumulation. Experiments were carried out in mutant HR inducible (100 μM/m^2/s PAR) and non inducible (3000 μM/m^2/s PAR) conditions (A). Similar, but less dramatic difference can be seen in 5 day old seedlings incubated in sucrose for 24 h (B). The lack of anthocyanin accumulation phenotype deviation in *exo70B1-2* is not suppressed by *npr1-1* mutation (C,F). Induction of anthocyanins in 5 day old seedlings of *exo70B1-2* mutants and WT treated with 1 mM naringenin (nar) or pre-treated with 100 μM 1-Chloro-2,4-dinitrobenzene (CDNB) to inhibit LT import pathway of anthocynins into the vacuole (D). Quantification of D (E). RT-PCR of chalcone synthase (CHS) mRNA in *exo70B1-2* mutant seedlings and WT after 0, 2 and 8 h of incubation in 3% sucrose. Actin (ACT) was used as a control (G).

indicating, that EXO70B1-positive compartments are really related to autophagosomes.

exo70B1-2 mutants show decreased amounts of intravacuolar autophagic bodies

To finally confirm the function of EXO70B1 in autophagic pathway, we have transformed ATG8f-RFP into *exo70B1-2* and WT plants. Then, we measured the amount of autophagic bodies inside of the vacuole of etiolated hypocotyls treated for 12 h with TM + ConcA. There was dramatic decrease of intravacuolar ATG8f-RFP bodies in the *exo70B1-2* as compared to WT (Figure 5).

As *exo70B1-2* mutant shows defects that are connected with the transport to the vacuole via the autophagy-related pathway we investigated 14 day old mutant leaves (complemented by *npr1-1*) by transmission electron microscopy (TEM) that were high pressure frozen and cryosubstituted and 26 days old, chemically fixed mutant leaves grown under daylight to prevent HR and under HR-inducible 100 μM/m^2/s PAR. In both conditions, these mutants often have exosomes in the apoplast (in young leaves) and multivesicular bodies (in older leaves), which strongly resemble paramural bodies (Figure S3). We did not observe any similar structures in the control WT sections. Ultrastructural phenotype deviation of *exo70B1-2* may be the result of insufficient autophagosome targeting to the vacuole, causing cytoplasmic autophagic bodies to fuse with the PM or with other autophagic bodies. However, the influence of SA signaling cannot be entirely ruled out at this point, despite the fact that we have prevented plants from ectopic HR formation with a second *npr1* mutation. This is a subject of our current studies.

EXO70B1 interacts with SEC5A and EXO84b and probably forms an exocyst subcomplex involved in the autophagic pathway

An important question is whether the exocyst subunit EXO70B1 functions alone or as a subunit of the exocyst subcomplex. We therefore performed yeast two-hybrid (Y2H) experiment with multiple exocyst subunits. In this experiment, we used GAL4 BD fused with EXO70B1 and several exocyst constructs displaying no autoactivation, as published previously (see *Materials and Methods*). We observed two interactions – with subunit SEC5A and with the N-terminal fragment of EXO84b (Figure 6). We confirmed these results by co-immunoprecipitation assay with YFP-EXO70B1. We also obtained signal with an AtSEC6 antibody (Figure S4A). These data are supported by observations that YFP-EXO70B1 displays co-localization with RFP-EXO84 (Figure S4B) and *sec5a-1* mutation

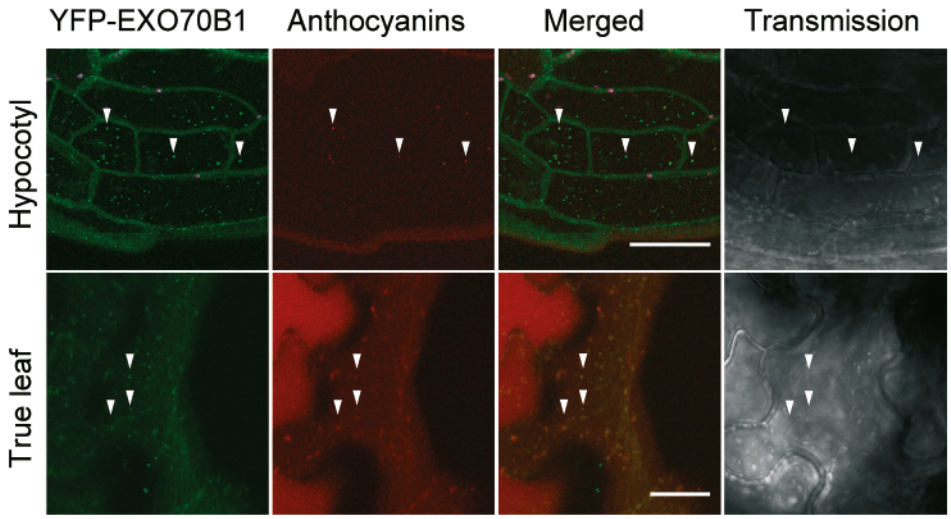

Figure 3: YFP-EXO70B1 co-localizes with anthocyanin containing compartments in etiolated hypocotyls and leaves. Plastids are indicated in magenta. Scale bars are 20 μm long.

shows synergism with *exo70B1-2* mutation in autophagic phenotype deviation (see above). As was previously shown, the *atsec5a-1/exo70A1-2* double mutant also shows enhancement of *exo70A1* phenotype (26).

Exocyst subunits EXO70A1 and EXO70B1 function in different pathways

To test the crucial question of functional specificity of these two EXO70 exocyst subunits, we observed *exo70B1-2/exo70A1-2* double mutant *Arabidopsis* plants. Phenotypic deviations of *exo70A1-2* mutant (33) were fully additive to *exo70B1-2* mutant, with no synergism – the double mutant plants exhibited the same size and anatomy as the *exo70A1-2* mutation alone, however, after 4 weeks, double mutants showed an ectopic hypersensitive reaction like *exo70B1-2* plants, along with the lack of anthocyanin accumulation (Figure S2B–D). Thus, both *exo70B1* and *exo70A1* mutations show no functional synergism, but both show enhancement of their specific mutant phenotypes when crossed with *sec5a-1*. This can be explained by SEC5 being the part of the core machinery which is used by multiple EXO70s involved in different pathways – EXO70A1 functions as expected in the exocyst complex specific for the tethering exocytotic vesicles at the PM (34), while unexpectedly EXO70B1 functions as a subunit of the exocyst subcomplex in the transport of autophagosome-like structures into the vacuole.

Discussion

In this study we provide evidence that EXO70B1 along with SEC5, EXO84B and likely also SEC6, form a sub complex, which plays a role in autophagic transport into the vacuole. Phenotypic deviations of *exo70B1* mutants, such as nitrogen starvation hypersensitivity and defective vesicular transportation of anthocyanins support the main arguments for EXO70B1 function in autophagy – co-localization of the autophagic marker ATG8 with YFP-EXO70B1 inside of the vacuole and the dramatic decrease of intravacuolar autophagic bodies in the *exo70B1-2* mutant upon the induction of autophagy by ER stress. This induction of autophagy, recently reported by (31), was a good option for us as it allowed us to perform treatments of well defined lengths with an exact start time. Autophagy induction by nitrogen starvation has given us similar, but less clear results. Differences in response to carbon starvation, as compared to *atg5*, suggests a possible role in specific autophagic responses, similar to what was shown recently for NBR1 (35). Another plausible explanation is dependence of this phenotype on developmental stage or growth conditions. Light dependence of lesion formation (suppression by higher light fluencies) indicates sensitivity of *exo70b1* mutants to carbohydrate pools.

Mechanistic details of EXO70B1 exocyst subcomplex function includes questions about the timing for which it acts during autophagosome biogenesis and transport is the topic of ongoing studies in our laboratory. Our current data strongly suggest that the EXO70B1 exocyst subcomplex is necessary for ER stress induced autophagosomes targeting into the vacuole. Extrapolating data from mammalian studies points at a defect in autophagosome biogenesis (21). However, we have observed abundant multivesicular bodies and exosomes in the *exo70B1-2* mutant. This suggests that the main EXO70B1 sensitive step could be autophagosome targeting into the vacuole. It was shown many times that when one endomembrane pathway is blocked, another pathway delivers cargo to the different ectopic destinations. For example CLV3 with vacuolar sorting signal, is normally transported into the vacuole, but becomes secreted in vacuolar trafficking mutants (36) or the pectin secretory mutant *echidna* accumulates pectins in the

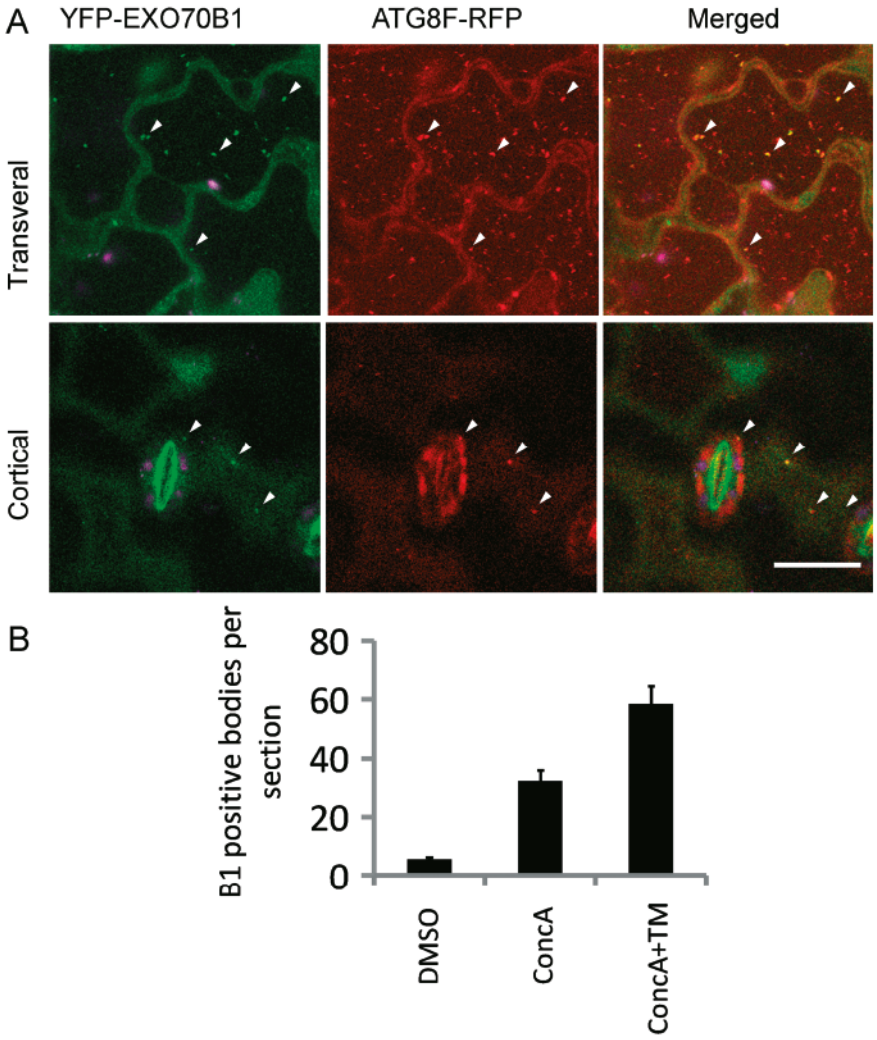

Figure 4: YFP-EXO70B1 co-localizes with ATG8f-RFP inside of the vacuole and in the cytoplasm of stably transformed *Arabidopsis* leaves, when treated for 12 h with 5 μg/mL TM and 1 μM ConcA. Plastids are indicated in magenta. Green signal was not detectable for all of ATG8f-RFP positive spots in this resolution, likely due to weak fluorescence of YFP-EXO70B1. (A). Quantification of intravacuolar autophagic bodies marked by ATG8f-RFP upon ER stress (treatments as indicated) (B). Scale bars are 20 μm long.

vacuoles (37). Similarly, abundant cytoplasmic autophagosomes/MVBs of *exo70B1* mutants could fuse together or be secreted to the apoplast. This model would also explain why *exo70B1* mutants have some similarities with *atg5-3* mutant, but some differences as well – with *atg5* mutant being defective in autophagosome biogenesis and *exo70B1-2* mutant in autophagosome vacuolar import resulting in an 'autophagic traffic jam'. In our study, we have shown co-localization of EXO70B1 with autophagic bodies, however, it is quite possible, that not all of them are EXO70B1 positive. There are eight ATG8 paralogs in *Arabidopsis* and 23 paralogs of EXO70, providing a big space for functional specialization.

EXO70B1 has previously been reported to be localized to the double membrane structures (30). Using mostly transient over-expression of selected Arabidopsis EXO70 subunits in suspension cells, the formation of EXO70A1, EXO70B1 and EXO70E2 positive double membrane bodies, which are explicitly distinct from autophagosome have been described (30). These bodies were named 'EXPO' (exocyst-positive organelle) and proposed to be exported out of cells in an exosome-like manner (30). However, most of the detailed analyses were done only on EXO70E2 subunit. According to (30), overexpressed GFP-EXO70E2 does not enter the vacuole visualized after the concanamycin treatment, in contrast to our observations on EXO70B1. Moreover, upon close inspection of Figure 12c from Ref. (30), partial nonaccidental co-localization with autophagosomal marker ATG8e is also visible. In this context, it is important to point out our observation that over-expression of exocyst subunits itself may cause stimulation of biogenesis of new exocyst-positive compartments, that are normally absent (Figure S5). We suppose that the increased production of exosomes in EXO70E2 over-expressing cells might be an outcome of a saturation – i.e. jam – of vacuolar import resulting in the increased exosome release as is the case in the *exo70B1* mutant described here. The question of EXO70E2 dependent pathway function is still open and needs deeper cytological and especially genetic evidence.

Our model, where different EXO70 proteins mediate targeting of membrane vesicles to different destinations

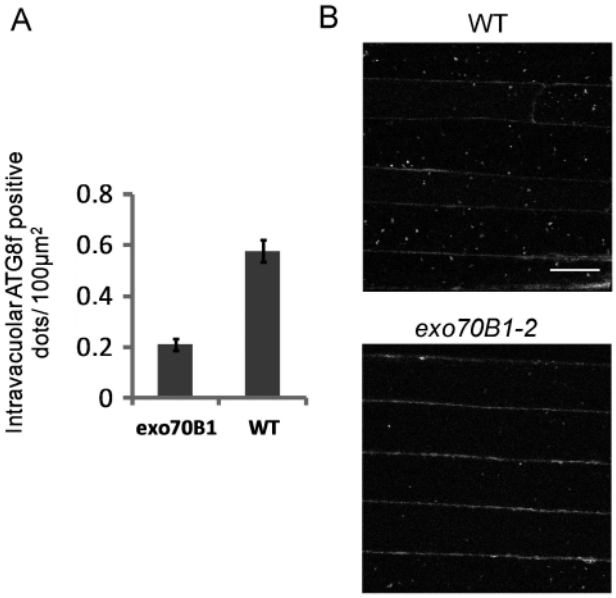

Figure 5: Autophagic defect of *exo70B1-2* mutant. Quantification of intravacuolar autophagic bodies in etiolated hypocotyls upon ER stress (5 µg/mL TM and 1 µM ConcA) marked by ATG8f-RFP in *exo70B1-2* and WT hypocotyls (A). Representative picture (B). Scale bar is 20 µm long.

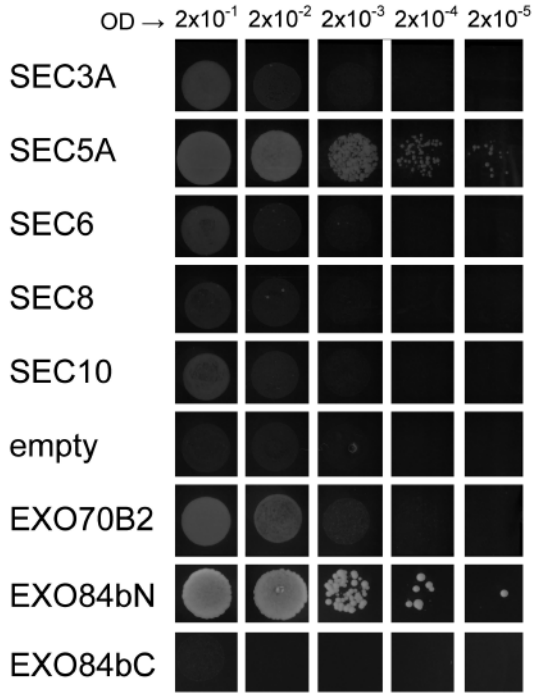

Figure 6: Yeast two-hybrid interactions of EXO70B1 fused with GAL4 BD interacts with SEC5A and N-terminal part of EXO4b fused with GAL4 AD (full-length EXO84b autoactivates).

in the same cell seems likely and raises further questions (39). For example, EXO70B2 – the closest paralog of EXO70B1, could target autophagy derived bodies (possibly MVBs) to the secretory papilla, as we have previously reported papilla formation abnormalities in *exo70B2-1* mutant (27). This mechanism may be similar to the one recently reported for the fungal (*Magnaporthe oryzae*) exocyst dependent pathway for secretion of cytoplasmic effectors (38).

Obviously, questions of possible EXO70s-dependent functional diversification of exocyst and its putative subcomplexes acting in exocytosis or in the autophagy in plant cells lay ahead. Despite that, we already bring first insights into this issue. We show that EXO70B1 interacts with SEC5a and EXO84. Also, the EXO70B2 paralog involved in the MAMP triggered immunity was shown to interact with *Arabidopsis* SEC5A subunits before (27) and EXO70A1 was shown to interact with EXO84B (34). A LOF mutant *sec5a-1* looks like WT under normal conditions (26) and mutations in both *exo70B1* and *exo70A1* show synergism with *sec5a-1*. However, there is no synergism between *exo70A1* and *exo70B1* mutations – EXO70A1 and EXO70B1 function in completely different membrane traffic pathways. The most parsimonious explanation for these observations is a model where the plant uses exocyst for various functions and a large EXO70 family is responsible for its subfunctionalizations, as EXO70 subunits are those binding the target membrane, functioning as the landmark for vesicle targeting/tethering (19,20). Mutations in core machinery, for example SEC5, would then cause defects in all processes mediated by exocyst, whereas mutations in EXO70 subunits would cause target membrane-specific deviations. This model has been suggested before (39) however, phagophore or tonoplast as a destination membrane for exocyst function has not been expected at all.

The fact that very recently also a breakthrough study on exocyst role in autophagy of mammals was published (21) brings the exocyst complex into a brand new light, giving it a second function – in the autophagy dependent endomembrane trafficking. This role might be as ancient in the eukaryote evolution as is its well established function in the exocytotic vesicles tethering. Positioned between biosynthetic membrane transport pathway to the cell surface and vacuolar biogenesis via autophagy-related pathway, exocyst might turn out to be one of the central coordinating regulatory knots of endomembrane transport.

Materials and Methods

Plant material and growth

GABIKAT T-DNA insertional lines of *Arabidopsis thaliana* ecotype Columbia-0 (Col0) were obtained from NASC Institute (40). We also used *sec5a-1* plants from (26,41). Mutant *npr1-1*, was a gift from Saskia van Wees (Utrecht University). If not specified otherwise in the results, plants were grown in soil or peat pellets (Jiffy) under long day (LD) conditions (16:8 h) with standard illumination of 100 µM/m^2/s PAR. For highest light intensities (750–3000 µM/m^2/s), direct sunlight was used as a source of light and

plant were grown in the June/July, which corresponds to LD 16:8 h. For anthocyanin induction experiments, surface sterilized seedlings were kept in 4°C for 2–3 days and for 1 day exposed to the light and 24°C. Then they were placed in liquid MS media without sucrose and grown in darkness with shaking at 100 rpm.

Genotype analysis

Following primer sets were used for genotyping:

exo70B1-1	LP: TTCGTTTATGGAGGTTTGTCG
(GABI_114C03)	RP: TGGTCATTTAGCAGGTGGTTC
exo70B1-2	LP: CGTGGCAGGAGTTAGAAGATG
(GABI_156G02)	RP: TTGTCTGCGTTTTTCCCTATG
o8474 (GABI LB)	ATAATAACGCTGCGGACATCTACATTTT
atg5-3	LP: AAAGACCACAGAACCCGAAAC
(SALK_020601)	RP: CCAAATTGAATCTTCACCAGG
LBB 1.3 (salk LB)	ATTTTGCCGATTTCGGAAC

sec5a-1 line was genotyped as previously (26).

Transcript detection and semi-quantitative RT-PCR

For detection of transcript in *exo70B1-2* mutant RNA was isolated from 100 mg of 7 day old seedlings growing on MS plates. RT-PCR was done by Fermentas First Strand cDNA Synthesis Kit with 1 μg of total RNA, which was double-DNAsed. Following primer pairs were used for transcript detection: CTGGATTTGGTAAGGCGTGT with ACGTTCGCTAGGAAACAGGA for detection of 5′ terminal region and TTGACGAGCAGCTGAAAGAA with CTTCCCGTGGTAGTCCCTTT for 3′ terminal region. All reactions were made in 24, 28 and 32 cycles. Twenty-eight cycle PCR products were used in images. After 32 cycles, weak band has appeared also in c-terminal part of EXO70B1 transcript. This was probably caused by genomic DNA contamination (EXO70B1 has a single exon, so it is impossible to get differential PCR products), despite the DNAse treatment, as genomic contamination appeared also at actin control. For semi-quantitative RT-PCR, total RNA was isolated from fresh rosette leaves of 28 day old plants, which not yet showed any lesions or defects. For extraction, Qiagen RNEasy Plant Mini kit was. RT-PCR was done by Fermentas First Strand cDNA Synthesis Kit with 1 μg of total RNA. For detection of HR, the following sets of primers were used:

PR1:	CTTGTAGGTGCTCTTGTTCTTCCC
	TGCCTCTTAGTTGTTCTGCGTAGC
VPEα	CGAAGAACGAGGAGAATCCAAGAC
	GACCGCTATCTACAACTTTCCCAC
VPEβ	CGGAAGATGGGTCAAGGAAGAAG
	ATCGTCAACCAAAGGCAAACC
VPEγ	GGAACAAACCCTGCCAATGAC
	GAACCTTCTGGTGCTTTTCGG
VPEδ	TTCTGGCTTGGTCAATCCGC
	GCTGTCCTGTTGTTCTTGTGGAAG
CHS	AGGCTCAGAGAGCTGATGGA
	GTAGTCAGCACCAGGCATGT

All reactions were made in 24, 28 and 32 cycles. Twenty-eight cycle PCR products were used in images.

Phytohormonal analysis

We utilized a modification of previously published (42) extraction and purification procedure, which separated the extracted hormones into two fractions, (i) fraction A – containing the hormones of acidic and neutral character, and (ii) fraction B – containing the hormones of basic character. Hormones were quantified using HPLC (Ultimate 3000, Dionex) coupled to hybrid triple quadrupole/linear ion trap mass spectrometer (3200 Q TRAP, Applied Biosystems) set in selected reaction monitoring mode. Fraction A was used. Experiment was done in triplicate.

TUNEL assay

Paraffin sections (11 μm thick) were subjected to TUNEL reaction with TMR red *in situ* cell death detection kit (Roche Diagnostic GmbH) according to manufacturer´s protocol with slight modification. Just prior to the TUNEL reaction, all samples were washed for 5 min in 25 mM Tris pH 6.6. Nuclei staining was done by incubation of the samples with 0.1 μg/mL Hoechst in 1x PBS for 10 min. Samples were observed under an epifluorescent microscope equipped with appropriate excitation and emission filters.

Fluorescent protein construction and transformation

EXO70B1 single exon was amplified from genomic DNA using primers: TATAC ACTGTCGACACATCTGTTTCAATCATG and CCTTCGAATTCTTCC-CGTGGTAGTCC and subcloned into pENTR1A (Invitrogen) using SalI and EcoRI restriction sites. Using Invitrogen gateway cloning system, this construct was used to create GFP and EOS n-terminal fusion construct, using pUBN:EOS and pUBN:YFP vectors (43). These constructs were transformed into *Agrobacterium tumefaciens GV3101* and used for infiltration *Nicotiana benthamiana* leaves, as well as for making stable transformants. Transient expression was performed as described in (44) with final OD for infiltration 0.05 and observations were made 48–72 h. after infiltration due to slower UBQ promoter. For stable transformants, progeny of heterozygotes in *EXO70B1-2* was transformed using floral dip method and selected on soil using BASTA selection. ATG8-RFP vector was obtained from (32). HDEL-GFP was obtained from (45). EXO84b constructs with GFP and or natural promoter were described at (34) EXO84b construct from (26) was transformed into binary 35S vector pK7RWG2 (46) using Invitrogen gateway cloning system to form EXO84b-RFP construct.

Co-immunoprecipitation

Protein complexes with EXO70B1-YFP and YFP (tagged with HDEL) as a control, were isolated using the μM ACS GFP tagged protein isolation kit (Miltenyi Biotec), according to the manufacturer's instructions, with some modifications. Approximately 1 g of 7-day-old *A. thaliana* seedlings were pulverized in liquid nitrogen, resuspended in 1 mL of Sec6/8 buffer [20 mM HEPES, pH 6.8, 150 mM NaCl, 1 mM EDTA, 1 mM DTT, and 0.5% Tween, supplemented with 13 protease inhibitor cocktail (Sigma-Aldrich); (26)], and centrifuged 10 000 × g for 10 min at room temperature. The anti-GFP microbeads, 75 μL, were added and incubated for 30 min on ice with occasional shaking. The Sec6/8 buffer, two times, and lysis buffer provided in the kit, two times, were used to wash the samples on the column, and immunoprecipitates were eluted with 70 μL of the elution buffer.

Several SDS–PAGEs were run with aliquots of eluted proteins loaded so that the amounts of tagged baits, EXO70B1-YFP and YFP were approximately equal. Subsequently, proteins were blotted onto a nitrocellulose membrane and blocked overnight at 4°C with 5% nonfat dry milk in PBS (137 mM NaCl, 2.7 mM KCl, 10 mM Na_2HPO_4, and 2 mM KH_2PO_4, pH 7.4) supplemented with 0.1% Tween 20. Primary antibodies used for immunodetection were commercially available anti-GFP antibody (Roche) and rabbit polyclonal antibodies (Agrisera), raised against peptides from SEC5a (CVRKPSMDEDEESEVE), EXO84b (CQRTDDLRRPLDRQN) and SEC6 (Ac-NPPKTGFVFPRVKC), diluted 1:5000, 1:10 000 and 1:10 000, respectively, and incubated with the membranes overnight, at 4°C, in the blocking solution. Horseradish peroxidase-conjugated secondary anti-rabbit antibody (Promega) was applied, followed by chemiluminescent ECL detection (Amersham).

Microscopy

Leaves of both *A. thaliana* and *N. benthamiana* were observed using LCS 510; Leica with a × 63/1.2 water immersion objective. Following excitation and emission settings were used [ex(nm)/em range(nm)]:

488/525–535 for GFP, YFP and nonconverted EOS, 514/580-620 nm for RFP photoconverted EOS and for anthocyanins. For co-localization experiments with anthocyanins, EXO84b and ATG8f we performed lambda scan to avoid misinterpretations.

For quantification of intravacuolar bodies, each section was taken three times and number of bodies was then averaged. We have used three independent transformed lines for each genotype. For evaluation, 90 pictures out of 30 plants have been used.

TEM microscopy

For TEM, leaf stripes were fixed for 24 h in 2.5% glutaraldehyde in 0.1 M cacodylate buffer (pH 7.2) in 4°C and postfixed in 2% OsO_4 in the same buffer. Fixed tissue was dehydrated through an ascending ethanol and acetone series and embedded in Epon-Araldite. For cryo-fixation, tiny pieces of Arabidopsis leaves were placed in specimen holders filled with a dense culture of Saccharomyces sp. and cryoimmobilized using the Balzers HPM 010 high pressure freezer (BAL-TEC Inc.). The samples were freeze-substituted for 17 h at 2908C in anhydrous acetone containing 2% OsO_4 and gradually brought to room temperature within 6 h. Following a wash in acetone, leaf pieces were embedded through stepwise infiltration into a mixture of Epon and Durcupan (Fluka). Thin sections were cut on a Reichert-Jung Ultracut E ultramicrotome and stained using uranyl acetate and lead citrate. We examined and photographed using Jeol JEM-1010 electron microscope with camera Veleta and software iTEM software (Olympus).

Anthocyanin extraction

Dry weight was measured and soaked overnight at room temperature in 50% methanol in water (v/v). We used 25 mg of dry weight/mL. Then, extraction was done according (5).

Yeast two-hybrid system

The yeast two-hybrid was performed as described previously (26). We used the Matchmaker GAL4 Two-Hybrid System 3 (Clontech), following manufacturer's instructions. We used constructs prepared by (26,27,34). EXO70B1 in pGBKT7 vector was prepared using fragment amplified with ACTGAATTCACATCTGTTTCAATCATG and AAGTCGACATTTTTGT-GTTCGTTACCT (EcoRI and SalI restriction sites).

Plant treatments

UV irradiation was made with soft UV irradiation (360 nm) approximately 2 W/m^2. We used 2 min UV pulse every hour. Concanamycin A and tunicamycin were used as described in (31). Naringenin and CDNB were used according to (5), with our seedlings being little bit older (5 DAG).

Picture analysis

For measuring of plant size and for taking plant pictures, we used Canon EOS 450D with objective EF-S 60 2.8/Macro. For size quantification, calculating area and number of objects, preparation and for projections of confocal images, we used open source FIJI software (47).

Acknowledgments

This work was supported by the Czech Science Foundation grant GACR P305/11/1629. Part of the V. Z. income is from project MSM0021620858 by Czech Ministry of Education. The authors would like to thank colleague from the Faculty of Science, Charles University – Fatima Cvrčková for the support in yeast two-hybrid screens and discussions of the work; we are grateful to Edita Janková-Drdová from the Institute of Experimental Botany ASCR for her help with the EM. ATG8-RFP marker is from the laboratory of Gad Galili (Weizmann Institute of Science, Israel). We are grateful for the important discussions with the Marco Trujillo (Leibniz Institute of Plant Biochemistry, Germany) and Ralph Hückelhoven (Technical University of Munich).

Supporting Information

Additional Supporting Information may be found in the online version of this article:

Figure S1: *exo70b1-1* mutant and WT on different light intensities. Light intensity values represent PAR radiation only. Mutant was rescued from lesion phenotype by radiations above 750 μM/m^2/s on both sunlight (A) and in growth chamber with 750 μM/m^2/s PAR (data not shown). Pictures were taken in the early stages of HR appearance, so that we could take all samples together. All experiments were done on long day (in case of sunlight, the day length varied from 15.81 to 16.12 h per day) (A). TUNEL staining of *exo70B1-2* mutants and WT. First column (Hoechst) indicates presence of nuclear DNA using Hoechst stain. dUTP marked with TMR red in second column – samples treated by terminal deoxynucleotidyl transferase (TdT) to visualize nucleosomal fragmented DNA by PCD. As a negative control, we used staining without addition of TdT (B). Scale bar is 20 μM long and valid for all frames (B). Lesions appearance on *in vitro* grown plants in standard light conditions (see *Materials and Methods*) (C).

Figure S2: *exo70B1-2* allele in the background of EOS-EXO70B1 and *exo70A1-2*. Complementation of *exo70B1-2* mutant phenotypic deviations by EOS-EXO70B1 transformation and genotyping of shown plants detecting presence of *exo70B1-2* allele (A). *exo70A1-2 x exo70B1-2* double mutant displays additive phenotypic deviations of both mutant genes with no synergism. First lesions on double mutant appear 40 DAG (B) and continue to spread (C, 54 DAG). Anthocyanin accumulation defect is present only in the *exo70A1-2 x exo70B1-2* double mutant (D).

Figure S3: Ultrastructural analysis of *exo70B1-2* mutants. High pressure freeze substituted (HPSF) TEM of leaf mesophyll cells of 14 days old *exo70B1-2* complemented by *npr1-1* showing exosomes in apoplast not observed in the WT (A, D). Chemically fixed TEM images of 26 days old *exo70B1-2* mutant grown on daylight to prevent HR. Arrows point at multivesicular bodies which strongly resemble paramural bodies in epidermal cells (B, C), which are present in mesophyll as well (E, F). No such bodies were spotted in WT plants. Scale bar is 0, 2 μm long (A, D), 2 μm long (B, E) and 1 μm long (C, F).

Figure S4: Co-immunoprecipitation of YFP-EXO70B1 with other exocyst subunits. Individual lines represent: M, marker; 1, coimmunoprecipitate with YFP-EXO70B1; 2, coimmunoprecipitate with control YFP; 3, total cell extract from YFP-EXO70B1 seedlings. A) Co-localization of YFP-EXO70B1 and EXO84B-RFP in transiently transformed *Nicotiana benthamiana*. Scale bar is 20 μm long (B).

Figure S5: Comparison of expression of EXO84b:GFP driven by 35 promoter (right) and WT promoter (left) in *Arabidopsis* root. Scale bar is 5 μm long.

References

1. Marty F. Plant vacuoles. Plant Cell 1999;11:587–599.
2. Rojo E, Denecke J. What is moving in the secretory pathway of plants? Plant Physiol 2008;147:1493–1503.
3. Paris N, Stanley CM, Jones RL, Rogers JC. Plant cells contain two functionally distinct vacuolar compartments. Cell 1996;85:563–572.
4. Frigerio L, Hinz G, Robinson DG. Multiple vacuoles in plant cells: rule or exception? Traffic 2008;9:1564–1570.
5. Poustka F, Irani NG, Feller A, Lu Y, Pourcel L, Frame K, Grotewold E. A trafficking pathway for anthocyanins overlaps with the endoplasmic reticulum-to-vacuole protein-sorting route in Arabidopsis and contributes to the formation of vacuolar inclusions. Plant Physiol 2007;145:1323–1335.
6. Jurgens G. Membrane trafficking in plants. Annu Rev Cell Dev Biol 2004;20:481–504.
7. Pourcel L, Irani NG, Lu Y, Riedl K, Schwartz S, Grotewold E. The formation of Anthocyanic Vacuolar Inclusions in Arabidopsis thaliana and implications for the sequestration of anthocyanin pigments. Mol Plant 2010;3:78–90.

8. Guiboileau A, Yoshimoto K, Soulay F, Bataillé M-P, Avice J-C, Masclaux-Daubresse C. Autophagy machinery controls nitrogen remobilization at the whole-plant level under both limiting and ample nitrate conditions in Arabidopsis. New Phytol 2012;194:732–740.
9. Hanaoka H, Noda T, Shirano Y, Kato T, Hayashi H, Shibata D, Tabata S, Ohsumi Y. Leaf senescence and starvation-induced chlorosis are accelerated by the disruption of an Arabidopsis autophagy gene. Plant Physiol 2002;129:1181–1193.
10. Xiong Y, Contento AL, Bassham DC. AtATG18a is required for the formation of autophagosomes during nutrient stress and senescence in Arabidopsis thaliana. Plant J Cell Mol Biol 2005;42:535–546.
11. Axe EL, Walker SA, Manifava M, Chandra P, Roderick HL, Habermann A, Griffiths G, Ktistakis NT. Autophagosome formation from membrane compartments enriched in phosphatidylinositol 3-phosphate and dynamically connected to the endoplasmic reticulum. J Cell Biol 2008;182:685–701.
12. Simonsen A, Stenmark H. Self-eating from an ER-associated cup. J Cell Biol 2008;182:621–622.
13. Phillips AR, Suttangkakul A, Vierstra RD. The ATG12-conjugating enzyme ATG10 is essential for autophagic vesicle formation in Arabidopsis thaliana. Genetics 2008;178:1339–1353.
14. Thompson AR, Doelling JH, Suttangkakul A, Vierstra RD. Autophagic nutrient recycling in Arabidopsis directed by the ATG8 and ATG12 conjugation pathways. Plant Physiol 2005;138:2097–2110.
15. Yoshimoto K, Jikumaru Y, Kamiya Y, Kusano M, Consonni C, Panstruga R, Ohsumi Y, Shirasu K. Autophagy negatively regulates cell death by controlling NPR1-dependent salicylic acid signaling during senescence and the innate immune response in Arabidopsis. Plant Cell 2009;21:2914–2927.
16. Chung T, Suttangkakul A, Vierstra RD. The ATG autophagic conjugation system in maize: ATG transcripts and abundance of the ATG8-lipid adduct are regulated by development and nutrient availability. Plant Physiol 2009;149:220–234.
17. Bassham DC. Plant autophagy – more than a starvation response. Curr Opin Plant Biol 2007;10:587–593.
18. Meijer WH, van der Klei IJ, Veenhuis M, Kiel JAKW. ATG genes involved in non-selective autophagy are conserved from yeast to man, but the selective Cvt and pexophagy pathways also require organism-specific genes. Autophagy 2007;3:106–116.
19. Heider MR, Munson M. Exorcising the exocyst complex. Traffic Cph Den 2012;13:898–907.
20. Munson M, Novick P. The exocyst defrocked, a framework of rods revealed. Nat Struct Mol Biol 2006;13:577–581.
21. Bodemann BO, Orvedahl A, Cheng T, Ram RR, Ou Y-H, Formstecher E, Maiti M, Hazelett CC, Wauson EM, Balakireva M, Camonis JH, Yeaman C, Levine B, White MA. RalB and the exocyst mediate the cellular starvation response by direct activation of autophagosome assembly. Cell 2011;144:253–267.
22. Cvrckova F, Grunt M, Bezvoda R, Hala M, Kulich I, Rawat A, Zarsky V. Evolution of the land plant exocyst complexes. Front Plant Sci 2012;3:159; doi: 10.3389/fpls.2012.00159.
23. Elias M. The exocyst complex in plants. Cell Biol Int 2003;27:199–201.
24. Cole RA, Synek L, Zarsky V, Fowler JE. SEC8, a subunit of the putative Arabidopsis exocyst complex, facilitates pollen germination and competitive pollen tube growth. Plant Physiol 2005;138:2005–2018.
25. Kulich I, Cole R, Drdová E, Cvrcková F, Soukup A, Fowler J, Zarsky V. Arabidopsis exocyst subunits SEC8 and EXO70A1 and exocyst interactor ROH1 are involved in the localized deposition of seed coat pectin. New Phytol 2010;188:615–625.
26. Hála M, Cole R, Synek L, Drdová E, Pečenková T, Nordheim A, Lamkemeyer T, Madlung J, Hochholdinger F, Fowler JE, Žárský V. An exocyst complex functions in plant cell growth in Arabidopsis and tobacco. Plant Cell 2008;20:1330–1345.
27. Pecenková T, Hála M, Kulich I, Kocourková D, Drdová E, Fendrych M, Toupalová H, Zársky V. The role for the exocyst complex subunits Exo70B2 and Exo70H1 in the plant–pathogen interaction. J Exp Bot 2011;62:2107–2116.
28. Kinoshita T, Yamada K, Hiraiwa N, Kondo M, Nishimura M, Hara-Nishimura I. Vacuolar processing enzyme is up-regulated in the lytic vacuoles of vegetative tissues during senescence and under various stressed conditions. Plant J Cell Mol Biol 1999;19:43–53.
29. Serrano M, Kanehara K, Torres M, Yamada K, Tintor N, Kombrink E, Schulze-Lefert P, Saijo Y. Repression of sucrose/ultraviolet B light-induced flavonoid accumulation in microbe-associated molecular pattern-triggered immunity in Arabidopsis. Plant Physiol 2012;158:408–422.
30. Wang J, Ding Y, Wang J, Hillmer S, Miao Y, Lo SW, Wang X, Robinson DG, Jiang L. EXPO, an exocyst-positive organelle distinct from multivesicular endosomes and autophagosomes, mediates cytosol to cell wall exocytosis in Arabidopsis and tobacco cells. Plant Cell 2010;22:4009–4030.
31. Liu Y, Burgos JS, Deng Y, Srivastava R, Howell SH, Bassham DC. Degradation of the endoplasmic reticulum by autophagy during endoplasmic reticulum stress in Arabidopsis. Plant Cell 2012;24:4635–4651.
32. Honig A, Avin-Wittenberg T, Ufaz S, Galili G. A new type of compartment, defined by plant-specific Atg8-interacting proteins, is induced upon exposure of Arabidopsis plants to carbon starvation. Plant Cell 2012;24:288–303.
33. Synek L, Schlager N, Eliáš M, Quentin M, Hauser M-T, Žárský V. AtEXO70A1, a member of a family of putative exocyst subunits specifically expanded in land plants, is important for polar growth and plant development. Plant J 2006;48:54–72.
34. Fendrych M, Synek L, Pečenková T, Toupalová H, Cole R, Drdová E, Nebesářová J, Šedinová M, Hála M, Fowler JE, Žárský V. The Arabidopsis Exocyst Complex Is Involved in Cytokinesis and Cell Plate Maturation. Plant Cell 2010;22:3053–3065.
35. Zhou J, Wang J, Cheng Y, Chi Y-J, Fan B, Yu J-Q, Chen Z. NBR1-mediated selective autophagy targets insoluble ubiquitinated protein aggregates in plant stress responses. Plos Genet 2013; doi: 10.1371/journal.pgen.1003196.
36. Sanmartín M, Ordóñez A, Sohn EJ, Robert S, Sánchez-Serrano JJ, Surpin MA, Raikhel NV, Rojo E. Divergent functions of VTI12 and VTI11 in trafficking to storage and lytic vacuoles in Arabidopsis. Proc Natl Acad Sci USA 2007;104:3645–3650.
37. Gendre D, McFarlane HE, Johnson E, Mouille G, Sjödin A, Oh J, Levesque-Tremblay G, Watanabe Y, Samuels L, Bhalerao RP. Trans-golgi network localized ECHIDNA/Ypt interacting protein complex is required for the secretion of cell wall polysaccharides in Arabidopsis. Plant Cell 2013; doi: 10.1105/tpc.113.112482.
38. Giraldo MC, Dagdas YF, Gupta YK, Mentlak TA, Yi M, Martinez-Rocha AL, Saitoh H, Terauchi R, Talbot NJ, Valent B. Two distinct secretion systems facilitate tissue invasion by the rice blast fungus Magnaporthe oryzae. Nat Commun 2013; doi: 10.1038/ncomms2996.
39. Zárský V, Cvrcková F, Potocký M, Hála M. Exocytosis and cell polarity in plants – exocyst and recycling domains. New Phytol 2009;183:255–272.
40. Kleinboelting N, Huep G, Kloetgen A, Viehoever P, Weisshaar B. GABI-Kat SimpleSearch: new features of the Arabidopsis thaliana T-DNA mutant database. Nucleic Acids Res 2012;40.
41. Alonso JM, Stepanova AN, Leisse TJ, Kim CJ, Chen H, Shinn P, Stevenson DK, Zimmerman J, Barajas P, Cheuk R, Gadrinab C, Heller C, Jeske A, Koesema E, Meyers CC, et al. Genome-wide insertional mutagenesis of Arabidopsis thaliana. Science 2003;301:653–657.
42. Dobrev PI, Kamínek M. Fast and efficient separation of cytokinins from auxin and abscisic acid and their purification using mixed-mode solid-phase extraction. J Chromatogr A 2002;950(1–2):21–29.
43. Grefen C, Donald N, Hashimoto K, Kudla J, Schumacher K, Blatt MR. A ubiquitin-10 promoter-based vector set for fluorescent protein tagging facilitates temporal stability and native protein distribution in transient and stable expression studies. Plant J Cell Mol Biol 2010;64:355–365.
44. Lavy M, Bracha-Drori K, Sternberg H, Yalovsky S. A cell-specific, prenylation-independent mechanism regulates targeting of type II RACs. Plant Cell 2002;14:2431–2450.
45. Petrásek J, Cerná A, Schwarzerová K, Elckner M, Morris DA, Zazímalová E. Do phytotropins inhibit auxin efflux by impairing vesicle traffic? Plant Physiol 2003;131:254–263.
46. Karimi M, Inzé D, Depicker A. GATEWAY^{TM} vectors for Agrobacterium-mediated plant transformation. Trends Plant Sci 2002;7:193–195.
47. Schindelin J, Arganda-Carreras I, Frise E, Kaynig V, Longair M, Pietzsch T, Pietzsch T, Preibisch S, Rueden C, Saalfeld S, Schmid B, Tinevez J-Y, White DJ, Hartenstein V, Eliceiri K, Tomancak P, Cardona A, et al. Fiji: an open-source platform for biological-image analysis. Nat Methods 2012;9:676–682.

New Phytologist

Microtubule-dependent targeting of the exocyst complex is necessary for xylem development in Arabidopsis

Nemanja Vukašinović[1,2], Yoshihisa Oda[3,4], Přemysl Pejchar[1], Lukáš Synek[1], Tamara Pečenková[1], Anamika Rawat[1,2], Juraj Sekereš[1,2], Martin Potocký[1] and Viktor Žárský[1,2]

[1]Institute of Experimental Botany, v.v.i., The Czech Academy of Sciences, 16502, Prague 6, Czech Republic; [2]Department of Experimental Plant Biology, Faculty of Science, Charles University in Prague, 128 44, Prague 2, Czech Republic; [3]Center for Frontier Research, National Institute of Genetics, 1111 Yata, Mishima, Shizuoka 411-8540, Japan; [4]Department of Genetics, School of Life Science, SOKENDAI (Graduate University for Advanced Studies), 1111 Yata, Mishima, Shizuoka 411-8540, Japan

Author for correspondence:
Viktor Žárský
Tel: +420221951683
Email: zarsky@ueb.cas.cz

Received: *15 July 2016*
Accepted: *13 September 2016*

New Phytologist (2017) **213:** 1052–1067
doi: 10.1111/nph.14267

Key words: conserved oligomeric Golgi (COG) complex, exocyst, microtubules, secondary cell wall, tracheary elements, xylem.

Summary

- Cortical microtubules (MTs) play a major role in the patterning of secondary cell wall (SCW) thickenings in tracheary elements (TEs) by determining the sites of SCW deposition. The EXO70A1 subunit of the exocyst secretory vesicle tethering complex was implicated to be important for TE development via the MT interaction. We investigated the subcellular localization of several exocyst subunits in the xylem of *Arabidopsis thaliana* and analyzed the functional significance of exocyst-mediated trafficking in TE development.
- Live cell imaging of fluorescently tagged exocyst subunits in TE using confocal microscopy and protein–protein interaction assays were performed to describe the role of the exocyst and its partners in TE development.
- In TEs, exocyst subunits were localized to the sites of SCW deposition in an MT-dependent manner. We propose that the mechanism of exocyst targeting to MTs involves the direct interaction of exocyst subunits with the COG2 protein. We demonstrated the importance of a functional exocyst subunit EXO84b for normal TE development and showed that the deposition of SCW constituents is partially compromised, possibly as a result of the mislocalization of secondary cellulose synthase in exocyst mutants.
- We conclude that the exocyst complex is an important factor bridging the pattern defined by cortical MTs with localized secretion of the SCW in developing TEs.

Introduction

The xylem vessel system is essential for water and nutrient transport of vascular plants and mechanical stability of their tissues (Fukuda, 1997). Mature xylem vessel elements, also called tracheary elements (TEs), display structured cell wall morphology with diversity of secondary thickening patterns – annular or spiral pattern in protoxylem, and reticulate or pitted pattern in metaxylem (Růžička *et al.*, 2015). TEs differentiate from procambial cells and this developmental switch is triggered by VASCULAR-RELATED NAC-DOMAIN 6 (VND6) and VND7 – master regulators of xylem development in Arabidopsis (Kubo *et al.*, 2005).

Further steps in xylem maturation, such as secondary cell wall (SCW) thickening and programmed cell death, are under the control of genes upregulated by VND6 and VND7 in metaxylem and protoxylem, respectively (Kubo *et al.*, 2005). A substantial role of microtubules (MTs) in scaffolding SCW thickening has been demonstrated in several studies. Dynamic cortical MTs reorganize before SCW deposition and serve as a scaffold for later events (Oda *et al.*, 2005). In metaxylem, the MT rearrangement is governed by local activity of the ROP11 small RHO-related GTPase, which recruits an MT-associated protein, MIDD1, to promote MT disassembly via Kinesin13-A. MIDD1/RIP3 (Mucha *et al.*, 2010) is a close homolog of the previously described ROP interacting protein ICR1/RIP1, which mediates the interaction of active ROPs with the SEC3a exocyst complex subunit (Lavy *et al.*, 2007). The balance between cortical MT domains and active ROP11 domains is maintained by their mutual inhibition (Oda & Fukuda, 2013). MAP70-5, another MT-associated protein, together with its binding partner MAP70-1, has also been shown to be essential for normal SCW patterning in xylem (Pesquet *et al.*, 2010).

During xylem SCW maturation, both localized cellulose deposition (Gardiner *et al.*, 2003; Wightman & Turner, 2008; Watanabe *et al.*, 2015) and lignin polymerization (Zhao *et al.*, 2013; Schuetz *et al.*, 2014) contribute to vessel SCW patterning. Cellulose is synthesized by cellulose synthase complexes (CSCs), which are first actively delivered along F-actin cables to sites marked by cortical MTs, and then move along MTs during cellulose synthesis in a similar manner to that extensively described for primary cell wall deposition (Paredez *et al.*, 2006; Wightman

et al., 2009; Watanabe *et al.*, 2015). Laccases, which drive lignin oxidative polymerization, are also selectively localized to sites of prospective thickening, thus suggesting targeted delivery (Schuetz *et al.*, 2014).

The exocyst is a conserved protein complex involved in the tethering of secretory vesicles to the plasma membrane (PM) (reviewed in He & Guo, 2009). It consists of eight subunits (Sec3, Sec5, Sec6, Sec8, Sec10, Sec15, Exo70 and Exo84) and represents one of the key regulators of localized secretion and cell polarity in eukaryotes (Hertzog & Chavrier, 2011; Heider & Munson, 2012). Sec3 and Exo70 subunits have been proposed to serve as landmarks in yeast and animals for the delivery of secretory vesicles because of their direct interactions not only with activated RHO GTPases, but also with membrane lipids (Boyd *et al.*, 2004; Wu *et al.*, 2008; Heider & Munson, 2012; Pleskot *et al.*, 2015; Bloch *et al.*, 2016). In plants, the exocyst has been shown to play a role in many cell polarity-related processes, including pollen tube growth, hypocotyl elongation (Cole *et al.*, 2005; Hála *et al.*, 2008), cell plate formation/maturation (Fendrych *et al.*, 2010; Rybak *et al.*, 2014), cell wall biogenesis and seed coat deposition (Kulich *et al.*, 2010, 2015), and recycling of PIN auxin transporters (Drdová *et al.*, 2013).

A specific feature of the exocyst in land plants is a prominent evolutionary multiplication of genes encoding the EXO70 subunit, with 13 paralogs in *Physcomitrella patens*, 15 in *Vitis vinifera*, 23 in *Arabidopsis thaliana* and 47 in *Oryza sativa* (Synek *et al.*, 2006; Cvrčková *et al.*, 2012). Such an extensive proliferation of EXO70s in plants provides a potential for the targeting of secretory vesicles into specific domains at the PM/endomembranes within one cell, whereas the differential expression of individual EXO70 paralogs could confer a functional specificity to certain tissues or cell types (Žárský *et al.*, 2009, 2013).

An interplay between the exocyst and cytoskeleton has been well described in several Opisthokonts, but only briefly addressed in plants (Fendrych *et al.*, 2013; reviewed in Synek *et al.*, 2014). Several recent studies have revealed links between the exocyst and MT-dependent xylem development. Oda *et al.* (2015) discovered that the EXO70A1 exocyst subunit is recruited to cortical MTs in cultured Arabidopsis xylem cells by novel coiled-coil proteins, named vesicle tethering 1 (VETH1) and VETH2, via an interaction with the conserved oligomeric Golgi complex 2 protein (COG2). Li *et al.* (2013) described impaired xylem cell wall morphogenesis, an accumulation of large vesicles in developing xylem elements, and a reduced xylem hydraulic conductance in *exo70A1* mutants. Derbyshire *et al.* (2015) identified several exocyst subunits in MT pull-downs on extracts from TEs in Arabidopsis suspension cultures. In the most recent study, Tu *et al.* (2015) showed the importance of functional OsEXO70A1 for TE development in rice.

Here, we describe a clear difference in exocyst MT-independent dynamics in epidermal cells vs cell type-specific MT-driven exocyst recruitment in developing xylem vessels. Importantly, we observed that an annular pattern of exocyst localization in developing xylem vessels follows previous formation of the MT annular scaffold, but precedes SCW deposition during xylem differentiation. Using the dwarf *exo84b-1* mutant, we demonstrate the importance of the functional exocyst complex for TE development by describing collapsed protoxylem vessels and a rescue of the defect by xylem-restricted expression of EXO84b. We further show that the secondary cellulose synthase (CESA) is partially mislocalized in the *exo84b* mutant. We also display interactions of several exocyst subunits with COG2, which possibly enable the exocyst complex binding to MTs. We conclude that the exocyst complex is an important factor bridging the pattern defined by cortical MT assembly, with localized secretion underlying structured deposition of the SCW in developing TEs.

Materials and Methods

Plant material and growth conditions

Arabidopsis thaliana plants of Col-0 were used. Lines expressing fluorescently labeled exocyst subunits were prepared previously (Fendrych *et al.*, 2010, 2013). VND7-VP16-GR, LAC17-mCherry and YFP-CESA7 plants were generated by Yamaguchi *et al.* (2010), Schuetz *et al.* (2014) and Watanabe *et al.* (2015), respectively. Seeds were surface sterilized, vernalized for 3 d at 4°C and plants were grown in a growth chamber at 21°C under long day conditions (16 h : 8 h, light : dark) on vertical agar plates with half-strength Murashige and Skoog salts (½MS; Duchefa Biochemie, Haarlem, the Netherlands) supplemented with 1% sucrose, vitamin mixture and 1.6% plant agar (Duchefa Biochemie). The F_1 generation of crosses between plants expressing fluorescently tagged proteins was used for the evaluation of possible co-localization and localization in VND7-induced TE. In the case of localization of LAC17-mCherry and YFP-CESA7 in *exo70A1-2* and *exo84b-1* backgrounds, heterozygous plants from the F_1 generation of crosses were selected, and the F_2 generation was analyzed. For co-localization of GFP-SEC8 and mCherry-TUA5 in VND7-induced TE, the F_1 generation of crosses between GFP-SEC8 and VND7-VP16-GR plants was crossed with plants expressing mCherry-TUA5, and next-generation plants were analyzed.

TE induction systems

In plants expressing VND7-VP16-GR, TE differentiation was induced as described by Watanabe *et al.* (2015). The stage of development was defined based on MT bundling, as described by Watanabe *et al.* (2015). Cell cultures of *A. thaliana* (Col-0) suspension cells for VND6-induced xylem differentiation have been described previously (Oda *et al.*, 2010).

Plasmid construction and generation of transgenic lines

Generation of *pSEC10a:GUS* was performed by PCR amplification of a promoter region 1.5 kbp upstream from the start codon of *SEC10a* (Vukašinović *et al.*, 2014) and cloned using *Sal*I and *Not*I enzymes to the pENTR3C vector for the Gateway system (Invitrogen). The generation of *pSEC6:GUS* was performed by PCR amplification of the promoter region 1 kbp upstream from

the start codon using specific primers, and reamplified using attB1 and attB2 primers. The PCR product was subsequently cloned by BP clonase II enzyme mix into pDONR201 (Invitrogen). Promoter regions were transferred using LR clonase II enzyme mix (Invitrogen) into pKGWFS7.0 binary vector (Karimi *et al.*, 2002).

To generate *pSEC10a:SEC10a-GFP* and *pSEC10b:SEC10b-mRFP*, *SEC10a* and *SEC10b* coding regions without a stop codon were PCR amplified, fused to the *SEC10a* and *SEC10b* promoters, respectively, by overlapping PCR and cloned using *Sal*I and *Not*I enzymes to the pENTR3C vector. The constructs were transferred by LR reaction to pB7FWG.0 in the case of *SEC10a* and to pK7RWG2.0 (modified by removing the 35S promoter) in the case of *SEC10b* (Karimi *et al.*, 2002).

To generate a *pIRX3:EXO84b-GFP* construct, *EXO84b-GFP* was PCR amplified from genomic DNA from the EXO84b-GFP line (Fendrych *et al.*, 2010), fused to the *IRX3* gene promoter by overlapping PCR and introduced to the pBAR1 vector (Holt *et al.*, 2002) using *Xma*I and *Sac*I enzymes.

For transient expression in *Nicotiana benthamiana* leaves, *SEC10a* and *COG2* coding sequences were PCR amplified and introduced to the pENTR3C vector using *Sal*I and *Not*I enzymes, and further transferred using LR clonase II enzyme mix (Invitrogen) into pGWB5 (provided by Tsuyoshi Nakagawa, Shimane University, Japan) and pUBC-RFP-DEST (Grefen *et al.*, 2010), respectively, to obtain green fluorescent protein (GFP) and monomeric red fluorescent protein (mRFP) fusions.

All PCRs were performed using the Phusion polymerase (New England BioLabs, Ipswich, MA, USA). Primers used for cloning are listed in Supporting Information Table S1. Col-0 plants were transformed by floral dipping (Clough & Bent, 1998).

β-Glucuronidase (GUS) histochemical assay

For GUS staining, 5-d-old seedlings were vacuum infiltrated with staining solution (50 mM sodium phosphate buffer, pH 7.2, 250 μM $K_3Fe(CN)_6$, 250 μM $K_4Fe(CN)_6$, 2% Triton-X and 1 mM 5-bromo-4-chloro-3-indolyl-β-D-glucuronic acid (X-GlcA); Duchefa Biochemie) for 1 h, and then incubated at 37°C for 5 h in darkness. After washing the staining solution out with phosphate buffer, seedlings were cleared in subsequent baths of 20%, 40% and 60% ethanol for 15 min each and overnight in 96% ethanol. Rehydration was performed in the same baths in reverse order and the samples were mounted in 50% glycerol for microscopic analysis using an Olympus BX-51 equipped with a DP50 color camera.

Microscopy

Microscopic analysis of Arabidopsis seedlings was performed using an inverted spinning disk confocal microscope (CSU-X1, Yokogawa, Tokyo, Japan on Nikon Ti-E platform, laser box MLC400 Agilent, Santa Clara, CA, USA, Zyla sCMOS camera by Andor, Belfast, UK). Nikon Plan Apochromat ×60 WI (NA = 1.2) and Plan Apochromat λ ×100 Oil (NA = 1.45) objective lenses were used for imaging. Fluorescence profiles and acquired images were exported from NIS Elements 4.1 software (Nikon, Tokyo, Japan) – identical settings were used for each series of comparable images. Figures were then assembled in Adobe Photoshop CS6. A cell culture of *A. thaliana* (Col-0) suspension cells was observed using an inverted spinning disk confocal microscope (Yokogawa CSU-W1 on an Olympus IX83-ZDC platform, iXon3 888 EM-CCD camera by Andor). An Olympus UPlanSApo ×60 WI (NA = 1.2) objective lens was used for imaging. Acquired images were digitally analyzed using MetaMorph (Molecular Devices, Sunnyvale, CA, USA) and ImageJ (http://rsbweb.nih.gov/ij/).

Cell wall staining and drug treatments

For cell wall staining, seedlings were incubated with propidium iodide (PI) (SIGMA P4170) (10 μg ml^{-1}) in liquid ½MS for 10 min and rinsed twice in water before microscopic analysis. For MT and actin depolymerization, seedlings or cell culture were incubated in a 10 μM solution of oryzalin (Fluka 36182; in dimethylsulfoxide (DMSO)) or LatB (Sigma L5288; in ethanol) in liquid ½MS. In control experiments, seedlings were incubated in a 0.1% solution of DMSO in liquid ½MS. For lignin staining, whole seedlings were stained in 0.0001% basic fuchsin in liquid ½MS for 5 min and rinsed twice in water before imaging. For the examination of lignified cell walls in stems, hand-cut sections were stained for 15 min with 1% phloroglucinol in 6 M HCl.

Transmission electron microscopy (TEM)

For TEM, 7-d-old wild-type, *exo84b-1*- and *exo84b-1*-expressing *pIRX3*:EXO84b-GFP seedlings were fixed for 24 h in 2.5% (v/v) glutaraldehyde in 0.1 M cacodylate buffer (pH 7.2) at 4°C, and postfixed in 2% (w/v) OsO_4 in the same buffer. Fixed samples were dehydrated through an ascending ethanol and acetone series and embedded in Epon-Araldite. Hypocotyl cross-sections were observed.

Yeast two-hybrid system

SEC10a and *COG2* coding regions were PCR amplified and cloned into pGADT7 by *Bam*HI and *Xho*I enzymes. *COG2* was also cloned into pGBKT7 by *Bam*HI and *Sal*I enzymes. The primers used for cloning are listed in Table S1. The yeast two-hybrid assay was performed as described previously (Hála *et al.*, 2008). All constructs with exocyst genes (SEC3a, SEC5a, SEC6, SEC8, SEC10b, SEC15b and EXO70A1) have been prepared by Hála *et al.* (2008) and Fendrych *et al.* (2010). Double-transformed yeasts were plated onto −Leu/−Trp selective medium and grown for 3–5 d at 30°C. A subset of the obtained colonies was subsequently transferred to −Leu/−Trp/−His/−Ade plates and grown under the same conditions. The strength of the interactions was compared with a positive control – single colonies were resuspended in 100 μl of sterile water and 10 μl of each dilution (1×, 30×, 900×) were dropped onto −Leu/−Trp/−His/−Ade plates.

Fluorescence energy transfer (FRET) – acceptor photobleaching analysis

Transfected leaf epidermal cells were analyzed for FRET between SEC10a-GFP (donor molecule) and COG2-mRFP (acceptor molecule) using a Zeiss LSM 880 confocal scanning microscope equipped with a Zeiss C-Apochromat ×40/1.2 water-corrected lens, at a 512 × 512 resolution format. GFP was excited with the 488-nm line of the argon multiline laser and mRFP was excited with the 561-nm DPSS laser. Fluorescence was detected between 499 and 540 nm or between 579 and 633 nm for GFP or mRFP, respectively. Acceptor photobleaching was performed at 561 nm with 100% laser intensity and photodestruction of the acceptor was 50% on average. FRET efficiency was calculated directly by ZEN II software using the following formula: FRET Eff. % = Delta D/D Post × 100.

Results

Exocyst subunit expression and localization in the vasculature

In order to characterize the expression pattern of exocyst subunits described previously (Hála *et al.*, 2008; Fendrych *et al.*, 2010; Vukašinović *et al.*, 2014), we fused promoter sequences of *SEC6* and *SEC10a* genes with the *GUS* reporter gene. Arabidopsis transformants from the T_2 generation were then analyzed for *GUS* expression. Expression profiles of *pSEC6:GUS* and *pSEC10a:GUS*, respectively, were consistent across multiple transgenic lines (Fig. S1a,h). In both *pSEC6:GUS* and *pSEC10a:GUS*, *GUS* expression was prominent in the root tip (Fig. S1d,k), developing lateral roots (Fig. S1g,n) and, markedly, in the root vasculature (Fig. S1e,f,l,m) and cotyledons (Fig. S1b,c,i,j). The GUS signal appeared in the root vasculature already after 1 h of staining, indicating a strong expression, which is in agreement with publicly available microarray data (Genevestigator; Zimmermann *et al.*, 2004). Interestingly, it has been shown that *EXO70A1* is also expressed during TE development (Li *et al.*, 2010, 2013), suggesting that the exocyst complex as a whole might be involved in the process of TE development.

Data on the localization of exocyst subunits in xylem have been limited to the EXO70A1 subunit and, to date, only in cultured xylem cells (Oda *et al.*, 2015), where EXO70A1 was associated with cortical MTs at the sites of SCW deposition. To test whether the entire exocyst complex is localized in the same pattern in developing protoxylem vessels in Arabidopsis roots, we used lines expressing EXO84b-GFP, SEC6-GFP, GFP-SEC8 and SEC10a-GFP, driven by their native promoters, and GFP-EXO70A1, under the 35S promoter. Both the spiral and annular cell wall thickenings in root protoxylem vessels are known to emit autofluorescence, and so we first optimized the acquisition settings of the spinning disk confocal microscope. The autofluorescence signal was first detected in an average position of 8.5 ± 0.7 cells (± represents SD) after onset of elongation (measured as described in Alassimone *et al.*, 2010) in both green and red channels using standard GFP and RFP filters, respectively (Fig. S2a). Despite the fact that the autofluorescence did not reach the level of GFP or RFP fluorescence in our setup (compare Fig. S2a with panels b and c, where images were taken and processed with the same settings), we decided to perform all imaging below the zone of autofluorescence, i.e. 5–7 cells after the onset of elongation (Fig. 1a).

All GFP-tagged exocyst subunits tested localized in the same manner to helical or annular PM domains beneath the SCW thickenings of protoxylem (Fig. 1b–f). In addition, in a line co-expressing GFP-SEC8 and EXO84b-mRFP, we documented full co-localization of these two exocyst subunits (Fig. 1g). Because any fluorescent imaging deep in the root tissue is compromised concerning image quality, we introduced an artificial xylem induction system. We crossed Arabidopsis lines expressing EXO84b-GFP, GFP-SEC8 or SEC10a-GFP with plants constitutively expressing VND7, a transcription factor controlling xylem vessel differentiation, fused to the activation domain of herpes virus VP16 protein and the glucocorticoid receptor (GR) (Yamaguchi *et al.*, 2010). On treatment with dexamethasone (DEX), most of the plant cells expressing VND7-VP16-GR trans-differentiate into xylem vessel-like cells. We focused on hypocotyl cells of etiolated seedlings, and performed microscopic analysis after DEX treatment. In this system, all inspected exocyst subunits localized to the sites of SCW thickenings stained with PI (Figs 1h; S2d,e). At the cell surface, the exocyst localization appeared to split to each side of an SCW thickening (Fig. 1h), but formed a U-shaped furrow curving around the SCW thickenings when observed in the mid-plane (Fig. 1h).

We also measured the cellular distance after onset of elongation for exocyst signal appearance. In plants expressing SEC10a-GFP, the signal started to organize in the annular pattern at 4.7 ± 0.6 cells after onset of elongation, on average, before any SCW thickenings were visible in the bright field (Figs 1a, S2b). To demonstrate that the exocyst arrives at the PM before SCW deposition, we stained plants expressing SEC10a-GFP with PI, which is commonly used for cell wall staining in Arabidopsis roots. The PI annular signal appeared 5.3 ± 0.8 cells after the onset of elongation, on average, considerably later than the SEC10a signal (Figs 1a, S2c). In addition, in early stages of TE trans-differentiation in VND7-VP16-GR plants, the exocyst signal was observed in an annular pattern at the PM before any SCW could be stained with PI (Fig. 2).

Together with data on protein–protein interactions between exocyst subunits (Hála *et al.*, 2008; Fendrych *et al.*, 2010), our observations indicate that the whole exocyst complex is present at the future sites of SCW deposition, and further support the concept of its involvement in SCW deposition during TE development.

The exocyst undergoes an MT-dependent switch in localization and dynamics during the induced differentiation of xylem cells

In young TEs, cortical MTs are localized at the PM, bordering the edges of developing bands of the SCW (Hepler & Newcomb, 1964; Oda *et al.*, 2005). Oda *et al.* (2015) reported that VETH1 and VETH2 proteins regulate the association of

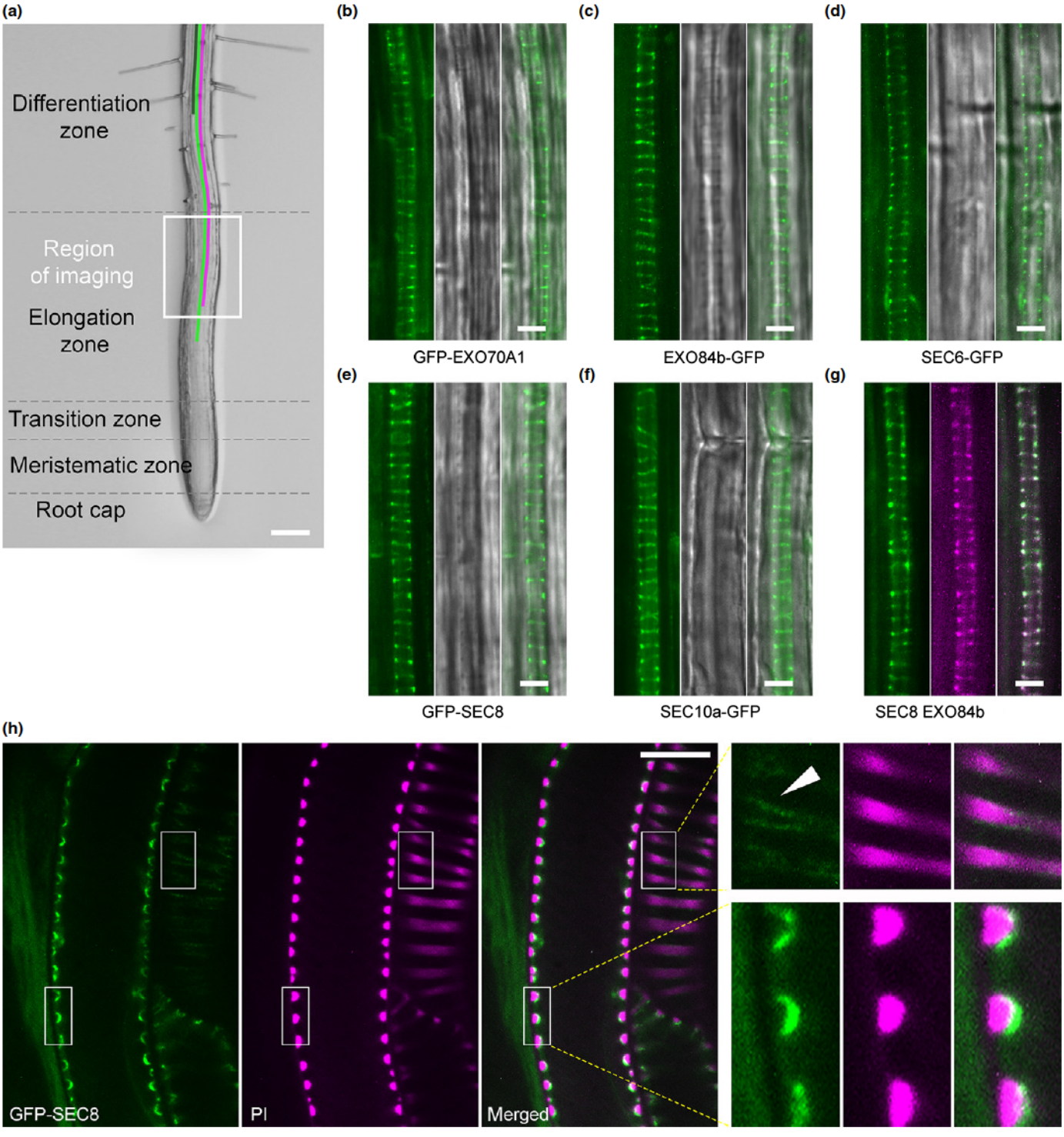

Fig. 1 The exocyst is localized at sites of secondary cell wall (SCW) deposition in developing tracheary elements (TEs). (a) Scheme of a root showing different root zones with the indicated region of imaging – between the fifth and seventh cell after the onset of elongation. Green, magenta and blue lines indicate start of exocyst, propidium iodide and autofluorescence signal, respectively. Bar, 100 μm. (b–f) Green fluorescent protein (GFP)-tagged exocyst subunits (EXO70A1, EXO84b, SEC6, SEC8 and SEC10a) localize to helical/annular plasma membrane (PM) domains in protoxylem in *Arabidopsis thaliana* roots. Each panel shows GFP, bright field and overlay. Bars, 5 μm. (g) GFP-SEC8 and EXO84b-mRFP completely co-localize in protoxylem in a helical/annular pattern. Bar, 5 μm. (h) GFP-SEC8 is localized at the sites of SCW deposition during VND7-induced protoxylem TE differentiation in etiolated hypocotyls. Higher magnification of developing SCWs is shown on the right. Arrowhead indicates a split of the exocyst signal. SCWs were stained with propidium iodide (PI). Bar, 10 μm.

EXO70A1-positive vesicle-like compartments with cortical MTs via COG2 protein in xylem culture cells. We therefore analyzed the dynamics of the GFP-SEC8 exocyst subunit expressed together with the mCherry-Tubulin alpha-5 (TUA5) MT marker (Gutierrez *et al.*, 2009) during VND7-induced protoxylem TE differentiation.

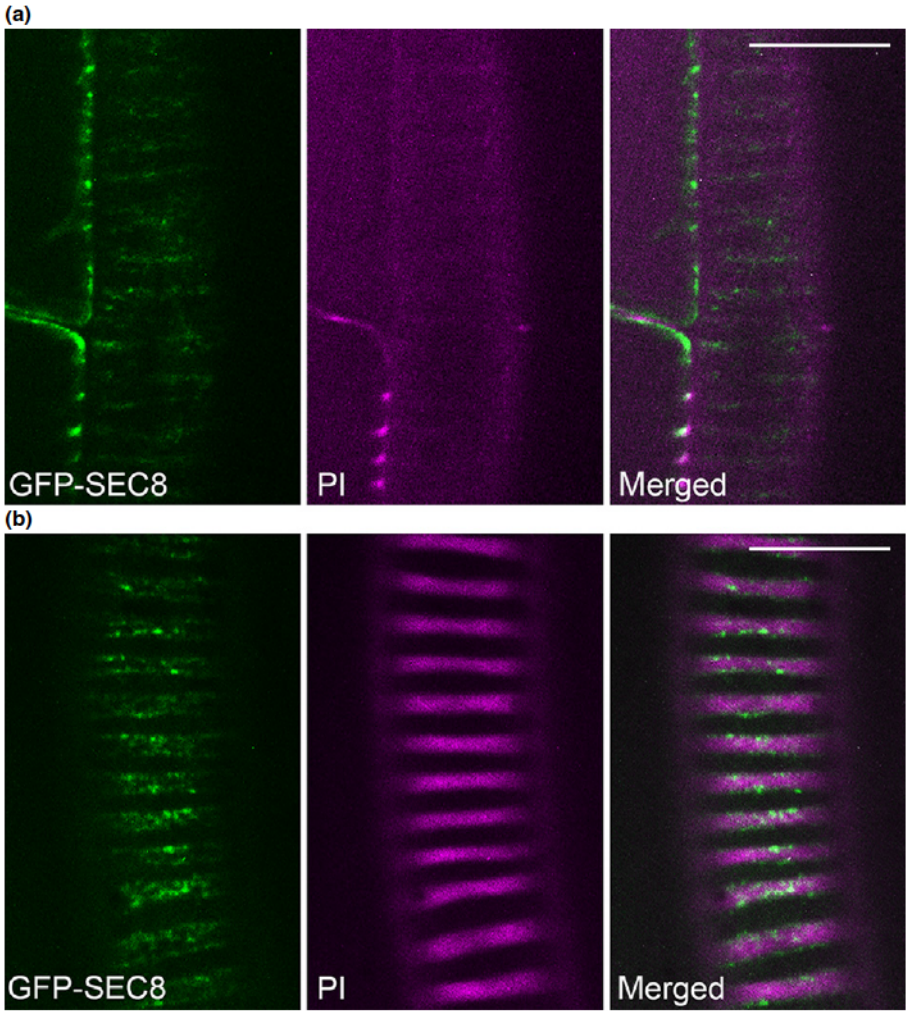

Fig. 2 The exocyst signal is present at the plasma membrane (PM) in an annular pattern before the secondary cell wall (SCW) is deposited. (a) In the early stages of xylem induction by VND7 expression in *Arabidopsis thaliana*, the GFP-SEC8 signal is present at the future SCW thickenings, before any SCW can be detected with PI staining. (b) In later stages of xylem development, the exocyst is localized at the SCW thickenings stained with propidium iodide (PI). Bars, 10 μm.

Over the course of TE differentiation, the exocyst and cortical MT distribution changed. Whereas, in uninduced hypocotyl epidermal cells, GFP-SEC8 foci were randomly distributed across the PM and did not co-localize with cortical MTs (Fig. 3a), during early xylem development, MTs began to bundle and GFP-SEC8 foci started to be associated with the emerging MT bundles. Later, in the mid-development stage, MTs were fully bundled and GFP-SEC8 foci were completely co-aligned (Fig. 3a). Finally, in late development, pushed by the nascent SCW, MT bands appeared to split and GFP-SEC8 localization followed this pattern (Fig. 3a).

We verified these findings using the *in vitro* VND6-induced metaxylem differentiation system, which enables the induction of synchronous and high-frequency TE differentiation in Arabidopsis suspension cells (Oda *et al.*, 2010). In the first stage, before or immediately after the induction of xylem differentiation, the EXO70A1-tagRFP exocyst subunit appeared as PM-associated foci (Fig. S3) and did not co-localize with MTs. In later stages, as cortical MTs gradually started to organize into regular bundles, EXO70A1-tagRFP assembled at the cell cortex, following the pattern of cortical MTs (Fig. S3).

Previously, it has been shown that exocyst localization at the PM in root epidermal cells is not dependent on MTs (Fendrych *et al.*, 2013). To determine the MT-dependent exocyst localization in VND7-induced protoxylem TEs, we treated plants expressing GFP-SEC8 and mCherry-TUA5 with oryzalin, an MT depolymerizing drug. Unlike in epidermal cells, clear changes in the exocyst localization in TEs were observed after a 45-min treatment: following MT depolymerization, GFP-SEC8-positive foci became aggregated, but were still present at the SCW sites (Fig. 3b). In control seedlings treated with DMSO, no changes in exocyst localization were observed (Fig. 3b). Similarly, in xylem culture cells, oryzalin treatment dispersed cortical MTs and caused the formation of EXO70A1-tagRFP aggregates at PM after 20 min (Fig. S4a). However, we found that EXO70A1-tagRFP neither co-localized with F-actin microfilaments nor was affected by LatB treatment in xylem culture cells (Fig. S4b), excluding actin-dependent localization/recruitment.

After documentation of the MT-dependent localization of exocyst subunits in TEs, we followed the dynamics of individual GFP-SEC8 foci associated with MTs in protoxylem cells using spinning disk confocal microscopy. We found that these foci are static and do not move along the MTs (Fig. 4a; Movie S1). In sharp contrast with the exocyst foci in root epidermal cells, which exhibited a median lifetime of ~10 s (Fendrych *et al.*, 2013), most of the exocyst-positive foci in TEs did not vanish over the

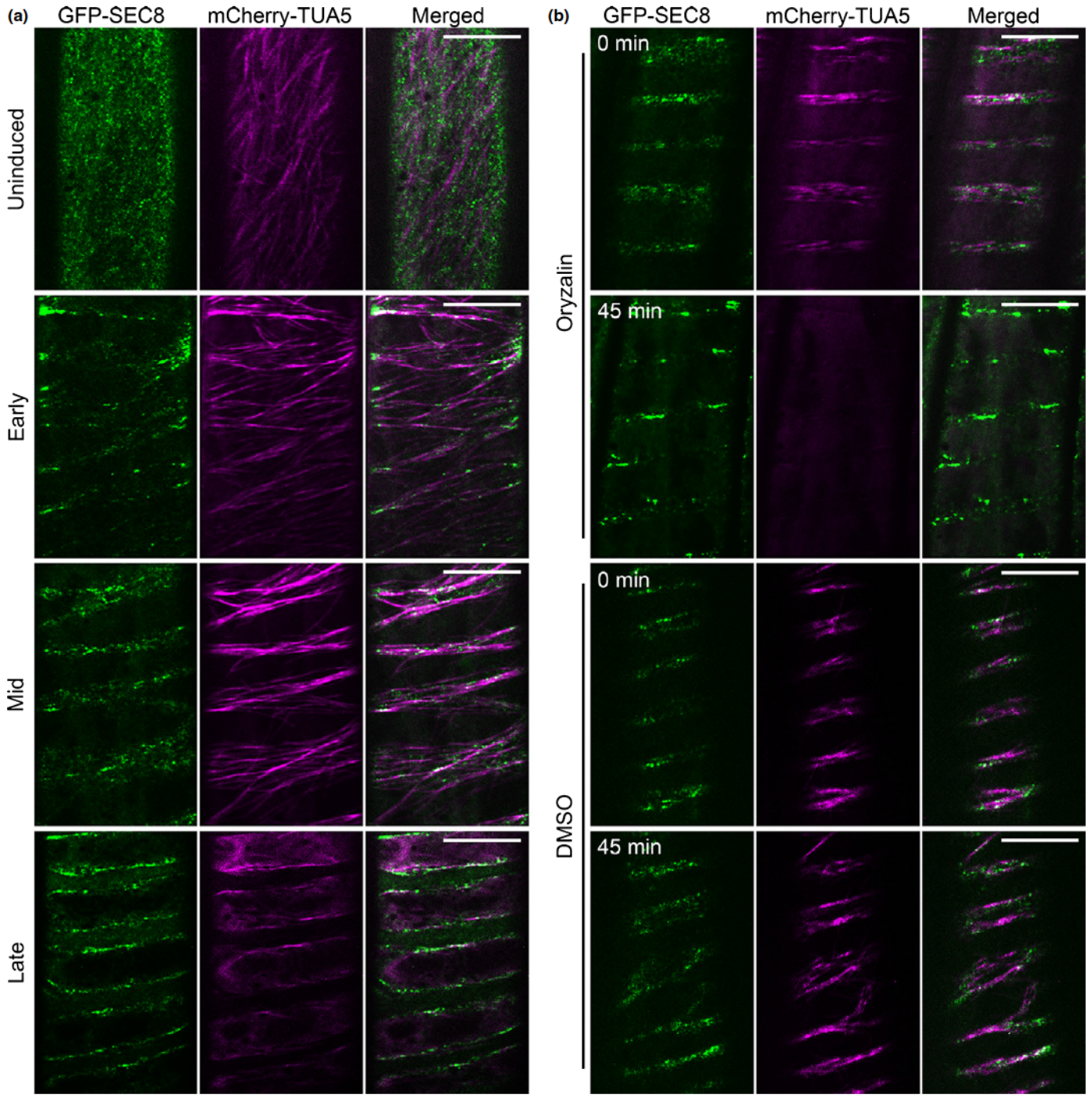

Fig. 3 Localization of the exocyst is microtubule (MT)-dependent during VND7-induced tracheary element (TE) differentiation in *Arabidopsis thaliana*. (a) Different stages of TE development are shown. In uninduced cells, GFP-SEC8 foci across the plasma membrane (PM) are randomly organized and do not co-localize with mCherry-TUA5-labeled MTs. In early stages of TE development, MTs start to bundle and co-localize with the exocyst. MTs are fully bundled in mid-development and co-localization with the exocyst signal is more pronounced. Finally, in late development, MT bundles appear to split and the exocyst signal exhibits the same pattern. Bars, 10 μm. (b) Localization of GFP-SEC8 in protoxylem TE before and after treatment with 10 μM oryzalin. After 45 min of treatment, MTs are dispersed and the exocyst signal becomes more focused. In control experiments, seedlings were treated with dimethylsulfoxide (DMSO). No change in exocyst localization was observed after 45 min. Bars, 10 μm.

course of time-lapse imaging (~ 120 s). This was also supported by kymograph analysis showing the exocyst dynamics in uninduced and VND7-induced hypocotyl cells expressing GFP-SEC8. The exocyst foci were more stable in differentiating TEs than in epidermal cells, which was visualized by longer lines in the kymographs (Fig. 4b).

These observations clearly show that the exocyst complex localization is coupled with cortical MTs in xylem, rather than with

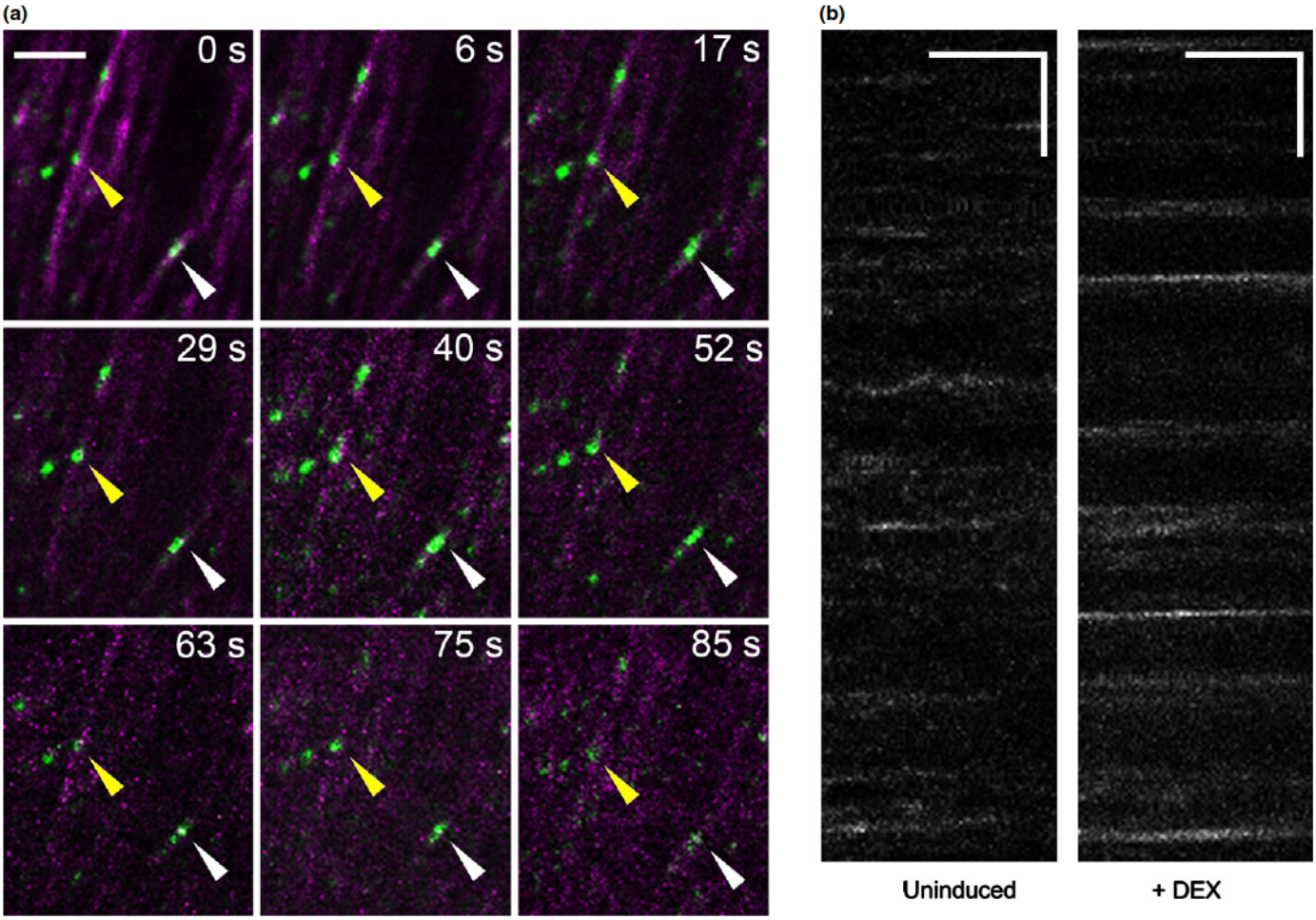

Fig. 4 The exocyst foci at the plasma membrane (PM) of tracheary elements (TEs) are static and stable. (a) Time-lapse images of mCherry-TUA5 and GFP-SEC8 in developing tracheary elements (TEs) in *Arabidopsis thaliana*. GFP-SEC8 foci are static and do not move along microtubules (MTs). Yellow and white arrowheads indicate two independent foci. Bar, 2 μm. (b) A kymographic representation of GFP-SEC8 foci at the PM of epidermal cells of etiolated hypocotyls. An uninduced cell and VND7-induced protoxylem cell are shown. Horizontal and vertical bars represent 60 s and 5 μm, respectively. DEX, dexamethasone.

the actin cytoskeleton, and that its localization is dynamically arranged depending on cortical MTs during TE differentiation. In addition, we show that, in TEs, the exocyst dynamics manifested by a longer dwell time at the PM and a complete lack of lateral membrane movement are distinct from those of other cell types.

Developing protoxylem TEs partially collapse in the *exo84b-1* mutant as a result of aberrant SCW deposition

Arabidopsis T-DNA insertional mutants in the *EXO84b* gene are sterile dwarfs with pleiotropic defects (Fendrych *et al.*, 2010). We inspected developing protoxylem vessels in this mutant after clearing of whole roots (Malamy & Benfey, 1997), and found that, in all mutant plants examined ($n > 20$), the autofluorescence signal of young protoxylem TE was interrupted close to the root tip and the interrupted TEs were also visible in the bright field (Fig. 5a). Such TE collapses were never observed in wild-type siblings ($n > 20$) (Fig. 5a). Further, we compared the thickness of SCW of TEs of wild-type and mutant plants at the ultrastructural level using TEM. In cross-sections of hypocotyls of 7-d-old wild-type plants, TEs were arranged in a single row of distinct cells with thick SCWs (Fig. 5b). However, in *exo84b-1* mutant seedlings, xylem cells had much thinner cell walls and were difficult to distinguish from the surrounding cells (Fig. 5b). As the observed TE phenotype in *exo84b-1* mutants is much more severe than in *exo70A1-1* (Li *et al.*, 2013), we compared the localization of several exocyst subunits in these two mutant backgrounds. Although SEC6-GFP, GFP-SEC8 and SEC10a-GFP were cytoplasmic in the protoxylem of the *exo84b-1* mutant (Fig. S5b), indicating an absence of the exocyst at the PM, SEC6-GFP, GFP-SEC8 and EXO84b-GFP partially remained at the PM beneath the sites of SCW secretion in the *exo70A1-2* mutant background (Fig. S5b). These findings correspond to the severity of phenotypic defects in TE development observed in *exo84b-1* relative to *exo70A1* mutants.

As at least two exocyst mutants show compromised auxin transport (Drdová *et al.*, 2013), which can lead to different secondary phenotypic defects, we wanted to test whether the collapse of protoxylem vessels is solely caused by a lack of functional

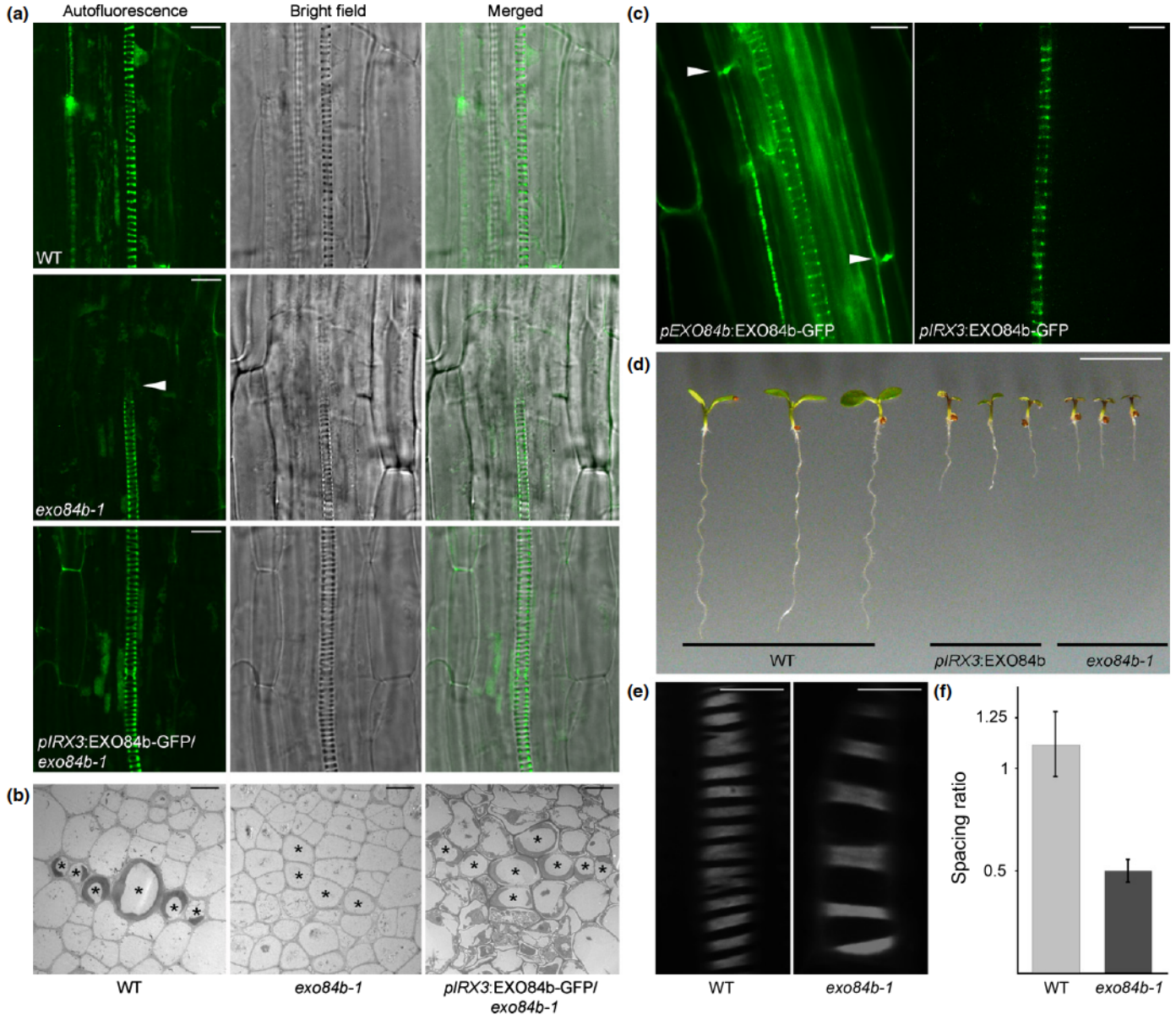

Fig. 5 EXO84b is needed for normal protoxylem development. (a) Autofluorescence of protoxylem vessels in cleared roots of *Arabidopsis thaliana*. The phenotypic defect of interrupted protoxylem vessels in the *exo84b-1* mutant (arrowhead) is completely restored in mutant plants expressing EXO84b-GFP under the *IRX3* promoter. Bars, 10 μm. (b) Transmission electron microscopy cross-sections of hypocotyls of wild-type (WT), *exo84b-1* and *exo84b-1* mutant plants carrying the *pIRX3*:EXO84b-GFP construct. Asterisks indicate xylem cells. Bars, 4 μm. (c) A comparison of the localization pattern of EXO84b-GFP expressed under its native or *IRX3* promoter, respectively. Arrowheads indicate the localization of EXO84b-GFP when expressed under its native promoter at forming Casparian strips in endodermal cells, whereas the EXO84b-GFP signal is restricted exclusively to secondary cell wall (SCW) deposition sites in protoxylem when expressed under the *IRX3* promoter. Bars, 10 μm. (d) The overall appearance of *exo84b-1* mutant plants and mutant plants carrying *pIRX3*:EXO84b-GFP is similar. No complementation of the mutant phenotype is observable at the whole-plant level. Bar, 10 mm. (e) A comparison of VND7-induced tracheary elements (TEs) in wild-type and *exo84b-1* etiolated hypocotyls. Bars, 10 μm. (f) The thickening to spacing width ratio is higher in wild-type than in *exo84b-1* TEs. Error bars indicate SEM.

exocyst complex in this cell type. To this end, we expressed EXO84b-GFP under the control of the *IRX3* xylem-specific promoter (Wightman & Turner, 2008) in wild-type and *exo84b-1* plants. When expressed under its native promoter, the EXO84b-GFP signal was detected in all cell types of the root central cylinder, including the endodermis (Fig. 5c). The signal was very prominent at forming Casparian strips in endodermal cells and annular thickenings in protoxylem vessels. On the contrary, when expressed under the *IRX3* promoter, the EXO84b-GFP signal was restricted solely to xylem cells (Fig. 5c), proving the specificity of the *IRX3* promoter. The overall phenotype of *exo84b-1* seedlings carrying the *pIRX3*:EXO84b-GFP construct was not obviously changed compared with the *exo84b-1* mutant seedlings (Fig. 5d). However, the protoxylem vessel collapses were fully complemented ($n > 20$) (Fig. 5a). TEM analysis confirmed these findings, as TEs were clearly visible in cross-sections of

hypocotyls of plants carrying the *pIRX3*:EXO84b-GFP construct. Although TEs were not aligned in a single row, the thickness of SCWs of the complemented line was comparable with that of the wild-type (Fig. 5b).

Finally, we compared VND7-induced protoxylem TEs of wild-type and *exo84b-1* mutant plants. In *exo84b-1*, the average width of the SCW thickenings was greater than that of the wild-type SCW thickenings, and also the spacing between them (Fig. 5e). As we analyzed TEs differentiated from the epidermal cells of etiolated hypocotyls, it should be taken into account that epidermal cells of *exo84b-1* were much shorter than those of the wild-type at the onset of differentiation. Therefore, we compared ratios of SCW and spacing widths between wild-type and mutant TEs. This ratio was much higher in wild-type plants, indicating altered SCW patterning in TEs of *exo84b-1* mutants (Fig. 5f).

Taken together, these data indicate that the functional exocyst complex subunit EXO84b is necessary for normal protoxylem development.

Lack of exocyst complex leads to imperfect localization of secondary CESAs in developing TEs

We investigated whether the collapse of protoxylem vessels could have been caused by irregular targeting of the secondary CESAs, which would lead to altered cellulose deposition in SCW. In agreement with previous reports, YFP-CESA7 was found in a spiral pattern at the sites of SCW deposition (Wightman & Turner, 2008) in wild-type xylem and co-localized perfectly with the SEC10b-mRFP exocyst subunit (Fig. S6a). By contrast, the strictly patterned localization of YFP-CESA7 was partially disturbed in the *exo70A1-2* and, especially, *exo84b-1* mutant background, where a considerable portion of YFP-CESA7 was found outside the sites of SCW thickening (Fig. 6a,b). Notably, the spiral pattern of YFP-CESA7 localization was completely lost in collapsed TEs of the *exo84b-1* mutant (Fig. 6a).

Next, we tested whether the collapse of protoxylem vessels caused by the disruption of the functional exocyst complex is a result of general mislocalization of the SCW components. To this end, we analyzed the localization of LACCASE17 (LAC17) – an oxidative enzyme directing lignification at the sites of SCW deposition in protoxylem (Schuetz *et al.*, 2014) in the *exo70A1-2* and *exo84b-1* mutants. Although EXO84b-GFP and LAC17-mCherry co-localize in developing protoxylem (Fig. S6b), the localization of LAC17-mCherry seems to be less affected in both the *exo70A1-2* and *exo84b-1* mutant background (Fig. 6c), with the exception of the collapsed regions of TEs of the *exo84b-1* mutant, where LAC17-mCherry is completely mislocalized (Fig. 6c). In addition, we observed the ectopic localization of LAC17-mCherry in the endodermis at forming Casparian strips (Fig. S6c). Basic fuchsin staining of *exo84b-1* and *exo70A1-2* mutant roots confirmed a similar level of lignification in the wild-type and mutant TEs (Fig. S6d). Further, we used phloroglucinol-HCl staining to assess the level of lignification in wild-type and *exo70A1-2* stem sections. Cell walls of interfascicular fibers and xylem cells in the *exo70A1-2* mutant were thinner, but exhibited normal red coloration on phloroglucinol-HCl staining (Fig. S6e).

Taken together, these data show that, although SCWs can still be formed in *exo70A1-2* and *exo84b-1* mutants, the factors involved in xylem SCW deposition are secreted in an aberrant manner in exocyst mutants.

Exocyst subunits interact directly with subunit 2 of the conserved oligomeric Golgi (COG) complex (COG2)

Oda *et al.* (2015) showed that COG2 protein recruits EXO70A1-positive compartments to cortical MTs in xylem via interaction with VETH1/2 adaptor proteins, and localizes to the sites of SCW deposition in xylem. Another recent study identified subunits of exocyst and COG complexes in proteome enrichments of affinity-purified RFP-RABF2b/ARA7 (Heard *et al.*, 2015). As no direct interaction of COG2 with any of the exocyst subunits has been observed, we wanted to test whether COG2 can bridge the exocyst with VETH1/2. We performed the GAL4-based pairwise yeast two-hybrid assay. When used as a bait, COG2 interacted with EXO70A1, SEC3a, SEC15b and SEC10a (Fig. 7a). As a prey, COG2 showed interactions only with SEC15b.

In the next step, we confirmed the interaction of SEC10a and COG2, which showed strongest interaction in the yeast two-hybrid system, in plant cells. We generated a fusion construct of SEC10a with GFP, driven by the 35S promoter, and COG2 with mRFP, driven by the ubiquitin promoter, and transiently expressed them in *N. benthamiana* leaves. When expressed alone in leaf epidermal cells, SEC10a-GFP showed typical exocyst localization, with PM-bound and cytoplasmic pools (Fig. 7b). However, when co-expressed with COG2-mRFP, SEC10a-GFP co-localized with COG2-mRFP in mobile intracellular organelles (Fig. 7b). We confirmed this interaction using FRET acceptor photobleaching analysis (Fig. 7c). The mean FRET efficiency for the SEC10a-GFP–COG2-mRFP pair was $5.57 \pm 0.56\%$, whereas a negative FRET efficiency of $-0.77 \pm 0.97\%$ was recorded in control experiments where SEC10a-GFP was co-expressed with free mRFP (Fig. 7d).

These findings identify COG2 as a direct exocyst interactor that probably physically links the exocyst to MTs via associated VETH1/2 proteins.

Discussion

An important role of the exocyst complex in polarized secretion in plants has been demonstrated in several studies (Fendrych *et al.*, 2010; Kulich *et al.*, 2010; Žárský *et al.*, 2013). Here, we show that two exocyst core subunits, SEC6 and SEC10a, are also strongly expressed in the central cylinder of roots and the vasculature of leaves. As a common feature of cell types forming the central cylinder, such as TEs, sieve tube elements and fibers, together with the endodermis which encircles them, is a prominent SCW deposition, the exocyst involvement is expected, because SCW synthesis requires intensive targeted secretion of cell wall material (Turner & Sieburth, 2003; Geldner, 2013; Heo *et al.*, 2014).

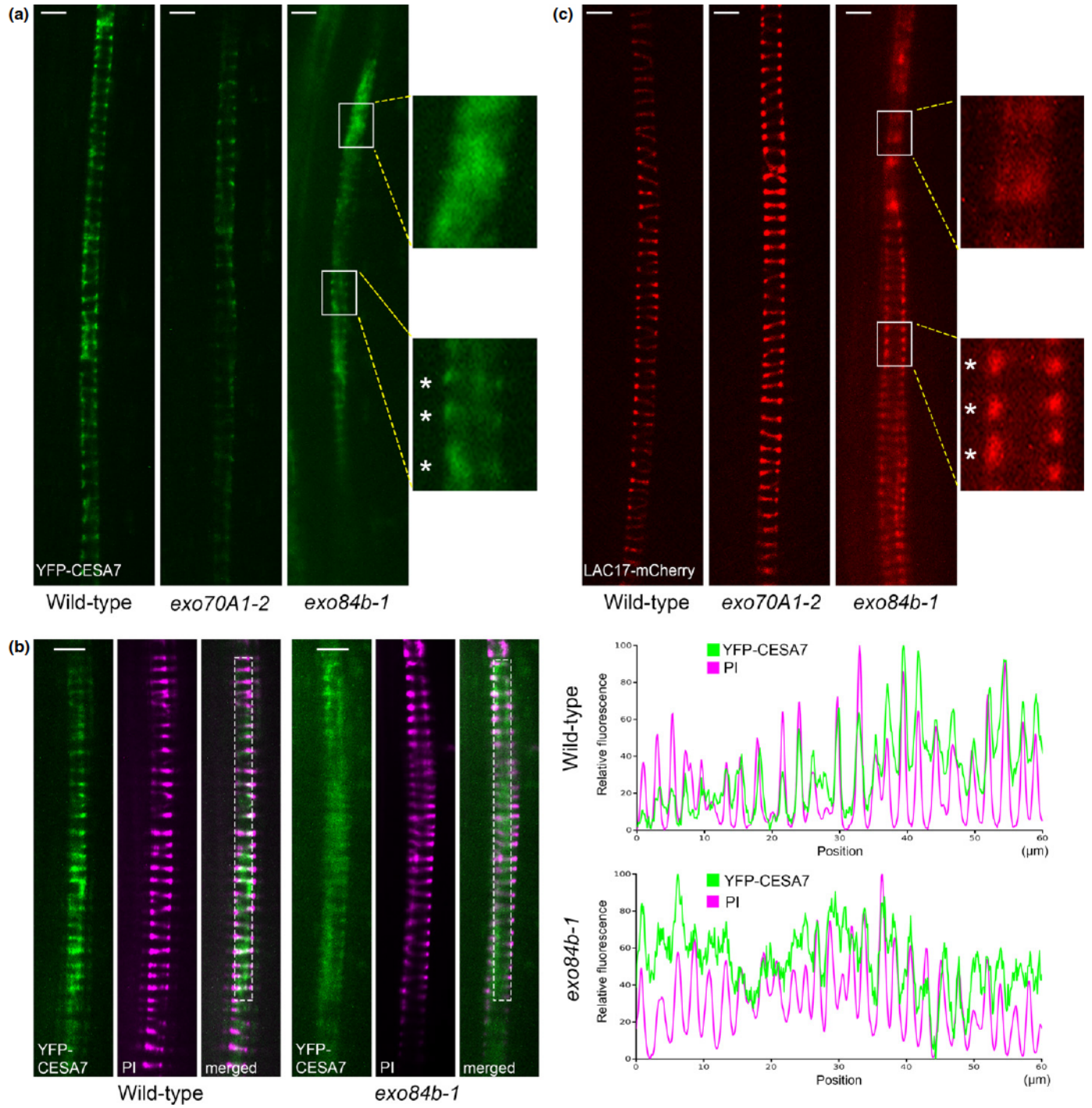

Fig. 6 Exocyst is involved in the correct targeting of secondary cell wall components. (a) Localization pattern of YFP-CESA7 is changed in *exo70A1-2* and *exo84b-1* mutant *Arabidopsis thaliana* plants. The insets show partly and completely mislocalized YFP-CESA7 in developed and collapsed tracheary elements (TEs) of the *exo84b-1* mutant, respectively. Asterisks indicate secondary cell wall (SCW) thickenings. (b) Relative intensity plots of YFP-CESA7 localization and SCW thickenings (visualized by propidium iodide (PI)) in developed TEs of wild-type (WT) and *exo84b-1* plants. The regions used for analyses are boxed. (c) Localization of LAC17-mCherry is mostly unchanged in *exo70A1-2* and *exo84b-1* mutant plants. The insets show details of correctly targeted and completely mislocalized LAC17-mCherry in developed and collapsed TEs of the *exo84b-1* mutant, respectively. Bars, 5 μm.

We show that exocyst subunits localize to the sites of SCW deposition in developing TEs, as soon as the secretory domains are established by MT rearrangement and well before SCW is deposited. Oda *et al.* (2015) have recently demonstrated the association of a single EXO70A1 exocyst subunit with cortical MT-marked domains in developing metaxylem cells. In another recent study, Derbyshire *et al.* (2015) detected SEC3a, SEC6, SEC10 and SEC15b exocyst subunits in the TE MT interactome. We confirmed and extended these findings by showing that exocyst subunits co-localize with MTs very early during VND6- and

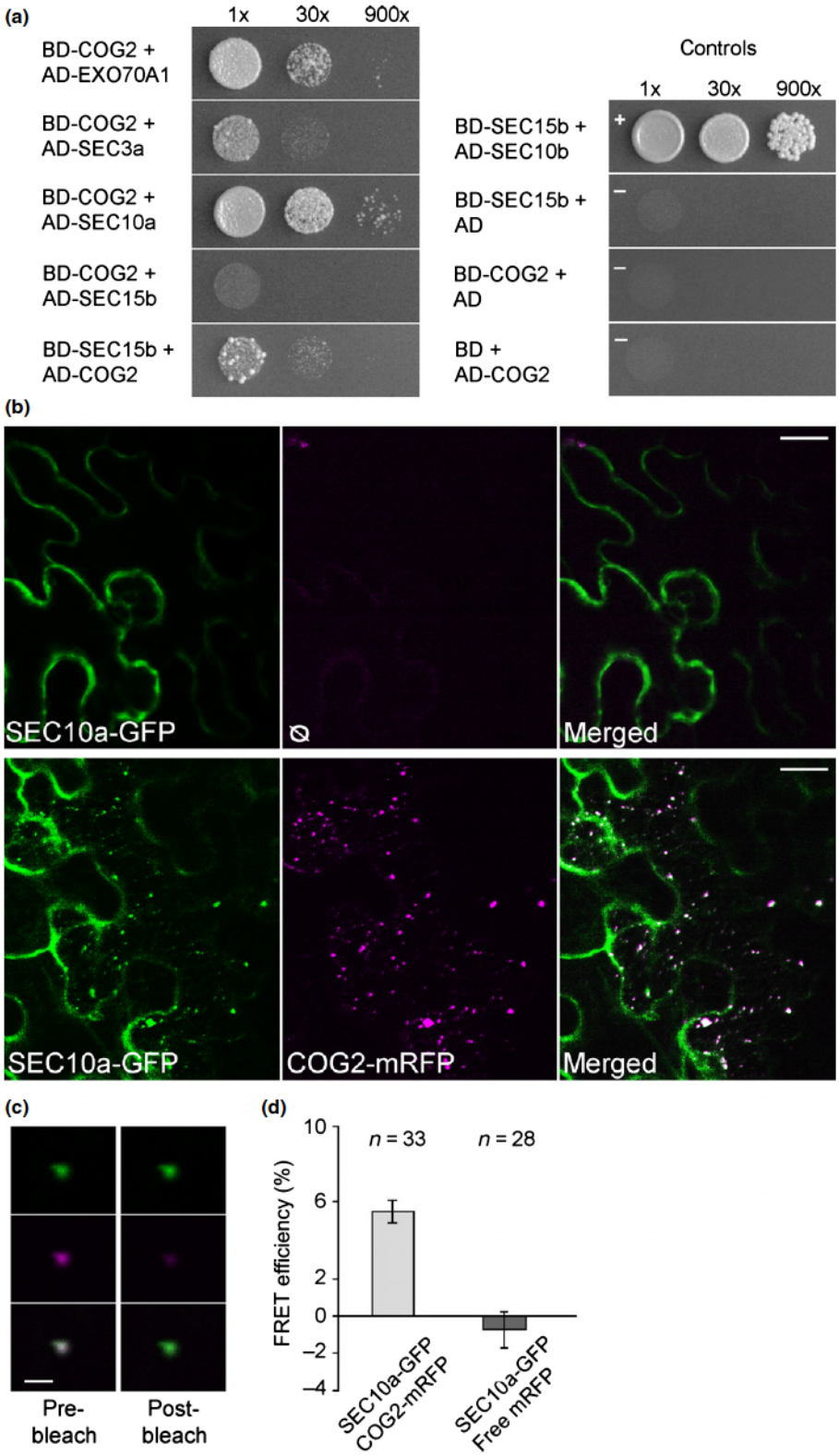

Fig. 7 Conserved oligomeric Golgi complex 2 protein (COG2) interacts with exocyst subunits. (a) On the left, positive pairwise interactions of COG2 with exocyst subunits EXO70A1, SEC3a, SEC10a and SEC15b in the yeast two-hybrid system. The strength of interactions is demonstrated by dilution series (indicated at the top). On the right, controls: BD-SEC15b + AD-SEC10b served as a positive control, whereas BD-SEC15b, BD-COG2 and AD-COG2 with the appropriate empty vector (AD or BD) served as negative controls. (b) Transient expression of SEC10a-GFP and COG2-mRFP in *Nicotiana benthamiana* leaves. When expressed alone, SEC10a-GFP is localized to the plasma membrane (PM) and cytoplasm (upper panel), whereas co-expression with COG2-mRFP causes relocalization of SEC10a-GFP to intracellular organelles (lower panel). Bars, 20 μm. (c) Fluorescence energy transfer (FRET) microscopy by acceptor photobleaching. Fluorescence intensities of SEC10a-GFP and COG2-mRFP before and after acceptor photobleaching. Bars, 5 μm. (d) Mean FRET efficiencies after acceptor photobleaching measured for cells co-expressing SEC10a-GFP and COG2-mRFP (region of interest (ROI), $n = 33$) and cells co-expressing SEC10a-GFP and free mRFP (ROI, $n = 28$). Data are means and bars indicate ± SEM.

VND7-induced TE differentiation. More specifically, we showed static GFP-SEC8-positive foci associated with cortical MTs, whose dwell time at the PM is at least nine times longer than that in root epidermal cells (Fendrych *et al.*, 2013). It is likely that individual exocyst foci observed during TE development do not represent single exocytotic events (as is possibly the case in Fendrych *et al.*, 2013), but are rather well-established secretory domains in which several subsequent exocytotic events occur in order to achieve rapid cell wall biogenesis-related material deposition during SCW development.

Unlike in root epidermal cells (Fendrych *et al.*, 2013), treatment with oryzalin confirmed that the correct exocyst localization to the future SCW site is at least partially dependent on intact cortical MTs in TEs, similar to CSCs in the same cell type (Gardiner *et al.*, 2003; Wightman & Turner, 2008; Watanabe *et al.*, 2015). It is intriguing that the exocyst aggregates formed at the PM domains beneath SCW thickenings are visible even after a relatively long oryzalin treatment, which indicates that the PM secretory domains are stable and only slowly disperse once they are established in an MT-dependent manner.

We have revealed that COG2, a putative subunit of the COG tethering complex, physically interacts with several exocyst tethering complex subunits and links the exocyst to VETH1/2 (Fig. 8). Exocyst-positive compartments only partially overlap with VETH1/2 compartments (Oda *et al.*, 2015), and this could explain why exocyst foci do not move along MTs. It is plausible to speculate that VETH/COG2-positive organelles move along the MTs until they reach the secretory domain at the PM; they then associate with the exocyst at the PM and targeted secretion takes place in such a site. Direct interaction of the exocyst with yet another tethering complex, TRAPII, has been described recently during cytokinesis in Arabidopsis (Rybak *et al.*, 2014), and so it is possible that different tethering complexes cooperate in certain multi-level cellular processes. The work of Oda *et al.* (2015) and our data presented here show that the COG complex subunits have gained additional functions in plants, compared with other organisms (Ungar *et al.*, 2006), which are unrelated to Golgi trafficking. COG2 is localized to the secretory sites of SCW deposition in xylem culture cells (Oda *et al.*, 2015), whereas its human homolog is localized to the Golgi apparatus in Chinese hamster ovary cells (Podos *et al.*, 1994). Whether the whole-plant COG complex gains this new function, or it is only a feature of the COG2 subunits, remains to be tested. COG2 and EXO70A1 are widely expressed throughout the plant body, but VETH1/2 are specifically expressed in xylem in Arabidopsis roots, and this could explain why the association of the exocyst with cortical MTs is observed exclusively in this cell type. The interesting shift in exocyst localization and dynamics, driven by tissue-specific interactors, such as VETH proteins, during cell differentiation could represent a more general mechanism underlying the role of the exocyst in the morphogenesis of different cell types. This might occur, for example, in seed coat cells, where the exocyst is essential for pectin deposition in pockets around volcano-shaped cell wall thickenings (Kulich *et al.*, 2010) – a domain that is spatially marked by a dense meshwork of MTs (McFarlane *et al.*, 2008).

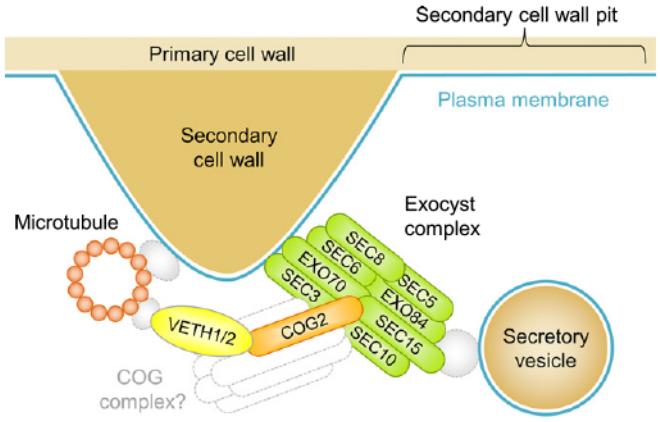

Fig. 8 Role of the exocyst in secondary cell wall (SCW) deposition in developing tracheary elements (TEs). Cortical microtubules (MTs) define the sites of SCW deposition. Several exocyst subunits interact with the conserved oligomeric Golgi complex 2 protein (COG2), which forms a complex with VETH1/2 associated with cortical MTs. Consequently, the exocyst complex promotes tethering of the secretory vesicle at the sites of SCW deposition.

Li *et al.* (2013) described irregular TE development in the *exo70A1-1* mutant, interpreting most of the growth phenotypes in dwarfish *exo70A1-1* mutants, in contradiction with Synek *et al.* (2006), to be caused exclusively by the defective xylem, and concluded that EXO70A1 is primarily expressed in developing TEs. Drdová *et al.* (2013) showed that polar auxin transport and distribution are severely affected in *exo70A1* mutants, and that EXO70A1 is required for recycling of PM proteins, including PIN auxin efflux carriers. As the disconnectivity of vascular strands is often observed when polar auxin transport is perturbed, either by chemical inhibitors or mutation in *PIN1* (Mattsson *et al.*, 1999), the phenotype observed in *exo70A1* and *exo84b* mutants might be enhanced indirectly by impaired PIN1 recycling. In comparison with *exo70A1*, we demonstrate here much stronger phenotypic changes in xylem development in the *exo84b-1* mutant. We show a thinner SCW and interruption of protoxylem TEs of mutant plants, and confirm by xylem-specific complementation that these phenotypic deviations are caused solely by the lack of functional EXO84b in this cell type. The differences between *exo70A1* and *exo84b-1* mutant phenotypes could be explained by partial recruitment of the exocyst complex to the sites of SCW deposition in the *exo70A1-2* background, whereas, in *exo84b-1* TEs, mutant exocyst subunits are localized only in the cytoplasm. Most importantly, in both *exo70A1-2* and *exo84b-1* mutant backgrounds, the localization of other exocyst subunits to the PM (and therefore also to the MT-patterned cortical domains) is partially or strongly compromised (Fig. S5). This corresponds with our previous observations for the rhizodermis in the *exo70A1* mutant (Fendrych *et al.*, 2013). Defective localization of core exocyst subunits in *exo70A1* mutant root epidermal cells (Fendrych *et al.*, 2013), impaired recycling of PIN proteins in *exo70A1* mutant roots (Drdová *et al.*, 2013) and the role of EXO70A1 in pectin secretion during seed coat formation (Kulich *et al.*, 2010) demonstrate the widespread function of EXO70A1 in different plant tissues. Although other EXO70 isoforms might be active in xylem, we conclude, in contrast with the xylem-exclusive interpretation of EXO70A1 function by Li *et al.* (2013), that EXO70A1 is a general EXO70 isoform functioning in xylem SCW deposition, as well as in many other exocytosis-dependent processes in different plant tissues.

In yeast, Exo70p interacts directly with phosphatidylinositol 4,5-bisphosphate and functions in concert with Sec3p to anchor the exocyst to the PM (He *et al.*, 2007). The fact that a proportion of the exocyst subunits tested remain in an annular/spiral

pattern in TEs of the *exo70A1-2* mutant can be explained by direct interactions of COG2 with the SEC3a, SEC10a or SEC15b subunit, as revealed in our yeast two-hybrid assay. It is possible that the other subunits are not associated with PM in the mutant background, but only with cortical MTs, and could still be visualized in an annular pattern. Alternatively, and very probably, one or more of the 23 EXO70 isoforms function redundantly to EXO70A1 in TEs. More than 10 EXO70 isoforms are expressed in TEs based on current transcriptomic data (GENEVESTIGATOR – Zimmermann *et al.*, 2004; eFP Browser – Winter *et al.*, 2007), with EXO70D3 and EXO70F1 showing the highest level of expression.

We demonstrate that the exocyst mutants *exo70A1-2* and *exo84b-1* do not exhibit impaired lignification of TE SCW, and that laccases, which direct lignification in this cell type (Schuetz *et al.*, 2014), have mostly normal localization in exocyst mutant backgrounds, with the exception of fully collapsing TE regions in *exo84b-1*. However, we show that secondary CESAs, represented by CESA7, which are responsible for cellulose synthesis in TEs, have differentially disturbed localization in exocyst mutants – from only partial mislocalization to the fully delocalized signal, or even possibly released from the PM. These findings are in full agreement with a recent study, in which the authors described large deviations in xylem cell wall biogenesis in *OsEXO70A1* rice mutant plants – collapsed vascular tissues and irregular SCW deposition (Tu *et al.*, 2015). It is possible that CESA mislocalization in exocyst mutants is a consequence of perturbations in cell wall or PM composition as a result of the lack of functional exocyst complex, and that CESAs are not a direct cargo for exocyst-mediated secretion.

In summary, our data show that, depending on the cell type, the role of the cytoskeleton in the targeting and spatio-temporal dynamics of the exocyst complex can be strikingly different. In addition, the cell-specific mechanism of exocyst subunit recruitment via the same subunit and specific adaptors expands significantly the potential of specific vesicle targeting via the exocyst, which was, until now, only implied by multiple EXO70 isoforms in land plants. Our results call for further analyses to elucidate the molecular details of the exocyst complex recruitment to the PM in TEs. Lastly, our report indicates possible cargos for exocyst-mediated exocytosis (especially CESA complexes); however, the secretion of numerous other cell wall components and modifying enzymes will need to be tested.

Acknowledgements

This work was supported by the Czech Science Foundation (GACR) 15-14886S and Grant Agency of Charles University (GAUK, project no. 1230214) to N.V., and MEXT KAKENHI (project nos. 26113505 and 15H01243), JSPS KAKENHI (project no. 25440128) and the Mitsubishi Foundation to Y.O. Part of the income and work of V.Z. and N.V. is supported by the Ministry of Education Youth and Sport of the Czech Republic (project no. NPUILO1417). We thank Lacey Samuels and Jan Petrášek for providing the plant material and Ivan Kulich for providing a modified pK7RWG2.0 vector.

Author contributions

N.V. designed the experiments, performed or took part in most of them, analyzed the data and wrote the manuscript. Y.O. designed and performed the experiments with suspension cells, assembled the figures and wrote parts of the manuscript. P.P. cloned most of the constructs used in this study and wrote parts of the manuscript. L.S. analyzed the data, assembled the figures and wrote parts of the manuscript. T.P. performed GUS and yeast two-hybrid experiments. A.R. performed plant crossing and microscopy. J.S. designed the experiments, analyzed the data and wrote parts of the manuscript. M.P. analyzed the data and wrote parts of the manuscript. V.Z. designed the research, analyzed the data and wrote the manuscript.

References

Alassimone J, Naseer S, Geldner N. 2010. A developmental framework for endodermal differentiation and polarity. *Proceedings of the National Academy of Sciences, USA* **107**: 5214–5219.

Bloch D, Pleskot R, Pejchar P, Potocký M, Trpkošová P, Cwiklik L, Vukašinović N, Sternberg H, Yalovsky S, Žárský V. 2016. Exocyst SEC3 and phosphoinositides define sites of exocytosis in pollen tube initiation and growth. *Plant Physiology* **172**: 980–1002.

Boyd C, Hughes T, Pypaert M, Novick P. 2004. Vesicles carry most exocyst subunits to exocytic sites marked by the remaining two subunits, Sec3p and Exo70p. *Journal of Cell Biology* **167**: 889–901.

Clough SJ, Bent AF. 1998. Floral dip: a simplified method for Agrobacterium-mediated transformation of *Arabidopsis thaliana*. *Plant Journal* **16**: 735–743.

Cole RA, Synek L, Zarsky V, Fowler JE. 2005. SEC8, a subunit of the putative Arabidopsis exocyst complex, facilitates pollen germination and competitive pollen tube growth. *Plant Physiology* **138**: 2005–2018.

Cvrčková F, Grunt M, Bezvoda R, Hála M, Kulich I, Rawat A, Žárský V. 2012. Evolution of the land plant exocyst complexes. *Frontiers in Plant Science* **3**: 159.

Derbyshire P, Ménard D, Green P, Saalbach G, Buschmann H, Lloyd CW, Pesquet E. 2015. Proteomic analysis of microtubule interacting proteins over the course of xylem tracheary element formation in Arabidopsis. *Plant Cell* **27**: 2709–2726.

Drdová EJ, Synek L, Pečenková T, Hála M, Kulich I, Fowler JE, Murphy A, Žárský V. 2013. The exocyst complex contributes to PIN auxin efflux carrier recycling and polar auxin transport in *Arabidopsis*. *Plant Journal* **73**: 709–719.

Fendrych M, Synek L, Pečenková T, Drdová EJ, Sekereš J, De Rycke R, Nowack MK, Žárský V. 2013. Visualization of the exocyst complex dynamics at the plasma membrane of *Arabidopsis thaliana*. *Molecular Biology of the Cell* **24**: 510–520.

Fendrych M, Synek L, Pečenková T, Toupalová H, Cole R, Drdová E, Nebesářová J, Šedinová M, Hála M, Fowler JE *et al.* 2010. The *Arabidopsis* exocyst complex is involved in cytokinesis and cell plate maturation. *Plant Cell* **22**: 3053–3065.

Fukuda H. 1997. Tracheary element differentiation. *Plant Cell* **9**: 1147–1156.

Gardiner JC, Taylor NG, Turner SR. 2003. Control of cellulose synthase complex localization in developing xylem. *Plant Cell* **15**: 1740–1748.

Geldner N. 2013. The endodermis. *Annual Review of Plant Biology* **64**: 531–558.

Grefen C, Donald N, Hashimoto K, Kudla J, Schumacher K, Blatt MR. 2010. A ubiquitin-10 promoter-based vector set for fluorescent protein tagging facilitates temporal stability and native protein distribution in transient and stable expression studies. *Plant Journal* **64**: 355–365.

Gutierrez R, Lindeboom JJ, Paredez AR, Emons AMC, Ehrhardt DW. 2009. Arabidopsis cortical microtubules position cellulose synthase delivery to the plasma membrane and interact with cellulose synthase trafficking compartments. *Nature Cell Biology* **11**: 797–806.

Hála M, Cole R, Synek L, Drdová E, Pečenková T, Nordheim A, Lamkemeyer T, Madlung T, Hochholdinger F, Fowler JE *et al.* 2008. An exocyst complex functions in plant cell growth in *Arabidopsis* and tobacco. *Plant Cell* **20**: 1330–1345.

He B, Guo W. 2009. The exocyst complex in polarized exocytosis. *Current Opinion in Plant Biology* **21**: 537–542.

He B, Xi F, Zhang X, Zhang J, Guo W. 2007. Exo70 interacts with phospholipids and mediates the targeting of the exocyst to the plasma membrane. *EMBO Journal* **26**: 4053–4065.

Heard W, Sklenar J, Tome DF, Robatzek S, Jones AM. 2015. Identification of regulatory and cargo proteins of endosomal and secretory pathways in *Arabidopsis thaliana* by proteomic dissection. *Molecular & Cellular Proteomics* **14**: 1796–1813.

Heider MR, Munson M. 2012. Exorcising the exocyst complex. *Traffic* **13**: 898–907.

Heo JO, Roszak P, Furuta KM, Helariutta Y. 2014. Phloem development: current knowledge and future perspectives. *American Journal of Botany* **101**: 1393–1402.

Hepler PK, Newcomb EH. 1964. Microtubules and fibrils in the cytoplasm of *Coleus* cells undergoing secondary wall deposition. *Journal of Cell Biology* **20**: 529–533.

Hertzog M, Chavrier P. 2011. Cell polarity during motile processes: keeping on track with the exocyst complex. *Biochemical Journal* **433**: 403–409.

Holt BF, Boyes DC, Ellerström M, Siefers N, Wiig A, Kauffman S, Grant MR, Dangl JL. 2002. An evolutionarily conserved mediator of plant disease resistance gene function is required for normal Arabidopsis development. *Developmental Cell* **2**: 807–817.

Karimi M, Inzé D, Depicker A. 2002. GATEWAY™ vectors for *Agrobacterium*-mediated plant transformation. *Trends in Plant Science* **7**: 193–195.

Kubo M, Udagawa M, Nishikubo N, Horiguchi G, Yamaguchi M, Ito J, Mimura T, Fukuda H, Demura T. 2005. Transcription switches for protoxylem and metaxylem vessel formation. *Genes & Development* **19**: 1855–1860.

Kulich I, Cole R, Drdová E, Cvrčková F, Soukup A, Fowler JE, Žárský V. 2010. Arabidopsis exocyst subunits SEC8 and EXO70A1 and exocyst interactor ROH1 are involved in the localized deposition of seed coat pectin. *New Phytologist* **188**: 615–625.

Kulich I, Vojtíková Z, Glanc M, Ortmannová J, Rasmann S, Žárský V. 2015. Cell wall maturation of *Arabidopsis* trichomes is dependent on exocyst subunit EXO70H4 and involves callose deposition. *Plant Physiology* **168**: 120–131.

Lavy M, Bloch D, Hazak O, Gutman I, Poraty L, Sorek N, Sternberg H, Yalovsky S. 2007. A novel ROP/RAC effector links cell polarity, root-meristem maintenance, and vesicle trafficking. *Current Biology* **17**: 947–952.

Li S, Chen M, Yu D, Ren S, Sun S, Liu L, Ketelaar T, Emons AMC, Liu CM. 2013. EXO70A1-mediated vesicle trafficking is critical for tracheary element development in Arabidopsis. *Plant Cell* **25**: 1774–1786.

Li S, van Os GM, Ren S, Yu D, Ketelaar T, Emons AMC, Liu CM. 2010. Expression and functional analyses of EXO70 genes in Arabidopsis implicate their roles in regulating cell type-specific exocytosis. *Plant Physiology* **154**: 1819–1830.

Malamy JE, Benfey PN. 1997. Organization and cell differentiation in lateral roots of Arabidopsis thaliana. *Development* **124**: 33–44.

Mattsson J, Sung ZR, Berleth T. 1999. Responses of plant vascular systems to auxin transport inhibition. *Development* **126**: 2979–2991.

McFarlane HE, Young RE, Wasteneys GO, Samuels AL. 2008. Cortical microtubules mark the mucilage secretion domain of the plasma membrane in *Arabidopsis* seed coat cells. *Planta* **227**: 1363–1375.

Mucha E, Hoefle C, Hückelhoven R, Berken A. 2010. RIP3 and AtKinesin-13A–a novel interaction linking Rho proteins of plants to microtubules. *European Journal of Cell Biology* **89**: 906–916.

Oda Y, Fukuda H. 2013. The dynamic interplay of plasma membrane domains and cortical microtubules in secondary cell wall patterning. *Frontiers in Plant Science* **4**: 511.

Oda Y, Iida Y, Kondo Y, Fukuda H. 2010. Wood cell-wall structure requires local 2D-microtubule disassembly by a novel plasma membrane-anchored protein. *Current Biology* **20**: 1197–1202.

Oda Y, Iida Y, Nagashima Y, Sugiyama Y, Fukuda H. 2015. Novel coiled-coil proteins regulate exocyst association with cortical microtubules in xylem cells via the conserved oligomeric Golgi-complex 2 protein. *Plant and Cell Physiology* **56**: 277–286.

Oda Y, Mimura T, Hasezawa S. 2005. Regulation of secondary cell wall development by cortical microtubules during tracheary element differentiation in Arabidopsis cell suspensions. *Plant Physiology* **137**: 1027–1036.

Paredez AR, Somerville CR, Ehrhardt DW. 2006. Visualization of cellulose synthase demonstrates functional association with microtubules. *Science* **312**: 1491–1495.

Pesquet E, Korolev AV, Calder G, Lloyd CW. 2010. The microtubule-associated protein AtMAP70-5 regulates secondary wall patterning in Arabidopsis wood cells. *Current Biology* **20**: 744–749.

Pleskot R, Cwiklik L, Jungwirth P, Žárský V, Potocký M. 2015. Membrane targeting of the yeast exocyst complex. *Biochimica et Biophysica Acta* **7**: 1481–1489.

Podos SD, Reddy P, Ashkenas J, Krieger M. 1994. LDLC encodes a brefeldin A-sensitive, peripheral Golgi protein required for normal Golgi function. *Journal of Cell Biology* **127**: 679–691.

Růžička K, Ursache R, Hejátko J, Helariutta Y. 2015. Xylem development – from the cradle to the grave. *New Phytologist* **207**: 519–535.

Rybak K, Steiner A, Synek L, Klaeger S, Kulich I, Facher E, Wanner G, Kuster B, Zarsky V, Persson S *et al.* 2014. Plant cytokinesis is orchestrated by the sequential action of the TRAPPII and Exocyst tethering complexes. *Developmental Cell* **29**: 607–620.

Schuetz M, Benske A, Smith RA, Watanabe Y, Tobimatsu Y, Ralph J, Demura T, Ellis B, Samuels AL. 2014. Laccases direct lignification in the discrete secondary cell wall domains of protoxylem. *Plant Physiology* **166**: 798–807.

Synek L, Schlager N, Eliáš M, Quentin M, Hauser MT, Žárský V. 2006. AtEXO70A1, a member of a family of putative exocyst subunits specifically expanded in land plants, is important for polar growth and plant development. *Plant Journal* **48**: 54–72.

Synek L, Sekereš J, Žárský V. 2014. The exocyst at the interface between cytoskeleton and membranes in eukaryotic cells. *Frontiers in Plant Science* **4**: 543.

Tu B, Hu L, Chen W, Li T, Hu B, Zheng L, Lv Z, You S, Wang Y, Ma B *et al.* 2015. Disruption of OsEXO70A1 causes irregular vascular bundles and perturbs mineral nutrient assimilation in rice. *Scientific Reports* **5**: 18609.

Turner SR, Sieburth LE. 2003. Vascular patterning. *The Arabidopsis Book/ American Society of Plant Biologists* **2**: e0073.

Ungar D, Oka T, Krieger M, Hughson FM. 2006. Retrograde transport on the COG railway. *Trends in Cell Biology* **16**: 113–120.

Vukašinović N, Cvrčková F, Eliáš M, Cole R, Fowler JE, Žárský V, Synek L. 2014. Dissecting a hidden gene duplication: the *Arabidopsis thaliana* SEC10 locus. *PLoS ONE* **9**: e94077.

Watanabe Y, Meents MJ, McDonnell LM, Barkwill S, Sampathkumar A, Cartwright HN, Demura T, Ehrhardt DW, Samuels AL, Mansfield SD. 2015. Visualization of cellulose synthases in Arabidopsis secondary cell walls. *Science* **350**: 198–203.

Wightman R, Marshall R, Turner SR. 2009. A cellulose synthase-containing compartment moves rapidly beneath sites of secondary wall synthesis. *Plant and Cell Physiology* **50**: 584–594.

Wightman R, Turner SR. 2008. The roles of the cytoskeleton during cellulose deposition at the secondary cell wall. *Plant Journal* **54**: 794–805.

Winter D, Vinegar B, Nahal H, Ammar R, Wilson GV, Provart NJ. 2007. An "Electronic Fluorescent Pictograph" browser for exploring and analyzing large-scale biological data sets. *PLoS ONE* **2**: e718.

Wu H, Rossi G, Brennwald P. 2008. The ghost in the machine: small GTPases as spatial regulators of exocytosis. *Trends in Cell Biology* **18**: 397–404.

Yamaguchi M, Goué N, Igarashi H, Ohtani M, Nakano Y, Mortimer JC, Nishikubo N, Kubo M, Katayama Y, Kakegawa K *et al.* 2010. VASCULAR-RELATED NAC-DOMAIN6 and VASCULAR-RELATED NAC-DOMAIN7 effectively induce transdifferentiation into xylem vessel elements under control of an induction system. *Plant Physiology* **153**: 906–914.

Žárský V, Cvrčková F, Potocký M, Hála M. 2009. Exocytosis and cell polarity in plants–exocyst and recycling domains. *New Phytologist* **183**: 255–272.

Žárský V, Kulich I, Fendrych M, Pečenková T. 2013. Exocyst complexes multiple functions in plant cells secretory pathways. *Current Opinion in Plant Biology* **16**: 726–733.

Zhao Q, Nakashima J, Chen F, Yin Y, Fu C, Yun J, Shao H, Wang X, Wang Z, Dixon RA. 2013. Laccase is necessary and nonredundant with peroxidase for lignin polymerization during vascular development in Arabidopsis. *Plant Cell* **25**: 3976–3987.

Zimmermann P, Hirsch-Hoffmann M, Hennig L, Gruissem W. 2004. GENEVESTIGATOR. *Arabidopsis* microarray database and analysis toolbox. *Plant Physiology* **136**: 2621–2632.

Supporting Information

Additional Supporting Information may be found online in the Supporting Information tab for this article:

Fig. S1 β-Glucuronidase (GUS) analysis of *SEC6* and *SEC10a* promoters.

Fig. S2 Appearance of autofluorescence, exocyst and propidium iodide (PI) signal in developing protoxylem of root and exocyst localization in VND7-induced tracheary elements (TEs).

Fig. S3 EXO70A1 follows the behavior of cortical microtubules (MTs) in cultured Arabidopsis xylem cells.

Fig. S4 Exocyst localization is dependent on the microtubule (MT) and not actin cytoskeleton.

Fig. S5 Localization of exocyst subunits in tracheary elements (TEs) of *exo84b-1* and *exo70A1-2* mutant plants.

Fig. S6 Co-localization of CESA7 and LAC17 with exocyst subunits, ectopic expression of LAC17-mCherry in *exo84b-1* mutant and lignin staining in exocyst mutants.

Table S1 Primer sequences used in this study

Movie S1 GFP-SEC8 foci at the plasma membrane (PM) are static and do not move along microtubules (MTs).

Please note: Wiley Blackwell are not responsible for the content or functionality of any Supporting Information supplied by the authors. Any queries (other than missing material) should be directed to the *New Phytologist* Central Office.

EXO70B2 containing exocyst complex mediates fungal non-host penetration resistance in Arabidopsis

Jitka Ortmannová[1,2], Tamara Pečenková[1,2], Juraj Sekereš[1,2], Ivan Kulich[2], Viktor Žárský[1,2*]

1 Laboratory of Cell Biology, Institute of Experimental Botany, Academy of Sciences of the Czech Republic, Rozvojova 263, 165 02, Prague 6, Czech Republic
2 Laboratory of Cell Morphogenesis, Department of Experimental Plant Biology, Charles University in Prague, Faculty of Science, 128 44 Vinicna 5, Prague 2, Czech Republic

* Correspondence: Viktor Žárský (zarsky@ueb.cas.cz)
Laboratory of Cell Biology, Institute of Experimental Botany, Academy of Science, Czech Republic, Rozvojova 263, 16502, Praha 6, Czech Republic, +420225106459

Running title: Exocyst complex mediates fungal non-host resistance in Arabidopsis

Abstract /200

Exocytosis is one of the basal mechanisms maintaining penetration resistance to a broad spectrum of non-adapted pathogens, such as biotrophic fungi. In defense, plant cells build cell wall reinforcing papillae and encasements in order to stop fungal growth. In Arabidopsis, syntaxin of plants SYP121/PEN1, member of SNARE complex at the plasma membrane, is essential for the proper papillae formation in time. Both SNARE and exocyst complexes orchestrate secretion, however, their cooperation is poorly understood. Here, we report a direct association between exocyst and SNARE complexes in penetration resistance. We observed diminished penetration resistance in several *Arabidopsis* mutant lines of exocyst subunits upon the infection with non-adapted fungal pathogens *Blumeria graminis* f. *sp. hordei (Bgh)*. We showed interaction between exocyst subunits and SYP121 in plant immunity. We provide evidence that SYP121 and EXO70B2 subunit of exocyst occur at the membrane domain

of papilla. In *exo70B2/syp121* double mutants we identified additive phenotype in plant sensitivity, confirming exocyst and SNARE cooperate in non-host resistance. Consistent with the importance of secretory pathway for the penetration resistance, we proved the substantial role of the exocyst complex hand by hand with SNARE complex in papillae and encasements formation.

Keywords: exocyst, encasement, papilla, penetration resistance, plant immunity, SNARE, SYP121

Introduction / 8000 (excluding the title page, references, figure legends, and tables)

In a struggle between a fungus and a plant, plant surface is the place where the battle starts. In the moment of detection of a pathogen/damage associated molecular patterns (PAMPs/DAMPs) and pressure, which a fungal pathogen exerts on the cell surface, plant cells start to react and re-polarize their secretory pathways to that point as a one of non-host resistance mechanisms (Schmelzer, 2002a; Lee et al., 2017). Through the massive secretion, plant cells form focal cell wall reinforcements called papillae (Bestwick et al., 1995). The papillae are composed of a mixture of the cell wall and antimicrobial components, such as callose (beta-1,3-glucan), pectins, lignins, reactive oxygen species (ROS), phytoalexins and thionins (Schmelzer, 2002b). Although all the components have structural and antimicrobial functions, based on recent observations the limiting steps for formation of successful papillae is their deposition in proper time and sufficient concentration (Assaad et al., 2004a; Nielsen et al., 2012a; Ellinger et al., 2014; Chowdhury et al., 2014a). Thus recruitment of adequate cargoes and proteins responsible for efficient vesicular fusion is essential for successful non-host penetration defence. Despite the surface barriers, some fungal hyphae may penetrate plant cells, creating feeding structures called haustoria, which are surrounded by specialized extrahaustorial membrane (EHM; Micali *et al.*, 2011). In return, plant cell may sequestrate the haustorium by secretion of an encasement, the defensive structure made of similar components as the papilla (Heath and Heath, 1971; Zeyen et al., 2002).

The non-host resistance remains sufficient against evolutionary non-adapted fungi to *Arabidopsis thaliana* host (further *Arabidopsis*) such as *Erysiphe pisi (Ep)* or *Blumeria graminis f.* sp. *hordei* (*Bgh*) ((Vogel and Somerville, 2000a; Consonni et al., 2006; Lipka et al., 2008). In *Arabidopsis PENETRATION1* (*PEN1/SYP121*) have been described as crucial for non-host resistance against biotrophic fungi (Collins et al., 2003a; Lipka et al., 2005; Stein et al., 2006). SYP121 belongs to family of plasma membrane Qa- Soluble N-ethylmaleimide-sensitive factor Attachment protein REceptors SNAREs. In vesicle fusion SYP121 forms ternary SNARE complex with cytoplasmic Qbc-SNARE SNAP33 (soluble N-ethylmaleimide-sensitive factor adaptor protein 33) and vesicle membrane bound R-SNARE VAMP721/722 (vesicle-associated membrane protein 721/722; Kwon *et al.*, 2008). This complex promotes exocytosis of secretory vesicles carrying so far unknown defence-related cargo to plant cell/fungus contact sites and mediates papillae formation (Assaad et al., 2004b; Kwon et al., 2008; Meyer et al., 2009). Besides GFP-SYP121 localisation to papillae and encasements, it also associates with exosomes in the extracellular matrix, the paramural space, of those structures (Nielsen et al., 2012a; Rutter and Innes, 2017). However, no functional impact of extracellular SYP121 on papilla or encasement function has been shown (Nielsen and Thordal-Christensen, 2012; Nielsen and Thordal-Christensen, 2013). Thus, the actual role of SYP121 takes place possibly on the membrane surrounding papilla and encasement after its transcytosis from its pool at the PM (Nielsen et al., 2017). The SYP121 operates also in a complex with the specific MVB (multivesicular body) R-SNARE VAMP727, which may play the crucial role in the Rab-GTPase ARA6 dependent exosome secretion into the papillary matrix, thus rapidly delivering recycled pre-synthesized material to papillae (Ebine et al., 2011; Nielsen et al., 2012b). Intriguingly, the ARA7 not ARA6 mediates the SYP121 transcytosis into the encasement, therefore two distinct MVB dependent secretory pathways may exist to distinguish between papilla and encasement formation (Nielsen et al., 2017).

In yeasts and mammals, SNARE proteins execute their function in cooperation with other proteins and protein complexes, one of them being the exocyst complex (Hsu

et al., 1996; Sivaram et al., 2005; Dubuke et al., 2015; Yue et al., 2017a). Exocyst is an octameric tethering complex, assembled from core subunits SEC5, SEC6, SEC8, SEC10, SEC15, EXO84 and PM associated subunits EXO70 and SEC3 (TerBush et al., 1996; Guo et al., 1997). In plants, the exocyst complex has been found first by *in silico* analysis and later on its function was confirmed by genetic, biochemical and microscopic analyses (Elias et al., 2003a; Cole et al., 2005a; Synek et al., 2006; Hala et al., 2008a; Fendrych et al., 2010; Fendrych et al., 2013a). Phenomenon of evolutionary multiplication of *EXO70* gene family giving rise e. g. in *Arabidopsis* to 23 genes, could be related the necessity to specify and redirect secretory pathway to distinct cortical PM domains of an immobile plant cell (Zárský et al., 2009a; Vukašinović and Žárský, 2016). Recently, the comparative study of tobacco EXO70 family members has shown a diversity of behaviour of EXO70 isoforms and their ability to bind different domains within a pollen tube (Sekereš et al., 2017a). Current data indicate the possibility of an existence of more than one variant of the exocyst complex in a single plant cell, dependent on an EXO70 isoform bound to the core of the complex (Zárský et al., 2013a). In *Arabidopsis*, EXO70B clade represents two isoforms EXO70B1 and EXO70B2 (Cvrčková et al., 2012). The EXO70B1, which mediates autophagy-related transport to the vacuole, is supposed to interfere with the effector-triggered immunity (Kulich et al., 2013; Cui et al., 2015; Zhao et al., 2015). The connection with basal pathogen-associated molecular patterns triggered immunity (PTI) driven by SYP121 pathway has been excluded for EXO70B1, although it directly interacts with SYP121 and SNAP33 (Zhao et al., 2015). On the contrary, EXO70B2, which also interacts with SNAP33, has been described as a positive regulator of PTI, the first layer of defence involved in penetration resistance (Pecenková et al., 2011; Stegmann et al., 2012a) and so far no work has addressed the possible connection of EXO70B2 and SYP121 pathway in penetration resistance.

Based on our previous observation of EXO70B2 mutant impairment in the proper formation of papillae (Pecenkova et al., 2011a), we hypothesized that exocyst complex containing EXO70B2 might localise at the fungal contact sites and possibly cooperates

with the SYP121 in non-host penetration resistance. To test the exocyst plays a role in non-host resistance, we analysed penetration rate of non-adapted powdery mildew fungi *Bgh* and *Ep* in several exocyst mutants. We showed an accumulation of a signal of the exocyst subunits tagged with GFP near papillae and in haustorial encasements. We detected defects in defensive papillae formation and overall decreased penetration resistance in tested mutants. Genetic analysis indicated the synergic action of EXO70B2 containing exocyst and SYP121, which also directly interacted and co-localised at the domain of papilla biogenesis. We conclude that the proper functioning of the exocyst complex involving isoform EXO70B2 is important for the penetration resistance, likely as a part of the previously characterised SYP121-dependent secretory pathway.

Results

EXO70B2 is specifically upregulated after the fungal attack

Pathogen recognition innittates reorientation of plant cell secretory pathway towards cell/pathogen contact sites where the associated proteins and cargoes accumulate and deposit papillae. Exocyst complex is involved in polarization of secretion in various cell types in Arabidopsis (Bloch et al., 2016; Kalmbach et al., 2017; Kulich et al., 2018). Subunit of exocyst EXO70B2 mRNA level was shown to be upregulated after various elicitor treatments in *Arabidopsis* and the protein is involved in papillae biogenesis (Pecenková et al., 2011; Stegmann et al., 2012a). Non-host resistance to fungal pathogens, where the papillae are formated, is a slow-mode process happening within hours. Therefore we suggest, EXO70B2 protein level might specifically response to a fungal attack and accumulate in papillae periphery. To be able to detect EXO70B2 protein, we used several stable lines expressing EXO70B2-GFP driven by the native promoter in *exo70B2* mutant background, which complemented its phenotype in penetration resistance (Fig. S1). In those plants, we examined a protein level of the core exocyst subunit SEC8, EXO70B2-GFP and it's paralogue EXO70A1 at

the early hours after *Bgh* treatment (Fig. 1A). The level of EXO70B2 protein grew significantly up at 4 hpi (Fig. 1A) and stayed unchanged even at 24 hpi *Bgh* (Fig. S2). The level of EXO70A1 slightly decreased, while the level of SEC8 stayed unchanged (Fig. 1B). This suggests a putative replacement of EXO70 isoforms in exocyst complex under specific conditions as proposed before (Zárský et al., 2013b). We examined also the response of GFP-EXO70B1 protein, the closest paralogue of EXO70B2. In contrast to EXO70B2-GFP, we did not detect an expression of GFP-EXO70B1 in the *exo70B1-1* background, comparing same protein concentrations (Fig. 1A). We observed only the mild positive response of GFP-EXO70B1 expression, increasing total extracts concentrations three times (Fig. S2). To be able to exclude influence of GFP-tag position, we compared GFP-EXO70B1 expression with GFP-EXO70B2 variant, which similarly to EXO70B2-GFP respond to the inoculation with fungus (Fig. S2).

In order to detect the earliest point of EXO70B2-GFP recruitment to the *Arabidopsis/Bgh* contact sites, we acquired images of infected *Arabidopsis* leaves every two hours starting from the 0 point of inoculation till 24 hpi. The very first signal of EXO70B2-GFP accumulated at the fungal attack site at 8-9 hpi unlike signal of GFP-EXO70B1, which we did not detect probably due to its low expression (Fig. 1B). In comparison with wild-type (WT) plants, we observed faint accumulation of GFP-EXO70A1 driven by 35S promotor in the contact sites. This results suggest the EXO70B2 specifically responses to a pathogen and focally accumulates at the contact sites rapidly upon stress exposition.

Figure 1

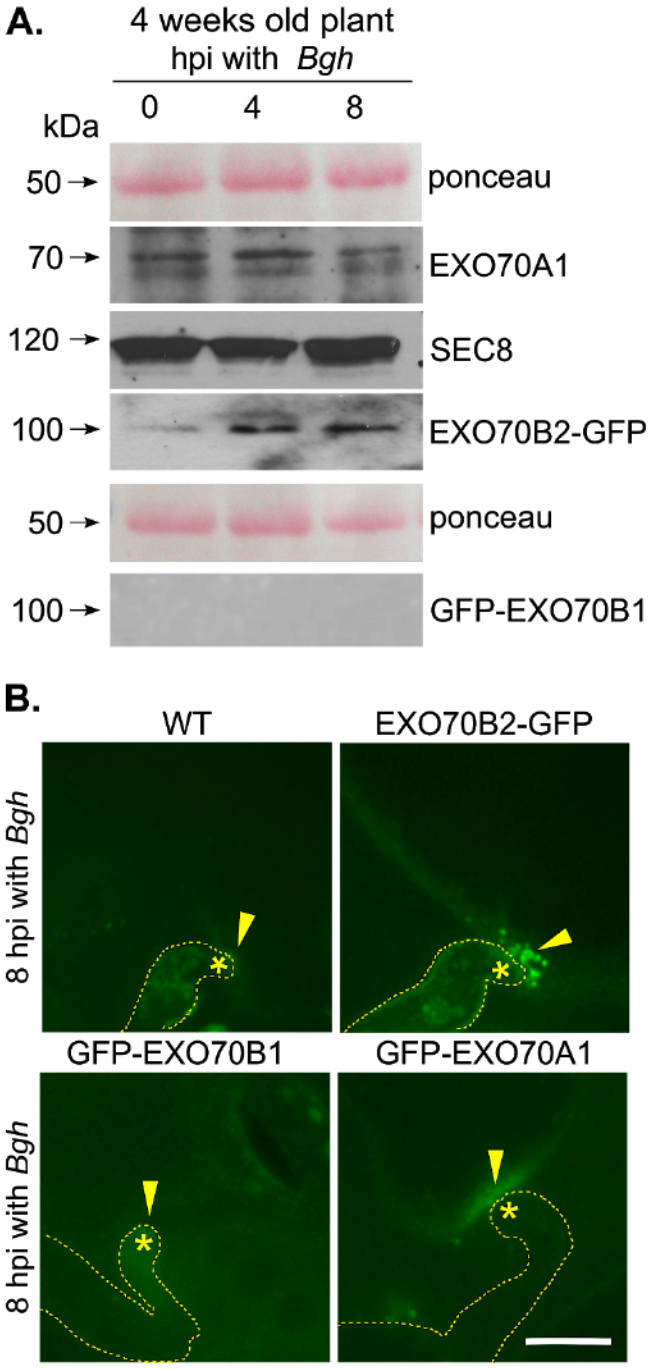
A.
4 weeks old plant
hpi with Bgh
0
4
8
kDa
50
ponceau
70
EXO70A1
120
SEC8
100
EXO70B2-GFP
50
ponceau
100
GFP-EXO70B1
B.
WT
EXO70B2-GFP
8 hpi with Bgh
GFP-EXO70B1
GFP-EXO70A1
8 hpi with Bgh

Exocyst subunits localise to the defensive papillae

Using spinning disc confocal microscopy, we aimed to compare the localisation and dynamic of EXO70B2-GFP at the fungal contact sites with several GFP-tagged exocyst subunits 24 hpi with *Bgh* (Fig. 2A). We used FM4-64 dye to stain PM and fungal structures. In parallel we observed localisation of exocyst subunits with positive control GFP-SYP121 (Kato et al., 2010), which hyper-accumulates at the membrane domain of papillae (incidence of accumulation 58%±10 of 50 spores) as well as in their paramural space (Assaad et al., 2004b; Nielsen et al., 2012c). The signal of exocyst complex core subunits tested – Ub:SEC5a-GFP (52%±5) and with natural promoters SEC6-GFP (60%±8), GFP-SEC8 (45%±12; (Fendrych et al., 2013b), SEC10a-GFP (62%±12; (Vukašinović et al., 2017) and EXO70B2-GFP (43%±12) was enriched at the contact sites with the fungus, at the membrane cortical domains of papillae (Fig. 2A, B). To avoid false positive exocyst localisation signals, we always compared the GFP signal maxima with the autofluorescence of non-transformed WT plants within papilla structure (Fig. 2B). Using the confocal microscope with lambda scan mode and linear unmixing tool, we confirmed that the accumulated signal observed in infected cells was true GFP and not an autofluorescence commonly upregulated in inoculated *Arabidopsis* leafs (Fig. S3).

Deposited papillae are stable structures as well pool of GFP-SYP121, which persists at the peripheral membrane domain as well in paramural space of papillae body (Meyer et al., 2009; Nielsen et al., 2012a). We compared dynamics of the EXO70B2-GFP and the SEC6-GFP localisation with the SYP121-GFP within the papilla structure. The kymographs generated from time series showed that the localisation of exocyst within the papilla is stationary (Fig. S4). Therefore, we compared this stable exocyst domain to previously described exocyst PM localisation in secondary cell wall deposition in tracheary elements (Vukašinović et al., 2017) in contrast to dynamic exocyst localisation at the lateral PM domains of rhizodermal cells (Fendrych *et al.*, 2013).

Figure 2

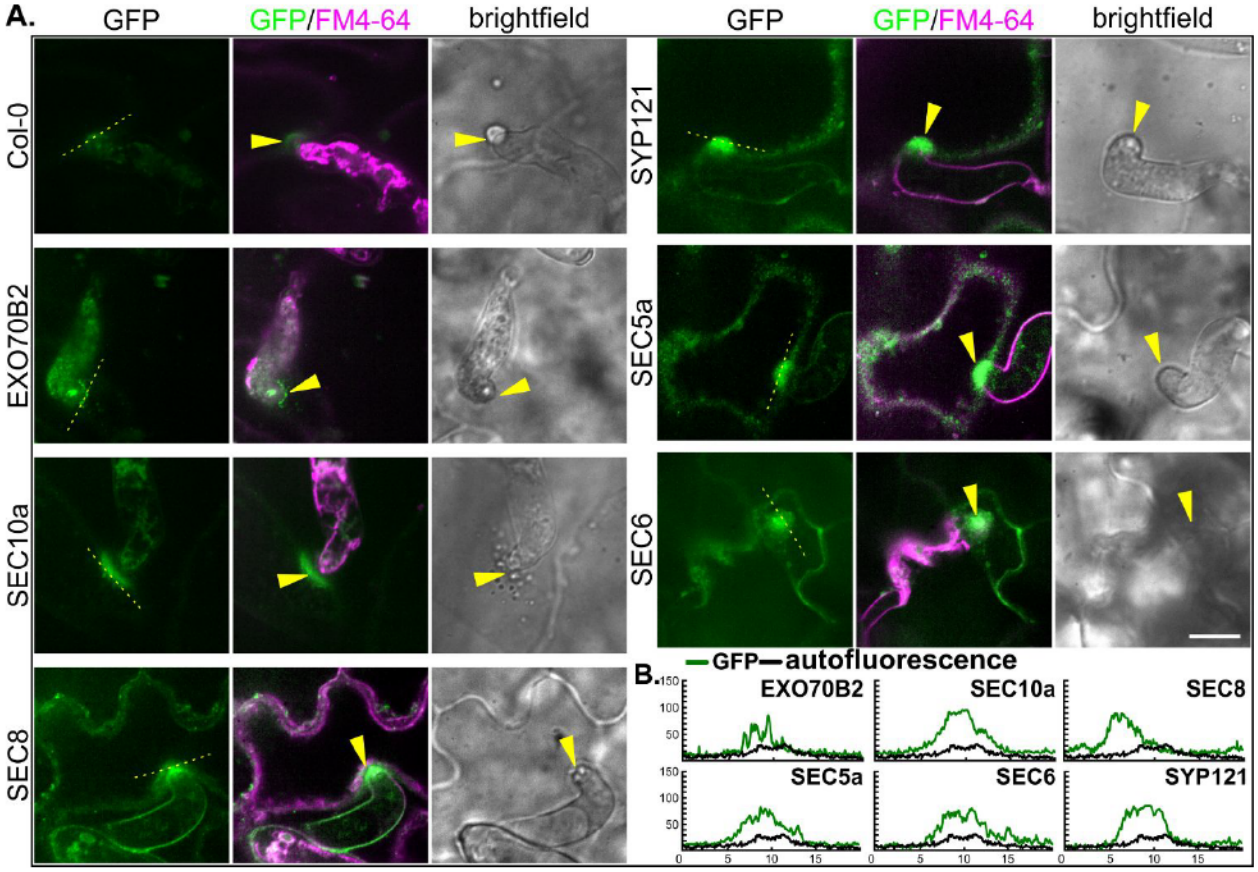
A.
GFP
GFP/FM4-64
brightfield
GFP
GFP/FM4-64
brightfield
Col-0
SYP121
EXO70B2
SEC5a
SEC10a
SEC6
SEC8
B.
GFP—autofluorescence
EXO70B2
SEC10a
SEC8
SEC5a
SEC6
SYP121
150
100
50
0
5
10
15

Exocyst colocalises with the growing structure of haustorial encasement

Bgh and *Ep* are both able to occasionally successfully penetrate non-host plant cell and develop haustoria, which become later encased. Using optical sectioning confocal microscopy, we observed GFP-fused exocyst subunits in haustorial encasements and their collars, the connective structure with the cell wall and PM. We inspected the surface of *Bgh* haustorium and showed signals of EXO70B2-GFP and core exocyst subunit SEC6-GFP label the encasements (Fig. 3). We observed that the EXO70B2-GFP signal outlined not only the papilla body (Fig. 3A) but also the collar of haustoria (Fig. 3B, yellow arrowheads) and the encasement itself (Fig. 3B). However, the signal was excluded from the part of haustoria lacking the encasement, i.e. it was not present at the extrahaustorial membrane (Fig. 3B, pink arrowheads). The very tips of haustoria were marked by EXO70B2-GFP only if they were in the stage of encasement closing. The same was true for SEC6-GFP representing the exocyst core subunit (Fig. 3D, pink arrowhead marks the enclosure of encasement). The maximum intensity of signals showed the difference between EXO70B2-GFP and the SEC6-GFP signal. The SEC6 displayed higher signal in papilla (Fig. 3C) or the collar (Fig. 3D, yellow arrowhead) than EXO70B2-GFP, and stayed excluded from the EHM (pink arrowhead in Fig. 3D). Similar to accumulation of signal at papillae, we verified this observation by lambda scan and subsequent linear unmixing analysis, where we confirmed exocyst is not internalised into paramural space of encasements (Fig. S3). These observations indicate that EXO70B2 containing exocyst complex may also have a specific role in encasement biogenesis.

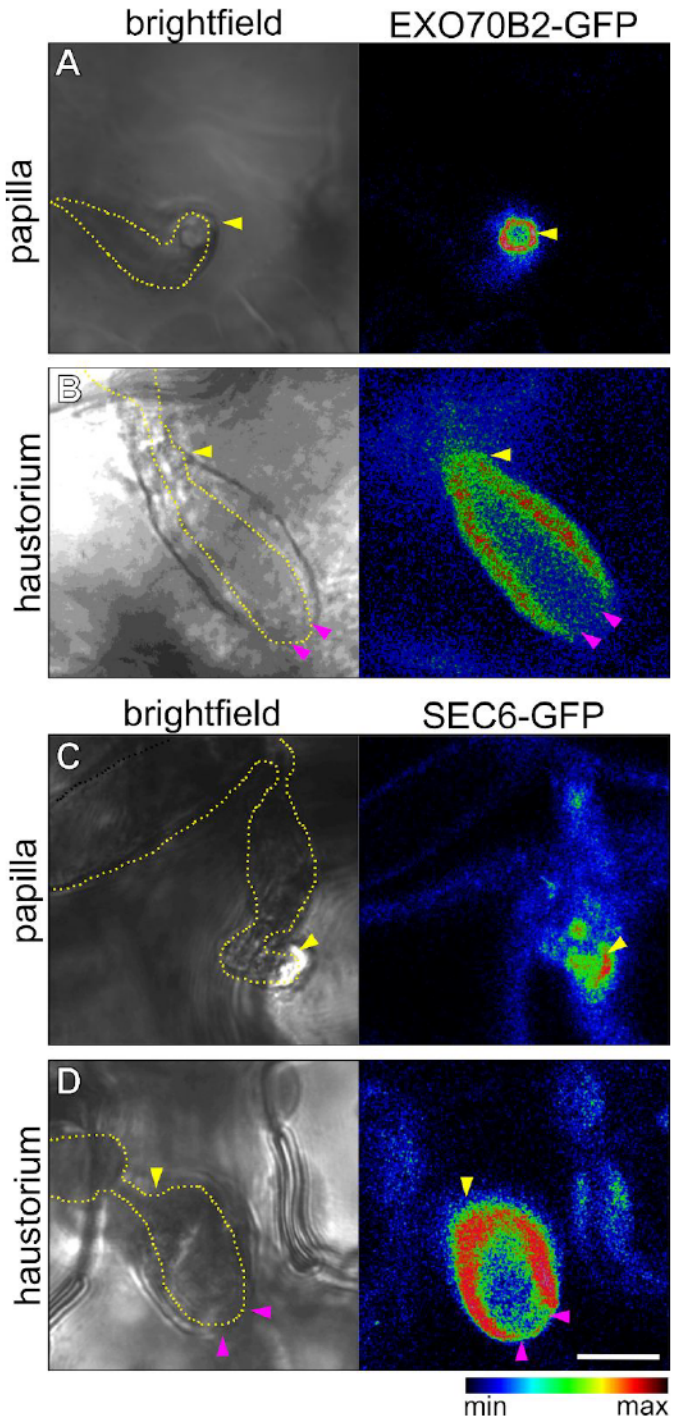
brightfield
EXO70B2-GFP
A
papilla
B
haustorium
brightfield
SEC6-GFP
C
papilla
D
haustorium
min
max

Figure 3

Exocyst subunits mutants display deviated papillae and impaired penetration resistance

Based on our localisation study, we examined interaction sites and penetrated cells on infected leaves of exocyst mutant lines using trypan blue and aniline blue staining (Fig. 4A). We aimed to work with mutants, which do not have obvious developmental defects. Therefore we chose mutants in exocyst core subunit genes, the knockout line (KO) *sec5a-1* (GABI_731C01, Fig. S5), knock-down line *sec8-m4* (Cole et al., 2005b)) and *exo70B2* line (*exo70B2-2* from (Pecenkova et al., 2011b) and *exo70B1* (Kulich et al., 2013), both representing *EXO70* gene involved in plant immunity. As a negative control, we used homozygous WT lines outcrossed from *exo70B2* and *exo70B1* background. Along with previously characterised types of fungal propagation, such as regular papilla, encased haustorium, unencased haustorium and dead cell, known from *Arabidopsis* wild-type (WT) leaves (Takemoto et al., 2006a), we observed two types of papillae deviation. The papillae with vesicular clump described before (Pecenková et al., 2011) and the enlarged papillae with diameter more than twice than regular papillae (Fig. 4A). We identified two distinct patterns of callose deposition defect as well. The vesicular clump category exhibited a reduction of callose and stacking of faint callose spots around the appressorium (Fig. 4A). In contrast, the enlarged papillae showed over accumulation of callose as well as bigger papillae body observed in the bright field (Fig. 4A). We quantified occurrence of two categories, the deviated papillae and penetrated cells at 24 and 48 hpi with *Bgh* and 116 hpi with *Ep* in chosen mutant lines (Fig. 4B). The penetration efficiency comprises cells with either developed haustoria or undergoing cell death (Fig. 4A). Since *Ep* spores germinate slowly but with higher penetration efficiency in *Arabidopsis*, we prolonged inoculation time for *Ep* penetration evaluation. In accordance with published data (Pečenková *et al.*, 2011), *exo70B2* demonstrated a higher occurrence of deviated papillae, but also increase of penetration success of *Ep* (Fig. 4B). Unlike *exo70B2*, *exo70B1* mutant showed only mild increase in penetration efficiency of *Bgh*, which might be connected with hypersensitivity of *exo70B1* mutant. The core exocyst mutant lines showed significant increase in the

formation of deviated papillae and penetration success of *Bgh* and *Ep* (Fig. 4B). Taken together, these results indicates exocyst complex mediates proper formation of defensive papille and is involved in non-host penetration resistance.

Figure 4

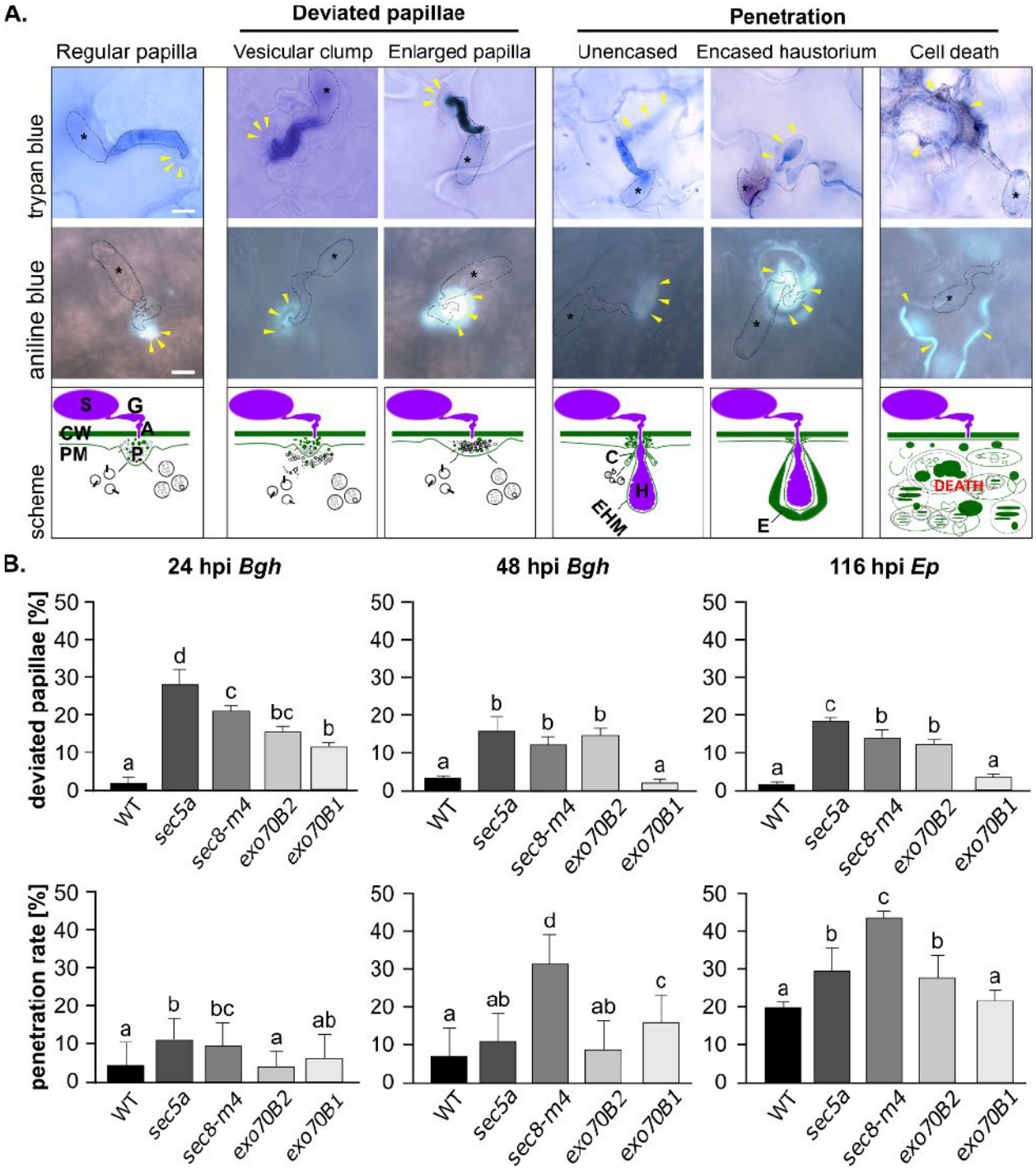
A.
Deviated papillae
Penetration
Regular papilla
Vesicular clump
Enlarged papilla
Unencased
Encased haustorium
Cell death
trypan blue
aniline blue
scheme
S
G
A
CW
PM
P
C
H
EHM
E
DEATH
B.
24 hpi Bgh
48 hpi Bgh
116 hpi Ep
deviated papillae [%]
penetration rate [%]
WT
sec5a
sec8-m4
exo70B2
exo70B1

Exocyst and SYP121 disruption cause similar defect in penetration resistance

Since the exocyst complex operates in the secretory pathway, we inspected if its role in the penetration defence could be similar to the previously reported role of SYP121, which is crucial for proper timing of papillae development and related callose deposition upon infection with *Bgh* (Assaad et al., 2004c; Nielsen et al., 2012d). We analysed the development of haustoria (Fig. 5A), as an obvious penetration marker, in leaves together with the activation of PCD (Fig. 5B) in *sec8-m4* core subunit mutant and in *exo70B2,* in comparison with control lines WT and *syp121* mutant. The knock-down mutant *sec8-m4* plants exhibited normal growth under standard cultivation conditions (Cole *et al.*, 2005). The same applies to the KO mutant *syp121*, under the optimal growth conditions (Collins et al., 2003b; Eisenach et al., 2012). In our experiment the mutant *sec8-m4* allowed faster penetration of *Bgh* than the WT, but slower than *syp121* (Fig. 5A). The *exo70B2* penetration was slightly higher than WT (Fig. 5A), thus its major defect upon the *Bgh* infection are papillae with the vesicular clump formation. Both *sec8-m4* and *syp121* mutants exhibited the same trend in the PCD rate - the PCD gradually increased until bursting at 72 hpi. This burst occurred also in WT and *exo70B2,* but with less intensity (Fig. 5B). In this time point, most of the previously attacked cells underwent the PCD, therefore the number of observed haustoria dropped down. This tendency showed that in both mutants the activation of PCD occurred normally as in WT. Since the higher penetration success of *Bgh* in *syp121* has been associated with the delay in callose deposition in early defensive papillae development, we verified the amount of papillary callose in our mutant lines (Fig. 5C). We observed the comparable delay in callose deposition for *sec8-m4* and *syp121* mutants, while *exo70B2* mutant exhibited the strongest inhibition. These results were in contrast with the relative weak penetration defect of *exo70B2* and *sec8-m4* mutants that reflects incidence of created haustoria and dead cells (Fig. 5A, C).

Figure 5

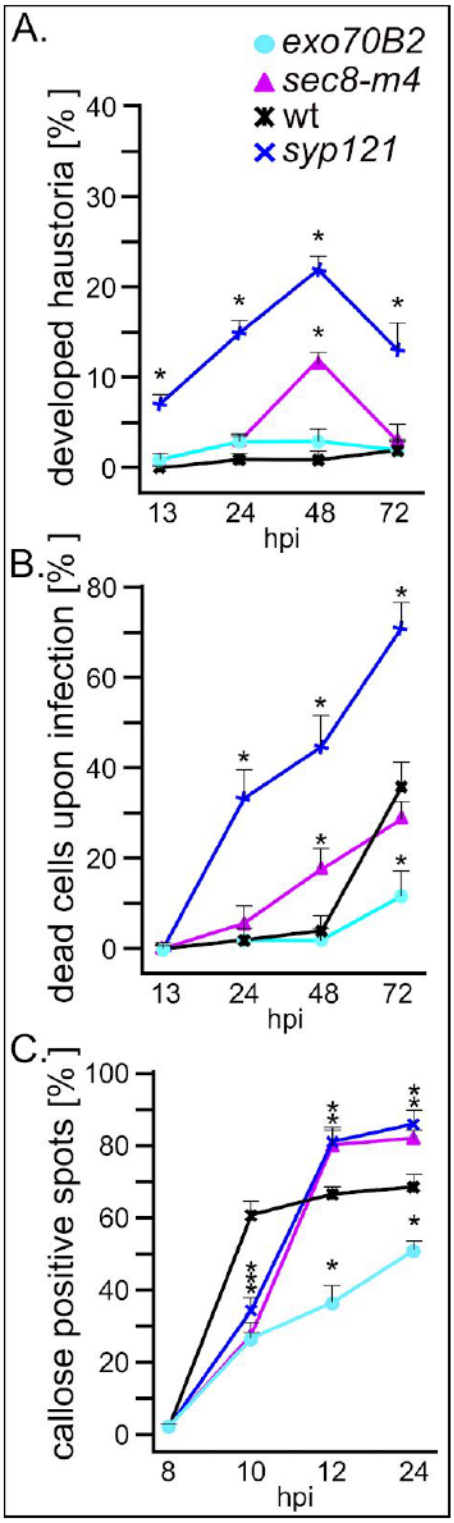
A.
exo70B2
sec8-m4
wt
syp121
developed haustoria [%]
40
30
20
10
0
13
24
48
72
hpi
B.
dead cells upon infection [%]
80
60
40
20
0
13
24
48
72
hpi
C.
callose positive spots [%]
100
80
60
40
20
0
8
10
12
24
hpi

The EXO70B2 containing exocyst complex interacts with SYP121

For non-host resistance, the proper functioning of SYP121 dependent secretory pathway is necessary. Our results indicate a connection between exocyst and SYP121 driven secretory pathways exists. Similar to SYP121, EXO70B2 expression response to non-adapted powdery mildew treatment and both accumulates in papilla and encasement structure (Meyer et al., 2009). However, the SYP121 has C-terminal transmembrane domain and as a permanent membrane protein undergoes extensive recycling from PM due to which ends in exosomes filling also papilla body (cit). In contrast, exocyst is cytoplasmic protein complex which may transiently associate with membrane (Hala et al. 2008, Fendrych et al. 2013). Thus, we suggest if EXO70B2 containing exocyst cooperates with functional pool of SYP121 they meet at the PM domain of papilla. To examine their common role, we observed the co-localisation of mRuby2-EXO70B2 with GFP-SYP121 upon *Bgh* attack (Fig. 6A). According to our hypothesis, both proteins co-localised at the papilla periphery (white colour) and their co-localisation vanished in plasmolysed cells, which documented the Pearson correlation test in graph (Fig. 6A).

To address the possible direct association between the EXO70B2 containing exocyst and SYP121, we tested their possible direct interaction. In the yeast-two-hybrid system, out of many pairs tested (AD-SYP121ΔC/BD-EXO70A1, EXO70B1, EXO70B2, EXO70H1, SEC3a, SEC5a, SEC6, SEC8, SEC10a, SEC15b, EXO84b) we detected only weak interaction of SYP121ΔC, free from transmembrane domain, with EXO70B2 and EXO70B1 (Fig. 6B). As the positive control, we used known SEC3a/EXO70A1 interaction pair (Hála (Hala et al., 2008b). Since the interaction in yeast represent rather structural ability of tested proteins to interact and might be biologically irrelevant, we further performed the co-immunoprecipitation assay in transgenic *Arabidopsis* plants expressing both GFP-SYP121 and mCherry-EXO70B2. To determine whether SYP121 interacts with EXO70B2 upon fungal attack, we treated plants with *Bgh* before sampling. With the same input concentration, GFP-SYP121 as a bait bound EXO70B2 in time 0, 4, and 8 hpi (Fig. 6C). Although, the interaction in time 0 was relatively weak, it

suggests the ability of SYP121 to interact with the exocyst complex in normal conditions. Therefore, we examined the GFP-SYP121 bound fraction with additional specific anti-exocyst antibodies. Hence we obtained in the eluted fraction from SYP121 two exocyst core subunits SEC6 and SEC3, which we did not detect in the control free-GFP bound fraction (Fig. 6D). According to published work exocyst form a complex in plants (Hala et al. 2008, Fendrych et al. 2013). Therefore, we propose wholle exocyst complex has the ability to interact with SYP121 and the EXO70B2 variant of it may possess eventual specialization of such interaction in non-host resistance in *Arabidopsis*.

EXO70B2 containing exocyst and SYP121 cooperate in penetration resistance

We decided to test further the relevance of its interaction on genetic level. Therefore we tested both double mutants *exo70B1/syp121* and *exo70B2/syp121* in penetration resistance to *Bgh*. Although there was not a significant difference in a total number of interactions (Fig. 7A), *exo70B2/syp121* double mutant had significantly decreased number of regular papillae in comparison with single *syp121* (Fig. 7B). Both double mutants had increased number of unencased haustoria (Fig. 7C). Only *exo70B2/syp121* double mutant, however, had decreased number of encased haustoria when compared to *syp121* single mutant (Fig. 7C). The pronounced double mutant phenotype of *exo70B2/syp121* was even more apparent with respect to the reduction of callose deposition signal in inoculated leaves (callose from haustoria and papillae; Fig. 7D). Thus, double mutant *exo70B2/syp121* had significantly reduced defence efficiency against *Bgh*, unlike the *exo70B1/syp121*, which did not differ from *syp121*.

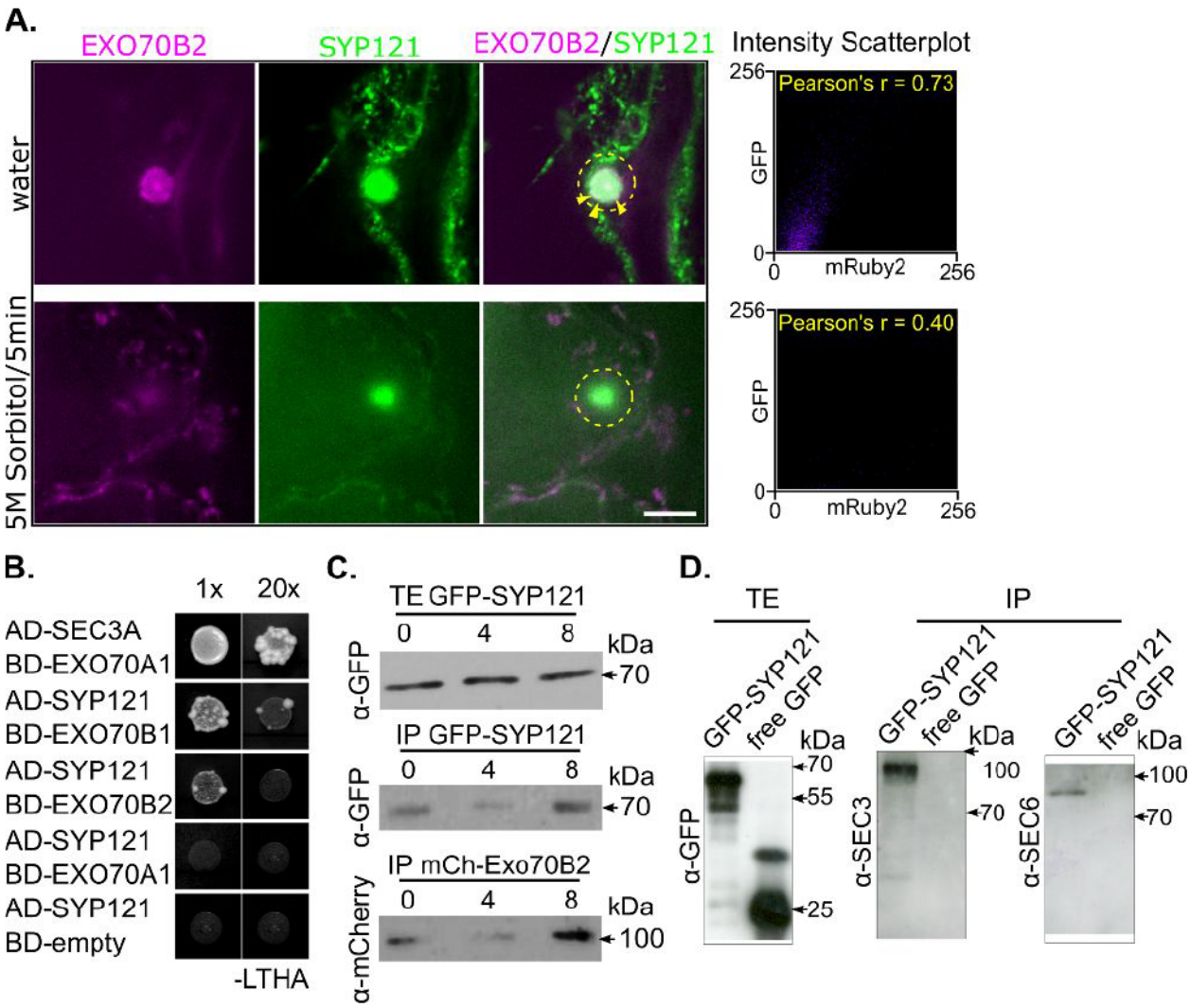
A.
EXO70B2
SYP121
EXO70B2/SYP121
Intensity Scatterplot
water
5M Sorbitol/5min
Pearson's r = 0.73
Pearson's r = 0.40
GFP
mRuby2
256
0
B.
1x
20x
AD-SEC3A
BD-EXO70A1
AD-SYP121
BD-EXO70B1
AD-SYP121
BD-EXO70B2
AD-SYP121
BD-EXO70A1
AD-SYP121
BD-empty
-LTHA
C.
TE GFP-SYP121
IP GFP-SYP121
IP mCh-Exo70B2
0
4
8
kDa
70
100
α-GFP
α-mCherry
D.
TE
IP
GFP-SYP121
free GFP
kDa
70
55
25
100
α-GFP
α-SEC3
α-SEC6

Figure 6

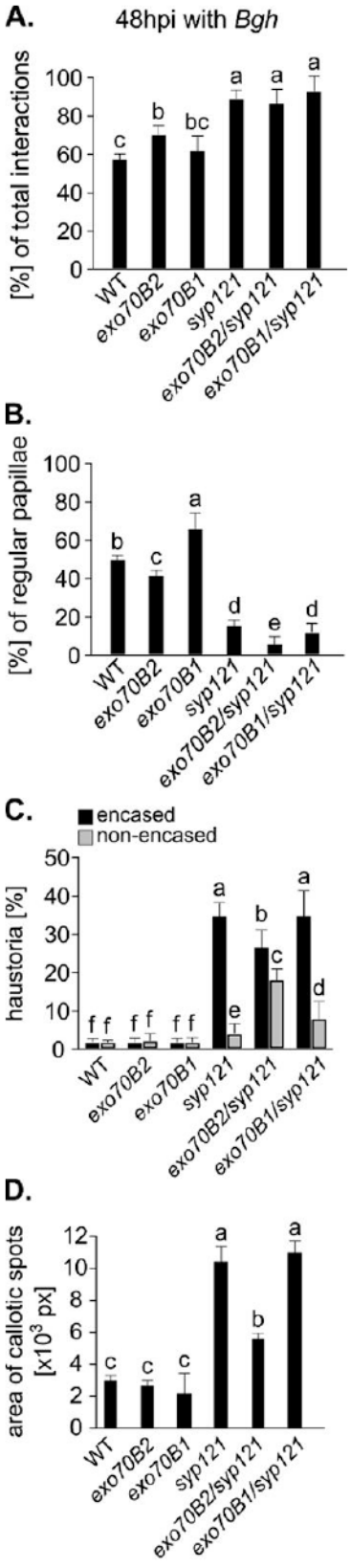
A.
48hpi with Bgh
[%] of total interactions
100
80
60
40
20
0
c
b
bc
a
a
a
WT
exo70B2
exo70B1
syp121
exo70B2/syp121
exo70B1/syp121
B.
[%] of regular papillae
100
80
60
40
20
0
b
c
a
d
e
d
WT
exo70B2
exo70B1
syp121
exo70B2/syp121
exo70B1/syp121
C.
encased
non-encased
haustoria [%]
50
40
30
20
10
0
f f
f f
f f
a
e
b
c
a
d
WT
exo70B2
exo70B1
syp121
exo70B2/syp121
exo70B1/syp121
D.
area of callotic spots [x10³ px]
12
10
8
6
4
2
0
c
c
c
a
b
a
WT
exo70B2
exo70B1
syp121
exo70B2/syp121
exo70B1/syp121

Figure 7

Figure 8

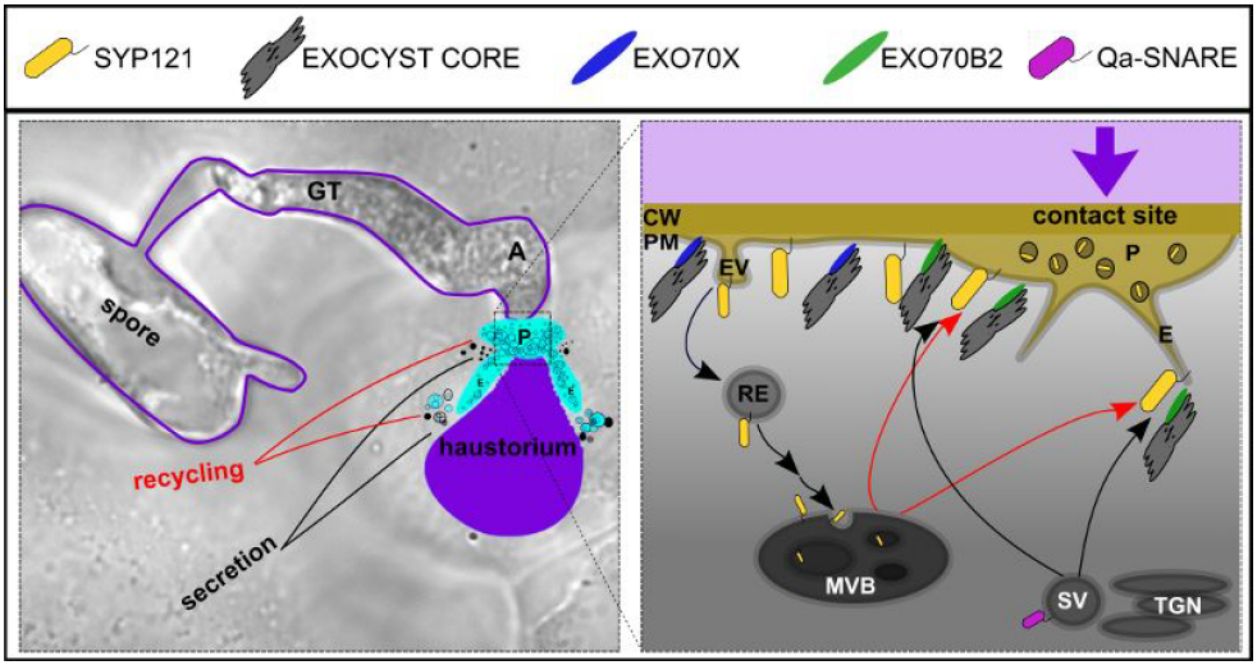

Discussion

The model system of interactions between non-host pathogen such as *Blumeria graminis* and *Arabidopsis thaliana* has been successfully used in studies of the role of the secretory pathway in the plant immunity before. In this report, we analysed the cell immunity phenotypes of several *Arabidopsis* lines mutated in exocyst subunit genes in defence response against *Bgh* and *Ep*. We showed that the exocyst complex involving EXO70B2 is required for full penetration resistance against non-adapted biotrophic fungi.

The exocyst is the major regulator of plant cell secretion and polarity, so disruption of the complex leads to severe growth phenotypes (Synek (Synek et al., 2006; Hala et al., 2008a), 2006; Hála (Synek et al., 2006; Hala et al., 2008a). In order to avoid pleiotropic mutation effects and to study the specific role of plant exocyst in reaction to fungal penetration, we worked with weak allele lines of core exocyst subunits *sec8-m4*, *sec5a-1* and *sec15b-1* that do not have severe growth phenotype. For these mutants, we were able to describe new interaction phenotypes resulting from a defence reaction of plant cells with impaired secretory machinery, apart from the previously

described stages of *Bgh* progression in WT (Takemoto (Takemoto et al., 2006b). Along with the vesicular clump, which has been previously characterised as a vesicular halo in the *exo70B2* mutants (Pečenková (Pecenkova et al., 2011c), we newly described the presence of enlarged papillae. Using aniline blue staining, we showed that in the papillae with the clump, the aniline blue positive signal was present in vesicular compartment surrounding the attack sites (Underwood, 2012; Chowdhury (Underwood, 2012; Chowdhury et al., 2014b). In contrast to faint aniline blue signal of papillae with the vesicular clump, the enlarged papillae reflected probably the ectopic callose deposition behind the regular papillae body (Fig. 1B). Such papillae resembled the phenotype of the overexpressing line PMR4 (Blümke et al., 2013). Although we categorized these papillae as deviated, we cannot exclude that they might be partly functional or transform into regular papillae or PCD as might be the case of *sec5a* mutant line (Fig. 1E, F). We also cannot exclude, that the enlarged callose deposition is the result of an impaired callose degradation. Even though all the exocyst mutants tested had diminished penetration resistance, they differed in some response categories. Therefore, we focused on mutant lines providing the most reproducible phenotype - the *exo70B2* and *sec8-m4*. We found that both have a distinct delay in penetration defence (Fig. 2), as well as the higher occurrence of successfully penetrated cells by haustoria (Fig. 1E, F). This phenotype resembles the more severe phenotype of *syp121*, in which major defect in penetration resistance is the delay of secretion marked by callose deposition in papillae (Assaad et al., 2004b; Nielsen et al., 2012c). The occurrence of deviated papillae, the lower penetration resistance, and the delayed callose deposition in the exocyst mutants reflected defects in the normal exocytotic machinery and importance of functional secretion pathway in defence over time. Recently, the exocyst and especially SEC5 role in callose secretion in PTI has been shown in tobacco (Du *et al.*, 2015; Du *et al.*, 2018). Here we showed that *exo70B2* and *sec8-m4* mutants have the delay in early callose deposition comparable to *syp121*, but their penetration resistance did not compromise so drastically. This result pointed to

the importance of secretion timing in penetration resistance but indicated callose as a possibly less important component in it.

The exocyst subunits have been demonstrated to work within the stable protein complex in yeast cells (Heider et al., 2015; Yue et al., 2017b; Picco et al., 2017). The *EXO70* gene has many paralogs in plant genomes (Elias et al., 2003b) and several EXO70 protein isoforms (ie EXO70B2) are targets of rapid proteolytic degradation (Stegmann et al., 2012b; Seo et al., 2016). Therefore we hypothesized, that the exocyst complex in plant cells is capable of exchanging EXO70 isoforms in order to target secretion to particular membrane domains as previously proposed (Zárský et al., 2009b; Zárský et al., 2013c). In this report, we focused on the EXO70B2, because it is the only exocyst subunit previously confirmed to be involved in the papillae formation and penetration resistance against non-adapted fungi. Its localisation has been analysed only transiently in *Nicotiana benthamiana* or *Arabidopsis* protoplast and never in papilla structure (Pecenkova et al., 2011d; Stegmann et al., 2012c). We compared the behaviour of EXO70B2, the closest paralog of EXO70B1 and the EXO70A1 (possibly major exocytotic EXO70 in Arabidopsis – Synek *et al.*, 2006), during the reaction to fungal penetration and confirmed the EXO70B2 is the isoform specifically involved in this particular process. We found only a faint cytoplasmic signal of the EXO70B2-GFP and the GFP-EXO70B1 at the edge of detection limit in non-treated seedlings or mature leaves. We spotted early protein upregulation and focal accumulation of the EXO70B2-GFP beneath the contact sites with *Bgh*. This was not a case of the GFP-EXO70B1 signal. Intriguingly, we showed that this increase in the EXO70B2-GFP protein level correlated with the EXO70A1 depletion, while the SEC8 stayed unchanged (Fig. 5). The level of EXO70B2 is thus tightly regulated in the context of a pathogen attack, as proposed before (Pecenková et al., 2011). This notion is in concert with previous discovery of both the EXO70A1 and the EXO70B2 being the target of regulated proteasomal degradation (Samuel et al., 2009; Stegmann et al., 2012d). After the recently reported different localisation of EXO70 isoforms in spatially different membrane domains of pollen tubes (Sekereš et al., 2017b), we thus indicate the

possible replacement of one EXO70 isoform by another one in time in response to a specific stimulus.

We demonstrated that both Arabidopsis EXO70Bs directly interact with soluble SYP121. We also showed that in defence against non-adapted powdery mildew, the simultaneous loss of EXO70B2 and SYP121 disturbed the penetration resistance and reduced the immunity response. Unlike the *exo70B1/syp121* double mutant, the *exo70B2/syp121* showed an additive phenotype in the penetration defence. This support a common role of SNARE and exocyst complexes in PTI. Nevertheless, the association between SYP121 and exocyst may found biological relevance in the canonical SNARE driven secretion, where different EXO70 may participate. The cooperation of EXO70B2 and SYP121 in non-host resistance has been proposed also based on their co-expression together with SNAP33 and VAMP722 (Humphry et al., 2010). However, the cooperation dynamics of the two proteins might differ in the papillae and the encasement formation, since we found the additive phenotype of *exo70B2/syp121* double mutant only for the encasement formation and not the papilla. It has been shown before, that the SYP121 transcytosis plays possibly an important role in the formation of both the defensive structures by two independent pathways. The formation of the encasement, but not the formation of papillae, relied on the function of ARA7, the GTPase closely related to ARA6 (Nielsen et al., 2017). The study has suggested a model in which the influence of the SYP121 on the papillae formation might be stronger than in the case of encasement formation, where another Qa-SNARE may take the main function (Hansen and Nielsen *et al.*, 2018). This would be in agreement with our results showing the *syp121* mutation epistasis over *exo70B2* mutation in papillae formation and the increased importance of the EXO70B2 function in the encasement formation (see model Fig. 7). Based on the localisation studies, our model introduces the membrane-localised EXO70B2 containing complex as a member of the secretory pathway, which drives a structural material towards papillae and encasements (Fig. 7). It remains to be further elucidated whether this reflects SYP121-dependent (cooperation on the level of the encasement formation) or - independent (SYP121

function in the papillae formation with subsequent EXO70B2 function in the encasement formation) process. One of the possible scenario is that exocyst role in MVB fusion with papilla and encasement membrane is reminiscent of the role of coiled-coil effector of ARA6 the PUF2, which is involved in targeting of RABs and VPS9a into endosomes and regulates vacuole loading (Ito et al., 2018)(Ito et al., 2018). A more detailed study is needed in order to assess these hypotheses.

The model situation of papillae development used in our study allowed us to demonstrate the functional relationship between SNARE and EXOCYST complexes. We conclude that our data on exocyst localisation and behaviour resembles dynamics of SYP121 SNARE complex. Moreover, our genetic analyses clearly indicate that the exocyst complex containing EXO70B2 is involved along with SYP121 in secretion process supporting the defence against non-adapted powdery mildew. It is possible, that the EXO70B2 containing exocyst complex recognizes the attack sites to target exocytosis and to regulate SYP121-mediated vesicle fusion there. Thus exocyst mediates the time-dependent focal secretion of papillae and encasements materials, including callose as one of the components. SYP121 localisation to the paramural space vs. exocyst absence in it indicates that additional mechanistic details and time sequence of exocyst vs. SNARE action will need further studies.

Material and Methods

Plant material

The seeds of *Arabidopsis thaliana* were sterilised and plated on 1/2 MS, 1% sucrose medium. The plants were grown in vitro for 10 days, and used for qRT-PCR, confocal imaging, or transferred into Jiffy tablets and grown in growth chamber under short day conditions (21°C, 10/14 light/dark h, 80% humidity and a light intensity of 125 µmol m^{-2} s^{-1} in a 400 - 700 nm range).

Pathogen inoculation and cytology

For pathogen inoculation experiments, plants were cultivated under short day conditions (21°C, 10/14 h, 75% humidity with a light intensity of 125 µmol m^{-2} s^{-1}). *Bgh* was cultivated continuously on fresh barley (Golden promise) grown under short day conditions (19°C, 10/14 h, 50% humidity, and a light intensity of 70 µmol m^{-2} s^{-1}). *Ep* was cultivated continuously on fresh pea (*Pisum sativum* variety petit provencal) cultivated under short day conditions (19°C, 10/14 h, 60% humidity and a light intensity of 70 µmol m^{-2} s^{-1}). The *Bgh* isolate A6 on barely genotype P01 was kindly provided by Laboratory of Pathological Plant Physiology. Max Planck Institute for Plant Breeding Research in Cologne Institute kindly provided the Ep isolate.

Plants, approximately 4 weeks old were inoculated by spreading of spores from infected barley or pea on the adaxial site of their leaves (from leaf to leaf). The 5th - 6th leaves were cut off at selected hpi and cleared with 96% ethanol or chloral hydrate. For callose visualisation cleared leaves were stained with an alkali solution of aniline blue (Eschrich and Currier, 1964). For penetration rate visualisation fungal structures were stained with 250 mg/ml trypan blue in lactophenol/ethanol solution (Vogel and Somerville, 2000b). For quantification purposes, we considered epidermal cells attacked by a single germinated spore. The additional protocol has been performed for the intense fungal structures staining as described by (Rate et al., 1999). Stained leaves were observed with classical epifluorescence microscopy or optical microscopy by Nikon Eclipse TE 2000-E inverted microscope.

Transcript detection and semiquantitative RT-PCR

RNA was isolated from 100-120 mg of 14 days old plants using the RNeasy kit (Qiagen). For PCR amplification, 2.5 µL of 20 × diluted cDNA was used and the gene-specific pairs of primers were used for semiquantitative PCR (Supplementary Table S8). The EXO70A1 was amplified as a cDNA quality control.

Plasmid construction and generation of transgenic lines

All constructs were prepared by Phusion PC (NEB, USA) reaction using as a template either genomic DNA for intronless genes and promoters or cDNA obtained from RNA as described in the previous passage. List of used primers is presented in table (S8), as well as lengths of amplified fragments, restriction sites used for cloning procedure and destination vectors.

The sequenced vectors were transformed into *Agrobacterium tumefaciens* GV3101 strain. *Arabidopsis* WT or respective mutants were transformed by *Agrobacterium*-mediated floral dip method (Clough and Bent, 1998).

Microscopy

Microscopic observation of Arabidopsis plantlets attacked with pathogens was done by an inverted spinning disk confocal microscope with a high-resolution camera (Yokogawa CSU-X1 on Nikon Ti-E platform, laser box Agilent MLC400, with sCMOS camera Andor Zyla CSU-X1). The dynamic study was done with a high-speed camera (with sCMOS Andor iXon DU-897), using filter stringent cubes for GFP and RFP. Nikon Plan Apochromat x60 WI (NA = 1.2) and Plan Apochromat x100 OI (NA = 1.45) objective lenses were used for imaging, using 488- and 561-nm laser lines. Exposure time was 700 ms, 488 nm laser power of 75%. Fluorescence profiles and acquired images were exported from NIS ELEMENTS 4.1 software (Nikon, Tokyo, Japan) – identical settings were used for each image. Figures were then analysed in ImageJ Fiji software (http://rsbweb.nih.gov/ij/). Microscopic analysis of tissue staining with aniline or trypan blue was performed using an Olympus BX51 microscope with attached DP50 camera x100 OI (NA = 1.35) objective (Olympus; Trypan blue) or Zeiss AxioImager ApoTome2 microscope 20x objective (Aniline blue). For fungal structure visualisation in vivo the propidium iodide PI 1:500 or FM4-64 dye 1:1000 diluted in water was used. To perform lambda scan the Zeiss LSM 880 confocal scanning microscope with a Zeiss C-Apochromat 40x (NA = 1.2) W Korr FCS M27 or C-Apochromat x63 OI (NA = 1.45) objective was used. Excitation wavelengths used were 488 nm for GFP and 561 nm for

mRuby2, PI and FM4-64. The linear unmixing was performed with the ZEISS BLACK software.

Yeast Two-Hybrid Assay

The SYP121 DNA (obtained from Riken) was amplified from cDNA with primers excluding the transmembrane domain and cloned into pGADT7 vector (Clontech Laboratories, Inc.). All the other exocyst constructs used in the study have already been described (Hala et al., 2008a; Pecenková et al., 2011; Zárský et al., 2013a; Vukašinović et al., 2014). Different pGBKTs with pGAD with an inserted non-coding piece of vector pENTR3C were used as negative controls. At least 10 positive colonies from –Leu/–Trp plates were resuspended in 150µl of sterile water, diluted 30x and 900x, and subsequently plated onto –Leu/–Trp/–His/-Ade plate.

Protein extraction, SDS Gel Electrophoresis and Western Blot

Total protein extracts were isolated from 2-4 weeks old plants transformed with EXO70B2-GFP in different time points 0-24 hpi *Bgh* or water (mock) inoculation. The protein extraction Sec6/8 buffer adjusted for the exocyst extraction was used (20 mM HEPES, pH 6.8, 150 mM NaCl, 1 mM EDTA, 1 mM DTT, and 0.5% Tween, supplemented with 13 protease inhibitor cocktail (Sigma-Aldrich). After one hour of lysis, the extracts were spinned down and the supernatants were boiled with 6x SDS loading buffer.

The proteins were loaded on 10% SDS-PAGE and blotted to a nitrocellulose membrane. The membrane was stained with ponceau S solution and blocked overnight with 5% non-fat dry milk in PBS (137 mM NaCl, 2.7 mM KCl, 10 mM Na2HPO4, and 2 mM KH2PO4, pH 7.4, 0.25% Tween 20). Primary antibody dilutions in PBS were as follows: monoclonal mouse mCherry (Novus Biologicals), 1:1000; polyclonal rabbit anti-GFP (Invitrogen), 1:800; polyclonal rabbit antibodies anti-AtSEC3, 1:5000; anti-AtSEC5, 1:5000; anti-AtSEC6 (Agrisera Sweeden), 1:10000; anti-AtSEC8 (Agrisera Sweeden), 1:8000; anti-AtSEC10, 1:10000; anti-AtSEC15a, 1:1000 and anti-AtEXO84b,

1:1000. Appropriate secondary horseradish peroxidase–conjugated antibodies (Promega, Madison, WI, USA) were applied followed by chemiluminescent ECL detection (Amersham, GE Healthcare, Chicago, IL, USA).

Coimmunoprecipitation

*Arabi*dopsis seedlings (1 g of 10-day-old) were used for the co-immunoprecipitation of proteins. Protein complexes with GFP-SYP121-GFP and freeGFP as a control, were isolated using the μMACS GFP-tagged protein isolation kit (Miltenyi Biotec), according to the manufacturer's instructions. The only exception was a utilisation of the Sec6/8 buffer (Hala et al., 2008a) as a wash buffer, two times and lysis buffer provided in the kit as a third more stringent wash. Bound proteins were eluted with 100 μL of the preheated elution buffer. In order to analyse bound proteins in an eluted fraction, SDS-PAGE and western blot were performed.

Acknowledgment

This work was supported by Czech Science Foundation (CSF/GACR) project GA15-14886S and by NPUILO1417 of MEYS CR. It was founded by terminated student project GAUK-1102214 by Grant Agency of Charles University. The Institute of Experimental Botany (IEB) Imaging Facility is supported by the Operational Programme Prague Competitiveness (OPPC) CZ.2.16/3.1.00/21519 and Czech-BioImaging large RI project (LM2015062 funded by MEYS CR).

Authors would like to thank Peter Sabol for help with text editing and cloning assistance, Martin Potocký for fruitful discussion and image software guidance and Jana Šťovíčková for reliable technical support.

Author Contributions

Conceived and designed the experiments: JO, TP, VZ. Performed the experiments: JO, TP. Analysed the data: JO. Contributed reagents/materials/analysis tools: JO, TP, JS, IK. Wrote the paper: JO, TP, JS, VZ.

References

Assaad, F. F., Qiu, J.-L., Youngs, H., Ehrhardt, D., Zimmerli, L., Kalde, M., Wanner, G., Peck, S. C., Edwards, H., Ramonell, K., et al. (2004a). The PEN1 syntaxin defines a novel cellular compartment upon fungal attack and is required for the timely assembly of papillae. *Mol. Biol. Cell* **15**:5118–5129.

Assaad, F. F., Qiu, J.-L., Youngs, H., Ehrhardt, D., Zimmerli, L., Kalde, M., Wanner, G., Peck, S. C., Edwards, H., Ramonell, K., et al. (2004b). The PEN1 syntaxin defines a novel cellular compartment upon fungal attack and is required for the timely assembly of papillae. *Mol. Biol. Cell* **15**:5118–5129.

Assaad, F. F., Qiu, J.-L., Youngs, H., Ehrhardt, D., Zimmerli, L., Kalde, M., Wanner, G., Peck, S. C., Edwards, H., Ramonell, K., et al. (2004c). The PEN1 syntaxin defines a novel cellular compartment upon fungal attack and is required for the timely assembly of papillae. *Mol. Biol. Cell* **15**:5118–5129.

Bestwick, C. S., Bennett, M. H., and Mansfield, J. W. (1995). Hrp Mutant of Pseudomonas syringae pv phaseolicola Induces Cell Wall Alterations but Not Membrane Damage Leading to the Hypersensitive Reaction in Lettuce. *Plant Physiol.* **108**:503–516.

Bloch, D., Pleskot, R., Pejchar, P., Potocký, M., Trpkošová, P., Cwiklik, L., Vukašinović, N., Sternberg, H., Yalovsky, S., and Žárský, V. (2016). Exocyst SEC3 and Phosphoinositides Define Sites of Exocytosis in Pollen Tube Initiation and Growth. *Plant Physiol.* **172**:980–1002.

Blümke, A., Somerville, S. C., and Voigt, C. A. (2013). Transient expression of the *Arabidopsis thaliana* callose synthase PMR4 increases penetration resistance to powdery mildew in barley. *Adv. Biosci. Biotechnol.* **04**:810–813.

Chowdhury, J., Henderson, M., Schweizer, P., Burton, R. A., Fincher, G. B., and Little, A. (2014a). Differential accumulation of callose, arabinoxylan and cellulose in nonpenetrated versus penetrated papillae on leaves of barley infected with Blumeria graminis f. sp. hordei. *New Phytol.* **204**:650–660.

Chowdhury, J., Henderson, M., Schweizer, P., Burton, R. A., Fincher, G. B., and Little, A. (2014b). Differential accumulation of callose, arabinoxylan and cellulose in nonpenetrated versus penetrated papillae on leaves of barley infected with Blumeria graminis f. sp. hordei. *New Phytol.* **204**:650–660.

Clough, S. J., and Bent, A. F. (1998). Floral dip: a simplified method forAgrobacterium-mediated transformation ofArabidopsis thaliana. *Plant J.* **16**:735–743.

Cole, R. A., Synek, L., Zarsky, V., and Fowler, J. E. (2005a). SEC8, a subunit of the putative Arabidopsis exocyst complex, facilitates pollen germination and competitive pollen tube growth. *Plant Physiol.* **138**:2005–2018.

Cole, R. A., Synek, L., Zarsky, V., and Fowler, J. E. (2005b). SEC8, a subunit of the putative Arabidopsis exocyst complex, facilitates pollen germination and competitive pollen tube growth. *Plant Physiol.* **138**:2005–2018.

Collins, N. C., Thordal-Christensen, H., Lipka, V., Bau, S., Kombrink, E., Qiu, J.-L., Hückelhoven, R., Stein, M., Freialdenhoven, A., Somerville, S. C., et al. (2003a). SNARE-protein-mediated disease resistance at the plant cell wall. *Nature* **425**:973–977.

Collins, N. C., Thordal-Christensen, H., Lipka, V., Bau, S., Kombrink, E., Qiu, J.-L., Hückelhoven, R., Stein, M., Freialdenhoven, A., Somerville, S. C., et al. (2003b). SNARE-protein-mediated disease resistance at the plant cell wall. *Nature* **425**:973–977.

Consonni, C., Humphry, M. E., Hartmann, H. A., Livaja, M., Durner, J., Westphal, L., Vogel, J., Lipka, V., Kemmerling, B., Schulze-Lefert, P., et al. (2006). Conserved requirement for a plant host cell protein in powdery mildew pathogenesis. *Nat. Genet.* **38**:716–720.

Cui, H., Tsuda, K., and Parker, J. E. (2015). Effector-Triggered Immunity: From Pathogen Perception to Robust Defense. *Annu. Rev. Plant Biol.* **66**:487–511.

Cvrčková, F., Grunt, M., Bezvoda, R., Hála, M., Kulich, I., Rawat, A., and Zárský, V. (2012). Evolution of the land plant exocyst complexes. *Front. Plant Sci.* **3**:159.

Dubuke, M. L., Maniatis, S., Shaffer, S. A., and Munson, M. (2015). The Exocyst Subunit Sec6 Interacts with Assembled Exocytic SNARE Complexes. *J. Biol. Chem.* **290**:28245–28256.

Ebine, K., Fujimoto, M., Okatani, Y., Nishiyama, T., Goh, T., Ito, E., Dainobu, T., Nishitani, A., Uemura, T., Sato, M. H., et al. (2011). A membrane trafficking pathway regulated by the plant-specific RAB GTPase ARA6. *Nat. Cell Biol.* **13**:853–859.

Eisenach, C., Chen, Z.-H., Grefen, C., and Blatt, M. R. (2012). The trafficking protein SYP121 of Arabidopsis connects programmed stomatal closure and K^+ channel activity with vegetative growth. *Plant J.* **69**:241–251.

Elias, M., Drdova, E., Ziak, D., Bavlnka, B., Hala, M., Cvrckova, F., Soukupova, H., and Zarsky, V. (2003a). The exocyst complex in plants. *Cell Biol. Int.* **27**:199–201.

Elias, M., Drdova, E., Ziak, D., Bavlnka, B., Hala, M., Cvrckova, F., Soukupova, H.,

and Zarsky, V. (2003b). The exocyst complex in plants. *Cell Biol. Int.* **27**:199–201.

Ellinger, D., Glöckner, A., Koch, J., Naumann, M., Stürtz, V., Schütt, K., Manisseri, C., Somerville, S. C., and Voigt, C. A. (2014). Interaction of the Arabidopsis GTPase RabA4c with its effector PMR4 results in complete penetration resistance to powdery mildew. *Plant Cell* **26**:3185–3200.

Eschrich, W., and Currier, H. B. (1964). Identification of Cauose by its Diachrome and Fluorochrome Reactions. *Stain Technol.* **39**:303–307.

Fendrych, M., Synek, L., Pecenková, T., Toupalová, H., Cole, R., Drdová, E., Nebesárová, J., Sedinová, M., Hála, M., Fowler, J. E., et al. (2010). The Arabidopsis exocyst complex is involved in cytokinesis and cell plate maturation. *Plant Cell* **22**:3053–3065.

Fendrych, M., Synek, L., Pecenková, T., Drdová, E. J., Sekeres, J., de Rycke, R., Nowack, M. K., and Zársky, V. (2013a). Visualization of the exocyst complex dynamics at the plasma membrane of Arabidopsis thaliana. *Mol. Biol. Cell* **24**:510–520.

Fendrych, M., Synek, L., Pecenková, T., Drdová, E. J., Sekeres, J., de Rycke, R., Nowack, M. K., and Zársky, V. (2013b). Visualization of the exocyst complex dynamics at the plasma membrane of Arabidopsis thaliana. *Mol. Biol. Cell* **24**:510–520.

Guo, W., Roth, D., Gatti, E., De Camilli, P., and Novick, P. (1997). Identification and characterization of homologues of the Exocyst component Sec10p. *FEBS Lett.* **404**:135–139.

Hala, M., Cole, R., Synek, L., Drdova, E., Kulich, I., Pecenkova, T., Hochholdinger, F., Cvrckova, F., Fowler, J., and Zarsky, V. (2008a). Exocyst complex functions in plant development. *Comp. Biochem. Physiol. A Mol. Integr. Physiol.* **150**:S189.

Hala, M., Cole, R., Synek, L., Drdova, E., Kulich, I., Pecenkova, T., Hochholdinger, F., Cvrckova, F., Fowler, J., and Zarsky, V. (2008b). Exocyst complex functions in plant development. *Comp. Biochem. Physiol. A Mol. Integr. Physiol.* **150**:S189.

Heath, M. C., and Heath, I. B. (1971). Ultrastructure of an immune and a susceptible reaction of cowpea leaves to rust infection. *Physiological Plant Pathology* **1**:277–287.

Heider, M. R., Gu, M., Duffy, C. M., Mirza, A. M., Marcotte, L. L., Walls, A. C., Farrall, N., Hakhverdyan, Z., Field, M. C., Rout, M. P., et al. (2015). Subunit connectivity, assembly determinants and architecture of the yeast exocyst complex. *Nat. Struct. Mol. Biol.* **23**:59–66.

Hsu, S. C., Ting, A. E., Hazuka, C. D., Davanger, S., Kenny, J. W., Kee, Y., and

Scheller, R. H. (1996). The mammalian brain rsec6/8 complex. *Neuron* **17**:1209–1219.

Humphry, M., Bednarek, P., Kemmerling, B., Koh, S., Stein, M., Göbel, U., Stüber, K., Pislewska-Bednarek, M., Loraine, A., Schulze-Lefert, P., et al. (2010). A regulon conserved in monocot and dicot plants defines a functional module in antifungal plant immunity. *Proc. Natl. Acad. Sci. U. S. A.* **107**:21896–21901.

Ito, E., Ebine, K., Choi, S.-W., Ichinose, S., Uemura, T., Nakano, A., and Ueda, T. (2018). Integration of two RAB5 groups during endosomal transport in plants. *Elife* **7**.

Kalmbach, L., Hématy, K., De Bellis, D., Barberon, M., Fujita, S., Ursache, R., Daraspe, J., and Geldner, N. (2017). Transient cell-specific EXO70A1 activity in the CASP domain and Casparian strip localization. *Nat Plants* **3**:17058.

Kato, N., Fujikawa, Y., Fuselier, T., Adamou-Dodo, R., Nishitani, A., and Sato, M. H. (2010). Luminescence detection of SNARE-SNARE interaction in Arabidopsis protoplasts. *Plant Mol. Biol.* **72**:433–444.

Kulich, I., Pečenková, T., Sekereš, J., Smetana, O., Fendrych, M., Foissner, I., Höftberger, M., and Zárský, V. (2013). Arabidopsis exocyst subcomplex containing subunit EXO70B1 is involved in autophagy-related transport to the vacuole. *Traffic* **14**:1155–1165.

Kulich, I., Vojtíková, Z., Sabol, P., Ortmannová, J., Neděla, V., Tihlaříková, E., and Žárský, V. (2018). Exocyst Subunit EXO70H4 Has a Specific Role in Callose Synthase Secretion and Silica Accumulation. *Plant Physiol.* **176**:2040–2051.

Kwon, C., Neu, C., Pajonk, S., Yun, H. S., Lipka, U., Humphry, M., Bau, S., Straus, M., Kwaaitaal, M., Rampelt, H., et al. (2008). Co-option of a default secretory pathway for plant immune responses. *Nature* **451**:835–840.

Lee, H.-A., Lee, H.-Y., Seo, E., Lee, J., Kim, S.-B., Oh, S., Choi, E., Choi, E., Lee, S. E., and Choi, D. (2017). Current Understandings of Plant Nonhost Resistance. *Mol. Plant. Microbe. Interact.* **30**:5–15.

Lipka, V., Dittgen, J., Bednarek, P., Bhat, R., Wiermer, M., Stein, M., Landtag, J., Brandt, W., Rosahl, S., Scheel, D., et al. (2005). Pre- and postinvasion defenses both contribute to nonhost resistance in Arabidopsis. *Science* **310**:1180–1183.

Lipka, U., Fuchs, R., and Lipka, V. (2008). Arabidopsis non-host resistance to powdery mildews. *Curr. Opin. Plant Biol.* **11**:404–411.

Meyer, D., Pajonk, S., Micali, C., O'Connell, R., and Schulze-Lefert, P. (2009). Extracellular transport and integration of plant secretory proteins into

pathogen-induced cell wall compartments. *Plant J.* **57**:986–999.

Nielsen, M. E., and Thordal-Christensen, H. (2012). Recycling of Arabidopsis plasma membrane PEN1 syntaxin. *Plant Signal. Behav.* **7**:1541–1543.

Nielsen, M. E., and Thordal-Christensen, H. (2013). Transcytosis shuts the door for an unwanted guest. *Trends Plant Sci.* **18**:611–616.

Nielsen, M. E., Feechan, A., Böhlenius, H., Ueda, T., and Thordal-Christensen, H. (2012a). Arabidopsis ARF-GTP exchange factor, GNOM, mediates transport required for innate immunity and focal accumulation of syntaxin PEN1. *Proc. Natl. Acad. Sci. U. S. A.* **109**:11443–11448.

Nielsen, M. E., Feechan, A., Böhlenius, H., Ueda, T., and Thordal-Christensen, H. (2012b). Arabidopsis ARF-GTP exchange factor, GNOM, mediates transport required for innate immunity and focal accumulation of syntaxin PEN1. *Proc. Natl. Acad. Sci. U. S. A.* **109**:11443–11448.

Nielsen, M. E., Feechan, A., Böhlenius, H., Ueda, T., and Thordal-Christensen, H. (2012c). Arabidopsis ARF-GTP exchange factor, GNOM, mediates transport required for innate immunity and focal accumulation of syntaxin PEN1. *Proc. Natl. Acad. Sci. U. S. A.* **109**:11443–11448.

Nielsen, M. E., Feechan, A., Böhlenius, H., Ueda, T., and Thordal-Christensen, H. (2012d). Arabidopsis ARF-GTP exchange factor, GNOM, mediates transport required for innate immunity and focal accumulation of syntaxin PEN1. *Proc. Natl. Acad. Sci. U. S. A.* **109**:11443–11448.

Nielsen, M. E., Jürgens, G., and Thordal-Christensen, H. (2017). VPS9a Activates the Rab5 GTPase ARA7 to Confer Distinct Pre- and Postinvasive Plant Innate Immunity. *Plant Cell* **29**:1927–1937.

Pecenkova, T., Hala, M., Kulich, I., Kocourkova, D., Drdova, E., Fendrych, M., Toupalova, H., and Zarsky, V. (2011a). The role for the exocyst complex subunits Exo70B2 and Exo70H1 in the plant-pathogen interaction. *J. Exp. Bot.* **62**:2107–2116.

Pecenkova, T., Hala, M., Kulich, I., Kocourkova, D., Drdova, E., Fendrych, M., Toupalova, H., and Zarsky, V. (2011b). The role for the exocyst complex subunits Exo70B2 and Exo70H1 in the plant-pathogen interaction. *J. Exp. Bot.* **62**:2107–2116.

Pecenkova, T., Hala, M., Kulich, I., Kocourkova, D., Drdova, E., Fendrych, M., Toupalova, H., and Zarsky, V. (2011c). The role for the exocyst complex subunits Exo70B2 and Exo70H1 in the plant-pathogen interaction. *J. Exp. Bot.* **62**:2107–2116.

Pecenkova, T., Hala, M., Kulich, I., Kocourkova, D., Drdova, E., Fendrych, M., Toupalova, H., and Zarsky, V. (2011d). The role for the exocyst complex subunits Exo70B2 and Exo70H1 in the plant-pathogen interaction. *J. Exp. Bot.* **62**:2107–2116.

Pecenková, T., Hála, M., Kulich, I., Kocourková, D., Drdová, E., Fendrych, M., Toupalová, H., and Zársky, V. (2011). The role for the exocyst complex subunits Exo70B2 and Exo70H1 in the plant-pathogen interaction. *J. Exp. Bot.* **62**:2107–2116.

Picco, A., Irastorza-Azcarate, I., Specht, T., Böke, D., Pazos, I., Rivier-Cordey, A.-S., Devos, D. P., Kaksonen, M., and Gallego, O. (2017). The In Vivo Architecture of the Exocyst Provides Structural Basis for Exocytosis. *Cell* **168**:400–412.e18.

Rate, D. N., Cuenca, J. V., Bowman, G. R., Guttman, D. S., and Greenberg, J. T. (1999). The gain-of-function Arabidopsis acd6 mutant reveals novel regulation and function of the salicylic acid signaling pathway in controlling cell death, defenses, and cell growth. *Plant Cell* **11**:1695–1708.

Rutter, B. D., and Innes, R. W. (2017). Extracellular Vesicles Isolated from the Leaf Apoplast Carry Stress-Response Proteins. *Plant Physiol.* **173**:728–741.

Samuel, M. A., Chong, Y. T., Haasen, K. E., Aldea-Brydges, M. G., Stone, S. L., and Goring, D. R. (2009). Cellular pathways regulating responses to compatible and self-incompatible pollen in Brassica and Arabidopsis stigmas intersect at Exo70A1, a putative component of the exocyst complex. *Plant Cell* **21**:2655–2671.

Schmelzer, E. (2002a). Cell polarization, a crucial process in fungal defence. *Trends Plant Sci.* **7**:411–415.

Schmelzer, E. (2002b). Cell polarization, a crucial process in fungal defence. *Trends Plant Sci.* **7**:411–415.

Sekereš, J., Pejchar, P., Šantrůček, J., Vukašinović, N., Žárský, V., and Potocký, M. (2017a). Analysis of Exocyst Subunit EXO70 Family Reveals Distinct Membrane Polar Domains in Tobacco Pollen Tubes. *Plant Physiol.* **173**:1659–1675.

Sekereš, J., Pejchar, P., Šantrůček, J., Vukašinović, N., Žárský, V., and Potocký, M. (2017b). Analysis of Exocyst Subunit EXO70 Family Reveals Distinct Membrane Polar Domains in Tobacco Pollen Tubes. *Plant Physiol.* **173**:1659–1675.

Seo, D. H., Ahn, M. Y., Park, K. Y., Kim, E. Y., and Kim, W. T. (2016). The N-Terminal UND Motif of the Arabidopsis U-Box E3 Ligase PUB18 Is Critical for the Negative Regulation of ABA-Mediated Stomatal Movement and Determines Its Ubiquitination Specificity for Exocyst Subunit Exo70B1. *Plant Cell* **28**:2952–2973.

Sivaram, M. V. S., Saporita, J. A., Furgason, M. L. M., Boettcher, A. J., and Munson, M. (2005). Dimerization of the exocyst protein Sec6p and its interaction with the t-SNARE Sec9p. *Biochemistry* **44**:6302–6311.

Stegmann, M., Anderson, R. G., Ichimura, K., Pecenkova, T., Reuter, P., Žársky, V., McDowell, J. M., Shirasu, K., and Trujillo, M. (2012a). The ubiquitin ligase PUB22 targets a subunit of the exocyst complex required for PAMP-triggered responses in Arabidopsis. *Plant Cell* **24**:4703–4716.

Stegmann, M., Anderson, R. G., Ichimura, K., Pecenkova, T., Reuter, P., Žársky, V., McDowell, J. M., Shirasu, K., and Trujillo, M. (2012b). The ubiquitin ligase PUB22 targets a subunit of the exocyst complex required for PAMP-triggered responses in Arabidopsis. *Plant Cell* **24**:4703–4716.

Stegmann, M., Anderson, R. G., Ichimura, K., Pecenkova, T., Reuter, P., Žársky, V., McDowell, J. M., Shirasu, K., and Trujillo, M. (2012c). The ubiquitin ligase PUB22 targets a subunit of the exocyst complex required for PAMP-triggered responses in Arabidopsis. *Plant Cell* **24**:4703–4716.

Stegmann, M., Anderson, R. G., Ichimura, K., Pecenkova, T., Reuter, P., Žársky, V., McDowell, J. M., Shirasu, K., and Trujillo, M. (2012d). The ubiquitin ligase PUB22 targets a subunit of the exocyst complex required for PAMP-triggered responses in Arabidopsis. *Plant Cell* **24**:4703–4716.

Stein, M., Dittgen, J., Sánchez-Rodríguez, C., Hou, B.-H., Molina, A., Schulze-Lefert, P., Lipka, V., and Somerville, S. (2006). Arabidopsis PEN3/PDR8, an ATP binding cassette transporter, contributes to nonhost resistance to inappropriate pathogens that enter by direct penetration. *Plant Cell* **18**:731–746.

Synek, L., Schlager, N., Eliás, M., Quentin, M., Hauser, M.-T., and Zárský, V. (2006). AtEXO70A1, a member of a family of putative exocyst subunits specifically expanded in land plants, is important for polar growth and plant development. *Plant J.* **48**:54–72.

Takemoto, D., Jones, D. A., and Hardham, A. R. (2006a). Re-organization of the cytoskeleton and endoplasmic reticulum in the Arabidopsis pen1-1 mutant inoculated with the non-adapted powdery mildew pathogen, Blumeria graminis f. sp. hordei. *Mol. Plant Pathol.* **7**:553–563.

Takemoto, D., Jones, D. A., and Hardham, A. R. (2006b). Re-organization of the cytoskeleton and endoplasmic reticulum in the Arabidopsis pen1-1 mutant inoculated with the non-adapted powdery mildew pathogen, Blumeria graminis f. sp. hordei. *Mol. Plant Pathol.* **7**:553–563.

TerBush, D. R., Maurice, T., Roth, D., and Novick, P. (1996). The Exocyst is a

multiprotein complex required for exocytosis in Saccharomyces cerevisiae. *EMBO J.* **15**:6483–6494.

Underwood, W. (2012). The plant cell wall: a dynamic barrier against pathogen invasion. *Front. Plant Sci.* **3**:85.

Vogel, J., and Somerville, S. (2000a). Isolation and characterization of powdery mildew-resistant Arabidopsis mutants. *Proc. Natl. Acad. Sci. U. S. A.* **97**:1897–1902.

Vogel, J., and Somerville, S. (2000b). Isolation and characterization of powdery mildew-resistant Arabidopsis mutants. *Proc. Natl. Acad. Sci. U. S. A.* **97**:1897–1902.

Vukašinović, N., and Žárský, V. (2016). Tethering Complexes in the Arabidopsis Endomembrane System. *Front Cell Dev Biol* **4**:46.

Vukašinović, N., Cvrčková, F., Eliáš, M., Cole, R., Fowler, J. E., Žárský, V., and Synek, L. (2014). Dissecting a Hidden Gene Duplication: The Arabidopsis thaliana SEC10 Locus. *PLoS One* **9**:e94077.

Vukašinović, N., Oda, Y., Pejchar, P., Synek, L., Pečenková, T., Rawat, A., Sekereš, J., Potocký, M., and Žárský, V. (2017). Microtubule-dependent targeting of the exocyst complex is necessary for xylem development in Arabidopsis. *New Phytol.* **213**:1052–1067.

Yue, P., Zhang, Y., Mei, K., Wang, S., Lesigang, J., Zhu, Y., Dong, G., and Guo, W. (2017a). Sec3 promotes the initial binary t-SNARE complex assembly and membrane fusion. *Nat. Commun.* **8**:14236.

Yue, P., Zhang, Y., Mei, K., Wang, S., Lesigang, J., Zhu, Y., Dong, G., and Guo, W. (2017b). Sec3 promotes the initial binary t-SNARE complex assembly and membrane fusion. *Nat. Commun.* **8**:14236.

Zárský, V., Cvrcková, F., Potocký, M., and Hála, M. (2009a). Exocytosis and cell polarity in plants - exocyst and recycling domains. *New Phytol.* **183**:255–272.

Zárský, V., Cvrcková, F., Potocký, M., and Hála, M. (2009b). Exocytosis and cell polarity in plants - exocyst and recycling domains. *New Phytol.* **183**:255–272.

Zárský, V., Kulich, I., Fendrych, M., and Pečenková, T. (2013a). Exocyst complexes multiple functions in plant cells secretory pathways. *Curr. Opin. Plant Biol.* **16**:726–733.

Zárský, V., Kulich, I., Fendrych, M., and Pečenková, T. (2013b). Exocyst complexes multiple functions in plant cells secretory pathways. *Curr. Opin. Plant Biol.*

16:726–733.

Zárský, V., Kulich, I., Fendrych, M., and Pečenková, T. (2013c). Exocyst complexes multiple functions in plant cells secretory pathways. *Curr. Opin. Plant Biol.* **16**:726–733.

Zeyen, R. J., Kruger, W. M., Lyngkjær, M. F., and Carver, T. L. W. (2002). Differential effects of D -mannose and 2-deoxy- D -glucose on attempted powdery mildew fungal infection of inappropriate and appropriate G ramineae. *Physiol. Mol. Plant Pathol.* **61**:315–323.

Zhao, T., Rui, L., Li, J., Nishimura, M. T., Vogel, J. P., Liu, N., Liu, S., Zhao, Y., Dangl, J. L., and Tang, D. (2015). A truncated NLR protein, TIR-NBS2, is required for activated defense responses in the exo70B1 mutant. *PLoS Genet.* **11**:e1004945.

Hansen LL and Nielsen ME. 2018. Plant exosomes: using an unconventional exit to prevent pathogen entry? *Journal of Experimental Botany* **1**: 59–68.

Du Y, Overdijk EJR, Berg JA, Govers F, Bouwmeester K. 2018. Solanaceous exocyst subunits are involved in immunity to diverse plant pathogens. *Journal of experimental botany.* **69:** 655-666

Supplementary 1

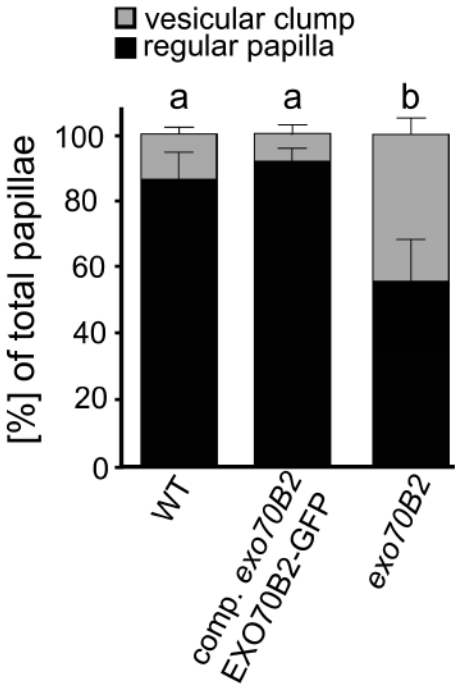

Supplementary 2

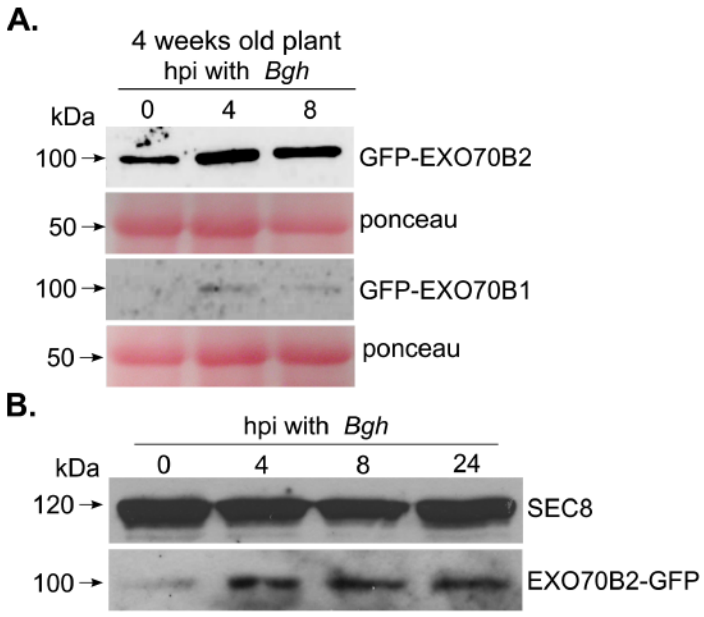

Supplementary 3

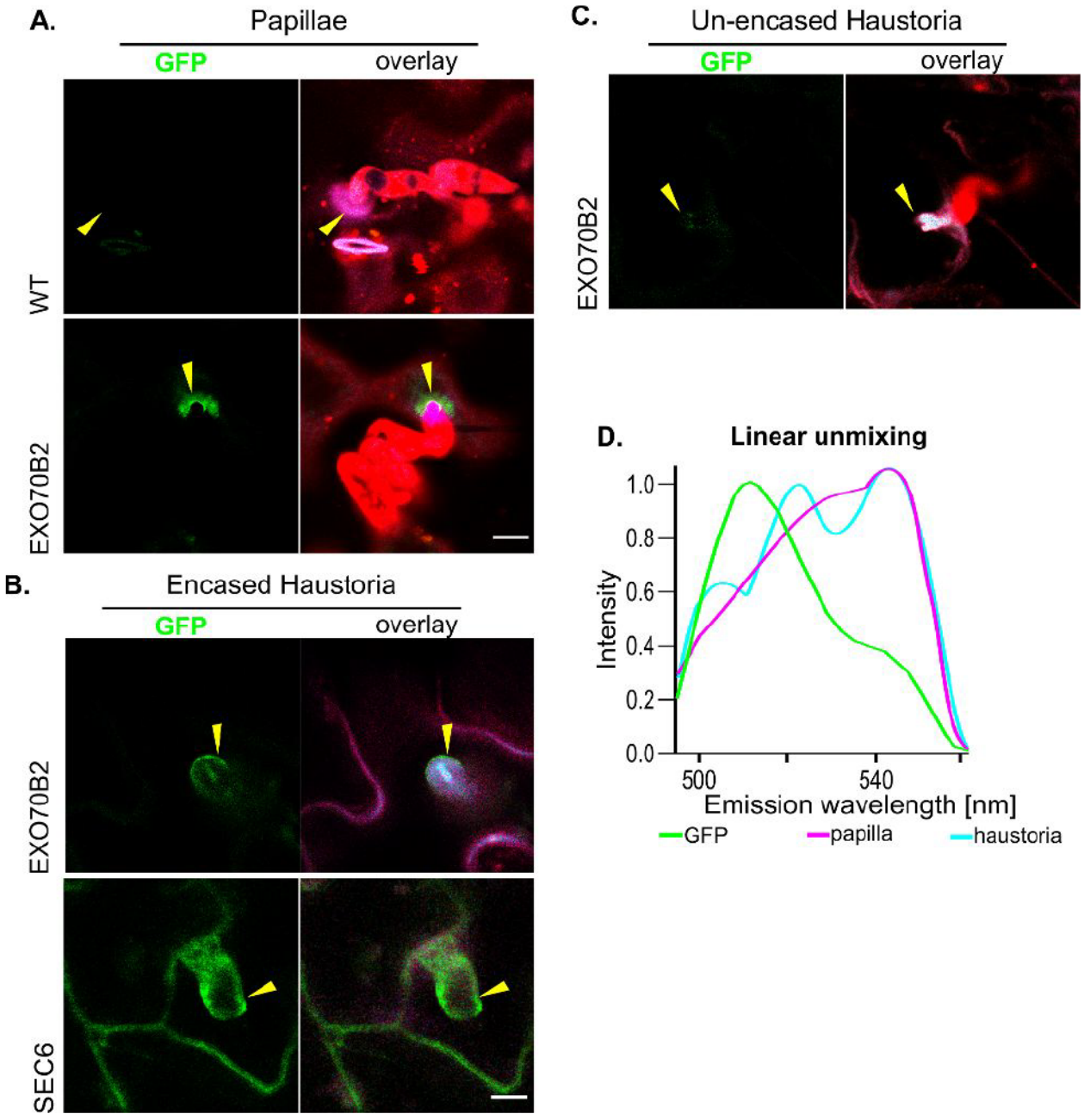

Supplementary 4

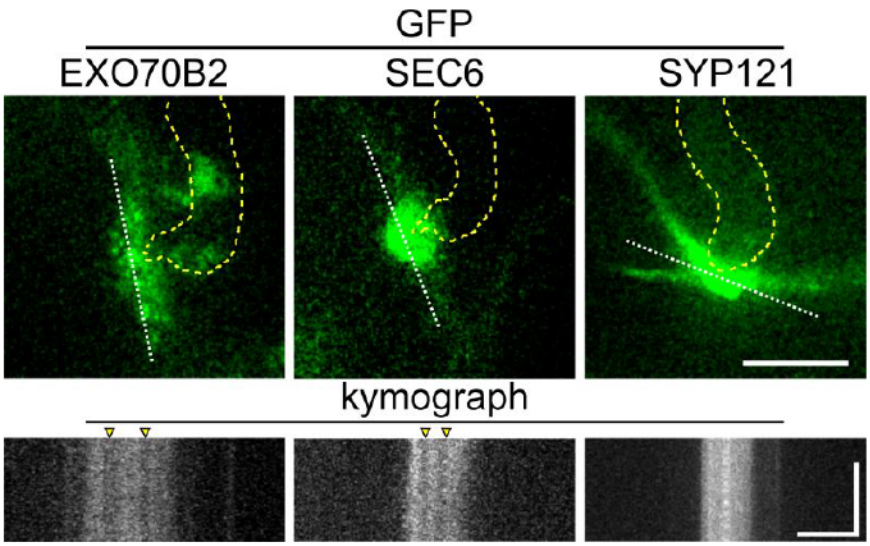

Figure 1 Category of interactions between exocyst mutants and non-host pathogens.

Bgh and *Ep* evoked the same types of reactions - in the columns: (A) Regular papillae; (B) Deviated papillae (either smaller than regular papilla but with vesicular clump or enlarged papilla); (C) Haustoria (completely unencased and partially or fully encased haustoria); (D) Cell death/isolated programmed cell death. From the top: the first row shows independent interactions visualized by hot-phenol trypan blue staining (blue colour visualizes fungal structures or dead cells); second row, aniline blue staining visualisation of the callose (different experiment); third row, schematic model of reactions to fungi (inspired by Meyer *et al.*, 2009). The phenotypic deviation in penetration resistance according to described interaction types is shown (E) 24 hpi or (F) 48 hpi with *Bgh*. The elevated total amount of interactions (A+B+C+D) highlights defects in plant immunity of exocyst core subunit mutants (E, F). The increased portion of deviated papillae indicates imbalanced secretion in pre-invasive basal resistance in exocyst mutants. A number of haustoria and cell death show the weakening in penetration resistance. The dataset for each genotype was counted from 100 germinated spores on defined leaf area, two leaves from each of five plants were analysed. For each column in the graph, the area complementary to 100 % presents the proportion of spores that did not provoke any reaction of the plant (empty bars). The experiment was repeated 4 times with similar results. The small letters indicate the significant difference calculated with one-way ANOVA (ANalysis Of VAriance) with post-hoc Tukey-Kramer HSD (Honestly Significant Difference), Z-score $p<0.01$. A appressorium; G germ tube; S spore; CW cell wall; PM plasma membrane; P papilla; C collar; EHM extrahaustorial membrane; H haustorium; E encasement. Yellow arrows mark outer borders of plant cell defensive structures. The black dashed line outlines fungal structures and the star marks a spore. Scale bars 5 µm.

Figure 2 Timescale analysis of penetration success of *Bgh*.

(A) cells with developed haustoria and (B) cells undergoing PCD in WT and *sec8-m4*, *exo70B2*, *syp121* mutant lines were counted on a defined leaf area. The data were taken at 13, 24, 48 and 72 hpi with *Bgh*. (C) the frequency of callose deposition counted on a defined leaf area at the sites of *Bgh* attack was followed at 8, 10, 12, 24 hpi. The experiment was repeated 3 times with similar trend. The asterisks indicate significant difference from WT in each time point if there are two or three the more genotypes were different in this time point. The statistical difference was calculated with one way ANOVA with post-hoc Tukey-Kramer HSD Z score $p<0.01$. Error bars represent standard error.

Figure 3 Exocyst subunits localised into defensive papilla.

(A) Signal accumulation of GFP-tagged exocyst subunits in papilla, for comparison the autofluorescence of fungal and plant cell structures are presented in the picture. The FM4-64 was used for visualisation of PM and fungal structures. For each line, the green channel (GFP/autofluorescence; left column), merged green and red channel (GFP with FM4-64 signal; middle) and brightfield channel (right) are shown. The Y-axis represents an intensity of a signal, the X-axis represents the length of the section. Yellow arrowheads point to the appressorium. Scale bar 10 μm. (B) The graphs represent an example of the difference between the GFP signal and the autofluorescence of papilla. (C) The colocalisation of EXO70B2-mRuby2 and GFP-SYP121 in a papilla. The transgenic plants with the EXO70B2-mRuby2 and GFP-SYP121 were observed at 16 hpi with *Bgh* in a normal water or hyperosmotic condition. Pictures represent one out of 15 papillae observed through the one experiment. Approximately 2/3 of observed spores appeared to have the similar effect on protein localisation after plasmolysis. Pearson's correlation graph of EXO70B2-mRuby2 (Ch1) and GFP-SYP121 (Ch2) for non-plasmolysed and plasmolysed cells. Scale bar 5μm.

The yellow dashed line marks the cross-section used for analysis.

Figure 4 Exocyst localised into the encasement of haustoria.

The panels represent a bright field and a signal intensity analysis of the three stages of defensive structures growth: the papilla (A, B), the partially encased haustorium (C, D) and the enclosing encasement (E, F). The signal of EXO70B2 surrounds the papilla (A), the collar (C, E, yellow arrowheads) and the encasement (C, E). The signal of SEC6-GFP marks strongly papilla (B), the collar or initiations of the encasement (D, F yellow arrowheads) and the encasement (F). Pink arrowheads are pointing where the haustoria end and where the signal of the Exocyst subunits is disappearing. Scale bar 10 µm; scale bar of signal intensities on the left. The yellow dashed line outlines fungal structures.

Figure 5 EXO70B2 was specifically induced on mRNA and protein level after *Bgh* inoculation.

(A) The relative transcript level, normalised to ubiquitin gene, of *EXO70B2* gene was elevated at 8 hpi with *Bgh*, in comparison to *SEC8*. (B) The protein level of EXO70B2-GFP in *exo70B2* mutant increased at 4 hpi with *Bgh* and stayed elevated during the time of interaction with the fungus, whereas the level of EXO70A1 dropped and the level of SEC8 stayed unchanged.The anti-GFP, anti-EXO70A1 and anti-SEC8 antibodies were used. (C) The early accumulation of EXO70B2-GFP signal in the cytoplasm in vesicle-like dots. The GFP signal labelled the papilla structure already at 8 hpi with *Bgh* in 3 weeks old plants. The asterisks indicate statistically significant differences calculated with nonparametric Tukey-Kramer HSD test at $p<0.01$. ($n = 3$ biological replicates). The error bars show standard deviation. The yellow arrowheads highlight signal maxima. The scale bar 5 µm.

Figure 6 SYP121 interacted with the EXO70B2 containing exocyst complex

Biochemical and genetic verification of SYP121 and EXO70B2 interaction. (A) The GFP-SYP121 seedlings were used for co-immunoprecipitation and the eluted fraction was tested for the exocyst subunits presence. For each gel, the arrangement of samples was always the same - on the left eluate of the GFP-SYP121 expressing

seedlings, and the eluate of the free GFP expressing seedlings as a control. (B) The direct interaction between the exocyst and SYP121 was examined in a yeast two-hybrid assay. Yeasts containing both the binding and activation domain were spotted on the selection SD-His, Trp, Ade, Leu plates in two dilutions, and left to grow for 5 days. (C) Four weeks old plants of *syp121*, e*xo70B2/syp121*, *exo70B1/syp121* mutant lines were inoculated with the spores of *Bgh*. The leaves were collected at 48 hpi and stained with trypan or aniline blue. The sum of all evoked interactions by pathogen described graph. (D) The graph shows the mean area of callose spots created after the interaction counted on the predefined leaf area. (E) The mean percentage of developed encased (fully or partially) or unencased haustoria. Error bars indicate SE (n = 3 biological replicates). Comparisons between multiple groups were performed by ANOVA followed by the Tukey-Kramer test. The same letter indicates that there are no significant differences ($P<0.01$).

Figure 7 The interaction scheme

The model describing our working hypothesis of two pathways involved in the basal resistance to the fungal non-adapted pathogen. The left scheme shows germinated spore which successfully penetrated a plant cell and created haustorium before the cell started the programmed cell death. The cell uses two major secretory pathway to develop defensive papilla and encasement, the secretion and recycling. In detail, we hypothesise that according to EXO70 comprised in the complex, exocyst helps to distinguish the defensive structures from PM. Exocyst containing EXO70B2 may help to establish the papilla membrane domain for SYP121 and similarly work for other Qa-SNARE in the encasement formation. The model also supports a variability of exocyst complex according to the bound EXO70X subunit. CW cell wall, PM plasma membrane, MVB multivesicular body, SE secretory vesicle, RV recycling vesicle, TGN trans-Golgi network, EV endocytosed vesicle, E encasement, P papilla, GT germ tube, A appressorium.

Supplementary Figure 1

Verification of the KO *sec5a-1* and KO *sec15b-1* mutants. The graphical illustration represents the genomic sequence of *Arabidopsis SEC5A* gene (A) and *SEC15B* (D) with the arrow point the place of insertion. The 1800 bp long segment of *SEC5A* was amplified from cDNA of 14 days old *sec5-1* mutant and WT seedlings (B). From the same cDNA samples, the 600 bp long fragment of control gene *EXO70B2* was amplified as the DNA quality control (C). The 1200 bp long segment of *SEC15B* was amplified as described above and the actin gene was used as a control. Primers used for the PCR were designed to cover the part with the insertion and to distinguish *SEC5A* from *SEC5B* or *SEC15B* from *SEC15A* (Table 10).

Supplementary Figure 2

Quantification of penetration resistance against *Ep* in exocyst mutants. The penetration resistance was analysed at 72 (A, C) and 116 hpi (B, D) with *Ep* in comparison to WT. The percentage of total interactions indicates changes in responsiveness to fungal attack (A, B). In detail, the penetration rate showed the changes in penetration resistance of exocyst mutants (C, D). The letters indicate the statistically significant difference performed by ANOVA followed by the post-hoc Tukey-Kramer test, Z-score calculations $p<0.01$, n = 3 biological replicates.

Supplementary Figure 3

The dynamics of exocyst subunits in papilla cross-section. Pictures on the left show the start section of time series used for kymographs (on the right); scale bar represents 10 µm. The yellow dash line defines the X-axis of the kymographs. Presented kymographs show the dynamics of GFP-tagged EXO70B2, SEC6 and SYP121. All proteins were expressed under their natural promoters. In kymograph, the vertical scale bar represents the 30s and the horizontal scale bar 3 µm. The white dashed line outlines fungal structures.

Supplementary Figure 4

(A) The accumulation of GFP signal and the overlay of GFP, autofluorescence of haustoria and papillae after the linear unmixing after lambda scan. The red colour shows the FM4-64 dye in an overlay picture. The non-transformed plants were used as the control to EXO70B2-GFP and SEC6-GFP expressing plants. (B) The unmixed channels represent the specific range of wavelengths described in the graph. Lambda scan was done to visualize GFP only with 488 nm argon laser with a range of 489-600 nm.

Supplementary Figure 5

(A) The localisation of EXO70B2-GFP/*exo70B2* and SEC6-GFP in the haustoria was done by linear unmixing of characterised spectra. Scale bar 10µm. The lambda scan was done to visualize GFP only with 488 nm argon laser with a range of 489-600 nm. (B) The graphical illustration of used spectra for GFP and fungal structures obtained from the control plants for linear unmixing picture processing.

Supplementary Figure 6

The isolated stacks from the Z-stack scanning showing localisation of GFP-SEC8 to the defensive structures papillae/collar or neck (A) and the growing encasement (B). The PI 1000x was used to visualise the fungal structure. The depth of a scan is indicated by yellow numbers, top right. Yellow arrowheads indicate the GFP maximum presence. Pink arrowhead shows the tip of haustoria. Scale bar 10µm.

Supplementary Figure 7

The graph shows the ability of EXO70B2-GFP to fully complement the defect of *exo70B2* mutant in papilla development. Leaves were stained with the trypan blue method. From the total number of created papillae on a leaf, the two categories (vesicular clump and regular papilla) were counted. Error bars represent SE. The small letters indicate statistically significant difference calculated with ANOVA test at $p<0.01$.

Supplementary table 8

The table presents a list of primers and constructs used in the study.

Discussion

PAPER 10:

Title: On the functional diversity and subcellular targeting of plant exocyst subunit EXO70 isoforms

Authors: Juraj Sekereš, Viktor Žárský and Martin Potocký

Rationale of the report: This work summarizes the vast and often contradictory knowledge about the roles of the EXO70 gene family and its massive expansion in angiosperm plant evolution

My contribution: I wrote most of the manuscript with contribution from Martin Potocký and Viktor Žárský.

Manuscript is being finalized for submission

The vesicle tethering complex exocyst is present throughout eukaryotes (Koumandou et al., 2007) and was repeatedly demonstrated to be the key cell polarity regulator in yeasts, animals and plants (Martin-Urdiroz et al., 2016; Zarsky et al., 2009; Zarsky et al., 2013). It consists of eight subunits (SEC3, SEC5, SEC6, SEC8, SEC10, SEC15, EXO84 and EXO70), and catalyzes SNARE complex - mediated membrane fusion. This process is mechanistically best understood in budding yeast model system, where the t-SNARE Sso2 directly interacts with Sec3p (Yue et al., 2017) and Sec9p with Sec6p (Sivaram et al., 2005). The cis-SNARE complex formation is further boosted by the direct interaction of Sec6p with the regulatory Sec1 protein (Morgera et al., 2012). Yeast and mammalian SEC3 and EXO70 subunits drive the complex to the plasma membrane by direct interaction with PIP_2 (He et al., 2007; Liu et al., 2007) and specific protein interactors like small GTPases (Pommereit and Wouters, 2007; Robinson et al., 1999). In animal systems, the complex functions of EXO70 have been addressed by many studies in various cell types. Besides functioning within the exocyst complex in processes like insulin secretion, neurite growth, cell migration, as well as midbody scission (Martin-Urdiroz et al., 2016) and phagosome

maturation (Rauch et al., 2014), EXO70 is involved in autophagy as part of exocyst subcomplex (Bodemann et al., 2011) and has several exocyst-independent roles documented. Surprisingly, it even regulates regulates pre-mRNA splicing (Dellago et al., 2011). Independently on the rest of exocyst, EXO70 stimulates Arp2/3-induced actin polymerization and branching (Liu et al., 2012) but it is also able to produce actin-free cell protrusions by oligomerization-induced negative membrane curvature (Zhao et al., 2013). Two different isoforms, the E-EXO70 and M-EXO70 result from mammalian EXO70 alternative splicing with only the M-EXO70 being able to activate the Arp2/3 complex. During the epithelial-mesenchymal transition, cells switch expression from E-EXO70 to M-EXO70, which facilitates invadopodia formation and cell migration. Few more mammalian EXO70 splice variants with differential tissue expression were documented (Dellago et al., 2011) but significance of these variants is unclear.

With so many functions executed by one or only a few isoforms in animals, it is surprising that angiosperm genomes encode vast amount of EXO70 variants (23 in Arabidopsis, 22 in diploid tobacco genomes, 47 in rice) distributed to nine subfamilies (A-I) (Elias et al., 2003; Cvrckova et al., 2012). The Arabidopsis EXO70 isoforms share residues implicated in plasma membrane binding to a different degree, which points to their putatively diverse roles in trafficking to different recycling membrane domains as part of different subtypes of the plant exocyst complex (Zarsky et al., 2009). The potential for diverse roles is further revealed by the differences in surface charge distribution predicted by structural homology modelling (Fig. 1). In this review, we further address the conundrum of the enormous plant EXO70 diversity by discussing current knowledge on the subcellular localization of plant EXO70 isoforms, their functions, mechanisms of regulation and molecular interactions with other subunits of plant exocyst, as well as other protein and lipid components.

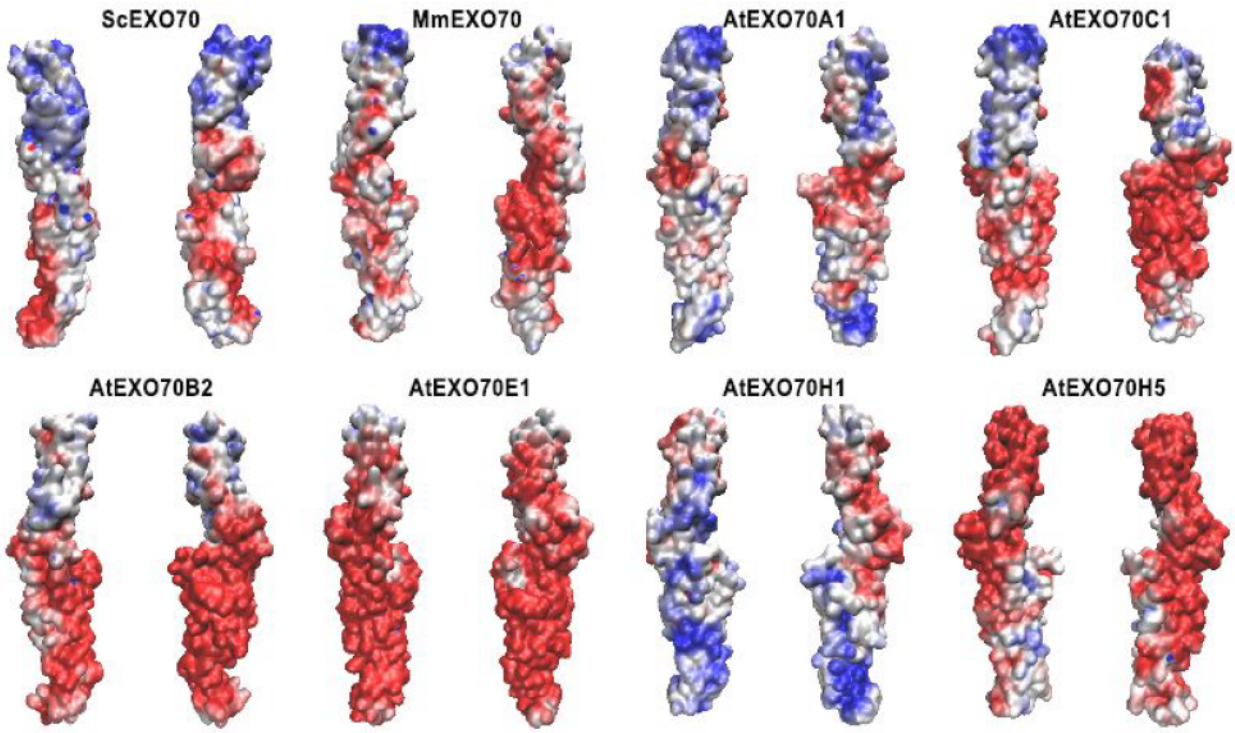

FIGURE 1. Structures of yeast and mammalian EXO70 protein are shown, together with predicted structures of selected Arabidopsis EXO70 isoforms. Indicated electrostatic potential mapped onto the solvent accessible surfaces spans from -5 (red) to +5 (blue) kbT/ec. 3D models of all Arabidopsis EXO70s were predicted using yeast (PDB code 2PVF), mouse (PDB code 2PFT) and partial Arabidopsis (PDB code 4RL5) structures as templates. Multiple structure-sequence alignment of 231 EXO70 sequences was used as a starting point for the individual predictions using MODELLER 9v8 software. For each Arabidopsis EXO70, 100 models were generated and evaluated with internal Modeller ranking algorithms (DOPE-HR, molpdf and Z). Five best models were further evaluated using Prosa (https://prosa.services.came.sbg.ac.at/prosa.php) and WhatIf (http://swift.cmbi.ru.nl/servers/html/index.html) algorithms, and the best models are shown. The pair of images is rotated 180° around y-axis. Courtesy of Martin Potocký

A subfamily EXO70 isoforms: the membrane targeting components (determinants) of canonical plat exocyst complex

Arabidopsis EXO70A1 is the first described and so far best characterized of plant EXO70 isoforms and phylogenetically closest to Opisthokont EXO70s (Synek et al., 2006). It is considered to be included in the variant of exocyst complex that regulates housekeeping and differentiation processes in most tissues, because it is strongly expressed across Arabidopsis sporophytic tissues (Synek et al., 2006; Hala et al., 2008;) and *exo70A1* mutant phenocopies defects of many mutants in one of the core exocyst subunits. The phenotypes shared between plant exocyst core subunit sporophytic mutants and *exo70A1* mutant are: slower hypocotyl elongation (Hala et al., 2008), thinner and collapsed xylem secondary cell wall (Vukasinovic et al., 2013), impaired seed coat deposition (Kulich et al., 2010), smaller stigmatic papillae (Synek et al., 2006; Safavian et al., 2015), reduced size of root apical meristem and slower root cell elongation (Cole et al., 2014), as well as impaired auxin transport due to slower PIN transporter recycling (Drdova EJ., 2013; Tan et al., 2016) and defective root hair growth (Synek et al., 2006; Wu et al., 2013). The elongation of *exo70A1* mutant root hairs is also less stimulated by presence of *Pseudomonas syringae* and the mutant seedling roots are more susceptible to colonization by the bacteria than wild type (Pecenkova et al., 2017). Furthermore, EXO70A1 shares subcellular localization with core exocyst subunits in many tissues, like root epidermis with polarization towards the outer lateral membrane domain (Fendrych et al., 2013), site of prospective Casparian strip deposition (Kalmbach et al., 2017) and maturating secondary cell wall in differentiating xylem (Vukasinovic et al., 2017).

Strikingly, there is a dramatic involvement of core exocyst subunits and only marginal role of EXO70A1 during cytokinesis. *exo84b* (Fendrych et al., 2010) and lat52:SEC6 complemented *sec6* (Wu et al., 2013) mutants have crippled seedlings and cell wall stubs resulting from defective cytokinesis. While EXO70A1 colocalizes with core subunits both during initial cytokinesis and cell plate maturation, only the former phase is affected in *exo70A1* mutant and the defect is later compensated, so *exo70A1* tissues bear no trace of cytokinesis defects. It is

possible that some yet uncharacterized EXO70 isoform acts redundantly with EXO70A1 during cytokinesis or that late cell plate recruits exocyst via one of its core subunits. Besides Arabidopsis, the mutant in EXO70A1 gene was also characterized in rice (Tu et al., 2015). The mutant plants are dwarfish with impaired cell elongation and collapsed vascular cell walls, which demonstrates conserved EXO70A1 function across angiosperms.

Arabidopsis EXO70A2, the sister isoform of the EXO70A1, is highly expressed in pollen (Loraine et al., 2013; Synek et al., 2017). It thus probably plays analogous role in recruiting the exocyst to the area of active secretion. In tobacco, NtEXO70A1a and to some extend NtEXO70A2 localize to the exact small subapical area of the pollen tube, where exocytosis occurs, while nonpollen NtEXO70A1b does not bind plasma membrane in tobacco pollen (Sekeres et al., 2017). A subfamily EXO70 isoforms are thus involved in exocytosis in many cell types with sporophyte-pollen division of labor between closely related isoforms.

B subfamily EXO70 isoforms: versatile mediators of autophagy-related processes and plasma membrane dynamics

Both members of Arabidopsis B subfamily of EXO70 isoforms, the EXO70B1 and EXO70B2, have been thoroughly investigated. Most angiosperm genomes contain either only one EXO70B paralogue or paralogues that arose from independent duplications with regard to evolution of Arabidopsis EXO70B1 and EXO70B2. Therefore, many of the functional properties of those proteins discussed here are most probably relevant mostly for Brassicaceae, at least in the case of EXO70B2, which is derived when compared to Arabidopsis EXO70B1 and other angiosperm members of B subfamily of EXO70s and therefore probably evolutionary novelty of Brassicaceae.

EXO70B1 is expressed across many sporophytic tissues and was at first characterized as part of autophagic machinery that plays role during nitrogen starvation, as well as constitutive transport in autophagy-related pathways from ER to vacuole that bypass Golgi apparatus (Kulich et al.,

2013). Such transport involves vesicular trafficking of anthocyanins. YFP:EXO70B1 colocalizes with the anthocyanin containing compartments, with the autophagy marker ATG8f and gets internalized to the vacuole. *exo70B1* mutant plants are nitrogen starvation sensitive, accumulate less autophagic bodies in the vacuole and accumulate paramural bodies in the apoplast, possibly due to the defective transport to the vacuole. Importantly, *exo70A1exo70B1* double mutant displays phenotypic deviations of both single mutants without any synergism, so there is no functional overlap between EXO70A1 and EXO70B1 (Kulich et al., 2013). *exo70B1* mutant plants also develop spontaneous lesions with cells undergoing programmed cell death due to SA hyperaccumulation (Kulich et al., 2013) and have reduced threshold for PCD initiation after pathogen infection (Stegmann et al., 2013; Zhao et al., 2015). The mutants are thus more resistant towards strictly biotrophic pathogens but display overly reduced fitness (Stegmann et al., 2013; Zhao et al., 2015). Since SA directly induces autophagy (Kulich and Zarsky, 2014), the hypersensitive phenotype of *exo70B1* is probably caused by impaired SA clearance due to its defective autophagy-related transport to the vacuole (Kulich et al., 2013). It was further discovered that TIR-NBS truncated NLR disease resistance protein TN2, a direct EXO70B1 interactor, is required for elevated SA level, H_2O_2 accumulation and spontaneous hypersensitive response in *exo70B1* mutant (Zhao et al., 2015). Later, the TN2 interactor calcium-dependent protein kinase 5 (CDPK5), unlike other closely related CDPKs, was shown to be involved in TN2-driven hypersensitive reaction and to directly phosphorylate EXO70B1 (Liu et al., 2017), probably in inhibitory manner. It was hypothesized that EXO70B1 is target of yet unknown pathogen effector and TN2 monitors EXO70B1 integrity triggering hypersensitive reaction when EXO70B1 becomes compromised. Alternatively, TN2 could be normally degraded by EXO70B1-dependent autophagy pathway to prevent excessive TN2-induced SA accumulation, which occurs when the pathway does not function properly due to EXO70B1 loss (Zhao et al., 2015), since autophagy has been proposed to be a general mechanism for negative regulation of R proteins (Pecenkova et al., 2016). Please note, that mechanisms postulating direct and indirect role of EXO70B1 in SA level control are not mutually exclusive. EXO70B1 could monitor TN2 activity under standard conditions but also facilitate degradation of excessive SA upon SA level

elevation. Autophagy-related pathway involving EXO70B1 could thus be a general traffic route of various secondary metabolites to the vacuole (Kulich and Zarsky, 2014).

Furthermore, EXO70B1 also regulates stomatal opening and closure. *Exo70B1* mutants exhibit slower light-induced stomatal opening than WT plants. EXO70B1 directly interacts with RIC7 and both proteins are translocated to PM by active ROP2 and held inside the cell by dominant negative ROP2 in *Vicia faba* stomata. Since Arabidopsis *ric7* mutants display faster light-induced opening than WT, RIC7 probably also acts as a negative regulator of EXO70B1 activity during stomatal opening (Hong et al., 2016). While mutation in EXO70B1 gene has no effect on ABA-induced stomatal closure upon treatment with 1μM ABA (Hong et al., 2016), the stomata of *exo70B1* close slower than those of WT plants when 10μM ABA or mannitol is applied, while plants overexpressing EXO70B1 close their stomata faster under same conditions (Seo et al., 2016). EXO70B1 is also translocated to PM by RIN4, the regulator of plant defence and guardee of many plant R-proteins, in Arabidopsis stomata (Sabol et al., 2017). EXO70B1 directly interacts with RIN4 and the interaction is specific for the EXO70B1 among tested EXO70 isoforms. Molecular details of EXO70B1 PM recruitment by RIN4 were further investigated in heterologous *Nicotiana benthamiana* system showing that full length RIN4 is required and upon RIN4 cleavage by AvrRpt2 protease, both RIN4 and EXO70B1 loss PM localization (Sabol et al., 2017).

Surprisingly, tobacco NtEXO70B1 was found to be natively transcribed in tobacco pollen (Sekeres et al., 2017; Conze et al., 2017) and tagged NtEXO70B1 localizes to a distinct sub-apical membrane domain in growing tobacco pollen tube (Sekeres et al., 2017). The NtEXO70B1 signal overlaps with zone of active endocytosis and localization of endocytic machinery, so the protein could play direct or indirect role in endocytosis. Alternatively, it could regulate an unknown minor secretory pathway in tobacco pollen, distinct from the bulk secretion regulated by A subfamily of EXO70s (Sekeres et al., 2017). To our knowledge, EXO70B1 expression has never been detected in Arabidopsis pollen. It is thus possible that the pollen function of EXO70B1 is limited to Solanacea.

EXO70B2 is the closest homolog of EXO70B1 in Arabidopsis, although out of all the Arabidopsis pairs of sister EXO70 paralogs, the EXO70B1-EXO70B2 has the lowest sequence similarity and EXO70B2 is highly derived when compared to EXO70B1 of Arabidopsis and other angiosperms. EXO70B2 is thus evolutionary novelty of Brassicaceae and what we know about its function might not be relevant for other angiosperm groups (for phylogenetic analysis of B subfamily of EXO70s, see Cvrckova et al., 2012). EXO70B2 mRNA level is induced by various elicitors (Pecenkova et al., 2011) and both EXO70B2 transcript and protein level increase upon fungal attack (Ortmannova et al., unpubl.). The *exo70B2* mutant plants are more susceptible to *Pseudomonas syringae* infection (Pecenkova et al., 2011; Stegmann et al., 2012), and oomycete *Hyaloperenospora arabidopsidis* (Stegmann et al., 2012) than WT plants. The mutants also exhibit deviations in defensive papilla buildup upon infection by fungi *Blumeria graminis* (Pecenkova et al., 2011; Ortmannova et al., unpubl.) and *Erysiphe pisi* (Ortmannova et al., unpubl.). Unlike WT plants, the *exo70B2* mutants do not upregulate expression of several markers after PAMP treatment, do not build up protection against Pseudomonas infection upon flg22 pretreatment and inhibition of their root growth by flg22 is less pronounced than in the case of WT plants (Stegmann et al., 2012). EXO70B2 does not play role in ABA-induced stomatal closure but it is employed in mannitol-induced stomatal closure (Seo et al., 2016). GFP-tagged EXO70B2 localizes to plasma membrane in root and cotyledon cells of young seedlings and relocalizes to autophagosomes after autophagy induction. The localization is BFA-sensitive, so the protein either passes GA/TGN or binds small vesicles that collapse into the BFA body (Teh et al., unpubl., available at BioRxiv preprint server). In fully grown leaves, detectable expression of EXO70B2 occurs only upon pathogen infection and EXO70B2 together with core exocyst subunits localizes to haustorial encasement and defensive papilla, where it interacts with the SNARE SYP121 (Ortmannova et al., unpubl.). EXO70B2 also plays role in stomatal dynamics but it seems to be limited to osmolyte-induced closure (Seo et al., 2016). Molecular determinants of EXO70B2 recruitment are unclear but unlike EXO70B1, the EXO70B2 is not translocated to PM when coexpressed with RIN4 in *N. benthamiana* leaves (Sabol et al., 2017). It, however, weakly interacts with RIN-domain containing protein NOI6 and

EXO70B2 could be recruited to PM by one of the many RIN-domain containing proteins (Afzal et al. 2013, Sabol et al., 2017).

C subfamily EXO70 isoforms: the conserved regulators of the tip growth

Arabidopsis EXO70C1 and EXO70C2 are specifically transcribed in trichoblasts and pollen (Synek et al., 2017) at very high level exceeding expression of core exocyst subunits on the level of transcripts. On the protein level, C subfamily EXO70s are the most abundant EXO70 isoforms in both Arabidopsis (Grobei et al., 2009) and tobacco (Sekeres et al., 2017) pollen. Surprisingly, unlike A subfamily EXO70 isoforms or core exocyst subunits, C subfamily EXO70s do not localize to plasma membrane and are purely cytoplasmic in Arabidopsis trichoblasts and Arabidopsis and tobacco pollen tubes, even upon overexpression (Sekeres et al., 2017; Synek et al., 2017). However, the overexpression in tobacco pollen tube causes phenotypes related to misregulated polarity (Sekeres et al., 2017) and *exo70C1* (Li et al., 2010) and *exo70C2* (Synek et al., 2017) mutants display male transmission defect. *exo70C2* pollen tubes growing in style and *in vitro* are shorter than wild type pollen tubes. Surprisingly, this is not due to shorter growth rate but it is the result of faster growth periods in mutant pollen tubes, which result into burst of their tips. Burst pollen tubes cease growth, regenerate, start new period of fast growth and burst again in cycles resulting in overall length shorter than that of WT pollen tubes (Synek et al., 2017). This phenomenon, probably resulting from thinning-out of some cell wall components at the apex, could be explained either by less cell wall delivered in the *exo70C2* mutant or by C subfamily EXO70 isoforms functioning as negative regulators of secretion and the *exo70C2* mutant pollen having disrupted balance between cellulose synthesis and exocytosis of other cell wall components (Synek et al., 2017).

Conundrums of E subfamily EXO70s: unconventional autophagy or overexpression artefacts?

Arabidopsis EXO70E2 localizes to cytoplasmic punctae when overexpressed in cell culture and the localization is unaffected by inhibitors commonly used to dissect plant cell membrane trafficking (Wang et al., 2010). The structures resemble inclusion bodies but turn to be double-membrane compartments reminiscent of autophagosomes that fuse with plasma membrane releasing a big exosome to the apoplast when assessed by electron microscopy (Wang et al., 2010). The structures sequester exocyst subunits and other proteins upon overexpression in Arabidopsis cell culture (Wang et al., 2010; Ding et al., 2014) but do not normally colocalize with known membrane compartment markers including the autophagy marker Atg8e (Wang et al., 2010). On the other hand, the structures containing EXO70E2 colocalize with Atg8e and Atg8f and move with them to vacuolar lumen after autophagy induction (Lin et al., 2015). NtEXO70E2 is not natively expressed in tobacco pollen and when YFP:NtEXO70E2 is ectopically expressed in growing tobacco pollen tube, it also localizes to mobile puncta with negligible cytoplasmic signal even upon low level of expression (Sekeres et al., 2017). Strangely, the EXO70E2 induces the double-membrane compartments even in mammalian cells - an extremely heterologous system for the plant specific protein (Ding et al., 2014). It is thus evident that the EXO70E2 protein either hijacks autophagy machinery in different species, directly strongly deforms membranes or forms aggregates that are very potent autophagy cargo in both animal and plant cells. It is difficult to figure out biological function of EXO70E2, because most subcellular localization data about the protein come from 35S promoter-driven overexpression in Arabidopsis plants or from cell cultures. Unless the protein is studied in native environment under physiological level of expression, the artifacts are difficult to be avoided and interpretation of the results is problematic. EXO70E2 could play role in specific subtype of autophagic processes connected to an unconventional secretory pathway but unlike in the case of the EXO70B1, no functional studies with mutant plants have been performed so far. NtEXO70E1b is natively expressed in tobacco pollen and YFP:NtEXO70E1b localizes to vesicular inverted

cone in growing tobacco pollen tube (Sekeres et al., 2017) but functional significance of this subcellular localization is unclear.

H subfamily EXO70 isoforms: Diversified dicot molecular players acting from cell wall secretory function to yet unclear roles in the nucleus

While encoded by only a few paralogs in monocot genomes, the H subfamily EXO70s are the most expanded subfamily in dicot genomes (Cvrckova et al., 2012). H subfamily EXO70s display the most striking example of independent EXO70 duplications specific for many angiosperm taxa (Cvrckova et al., 2013). It is also noteworthy that rate of substitution detected between EXO70 genes from tobacco and its parental species (*N. sylvestris* and *N. tomentosiformis*) was very low for the A subfamily EXO70s and highest for the H subfamily EXO70s (Sekeres et al., 2017). H subfamily EXO70s thus seem to be subject of rapid evolution in dicot plants when compared to other EXO70 subfamilies. Also, different isoforms of H subfamily EXO70s are expressed in Arabidopsis and tobacco pollen (Sekeres et al., 2017; Synek et al., 2017), further pointing at rapid evolution of this EXO70 subfamily. Functionally best characterized member of the H subfamily is the Arabidopsis EXO70H4. It is one of the most expressed genes in developing trichomes, where it regulates cell wall deposition during thickening and buildup of the Ortmannian ring, the structure at the trichome base enriched in callose and other cell wall components (Kulich et al., 2015). EXO70H4 localizes to sites of prospective cell wall deposition in trichomes together with other exocyst subunits and recruits callose synthases PMR4 and Cals9 to these sites (Kulich et al., 2018). Importantly, function of the EXO70H4 in trichomes can not be supplemented by any other of the Arabidopsis EXO70 isoforms (Kulich et al., 2018). While limited to trichomes under normal conditions, EXO70H4 expression is induced in pavement epidermal cells upon flg22 or chitin treatment, suggesting role of the EXO70H4 in callose deposition during reaction to pathogen attack (Kulich et al., 2018). Role in defence against pathogens has also been described in case of the EXO70H1, which is expressed upon elf18 peptide treatment and mutation in the EXO70H1 leads to enhanced susceptibility towards *Pseudomonas syringae* (Pecenkova et al., 2011). However, the mechanism

of EXO70H1 action is unknown. The Arabidopsis EXO70H1 localizes to the nucleus when expressed in *Nicotiana benthamiana* epidermis (Pecenkova et al., 2011) and tobacco NtEXO70H1/2 and NtEXO70H5-8b localize to the nucleus in growing pollen tube (Sekeres et al., 2017). The high ratio of nuclear to cytoplasmic localization of selected tobacco H subfamily EXO70 isoforms suggests they function within the nucleus. This is further supported by richness of nuclear proteins among the putative Arabidopsis EXO70H1 interactome (Zarsky et al., 2013).

EXO70s subfamilies absent in Arabidopsis

While most of the EXO70 subfamilies are represented in genome of the most common plant model *Arabidopsis thaliana*, some are missing in Arabidopsis, mostly because they are taxonomically restricted. Analogous to the case of H subfamily of EXO70s in dicots, the monocot F EXO70s and their FX subclade have undergone massive expansion (Cvrckova et al., 2012). Silencing of one of the barley F subfamily EXO70s leads to increased susceptibility towards grass powdery mildew (Ostertag et al., 2013), rice OsEXO70-F2 and OsEXO70-F3 form complexes with the avirulence factor AVR-Pii and the OsEXO70-F3 contributes to *Pii*-mediated resistance against incompatible *Magnaporthe oryzae* strains expressing *AVR-Pii* (Fujisaki et al., 2015), which suggests that the expansion of the F and Fx EXO70 subfamily in monocots might be result of their general role in immunity.

While nine EXO70 subfamilies present within angiosperms have been acknowledged since the discovery of the plant exocyst (Elias et al., 2003), the I subfamily of EXO70s is not present in the Arabidopsis genome. It belongs to one of the 3 EXO70 subgroups that also includes G subfamily EXO70s, which are present in Arabidopsis but have not been properly characterized even in this model system yet. In *Medicago truncatula*, expression of EXO70I is induced by arbuscular mycorrhizal symbiosis and in *exo70i* mutant plants, the branching of developing arbuscules is aberrant and incorporation of membrane cargo to the periarbuscular membrane impaired (Zhang et al., 2015). EXO70I:YFP specifically accumulates near the hyphal tips of developing arbuscules. The EXO70I-mediated trafficking to the developing periarbusculat

membrane is likely to involve the whole EXO70I-containing exocyst complex, because the core exocyst subunit EXO84b also localized to sites of symbiotic fungal penetration in Medicago and *Daucus carota*. Unlike mature arbuscules, the developing arbuscules recruit GFP:EXO84b to tips and branches in *Daucus carota* (Genre et al., 2012). Although the GFP:EXO70I was also reported to accumulate near tips of the infection threads during rhizobial nodulation of Medicago cells (Gavrin et al., 2017), mutation in the Medicago EXO70I does not affect symbiotic interactions with nodule bacteria (Zhang et al., 2015).

A legume-specific group of EXO70 domain containing proteins was discovered in soybean (Chi et al., 2015). The EXO70 domain is derived from B subfamily EXO70s but the 12 proteins form a distinct phylogenetic subgroup, so they were named EXO70J subfamily. Many of them contain transmembrane domain homologous to one from WRKY-related protein. The transmembrane domain containing GmEXO70J1, 6, 7, 10 and 12 localize to Golgi apparatus when expressed in *N. benthamiana*, unlike the GmEXO70J3, which does not contain the transmembrane domain. Their cellular function is unknown but J subfamily EXO70s were hypothesized to play role in Golgi apparatus restructuralization and fragmentation (Chi et al., 2015). This would be in agreement with capability of the animal EXO70 to directly deform membrane (Zhao et al., 2013). Expression of J subfamily EXO70s increases in leaves during senescence (Chi et al., 2015) but they are also expressed in many other tissues (Wang et al., 2016). Viral-induced silencing of either transmembrane domain (TMD) containing GmEXO70J7 or soluble GmEXO70J8 leads to premature leaf senescence. Furthermore, amiRNA- silencing of TMD-containing GmEXO70J7 or GmEXO70J9 leads to reduced number of nodules (Wang et al., 2016). Strangely, the native expression of GmEXO70J7 and GmEXO70J9 normally decreases upon soybean inoculation with *Rhizobium* (Wang et al., 2016). There are many hypotheses about physiological role of J subfamily EXO70s, including nitrogen transport, senescence regulation, nutrient elongation and cell elongation (Chi et al., 2015; Wang et al., 2016) but they have been so far speculative and more detailed functional studies will be needed.

Mechanisms of EXO70 targeting to their subcellular destinations

Since the EXO70 subunit, together with the SEC3, is responsible for polar targeting of the whole yeast and mammalian exocyst, mechanisms of Opisthokont EXO70 membrane recruitment are of utmost interest. So far, many peripheral membrane proteins, mainly small GTPases, have been discovered to recruit Opisthokont EXO70 (He et al., 2007; Liu et al., 2007). Moreover, both yeast and mammalian EXO70 are recruited by PIP_2 and in return, PIP_2 molecules are predicted to be clustered by EXO70 (Pleskot et al., 2015), which could facilitate membrane fusion directly by changing local membrane properties and indirectly by clustering effector proteins. It has been proposed that local membrane composition recruits different EXO70s to particular recycling domains (Žárský et al., 2009) but partly because there are so many different EXO70 isoforms in plant cells, insight into mechanisms of plant EXO70s targeting to their destinations of action is limited when compared to the scenario in animal and yeast cells. With the exception of the EXO70A1, no experiments proving targeting of an EXO70 isoform to target membrane domain by specific phospholipid composition are available and only few protein interactors possibly involved in specific targeting of plant EXO70s have been verified. The case study of EXO70A1 targeting to plasma membrane combining *in vivo* experiments, *in vitro* lipid binding assays and molecular dynamic simulations (Synek, Sekereš et al., unpublished) revealed involvement of multiple anionic phospholipids, namely PA, PI4P and PIP_2 in this process, which is thus possibly based on general electrostatic interaction. Interactions of other EXO70 isoforms, which are supposed to be more functionally specialized than EXO70A1 delivering secretory cargo under many circumstances, might be more specific towards particular phospholipid species. Even in the case of EXO70A1, which binds PA, PI4P and PIP_2 *in vitro*, the phospholipids responsible for its recruitment *in vivo* vary according to cell type and membrane domain. While PIP_2 and PA recruit NtEXO70A1a to PM in tobacco pollen tube, PI4P and PA are the major lipid contributors for EXO70A1 PM binding in Arabidopsis root epidermis (Synek, Sekereš et al., unpublished), probably due to PI4P and PA being major determinants of PM negative charge in Arabidopsis root cells (Simon et al., 2016; Platre et al., 2018). PIP_2 is also likely to recruit EXO70A1 in differentiating endodermis to membrane domain of prospective casparian strip formation

(Kalmbach et al., 2017). On the other hand, activity of exocyst complex at sites of prospective secondary cell wall formation in differentiating xylem depends on tethering of EXO70A1 and other exocyst subunits to cortical microtubules via VETH-COG2 protein pair (Oda et al., 2015; Vukasinovic et al., 2017) and could be independent on interaction of EXO70A1 with PM lipids. Tobacco NtEXO70B1 could be targeted to PM via interaction with PA in growing pollen tube, since its localization largely overlaps with the PA maximum (Sekeres et al., 2017) but the direct interaction has not been demonstrated so far. PM targeting of Arabidopsis EXO70B1 can be driven by various protein interactors like RIN4 (Sabol et al., 2017) and RIC7 in stomatal guard cells (Hon et al., 2016). Direct experiments and data from protein-protein interaction databases implicate that different EXO70 isoforms interact with different NOI-domain containing proteins to a different degree (Afzal et al., 2013; Sabol et al., 2017). For example, unlike its closest homolog EXO70B1, the EXO70B2 is not recruited to PM by RIN4 in tobacco cells (Sabol et al., 2017). Molecular determinants of EXO70B2 localization are unclear but it might be fully dependent on protein-based targeting, because of apparent lack of phospholipid-interacting residues (Zarsky et al., 2009). Scaffold protein vampyrin colocalizes with the EXO70I in *Medicago truncatula* and specifically interacts with this isoform unlike with the EXO70A1 or EXO70B2 (Zhang et al., 2015), so it likely acts in EXO70I recruitment to its target membrane domain. The exotic EXO70J isoforms of legumes with transmembrane domain probably reach their target destination by progressing through the secretory pathway and being trapped in a specific membrane due to interaction with local compartment identity determinants and hydrophobic mismatch of the transmembrane alpha-helix and lipid bilayer thickness like in many other transmembrane proteins (Cosson et al., 2013).

Bioinformatic analyses have uncovered over-representation of Atg8-interacting motifs (AIMs) in exocyst subunits including many EXO70 isoforms (Tzafadia and Gallili, 2013; Cvrckova and Zarsky, 2013). While the AIM motifs can serve in targeting of the particular EXO70 isoforms for regulated degradation, they may also, possibly together with specific lipid species, drive certain isoforms to autophagosome to play direct role in autophagy like the EXO70B1 does (Kulich et al., 2013). As in the case of yeast and mammalian EXO70, the various plant EXO70 isoforms are

thus probably targeted to distinct membrane domains by coincidence detection of protein interactors and particular lipid species. The combination of factors may differ according to cell type, as evident in case of EXO70A1 (Sekeres et al., 2017; Synek, Sekereš et al., unpublished) and EXO70B1 (Hong et al., 2016; Sabol et al., 2017). Majority of the protein interactors responsible for targeting of EXO70 isoforms to their destinations is still uncharacterized but public protein-protein interaction databases suggest many candidates for future investigations (Zarsky et al., 2013).

Exocyst-dependent and independent roles of plant EXO70 isoforms and regulation of plant cell EXO70 repertoire

Since animal EXO70 has also functions not executed within the exocyst complex but in exocyst subcomplex (Bodemann et al., 2011) and has roles totally independent on the rest of the exocyst (Dellago et al., 2011; Liu et al., 2012; Zhao et al., 2013), it is reasonable to suppose that some functions of plant EXO70 isoforms are partly or fully independent on other exocyst subunits. In some cases, the function of an EXO70 within exocyst particle can be inferred from colocalization of core exocyst subunits and the EXO70 during a specific process and from the fact that mutants in genes encoding core exocyst subunits share phenotype with the mutant defective in the particular EXO70 paralog. Besides EXO70A1, both colocalization of core exocyst subunits with the EXO70 and shared phenotypic defect was demonstrated for the EXO70B2 in its role in defensive papilla buildup (Ortmannova et al., unpubl.). Core exocyst subunits SEC8 and EXO84b colocalize with the EXO70H4 in specific membrane domains of maturing trichomes (Kulich et al., 2018). In case of EXO70A1 (Hala et al., 2008) and EXO70B1 (Kulich et al., 2013) genetic interaction with core exocyst subunits was detected, which also points at function of those EXO70s within an exocyst (sub)complex. In other cases however, the only indicator that an EXO70 works within exocyst complex or subcomplex comes from protein-protein interaction data between the EXO70 and core exocyst subunits. The architecture of plant exocyst is best understood for the complex containing EXO70A1, which consists of two subcomplexes in analogous manner to the situation in yeast and animal exocyst (Synek, Sekereš

et al., unpublished). In yeast two hybrid test (Y2H), the EXO70A2 interacts with the same core subunits as EXO70A1 does (Hala et al., 2008; Synek et al., 2017), so it likely functions in identical manner but in gametophytic tissues. However, other EXO70 isoforms, namely B1,B2,H1 and H4, differ from the EXO70A1 and from each other in interactions with certain core subunits. SEC5 appears as direct interaction partner of all these isoforms (Pecenkova et al., 2011; Kulich et al., 2013; Kulich et al., 2015) and SEC6 interacts with the EXO70H4 (Kulich et al., 2015), while none of these core subunit directly interacts with A subfamily EXO70s (Hala et al., 2008; Synek et al., 2017). Significance of these differential interaction patterns is not clear but it is tempting to speculate that by directly binding different core subunits, different EXO70 isoforms could lock the exocyst complex in a slightly different conformation. It is known that while some of the inter-subunit links within the exocyst are stable, parts of the complex are mobile and can exist in different conformations (Picco et al., 2017). If different EXO70s could influence details of the exocyst conformation, they would not only act as adaptors for targeting of the complex to a specific compartment but would also influence orientation of peripheral residues of the core subunits and thus determine which of their potential protein-protein interactions with components outside the exocyst are possible for the particular type of exocyst complex. It needs to be emphasized that experimental data addressing putative differential architecture of exocyst complexes containing different EXO70 isoforms are missing, because the architecture is partly solved only for the EXO70A1 containing plant exocyst complex (Synek, Sekereš et al., unpublished).

It is not entirely clear which of the plant EXO70 isoforms function in exocyst-independent manner but in case of some isoforms there are hints for activity outside the complex. It also needs to be stressed that a particular EXO70 isoform could have more functions with some executed within the exocyst particle and some independently, like in the case of the mammalian EXO70. C subfamily EXO70s do not interact with any core subunit in the yeast two hybrid assay (Synek et al., 2017), so they probably do not directly associate with the exocyst complex. They could possibly regulate the exocyst function by competing for a common interactor like the ROH1 (Kulich et al., 2010, Synek et al., 2017). Some members of the H subfamily EXO70s

localize to the nucleus (Pecenkova et al., 2011; Sekeres et al., 2017) and although their precise role there is not clear, it definitely differs from regulation of vesicle fusion with target membrane and is thus probably independent on the exocyst. The J subfamily EXO70s specific for legumes also probably act in exocyst-independent manner, because their N terminus, which links EXO70 to the rest of exocyst complex in case of A subfamily EXO70s (Synek et al., unpub.), is linked to the Golgi complex membrane (Chi et al., 2015).

Besides coexistence of exocyst complexes containing different EXO70 isoform within a cell (Zarsky et al., 2009), it has also been proposed that EXO70 isoforms of the complexes can be replaced according to needs of a cell due to biotic and abiotic stimuli by induced expression of required isoforms and regulated proteolysis of those not required under the particular circumstances (Zarsky et al., 2013). Experimental evidence supporting this concept has been gradually accumulated. Recently, switch of EXO70 isoforms within exocyst in time has been documented for the first time with EXO70B2 transcription and translation being induced by pathogen attack with concomitant degradation of the EXO70A1 (Ortmannova et al., unpubl.).

The degradation of EXO70B2 (but not of EXO70A1) is regulated by its direct interactor, the E3 poly-ubiquitin ligase PUB22 and the related isoform PUB21 (Stegmann et al., 2012). The PUB22 is itself subject to proteasomal degradation but it is stabilized by flg22 treatment, so flg22 presence increases ubiquitin ligase activity of the PUB22. It is thus probably component of a negative feedback loop, which clears EXO70B2 once it is not needed any more (Stegmann et al., 2012). On the other hand, PUB18 and its related isoform PUB19 induce proteolytic degradation of the EXO70B1 in ABA-regulated manner, which regulates EXO70B1 function in ABA-induced stomatal closure. Like PUB22, the PUB18 is itself targeted to degradation due to self-ubiquitination (Seo et al., 2016) and thus also forms a tight regulatory feedback loop between a stress signalling mediator, EXO70 isoform and a specific E3 ubiquitin ligase. Interestingly, the specificity of EXO70B1-PUB18 and EXO70B2-PUB22 interactions is dependent on the UND domain of the PUB18 and upon swapping of the domain to PUB22, the specificity of interaction with the EXO70 isoforms is reversed (Seo et al., 2016). The fact that

division of labor between EXO70B1 and EXO70B2 is probably specific to Brassicaceae and thus relatively recent on evolutionary time scale demonstrates that specific hardwiring of machinery regulating degradation of EXO70 isoforms can evolve rapidly and might be taxon-specific in many cases. This notion is further coined by the fact, that while E3 ubiquitin ligase ARC1 directly binds (Samuel et al., 2009; Liu et al., 2016) and primes for degradation (Samuel et al., 2009) EXO70A1 in Brassica, the Arabidopsis ARC1 is a nonfunctional pseudogene (Kitashiba et al., 2011), so the EXO70A1 is subject to different regulatory mechanisms even in closely related genera.

Since most EXO70s contain one or more AIMs, they could also serve as autophagy cargo degraded in vacuole besides being targets for proteasomal degradation. This has been recently suggested for Arabidopsis EXO70B2 (Teh et al., unpubl., available at BioRxiv preprint server). Besides induction of its proteasomal degradation, flg22 treatment also induces EXO70B2 relocalization to microsomal fraction, colocalization with autophagosomes, which is dependent on C-terminal AIMs of the EXO70B2, and its vacuolar degradation (Teh et al., unpubl., available at BioRxiv preprint server). It is not clear why peripheral membrane proteins would be degraded by autophagic clearance, which usually targets larger cargo like inclusion bodies, whole compartments and viruses. Hypothetically, the regulated autophagy could destroy the vesicles containing specific secretory cargo together with the interacting EXO70 isoform. Cells would thus rapidly switch off trafficking to a particular membrane domain not only by degradation of the EXO70 regulating the trafficking but also by quickly removing compartments with cargo involved in the secretory pathway being switched off.

Conclusions and future perspectives

Albeit the research of plant exocyst complex has advanced tremendously during the past years and pieces of evidence addressing function of various EXO70 isoforms are accumulating, there are still many questions to be answered. While some EXO70 clades have been functionally characterized to a reasonable degree, others still constitute a mystery. For example, several

studies addressing Arabidopsis EXO70E2 exist but physiological function of the protein is still completely unknown. Other EXO70 subfamilies like D and G have not been functionally investigated at all and with exception of public expression data we do not known anything about action of these genes. On the other hand, several previously proposed concepts regarding the vast diversity of EXO70 isoforms are getting more and more support. It is now evident that more EXO70 isoforms can coexist within the same cell as part of different exocyst complex or subcomplex variants. The study addressing mechanism of Arabidopsis EXO70A1 membrane targeting (Synek, Sekereš et al., unpublished) by combination of advanced live cell imaging, *in vitro* lipid binding assays and computational methods not only uncovered phospholipid binding properties different from the Opisthokont EXO70 counterpart (yet meaningful in the context of plant PM lipid composition) but also opened door for detailed comparison of different EXO70 isoform targeting mechanisms to specific membrane domains. Detailed understanding of differential targeting of EXO70 isoforms will also require further evaluation of predicted and screening for novel specific protein interactors of the particular isoforms. Evidence of targeted proteolytic degradation as rapid regulatory switch between EXO70 isoforms within a cell is also accumulating. Fact that the ubiquitin ligase machinery can differ even for closely related isoforms like Arabidopsis EXO70B1 and EXO70B2 demonstrates tight and specifically fine tuned regulation, which can undergo rapid evolution, for different EXO70 isoforms. Because of overrepresentation of AIMs in most EXO70 isoforms and clear role of exocyst subcomplex in autophagy in different eukaryotes, it will be interesting to investigate which of the EXO70 isoforms play direct role in autophagy and which of them are degraded by autophagic machinery as a cargo. Sice EXO70 can in general act both as part of exocyst complex and in an exocyst-independent way, future studies of EXO70 isoforms function should also focus on validating or disproving involvement of core exocyst subunits in the particular process by careful comparison of phenotypes between plants with mutated genes encoding core exocyst subunits and with mutated particular EXO70 paralogs in the investigated process. Despite the amount of accumulated data, it is still difficult to build a clear picture about functional evolution of the EXO70 family in plants, mostly because of majority of the functional studies being focused on Arabidopsis EXO70s. The well characterized animal EXO70 has many documented functions, so

it is not entirely clear to which degree ancestral plant EXO70 has subfunctionalized into many isoforms by differential loss of original functions versus EXO70 subfamily specific neofunctionalization. Most probably, the diversity of roles observed in extant EXO70 isoforms resulted from combination of both processes. A and C subfamilies of EXO70 isoforms are likely to have conserved cellular functions among angiosperms. On the other hand, H subfamily EXO70s have definitely been subject to rapid diversification and seem to play functions in various cellular compartments. Interestingly, all 3 major clades involve EXO70 isoforms with clear secretory function, as is evident from many studies focused on A subfamily EXO70s and from secretory roles of Arabidopsis EXO70B2, EXO70H4 and Medicago EXO70I. It is thus evident that secretory function of ancestral Streptophyte EXO70 was retained in case of some isoforms but most probably lost in case of others. The details of this evolutionary process are blurred, mostly because critical lack of functional studies outside angiosperms. The only notable exception is the recent study (Rawat et al., 2017) addressing role of *Physcomitrella patens* EXO70.3d. It belongs to the same EXO70 subfamily as angiosperm G/I EXO70s and its disruption results, together with pleiotropic defects related to cell growth, cytokinesis and auxin signaling, into abnormal egg cell development and collapse during gametophore development (Rawat et al., 2017). More comparative studies will be necessary in order to elucidate the process of EXO70 paralogs subfuncialization during plant phylogeny. In summary, functional diversification of plant EXO70 isoforms provides not only important challenge for uncovering general mechanism of angiosperm cell morphogenesis but also an interesting model case of a versatile gene family rapidly evolving in specific contexts.

Conclusions

Our pioneering study provided the first large scale comparison of the localization of all EXO70 isoforms within a single plant cell type, the growing tobacco pollen tube. We performed phylogenetic analysis of the EXO70 family in *Solanaceae* and discussed both similarities and differences of EXO70 genes between plant taxa. While some EXO70 subfamilies tend to diverge only little and probably have conserved function within angiosperms, other subfamilies can differ in number and sequence of paralogs even among closely related taxa and probably play functionally divergent roles, which is most conspicuous in the case of EXO70H subfamily. We analyzed expression of EXO70 isoforms in tobacco pollen both on the level of mRNA transcripts and on proteomic level. We detected expression of several isoforms with the members of A and C subfamilies most abundant on the protein level. Subsequently, we analyzed subcellular localization of the YFP-tagged EXO70 isoforms in growing tobacco pollen tube. Surprisingly, the isoforms with interesting intracellular localization largely overlapped with those natively expressed in tobacco pollen. This observation suggests that EXO70 isoforms should be studied in their native cell types and under physiological conditions in the future, because their expression in heterologous cell type might not result in proper subcellular localization. We observed localization of EXO70 isoforms to various compartments including the vesicle-enriched inverted cone and nucleus but most importantly, we discovered that NtEXO70A1a and NtEXO70B1 localize to mutually exclusive plasma membrane domains. Localization of both isoforms overlapped with the plasma membrane region bound by tobacco SEC3 exocyst subunits, so these EXO70s possibly form parts of distinct types of exocyst complex. Localization of the NtEXO70A1a matches with previously characterized hotspot of exocytosis in tobacco pollen tube. Members of both EXO70 subfamilies enriched in pollen result in morphological deviations characteristic for perturbed cell polarity regulation upon overexpression, which indicates their active role in cell polarity driving processes. Interestingly, despite their effect on cell polarity regulation, the members of EXO70C subfamily do not localize to plasma membrane even upon increased phosphatidylinositol-4,5-bisphosphate level or when the EXO70C proteins are

overexpressed. These observations suggest that the EXO70C isoforms play regulatory role in tip growing cells, which is further supported by work of Synek et al. 2017.

Our follow-up study combined advanced live cell imaging of two model systems, the tobacco pollen tube and Arabidopsis root epidermis, genetics, molecular pharmacology, molecular dynamics simulations, *in vitro* lipid binding and *in vivo* lipid recruitment assays in order to provide detailed analysis of mechanisms of the canonical exocyst EXO70 isoform EXO70A1 targeting to plasma membrane. We showed that all analyzed GFP-tagged exocyst subunits lose their proper plasma membrane localization when the *EXO70A1* gene is mutated. We further analyzed importance of EXO70A1 protein domains for its localization to plasma membrane and discovered that both the N-terminal part, which is involved in interaction with other exocyst subunits, and the C-terminal part that plays role in interaction with the plasma membrane lipids are essential for proper EXO70A1 localization and function. Because EXO70 in Opisthokonts are known to directly bind phosphatidylinositol-4,5-bisphosphate, we further analyzed the propensity of EXO70A1 interaction with different anionic phospholipids. We initiated this analysis by *in vitro* protein lipid binding assay testing ability of the purified GST-tagged EXO70A1 to bind large unilamellar vesicles of various lipid composition. We discovered that EXO70A1 binds *in vitro* phosphatidylinositol-4-phosphate, phosphatidylinositol-4,5-bisphosphate and surprisingly the phosphatidic acid, the anionic phospholipid which is generally neglected in yeast and mammalian cell biology research but enriched and potentially essential in several plant tissues and under specific conditions. We further took advantage of the growing tobacco pollen tube model system that is amenable to transient transformation with constructs encoding phospholipid modifying enzymes leading to altered levels of particular membrane phospholipid species. We monitored localization of the native tobacco NtEXO70A1a upon increased level of phosphatidylinositol-4,5-bisphosphate or phosphatidic acid in comparison to control pollen tubes. Our experiments demonstrated that elevated levels of both tested phospholipids in the growing pollen tube leads to overaccumulation of NtEXO70A1a at the plasma membrane. We further analyzed the role of phosphatidylinositol-4,5-bisphosphate in EXO70A1 recruitment to plasma membrane in

Arabidopsis cells by introducing the GFP-tagged EXO70A1 into Arabidopsis *pip5k1pip5k2* double mutants with dramatically reduced phosphate 5 kinase activity in sporophytic tissues. Surprisingly, we did not observe and difference in EXO70A1 recruitment to plasma membrane in these lines. We thus further inspected importance of the other two anionic phospholipids in EXO70A1 membrane recruitment by molecular pharmacology and concluded that both diacylglycerol kinase-produced pool of phosphatidic acid and the phosphatidylinositol-4 phosphate contribute to EXO70A1 recruitment to the outer lateral plasma membrane of Arabidopsis root epidermal cells. For the sake of even more detailed analysis of EXO70A1 interaction with the anionic phospholipids, our team employed series of molecular dynamic simulations of EXO70A1 interaction with virtual phosphatidic acid-enriched membrane, uncovering the positively charged lysine residues, that are critical for the interaction. We subsequently experimentally confirmed the importance of computationally predicted residues for EXO70A1 recruitment to the plasma membrane in both Arabidopsis and tobacco. Our pioneering work thus paves the way for the future detailed comparative analyses of targeting different EXO70 isoforms to various membrane domains.

The thesis further includes several studies analysing role of selected EXO70 isoforms in plant exocyst targeting. Our team provided analysis of plant exocyst dynamics in the cortical region of root epidermis outer lateral domain showing that EXO70A1 is essential for the exocyst targeting to this region. We also showed that EXO70B1 plays role in autophagy as a part of specialized exocyst complex or subcomplex. Interestingly, while the exocyst targeting is independent on microtubular cytoskeleton in root epidermis, the microtubules play essential role in focusing exocyst complex and vesicular trafficking to sites of secondary cell wall deposition in differentiating xylem cells. Furthermore, we provided comprehensive study of plant exocyst role during defence against fungal pathogens. We showed that EXO70B2 isoform is specifically upregulated during this process and important for deposition of the secretory papilla. Finally, the discussion part of the thesis provides a comprehensive review of the published works addressing targeting and function of plant EXO70 isoforms.

Závěr

Naše srovnávací práce byla zaměřena na systematickou studii vnitrobuněčné lokalizace všech izoforem EXO70 v rámci klíčící tabákové láčky. Fylogenetická analýza genové rodiny EXO70 lilkovitých rostlin poukázala na rozdíly i podobnosti evoluce jednotlivých podrodin EXO70 u krytosemenných rostlin. Některé podrodiny EXO70 vykazují mezi taxony krytosemenných rostlin pouze malé rozdíly, kdežto jiné podrodiny EXO70 se značně liší počtem paralogů i jejich sekvencí i mezi příbuznými druhy. Největší rozmanitost vykazuje podrodina EXO70H, jejíž členové podléhají rychlé evoluci a patrně zastávají u různých skupin rostlin rozdílné specializované funkce. Pomocí transkripční a proteomické analýzy jsme analyzovali expresi izoforem EXO70 v tabákovém pylu a zjistili přítomnost několika izoforem s největším zastoupením členů podrodin EXO70A a EXO70C. Poté jsme s využitím fluorescenční konfokální mikroskopie studovali vnitrobuněčnou lokalizaci fluorescenčně značených izoforem EXO70. Dospěli jsme k zajímavému zjištění, že izoformy přirozeně exprimované v pylu tabáku vesměs lokalizují do specifických buněčných kompartmentů, kdežto izoformy, které běžně v pylové láčce nejsou exprimovány většinou nevykazují specifickou vnitrobuněčnou lokalizaci. Izoformy EXO70 je tedy vhodné studovat v jejich přirozeném buněčném prostředí. Pozorovali jsme lokalizaci vybraných izoforem EXO70 do rozličných částí buňky, včetně oblasti bohaté na sekretorické váčky blízko růstového vrcholu buňky a buněčného jádra. Nejzajímavější bylo zjištění, že izoformy NtEXO70A1a a NtEXO70B1 lokalizují do rozdílných domén plazmatické membrány. Obě izoformy částečně kolokalizují s podjednotkou exocystu SEC3 a mohou tedy být součástí různých typů komplexu exocyst. NtEXO70A1a lokalizuje to malé oblasti, která odpovídá dříve popsané zóně intenzivní buněčné sekrece řídící růst pylové láčky. Pomocí genové overexprese jsme dále analyzovali funkci členů podrodin EXO70A a EXO70C v polárním růstu a zjistili, že navýšené množství daných izoforem EXO70 vede k poruchám polárního růstu. Izoformy podrodiny EXO70C překvapivě nelokalizují na plazmatickou membránu a to ani při jejich zvýšené expresi nebo při zvýšené koncentraci fosfatidylinositol-4,5-bisfosfátu. Izoformy

EXO70C zůstávají v cytoplazmě a pravděpodobně mají regulační funkci, což bylo dále potvrzeno studií Synek a kol., 2017.

V další práci jsme se zaměřili na podrobnou analýzu vazby izoformy EXO70A1 na membránu. V této studii jsme propojili pokročilou fluorescenční mikroskopii v experimentálních modelech buněk kořene huseníčku a klíčící tabákové láčky s genetickou analýzou mutantů huseníčku, molekulární farmakologií, biochemickými analýzami vazby EXO70A1 na umělé membránové váčky rozličného složení a počítačovými simulacemi vazby EXO70A1 na membránu. Ukázali jsme, že v mutantech huseníčku s nefunkčním genem EXO70A1 další podjednotky exocyst nelokalizují v dostatečném množství na plasmatickou membránu. Dále jsme studovali význam jednotlivých proteinových domén EXO70A1 pro vazbu proteinu na membránu a zjistili, že jak N-terminální část proteinu, která odpovídá za jeho interakci s dalšími podjednotkami komplexu exocyst, tak C-terminální část, jež váže plazmatickou membránu, jsou nezbytné pro správnou lokalizaci a funkci EXO70A1. Jelikož podjednotka EXO70 váže fosfatidylinositol-4,5-bisfosfát v savčích i kvasinkových buňkách, studovali jsme schopnost EXO70A1 vázat záporně nabité fosfolipidy. Nejprve jsme testovali schopnost purifikovaného proteinu EXO70A1 vázat *in vitro* umělé membránové váčky definovaného složení a zjistili, že EXO70A1 interaguje s fosfatidylinositol-4-fosfátem, fosfatidylinositol-4,5-bisfosfátem i s fosfatidovou kyselinou, která je v zavedených Opistokontních buňkách poměrně málo studovaná, ale pravděpodobně hraje klíčovou úlohu v mnoha rostlinných pletivech. Výsledky biochemické analýzy jsme dále ověřili *in vivo*, nejprve pomocí modelového systému klíčící láčky tabáku, kde lze pomoci overexprese příslušných enzymů fosfolipidového metabolismu cíleně zvýšit koncentraci vybraných fosfolipidů. Zjistili jsme, že tabáková izoforma EXO70A1a váže v klíčící pylové láčce fosfatidylinositol-4,5-bisfosfát i fosfatidovou kyselinu. Dále jsme testovali, jestli je fosfatidylinositol-4,5-bisfosfát odpovědný za membránovou lokalizaci EXO70A1 i v kořenech huseníčku. Pozorovali jsme vnitrobuněčnou lokalizaci fluorescenčně značené EXO70A1 v kořenech mutantů *pip5k1pip5k2* s výrazně sníženou celkovou aktivitou fosfatidylinositol-4-fosfát 5 kinázy a tedy sníženým množstvím fosfatidylinositol-4,5-bisfosfátu. Překvapivě jsme nezjistili žádné snížení vazby EXO70A1 na membránu. Dále jsme tedy zkoumali roli dalších záporně

nabitých fosfolipidů ve vazbě EXO70A1 v kořenech huseníčku pomocí specifické farmakologické inhibice enzymů modifikujících membránové fosfolipidy. Tyto experimenty ukázaly, že na vazbě EXO70A1 v kořenech huseníčku se společně podílejí fosfatidylinositol-4-fosfát a fosfatidová kyselina produkovaná diacylglycerolkinázou. Abychom prostudovali mechanismus vazby EXO70A1 na membránu na molekulární úrovni, provedli jsme sadu počítačových simulací interakce EXO70A1 s membránou pomocí metod molekulární dynamiky. Simulace ukázaly významnou roli několika kladně nabitých postranních řetězců aminokyseliny lysinu pro vazbu záporně nabitých fosfolipidů. Závěr z počítačových simulací jsme poté ověřili *in vitro* pomocí lipid-vazebných experimentů a *in vivo* v klíčící pylové láčce tabáku i v buňkách kořene huseníčku. Výsledky naší práce poskytují metodickou a intelektuální platformu pro rozsáhlejší srovnávací studie mechanismů vnitrobuněčného zacílení rozličných izoforem EXO70 do různých membránových domén.

Doktorská práce dále zahrnuje několik publikací se zaměřením na roli vybraných izoforem EXO70 při zacílení komplexu exocyst. Náš kolektiv provedl první studii dynamiky podjednotek komplexu exocyst rostlin na vnější laterální membránové doméně buněk kořene a prokázal klíčovou funkci EXO70A1 v rámci zacílení komplexu na membránu. Další práce prokázala funkci EXO70B1 v autofagii v rámci komplexu či subkomplexu zahrnujícím další podjednotky exocystu. Zjistili jsme rovněž, že ačkoliv komplex exocyst správně lokalizuje na membránu v epidermálních buňkách kořene i při narušení mikrotubulárního cytoskeletu, mikrotubuly jsou nezbytné pro lokalizovanou buněčnou sekreci řízené komplexem exocyst v buňkách xylému. Prokázali jsme také, že izoforma EXO70B2 hraje klíčovou roli v tvorbě sekretorické papily v rámci obrany rostlinných buněk vůči patogenním houbám. Závěr práce poskytuje rozsáhlou diskuzi shrnující dosavadní publikace týkající se vnitrobuněčné lokalizace a funkce rostlinných izoforem EXO70.

References

Afzal AJ, Kim JH, Mackey D. 2013. The role of NOI-domain containing proteins in plant immune signaling. *BMC Genomics* **14**: 327.

Bodemann BO, Orvedahl A, Cheng T, Ram RR, Ou Y-H, Formstecher E, Maiti M, Hazelett CC, Wauson EM, Balakireva M, *et al.*. 2011. RalB and the Exocyst Mediate the Cellular Starvation Response by Direct Activation of Autophagosome Assembly. *Cell* **144**: 253–267.

Chi Y, Yang Y, Li G, Wang F, Fan B, Chen Z. 2015. Identification and characterization of a novel group of legume-specific, Golgi apparatus-localized WRKY and Exo70 proteins from soybean. *Journal of Experimental Botany* **66**: 3055–3070.

Conze LL, Berlin S, Bail AL, Kost B. 2017. Transcriptome profiling of tobacco (Nicotiana tabacum) pollen and pollen tubes. *BMC Genomics* **18(1):** 581.

Cosson P, Perrin J, Bonifacino JS. 2013. Anchors aweigh: protein localization and transport mediated by transmembrane domains. *Trends in Cell Biology* **23**: 511–517.

Cvrčková F, Grunt M, Bezvoda R, Hála M, Kulich I, Rawat A, Žárský V. 2012. Evolution of the Land Plant Exocyst Complexes. *Frontiers in Plant Science* **3**: 159

Cvrčková F, Žárský V. 2013. Old AIMs of the exocyst: evidence for an ancestral association of exocyst subunits with autophagy-associated Atg8 proteins. *Plant Signaling & Behavior* **8(11)**: e27099.

Dellago H, Löscher M, Ajuh P, Ryder U, Kaisermayer C, Grillari-Voglauer R, Fortschegger K, Gross S, Gstraunthaler A, Borth N, *et al.*. 2011. Exo70, a subunit of the exocyst complex, interacts with SNEVhPrp19/hPso4and is involved in pre-mRNA splicing. *Biochemical Journal* **438**: 81–91.

Ding Y, Wang J, Lai JHC, Chan VHL, Wang X, Cai Y, Tan X, Bao Y, Xia J, Robinson DG, *et al.*. 2014. Exo70E2 is essential for exocyst subunit recruitment and EXPO formation in both plants and animals. *Molecular Biology of the Cell* **25**: 412–426.

Drdová EJ, Synek L, Pečenková T, Hála M, Kulich I, Fowler JE, Murphy AS, Žárský V. 2013. The exocyst complex contributes to PIN auxin efflux carrier recycling and polar auxin transport in Arabidopsis. *The Plant Journal* **73**: 709–719.

Eliáš M. 2003. The exocyst complex in plants. *Cell Biology International* **27**: 199–201.

Fendrych M, Synek L, Pečenková T, Toupalová H, Cole R, Drdová E, Nebesářová J, Šedinová M, Hála M, Fowler JE, *et al.*. 2010. The Arabidopsis Exocyst Complex Is Involved in Cytokinesis and Cell Plate Maturation. *The Plant Cell* **22**: 3053–3065.

Fendrych M, Synek L, Pečenková T, Drdová EJ, Sekereš J, Rycke RD, Nowack MK, Žárský V. 2013. Visualization of the exocyst complex dynamics at the plasma membrane of Arabidopsis thaliana. *Molecular Biology of the Cell* **24**: 510–520.

Fujisaki K, Abe Y, Ito A, Saitoh H, Yoshida K, Kanzaki H, Kanzaki E, Utsushi H, Yamashita T, Kamoun S, *et al.*. 2015. Rice Exo70 interacts with a fungal effector,AVR-Pii, and is required for AVR-Pii-triggered immunity. *The Plant Journal* **83**: 875–887.

Gavrin A, Kulikova O, Bisseling T, Fedorova EE. 2017. Interface Symbiotic Membrane Formation in Root Nodules of Medicago truncatula: the Role of Synaptotagmins MtSyt1, MtSyt2 and MtSyt3. *Frontiers in Plant Science* **8**: 201

Genre A, Ivanov S, Fendrych M, Faccio A, Žárský V, Bisseling T, Bonfante P. 2011. Multiple Exocytotic Markers Accumulate at the Sites of Perifungal Membrane Biogenesis in Arbuscular Mycorrhizas. *Plant and Cell Physiology* **53**: 244–255.

Grobei MA, Qeli E, Brunner E, Rehrauer H, Zhang R, Roschitzki B, Basler K, Ahrens CH, Grossniklaus U. 2009. Deterministic protein inference for shotgun proteomics data provides new insights into Arabidopsis pollen development and function. *Genome Research* **19**: 1786–1800.

Hála M, Cole R, Synek L, Drdová E, Pečenková T, Nordheim A, Lamkemeyer T, Madlung J, Hochholdinger F, Fowler JE, *et al.*. 2008. An Exocyst Complex Functions in Plant Cell Growth in Arabidopsis and Tobacco. *The Plant Cell Online* **20**: 1330–1345.

He B, Xi F, Zhang X, Zhang J, Guo W. 2007. Exo70 interacts with phospholipids and mediates the targeting of the exocyst to the plasma membrane. *The EMBO Journal* **26**: 4053–4065.

Hong D, Jeon BW, Kim SY, Hwang J-U, Lee Y. 2015. The ROP2-RIC7 pathway negatively regulates light-induced stomatal opening by inhibiting exocyst subunit Exo70B1 in Arabidopsis. *New Phytologist* **209**: 624–635.

Kalmbach L, Hématy K, Bellis DD, Barberon M, Fujita S, Ursache R, Daraspe J, Geldner N. 2017. Transient cell-specific EXO70A1 activity in the CASP domain and Casparian strip localization. *Nature Plants* **3**: 17058.

Kitashiba H, Liu P, Nishio T, Nasrallah JB, Nasrallah ME. 2011. Functional test of Brassica self-incompatibility modifiers in Arabidopsis thaliana. *Proceedings of the National Academy of Sciences* **108**: 18173–18178.

Koumandou VL, Dacks JB, Coulson RM, Field MC. 2007. Control systems for membrane fusion in the ancestral eukaryote; evolution of tethering complexes and SM proteins. *BMC Evolutionary Biology* **7**:29.

Kulich I, Cole R, Drdová E, Cvrčková F, Soukup A, Fowler J, Žárský V. 2010. Arabidopsis exocyst subunits SEC8 and EXO70A1 and exocyst interactor ROH1 are involved in the localized deposition of seed coat pectin. *New Phytologist* **188**: 615–625.

Kulich I, Pečenková T, Sekereš J, Smetana O, Fendrych M, Foissner I, Höftberger M, Žárský V. 2013. Arabidopsis exocyst subcomplex containing subunit EXO70B1 is involved in the autophagy-related transport to the vacuole. *Traffic*. **14(11):**1155-65.

Kulich I, Žárský V. 2014. Autophagy-Related Direct Membrane Import from ER/Cytoplasm into the Vacuole or Apoplast: A Hidden Gateway also for Secondary Metabolites and Phytohormones? *International Journal of Molecular Sciences* **15**: 7462–7474.

Kulich I, Vojtíková Z, Glanc M, Ortmannová J, Rasmann S, Žárský V. 2015. Cell Wall Maturation of Arabidopsis Trichomes Is Dependent on Exocyst Subunit EXO70H4 and Involves Callose Deposition. *Plant Physiology* **168**: 120–131.

Kulich I, Vojtíková Z, Sabol P, Ortmannová J, Neděla V, Tihlaříková E, Žárský V. 2018. Exocyst Subunit EXO70H4 Has a Specific Role in Callose Synthase Secretion and Silica Accumulation. *Plant Physiology* **176**: 2040–2051.

Li S, Os GMAV, Ren S, Yu D, Ketelaar T, Emons AMC, Liu C-M. 2010. Expression and Functional Analyses of EXO70 Genes in Arabidopsis Implicate Their Roles in Regulating Cell Type-Specific Exocytosis. *Plant Physiology* **154**: 1819–1830.

Lin Y, Ding Y, Wang J, Shen J, Kung CH, Zhuang X, Cui Y, Yin Z, Xia Y, Lin H, Robinson DG, Jiang L. 2015. Exocyst-Positive Organelles and Autophagosomes Are Distinct Organelles in Plants. *Plant Physiology* **169(3)**:1917-32.

Liu J, Zuo X, Yue P, Guo W. 2007. Phosphatidylinositol 4,5-Bisphosphate Mediates the Targeting of the Exocyst to the Plasma Membrane for Exocytosis in Mammalian Cells. *Molecular Biology of the Cell* **18**: 4483–4492.

Liu J, Zhang H, Lian X, Converse R, Zhu L. 2015. Identification of Interacting Motifs Between Armadillo Repeat Containing 1 (ARC1) and Exocyst 70 A1 (Exo70A1) Proteins in Brassica oleracea. *The Protein Journal* **35**: 34–43.

Liu N, Hake K, Wang W, Zhao T, Romeis T, Tang D. 2017. CALCIUM-DEPENDENT PROTEIN KINASE5 Associates with the Truncated NLR Protein TIR-NBS2 to Contribute to exo70B1- Mediated Immunity. *The Plant Cell* **29**: 746–759.

Martin-Urdiroz M, Deeks MJ, Horton CG, Dawe HR, Jourdain I. 2016. The Exocyst Complex in Health and Disease. *Frontiers in Cell and Developmental Biology* **4**:24

Oda Y, Iida Y, Nagashima Y, Sugiyama Y, Fukuda H. 2014. Novel Coiled-Coil Proteins Regulate Exocyst Association with Cortical Microtubules in Xylem Cells via the Conserved Oligomeric Golgi-Complex 2 Protein. *Plant and Cell Physiology* **56**: 277–286.

Ortmannová J, Pečenková T, Sekereš J, Kulich I, Šantrůček J, Žárský V. Exocyst complex mediates non-host resistance against powdery mildew in Arabidopsis. *Submitted to Molecular Plant*

Ostertag M, Stammler J, Douchkov D, Eichmann R, Hückelhoven R. 2012. The conserved oligomeric Golgi complex is involved in penetration resistance of barley to the barley powdery mildew fungus. *Molecular Plant Pathology* **14**: 230–240.

Pečenková T, Hála M, Kulich I, Kocourková D, Drdová E, Fendrych M, Toupalová H, Žárský V. 2011. The role for the exocyst complex subunits Exo70B2 and Exo70H1 in the plant–pathogen interaction. *Journal of Experimental Botany* **62**: 2107–2116.

Pečenková T, Marković V, Sabol P, Kulich I, Žárský V. 2017. Exocyst and autophagy-related membrane trafficking in plants. *Journal of Experimental Botany* **69**: 47–57.

Picco A, Irastorza-Azcarate I, Specht T, Böke D, Pazos I, Rivier-Cordey A-S, Devos DP, Kaksonen M, Gallego O. 2017. The In Vivo Architecture of the Exocyst Provides Structural Basis for Exocytosis. *Cell* **168(3)**:400-412.e18.

Platre MP, Noack LC, Doumane M, Bayle V, Simon MLA, Maneta-Peyret L, Fouillen L, Stanislas T, Armengot L, Pejchar P, *et al.*. 2018. A Combinatorial Lipid Code Shapes the Electrostatic Landscape of Plant Endomembranes. *Developmental Cell* **45**:465-480.e11.

Pleskot R, Cwiklik L, Jungwirth P, Žárský V, Potocký M. 2015. Membrane targeting of the yeast exocyst complex. *Biochimica et Biophysica Acta (BBA) - Biomembranes* **1848**: 1481–1489.

Pommereit D, Wouters FS. 2007. An NGF-induced Exo70-TC10 complex locally antagonises Cdc42-mediated activation of N-WASP to modulate neurite outgrowth. *Journal of Cell Science* **120**: 2694–2705.

Rauch L, Hennings K, Aepfelbacher M. 2014. A Role for Exocyst in Maturation and Bactericidal Function of Staphylococci-Containing Endothelial Cell Phagosomes. *Traffic* **15**: 1083–1098.

Rawat A, Brejšková L, Hála M, Cvrčková F, Žárský V. 2017. The Physcomitrella patens exocyst subunit EXO70.3d has distinct roles in growth and development, and is essential for completion of the moss life cycle. *New Phytologist* **216**: 438–454.

Robinson NGG, Guo L, Imai J, Toh-E A, Matsui Y, Tamanoi F. 1999. Rho3 of Saccharomyces cerevisiae, Which Regulates the Actin Cytoskeleton and Exocytosis, Is a GTPase Which Interacts with Myo2 and Exo70. *Molecular and Cellular Biology* **19**: 3580–3587.

Sabol P, Kulich I, Žárský V. 2017. RIN4 recruits the exocyst subunit EXO70B1 to the plasma membrane. *Journal of Experimental Botany* **68**: 3253–3265.

Samuel MA, Chong YT, Haasen KE, Aldea-Brydges MG, Stone SL, Goring DR. 2009. Cellular Pathways Regulating Responses to Compatible and Self-Incompatible Pollen in Brassica and Arabidopsis Stigmas Intersect at Exo70A1, a Putative Component of the Exocyst Complex. *The Plant Cell* **21**: 2655–2671.

Sekereš J, Pejchar P, Šantrůček J, Vukašinović N, Žárský V, Potocký M 2017. Analysis of Exocyst Subunit EXO70 Family Reveals Distinct Membrane Polar Domains in Tobacco Pollen Tubes. *Plant Physiology* **173(3)**:1659-1675

Seo DH, Ahn MY, Park KY, Kim EY, Kim WT. 2016. The N-Terminal UND Motif of the Arabidopsis U-Box E3 Ligase PUB18 Is Critical for the Negative Regulation of ABA-Mediated Stomatal Movement and Determines Its Ubiquitination Specificity for Exocyst Subunit Exo70B1. *The Plant Cell* **28**: 2952–2973.

Simon MLA, Platre MP, Marquès-Bueno MM, Armengot L, Stanislas T, Bayle V, Caillaud M-C, Jaillais Y. 2016. A PtdIns(4)P-driven electrostatic field controls cell membrane identity and signalling in plants. *Nature Plants* **2**: 16089.

Stegmann M, Anderson RG, Ichimura K, Pecenkova T, Reuter P, Žárský V, Mcdowell JM, Shirasu K, Trujillo M. 2012. The Ubiquitin Ligase PUB22 Targets a Subunit of the Exocyst Complex Required for PAMP-Triggered Responses in Arabidopsis. *The Plant Cell* **24**: 4703–4716.

Stegmann M, Anderson RG, Westphal L, Rosahl S, Mcdowell JM, Trujillo M. 2013. The exocyst subunit Exo70B1 is involved in the immune response of Arabidopsis thaliana to different pathogens and cell death. *Plant Signaling & Behavior* **8(12)**: e27421.

Synek L, Schlager N, Eliáš M, Quentin M, Hauser M-T, Žárský V. 2006. AtEXO70A1, a member of a family of putative exocyst subunits specifically expanded in land plants, is important for polar growth and plant development. *The Plant Journal* **48**: 54–72.

Synek L, Vukašinović N, Kulich I, Hála M, Aldorfová K, Fendrych M, Žárský V. 2017. EXO70C2 Is a Key Regulatory Factor for Optimal Tip Growth of Pollen. *Plant Physiology* **174**: 223–240.

Synek L, Sekereš J, Pleskot R, Aldorfová K, Marković V, Ortmannová J, Pečenková T, Pejchar P, Růžičková M, Soukupová H, Šantrůček J, Vukašínović N, Žárský V, Potocký M. Molecular architecture of the Arabidopsis exocyst complex reveals EXO70A1 as the key subunit required for

targeting of the plant exocyst to the plasma membrane through the direct interaction with anionic phospholipids. *In prep.*

Teh O, Lee C, Ditengou FA, Klecker T, Furlan G, Zietz M, Hause G, Eschen-Lippold L, Hoehenwarter W, Lee J, Ott T, Trujillo M. Phosphorylation of the exocyst subunit EXO70B2 contributes to the regulation of its function. *BioRxiv preprint server*

Tzfadia O, Galili G. 2013. The Arabidopsis exocyst subcomplex subunits involved in a golgi-independent transport into the vacuole possess consensus autophagy-associated atg8 interacting motifs. *Plant Signaling & Behavior* **8**.

Vukašinović N, Oda Y, Pejchar P, Synek L, Pečenková T, Rawat A, Sekereš J, Potocký M, Žárský V. 2016. Microtubule-dependent targeting of the exocyst complex is necessary for xylem development in Arabidopsis. *New Phytologist* **213**: 1052–1067.

Wang J, Ding Y, Wang J, Hillmer S, Miao Y, Lo SW, Wang X, Robinson DG, Jiang L. 2010. EXPO, an Exocyst-Positive Organelle Distinct from Multivesicular Endosomes and Autophagosomes, Mediates Cytosol to Cell Wall Exocytosis in Arabidopsis and Tobacco Cells. *The Plant Cell* **22**: 4009–4030.

Wang Z, Li P, Yang Y, Chi Y, Fan B, Chen Z. 2016. Expression and Functional Analysis of a Novel Group of Legume-specific WRKY and Exo70 Protein Variants from Soybean. *Scientific Reports* **6:** 32090.

Žárský V, Cvrčková F, Potocký M, Hála M. 2009. Exocytosis and cell polarity in plants - exocyst and recycling domains. *New Phytologist* **183**: 255–272.

Žárský V, Kulich I, Fendrych M, Pečenková T. 2013. Exocyst complexes multiple functions in plant cells secretory pathways. *Current Opinion in Plant Biology* **16**: 726–733.

Zhang X, Pumplin N, Ivanov S, Harrison MJ. 2015. EXO70I Is Required for Development of a Sub-domain of the Periarbuscular Membrane during Arbuscular Mycorrhizal Symbiosis. *Current Biology* **25**: 2189–2195.

Zhao Y, Liu J, Yang C, Capraro BR, Baumgart T, Bradley RP, Ramakrishnan N, Xu X, Radhakrishnan R, Svitkina T, *et al.*. 2013. Exo70 Generates Membrane Curvature for Morphogenesis and Cell Migration. *Developmental Cell* **26**: 266–278.

Zhao T, Rui L, Li J, Nishimura MT, Vogel JP, Liu N, Liu S, Zhao Y, Dangl JL, Tang D, *et al.*. 2015. A Truncated NLR Protein, TIR-NBS2, Is Required for Activated Defense Responses in the exo70B1 Mutant. *PLOS Genetics* **11(1)**:e1004945.